Osvaldo Gervasi · Beniamino Murgante ·
Chiara Garau · David Taniar ·
Ana Maria A. C. Rocha ·
Maria Noelia Faginas Lago (Eds.)

LNCS 14816

Computational Science and Its Applications – ICCSA 2024 Workshops

Hanoi, Vietnam, July 1–4, 2024
Proceedings, Part II

2 Part II



Springer

Lecture Notes in Computer Science **14816**

Founding Editors

Gerhard Goos
Juris Hartmanis

Editorial Board Members

Elisa Bertino, *Purdue University, West Lafayette, IN, USA*
Wen Gao, *Peking University, Beijing, China*
Bernhard Steffen, *TU Dortmund University, Dortmund, Germany*
Moti Yung, *Columbia University, New York, NY, USA*

The series Lecture Notes in Computer Science (LNCS), including its subseries Lecture Notes in Artificial Intelligence (LNAI) and Lecture Notes in Bioinformatics (LNBI), has established itself as a medium for the publication of new developments in computer science and information technology research, teaching, and education.

LNCS enjoys close cooperation with the computer science R & D community, the series counts many renowned academics among its volume editors and paper authors, and collaborates with prestigious societies. Its mission is to serve this international community by providing an invaluable service, mainly focused on the publication of conference and workshop proceedings and postproceedings. LNCS commenced publication in 1973.

Osvaldo Gervasi · Beniamino Murgante ·
Chiara Garau · David Taniar ·
Ana Maria A. C. Rocha ·
Maria Noelia Faginas Lago
Editors

Computational Science and Its Applications – ICCSA 2024 Workshops

Hanoi, Vietnam, July 1–4, 2024
Proceedings, Part II

Springer

Editors
Osvaldo Gervasi
Department of Mathematics and Computer Science
University of Perugia
Perugia, Italy

Chiara Garau
Department of Civil and Environmental Engineering and Architecture
University of Cagliari
Cagliari, Italy

Ana Maria A. C. Rocha
Algoritmi Research Centre
University of Minho
Braga, Portugal

Beniamino Murgante
School of Engineering
University of Basilicata
Potenza, Italy

David Taniar
Faculty of Information Technology
Monash University Clayton Campus
Clayton, VIC, Australia

Maria Noelia Faginas Lago
Department of Chemistry, Biology and Biotechnology
University of Perugia
Perugia, Italy

ISSN 0302-9743 ISSN 1611-3349 (electronic)
Lecture Notes in Computer Science
ISBN 978-3-031-65222-6 ISBN 978-3-031-65223-3 (eBook)
https://doi.org/10.1007/978-3-031-65223-3

© The Editor(s) (if applicable) and The Author(s), under exclusive license to Springer Nature Switzerland AG 2024

This work is subject to copyright. All rights are solely and exclusively licensed by the Publisher, whether the whole or part of the material is concerned, specifically the rights of translation, reprinting, reuse of illustrations, recitation, broadcasting, reproduction on microfilms or in any other physical way, and transmission or information storage and retrieval, electronic adaptation, computer software, or by similar or dissimilar methodology now known or hereafter developed.
The use of general descriptive names, registered names, trademarks, service marks, etc. in this publication does not imply, even in the absence of a specific statement, that such names are exempt from the relevant protective laws and regulations and therefore free for general use.
The publisher, the authors and the editors are safe to assume that the advice and information in this book are believed to be true and accurate at the date of publication. Neither the publisher nor the authors or the editors give a warranty, expressed or implied, with respect to the material contained herein or for any errors or omissions that may have been made. The publisher remains neutral with regard to jurisdictional claims in published maps and institutional affiliations.

This Springer imprint is published by the registered company Springer Nature Switzerland AG
The registered company address is: Gewerbestrasse 11, 6330 Cham, Switzerland

If disposing of this product, please recycle the paper.

Preface

These 11 volumes (LNCS volumes 14815–14825) consist of the peer-reviewed papers from the 55 Workshops of the 2024 International Conference on Computational Science and Its Applications (ICCSA 2024) which took place during July 1–4, 2024 in Hanoi (Vietnam). The peer-reviewed papers of the main conference tracks are published in a separate set consisting of two volumes (LNCS 14813–14814).

The conference was held in a hybrid form, with some participants present in person, hosted in Hanoi, Vietnam, by the Thuy Loi University. We enabled virtual participation for those who were unable to attend the event, due to logistical, political and economic problems, by adopting a technological infrastructure based on open source software (jitsi + riot), and a commercial Cloud infrastructure.

ICCSA 2024 was another successful event in the International Conference on Computational Science and Its Applications (ICCSA) conference series, previously held in Athens, Greece (2023), Malaga, Spain (2022), Cagliari, Italy (hybrid with few participants in presence in 2021 and completely online in 2020), whilst earlier editions took place in Saint Petersburg, Russia (2019), Melbourne, Australia (2018), Trieste, Italy (2017), Beijing. China (2016), Banff, Canada (2015), Guimaraes, Portugal (2014), Ho Chi Minh City, Vietnam (2013), Salvador, Brazil (2012), Santander, Spain (2011), Fukuoka, Japan (2010), Suwon, South Korea (2009), Perugia, Italy (2008), Kuala Lumpur, Malaysia (2007), Glasgow, UK (2006), Singapore (2005), Assisi, Italy (2004), Montreal, Canada (2003), and (as ICCS) Amsterdam, The Netherlands (2002) and San Francisco, USA (2001).

Computational Science is the main pillar of most of the present research, industrial and commercial applications, and plays a unique role in exploiting ICT innovative technologies, and the ICCSA conference series have been providing a venue to researchers and industry practitioners to discuss new ideas, to share complex problems and their solutions, and to shape new trends in Computational Science. As the conference mirrors society from a scientific point of view, this year's undoubtedly dominant theme was the machine learning and artificial intelligence and their applications in the most diverse economic and industrial fields.

The ICCSA 2024 conference is structured in 6 general tracks covering the fields of computational science and its applications: Computational Methods, Algorithms and Scientific Applications – High Performance Computing and Networks – Geometric Modeling, Graphics and Visualization – Advanced and Emerging Applications – Information Systems and Technologies – Urban and Regional Planning. In addition, the conference consisted of 55 workshops, focusing on very topical issues of importance to science, technology and society: from new mathematical approaches for solving complex computational systems, to information and knowledge in the Internet of Things, new statistical and optimization methods, several Artificial Intelligence approaches, sustainability issues, smart cities and related technologies.

In the Workshops proceedings we accepted 281 full papers, 17 short papers and 2 PhD Showcase papers. In the Main Conference Proceedings we accepted 53 full papers, 6 short papers and 3 PhD Showcase papers from 207 submissions to the General Tracks of the conference (acceptance rate 30%). We would like to express our appreciation to the workshops chairs and co-chairs for their hard work and dedication.

The success of the ICCSA conference series in general, and of ICCSA 2024 in particular, vitally depends on the support of many people: authors, presenters, participants, keynote speakers, workshop chairs, session chairs, organizing committee members, student volunteers, Program Committee members, Advisory Committee members, International Liaison chairs, reviewers and others in various roles. We take this opportunity to wholehartedly thank them all.

We also wish to thank our publisher, Springer, for their acceptance to publish the proceedings, for sponsoring part of the best papers awards and for their kind assistance and cooperation during the editing process.

We cordially invite you to visit the ICCSA website https://iccsa.org where you can find all the relevant information about this interesting and exciting event.

July 2024

Osvaldo Gervasi
Beniamino Murgante
Chiara Garau

Welcome Message from Organizers

After the very hard times of COVID, ICCSA continues its successful scientific endeavors in 2024, hosted in Hanoi, Vietnam. This time, ICCSA moved from the Mediterranean Region to Southeast Asia and was held in the metropolitan city of Hanoi, the capital of Vietnam. Hanoi is a vibrant urban environment known for the hospitality of its citizens, its rich history, vibrant culture, and dynamic urban life. Located in the northern part of the country, Hanoi is a bustling metropolis that combines the old with the new, offering a unique blend of ancient traditions and modern development.

ICCSA 2024 took place in a secure environment, allowing for safe and vibrant in-person participation. Combined with the active engagement of the ICCSA 2024 scientific community, this set the stage for highly motivating discussions and interactions regarding the latest developments in computer science and its applications in the real world for improving communities' quality of life.

Thuyloi University, also known as the Water Resources University, is a prominent institution in Hanoi, Vietnam, with a strong reputation in engineering and technical education, particularly in water resources and environmental engineering. In recent years, the University has expanded its academic offerings to include computer science, reflecting the growing importance of technology and digital skills in all sectors. This year, Thuyloi University had the honor of hosting ICCSA 2024. The Local Organizing Committee felt the burden and responsibility of such a demanding task and put all necessary energy into meeting participants' expectations and establishing a friendly, creative, and inspiring scientific and social/cultural environment that allowed for new ideas and perspectives to flourish.

Since all ICCSA participants, whether informatics-oriented or application-driven, realize the tremendous advancements in computer science over the last few decades and the huge potential these advancements offer in coping with the enormous challenges of humanity in a globalized, 'wired,' and highly competitive world, the expectations for ICCSA 2024 were high. The goal was to successfully match computer science progress with communities' aspirations, achieving progress that serves real, place- and people-based needs and paves the way towards a visionary, smart, sustainable, resilient, and inclusive future for both current and future generations.

On behalf of the Local Organizing Committee, I would like to sincerely thank all of you who contributed to ICCSA 2024.

Nguyen Canh Thai

Organization

ICCSA 2024 was organized by Thuyloi University (Vietnam), the University of Perugia (Italy), the University of Basilicata (Italy), Monash University (Australia), Kyushu Sangyo University (Japan), the University of Minho (Portugal), and the University of Cagliari (Italy).

Honorary General Chairs

Norio Shiratori	Chuo University, Japan
Kenneth C. J. Tan	Sardina Systems, UK

General Chairs

Nguyen Canh Thai	Thuyloi University, Vietnam
Osvaldo Gervasi	University of Perugia, Italy
David Taniar	Monash University, Australia

Program Committee Chairs

Beniamino Murgante	University of Basilicata, Italy
Chiara Garau	University of Cagliari, Italy
Ana Maria A. C. Rocha	University of Minho, Portugal
Bernady O. Apduhan	Kyushu Sangyo University, Japan

International Advisory Committee

Jemal Abawajy	Deakin University, Australia
Dharma P. Agarwal	University of Cincinnati, USA
Rajkumar Buyya	Melbourne University, Australia
Claudia Bauzer Medeiros	University of Campinas, Brazil
Manfred M. Fisher	Vienna University of Economics and Business, Austria
Pierre Frankhauser	University of Franche-Comté/CNRS, France
Marina L. Gavrilova	University of Calgary, Canada

Sumi Helal	University of Florida, USA & University of Lancaster, UK
Bin Jiang	University of Gävle, Sweden
Yee Leung	Chinese University of Hong Kong, China

International Liaison Chairs

Ivan Blečić	University of Cagliari, Italy
Giuseppe Borruso	University of Trieste, Italy
Elise De Donker	Western Michigan University, USA
Maria Noelia Faginas Lago	University of Perugia, Italy
Maria Irene Falcão	University of Minho, Portugal
Robert C. H. Hsu	Chung Hua University, Taiwan
Yeliz Karaca	University of Massachusetts Medical School, Worcester, USA
Tae-Hoon Kim	Zhejiang University of Science and Technology, China
Vladimir Korkhov	Saint Petersburg University, Russia
Takashi Naka	Kyushu Sangyo University, Japan
Rafael D. C. Santos	National Institute for Space Research, Brazil
Maribel Yasmina Santos	University of Minho, Portugal
Anastasia Stratigea	National Technical University of Athens, Greece

Workshop and Session Organizing Chairs

Beniamino Murgante	University of Basilicata, Italy
Chiara Garau	University of Cagliari, Italy

Award Chair

Wenny Rahayu	La Trobe University, Australia

Publicity Committee Chairs

Elmer Dadios	De La Salle University, Philippines
Nataliia Kulabukhova	Saint Petersburg University, Russia

Daisuke Takahashi	Tsukuba University, Japan
Shangwang Wang	Beijing University of Posts and Telecommunications, China

Local Organizing Committee Chairs

Doan Quang Tu	Academy of Military Science and Technology, Hanoi, Vietnam
Ho Sy Tam	Thuyloi University, Vietnam
Le Quang Tuan	Thuyloi University, Vietnam
Nguyen Huu Quynh	Thuyloi University, Vietnam
Ta Quang Chieu	Thuyloi University, Vietnam

Technology Chair

Damiano Perri	University of Perugia, Italy

Program Committee

Vera Afreixo	University of Aveiro, Portugal
Vladimir Alarcon	Northern Gulf Institute, USA
Filipe Alvelos	University of Minho, Portugal
Debora Anelli	Polytechnic University of Bari, Italy
Hartmut Asche	Hasso-Plattner-Institut für Digital Engineering, Germany
Ginevra Balletto	University of Cagliari, Italy
Socrates Basbas	Aristotle University of Thessaloniki, Greece
David Berti	ART SpA, Italy
Michela Bertolotto	University College Dublin, Ireland
Debnath Bhattacharyya	Koneru Lakshmaiah University, India
Sandro Bimonte	CEMAGREF, TSCF, France
Ana Cristina Braga	University of Minho, Portugal
Tiziana Campisi	Kore University of Enna, Italy
Yves Caniou	Lyon University, France
José A. Cardoso e Cunha	Universidade Nova de Lisboa, Portugal
Rui Cardoso	University of Beira Interior, Portugal
Leocadio G. Casado	University of Almeria, Spain
Mete Celik	Erciyes University, Turkey
Maria Cerreta	University of Naples Federico II, Italy
Mauro Coni	University of Cagliari, Italy

Florbela Maria da Cruz Domingues Correia	Polytechnic Institute of Viana do Castelo, Portugal
Roberto De Lotto	University of Pavia, Italy
Marcelo De Paiva Guimaraes	Federal University of Sao Paulo, Brazil
Frank Devai	London South Bank University, UK
Joana Matos Dias	University of Coimbra, Portugal
Laila El Ghandour	Heriot Watt University, UK
Rafida M. Elobaid	Canadian University Dubai, United Arab Emirates
Maria Irene Falcao	University of Minho, Portugal
Florbela P. Fernandes	Polytechnic Institute of Bragança, Portugal
Paula Odete Fernandes	Polytechnic Institute of Bragança, Portugal
Adelaide de Fátima Baptista Valente Freitas	University of Aveiro, Portugal
Valentina Franzoni	University of Perugia, Italy
Andreas Fricke	University of Potsdam, Germany
Raffaele Garrisi	Centro Operativo per la Sicurezza Cibernetica, Italy
Maria Giaoutzi	National Technical University, Athens, Greece
Salvatore Giuffrida	University of Catania, Italy
Teresa Guarda	Universidad Estatal Peninsula de Santa Elena, Ecuador
Sevin Gümgüm	Izmir University of Economics, Turkey
Malgorzata Hanzl	Technical University of Lodz, Poland
Maulana Adhinugraha Kiki	Telkom University, Indonesia
Clement Ho Cheung Leung	Chinese University of Hong Kong, China
Andrea Lombardi	University of Perugia, Italy
Marcos Mandado Alonso	University of Vigo, Spain
Ernesto Marcheggiani	Katholieke Universiteit Leuven, Belgium
Antonino Marvuglia	Luxembourg Institute of Science and Technology, Luxembourg
Michele Mastroianni	University of Salerno, Italy
Hideo Matsufuru	High Energy Accelerator Research Organization, Japan
Alfredo Milani	University of Perugia, Italy
Fernando Miranda	Universidade do Minho, Portugal
Giuseppe Modica	University of Reggio Calabria, Italy
Louiza de Macedo Mourelle	State University of Rio de Janeiro, Brazil
Nadia Nedjah	State University of Rio de Janeiro, Brazil
Paolo Nesi	University of Florence, Italy
Rajdeep Niyogi	Indian Institute of Technology Roorkee, India
Suzan Obaiys	University Malaya, Malaysia
Marcin Paprzycki	Polish Academy of Sciences, Poland

Eric Pardede	La Trobe University, Australia
Ana Isabel Pereira	Polytechnic Institute of Bragança, Portugal
Damiano Perri	University of Perugia, Italy
Massimiliano Petri	University of Pisa, Italy
Telmo Pinto	University of Coimbra, Portugal
Maurizio Pollino	ENEA, Italy
Alenka Poplin	Iowa State University, USA
Marcos Quiles	Federal University of São Paulo, Brazil
Humberto Rocha	University of Coimbra, Portugal
Marzio Rosi	University of Perugia, Italy
Manna Sheela Rani Chetty	Koneru Lakshmaiah University, India
Lucia Saganeiti	University of L'Aquila, Italy
Tamie Salter	Citizen Alerts Inc., Canada
Francesco Scorza	University of Basilicata, Italy
Marco Paulo Seabra dos Reis	University of Coimbra, Portugal
Jie Shen	University of Michigan, USA
Chien Sing Lee	Sunway University, Malaysia
Francesco Tajani	Sapienza University of Rome, Italy
Rodrigo Tapia-McClung	Centro de Investigación en Ciencias de Información Geoespacial, Mexico
Eufemia Tarantino	Polytechnic of Bari, Italy
Sergio Tasso	University of Perugia, Italy
Ana Paula Teixeira	Universidade do Minho, Portugal
Maria Filomena Teodoro	IST ID, Instituto Superior Técnico, Portugal
Yiota Theodora	National Technical University of Athens, Greece
Carmelo Torre	Polytechnic of Bari, Italy
Giuseppe A. Trunfio	University of Sassari, Italy
Toshihiro Uchibayashi	Kyushu University, Japan
Marco Vizzari	University of Perugia, Italy
Frank Westad	Norwegian University of Science and Technology, Norway
Fukuko Yuasa	High Energy Accelerator Research Organization, Japan
Ljiljana Zivkovic	Republic Geodetic Authority, Serbia

Workshops

Advances in Artificial Intelligence Learning Technologies: Blended Learning, STEM, Computational Thinking and Coding (AAILT 2024)

Workshop Organizers

Alfredo Milani	University of Perugia, Italy
Valentina Franzoni	University of Perugia, Italy
Sergio Tasso	University of Perugia, Italy

Workshop Program Committee Members

Li Yuanxi	Hong Kong Baptist University, Hong Kong, China
Valentino Santucci	University for Foreigners, Perugia, Italy
Krassimir Markov	Institute of Information Theories and Applications, Sofia, Bulgaria
Clement Leung	Chinese University of Hong Kong, China
Rajdeep Niyogi	Indian Institute of Technology, Rooorkee, India

Advanced and Innovative Web Apps 2024 (AIWA 2024)

Workshop Organizers

Osvaldo Gervasi	University of Perugia, Italy
Damiano Perri	University of Perugia, Italy

Workshop Program Committee Members

Tamie Salter	Citizen Alert Inc., Canada
Paolo Nesi	University of Florence, Italy
Tae Hoon Kim	Zhejiang University of Science and Technology, China
Debnath Bhattacharyya	Koneru Lakshmaiah Education Foundation, India
David Berti	ART SpA, Italy

Advanced Processes of Mathematics and Computing Models in Complex Computational Systems (ACMC 2024)

Workshop Organizers

Yeliz Karaca	University of Massachusetts Chan Medical School and Massachusetts Institute of Technology, USA
Dumitru Baleanu	Cankaya University, Turkey
Osvaldo Gervasi	University of Perugia, Italy
Yudong Zhang	University of Leicester, UK
Majaz Moonis	University of Massachusetts Medical School, USA

Workshop Program Committee Members

Tamie Salter	Citizen Alert Inc., Canada
TaiHoon Kim	Konkuk University, South Korea
Debnath Bhattacharyya	Koneru Lakshmaiah Education Foundation, India
Massimiliano Nicolini	OliTec Foundation, Italy
Martin Bohner	Missouri University of Science and Technology, Missouri, USA
René Lozi	Université Côte d'Azur, France
Ravi P. Agarwal	Texas A&M University-Kingsville, USA
Aziz Dursun	Virginia Tech, USA
Muhammad Attique Khan	HITEC University, Pakistan and Lebanese American University, Lebanon
Rasulova Mukhayo	National University Uzbekistan, Uzbekistan

Advances in Information Systems and Technologies for Emergency Management, Risk Assessment and Mitigation Based on the Resilience Concepts (ASTER 2024)

Workshop Organizers

Maurizio Pollino	Italian National Agency for New Technologies, Energy and Sustainable Economic Development, Italy
Marco Vona	University of Basilicata, Italy

Alessandro Giocoli	Italian National Agency for New Technologies, Energyand Sustainable Economic Development, Italy
Chiara Ormando	Italian National Agency for New Technologies, Energy and Sustainable Economic Development, Italy
Angelo Anelli	Italian National Research Council, Italy

Workshop Program Committee Members

Gregorio D'Agostino	Italian National Agency for New Technologies, Energy and Sustainable Economic Development, Italy
Christian Bignami	INGV, Italy
Paolo Clemente	Anti-Seismic Systems International Society, ASSISI, USA
Sonia Giovinazzi	Italian National Agency for New Technologies, Energy and Sustainable Economic Development, Italy

Advances in Web-Based Learning 2024 (AWBL 2024)

Workshop Organizers

Mustafa Inceoglu	Ege University, Turkey
Birol Ciloglugil	Ege University, Turkey

Workshop Program Committee Members

Birim Balci	Celal Bayar University, Turkey
Burak Galip Aslan	Izmir Yuksek Teknoloji University, Turkey
Mahmut Unan	University of Alabama, USA
Nisha S. Raj	Global Indian International School, Japan
Oylum Alatlı	Ege University, Turkey

Blockchain and Distributed Ledgers: Technologies and Applications (BDLTA 2024)

Workshop Organizers

Vladimir Korkhov	Saint Petersburg State University, Russia
Elena Stankova	Saint Petersburg State University, Russia
Nataliia Kulabukhova	Saint Petersburg State University, Russia

Workshop Program Committee Members

Vasily Solodkov	Higher School of Economics Banking Institute
Alexander Bogdanov	St. Petersburg State University, Russia
Alexander Degtyarev	St. Petersburg State University, Russia
Dmitry Vasiunin	Deutsche Telekom Cloud Services E.P.E., Greece
Serob Balyan	National Academy of Sciences of Armenia, Armenia
Suren Abrahamyan	Osensus Arm LLC, Armenia
Ashot Gevorkyan	National Academy of Sciences of Armenia, Armenia
Martin Vala	Univerzita Pavla Jozefa Šafárika Košiciach, Košice, Slovakia
Nodir Zaynalov	Tashkent University of Information Technologies, Uzbekistan
Michail Panteleyev	St. Petersburg Electrotecnical University, Russia
Nikolay Peryazev	Irkutsk State University, Irkutsk, Russia

Computational and Applied Mathematics (CAM 2024)

Workshop Organizers

Maria Irene Falcao	University of Minho, Portugal
Fernando Miranda	University of Minho, Portugal

Workshop Program Committee Members

Ricardo Severino	University of Minho, Portugal
Helmuth Malonek	University of Aveiro, Portugal
Isabel Cacao	University of Aveiro, Portugal
Graça Tomaz	Polytechnic of Guarda, Portugal

Rosário Fernandes	University of Minho, Portugal
Lidia Aceto	University of Piedmont Oriental, Italy
Patrícia Beites	University of Beira Interior, Portugal
Regina de Almeida	University of Trás-os-Montes e Alto Douro, Portugal
Luís Ferrás	University of Porto, Portugal
Helmuth Malonek	University of Aveiro, Portugal
João Morais	Autonomous Technological Institute of Mexico, Mexico
Yilmaz Simsek	Akdeniz University, Turkey

Computational and Applied Statistics (CAS 2024)

Workshop Organizer

Ana Cristina Braga	University of Minho, Portugal

Workshop Program Committee Member

Adelaide Freitas	University of Aveiro, Portugal
Ângela Silva	University of Minho, Portugal
Arminda Manuela Gonçalves	University of Minho, Portugal
Arunasalam Rahunanthan	Central State University, USA
Elisete Correia	University of Trás-os-Montes e Alto Douro, Portugal
Frank Westad	Norwegian University of Science and Technology, Norway
Humberto Rocha	University of Coimbra, Portugal
Ivan Rodriguez Conde	University of Arkansas, USA
Lino Costa	University of Minho, Portugal
Marco Reis	University of Coimbra, Portugal
Maria Filipa Mourão	Polytechnic Institute of Viana do Castelo, Portugal
Martín Pérez Pérez	University of Vigo, Spain
Michal Abrahamowicz	McGill University, Canada
Vanda Lourenço	New University of Lisbon, Portugal
Vera Afreixo	University of Aveiro, Portugal

Cyber Intelligence and Applications (CIA 2024)

Workshop Organizer

Gianni D'Angelo	University of Salerno, Italy

Workshop Program Committee Members

Massimo Ficco	University of Salerno, Italy
Marcello Trovati	Edge Hill University, UK
Michal Choras	Bydgoszcz University of Science and Technology, Poland

Computational Methods, Statistics and Industrial Mathematics (CMSIM 2024)

Workshop Organizers

Maria Filomena Teodoro	University of Lisbon and Portuguese Naval Academy, Portugal
Marina A. P. Andrade	University Institute of Lisbon, Portugal
Maria de Fátima Alves de Pina	University Institute of Lisbon, Portugal

Workshop Program Committee Members

Ricardo Moura	University of Lisboa and FCT, Portugal
Aldina Correia	Escola Superior de Tecnologia e Gestão, Portugal
Eliana Costa	Escola Superior de Tecnologia e Gestão, Portugal
Ana Borges	Escola Superior de Tecnologia e Gestão, Portugal
Cristina Lopes	ISCAP, Portugal
Fernando Carapau	University of Evora, Portugal
Fernanda Costa	University of Minho, Portugal
Maria Luísa Morgado	University of Trás os Montes e Alto Douro and University of Lisboa, Portugal
Ana Isabel Pereira	Instituto Politécnico de Bragança, Portugal
Bruna Ramos	University of Minho, Portugal
Rosário Ramos	Universidade Aberta, Portugal
Elisabete Carolino	Escola Superior da Saúde de Lisboa, Portugal
Sofia Rézio	Instituto Politécnico de Lisboa, Portugal
Matteo Sacchet	University of Turin, Italy

Marina Marchisio Conte	University of Turin, Italy
António Seijas-Macias	University of Coruña, Spain
Luís F. A. Teodoro	University of Glasgow, UK and University of Oslo, Norway
Christos Kitsos	University of West Attica, Greece

Computational Optimization and Applications (COA 2024)

Workshop Organizers

Ana Maria A. C. Rocha	University of Minho, Portugal
Humberto Rocha	University of Coimbra, Portugal

Workshop Program Committee Members

Eligius M. T. Hendrix	University of Málaga, Spain
Joana Matos Dias	University of Coimbra, Portugal
Ana Isabel Pereira	Polytechnic Institute of Bragança, Portugal
Filipe Alvelos	Univeristy of Minho, Portugal
Emerson José de Paiva	Federal University of Itajubá, Brazil

Computational Astrochemistry (CompAstro 2024)

Workshop Organizers

Marzio Rosi	University of Perugia, Italy
Nadia Balucani	University of Perugia, Italy
Daniela Ascenzi	University of Trento, Italy
Stefano Falcinelli	University of Perugia, Italy

Workshop Program Committee Members

Albert Rimola	Universitat Autònoma de Barcelona, Spain
Dimitrios Skouteris	Master-Tec, Perugia, Italy
Piero Ugliengo	University of Turin, Italy
Andrea Lombardi	University of Perugia, Italy
Piergiorgio Casavecchia	University of Perugia, Italy
Fernando Pirani	University of Perugia, Italy
Costanza Borghesi	University of Perugia, Italy

Gabriella Digenova	University of Perugia, Italy
Lisa Giani	Grenoble Alpes University, France
Marco Parriani	University of Perugia, Italy
Cecilia Coletti	University of Chieti, Italy
Massimiliano Aschi	University of L'Aquila, Italy
Emilia Dearagao	University of Perugia, Italy
Giacomo Pannacci	University of Perugia, Italy
Gianmarco Vanuzzo	University of Perugia, Italy

Computational Methods for Porous Geomaterials (CompPor 2024)

Workshop Organizers

Vadim Lisitsa	Russian Academy of Science, Russia
Evgeniy Romenski	Russian Academy of Science, Russia

Workshop Program Committee Members

Kirill Gadylshin	Russian Academy of Science, Russia
Tayana Khachkova	Russian Academy of Science, Russia
Dmitri Prokhorov	Russian Academy of Science, Russia
Mikahil Novikov	Russian Academy of Science, Russia

Workshop on Computational Science and HPC (CSHPC 2024)

Workshop Organizers

Elise De Doncker	Western Michigan University, USA
Fukuko Yuasa	High Energy Accelerator Research Organization, Japan
Hideo Matsufuru	High Energy Accelerator Research Organization, Japan

Workshop Program Committee Members

Tadashi Ishikawa	High Energy Accelerator Research Organization, Japan
Hiroshi Daisaka	Hitotsubashi University, Japan
Naohito Nakasato	University Aizu, Japan

Takahiro Ueda	Juntendo University, Japan
Khiem Hong Phan	Duy Tan University, Vietnam
Naohito Nakasato	University Aizu, Japan
Tasnim Gharaibeh	Kalamazoo College, USA
Robert Makin	Western Michigan University, USA

Cities, Technologies and Planning (CTP 2024)

Workshop Organizers

Beniamino Murgante	University of Basilicata, Italy
Giuseppe Borruso	University of Trieste, Italy
Malgorzata Hanzl	Lodz University of Technology, Poland
Anastasia Stratigea	National Technical University of Athens, Greece
Ljiljana Zivkovic	Republic Geodetic Authority, Serbia
Ginevra Balletto	University of Cagliari, Italy

Workshop Program Committee Members

Silvia Battino	University of Sassari, Italy
Mara Ladu	University of Cagliari, Italy
Maria del Mar Munoz Leonisio	University of Cadiz, Spain
Ahinoa Amaro Garcia	Univeristy of Las Palmas of Gran Canaria, Spain
Maria Attard	University of Malta, Malta
Enrico Dagostini	University of Malta, Malta
Francesca Krasna	University of Trieste, Italy
Brisol García García	Polytechnic University of Quintana Roo, Mexico
Tu Anh Trinh	College of Technology and Design for UEH University, Vietnam
Giovanni Mauro	University of Campania Luigi Vanvitelli, Italy
Maria Ronza	University of Naples, Federico II, Italy
Massimiliano Bencardino	University of Salerno, Italy

Sustainable Digital Circular Economy (DiCE 2024)

Workshop Organizers

Ginevra Balletto	University of Cagliari, Italy
Stefano Epifani	Digital Sustainability Foundation, Italy

Stefano Carboni	University of Sassari, Italy
Francesca Sinatra	University of Cagliari, Italy
Salvatore Dore	University of Sassari, Italy
Andrea Gallo	University of Trieste, Italy

Workshop Program Committee Members

Giuseppe Borruso	University of Trieste, Italy
Silvia Battino	University of Sassari, Italy
Beniamino Murgante	University of Basilicata, Italy
Mara Ladu	University of Cagliari, Italy
Luigi Mundula	University of Perugia, Italy
Maria Attard	University of Malta, Malta
Enrico Dagostini	University of Malta, Malta
Emilio Ghiani	University of Cagliari, Italy
Marco Naseddu	University of Cagliari, Italy
Balázs Kulcsaár	University of Debrecen, Hungary
Tu Anh Trinh	College of Technology and Design for UEH University, Vietnam
Giovanni Mauro	University of Campania Luigi Vanvitelli, Italy
Maria Ronza	University of Naples, Federico II, Italy
Massimiliano Bencardino	University of Salerno, Italy

Evaluating Inner Areas Potentials (EIAP 2024)

Workshop Organizers

Diana Rolando	Polytechnic of Turin, Italy
Alice Barreca	Polytechnic of Turin, Italy
Manuela Rebaudengo	Polytechnic of Turin, Italy
Giorgia Malavasi	Polytechnic of Turin, Italy

Workshop Program Committee Members

John Accordino	Virginia Commonwealth University, USA
Sara Favargiotti	University of Trento, Italy
Maddalena Ferretti	Polytechnic University of Marche, Italy
Daniel Laven	Mid Sweden University, Sweden
Barbara Lino	University of Palermo, Italy
Umberto Mecca	Polytechnic University of Turin, Italy

Lorenzo Savio	Polytechnic University of Turin, Italy
Asja Aulisio	Polytechnic University of Turin, Italy

Econometrics and Multidimensional Evaluation of Urban Environment (EMEUE 2024)

Workshop Organizers

Carmelo Maria Torre	Polytechnic of Bari, Italy
Francesco Tajani	Sapienza University of Rome, Italy
Pierluigi Morano	Polytechnic of Bari, Italy
Simona Panaro	University of Sussex, UK
Maria Cerreta	University of Naples Federico II, Italy
Debora Anelli	Polytechnic of Bari, Italy

Workshop Program Committee Members

Pierfrancesco de Paola	University of Naples Federico II, Italy
Daniela Tavano	University of Calabria, Italy
Giuseppe Cerullo	Sapienza University of Rome, Italy
Francesco Paolo del Giudice	Sapienza University of Rome, Italy
Marco Locurcio	Polytechnic University of Bari, Italy
Maria Rosa Trovato	University of Catania, Italy
Felicia di Liddo	Polytechnic University of Bari, Italy
Maria Paz Saez Perez	University of Granada, Spain
Yasmine Selim	Ain Shams University, Cairo
Hasan Mara	Indian Institute of Technology Roorkee, India
Philipp Wiesner	Technical University of Berlin, Germany
Maria Gamboa Perez	Complutense University of Madrid, Spain
Manuel Yanez	Universidad Autónoma de Madrid, Spain
Lucia Ika Fitriastuti	Solusi Bisnis Indonesia, Indonesia
Frank Devai	London South Bank University, UK
Frank Westad	Norwegian University of Science and Technology, Norway
Eugenio Muccio	University of Naples Federico II, Italy
Chiara Mazzarella	TU Delft, The Netherlands
Daniele Cannatella	TU Delft, The Netherlands
Sabrina Sacco	University of Naples Federico II, Italy
Piero Zizzania	University of Naples Federico II, Italy
Stefano Cuntò	University of Naples Federico II, Italy

Sveva Ventre	University of Naples Federico II, Italy
Caterina Loffredo	University of Naples Federico II, Italy
Giuseppe Ciciriello	University of Naples Federico II, Italy
Maria Somma	University of Naples Federico II, Italy
Ludovica La Rocca	University of Naples Federico II, Italy
Gaia Daldanise	National Research Council, Italy
Giuliano Poli	University of Naples Federico II, Italy

Environmental, Social, Governance of Energy Planning (ESGEP 2024)

Workshop Organizers

Ginevra Balletto	University of Cagliari, Italy
Emilio Ghiani	University of Cagliari, Italy
Roberto De Lotto	University of Pavia, Italy
Alessandra Marra	University of Salerno, Italy
Riccardo Trevisan	University of Cagliari, Italy
Balázs Kulcsár	University of Debrecen, Hungary

Workshop Program Committee Members

Jacopo Torriti	University of Reading, UK
Roberto Gerundo	University of Salerno, Italy
Luigi Mundula	University of Perugia, Italy
Mara Ladu	University of Cagliari, Italy
Giuseppe Borruso	University of Trieste, Italy
Tu Anh Trinh	College of Technology and Design for UEH University, Vietnam
Giovanni Mauro	University of Campania Luigi Vanvitelli, Italy
Maria Ronza	University of Naples, Federico II, Italy
Massimiliano Bencardino	University of Salerno, Italy

Ecosystem Services in Spatial Planning for Resilient Urban and Rural Areas (ESSP 2024)

Workshop Organizers

Sabrina Lai	University of Cagliari, Italy
Corrado Zoppi	University of Cagliari, Italy
Francesco Scorza	University of Basilicata, Italy

Beniamino Murgante	University of Basilicata, Italy
Floriana Zucaro	University of Naples Federico II, Italy
Carmela Gargiulo	University of Naples Federico II, Italy

Workshop Program Committee Members

Carmen Guida	University of Naples Federico II, Italy
Irina Di Ruocco	Insubria University, Italy
Silvia Rossetti	University of Parma, Italy
Barbara Caselli	University of Parma, Italy
Gloria Pellicelli	University of Parma, Italy
Federica Leone	University of Cagliari, Italy
Federica Isola	University of Cagliari, Italy
Francesca Leccis	University of Cagliari, Italy
Francesca Perrone	Sapienza University of Rome, Italy
Angela Pilogallo	Italian National Research Council, Italy
Alfonso Annunziata	University of Basilicata, Italy
Alessandro Marucci	University of L'Aquila, Italy
Francesco Zullo	University of L'Aquila, Italy
Gizem Dinç	Süleyman Demirel University, Turkey
Atila Gul	Süleyman Demirel University, Turkey
Sarah Scheiber	University of Malta, Malta
Matteo Caglioni	Université Côte d'Azur, France

Ethical AI Applications for a Human-Centered Cyber Society (EthicAI 2024)

Workshop Organizers

Valentina Franzoni	University of Perugia, Italy
Alfredo Milani	University of Perugia, Italy
Jordi Vallverdu	University Autonoma Barcelona, Spain

Workshop Program Committee Members

Sergio Tasso	University of Perugia, Italy
Yuanxi Li	Hong Kong Baptist University, Hong Kong, China
Daniele Mezzetti	Santa Maria della Misericordia Hospital of Perugia, Italy
Abeer Dyoub	L'Aquila University, Italy

14th International Workshop on Future Computing System Technologies and Applications (FiSTA 2024)

Workshop Organizers

Bernady Apduhan	Kyushu Sangyo University, Japan
Rafael Santos	National Institute for Space Research, Brazil

Workshop Program Committee Members

Agustinus Borgy Waluyo	Monash University, Australia
Andre Ricardo Abed Grégio	Federal University of Parana, Brazil
Earl Ryan Aleluya	MSU-Iligan Institute of Technology, Philippines
Kai Cheng	Kyushu Sangyo University, Japan
Alvaro Fazenda	Federal University of São Paulo, Brazil
Yusuke Gotoh	Okayama University, Japan
Eric Pardede	La Trobe University, Australia
Yasuaki Sumida	Kyushu Sangyo University, Japan
Kazuaki Tanaka	Kyushu Institute of Technology, Japan
Toshihiro Uchibayashi	Kyushu University, Japan
Toshihiro Yamauchi	Okayama University, Japan
Fenghui Yao	Tennessee State University, USA

Geographical Analysis, Urban Modeling, Spatial Statistics (Geog-An-Mod 2024)

Workshop Organizers

Beniamino Murgante	University of Basilicata, Italy
Giuseppe Borruso	University of Trieste, Italy
Harmut Asche	Hasso-Plattner-Institut für Digital Engineering, Germany
Andreas Fricke	Hasso-Plattner-Institut für Digital Engineering, Germany
Rodrigo Tapia McClung	Centro de Investigación en Ciencias de Información Geoespacial, Mexico

Workshop Program Committee Members

Ginevra Balletto	University of Cagliari, Italy
Silvia Battino	University of Sassari, Italy
Mara Ladu	University of Cagliari, Italy
Marco Mazzarino	IUAV Univeristy Venice, Italy
Maria del Mar Munoz Leonisio	Univeristy of Cadiz, Spain
Ahinoa Amaro Garcia	University of Las Palmas of Gran Canaria, Spain
Veronica Camerada	University of Sassari, Italy
Maria Attard	University of Malta, Malta
Enrico Dagostini	University of Malta, Malta
Francesca Krasna	University of Trieste, Italy
Malgorzata Hanzl	Lodz University of Technology, Poland
Anastasia Stratigea	National Technical University of Athens, Greece
Tu Anh Trinh	College of Technology and Design for UEH University, Vietnam
Giovanni Mauro	University of Campania Luigi Vanvitelli, Italy
Maria Ronza	University of Naples, Federico II, Italy
Massimiliano Bencardino	University of Salerno, Italy

Geomatics for Resource Monitoring and Management (GRMM 2024)

Workshop Organizers

Alessandra Capolupo	Polytechnic of Bari, Italy
Eufemia Tarantino	Polytechnic of Bari, Italy
Alberico Sonnessa	Polytechnic of Bari, Italy

Workshop Program Committee Members

Umberto Fratino	Polytechnic of Bari, Italy
Valeria Monno	Polytechnic of Bari, Italy
Antonino Maltese	University of Palermo, Italy
Athos Agapiou	Cyprus University of Technology, Cyprus
Michele Mangiameli	University of Catania, Italy
Angela Gorgoglione	University of la República de Uruguay, Uruguay
Roberta Ravanelli	Sapienza University of Rome, Italy
Alessandra Mascitelli	D'Annunzio University of Chieti–Pescara, Italy
Ester Scotto di Perta	University of Naples, Federico II, Italy

Giacomo Caporusso	National Research Council, Italy
Andrea Montanino	University of Naples, Federico II, Italy
Antonino Iannuzzo	University of Sannio, Benevento, Italy
Silvano Dal Sasso	University of Basilicata, Potenza, Italy
Laura Mirra	National Research Council, Water Research Institute, Italy
Alessandro Pagano	National Research Council, Water Research Institute, Italy
Francesco Chiaravalloti	National Research Council, Water Research Institute, Italy
Francesco Di Capua	University of Basilicata, Italy
Stefania Santoro	National Research Council, Water Research Institute, Italy
Cinzia Albertini	National Research Council, IREA, Italy
Alessandra Saponieri	University of Salento, Italy

International Workshop on Information and Knowledge in the Internet of Things (IKIT 2024)

Workshop Organizers

Teresa Guarda	Peninsula State University of Santa Elena, Ecuador
José María Díaz Nafría	Madrid Open University, Spain
Filipe Portela	University of Minho, Portugal

Workshop Program Committee Members

Arnulfo Alanis	Instituto Tecnologico de Tijuana, Mexico
Bruno Sousa	University of Coimbra, Portugal
Carlos Balsa	Instituto Politécnico de Bragança, Portugal
Filipe Mota Pinto	Instituto Politécnico de Leiria, Portugal
Gustavo Gatica	Universidad Andrés Bello, Chile
Isabel Lopes	Instituto Politécnico de Bragança, Portugal
José María Díaz Nafría	Universidad a Distancia, Spain
Maria Fernanda Augusto	BiTrum Research Group, Spain
Maria Isabel Ribeiro	Instituto Politécnico Bragança, Portugal
Modestos Stavrakis	University of the Aegean, Greece
Simone Belli	Universidad Complutense de MadridSpain
Walter Lopes Neto	Instituto Federal de Educação, Brazil

Regenerating Brownfields Enhancing Urban Resilience Appeal (INFERENCE 2024)

Workshop Organizers

Francesca Moraci	Mediterranea University of Reggio Calabria, Italy
Maurizio Oddo	University of Enna Kore, Italy
Antonella Versaci	University of Enna Kore, Italy
Celestina Fazia	University of Enna Kore, Italy
Tiziana Campisi	University of Enna Kore, Italy
Kh Md Nahiduzzaman	University of British Columbia, Canada

Workshop Program Committee Members

Alessandro Baracco	University of Enna Kore, Italy
Kaoutare Amini Alaoui	Mohammed VI Polytechnic University, UM6P, Morocco
Maurizio Errigo	Sapienza University of Rome, Italy
Marsia Marino	Sapienza University of Rome, Italy
Nessrine Moumen	Mohammed VI Polytechnic University, UM6P, Morocco
Francesca Perrone	Sapienza University of Rome, Italy
Pasquale Pizzimenti	Mediterranea University of Reggio Calabria, Italy
Barbara Scala	University of Brescia, Italy
Clarastella Vicari Aversa	Mediterranea University of Reggio Calabria, Italy

International Workshop on Territorial Planning to Integrate Risk and Urban Ontologies (IWPRO 2024)

Workshop Organizers

Elisabetta Maria Venco	University of Pavia, Italy
Beniamino Murgante	University of Basilicata, Italy
Roberto De Lotto	University of Pavia, Italy
Caterina Pietra	University of Pavia, Italy

Workshop Program Committee Members

Stefano Borgo	National Research Council, Italy
Valentina Costa	University of Genoa, Italy
Pajouh Danesh	Middle East Technical University, Turkey

Ilaria Delponte	University of Genoa, Italy
Lorena Fiorini	University of L'Aquila, Italy
Veronica Gazzola	Polytechnic of Milan, Italy
Ghazaleh Goodarzi	Islamic Azad University, Iran
Michele Grimaldi	University of Salerno, Italy
Alessandra Marra	University of Salerno, Italy
Naghmeh Mohammadpourlima	Akademi University, Finland
Francesca Pirlone	University of Genoa, Italy
Silvia Rossetti	University of Parma, Italy
Lucia Saganeiti	University of L'Aquila, Italy
Bahareh Shahsavari	University of Minnesota, USA
Ilenia Spadaro	University of Genoa, Italy
Maria Rosaria Stufano Melone	Polytechnic of Bari, Italy

MaaS Solutions for Airports, Cities and Regional Connectivity (MaaS 2024)

Workshop Organizers

Gianfranco Fancello	University of Cagliari, Italy
Francesco Piras	University of Cagliari, Italy
Tanja Congiu	University of Sassari, Italy
Mara Ladu	University of Cagliari, Italy
Martina Sinatra	University of Cagliari, Italy
Ginevra Balletto	University of Cagliari, Italy

Workshop Program Committee Members

Italo Meloni	University of Cagliari, Italy
Tu Anh Trinh	College of Technology and Design for UEH University, Vietnam
Giuseppe Borruso	University of Trieste, Italy
Luigi Mundula	University of Perugia, Italy
Francesca Sinatra	University of Trieste, Italy
Salvatore Dore	University of Trieste, Italy
Andrea Gallo	University of Trieste, Italy
Marcello Tadini	University of Eastern Piedmont, Italy
Marco Mazzarino	IUAV Univeristy Venice, Italy
Maria del Mar Munoz Leonisio	University of Cadiz, Spain
Veronica Camerada	Univeristy of Sassari, Italy

Brunella Brundu	Univerisity of Sassari, Italy
Maria Attard	University of Malta, Malta
Enrico Dagostini	University of Malta, Malta
Giovanni Mauro	University of Campania Luigi Vanvitelli, Italy
Maria Ronza	University of Naples, Federico II, Italy
Massimiliano Bencardino	University of Salerno, Italy

Development of Urban Mobility Management and Risk Assessment (MAINTAIN 2024)

Workshop Organizers

Tiziana Campisi	University of Enna Kore, Italy
Massimo Di Gangi	University of Messina, Italy
Antonio Comi	University of Rome Tor Vergata, Italy
Grigorios Fountas	Aristotle University of Thessaloniki, Greece
Jesús González-Feliu	Excelia Business School, La Rochelle, France

Workshop Program Committee Members

Paola Panuccio	Mediterranea University of Reggio Calabria, Italy
Domenica Savia Pellicano	Mediterranean University of Reggio Calabria, Italy
Alexandros Nikitas	University of Huddersfield, UK
Antonio Polimeni	University of Messina, Italy
Orlando Belcore	University of Messina, Italy
Marinella Giunta	Mediterranea University of Reggio Calabria, Italy
Borja Alonso	University of Cantabria, Spain
Luigi Dall'Olio	University of Cantabria, Santander, Spain
Kh Md Nahiduzzaman	UBC, Canada

Multidimensional Evolutionary Evaluations for Transformative Approaches (MEETA 2024)

Workshop Organizers

Maria Cerreta	University of Naples Federico II, Italy
Giuliano Poli	University of Naples Federico II, Italy
Daniele Cannatella	TU Delft, The Netherlands

Ludovica Larocca	University of Naples Federico II, Italy
Maria Somma	University of Naples Federico II, Italy
Gaia Daldanise	National Research Council, Italy

Workshop Program Committee Members

Maria Lucia Raiola	University of Naples Federico II, Italy
Eugenio Muccio	University of Naples Federico II, Italy
Chiara Mazzarella	TU Delft, The Netherlands
Sabrina Sacco	University of Naples Federico II, Italy
Piero Zizzania	University of Naples Federico II, Italy
Stefano Cuntò	University of Naples Federico II, Italy
Sveva Ventre	University of Naples Federico II, Italy
Caterina Loffredo	University of Naples Federico II, Italy
Giuseppe Ciciriello	University of Naples Federico II, Italy
Laura Di Tommaso	University of Naples Federico II, Italy
Benedetta Grieco	University of Naples Federico II, Italy
Simona Panaro	University of Sussex, UK

Building Multi-dimensional Models for Assessing Complex Environmental Systems (MES 2024)

Workshop Organizers

Vanessa Assumma	University of Bologna, Italy
Caterina Caprioli	Politechnic of Turin, Italy
Giulia Datola	Politechnic of Turin, Italy
Federico Dell'Anna	Politechnic of Turin, Italy
Marta Dell'Ovo	Politechnic of Milan, Italy
Marco Rossitti	Politechnic of Milan, Italy

Workshop Program Committee Members

Maksims Feofilovs	Riga Technical University, Latvia
Ossama Abdelwahab	University of Bari, Italy
Mariarosaria Angrisano	Pegaso Telematic University, Italy
Francesca Torrieri	Polytechnic of Milan, Italy
Maurizio Pioletti	University of Padua, Italy
Daniela Tavano	University of Calabria, Italy
Simone Persico	Polytechnic of Turin, Italy

Chiara D'Alpaos	University of Padua, Italy
Ezgi Şahin	Mersin University, Turkey
Giorgia Sugoni	LINKS Foundation, Italy
Rubina Canesi	University of Padua, Italy
Giulia Marzani	University of Bologna, Italy
Danny Casprini	Polytechnic of Milan, Italy
Simona Barbaro	University of Palermo, Italy
Giulio Cavana	Polytechnic of Turin, Italy
Diana Rolando	Polytechnic of Turin, Italy
Giuliano Poli	University of Naples Federico II, Italy
Francesco Sica	University of Rome La Sapienza, Italy
Sabrina Lai	University of Cagliari, Italy

Models and Indicators for Assessing and Measuring the Urban Settlement Development in the View of Zero Net Land Take by 2050 (MOVEto0 2024)

Workshop Organizers

Lucia Saganeiti	University of L'Aquila, Italy
Lorena Fiorini	University of L'Aquila, Italy
Angela Pilogallo	University of L'Aquila, Italy
Francesco Zullo	University of L'Aquila, Italy
Alessandro Marucci	University of L'Aquila, Italy

Workshop Program Committee Members

Ginevra Balletto	University of Cagliari, Italy
Giuseppe Borruso	University of Trieste, Italy
Chiara Garau	University of Cagliari, Italy
Beniamino Murgante	University of Basilicata, Italy
Ljiljana Zivkovic	MBA, Republic Geodetic Authority, Serbia
Ilaria Del Ponte	University of Genoa, Italy
Carmen Guida	University of Naples Federico II, Italy
Chiara Di Dato	University of L'Aquila, Italy

4th Workshop on Privacy in the Cloud/Edge/IoT World (PCEIoT 2024)

Workshop Organizers

Michele Mastroianni	University of Salerno, Italy
Mauro Iacono	University of Campania Luigi Vanvitelli, Italy
Lelio Campanile	University of Campania Luigi Vanvitelli, Italy

Workshop Program Committee Members

Maria Ganzha	Warsaw University of Technology, Poland
Armando Tacchella	University of Genoa, Italy
Alessio Merlo	School for Advanced Defense Studies, Italy
Antonio Iannuzzi	Roma Tre University, Italy
Arcangelo Castiglione	University of Salerno, Italy
Daniel Grzonka	Cracow University of Technology, Poland
Davide Cerotti	University of Piedmont Oriental, Italy

Scientific Computing Infrastructure (SCI 2024)

Workshop Organizers

Vladimir Korkhov	St. Petersburg University, Russia
Elena Stankova	St. Petersburg State University, Russia

Workshop Program Committee Members

Adam Belloum	University of Amsterdam, the Netherlands
Dmitry Vasiunin	Deutsche Telekom Cloud Services E.P.E., Greece
Serob Balyan	National Academy of Sciences of Armenia, Armenia
Suren Abrahamyan	Osensus Arm LLC, Armenia
Ashot Gevorkyan	National Academy of Sciences of Armenia, Armenia
Michal Hnatic	Univerzita Pavla Jozefa Šafárika v Košiciach, Slovakia
Martin Vala	Univerzita Pavla Jozefa Šafárika v Košiciach, Slovakia
Nodir Zaynalov	Tashkent University of Information Technologies, Uzbekistan
Michail Panteleyev	St. Petersburg Electrotecnical University, Russia

Nikolay Peryazev	Irkutsk State University, Irkutsk, Russia
Alexander Degtyarev	St. Petersburg State University, Russia
Alexander Bogdanov	St. Petersburg State University, Russia
Nataliia Kulabukhova	SberAutoTech, Russia

Downscale Agenda 2030 (SDGscale 2024)

Workshop Organizers

Anna Richiedei	University of Brescia, Italy
Michele Pezzagno	University of Brescia, Italy
Ginevra Balletto	University of Cagliari, Italy
Francesca Sinatra	University of Trieste, Italy
Federico Martellozzo	University of Florence, Italy
Tú Anh Trinh	University of Economics Ho Chi Minh City, Vietnam

Workshop Program Committee Members

Giuseppe Borruso	University of Trieste, Italy
Elisabetta Maria Venco	University of Pavia, Italy
Riccardo Privitera	University of Catania, Italy
Elisa Conticelli	University of Bologna, Italy
Giovanni Marinelli	Polytechnic University of Marche, Italy
Francesca Sinatra	University of Trieste, Italy
Salvatore Dore	University of Trieste, Italy
Maria Attard	University of Malta, Malta
Giovanni Mauro	University of Campania Luigi Vanvitelli, Italy
Maria Ronza	University of Naples, Federico II, Italy
Massimiliano Bencardino	University of Salerno, Italy

Socio-Economic and Environmental Models for Land Use Management (SEMLUM 2024)

Workshop Organizers

Debora Anelli	Polytechnic of Bari, Italy
Pierluigi Morano	Polytechnic of Bari, Italy
Benedetto Manganelli	University of Basilicata, Italy
Francesco Paolo Del Giudice	Sapienza University of Rome, Italy

Workshop Program Committee Members

Laura Gabrielli	University of Ferrara, Italy
Sergio Copiello	University of Venice, Italy
Antonio Nesticò	University of Salerno, Italy
Pierfrancesco De Paola	University of Napoli, Italy
Elena Fregonara	Polytechnic of Turin, Italy
Paola Amoruso	LUM, Italy

Ports of the Future - Smartness and Sustainability (SmartPorts 2024)

Workshop Organizers

Giuseppe Borruso	University of Trieste, Italy
Gianfranco Fancello	University of Cagliari, Italy
Patrizia Serra	University of Cagliari, Italy
Silvia Battino	University of Sassari, Italy
Marco Petrelli	Roma Tre University, Italy

Workshop Program Committee Members

Ginevra Balletto	University of Cagliari, Italy
Beniamino Murgante	University of Basilicata, Italy
Marco Mazzarino	IUAV University Venice, Italy
Maria del Mar Munoz Leonisio	University of Cadiz, Spain
Ahinoa Amaro Garcia	University of Las Palmas of Gran Canaria, Spain
Veronica Camerada	University of Sassari, Italy
Brunella Brundu	University of Sassari, Italy
Maria Attard	University of Malta, Malta
Enrico Dagostini	University of Malta, Malta
Tu Anh Trinh	College of Technology and Design for UEH University, Vietnam
Giovanni Mauro	University of Campania Luigi Vanvitelli, Italy
Maria Ronza	University of Naples, Federico II, Italy
Massimiliano Bencardino	University of Salerno, Italy

Smart Transport and Logistics - Smart Supply Chains (SmarTransLog 2024)

Workshop Organizers

Giuseppe Borruso	University of Trieste, Italy
Marcello Tadini	University of Eastern Piedmont, Italy
Maria del Mar Munoz Leonisio	University of Cádiz, Spain
Maria Attard	University of Malta, Malta
Veronica Camerada	University of Sassari, Italy
Brunella Brundu	University of Sassari, Italy

Workshop Program Committee Members

Ginevra Balletto	University of Cagliari, Italy
Silvia Battino	University of Sassari, Italy
Gianfranco Fancello	University of Cagliari, Italy
Mara Ladu	University of Cagliari, Italy
Martina Sinatra	University of Cagliari, Italy
Francesca Sinatra	University of Trieste, Italy
Salvatore Dore	University of Trieste, Italy
Andrea Gallo	University of Trieste, Italy
Marco Mazzarino	IUAV University Venice, Italy
Enrico Dagostini	University of Malta, Malta
Marco Naseddu	University of Cagliari, Italy
José Ángel Hernández Luis	University of Las Palmas de Gran Canaria, Spain
Maurizio Cociancich	Adriafer, Italy
Giovanni Longo	University of Trieste, Italy
Luca Toneatti	University of Trieste, Italy
Giovanni Mauro	University of Campania Luigi Vanvitelli, Italy
Maria Ronza	University of Naples, Federico II, Italy
Massimiliano Bencardino	University of Salerno, Italy

Smart Tourism (SmartTourism 2024)

Workshop Organizers

Silvia Battino	University of Sassari, Italy
Francesca Krasna	University of Trieste, Italy
Maria del Mar Munoz Leonisio	University of Cadiz, Spain

Ginevra Balletto	University of Cagliari, Italy
Brisol García García	Polytechnic University of Quintana Roo, Mexico
Ainhoa Amaro Garcia	University of Las Palmas of Gran Canarias, Spain

Workshop Program Committee Members

Giuseppe Borruso	University of Trieste, Italy
Beniamino Murgante	University of Basilicata, Italy
Gianfranco Fancello	University of Cagliari, Italy
Mara Ladu	University of Cagliari, Italy
Martina Sinatra	University of Cagliari, Italy
Salvatore Dore	University of Trieste, Italy
Veronica Camerada	University of Sassari, Italy
Brunella Brundu	University of Sassari, Italy
Maria Attard	University of Malta, Malta
Tu Anh Trinh	College of Technology and Design for UEH University, Vietnam
Giovanni Mauro	University of Campania Luigi Vanvitelli, Italy
Maria Ronza	University of Naples, Federico II, Italy
Massimiliano Bencardino	University of Salerno, Italy

Sustainable Evolution of Long-Distance Freight Passenger Transport (SOLIDEST 2024)

Workshop Organizers

Tiziana Campisi	University of Enna Kore, Italy
Socrates Basbas	Aristotle University of Thessaloniki, Greece
Massimo Di Gangi	University of Messina, Italy
Antonio Comi	University of Rome Tor Vergata, Italy
Francesco Russo	Mediterranea University of Reggio Calabria, Italy
Giovanni Tesoriere	University of Enna Kore, Italy

Workshop Program Committee Members

Antonio Polimeni	University of Messina, Italy
Orlando Belcore	University of Messina, Italy
Filippo G. Praticò	Mediterranea University of Reggio Calabria, Italy
Borja Alonso	University of Cantabria, Spain
Luigi Dall'Olio	University of Cantabria, Spain
Antonio Russo	University of Enna Kore, Italy

Sustainability Performance Assessment: Models, Approaches, and Applications Toward Interdisciplinary and Integrated Solutions (SPA 2024)

Workshop Organizers

Francesco Scorza	University of Basilicata, Italy
Sabrina Lai	University of Cagliari, Italy
Jolanta Dvarioniene	Kaunas University of Technology, Lithuania

Workshop Program Committee Members

Carmela Gargiulo	University of Naples Federico II, Italy
Floriana Zucaro	University of Naples Federico II, Italy
Corrado Zoppi	University of Cagliari, Italy
Federica Leone	University of Cagliari, Italy
Federica Isola	University of Cagliari, Italy
Francesca Leccis	University of Cagliari, Italy
Francesca Perrone	Sapienza University of Rome, Italy
Angela Pilogallo	Italian National Research Council, Italy
Alfonso Annunziata	University of Basilicata, Italy
Luigi Santopietro	Italian National Research Council, Italy
Beniamino Murgante	University of Basilicata, Italy
Alessandro Marucci	University of L'Aquila, Italy
Francesco Zullo	University of L'Aquila, Italy
Monica Salvia	Italian National Research Council, Italy
Fulvia Pietrapertosa	Italian National Research Council, Italy
Valentin Grecu	Lucian Blaga University, Romania
Georgia Pozoukidou	Aristotle University of Thessaloniki, Greece
Giampiero Lombardini	University of Genoa, Italy

Specifics of Smart Cities Development in Europe (SPEED 2024)

Workshop Organizers

Chiara Garau	University of Cagliari, Italy
Katarína Vitálišová	Matej Bel University, Slovakia
Paolo Nesi	University of Florence, Italy
Anna Vaňová	Matej Bel University, Slovakia
Kamila Borsekova	Matej Bel University, Slovakia
Paola Zamperlin	University of Florence, Italy

Workshop Program Committee Members

Tiziana Campisi	University of Enna Kore, Italy
Giovanna Concu	University of Cagliari, Italy
Claudia Loggia	University of KwaZulu-Natal, South Africa
Alessandro Plaisant	University of Sassari, Italy
Francesca Maltinti	University of Cagliari, Italy
Silvia Rossetti	University of Parma, Italy
Gerardo Carpentieri	University of Naples Federico II, Italy
Carmen Guida	University of Naples Federico II, Italy
Anastasia Stratigea	National Technical University of Athens, Greece
Yiota Theodora	National Technical University of Athens, Greece
Marco Fanfani	University of Florence, Italy
Emanuele Bellini	University of Rome 3, Italy

Smart, Safe and Health Cities (SSHC 2024)

Workshop Organizers

Chiara Garau	University of Cagliari, Italy
Gerardo Carpentieri	University of Naples Federico II, Italy
Carmen Guida	University of Naples Federico II, Italy
Floriana Zucaro	University of Naples Federico II, Italy
Tanja Congiu	University of Sassari, Italy
Martina Carra	University of Brescia, Italy
Benedetto Barabino	University of Brescia, Italy

Workshop Program Committee Members

Rosaria Battarra	Italian National Research Council, Italy
Barbara Caselli	University of Parma, Italy
Francesca Maltinti	University of Cagliari, Italy
Romano Fistola	University of Naples Federico II, Italy
Sabrina Lai	University of Cagliari, Italy
Claudia Loggia	University of KwaZulu-Natal, South Africa
Alessandro Plaisant	University of Sassari, Italy
Silvia Rossetti	University of Parma, Italy
Michela Tiboni	University of Brescia, Italy
John Zacharias	Peking University, China
Thomas Buhler	University of Franche-Comté, France

Aynaz Lotfata	University of California, USA
Lucia Saganeiti	University of L'Aquila, Italy
Francesco Zullo	University of L'Aquila, Italy
Paola Zamperlin	University of Florence, Italy
Katarína Vitálišová	Matej Bel University, Faculty of Economics, Slovakia
Tiziana Campisi	University of Enna Kore, Italy
Caterina Pietra	University of Pavia, Italy
Elisabetta Maria Venco	University of Pavia, Italy
Vincenza Torrisi	University of Catania, Italy

Smart and Sustainable Island Communities (SSIC 2024)

Workshop Organizers

Chiara Garau	University of Cagliari, Italy
Anastasia Stratigea	National Technical University of Athens, Greece
Yiota Theodora	National Technical University of Athens, Greece
Giovanna Concu	University of Cagliari, Italy

Workshop Program Committee Members

Milena Metalkova-Markova	University of Portsmouth, UK
Tarek Teba	University of Portsmouth, UK
Despina Dimelli	Technical University of Crete, Greece
Gerardo Carpentieri	University of Naples Federico II, Italy
Carmen Guida	University of Naples Federico II, Italy
Floriana Zucaro	University of Naples Federico II, Italy
Anestis Gourgiotis	University of Thessaly, Greece
George Tsilimigkas	University of the Aegean, Greece
Maria Panagiotopoulou	National Technical University of Athens, Greece
George Somarakis	National Technical University of Athens, Greece
Harry Kyriakidis	National Technical University of Athens, Greece
Apostolos Lagarias	Univ. of Thessaly, Greece
Paola Zamperlin	University of Florence, Italy
Giuseppina Vacca	University of Cagliari, Italy
Roberto Minunno	Curtin University, Perth, Australia
Claudia Loggia	University of KwaZulu-Natal, South Africa
Francesca Maltinti	University of Cagliari, Italy
Elisabetta Maria Venco	University of Pavia, Italy

From Street Experiments to Planned Solutions (STEPS 2024)

Workshop Organizers

Silvia Rossetti	University of Parma, Italy
Angela Ricciardello	University of Enna Kore, Italy
Francesco Pinna	University of Cagliari, Italy
Chiara Garau	University of Cagliari, Italy
Tiziana Campisi	University of Enna Kore, Italy
Vincenza Torrisi	University of Catania, Italy

Workshop Program Committee Members

Martina Carra	University of Brescia, Italy
Barbara Caselli	University of Parma, Italy
Tanja Congiu	University of Sassari, Italy
Gabriele D'Orso	University of Palermo, Italy
Matteo Ignaccolo	University of Catania, Italy
Md Kh Nahiduzzaman	University of British Columbia, Canada
Muhammad Ahmad Al-Rashid	University of Malaya, Malesia
Alessandro Plaisant	University of Sassari, Italy
Marianna Ruggieri	University of Enna Kore, Italy
Michele Zazzi	University of Parma, Italy

Sustainable Development of Ports (SUSTAINABLEPORTS 2024)

Workshop Organizers

Giuseppe Musolino	Mediterranea University of Reggio Calabria, Italy
Tiziana Campisi	University of Enna Kore, Italy
Efstathios Bouhouras	Aristotle University of Thessaloniki, Greece
Elena Cocuzza	University of Catania, Italy
Gianfranco Fancello	University of Cagliari, Italy
Massimo Di Gangi	University of Messina, Italy

Workshop Program Committee Members

Georgios Vaggelas	National and Kapodistrian University of Athens, Greece
Antonio Polimeni	University of Messina, Italy

Orlando Belcore	University of Messina, Italy
Lucia Dalla Spina	Mediterranea University of Reggio Calabria, Italy
Elen Twerdy	University of Lubljana, Slovenia
Claudia Caballini	Polytechnic University of Turin, Italy

Theoretical and Computational Chemistry and Its Applications (TCCMA 2024)

Workshop Organizers

Noelia Faginas-Lago	University of Perugia, Italy
Andrea Lombardi	University of Perugia, Italy
Marcos Mandado	University of Vigo, Spain

Workshop Program Committee Members

Ángel Martín Pendás	University of Oviedo, Spain
Ernesto Garcia Para	University of Basque Country, Spain
Giovanni Bistoni	University of Perugia, Italy
Juan Jose Nogueira Perez	University Autonoma of Madrid, Spain
Jose Hermida	Universidade di Vigo, Spain
Luca Mancini	University of Perugia, Italy

Transport Infrastructures for Smart Cities (TISC 2024)

Workshop Organizers

Francesca Maltinti	University of Cagliari, Italy
Mauro Coni	University of Cagliari, Italy
Francesco Pinna	University of Cagliari, Italy
Chiara Garau	University of Cagliari, Italy
Nicoletta Rassu	University of Cagliari, Italy
James Rombi	University of Cagliari, Italy

Workshop Program Committee Members

Benedetto Barabino	University of Brescia, Italy
Martina Carra	University of Brescia, Italy

Mauro D'Apuzzo	University of Cassino, Italy
Roberto Minunno	Curtin University, Australia
Claudia Loggia	University of KwaZulu-Natal, South Africa
Amir Kavussi	Tarbiat Modares University, Iran
Tiziana Campisi	University of Enna Kore, Italy
Alessandro Plaisant	University of Sassari, Italy
Elena Cocuzza	University of Catania, Italy
Vincenza Torrisi	University of Catania, Italy

From Structural to Transformative-Change of City Environment: Challenges and Solutions and Perspectives (TRACE 2024)

Workshop Organizers

Maria Rosaria Guarini	Sapienza University of Rome, Italy
Francesco Sica	Sapienza University of Rome, Italy
Carmelo Maria Torre	Polytechnic University of Bari, Italy
Francesco Tajani	Polytechnic University of Bari, Italy

Workshop Program Committee Members

Angela Pilogallo	Italian National Research Council, Italy
Maria Cerreta	University of Naples Federico II, Italy
Giuseppe Cerullo	Sapienza University of Rome, Italy

Transport and Digital Multiscale Sustainable Network for Circular Economy (TransNet 2024)

Workshop Organizers

Andrea Gallo	University of Trieste, Italy
Mara Ladu	University of Cagliari, Italy
Enrico Dagostini	University of Malta, Malta
Salvatore Dore	University of Trieste, Italy
Martina Sinatra	University of Cagliari, Italy
Francesca Sinatra	University of Trieste, Italy

Workshop Program Committee Members

Martina Carra	University of Brescia, Italy
Ginevra Baletto	University of Cagliari, Italy
Giuseppe Borruso	University of Trieste, Italy
Beniamino Murgante	University of Basilicata, Italy
Maria del Mar Munoz Leonisio	Univeristy of Cadiz, Spain
Ahinoa Amaro Garcia	Univeristy of Las Palmas of Gran Canaria, Spain
Malgorzata Hanzl	Lodz University of Technology, Poland
Balázs Kulcsár	University of Debrecen, Hungary

Temporary Real Estate Management: Approaches and Methods for Time-Integrated Impact Assessments and Evaluations (TREAT 2024)

Workshop Organizers

Chiara Mazzarella	TU Delft, The Netherlands
Hilde Remoy	TU Delft, The Netherlands
Maria Cerreta	University of Naples Federico II, Italy

Workshop Program Committee Members

Maria Lucia Raiola	University of Naples Federico II, Italy
Eugenio Muccio	University of Naples Federico II, Italy
Daniele Cannatella	TU Delft, The Netherlands
Sabrina Sacco	University of Naples Federico II, Italy
Piero Zizzania	University of Naples Federico II, Italy
Stefano Cuntò	University of Naples Federico II, Italy
Sveva Ventre	University of Naples Federico II, Italy
Caterina Loffredo	University of Naples Federico II, Italy
Giuseppe Ciciriello	University of Naples Federico II, Italy
Maria Somma	University of Naples Federico II, Italy
Ludovica La Rocca	University of Naples Federico II, Italy
Laura Di Tommaso	University of Naples Federico II, Italy
Benedetta Grieco	University of Naples Federico II, Italy
Gaia Daldanise	National Research Council, Italy
Simona Panaro	University of Sussex, UK
Giuliano Poli	University of Naples Federico II, Italy

Urban Regeneration: Innovative Tools and Evaluation Model (URITEM 2024)

Workshop Organizers

Fabrizio Battisti	University of Florence, Italy
Giovanna Acampa	University of Florence and University of Enna Kore, Italy
Orazio Campo	La Sapienza University of Rome, Italy

Workshop Program Committee Members

Alice Barreca	Polytechnic of Turin, Italy
Marco Rossitti	Polytechnic of Milan, Italy
Celestina Fazia	University of Enna Kore, Italy

Urban Space Accessibility and Mobilities (USAM 2024)

Workshop Organizers

Chiara Garau	University of Cagliari, Italy
Alessandro Plaisant	University of Sassari, Italy
Barbara Caselli	University of Parma, Italy
Gabriele D'Orso	University of Palermo, Italy
Mauro D'Apuzzo	University of Cassino, Italy
Matteo Ignaccolo	University of Catania, Italy

Workshop Program Committee Members

Ivan Blečić	University of Cagliari, Italy
Mauro Coni	University of Cagliari, Italy
Martina Carra	University of Brescia, Italy
Tiziana Campisi	University of Enna Kore, Italy
Tanja Congiu	University of Sassari, Italy
Francesca Maltinti	University of Cagliari, Italy
Silvia Rossetti	University of Parma, Italy
Angela Pilogallo	Italian National Research Council, Italy
Lorena Fiorini	University of L'Aquila, Italy
Francesco Pinna	University of Cagliari, Italy

Aime Tsinda	University of Rwanda, Rwanda
Nicoletta Rassu	University of Cagliari, Italy
Youssef El Ganadi	International University of Rabat, Morocco
Marco Migliore	University of Palermo, Italy
Elena Cocuzza	University of Catania, Italy
Alessio Salvatore	Italian National Research Council, Italy
Giuseppe Stecca	Italian National Research Council, Italy
Gerardo Carpentieri	University of Naples Federico II, Italy
Carmen Guida	University of Naples Federico II, Italy
Floriana Zucaro	University of Naples Federico II, Italy

Virtual Reality and Augmented Reality and Applications (VRA 2024)

Workshop Organizers

Osvaldo Gervasi	University of Perugia, Italy
Damiano Perri	University of Florence, Italy
Sergio Tasso	University of Perugia, Italy

Workshop Program Committee Members

Massimiliano Nicolini	OliTec Foundation, Italy
JungYoon Kim	Gachon University, South Korea
Paolo Nesi	University of Florence, Italy
David Berti	ART SpA, Italy
Tamie Salter	Citizen Alert Inc., Canada
Marcelo Guimarães	Federal University of São Paulo, Brazil

Workshop on Advanced and Computational Methods for Earth Science Applications (WACM4ES 2024)

Workshop Organizers

Luca Piroddi	University of Malta, Malta
Patrizia Capizzi	University of Palermo, Italy
Marilena Cozzolino	Università Del Molise, Italy
Sebastiano D'Amico	University of Malta, Malta
Chiara Garau	University of Cagliari, Italy
Giuseppina Vacca	University of Cagliari, Italy

Workshop Program Committee Members

Andrea Angelini	ISPC, CNR, Italy
Raffaele Martorana	University of Palermo, Italy
Paolo Mauriello	University of Molise, Italy
Raffaele Persico	University of Calabria, Italy
Eufemia Tarantino	Polytechnic of Bari, Italy
Roberto Ricciu	University of Cagliari, Italy
Stefano Sfarra	University of L'Aquila, Italy
Peter Iregbeyen	University of Malta, Malta
Elisa Pilia	University of Cagliari, Italy
Emanuele Colica	Ministry for Transport, Infrastructure and Public Works, Malta
Luciano Galone	University of Malta, Malta
Sergio Vincenzo Calcina	University of Cagliari, Italy
Maria Brovelli	Polytechnic of Milan, Italy
Francesca Trevisiol	University of Bologna, Italy

Additional Reviewers

Burak Aslan	Izmir Institute of Technology, Turkey
Birim Balcı	Manisa Celal Bayar University, Turkey
Atrin Barzegar	Università degli Studi della Campania L. Vanvitelli, Italy
Manuel Carlos Figueiredo	University of Minho, Portugal
Chiara Chioni	University of Trento, Italy
Annalisa Contato	University of Palermo, Italy
Aurora Costales	Universidad de Oviedo, Spain
Hamid Daneshpajouh	Middle East Technical University, Turkey
Vito Dario Camiola	Università di Catania, Italy
Roberta De Fazio	Università degli Studi della Campania Luigi Vanvitelli, Italy
Michele Di Giovanni	Università degli Studi della Campania, Italy
David Ferro Costas	University of Santiago de Compostela, Spain
Michal Hnatič	P.J. Šafarik University in Košice, Slovak Republic
Francesco Loddo	Henge S.r.l., Italy
Caterina Loffredo	University of Naples Federico II, Italy
Vanda Lourenco	Universidade Nova de Lisboa, Portugal
Ángel Martín Pendás	Universidad de Oviedo, Spain
Maria Mourao	Polytechnic Institute of Viana do Castelo, Portugal

Martin Perez Perez	University of Vigo, Spain
Marco Pezzella	University of Perugia, Italy
Maria Polidoro	ESTG IPP, Portugal
Josef Rebenda	Brno University of Technology, Czech Republic
Donatella Rita Fiorino	University of Cagliari, Italy
Evgeniy Romenskiy	Sobolev Institute of Mathematics, Russia
Ezgi Sahin Toptal	Mersin University, Turkey
Domenica Savia Pellicanò	Mediterranean University of Reggio Calabria, Italy
Carina Silva	ESTeSL-IPL, Portugal
Paula Simões	CMA FCT UNL CINAMIL, Portugal
Francesca Sinatra	University of Trieste, Italy
Ana Sofia Rézio	Iscal, Portugal
Alexandra Stankulova	Politecnico di Torino, Italy
Maria Stella De Biase	Università della Campania Luigi Vanvitelli, Italy
Guan Yue Hong	Western Michigan University, USA

Sponsoring Organizations

ICCSA 2024 would not have been possible without the tremendous support of many organizations and institutions, for which all organizers and participants of ICCSA 2024 express their sincere gratitude:



Springer Nature Switzerland AG, Switzerland
(https://www.springer.com)



Computers Open Access Journal
(https://www.mdpi.com/journal/computers)



Thuyloi University, Hanoi, Vietnam
(https://en.tlu.edu.vn/)





University of Perugia, Italy
(https://www.unipg.it)



University of Basilicata, Italy
(http://www.unibas.it)



Monash University, Australia
(https://www.monash.edu/)



Kyushu Sangyo University, Japan
(https://www.kyusan-u.ac.jp/)

Universidade do Minho
Escola de Engenharia

University of Minho, Portugal
(https://www.uminho.pt/)

University of Cagliari, Italy
(https://en.unica.it/en)

Venue

ICCSA 2024 took place on the main campus of Thuyloi University in Hanoi, Vietnam.



Plenary Lectures

Harnessing Artificial Intelligence for Enhanced Spatial Analysis of Natural Hazard Assessments



Prof. Dr. Biswajeet Pradhan

Director - Centre for Advanced Modelling and Geospatial Information Systems (CAMGIS), School of Civil and Environmental Engineering, Faculty of Engineering and IT, University of Technology Sydney, Australia

Abstract. In the realm of natural hazard assessments within spatial domains, the advent of Artificial Intelligence (AI) represents a paradigm shift, revolutionizing the way we conceptualize, model, and interpret environmental risks. This keynote address illuminates the profound impact of AI technologies, particularly machine learning algorithms and data-driven approaches, in reshaping our understanding and prediction capabilities concerning natural disasters.

By assimilating and scrutinizing vast spatial datasets, AI-driven models offer unparalleled accuracy and efficiency, facilitating timely and precise hazard assessments. Real-time processing of geospatial information not only enables rapid predictions but also forms the cornerstone of proactive disaster management strategies. Furthermore, AI's capacity lies in its adeptness at deciphering intricate spatial patterns inherent to natural hazards, unraveling subtle cues and previously unnoticed correlations within the data fabric.

This keynote delves into how AI's nuanced interpretation, coupled with advanced algorithms, elevates hazard modeling, providing deeper insights into the spatial dynamics of environmental risks. By augmenting traditional methodologies and revealing hidden patterns, AI fosters comprehensive risk assessments, fostering informed decision-making processes. The fusion of AI and natural hazard assessments in spatial domains heralds a more resilient approach to disaster preparedness and response.

Join us in embracing this transformative era, where AI's sophisticated modeling techniques and precise spatial interpretations converge, heralding proactive and effective mitigation strategies amidst the ever-evolving landscape of environmental challenges.

Short Bio. Distinguished Professor Dr. Biswajeet Pradhan is an internationally established scientist in the field of Geospatial Information Systems (GIS), remote sensing and image processing, complex modelling/geo-computing, machine learning and soft-computing applications, natural hazards and environmental modelling. He is the Director of the Centre for Advanced Modelling and Geospatial Information Systems (CAMGIS) at the Faculty of Engineering and IT at the University of Technology, Sydney (Australia). He was listed as the World's Most Highly Cited Researcher by the Clarivate Analytics Report for five consecutive years, 2016–2020, as one of the world's most influential minds.

He ranked number one (1) in the field of "Geological & Geomatics Engineering" during the calendar year 2021–2023, according to the list published by Stanford University Researchers, USA. This list ranks the world's top 2% most highly cited researchers based on Scopus data. In 2018–2020, he was awarded as World Class Professor by the Ministry of Research, Technology and Higher Education, Indonesia. He is a recipient of the Alexander von Humboldt Research Fellowship from Germany. Between 2015–2021, he served as "Ambassador Scientist" for the Alexander Humboldt Foundation, Germany.

Professor Pradhan has received 58 awards since 2006 in recognition of his excellence in teaching, service and research. Out of his more than 850 articles (Google Scholar citation: 70,000, H-index: 129), more than 750 have been published in science citation index (SCI/SCIE) technical journals. He has authored/co-authored ten books and thirteen book chapters.

Software Engineering Research in a New Situation



Prof. Carl K. Chang

Professor Emeritus, Iowa State University, USA

Abstract. With the rise of Generative Artificial Intelligence (GAI), epitomized by Large Language Models (LLMs), a profound shift has unfolded in software engineering research. In this presentation, I will traverse my four-decade journey in software engineering research, focusing on situational awareness in the era of the Internet of Things (IoT). I have witnessed the turbulence brought forth by the AI community that demands changes in our approaches. Meanwhile, owing to the pervasiveness of services computing, services became the first-class citizen in modern-day software engineering methodologies.

I argue that situational awareness must permeate the entire lifecycle to consistently deliver software services that align with the dynamic needs of users and the ever-evolving environments. I will elucidate this argument by reviewing the Situ framework, offering a comprehensive illustration of my perspective. Furthermore, I will outline my vision regarding the formidable research challenges considering the rapidly shifting landscape dominated by an irresistible and profoundly disruptive generative AI tsunami.

Short Bio. Carl K. Chang is a former department chair and Professor Emeritus of Computer Science at Iowa State University. His research interests include requirements engineering, net-centric computing, situational software engineering and digital health. Chang was the 2004 President of the IEEE Computer Society. Previously he served as the Editor-in-Chief for IEEE Software (1991–1994), and as the Editor-in-Chief of IEEE Computer (2007–2010). He was the 2012 recipient of the Richard E. Merwin Medal from the IEEE Computer Society. Chang is a Life Fellow of IEEE, a Fellow of AAAS, and a Life Member of the European Academy of Sciences (EurASc).

Interpretability and Privacy Preservation in Large Language Models (LLMs)



Prof. My Thai

University of Florida (UF) Research Foundation Professor
Associate Director of UF Nelms Institute for the Connected World

Abstract. Large Language Models (LLMs) have transformed the AI landscape, captivating researchers and practitioners with their remarkable ability to generate human-like text and perform complex tasks. However, this transformative power comes with a set of critical challenges, particularly in the realms of interpretability and privacy preservation. In this keynote, we embark on an exploration of these pressing issues, shedding light on how LLMs operate, their limitations, and the strategies we can employ to mitigate risks. We begin by examining the interpretability in LLMs, which often function as enigmatic "black boxes." Their complex neural architectures make it challenging to understand how they arrive at specific outputs. This lack of transparency raises questions of trust and accountability. When deploying LLMs in real-world applications—whether for chatbots, content generation, or decision-making—it becomes crucial to demystify their decision paths.

We will use explainable AI (XAI) to offer faithful explanations, from the black-box to white-box models, and from feature-based [1, 2] to neuron circuits-based [3, 4] explanations. By visualizing attention mechanisms, feature importance, and saliency maps, we empower users to comprehend LLM predictions. XAI not only fosters trust but also encourages responsible utilization of LLMs.

We next turn our attention to one of the utmost concerns and challenges: data privacy. LLMs process vast amounts of data, raising risks of data leakage, model inversion, the right to be forgotten, and inadvertent exposure of sensitive information. Furthermore, the integration of LLMs into diverse applications also significantly brings these challenges to the next level [5]. This talk explores strategies to protect privacy, including differential privacy, federated learning, and data encryption.

Short Bio. My T. Thai is a University of Florida (UF) Research Foundation Professor, Associate Director of UF Nelms Institute for the Connected World, and a Fellow of IEEE and AAIA. Dr. Thai is a leading authority who has done transformative research in Trustworthy AI and Optimization, especially for complex systems with applications to healthcare, social media, critical networking infrastructure, and cybersecurity. The results of her work have led to 7 books and 350+ publications in highly ranked international journals and conferences, including several best paper awards from the IEEE, ACM, and AAAI.

In responding to a world-wide call for responsible and safe AI, Dr. Thai is a pioneer in designing deep explanations for black-box ML models, while defending against explanation-guided attacks, evident by her Distinguished Papers Award at the Association for the Advancement of Artificial Intelligence (AAAI) conference in 2023. At the same year, she was also awarded an ACM Web Science Trust Test-of-Time award, for her landmark work on combating misinformation in social media. In 2022, she received an IEEE Big Data Security Women of Achievement Award. In 2009, she was awarded the Young Investigator (YIP) from the Defense Threat Reduction Agency (DTRA), and in 2010 she won the NSF CAREER Award. She is presently the Editor-in-Chief of the Springer Journal of Combinatorial Optimization and the IET Blockchain Journal, and editor of the Springer book series Optimization and Its Applications.

References

1. Vu, M., Thai, M.T.: PGM-explainer: probabilistic graphical model explanations for graph neural networks. In: Advances in Neural Information Processing Systems (NeurIPS) (2020)
2. Nguyen, T., Lai, P., Phan, H., Thai, M.T.: XRand: differentially private defense against explanation-guided attacks. In: AAAI Conference on Artificial Intelligence (AAAI) (2023)
3. Vu, N., Nguyen, T., Thai, M.T.: NeuCEPT: learn neural networks' mechanism via critical neurons with precision guarantee. In: IEEE International Conference on Data Mining (ICDM) (2022)

4. Conmy, A., Mavor-Parker, A., Heimersheim, S., Garriga-Alonso, A.: Towards automated circuit discovery for mechanistic interpretability. In: Advances in Neural Information Processing Systems (NeurIPS) (2023)
5. Vu, M., Nguyen, T., Jeter, T., Thai, M.T.: Analysis of privacy leakages in federated large language models. In: International Conference on Artificial Intelligence and Statistics (AISTATS) (2023)

Contents – Part II

Advances in Information Systems and Technologies for Emergency Management, Risk Assessment and Mitigation Based on the Resilience Concepts (ASTER 2024)

Community Resilience Analysis for the Formulation of a Seismic Mitigation Strategy at Inter-municipal Level 3
Angelo Anelli, Marco Vona, Paolo Harabaglia, and Massimiliano Moscatelli

Advances in Web Based Learning (AWBL 2024)

Exploring the Navigation Patterns of Learners on an Educational Recommender System 23
Cevat Aktas and Birol Ciloglugil

Improving Efficiency of Natural-Language Text Generation for Automatic Pedagogical Questions 37
Yulia Gomazkova, Oleg Sychev, and Marat Gumerov

Cyber Intelligence and Applications (CIA 2024)

An Android Malware Multi-class Classification Explained Through Genetic Programming 53
Gianni D'Angelo, Francesco Palmieri, and Antonio Robustelli

TinyIDS - An IoT Intrusion Detection System by Tiny Machine Learning 71
Pietro Fusco, Gennaro Pio Rimoli, and Massimo Ficco

A General Study on the Malware Propagation Models in Wireless Sensor Networks 83
Eslam Farsimadan, Leila Moradi, and Francesco Palmieri

Comparative Analysis of AI-Based Methods for Enhancing Cybersecurity Monitoring Systems 100
Federica Uccello, Marek Pawlicki, Salvatore D'Antonio, Rafał Kozik, and Michał Choraś

A Predictive Model for Phishing Attacks on Mobile Intelligent Agent Systems 113
Mashako D. Manyama and Okuthe P. Kogeda

Computational Methods, Statistics and Industrial Mathematics (CMSIM 2024)

Metabolic Cost of Load Carriage in a Special Forces Team – A Non-parametric Approach 131
Rui Lucena, Nuno Almeida, and Paula Simões

Performance Evaluation of Information Systems in Portuguese Municipalities 144
Domingos Martinho, Inês Góis, Pedro Sobreiro, and António Pratas

Portuguese Service Electricity Continuity Indicators: Municipality Code and Quality Service Zones Evaluation – 2014 to 2022 162
Marina A. P. Andrade and M. Filomena Teodoro

Spatial and Multivariate Statistics in Assessing Water Quality in the North Sea 177
Christopher Ody, M. Rosário Ramos, and E. Carolino

Enhancement of Database Access Performance by Improving Data Consistency in a Non-relational Database System (NoSQL) 194
Adam A. E. Alflahi, Mohammed A. Y. Mohammed, and Abdallah Alsammani

Algorithm of Determining Errors of Gimballed Inertial Navigation System 206
Olha Sushchenko, Yurii Bezkorovainyi, Oleksandr Solomentsev, Maksym Zaliskyi, Oleksii Holubnychyi, Ivan Ostroumov, Yuliya Averyanova, Viktoriia Ivannikova, Borys Kuznetsov, Ihor Bovdui, Tatyana Nikitina, Roman Voliansky, Kostiantyn Cherednichenko, and Olena Sokolova

Crossover Design on the Bioequivalence of Pharmaceuticals - A Case of Study 219
M. Filomena Teodoro, Marina A. P. Andrade, and Teresa A. Oliveira

Mathematical and Statistical Frameworks Fostering Advances in AI Systems and Computing 235
Teresa A. Oliveira and Maria Filomena Teodoro

Information Management's Influence on Telework Efficiency and Leadership: Perspectives from a Study in Portugal 247
Jaime Santos, João Farinha, Maria de Fátima Pina, and Rui Martins

The Fish Biology and Firms' Internationalisation: The Process Explained Through a Metaphor 266
Rui Martins, Maria de Fátima Pina, and João Farinha

A New Probability Distribution: Theory, Simulation and Real Application 284
Nadia Hashim Al-Noor, Rafida M. Elobaid, and Suzan J. Obaiys

Computational Optimization and Applications (COA 2024)

Digitalization of Restrictions for Assigning Workstations 299
Francisca Santos, Ana Ribeiro, and Carina Pimentel

A Firefighting Resource Dispatch Problem Optimization Using Metaheuristics 313
Marina A. Matos, Rui Gonçalves, Ana Maria A. C. Rocha, Lino A. Costa, and Filipe Alvelos

Robust Optimization for IMPT: Introducing and Comparing Different Automated Approaches 324
Joana Neves, Humberto Rocha, Brígida Ferreira, and Joana Dias

Enhancing Medical Imaging Through Data Augmentation: A Review 341
Beatriz Teixeira, Gonçalo Pinto, Vitor Filipe, and Ana Teixeira

Unveiling Key Parameters: Time Windows and Travel Times in Capacitated Waste Collection 355
A. S. Silva, J. Lima, A. M. T. Silva, H. T. Gomes, and A. I. Pereira

Multi-objective Scheduling Optimization in Job Shop with Unrelated Parallel Machines Using NSGA-III 370
Francisco dos Santos, Lino Costa, and Leonilde Varela

A Simulation-Based Optimization Approach to the Firefighting Resource Scheduling Problem 383
Emerson J. Paiva, Marina A. Matos, and Ana Maria A. C. Rocha

On Polytopal Branch and Bound with Monotonicity 397
E. M. T. Hendrix, L. G. Casado, B. G.-Tóth, and F. Messine

Author Index 415

Advances in Information Systems and Technologies for Emergency Management, Risk Assessment and Mitigation Based on the Resilience Concepts (ASTER 2024)

Community Resilience Analysis for the Formulation of a Seismic Mitigation Strategy at Inter-municipal Level

Angelo Anelli[1(✉)], Marco Vona[2], Paolo Harabaglia[2], and Massimiliano Moscatelli[1]

[1] Italian National Research Council – IGAG, 00010 Montelibretti, Italy
angelo.anelli@igag.cnr.it, massimiliano.moscatelli@cnr.it
[2] School of Engineering, University of Basilicata, 85100 Potenza, Italy
{marco.vona,paolo.harabaglia}@unibas.it

Abstract. In recent years, community resilience assessment has also become a central issue in earthquake risk mitigation. However, the application of resilience concepts is extremely complex. In the study of seismic risk, applications are highly multidisciplinary. Consequently, they are often incomplete or partial. Although new rigorous mathematical models have been developed, most applications are extremely complicated and susceptible to the input data and skill of the user. Even more so, applications to real large-scale contexts are much more complex than applications on a local scale or on single structures. New models and procedures are needed to apply resilience principles in the formulation of mitigation strategies at regional or sub-regional scales. In the present study, the impact of a highway on a set of communities is evaluated. The seismic resilience of communities is assessed by integrating the seismic performances of bridges and viaducts with those of the connected housing systems. The latter are estimated by modelling their physical damage with vulnerability curves for buildings. The main results are illustrated and discussed.

Keywords: Seismic Risk Mitigation Strategies · Resilience · Decision-Making

1 Introduction

Medium- and strong-intensity earthquakes continuously demonstrate the considerable vulnerability of existing buildings (private, public and strategic), as well as of other civil structures and infrastructures (e.g., [1–4]). The consequent social and economic losses are becoming too risky and no longer acceptable (e.g., [5–7]). Since the times and costs of reconstruction are exorbitant (e.g., [8, 9]), seismic risk mitigation strategies should be carefully planned and performed defining prioritizations and intervention measures at different territorial scales [10].

Many recent studies in the seismic risk field have detected the key role of resilience in the definition of mitigation strategies [e.g., 11–13]. To mitigate the seismic risk and therefore reduce the direct and indirect losses with a resilient perspective, competent

© The Author(s), under exclusive license to Springer Nature Switzerland AG 2024
O. Gervasi et al. (Eds.): ICCSA 2024 Workshops, LNCS 14816, pp. 3–20, 2024.
https://doi.org/10.1007/978-3-031-65223-3_1

authorities should establish financial resources and acceptable performance levels in a clear and transparent way and in accordance with the needs of all stakeholders [14]. However, the operative implementation of resilience concept at different territorial and decisional levels is a hard work, especially in complex and strongly heterogeneous systems (urban sub-systems, cities, city's systems, regions, etc.).

The resilience concept in seismic mitigation strategies is usually understood as the ability of a system to absorb disaster impacts and quickly return to normal socioeconomic activities. To this aim, undamaged facilities (public and private) and lifelines (communication, transportation and utilities networks) are crucial to ensure the recovery phase in the aftermath of a disastrous earthquake. Rigorous theoretical and analytical frameworks on these issues have significantly developed in recent years [e.g., 15–19] but, in many cases, their applications to real case studies focus on a local scale (neighborhood, district, city) and/or single structures [20]. Most of these frameworks are based on the seminal work of Bruneau et al. [21], who developed a general framework to quantitatively evaluate and improve the seismic resilience of communities by analyzing four resilience dimensions: technical, organizational, social, and economic (TOSE).

Basically, the resilience concept is used to offer strongly multidisciplinary solutions capable of capturing the beneficial impact of prioritizations and intervention types on the seismic response of vulnerable communities. In this direction, interesting studies based on the use of Multi-Criteria Decision-Making (MCDM) analysis are recently presented to conciliate resilience assessments in the mitigation strategy definition on a large territorial scale [14, 22, 23]. These studies link the post-earthquake functionality of a system (urban sub-system, city, city's system, region) and therefore its resilience to three main aspects that embody groups of interwoven TOSE dimensions: i) seismic risk, ii) emergency management and recovery, iii) integration and social cohesion.

In the present work, a concrete application of this MCDM analysis to thirty-three municipalities located in Basilicata region is reported. In particular, the work investigates the functional interdependencies of the housing systems of these municipalities with the State Highway 407, namely a road network segment that is crucial for the emergency management of Basilicata region. Census data and seismic risk assessments incorporating stratigraphic amplification effects are used to define a resilience prioritization of the exanimated municipalities. The analysis is carried out on the basis of the data obtained from the individual bridge or viaduct, census section and/or municipality. It is evolving and the multidisciplinary and multidimensional connection between housing systems and the strategic infrastructural network may be seen as the main outcome of this work.

2 Case Study Analysis

Basilicata is a region in southern Italy with 131 municipalities (one hundred belong to the province of Potenza and thirty-one belong to the province of Matera) and a total population slightly under 600,000 people according to the National Institute of Statistics (ISTAT) [24]. Basilicata can be considered as the most mountainous region in the south of Italy. In fact, it covers an area of approximately 10,000 km^2, most of which is covered by mountains (47%) and hills (45%). An extensive part of this region is covered by the southern Apennine Mountains, an area where seismic activity is well known. Among

the most destructive earthquakes to have occurred in this area in the last centuries, the 1694 Irpinia–Basilicata earthquake destroyed many towns in the north-west of the region causing about 6,000 casualties, while the 1857 Basilicata earthquake devastated much of the region causing about 19,000 casualties. More recently, the 1930 and 1980 Irpinia earthquakes widely affected Basilicata, Campania and Puglia region, destroying many towns between Basilicata and Campania and causing 1,404 and 2,914 casualties, respectively.

The 1980 Irpinia earthquake is the most disastrous Italian seismic event in the last hundred years. The main shock (6.8 on the Richter scale) occurred on Sunday 23 November at 7:35pm (local time) and the subsequent aftershocks devastated 687 municipalities (8.7% of current Italian municipalities) in just a few hours. According to a Fire Brigade report [25], a consistent part of the national fire brigade worked continuously for 48 days, when the search and excavation operations were completed and the last victim was found. However, the adverse geomorphological and atmospheric conditions together with the occurrence of landslides (which compromised the existence of some towns and affected the transportation network) and damaged infrastructure had a negative impact on the rescue action during the first 10 crucial days. The delay in relief efforts led to the birth of the modern Italian Civil Protection system. For the first time, civil protection is defined as a primary task of the Italian State following four main directions: prediction, prevention, rescue, restoration of normality.

More recently, after the emergency caused by 2009 L'Aquila earthquake, the Italian government introduced the article 11 of Law No 77 of 24 June 2009 to promote interventions for seismic risk prevention. The government instructed the Italian Civil Protection Department (ICPD) to implement article 11, and ICPD issued eight ordinances, according to which a total of 1.115 billion euros were distributed among the Italian Regions to finance seismic prevention in their territories for the years 2010–2021 [23]. In particular, Ordinance n. 4007/2012 [26] introduced the analysis of the Emergency Limit Condition (ELC) to examine the main physical elements of the emergency management system defined at municipal level in the civil protection plan.

Starting from the ELC analysis, Territorial Contexts (TCs) have recently been defined in Basilicata, Calabria, Campania, Puglia, and Sicily regions, and their fundamental physical elements, i.e. strategic buildings, aggregates and structural units, emergency areas and accessibility/connection infrastructures, are therefore identified. These physical elements define the TC emergency structural system at municipal and inter-municipal level. More specifically, a set of neighboring municipalities is grouped in each TC according to the labor market areas [27] and considering each municipality as a homogeneous unit of reference. In this way, emergency planning and management activities and risk mitigation strategies may be implemented cooperatively among municipalities in a TC [28].

TCs govern the emergency management system of a region and are useful for the territorial resilience assessment and planning. In Basilicata region, fourteen TCs may be found. Examining the accessibility/connection infrastructures of these TCs by means of the ELC information available on the web-GIS platform [29], the State Highway 407 plays a key role in the emergency management of Basilicata region, especially for eight TCs. Consequently, the State Highway 407 and thirty-three municipalities belonging to

these eight TCs are analyzed hereafter. As shown in Fig. 1, the considered municipalities are directly crossed by the State Highway 407 or are close to it.

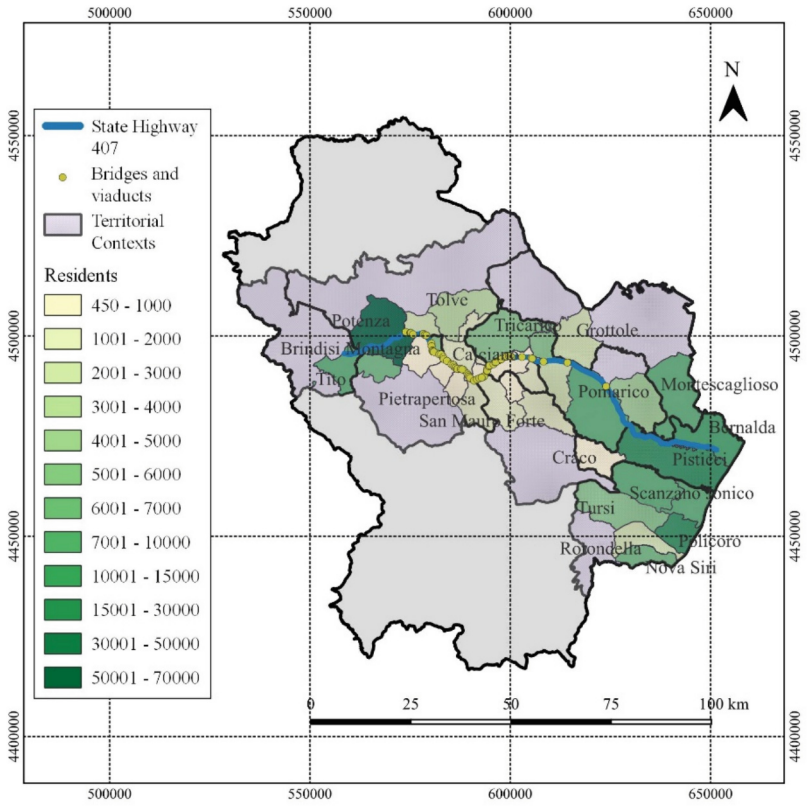

Fig. 1. Bridges and viaducts of State Highway 407 and connected territorial contexts with residents of neighboring housing systems.

The State Highway 407 connects Potenza with Metaponto (a hamlet of the municipality of Bernalda) following the course of the Basento river, entirely in Basilicata. Due to the complexity of the region's orography, the route in the province of Potenza is characterized by numerous bridges and viaducts. Along the route, there are a total of 89 bridges and viaducts considering both directions (Fig. 1). These structures are essential components to ensure the transportation system in the study area, especially for small mountain municipalities. In fact, according to ISTAT census data [30], the percentage of the resident population that moves outside these municipalities for study and work is the highest (Fig. 2).

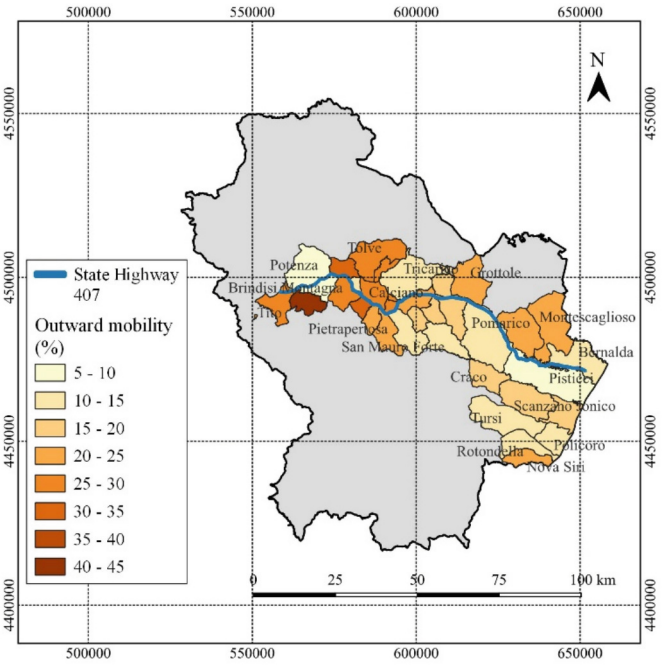

Fig. 2. Mobility outside the municipality for study or work.

To estimate the performance concerning the fundamental physical elements of a TC, a Territorial Context Structural Operational (TCSO) index and additional indicators are presented in a recent study [31]. In such study, the performance of accessibility/connection infrastructures is quantified by estimating the probabilities of interference due to possible coseismic effects, i.e. landslides and liquefactions, and the collapse probabilities of interfering buildings from fragility curves. For this last purpose, fragility curves for urban road networks are derived from fragility and vulnerability curves of interfering buildings [32].

Fragility and vulnerability curves are essential tools to estimate the seismic risk of exposed assets in terms of damage probabilities and damage factors (or losses), respectively. These curves describe the aforementioned values for a given earthquake intensity measure, usually defined in terms of Peak Ground Acceleration (PGA).

The analyzed bridges and viaducts were built in the years 1960–1970 with isostatic spans. Decks consist of pre-stressed Reinforced Concrete (RC) beams covered with a RC slab. They are simply supported on RC piers by means of isolated pier-to-deck connections. According to a Syner-G report [33], bridges and viaducts are one of the most seismically vulnerable structures in a highway system, and after a literature review on the topic, a set of mean fragility curves was proposed for representative RC bridge types. Depending on this set and the main characteristics of the considered bridges and viaducts, a mean fragility curve for collapse limit state is selected and used in order to estimate their seismic performance in the study area (Fig. 3).

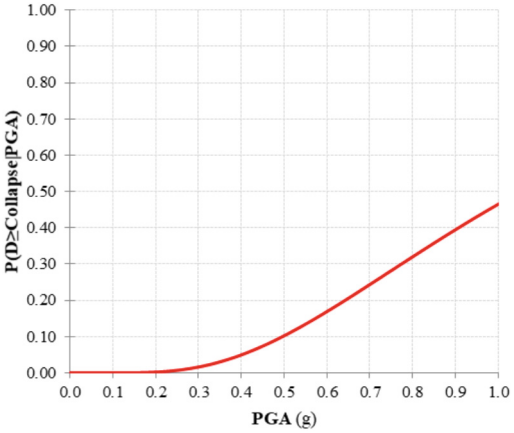

Fig. 3. Mean fragility curve for collapse limit state of regular or semi-regular RC bridges type with isolated pier-to-deck connection [33].

For a return period of 100 and 475 years (39% and 10% probability of exceedance in 50 years, respectively), the corresponding PGA demand of the *i*-th bridge or viaduct is estimated by multiplying the PGA at the outcropping engineering bedrock (deduced from the Italian seismic hazard assessment MPS04 [34, 35]) by the respective average amplification factor recently defined at national level with a regular grid of 50 × 50 m [36]. Then, the collapse probability ($P(D \geq Collapse|PGA)$) of the *i*-th bridge or viaduct is evaluated by entering with the estimated PGA value on the PGA values axis of the mean fragility curve of Fig. 3. Consequently, the seismic robustness of the *i*-th bridge or viaduct can be considered as the probability of non-collapse limit states ($P(D < Collapse|PGA)$). It is calculated as follows (Fig. 4):

$$P(D < Collapse|PGA)_i = 1 - P(D \geq Collapse|PGA)_i \tag{1}$$

The bridges and viaducts belonging to an accessibility infrastructure segment can be assumed to work in series within a TC. Thus, the Accessibility Infrastructure segment Robustness (*AIR*) in the *k*-th TC is based on the product among the probabilities of non-collapse limit states of the concerning bridges and viaducts. Mathematically, this can be expressed as follows:

$$AIR_k = \prod_{i=1}^{n} P(D < Collapse|PGA)_i, \ i \in k \tag{2}$$

where *n* is the number of bridges or viaducts belonging to the accessibility infrastructure segment of the *k*-th TC. Obviously, in addition to the damage to bridges or viaducts, other causes of mobility disruption may be co-present (i.e. landslides, liquefactions and damage to interfering buildings, retain walls, overpasses, underpasses, etc.). Also in these cases, Eq. (2) may be applied because the corresponding fragility curves can be assumed to work in series [32]. Figure 4 summarizes the robustness values of bridges and viaducts together with the *AIR* values of the eight TCs analyzed.

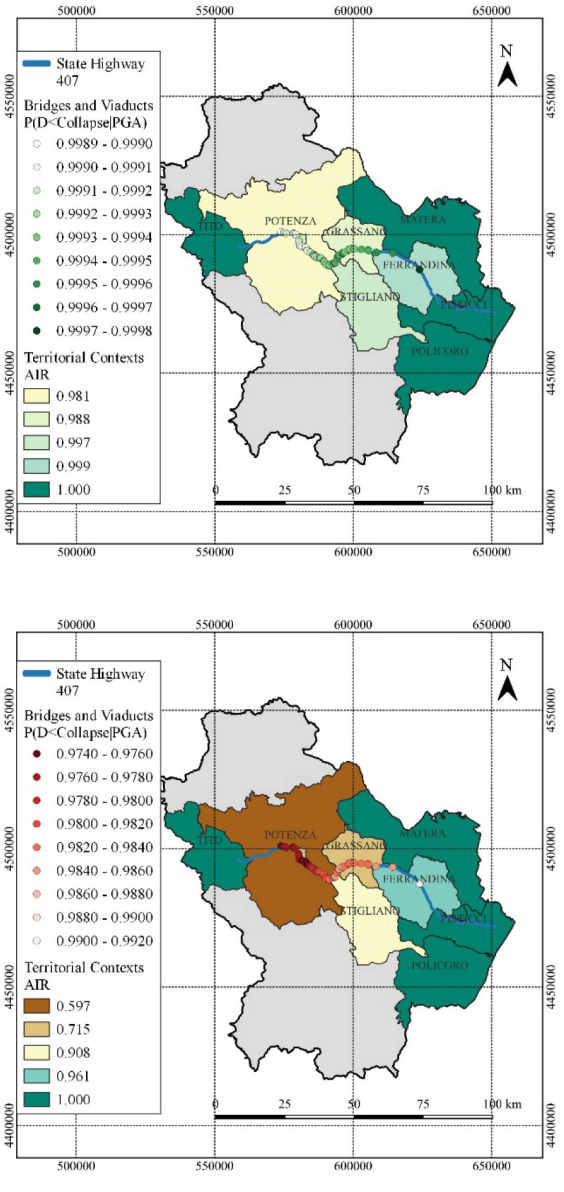

Fig. 4. Accessibility infrastructure robustness for a return period of 100 (a) and 475 years (b).

The robustness of housing systems in the study area (Fig. 5) is estimated by using the procedure of Anelli et al. [37] and data of a probabilistic seismic risk assessment (PSRA). The latter is carried out through the convolution of seismic hazard, vulnerability and exposure models.

The seismic hazard model was determined by integrating the Italian seismic hazard assessment framework [34, 35] with the stratigraphic amplification effects. These effects are evaluated by merging the national map of shear-wave velocity to 30 m depth [38] with a new generation of Ground Motion Prediction Equation (GMPE) [39]. An event based analysis with OpenQuake-engine software [40] was performed to assess the total hazard at the exposure site model.

Two set of vulnerability curves [37, 41] are used as vulnerability model to take in account the uncertainties concerning the structural response of residential buildings. Both sets of vulnerability curves are valid for masonry and RC buildings. More in detail, they categorize the Italian residential building stock in fourteen building types defined in terms of vulnerability and height classes: i) seven macroseismic vulnerability classes (A, B, C1, D1 for masonry buildings and C2, D2, E for RC buildings), ii) two height classes, i.e. low-rise buildings (L = 1-2 storeys) and medium/high-rise buildings (MH $\geq$ 3 storeys).

ISTAT census data on population and buildings [24] and the criteria provided by the National Risk Assessment [42] are used to determine the exposure model. For each municipality, buildings and their occupants are grouped into fourteen taxonomies according to the building types considered in the vulnerability model.

Seismic losses are calculated for both set of vulnerability curves by using the OpenQuake-engine software with a probabilistic event-based risk calculator. In such manner, loss exceedance curves and probabilistic loss maps are developed for a return period of 50, 100, 250, 500, 750, 1000 and 2000 years. Then, the procedure suggested by Anelli et al. [37] is used to estimate the seismic robustness of each municipality according to the calculated seismic losses. Figure 5 summarizes the seismic robustness of the considered housing systems for a return period of 100 and 500 years by averaging the housing robustness associated with the two sets of vulnerability curves.

Depending on the calculated robustness values of housing systems, the maximum restoration time is assessed for each return period by using the formulation proposed in recent studies [20, 23]. Figure 6 condenses the average results for a return period of 100, 250 and 500 years.

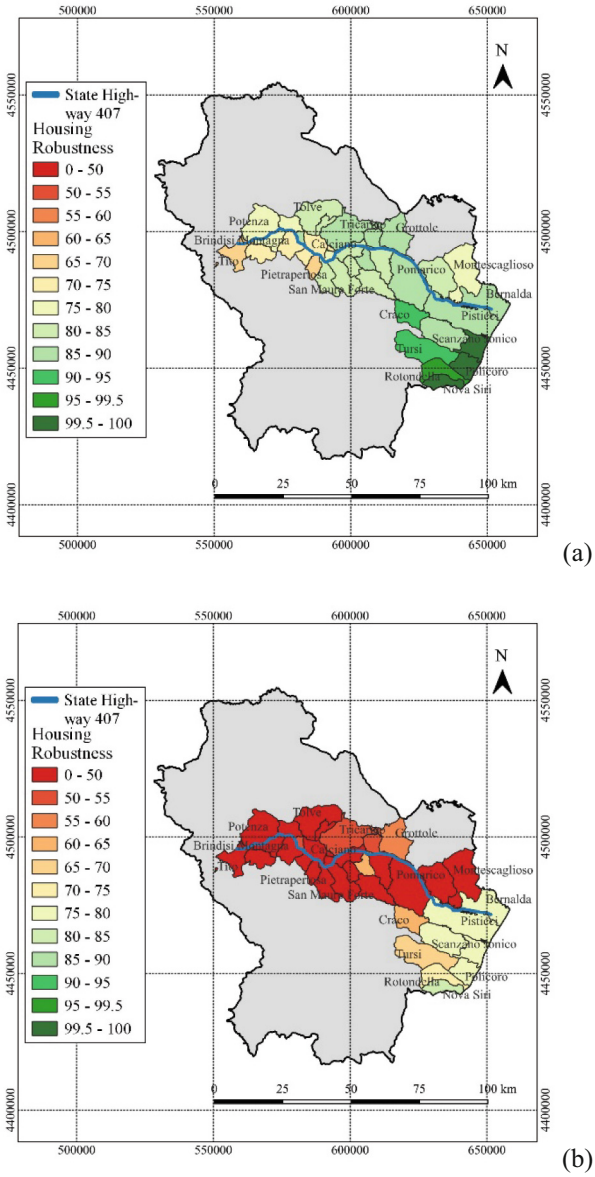

Fig. 5. Seismic robustness of housing systems for a return period of 100 (a) and 500 years (b).

3 Resilience Prioritization

To establish a resilience prioritization among the investigated municipalities, sixteen quantitative criteria (Table 1) and thirty-seven political scenarios or criteria weight vectors (Table 2) are considered herein. They are defined based on three main resilience

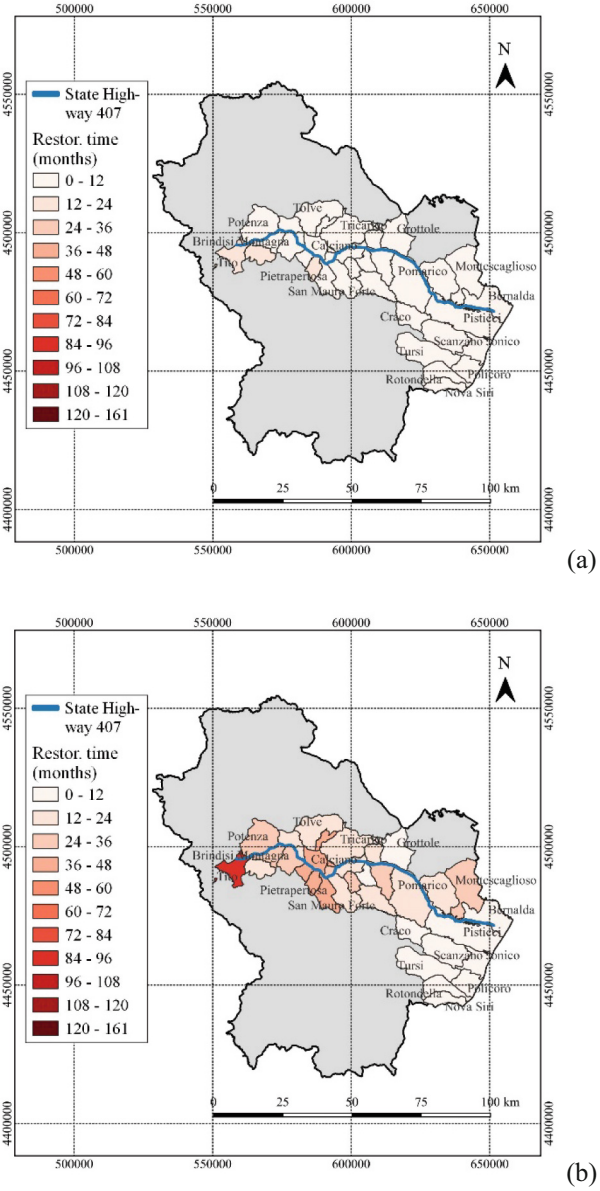

Fig. 6. Restoration time of housing systems for a return period of 100 (a), 250 (b), and 500 years (c).

aspects [14, 22, 23, 37]: i) seismic risk, ii) emergency management and recovery, iii) integration and social cohesion.

The thirty-three municipalities are assessed according to the judgement criteria reported in Table 1, from which the connection between the main resilience aspects

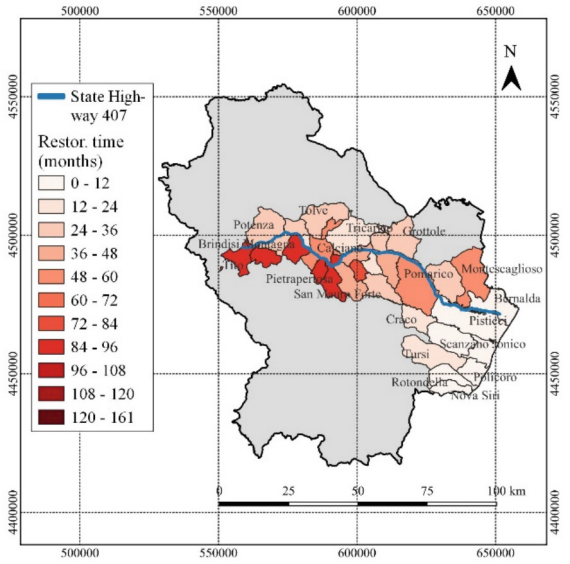

(c)

Fig. 6. (*continued*)

and the considered criteria can also be deduced. In particular, the seismic risk criteria – C_1, C_2, C_3, C_4 – and the emergency management and recovery criteria – C_6, C_7, C_8, C_9 – are described and evaluated in the previous Section (Figs. 2, 4, 5, 6).

When analyzing the municipalities with respect to the C_1 and C_2 criteria, the *AIR* values of the eight TCs (Fig. 4) are extended to all municipalities of the same TC because, as discussed in Sect. 1, emergency planning and management activities and risk mitigation strategies can be implemented cooperatively and uniformly across all municipalities in a TC.

Criterion C_5 aims to evaluate the specific exposure conditions in the compared municipalities. To this aim, ISTAT census data on population and buildings [24] are used. In criterion C_{10}, each municipality is analyzed by using a Geographic Information System (GIS) to identify its organizational relationships with the closest accessibility infrastructure.

ISTAT census data are also employed to analyze the municipalities with respect to the criteria of integration and social cohesion. More in detail, for the C_{11} criterion, the Average Population Growth Rate (*APGR*) of the *m*-th municipality is calculated as follows:

$$APGR_m = \frac{P(t + \Delta t)_m - P(t)_m}{P(t)_m \cdot \Delta t} \tag{3}$$

where Δt is assumed to be equal to ten years, while $P(t)$ and $P(t + \Delta t)$ is the number of inhabitants obtained from the ISTAT population census data for the years 2001 and 2011, respectively. This criterion aims to consider the risk of depopulation of a municipality. It is a significant and very worrying risk for Basilicata region.

Table 1. Resilience prioritization criteria.

Seismic Risk	C_1	Accessibility infrastructure robustness for a return period of 100 years
	C_2	Accessibility infrastructure robustness for a return period of 475 years
	C_3	Housing robustness for a return period of 100 years
	C_4	Housing robustness for a return period of 500 years
	C_5	Inhabitant per built area
Emergency Management & Recovery	C_6	Mobility outside the municipality for study or work
	C_7	Restoration time for a return period of 100 years
	C_8	Restoration time for a return period of 250 years
	C_9	Restoration time for a return period of 500 years
	C_{10}	Travel time from the nearest main accessibility infrastructure
Integration & Social Cohesion	C_{11}	Average population growth rate
	C_{12}	Incidence of foreign residents
	C_{13}	Incidence of young couples with children
	C_{14}	Participation in the job market
	C_{15}	Social and material vulnerability
	C_{16}	Unemployment rate

Municipal data concerning the remaining criteria – C_{12}, C_{13}, C_{14}, C_{15}, C_{16} – are directly taken from ISTAT database [30]. These criteria are able to take into account the social and economic dimensions of the communities involved. Among these, criterion C_{15} deserves particular attention because it is able to examine the overall socio-economic vulnerability of each municipality according to seven socio-economic indicators (for more details, see [43]).

A decision matrix (33x16) is used to capture the relationships between the thirty-tree municipalities and sixteen criteria considered.

To take into account the possible uncertainties involved in the decision-making process, thirty-seven political scenarios are defined based on the consistent comparisons of the three main resilience aspects (for more details, see [14, 22]). Then, the same relative importance is assigned to the criteria of each resilience aspect in order to simplify the procedure [23].

As shown in Table 2, the first twelve political scenarios emphasize the importance of seismic risk criteria, the second twelve place more emphasis on the emergency management and recovery criteria, the third twelve give greater importance to the criteria of integration and social cohesion, and, finally, the last political scenario attributes the same importance to the different resilience aspects.

Once the decision matrix and the political scenarios have been defined, the MCDM procedure suggested by Anelli et al. [23] is applied to calculate a Relative Resilience

Table 2. Political scenarios or criteria weight vectors.

$\mathbf{W}_1{}^{\mathrm{T}} =$	{0.108,0.108,0.108,0.108,0.108,0.059,0.059,0.059,0.059,0.059,0.027,0.027,0.027,0.027,0.027,0.027}^{T}
$\mathbf{W}_2{}^{\mathrm{T}} =$	{0.108,0.108,0.108,0.108,0.108,0.033,0.033,0.033,0.033,0.033,0.049,0.049,0.049,0.049,0.049,0.049}^{T}
$\mathbf{W}_3{}^{\mathrm{T}} =$	{0.127,0.127,0.127,0.127,0.127,0.052,0.052,0.052,0.052,0.052,0.017,0.017,0.017,0.017,0.017,0.017}^{T}
$\mathbf{W}_4{}^{\mathrm{T}} =$	{0.127,0.127,0.127,0.127,0.127,0.021,0.021,0.021,0.021,0.021,0.043,0.043,0.043,0.043,0.043,0.043}^{T}
$\mathbf{W}_5{}^{\mathrm{T}} =$	{0.132,0.132,0.132,0.132,0.132,0.053,0.053,0.053,0.053,0.053,0.013,0.013,0.013,0.013,0.013,0.013}^{T}
$\mathbf{W}_6{}^{\mathrm{T}} =$	{0.132,0.132,0.132,0.132,0.132,0.016,0.016,0.016,0.016,0.016,0.044,0.044,0.044,0.044,0.044,0.044}^{T}
$\mathbf{W}_7{}^{\mathrm{T}} =$	{0.143,0.143,0.143,0.143,0.143,0.043,0.043,0.043,0.043,0.043,0.011,0.011,0.011,0.011,0.011,0.011}^{T}
$\mathbf{W}_8{}^{\mathrm{T}} =$	{0.143,0.143,0.143,0.143,0.143,0.013,0.013,0.013,0.013,0.013,0.036,0.036,0.036,0.036,0.036,0.036}^{T}
$\mathbf{W}_9{}^{\mathrm{T}} =$	{0.150,0.150,0.150,0.150,0.150,0.036,0.036,0.036,0.036,0.036,0.012,0.012,0.012,0.012,0.012,0.012}^{T}
$\mathbf{W}_{10}{}^{\mathrm{T}} =$	{0.150,0.150,0.150,0.150,0.150,0.014,0.014,0.014,0.014,0.014,0.030,0.030,0.030,0.030,0.030,0.030}^{T}
$\mathbf{W}_{11}{}^{\mathrm{T}} =$	{0.164,0.164,0.164,0.164,0.164,0.018,0.018,0.018,0.018,0.018,0.015,0.015,0.015,0.015,0.015,0.015}^{T}
$\mathbf{W}_{12}{}^{\mathrm{T}} =$	{0.200,0.200,0.200,0.200,0.200,0.000,0.000,0.000,0.000,0.000,0.000,0.000,0.000,0.000,0.000,0.000}^{T}
$\mathbf{W}_{13}{}^{\mathrm{T}} =$	{0.059,0.059,0.059,0.059,0.059,0.108,0.108,0.108,0.108,0.108,0.027,0.027,0.027,0.027,0.027,0.027}^{T}
$\mathbf{W}_{14}{}^{\mathrm{T}} =$	{0.033,0.033,0.033,0.033,0.033,0.108,0.108,0.108,0.108,0.108,0.049,0.049,0.049,0.049,0.049,0.049}^{T}
$\mathbf{W}_{15}{}^{\mathrm{T}} =$	{0.052,0.052,0.052,0.052,0.052,0.127,0.127,0.127,0.127,0.127,0.017,0.017,0.017,0.017,0.017,0.017}^{T}
$\mathbf{W}_{16}{}^{\mathrm{T}} =$	{0.021,0.021,0.021,0.021,0.021,0.127,0.127,0.127,0.127,0.127,0.043,0.043,0.043,0.043,0.043,0.043}^{T}
$\mathbf{W}_{17}{}^{\mathrm{T}} =$	{0.053,0.053,0.053,0.053,0.053,0.132,0.132,0.132,0.132,0.132,0.013,0.013,0.013,0.013,0.013,0.013}^{T}
$\mathbf{W}_{18}{}^{\mathrm{T}} =$	{0.016,0.016,0.016,0.016,0.016,0.132,0.132,0.132,0.132,0.132,0.044,0.044,0.044,0.044,0.044,0.044}^{T}
$\mathbf{W}_{19}{}^{\mathrm{T}} =$	{0.043,0.043,0.043,0.043,0.043,0.143,0.143,0.143,0.143,0.143,0.011,0.011,0.011,0.011,0.011,0.011}^{T}
$\mathbf{W}_{20}{}^{\mathrm{T}} =$	{0.013,0.013,0.013,0.013,0.013,0.143,0.143,0.143,0.143,0.143,0.036,0.036,0.036,0.036,0.036,0.036}^{T}
$\mathbf{W}_{21}{}^{\mathrm{T}} =$	{0.036,0.036,0.036,0.036,0.036,0.150,0.150,0.150,0.150,0.150,0.012,0.012,0.012,0.012,0.012,0.012}^{T}
$\mathbf{W}_{22}{}^{\mathrm{T}} =$	{0.014,0.014,0.014,0.014,0.014,0.150,0.150,0.150,0.150,0.150,0.030,0.030,0.030,0.030,0.030,0.030}^{T}
$\mathbf{W}_{23}{}^{\mathrm{T}} =$	{0.018,0.018,0.018,0.018,0.018,0.164,0.164,0.164,0.164,0.164,0.015,0.015,0.015,0.015,0.015,0.015}^{T}
$\mathbf{W}_{24}{}^{\mathrm{T}} =$	{0.000,0.000,0.000,0.000,0.000,0.200,0.200,0.200,0.200,0.200,0.000,0.000,0.000,0.000,0.000,0.000}^{T}
$\mathbf{W}_{25}{}^{\mathrm{T}} =$	{0.059,0.059,0.059,0.059,0.059,0.033,0.033,0.033,0.033,0.033,0.090,0.090,0.090,0.090,0.090,0.090}^{T}
$\mathbf{W}_{26}{}^{\mathrm{T}} =$	{0.059,0.059,0.059,0.059,0.059,0.033,0.033,0.033,0.033,0.033,0.090,0.090,0.090,0.090,0.090,0.090}^{T}
$\mathbf{W}_{27}{}^{\mathrm{T}} =$	{0.052,0.052,0.052,0.052,0.052,0.021,0.021,0.021,0.021,0.021,0.106,0.106,0.106,0.106,0.106,0.106}^{T}
$\mathbf{W}_{28}{}^{\mathrm{T}} =$	{0.021,0.021,0.021,0.021,0.021,0.052,0.052,0.052,0.052,0.052,0.106,0.106,0.106,0.106,0.106,0.106}^{T}
$\mathbf{W}_{29}{}^{\mathrm{T}} =$	{0.053,0.053,0.053,0.053,0.053,0.016,0.016,0.016,0.016,0.016,0.110,0.110,0.110,0.110,0.110,0.110}^{T}
$\mathbf{W}_{30}{}^{\mathrm{T}} =$	{0.016,0.016,0.016,0.016,0.016,0.053,0.053,0.053,0.053,0.053,0.110,0.110,0.110,0.110,0.110,0.110}^{T}
$\mathbf{W}_{31}{}^{\mathrm{T}} =$	{0.043,0.043,0.043,0.043,0.043,0.013,0.013,0.013,0.013,0.013,0.120,0.120,0.120,0.120,0.120,0.120}^{T}
$\mathbf{W}_{32}{}^{\mathrm{T}} =$	{0.013,0.013,0.013,0.013,0.013,0.043,0.043,0.043,0.043,0.043,0.120,0.120,0.120,0.120,0.120,0.120}^{T}
$\mathbf{W}_{33}{}^{\mathrm{T}} =$	{0.036,0.036,0.036,0.036,0.036,0.014,0.014,0.014,0.014,0.014,0.125,0.125,0.125,0.125,0.125,0.125}^{T}
$\mathbf{W}_{34}{}^{\mathrm{T}} =$	{0.014,0.014,0.014,0.014,0.014,0.036,0.036,0.036,0.036,0.036,0.125,0.125,0.125,0.125,0.125,0.125}^{T}
$\mathbf{W}_{35}{}^{\mathrm{T}} =$	{0.018,0.018,0.018,0.018,0.018,0.018,0.018,0.018,0.018,0.018,0.136,0.136,0.136,0.136,0.136,0.136}^{T}
$\mathbf{W}_{36}{}^{\mathrm{T}} =$	{0.000,0.000,0.000,0.000,0.000,0.000,0.000,0.000,0.000,0.000,0.167,0.167,0.167,0.167,0.167,0.167}^{T}
$\mathbf{W}_{37}{}^{\mathrm{T}} =$	{0.067,0.067,0.067,0.067,0.067,0.067,0.067,0.067,0.067,0.067,0.056,0.056,0.056,0.056,0.056,0.056}^{T}

Index (RRI). This procedure was implemented to define a ranking of all TCs of Basilicata, Calabria, Campania, Puglia, and Sicily regions according to a wide range of political scenarios. Depending on the RRI values, funds among TCs and regions can also be distributed. For more details on the RRI calculation, please see the reference document above.

In the case study, the same procedure is applied to establish a resilience prioritization among the analyzed municipalities (Fig. 7). More specifically, in the RRI calculation, criteria – C_1, C_2, C_3, C_4, C_{11}, C_{13} – are considered as cost criteria (their minimization is the objective), while the remaining criteria are processed as benefit criteria (their maximization is the goal). Consequently, a maximization of RRI values is sought to obtain a ranking of the municipalities from the least resilient to the most resilient. As can be deduced from Fig. 7, the municipality of Castelmezzano (depicted in dark blue, RRI = 0.0428) is the least resilient among the municipalities investigated. It is followed by the municipalities of Pietrapertosa (RRI = 0.0415) and Albano di Lucania (RRI = 0.0400). On the contrary, the municipality of Policoro (depicted in light yellow, RRI = 0.0138) is the most resilient. It is preceded by the municipalities of Scanzano Jonico (RRI = 0.0167), Nuova Siri (RRI = 0.0171) and Bernalda (RRI = 0.0195), all located along the Ionian coast of the Basilicata region.

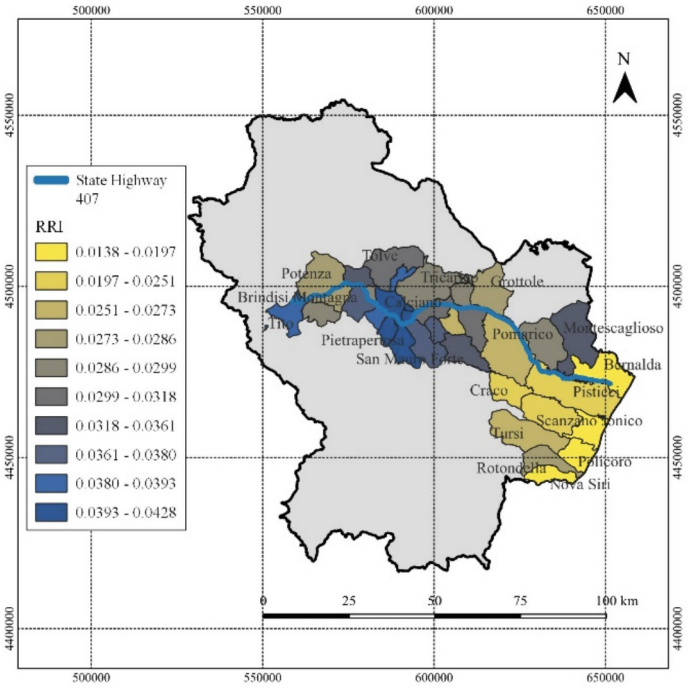

Fig. 7. Resilience prioritization of the municipalities according to their RRI value.

4 Conclusions

In this paper, a resilience prioritization among thirty-three municipalities in Basilicata region is proposed to show how resilience principles can be applied in the formulation of mitigation strategies on an inter-municipal level. At this territorial scale, the main

contribution to the field is the analysis of the functional interdependencies between housing systems and the main infrastructure system, especially in terms of emergency response.

Census data and seismic risk assessments incorporating stratigraphic amplification effects are used to analyze, with a transparent and multidisciplinary approach, the different resilience dimensions of the investigated systems. These data are integrated in the decision-making process by using a multi-criteria procedure that is able to rank the compared municipalities in relation to a large number of criteria and political scenarios.

Sixteen resilience prioritization criteria and thirty-seven political scenarios are considered, and then relative resilience measurements (RRI values) among the municipalities are determined with the procedure used. In this way, a resilience assessment of the municipalities is obtained in relative terms and a final ranking is defined according to their resilience values. The latter take into account the possible uncertainties involved in the decision-making process thanks to the ability of the procedure to find solutions based on multiple criteria and political scenarios.

The used procedure could become a main tool to define priorities and allocate funds among regions, TCs and municipalities for emergency planning and prevention purposes. By using this procedure at different territorial scales, a new and rational seismic risk mitigation policy can be developed to build resilience communities. Moreover, the procedure can be further enriched by analyzing the different urban systems. This last aspect can be considered the main limitation of the present work, but it can be further improved in future studies using the present methodological approach.

Acknowledgments. This research was supported by the Italian Civil Protection Department within the project "ART. 11 ORD.780" and partially supported by 2020 MIUR PON R&I 2014–2020 Program (project MITIGO, ARS01_00964).

Disclosure of Interests. The authors have no competing interests to declare that are relevant to the content of this article.

References

1. Dolce, M., Kappos, A.J., Masi, A., Penelis, G., Vona, M.: Vulnerability assessment and earthquake scenarios of the building stock of Potenza (Southern Italy) using the Italian and Greek methodologies. Eng. Struct. **28**(3), 357–371 (2006). https://doi.org/10.1016/j.engstruct.2005.08.009
2. Goretti, A., Sarli, V.: Road network and damaged buildings in urban areas: short and long-term interaction. Bull. Earthquake Eng. **4**(2), 159–175 (2006). https://doi.org/10.1007/s10518-006-9004-3
3. Dolce, M., Giovinazzi, S., Iervolino, I., Nigro, E., Tang, A.: Emergency management for lifelines and rapid response after L'Aquila earthquake. Progettazione Sismica **3**(2009 ISSN 1973–7432), 209–217 (2009)
4. Chiauzzi, L., et al.: Building damage scenarios based on exploitation of Housner intensity derived from finite faults ground motion simulations. Bull. Earthq. Eng. **10**(2), 517–545 (2012). https://doi.org/10.1007/s10518-011-9309-8

5. Vona, M., Murgante, B.: Seismic retrofitting of strategic buildings based on multi-criteria decision-making analysis. In: Furuta, H., Frangopol, D.M., Akiyama, M. (eds.) IALCCE 2014 Symposium, Tokyo, Japan, Volume: Life-Cycle of Structural Systems: tsuyosh Akiyama. TAYLOR and FRANCIS GROUP, London, UK, ISBN: 978-1-138-00120-6 (2014)
6. Vona, M., Harabaglia, P., Murgante, B.: Thinking about resilient cities: studying Italian earthquakes. Proc. Inst. Civil Eng. - Urban Des. Plan. **169**(4), 185–199 (2016). https://doi.org/10.1680/udap.14.00007
7. Vona, M., Anelli, A., Mastroberti, M., Murgante, B., Santa-Cruz., S.: Prioritization strategies to reduce the seismic risk of the public and strategic buildings. Disaster Adv. **10**(4), 1–15 (2017)
8. Cosenza, E., et al.: The Italian guidelines for seismic risk classification of constructions technical principles and validation. Bull. Earthq. Eng. **16**, 5905–5935 (2018). https://doi.org/10.1007/s10518-018-0431-8
9. Basaglia, A., Aprile, A., Spacone, E., Pelà, L.: Assessing community resilience, housing recovery and impact of mitigation strategies at the urban scale: a case study after the 2012 Northern Italy Earthquake. Bull. Earthq. Eng. **18**, 6039–6074 (2020). https://doi.org/10.1007/s10518-020-00919-8
10. Anelli, A., Vona, M., Santa-Cruz, S.: Comparison of different intervention options for massive seismic upgrading of essential facilities. Buildings **10**(7), 125 (2020). https://doi.org/10.3390/buildings10070125
11. Vona, M., Mastroberti, M., Mitidieri, L., Tataranna, S.: New resilience model of communities based on numerical evaluation and observed post seismic reconstruction process. Int. J. Disaster Risk Reduct. **28**, 602–609 (2018). https://doi.org/10.1016/j.ijdrr.2018.01.010
12. Vona, M., Manganelli, B., Tataranna, S.: Conservation, enhancement and resilience of historical and cultural heritage exposed to natural risks and social dynamics. In: Calabrò, F., Spina, L.D., Bevilacqua, C. (eds.) New Metropolitan Perspectives: Local Knowledge and Innovation Dynamics Towards Territory Attractiveness Through the Implementation of Horizon/E2020/Agenda2030 – Volume 2, pp. 426–433. Springer International Publishing, Cham (2019). https://doi.org/10.1007/978-3-319-92102-0_45
13. Vona, M.: Proactive actions based on a resilient approach to urban seismic risk mitigation. Open Construct. Build. Technol. J. **14**, 321–335 (2020). https://doi.org/10.2174/1874836802014010321
14. Anelli, A., Santa-Cruz, S., Vona, M., Tarque, N., Laterza, M.: A proactive and resilient seismic risk mitigation strategy for existing school buildings. Struct. Infrastruct. Eng. **15**(2), 137–151 (2019). https://doi.org/10.1080/15732479.2018.1527373
15. Cimellaro, G.P., Renschler, C., Reinhorn, A.M., Arendt, L.: Peoples: a framework for evaluating resilience. J. Struct. Eng. **142**(10), 04016063 (2016). https://doi.org/10.1061/(asce)st.1943-541x.0001514
16. Sharma, N., Tabandeh, A., Gardoni, P.: Resilience analysis: a mathematical formulation to model resilience of Engineering Systems. Sustain. Resilient Infrastruct. **3**(2), 49–67 (2018). https://doi.org/10.1080/23789689.2017.1345257
17. Battegazzorre, E., Bottino, A., Domaneschi, M., Cimellaro, G.P.: IdealCity: a hybrid approach to seismic evacuation modeling. Adv. Eng. Softw. **153**, 102956 (2021). https://doi.org/10.1016/j.advengsoft.2020.102956
18. Marasco, S., Cardoni, A., Zamani Noori, A., Kammouh, O., Domaneschi, M., Cimellaro, G.P.: Integrated platform to assess seismic resilience at the community level. Sustain. Cities Soc. **64**, 102506 (2021). https://doi.org/10.1016/j.scs.2020.102506
19. Jiang, H., Bu, H., He, L.: A new method for function-loss based seismic resilience assessment of Buildings. Eng. Struct. **266**, 114613 (2022). https://doi.org/10.1016/j.engstruct.2022.114613

20. Anelli, A., Vona, M., Mori, F., Moscatelli, M.: Measuring the seismic resilience of housing systems in Italy. Appl. Sci. **13**(15), 8944 (2023). https://doi.org/10.3390/app13158944
21. Bruneau, M., et al.: A framework to quantitatively assess and enhance the seismic resilience of communities. Earthq. Spectra **19**(4), 733–752 (2003). https://doi.org/10.1193/1.1623497
22. Anelli, A., Santa-Cruz, S., Vona, M., Laterza, M.: Spatial analysis and ranking for retrofitting of the School Network in Lima, Peru. In: Gervasi, O., Murgante, Beniamino, Misra, Sanjay, Borruso, Giuseppe, Torre, Carmelo M., Ana Maria, A.C., Rocha, David Taniar, Apduhan, Bernady O., Stankova, Elena, Cuzzocrea, Alfredo (eds.) Computational Science and Its Applications – ICCSA 2017: 17th International Conference, Trieste, Italy, July 3-6, 2017, Proceedings, Part II, pp. 310–325. Springer International Publishing, Cham (2017). https://doi.org/10.1007/978-3-319-62395-5_22
23. Anelli, A., Mori, F., Mendicelli, A., Vona, M., Moscatelli, M.: A large-scale prioritisation to strengthen the resilience of communities in Italian territorial contexts. Struct. Infrastruct. Eng. (2023). https://doi.org/10.1080/15732479.2023.2266817
24. Italian National Institute of Statistics (ISTAT). http://www.istat.it/it/archivio/104317. Accessed 1 March 2024
25. Fire Brigade report. http://www.vigilfuoco.it/aspx/ReturnDocument.aspx?IdDocumento=406. Accessed 1 Feb 2024
26. OPCM No. 4007/2012. https://rischi.protezionecivile.gov.it/it/sismico/attivita/piano-nazionale-la-prevenzione-del-rischio-sismico/annualita-2011. . Accessed 1 June 2024
27. Labour market areas (ISTAT). https://www.istat.it/en/labour-market-areas. Accessed 1 March 2024
28. Fontana, C., Cianci, E., Moscatelli, M.: Assessing seismic resilience of school educational sector. An attempt to establish the initial conditions in Calabria Region, southern Italy. Int. J. Disaster Risk Reduct. **51**, 101936 (2020). https://doi.org/10.1016/j.ijdrr.2020.101936
29. Web MS-CLE. http://www.webms.it/servizi/viewer.php. Accessed 1 Feb 2024
30. ISTAT census data. https://ottomilacensus.istat.it/download-dati/. Accessed 1 Feb 2024
31. Mori, F., Gena, A., Mendicelli, A., Naso, G., Spina, D.: Seismic emergency system evaluation: the role of seismic hazard and local effects. Eng. Geol. **270**, 105587 (2020). https://doi.org/10.1016/j.enggeo.2020.105587
32. Anelli, A., Mori, F., Vona, M.: Fragility curves of the urban road network based on the debris distributions of interfering buildings. Appl. Sci. **10**(4), 1289 (2020). https://doi.org/10.3390/app10041289
33. Syner-G report. https://op.europa.eu/en/publication-detail/-/publication/d521b119-1865-4177-a478-9f332f3cc827/language-en. Accessed 1 May 2024
34. CPTI Working Group, https://emidius.mi.ingv.it/CPTI04/. Accessed 1 March 2024
35. Stucchi, M., Meletti, C., Montaldo, V., Crowley, H., Calvi, G.M., Boschi, E.: Seismic Hazard Assessment (2003–2009) for the Italian Building Code. Bull. Seismol. Soc. Am. **101**(4), 1885–1911 (2011). https://doi.org/10.1785/0120100130
36. Mendicelli, A., et al.: Italian seismic amplification factors for peak ground acceleration and peak ground velocity. J. Maps **18**(2), 497–507 (2022). https://doi.org/10.1080/17445647.2022.2101947
37. Anelli, A., Mori, F., Mendicelli, A., Bramerini, F.: Mapping urban limit conditions in the perspective of disaster risk prevention and land management. Italian J. Geosci. **141**, 167–183 (2022). https://doi.org/10.3301/IJG.2022.11
38. Mori, F., Mendicelli, A., Moscatelli, M., Romagnoli, G., Peronace, E., Naso, G.: A new VS30 map for Italy based on the seismic microzonation dataset. Eng. Geol. **275**, 105745 (2020). https://doi.org/10.1016/j.enggeo.2020.105745

39. Bindi, D., et al.: Pan-European ground-motion prediction equations for the average horizontal component of PGA, PGV, and 5%-damped PSA at spectral periods up to 3.0 s using the RESORCE dataset. Bull. Earthquake Eng. **12**, 391–430 (2013). https://doi.org/10.1007/s10518-013-9525-5
40. Pagani, M., et al.: OpenQuake engine: an open hazard (and risk) software for the global earthquake model. Seismol. Res. Lett. **85**(3), 692–702 (2014). https://doi.org/10.1785/0220130087
41. Anelli, A., Mori, F., Moscatelli, M.: Seismic fragility and vulnerability curves for the Italian residential building stock. Struct. Infrastruct. Eng. **19**(1), 113–133 (2023). https://doi.org/10.1080/15732479.2021.1936568
42. Dolce, M., et al.: Seismic risk assessment of residential buildings in Italy. Bull. Earthq. Eng. **19**, 2999–3032 (2021). https://doi.org/10.1007/s10518-020-01009-5
43. Didkovskyi, O., Azzone, G., Menafoglio, A., Secchi, P.: Social and material vulnerability in the face of seismic hazard: an analysis of the Italian case. J. R. Stat. Soc. Ser. A Stat. Soc. **184**(4), 1549–1577 (2021). https://doi.org/10.1111/rssa.12739

Advances in Web Based Learning (AWBL 2024)

Exploring the Navigation Patterns of Learners on an Educational Recommender System

Cevat Aktas[1] and Birol Ciloglugil[2(✉)]

[1] Institute of Natural Sciences, Department of Computer Engineering, Ege University, 35100 Bornova, Izmir, Turkey
[2] Department of Computer Engineering, Ege University, 35100 Bornova, Izmir, Turkey
birol.ciloglugil@ege.edu.tr

Abstract. In this study, the interaction of students with an educational recommender system has been analyzed based on log data. Considering the fact that it is quite a challenging task to measure and model how learning actually takes place, the main contribution of this paper is to provide insights into the learning processes of learners based on interaction data. Various types of factors about learners such as prior knowledge level, motivation level, and learning styles can affect their learning processes and the learning outcomes directly. These factors also affect the usability of educational systems among other system-related aspects. In this regard, analyzing the usage data of adaptive e-learning systems can provide valuable information about the effectiveness of recommendations and the learning processes of learners. With this motivation, we collected and analyzed the interaction data of a semantic web-based educational recommender system. The educational recommender system was used as a supplementary tool by 172 voluntary students who took the Digital Computer Design course of the Computer Engineering curriculum at a public university in Turkey. Different types of learning resources such as presentations, videos (for teaching theoretical subjects and demonstrating different examples), exercises, and quizzes have been used as learning materials. Users can directly access the learning materials in whichever order they prefer or may follow the recommendations of the e-learning system. We analyzed the system interaction data to provide descriptive statistics and insights on various aspects such as learning material usage patterns of learners, popularity of learning materials based on learning material types, success levels at quizzes, and whether the learners were likely to follow recommendations given as hints after wrong answers at quizzes. The results are promising; however, considering the limited application size of a single course, further studies should be conducted to support the findings.

Keywords: E-Learning · Recommender Systems · Student Behaviour · Navigation Patterns

© The Author(s), under exclusive license to Springer Nature Switzerland AG 2024
O. Gervasi et al. (Eds.): ICCSA 2024 Workshops, LNCS 14816, pp. 23–36, 2024.
https://doi.org/10.1007/978-3-031-65223-3_2

1 Introduction

Educational recommender systems aim to improve the learning processes of learners by observing their interaction with learning materials and guiding them to use other relevant learning materials [1–4]. In this regard, individual differences of learners such as prior knowledge level, motivation level, and learning styles are modeled to provide enhanced learning experiences to learners [5–8]. Monitoring the interaction of learners with recommended learning materials is important to assess if the recommendations are useful for the learners [9–11]. Since it is a challenging task to model and/or understand the learning process, evaluation of log data can provide meaningful insights about the learning processes of learners [12].

Semantic web technologies and ontologies are widely used for knowledge representation purposes to model learners and educational resources [13,14]. Individual differences of learners are often utilized to provide adaptation and/or personalization in e-learning systems [15,16]. The learner model ontologies and interaction data of learners with e-learning systems provide valuable data for recommender systems to operate on [17–20]. Various artificial intelligence methods can also be used for educational data mining to analyze the data collected by recommender systems [21–24].

In this paper, we collected interaction data by using a semantic web-based educational recommender system [25] that models individual differences of learners with an ontology based on previous knowledge levels and learning styles of learners. Then, we analyzed the collected data to provide insights into the learning processes of learners and enhance their learning experiences in future interactions.

The rest of the paper is organized as follows; Sect. 2 briefly discusses the related work, and Sect. 3 introduces the web-based educational recommender system and the course that provides the data analyzed in this paper. Section 4 presents and discusses the statistical findings obtained by the analysis of the log data of the utilized educational recommender system. Finally, Sect. 5 concludes the paper with a brief discussion of the findings, limitations of the study, and possible further work directions.

2 Related Work

The importance of recommendation systems in the field of education is increasing, and in order to improve the effectiveness of these systems, it is of great importance to understand the users' browsing behavior among learning materials. Some important studies on this subject are briefly discussed below:

Students' navigation behavior through learning materials was analyzed by [26], and the results of this analysis were used as a basis to determine students' skill levels and suggest appropriate problems to practice based on the skill levels of students. This approach aims to introduce an improved recommendation system to provide more personalized and effective learning experiences to students.

A recommender system for learning activities was developed by [27] by utilizing knowledge graphs. Knowledge graphs are employed to model relationships between learning materials, concepts, and learning objectives. These graphs define the learning path a student should follow to achieve a specific learning objective. The recommender system determines the most suitable learning paths, taking into account the student's current level of knowledge and learning objectives, and suggests learning materials based on these learning paths. This system demonstrates the potential of using knowledge graphs to optimize the learning processes of students and help them progress more effectively.

Adaptive and personalized learning approaches were explored by [28] based on students' cognitive characteristics. Traditional educational methods often fail to consider that each student has different learning styles, skills, and needs. Therefore, a new learning approach aimed at enhancing learning experiences by understanding students' cognitive characteristics was introduced by [28]. Students' cognitive characteristics were assessed by using various tools, and methods, and used as an information source to provide adaptive and personalized learning content. The practical applications of this approach were discussed by examining how it can improve students' learning processes and enhance learning outcomes.

The main objective of [29] is to understand learning behavior patterns in social adaptive personalized e-learning systems. Students' learning behaviors in these systems were examined by combining social and personalized elements of e-learning. The use of various analyses and methods to understand student interactions and learning processes in such e-learning systems was discussed. Additionally, the impact of social interactions and personalized learning content on student success was investigated. Thus, this study aims to understand how the integration of social media and personalized learning technologies affects e-learning experiences.

It was aimed to utilize learning analytics to support both learners and teachers in [30]. The importance of using learning analytics tools to meet the needs of students and enhance their educational experiences was emphasized. Specifically, interactions and behaviors of students throughout their learning process were examined by adopting navigation among contents as a model. This model aims to understand how students navigate among learning materials and the impact of these navigation patterns on student success. Additionally, it may assist teachers in tracking students' progress and guiding their learning experiences more effectively.

It was aimed to predict student performance in higher educational institutions by utilizing video learning analytics and data mining techniques in [31]. It was sought to contribute to the exploration of new and effective methods for determining student success as digital technologies become increasingly integrated into education. Providing insight into how such analysis and predictions can be used to enhance teaching and learning processes in higher educational institutions was investigated.

3 The Educational Recommender System and Learning Materials Used for Data Collection

The semantic web-based educational recommender system utilized for data collection is presented in the following subsection. Then, the Digital Computer Design course is introduced and the learning materials prepared for this course are explained.

3.1 The Semantic Web-Based Educational Recommender System

The data used in this study is collected with a semantic web-based educational recommender system [25]. This recommender system was used as a supplementary tool to support Computer Engineering students at the Digital Computer Design course of a public university in Turkey. The recommender system was used by 172 voluntary students for two weeks and interaction data of learners with learning materials were collected from logs and used as the main data source to analyze the behaviours of learners.

The semantic web-based educational recommender system models individual differences of learners by using prior knowledge levels and learning styles. Learners were modeled with a learner modeling ontology that contains demographic information of learners, their grades at related courses, CGPA scores, and learner styles based on the Felder and Silverman learning style model [32]. A screenshot of the utilized educational recommender system is given in Fig. 1.

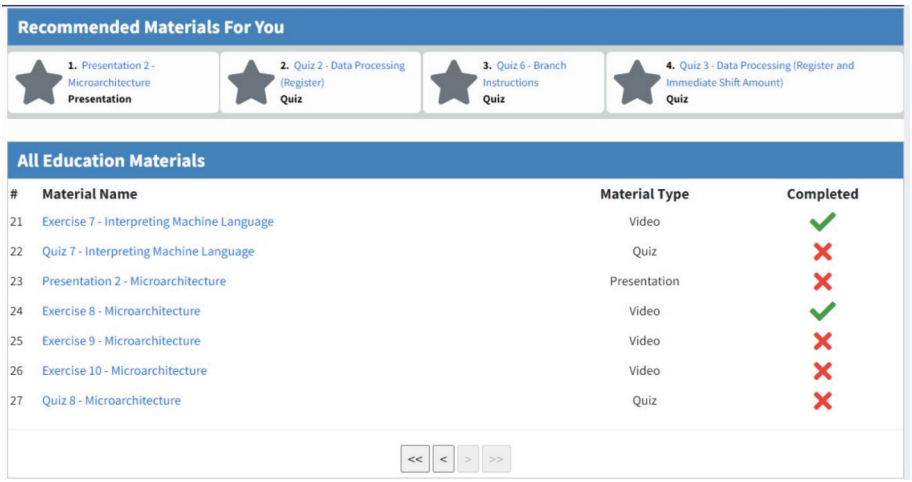

Fig. 1. A screenshot of the utilized educational recommender system [25]

This recommender system utilizes association rule mining to detect navigation patterns of learners [33]. In this regard, Frequent Pattern Growth (FP-Growth) algorithm [34,35], which is a popular algorithm that provides high

performance, is used by the recommender system to analyze log data and detect meaningful patterns among learning materials.

3.2 Learning Materials of Digital Computer Design Course

Digital Computer Design course is one of the main hardware courses of the computer engineering curriculum [36]. It is closely related to the Logic Design course which is part of the previous semester of the curriculum. Even though there is not an official prerequisite relationship between these two courses, the topics covered in the Digital Computer Design course can be thought of as a continuation of the topics of the Logic Design course. Thus, the success levels of students at the Logic Design course can be a good indicator of the success levels of students at the Digital Computer Design course. That's why we used the grades of students from the Logic Design course to model previous knowledge levels of students.

Learning materials were prepared for two topics of the Digital Computer Design course; Machine Language Instruction Encodings and Microarchitecture; that were taught after the midterm exam. Therefore, we also used the midterm grades of students at the Digital Computer Design course to model the previous knowledge levels of students. Finally, we also used the CGPA scores of learners until the semester the Digital Computer Design course was taught as another data source. Thus, the knowledge levels of learners were determined based on three parameters; CGPA scores of learners, grades of the Logic Design course, and grades of the midterm exam of the Digital Computer Design course.

Four types of learning materials were prepared for the Digital Computer Design course. The statistics related to learning material types and the amount of available learning materials from each learning material type are listed in ascending order at Table 1.

Table 1. Learning Material Types and The Amount of Available Learning Materials from Each Learning Material Type

No	Learning Material Type	The Amount of Learning Materials
1	Presentation	2
2	Video	7
3	Quiz	8
4	Exercise	10

Two presentations were prepared as ".pdf" files for the two topics of the Digital Computer Design course covered by the educational recommender system. These two presentations are listed below:

- "Presentation 1 - Instruction Encoding"
- "Presentation 2 - Microarchitecture"

In addition to presentations, seven video files that cover the theoretical background of some important subtopics were prepared. We tried to focus on important aspects and keep the video lengths as short as possible, i.e. less than 10 min. The videos were named based on the subtopics they focused on, and listed below:

- "Video 1 - Data Processing Instructions (Immediate)"
- "Video 2 - Data Processing Instructions (Register)"
- "Video 3 - Data Processing Instructions (Register and Immediate Shift Amount)"
- "Video 4 - Data Processing Instructions (Register Shifted Register)"
- "Video 5 - Memory Instructions"
- "Video 6 - Branch Instructions"
- "Video 7 - Interpreting Machine Language"

Exercise videos that cover applied examples of some important subtopics were also prepared. We focused on the most important aspects and prepared more than one exercise video for some subtopics, while we decided not to include any exercise video for some subtopics as their theoretical videos were thought to be enough to cover those subtopics. We kept the exercise video lengths less than 10 min, too. The exercise videos were named based on the subtopics they focused on, and listed below:

- "Exercise 1 - Data Processing Instructions (Register)"
- "Exercise 2 - Data Processing Instructions (Register)"
- "Exercise 3 - Memory Instructions"
- "Exercise 4 - Branch Instructions"
- "Exercise 5 - Interpreting Machine Language"
- "Exercise 6 - Interpreting Machine Language"
- "Exercise 7 - Interpreting Machine Language"
- "Exercise 8 - Microarchitecture"
- "Exercise 9 - Microarchitecture"
- "Exercise 10 - Microarchitecture"

Eight quizzes were prepared to assess the knowledge levels of learners at each subtopic of the Digital Computer Design course covered by the educational recommender system. The quizzes are listed below:

- "Quiz 1 - Data Processing Instructions (Immediate)"
- "Quiz 2 - Data Processing Instructions (Register)"
- "Quiz 3 - Data Processing Instructions (Register and Immediate Shift Amount)"
- "Quiz 4 - Data Processing Instructions (Register Shifted Register)"
- "Quiz 5 - Memory Instructions"
- "Quiz 6 - Branch Instructions"
- "Quiz 7 - Interpreting Machine Language"
- "Quiz 8 - Microarchitecture"

The number of questions available at each quiz is listed at Table 2. A total of 20 distinct question types were distributed to eight quizzes based on the subtopics they are related to. We wanted the students to have a more focused experience at each quiz. Thus, we tried to keep the number of questions at quizzes at a relatively low amount.

Table 2. The Amount of Questions Available at Each Quiz

Quiz No	The Number of Questions
Quiz 1	3
Quiz 2	2
Quiz 3	2
Quiz 4	2
Quiz 5	2
Quiz 6	3
Quiz 7	3
Quiz 8	3
Total	20

4 Statistical Findings of the Educational Recommender System Usage by Learners

The data collected by the semantic web-based educational recommender system were analyzed to provide insights regarding the learning processes of learners, and the findings are presented in this section. First, the statistical findings regarding the usage of the recommender system by learners are given. Then, the success levels of students at quizzes are discussed. Finally, the interaction of learners with recommended learning materials based on hints after wrong answers at quizzes is analyzed.

The log data of the educational recommender system were analyzed to provide statistics about the learner-system interaction. The usage ratios of each learning material over 100% are listed in descending order at Table 3.

"Quiz 1 - Data Processing Instructions (Immediate)" is the most commonly accessed learning material with 16.57%. "Presentation 1 - Instruction Encoding" is the second accessed learning material with 12.93%. "Quiz 7 - Interpreting Machine Language" is the third accessed learning material with 4.97%; however, its usage percentage is quite low compared to the first two highly-accessed learning materials.

The first and the second highly-accessed learning materials account for 29.5% of the overall learning material access in total. Considering the fact that the recommender system has 27 learning materials in total, it can be concluded that

Table 3. A List of Most Commonly Accessed Learning Materials

Learning Material Name	Usage Ratio of the Learning Material
Quiz 1 - Data Processing Instructions (Immediate)	16.57/100
Presentation 1 - Instruction Encoding	12.93/100
Quiz 7 - Interpreting Machine Language	4.97/100
Quiz 2 - Data Processing Instructions (Register)	4.95/100
Quiz 6 - Branch Instructions	4.86/100
Exercise 2 - Data Processing Instructions (Register)	4.63/100
Exercise 4 - Branch Instructions	4.56/100
Quiz 8 - Microarchitecture	4.02/100
Quiz 3 - Data Processing Instructions (Register and Immediate Shift Amount)	3.72/100
Quiz 4 - Data Processing Instructions (Register Shifted Register)	3.7/100
Video 1 - Data Processing Instructions (Immediate)	3.1/100
Quiz 5 - Memory Instructions	3.01/100
Exercise 1 - Data Processing Instructions (Register)	2.58/100
Video 2 - Data Processing Instructions (Register)	2.32/100
Video 4 - Data Processing Instructions (Register Shifted Register)	2.3/100
Video 3 - Data Processing Instructions (Register and Immediate Shift Amount)	2.13/100
Video 6 - Branch Instructions	2.09/100
Exercise 8 - Microarchitecture	1.87/100
Video 5 - Memory Instructions	1.85/100
Exercise 9 - Microarchitecture	1.79/100
Exercise 3 - Memory Instructions	1.79/100
Presentation 2 - Microarchitecture	1.74/100
Exercise 7 - Interpreting Machine Language	1.72/100
Exercise 10 - Microarchitecture	1.72/100
Exercise 6 - Interpreting Machine Language	1,72/100
Exercise 5 - Interpreting Machine Language	1.7/100
Video 7 - Interpreting Machine Language	1.66/100

two of them dominated the others. However, the reason behind this domination can be easily observed when we check the contents of the first two highly-used learning materials. “Quiz 1 - Data Processing Instructions (Immediate)” is the first quiz learners can access and is involved with the first type of data processing instruction encoding. Thus, it is not surprising to see it at the top of the list

as learners could have probably wanted to test their knowledge level by starting with this quiz. The second most accessed learning material "Presentation 1 - Instruction Encoding" is the first of the two presentation files available at the system. Besides, it is the first learning material listed on the user interface. Thus, it can be expected for it to have a high level of user access as some of the learners might have wanted to start learning from the beginning and follow the order of the listed materials.

We can also analyze the usage ratios of learning materials based on learning material types. There are four types of supported learning materials in the recommendation system, which are stated at Table 1.

As the first type of learning material, there are two presentations available in the recommender system. The usage ratio of "Presentation 1 - Instruction Encoding" is relatively high at 12.93% as it is the second highest used learning material, whereas the usage ratio of "Presentation 2 - Microarchitecture" is quite low at 1.74% as it is ranked as the 23rd highly-accessed learning material among the 27 learning materials available at the system (Table 3). There may be a lot of reasons that contributed to this finding. First of all, "Presentation 1 - Instruction Encoding" covers most of the available learning materials as 22 of the 27 materials are related to it, while "Presentation 2 - Microarchitecture" is involved with the remaining 5 learning materials. The second reason may be the order of the learning materials as "Presentation 1 - Instruction Encoding" is listed as the first learning material at the user interface.

Videos are the second learning material type supported by the recommender system, and their usage statistics can be seen in Table 3. "Video 1 - Data Processing Instructions (Immediate)" has the highest usage ratio with 3.1%. "Video 2 - Data Processing Instructions (Register)" and "Video 4 - Data Processing Instructions (Register Shifted Register)" are the second and the third highly watched videos with very close percentages at 2.32% and 2.3%, respectively. "Video 3 - Data Processing Instructions (Register and Immediate Shift Amount)" and "Video 6 - Branch Instructions" follow them with close ratios to each other at 2.13% and 2.09%, respectively. "Video 5 - Memory Instructions" is ranked as the 6th most watched video with 1.85% and it is the 19th most accessed learning material. Finally, "Video 7 - Interpreting Machine Language" is the least watched video with 1.66% and it is also the least accessed learning material on the overall list as it is the lowest ranked learning material at the 27th position. The reason for this last position can be related to the order of the subtopics as it is the video related to the last subtopic. On the other hand, learners could have liked to engage with other learning material types more than videos.

As the third learning material type of the recommender system, the usage statistics of exercises can be seen at Table 3. "Exercise 2 - Data Processing Instructions (Register)" and "Exercise 4 - Branch Instructions" are the most accessed exercises with 4.63% and 4.56%, respectively. They are followed by "Exercise 1 - Data Processing Instructions (Register)" at the third position with a 2.58% access ratio, while the rest of the exercises have quite close usage ratios ranging between 1.87% and 1.7%. It is an interesting finding to see "Exercise 1 - Data Processing Instructions (Register)" at the third position, because the

first presentation and the first video were at the top positions for their learning material type. This finding may be related to quizzes as some learners might have wanted to check some exercises after wrong answers to some questions of the related quizzes.

The fourth and final learning material type supported by the recommender system is quizzes. The access ratios for each quiz can be observed at Table 3. "Quiz 1 - Data Processing Instructions (Immediate)" is by far the most accessed quiz with 16.57% access ratio. It is followed by "Quiz 7 - Interpreting Machine Language", "Quiz 2 - Data Processing Instructions (Register)", and "Quiz 6 - Branch Instructions" at the second, third, and fourth positions with close ratios at 4.97%, 4.95%, and 4.86%, respectively. "Quiz 8 - Microarchitecture" is at the fifth position with 4.02% usage ratio, while "Quiz 3 - Data Processing Instructions (Register and Immediate Shift Amount)" and "Quiz 4 - Data Processing Instructions (Register Shifted Register)" are at the sixth and seventh positions with 3.72%, and 3.7%, respectively. Finally, "Quiz 5 - Memory Instructions" is at the last position with access ratio of 3.01%.

"Quiz 5 - Memory Instructions" is the least accessed quiz; however, it is ranked as the 12th most accessed learning material on the overall learning material access list. Since there are 8 quizzes in total, it is a valuable finding to see that 8 of the top 12 positions are filled with quizzes. That shows that quizzes are the most accessed and the most popular learning material type.

Average grades of students at quizzes are listed in descending order at Table 4. Learners were more successful at "Quiz 1 - Data Processing Instructions (Immediate)", "Quiz 2 - Data Processing Instructions (Register)", and "Quiz 3 - Data Processing Instructions (Register and Immediate Shift Amount)" with very close scores at 67, 66, and 66 over 100 points, respectively. The least successful quizzes were "Quiz 5 - Memory Instructions" and "Quiz 8 - Microarchitecture" with very close average scores at 49, and 51 points, respectively. It should be noted that the learners can take the same quizzes over and over again, and the average grades listed at Table 4 were calculated by taking into account each quiz activity.

Table 4. Average Grades of Learners at Quizzes

Quiz Name	Average Grade
Quiz 1 - Data Processing Instructions (Immediate)	67/100
Quiz 2 - Data Processing Instructions (Register)	66/100
Quiz 3 - Data Processing Instructions (Register and Immediate Shift Amount)	66/100
Quiz 4 - Data Processing Instructions (Register Shifted Register)	58/100
Quiz 7 - Interpreting Machine Language	55/100
Quiz 6 - Branch Instructions	54/100
Quiz 8 - Microarchitecture	51/100
Quiz 5 - Memory Instructions	49/100

Learners can check the correct answers after taking quizzes. If the answer to a question in the quiz is wrong, the recommender system guides the learners to suitable learning materials by giving them hints. The log data is analyzed to check if the learners followed the hints and clicked the suggested learning materials after each quiz. The results are listed at Table 5.

Table 5. Number of Clicks to Suggested Learning Materials After Each Quiz Based on Hints

Quiz Name	Number of Clicks To Suggestions
Quiz 1 - Data Processing Instructions (Immediate)	64
Quiz 2 - Data Processing Instructions (Register)	16
Quiz 3 - Data Processing Instructions (Register and Immediate Shift Amount)	19
Quiz 4 - Data Processing Instructions (Register Shifted Register)	7
Quiz 5 - Memory Instructions	2
Quiz 6 - Branch Instructions	16
Quiz 7 - Interpreting Machine Language	22
Quiz 8 - Microarchitecture	6

It is observed that users were the most likely to follow the hints after "Quiz 1 - Data Processing Instructions (Immediate)" with 64 clicks detected. Even though it is not certain whether the suggested learning material was clicked because of following the hints, based on recommendations at the user interface, or as a result of random navigation, there seems to be a correlation between usage ratios of quizzes and the number of clicks to suggested learning materials based on hints at the quizzes. "Quiz 1 - Data Processing Instructions (Immediate)" is at the top of both statistics, and "Quiz 7 - Interpreting Machine Language" is the second item on both of the lists. However, the number of clicks to suggested learning materials based on hints after taking quizzes is relatively low. Thus, we should point out that there is not enough interaction data to support the generalization of this finding. In this regard, the limited number of available log data is one of the main limitations of this study.

5 Discussion and Conclusion

In this paper, we analyzed the interaction data of learners with an educational recommender system to provide insights into how learners navigated through the system. The recommender system included learning materials prepared for a subset of topics of the Digital Computer Design course. The data used in this study was collected by utilizing the recommender system as a supplementary tool as part of the Digital Computer Design course of the Computer Engineering

curriculum at a public university in Turkey for two weeks during which the related subtopics were covered at the class.

The findings were discussed thoroughly to provide insights regarding the learning processes of learners. It is observed that learners were more likely to interact with quizzes than other types of learning materials. The fact that the recommender system was used as a supplementary tool and the students were already familiar with the subjects from the theoretical lectures might have been a factor in decreasing the popularity of other learning materials. In addition, there seems to be a correlation between quiz access ratios of students and the number of clicks to suggested learning materials based on the hints of wrong answers after taking quizzes; however, this finding needs to be supported by conducting new experiments with higher number of students, which is planned as future work.

In this regard, the study's reliance on data collected from a single course for a short duration is the main limitation of this study. Thus, the findings may have limited generalizability due to the specific context the data was collected. Even though the results are promising and in line with previous studies [21,29], the findings may not be representative of learner behavior in other educational settings or over longer time frames. Therefore, further studies should be conducted to support the findings of this study.

Future work directions can be discussed from learning design and system design perspectives. From the learning design perspective, instead of being used as a supplementary tool, the educational recommender system can be integrated with the theoretical lectures of the course to provide enhanced learning experiences. Feedback about the quality of the learning materials can be gathered and utilized to update them appropriately. In this regard, it is planned to work with learners more closely and also collect qualitative data by conducting focus group interviews. A comparison or control group against which to benchmark the observed navigation patterns could also be useful for achieving meaningful results in further studies.

From the system design perspective, the functionalities of the educational recommender system can be improved and new functionalities can be added. For example, instead of providing hints at the end of quizzes and checking whether the students followed the recommendations, the quiz feature can be enhanced to provide question-level interactions dynamically in case of a wrong answer. There are also plans to make technical adjustments to enhance the recommendation capability of the recommender system.

References

1. Aktas, C., Ciloglugil, B.: A survey of semantic web based recommender systems for E-Learning. In: Gervasi, O., et al. (eds.) ICCSA 2023. LNCS, vol. 14104, pp. 494–506. Springer, Cham (2023). https://doi.org/10.1007/978-3-031-37105-9_33
2. Rahayu, N.W., Ferdiana, R., Kusumawardani, S.S.: A systematic review of ontology use in E-Learning recommender system. Comput. Educ. Artif. Intell. **3**, 100047 (2022)

3. George, G., Lal, A.M.: Review of ontology-based recommender systems in e-learning. Comput. Educ. **142**, 103642 (2019)
4. Tarus, J.K., Niu, Z., Mustafa, G.: Knowledge-based recommendation: a review of ontology-based recommender systems for e-learning. Artif. Intell. Rev. **50**, 21–48 (2018)
5. Ciloglugil, B.: Adaptivity based on felder-silverman learning styles model in E-Learning systems. In: 4th International Symposium on Innovative Technologies in Engineering and Science, ISITES 2016, pp. 1523–1532 (2016)
6. Essalmi, F., Ayed, L. J. B., Jemni, M., Kinshuk, Graf, S.: A fully personalization strategy of e-learning scenarios. Comput. Hum. Behav. **26**(4), 581–591 (2010)
7. Ciloglugil, B., Inceoglu, M.M.: User modeling for adaptive e-learning systems. In: Murgante, B., Gervasi, O., Misra, S., Nedjah, N., Rocha, A.M.A.C., Taniar, D., Apduhan, B.O. (eds.) ICCSA 2012. LNCS, vol. 7335, pp. 550–561. Springer, Heidelberg (2012). https://doi.org/10.1007/978-3-642-31137-6_42
8. Truong, H.M.: Integrating learning styles and adaptive e-learning system: current developments, problems and opportunities. Comput. Hum. Behav. **55**, 1185–1193 (2015)
9. Ciloglugil, B., Inceoglu, M.M.: A learner ontology based on learning style models for adaptive e-learning. In: Gervasi, O., et al. (eds.) ICCSA 2018. LNCS, vol. 10961, pp. 199–212. Springer, Cham (2018). https://doi.org/10.1007/978-3-319-95165-2_14
10. Ozyurt, O., Ozyurt, H.: Learning style based individualized adaptive e-learning environments: content analysis of the articles published from 2005 to 2014. Comput. Hum. Behav. **52**, 349–358 (2015)
11. Ciloglugil, B., Inceoglu, M.M.: Exploring the state of the art in adaptive distributed learning environments. In: Taniar, D., Gervasi, O., Murgante, B., Pardede, E., Apduhan, B.O. (eds.) ICCSA 2010. LNCS, vol. 6017, pp. 556–569. Springer, Heidelberg (2010). https://doi.org/10.1007/978-3-642-12165-4_44
12. Khanal, S.S., Prasad, P.W.C., Alsadoon, A., Maag, A.: A systematic review: machine learning based recommendation systems for e-learning. Educ. Inf. Technol. **25**, 2635–2664 (2020)
13. Al-Yahya, M., George, R., Alfaries, A.: Ontologies in E-learning: review of the literature. Int. J. Softw. Eng. Appl. **9**(2), 67–84 (2015)
14. Ciloglugil, B., Inceoglu, M.M.: Ontology usage in e-learning systems focusing on metadata modeling of learning objects. In: International Conference on New Trends in Education, ICNTE 2016, pp. 80–96 (2016)
15. Tapia-Leon, M., Rivera, A. C., Chicaiza, J., & Luján-Mora, S.: Application of ontologies in higher education: a systematic mapping study. In: 2018 IEEE Global Engineering Education Conference (EDUCON), pp. 1344–1353. IEEE (2018)
16. Ciloglugil, B., Inceoglu, M. M.: Developing adaptive and personalized distributed learning systems with semantic web supported multi agent technology. In: 10th IEEE International Conference on Advanced Learning Technologies, ICALT 2010, Sousse, Tunesia, 5–7 July 2010, pp. 699–700. IEEE Computer Society (2010)
17. Klašnja-Milićević, A., Ivanović, M., Nanopoulos, A.: Recommender systems in e-learning environments: a survey of the state-of-the-art and possible extensions. Artif. Intell. Rev. **44**, 571–604 (2015)
18. Khalid, A., Lundqvist, K., Yates, A.: A literature review of implemented recommendation techniques used in Massive Open online Courses. Expert Syst. Appl. **187**, 115926 (2022)
19. Rahayu, N.W., Ferdiana, R., Kusumawardani, S.S.: A systematic review of learning path recommender systems. Educ. Inf. Technol. 1–24 (2022)

20. Ciloglugil, B., Inceoglu, M.M.: A Felder and Silverman learning styles model based personalization approach to recommend learning objects. In: Gervasi, O., et al. (eds.) ICCSA 2016. LNCS, vol. 9790, pp. 386–397. Springer, Cham (2016). https://doi.org/10.1007/978-3-319-42092-9_30
21. Premlatha, K.R., Geetha, T.V.: Learning content design and learner adaptation for adaptive e-learning environment: a survey. Artif. Intell. Rev. **44**, 443–465 (2015)
22. Murtaza, M., Ahmed, Y., Shamsi, J.A., Sherwani, F., Usman, M.: AI-based personalized e-learning systems: issues, challenges, and solutions. IEEE Access **10**, 81323–81342 (2022)
23. Chen, X., Xie, H., Zou, D., Hwang, G.J.: Application and theory gaps during the rise of artificial intelligence in education. Comput. Educ. Artif. Intell. **1**, 100002 (2020)
24. Hwang, G.J., Xie, H., Wah, B.W., Gašević, D.: Vision, challenges, roles and research issues of Artificial Intelligence in Education. Comput. Educ. Artif. Intell. **1**, 100001 (2020)
25. Aktaş, C.: Uyarlanabilir E-Öğrenme İçin Ontoloji Tabanlı Bir Öneri Sistemi. Yüksek lisans tezi. Ege Üniversitesi, Fen Bilimleri Enstitüsü, İzmir (2023)
26. Ramesh, P. N., Kannimuthu, S.: Context-aware practice problem recommendation using learners' skill level navigation patterns. Intell. Autom. Soft Comput. **35**(3) (2023)
27. Troussas, C., Krouska, A.: Path-based recommender system for learning activities using knowledge graphs. Information **14**(1), 9 (2022)
28. Chang, T. W., Kurcz, J., El-Bishouty, M. M., Kinshuk, Graf, S.: Adaptive and personalized learning based on students' cognitive characteristics. Ubiq. Learn. Environ. Technol. 77–97 (2015)
29. Shi, L., Cristea, A.I., Awan, M.S.K., Hendrix, M., Stewart, C.: Towards understanding learning behavior patterns in social adaptive personalized e-learning systems. In: Proceedings of the 19th Americas Conference on Information Systems (AMCIS 2013). (2013)
30. Miranda, S., Vegliante, R.: Learning Analytics to support learners and teachers: the navigation among contents as a model to adopt. J. e-Learn. Knowl. Soc. **15**(3), 101–116 (2019)
31. Hasan, R., Palaniappan, S., Mahmood, S., Abbas, A., Sarker, K.U., Sattar, M.U.: Predicting student performance in higher educational institutions using video learning analytics and data mining techniques. Appl. Sci. **10**(11), 3894 (2020)
32. Felder, R.M., Silverman, L.K.: Learning and teaching styles in engineering education. Eng. Educ. **78**(7), 674–681 (1988)
33. Agrawal, R., Imieliński, T., Swami, A.: Mining association rules between sets of items in large databases. In: Proceedings of the 1993 ACM SIGMOD International Conference on Management of Data, pp. 207–216 (1993)
34. Hunyadi, D.: Performance comparison of Apriori and FP-Growth algorithms in generating association rules. In: Proceedings of the 5th European Conference on European Computing Conference, pp. 376–381 (2011)
35. Shawkat, M., Badawi, M., El-ghamrawy, S., Arnous, R., El-desoky, A.: An optimized FP-growth algorithm for discovery of association rules. J. Supercomput. **78**(4), 5479–5506 (2022)
36. Balcı, B., Çiloğlugil, B., Murat İnceoğlu, M.: Open courseware-based logic design course. Croatian J. Educ. Hrvatski časopis za odgoj i obrazovanje **22**(2), 515–562 (2020)

Improving Efficiency of Natural-Language Text Generation for Automatic Pedagogical Questions

Yulia Gomazkova, Oleg Sychev(✉), and Marat Gumerov

Volgograd State Technical University, Lenin Avenue, 28, Volgograd 400005, Russia
o_sychev@vstu.ru

Abstract. When learning new skills, students may experience problems in understanding the course material and may require a tutor's help in the form of educational scaffolding. That can be organized in the form of learning dialogue consisting of closed-answer questions and explanations for answers to them. However, designing Intelligent Tutoring Systems that support generating pedagogical questions is very labor-intensive. In this paper, we propose a method of improving template-based generation of pedagogical questions by moving the templates from the level of nodes of Thought Process Tree describing the problem-solving reasoning process to the smaller elements like expressions, domain objects, their classes, properties, and relationships. The method allowed to reduce the number of templates used in the intelligent tutoring system for learning programming-language expressions by about half and the number of words used in templates by about 60%.

Keywords: Natural language generation · Pedagogical questions · Intelligent Tutoring Systems

1 Introduction

It is one of the most important tasks of any tutor to guide students through their learning process, particularly when they encounter obstacles or misconceptions [4], which is why effectiveness of conducted pedagogical interventions is very important [7,23].

The question-based approach to teaching allows teachers to build individualized dialogues with students, assessing the level of their knowledge and adjusting the explanations of the topic. That approach helps to develop the mastery of new educational material more than the usual explanatory monologue [16,22].The role of questions in learning has been repeatedly considered in earlier pedagogical studies, confirming their effectiveness [3,17]. It has been shown that questions asked after studying certain text materials have a significant effect on students' memory and understanding of the source text [3,6].

With rising demand for high-complexity tutoring systems, a growing body of research emerges that focuses on providing increasingly more efficient electronic

© The Author(s), under exclusive license to Springer Nature Switzerland AG 2024
O. Gervasi et al. (Eds.): ICCSA 2024 Workshops, LNCS 14816, pp. 37–50, 2024.
https://doi.org/10.1007/978-3-031-65223-3_3

tutors capable of performing more tasks that were previously done only by human tutors [8,21]. Today, many such systems aim to provide students with contextualized feedback based on the problem at hand and the individuality of the student. But despite their promising results [9], widespread integration of Intelligent Tutoring Systems (ITS) has been hindered by the substantial effort required to author courses and exercises. Estimates in [2] suggest that the creation of one hour of ITS content requires 200–300 h of expert design input. Reduction of that authoring effort is the focus of a lot of ongoing research in the field.

So, whether delivered by human instructors or sophisticated software systems, the ability to provide clear and comprehensive pedagogical support is paramount in facilitating student comprehension and retention, yet constructing the modern ITS to utilize such methods remains a labor-intensive process. Generating pedagogical dialogue as a set of questions and explanations is particularly challenging in that regard [19]. In this work, we are focusing on improving automatic generation of pedagogical questions with the goal of reducing the effort required to allow the system to engage the student in a natural-language dialogue about the rules of a new subject domain.

2 Related Works

The use of natural-language dialogue in tutoring systems goes back at least several decades, with a solid body of research going into it. The approaches to the problem of providing a student with a consistently readable and helpful text are varied across applications, but certain broad groups definitely emerge.

The simplest approach used when creating such systems is relying on the author's expertise by making them provide the questions and/or explanations shown to students explicitly. Such approaches, while straight-forward, can still provide a lot of complexity and adaptability, depending on the method used and the amount of effort spent. A major example of this approach can be seen with applications of the Knowledge Construction Dialogues (KCD) framework in works such as Atlas [5], ProPL [10], and Rimac [1]. With KCD, the author defines both the textual formulations of the questions shown as well as the structure of responses anticipated from the students, with each response either linked to another KCD responsible for providing remedial guidance or categorized as a correct answer. That process results in a hierarchical structure where the main line of dialogue can branch off into sub-dialogues for the purposes of correcting student's mistakes made at the higher level. With that, a number of automatic tutors can be constructed, which can provide a student with educational scaffolding that can help them during misunderstandings, but the authoring effort of such approaches is high.

There was effort in improving that approach. In the already-mentioned Rimac system [1], for example, an effort was made to increase the system's adaptability to student progress by utilizing a student model based on the Instructional Factor Analysis Model, which would continuously update after each dialogue session.

In more specialized domains, their rules can be utilized to reduce the amount of work necessary to create the teaching dialogue. In Jeliot 3 [13,14], a tutor

aimed at teaching Java programming language via code execution visualization, an approach was proposed for providing students with questions during the code execution. There, a code statement could be assigned a question about the result of its execution, which could then be displayed to the student during the visualization, allowing them to check their understanding. With this approach, the question structure arises naturally from the code execution sequence, and any given question can be reused every time the relevant statement is executed, while its answer options are dynamically adapted to match the context of program execution.

However, manually crafted systems of pedagogical questions remain very labor-intensive to construct. That can be solved by automating the generation of pedagogical questions. There are two broad approaches to the automatic generation of pedagogical questions: the transformational approach and the template approach. Question generation systems using the transformational approach operate on the following premise: a text source (such as a textbook chapter) is used as an input, its sentences are automatically parsed and structurally transformed into questions, keeping the semantics of the source text, in order to assess the student's understanding of it.

An example of such a system can be seen in [18], where textual analysis and transformation are used in order to create "fill in the blank" style questions given a corpus of Wikipedia articles related to the topic. There, the textual transformation is used in its simplest form: replacing a dynamically determined keyword with a blank. However, an interesting approach of analyzing and comparing the context the words appear in is used to determine a set of distractors, which also fit into the blank and can serve as possible answers in multiple-choice questions.

A more complex approach to text transformation is explored in [12]. Mazidi and Tarau propose introducing a Natural Language Understanding aspect into the question generation system. By analyzing the sentences of the input text by the type and arrangement of their syntactic elements, the system classifies sentences into 8 categories.For each of those categories, an internal template can then be defined and used to transform the sentence from a statement to a question while correctly handling its syntactic and semantic contents. The chief problem with that approach is that the questions remain very closely related to single sentences of the input text; they do not use the broad knowledge of the subject domain.

The use of templates defined specifically for a given problem or domain is another approach used in many question-generating systems. The systems in this category generally rely on the human author to provide some natural-language text templates in order to create their questions, rather than gathering this information from an input text. This generally leads to more nuanced questions but requires a lot more effort. Despite that, a study [11] of question generation methods tailored for educational purposes revealed that approaches relying on templates tended to outperform systems that relied on syntactic transformation of the source text.

A promising approach was chosen by O'Rourke et al. [15], who used a formalization of the student's thought process in the form of a custom programming language called Thought Process Language (TPL). The TPL code would describe the actions a student needed to perform to solve a problem, and the structure of the code could be used to generate explanations in a natural language by using predefined textual templates assigned to each type of TPL statement. Those templates could then be populated by the objects from the formal definition of the learning problem that the learner tries to solve in order to create explanations of the actions shown to the learner.

A possible improvement on this approach was proposed in [19], where the similar concept of assigning textual templates to an algorithm-defining structure was used to create sequences of questions, guiding the student through the necessary reasoning steps. This system allowed for a more human-like representation of a Thought Process than TPL, using a specialized tree-like formalization instead of code; it also used a more expressive template system. However, it still required manual creation of a lot of natural-language templates of several kinds.

3 Method

3.1 Existing Approach and its Flaws

We based this study on the results of automatic generation of pedagogical questions from templates obtained by Sychev and Gumerov [19]. In that approach, single-choice or multiple-choice questions are used, so the natural-language subsystem should generate three kinds of strings (see Fig. 1):

1. question formulations,
2. answer options (both correct answers and distractors),
3. explanations (reply) shown to the student (for wrong answer options).

That method uses Thought Process Trees to represent the reasoning paths a student must follow to correctly solve any problem in the given domain or determine why some solutions are incorrect. That representation is used together with the dictionaries of domain-specific entities (classes, class and object properties and kinds of relationships), and the formal problem formulation containing actual object instances and their relationships is then utilized to construct a sequence of questions which allows to detect where the student strayed from the correct solution path and explain their error.

That approach focuses on using the nodes of Thought Process Trees to generate pedagogical questions. That is, the majority of the natural-text templates necessary to generate the pedagogical dialogue are assigned to nodes. That allows for a nuanced control of the formulations presented to students, as the node's human-formulated meaning is often simpler than the literal translation of the expression defining the formal meaning of the node, so it was important to provide separate templates for each node. But assigning templates mostly to nodes did not allow generalizing templates for similar nodes, or indeed for any nodes at all.

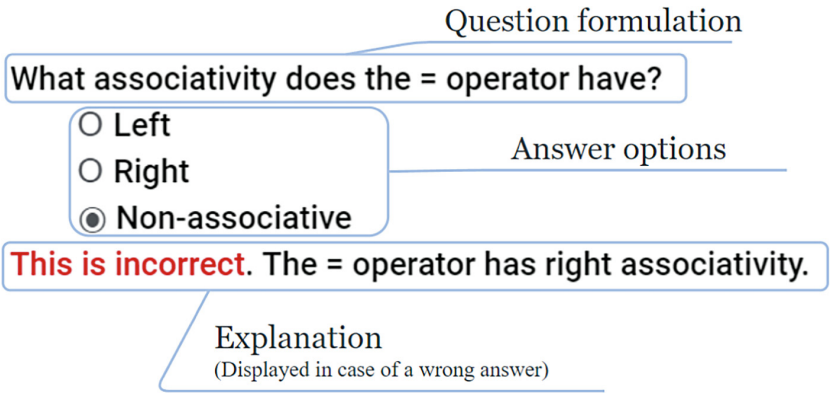

Fig. 1. The structure of generated pedagogical questions: the question formulation, answer options and explanation of the chosen answer.

Subject domains often contain similar branches of reasoning. For example, in the task of determining the order of evaluation of a programming-language expression [20], there are two similar branches concerned with the possible competing operators to the left and right of the current operator. The branches of thought were almost identical except that the relations between the operators were changed from "to the left" ("less than") to "to the right" ("more than") and vice versa [19]. But the nodes of the resulting branches were distinct, so there was no way to generalize their descriptions, and so the domain expert (the one responsible for authoring the Thought Process Tree) had to enter almost twice as many templates than was absolutely necessary.

The same problem is even more evident on the level of expressions determining the reasoning and their operands. Many class and object properties and relationships are used in multiple nodes, so their natural-language descriptions should be entered many times.

3.2 Improvements

In this study, our main focus was to reduce the amount of work needed to allow the system to generate pedagogical questions and explanations for different answers to them. As it was mentioned before, the previously described methods lacked a way to generalize the text generation for nodes with similar underlying logic, which is what we tried to address.

In the previous work, four kinds of generated questions are defined to be generated by the system:

- Variable Value questions ("What is the value of <variable>?")
- Final Node questions ("Which <reasoning step> determines the outcome in the current situation?")
- Node questions ("What is the outcome of this <reasoning step>?")

– Structural questions("Given the <answer to a node question> what should you do next?")

For the goals of this study, it is important to analyze how those question types relate to nodes and expressions they contain.

Variable Value questions are directly tied to Action Nodes: an action node introduces the relevant variable and contains the expression that determines the value of that variable. Variable Value questions can be generated by either assigning a description to the variable (which would produce more semantically-oriented questions) or deriving the description from the expression used in the node (which would produce a more direct, matter-of-fact question). Generally, the first approach is preferable because students usually refer to temporary values used in reasoning (represented as variables) by their semantic role instead of the exact way needed to determine them.

For example, let us consider the process of determining the order of evaluation of an expression. One of the important variables when considering if the given operator (X) can be evaluated right now is the competing operator to the left (A), which can prevent the given operator's evaluation if the competing operator must be evaluated first. Consider the action node which finds the competing operator—the closest unevaluated operator standing to the left of X—and assigns it to the variable A. The expression for that node is:

```
findExtreme operand A[
    not exists a' in A' {a'->isCloserToThan(X, A)}
]
among operand A' {
    A'->isLeftOf(X)
    AND A'.state == unevaluated
}
```

Our goal is to generate a question verifying that the student determined the value of A correctly in the given circumstances because it is crucial to verifying the further line of reasoning using A.

As mentioned, one approach is to define the textual description for the variable A itself—for example, "the competing left operator of ${X}" (where ${} denotes a sub-template—in this case, the textual description of the object contained in variable X). With this, a question asking to "Find the competing left operator of ${X}" can be generated by utilizing a higher-level template "Find ${variableDescription}" assigned to the variable value question. The answer options for this question are then generated from the textual descriptions of actual operators present in a given problem, including the actual correct value of A.

Another approach is to use the search expression in order to generate the description of A. As all the properties and relationships used in expressions in the Thought Process tree are defined in dictionaries by the problem-solving domain's author, the system can utilize that information to analyze expressions

and generate natural-language descriptions based on their structure and the used concepts. In the example above, the system can recognize the following pattern:

```
findExtreme <class> <extremeVariable>[
    not exists <rangeVariable> in <variableRange> {
        <rangeVariable>-><comparativeRelationship>(
            <otherVariable>,
            <extremeVariable>
        )
    }
]
among <class> <variableRange> {
    ...
}
```

meaning that <extremeVariable> should be described using an extreme formulation assigned to <comparativeRelationship>—(in this case, A) can be described as "${obj} closest to ${X}" based on the template assigned to the `isCloserToThan` relationship. The conditions in the `among` block can similarly be analyzed to get the "$obj to the left of ${X}" and "unevaluated ${obj}" templates, which, along with the variable's class name, could then be combined into the A's final description "unevaluated operator closest to ${X} to the left of it', which can then be used in the question template shown above.

The system we developed allows for both described approaches because they have their advantages and disadvantages. Directly assigning the text to a variable is conceptually simpler; it allows for more nuanced and semantically correct descriptions, which is especially necessary in cases where the meaning (role) of the variable is more important than and different from the procedure of determining its value. It, however, requires more effort from the domain expert and does not allow reusing the textual descriptions. The generation of text based on the structure of expressions has the opposite set of characteristics: while it generally requires less authoring effort, it is strictly tied to the expression's structure, unable to grasp the overall meaning of the variable. The two kinds of questions play different pedagogical roles and can be used in different circumstances. The question using the semantic role of the variables verifies if the student knows how to determine the object for that semantic role (e.g., a competing operator to the left) in the given circumstances. The question generated from the node expression only verifies if the student can perform the instructions for finding an object satisfying certain criteria well without understanding the semantic role of the found object.

Another problem to consider is the ability of the text-generation algorithm to handle arbitrarily complex expressions. Currently, our method can recognize relatively simple patterns in the expressions' structure: a unique object among a set of others, an object related in a certain way to another object, an object with a given property, an object of a given class, and their combinations. If no relevant pattern was detected, the tutoring system must ask for the expert's support

because no reliable way to translate that expression into natural-language text has been found as of yet.

Our work was based on the analysis of seven subject domains that were created for the tutoring system mentioned above: determining the order of a programming-language expression's evaluation; determining the order of adjectives in the English language; determining object visibility in the C++ programming language; constructing access expressions in the C++ programming language; determining the control flow of a given algorithm; determining the lifetime of a variable; determining the data types of expressions in programming languages. Reviewing the Thought Process Trees constructed for those domains allowed us to draw conclusions on the commonalities and patterns occurring within them. They also allowed us to test the method in different situations and make sure it could be generalized to other subject domains.

Generating text from the structure of expression is particularly important for Question Nodes, which represent questions that determine the line of reasoning in the given circumstances. Together, Question Nodes and Action Nodes constitute the majority of nodes in a typical Thought Process Tree (about 92% out of all nodes) so improving text generation for them is more important. Also, question nodes cannot be linked to a variable with certain semantic role so their only source of information is the node expression.

In order to generate Node Questions for Question Nodes, we had to classify the kinds of questions used in the nodes in Thought Process Trees. Based on the trees from the domains that we used, we identified the following kinds of questions:

- Checking a class's or object's property: further reasoning depends on the value of an object's property.
- Comparing a class's or object's property to a constant: further reasoning depends on how the value of an object's property relates to some explicit value.
- Comparing values of the same property of different objects: further reasoning depends on how the properties of the objects relate to each other.
- Checking for the existence of a relationship between two objects.
- Checking for the existence of an object defined by certain criteria: further reasoning depends on if such an object exists in the given learning situation or not.
- Checking for an object's class; the further reasoning depends on the class.

This classification allows to choose the appropriate meta-patterns for dynamically constructing question formulation for question nodes. This is done as follows.

Question nodes that check an object's property are defined by the expression of the following structure: <variable>.<property> (For example, 'X.associativity'). Those questions have a simple structure, but there are different kinds of properties and in natural languages, different syntactic templates are used for them. So, in this case, we propose to assign a question template to the property. For example, the template "What associativity does ${class}

have?" fits the `associativity` property of operators. Other examples are "How many tokens does $obj} have?" for integer property `countOfTokens` and "Does ${class} need a left operand?" for boolean property `needsLeftOperand`. If no template is defined for the class or object property, the system can use the default template "What is the ${property name} of ${class/object}?", which uses the textual description of the property. Properties can belong either to individual objects or their classes (static properties). So the templates use either the class description ("operator +") or the object description ("operator + at position 5") in the question.

The answer options for this type of questions can be created from all the possible values of the property depending on its type—or, when the value range of the property is large, some subset of the values close to the actual value of the property for the corresponding object and, possibly, some nearby objects in the same learning problem. The explanations, then, are constructed like the question formulation: when the student chooses an incorrect value for the checked value, the system can create a reply like "That is incorrect, because ${statement}.", where the `statement` placeholder is either constructed from the statement template assigned to the property itself (e.g., "${obj} has ${value} associativity"), or from the default "${propertyName} of ${class/object} is ${value}" template.

When comparing a class's or object's property to a constant, the expressions look like <object/variable>.<property> <operator> <constant> (for example, 'X.associativity == left'). For boolean and enumerated properties, which support only equality and inequality comparisons, the statement template assigned to the property can be reused. The questions then take the form "Is it true that ${statement}?", with the `statement` placeholder being filled in as mentioned above, just inserting the description of the constant in question in place of the `value` placeholder. With numeric (or other linear-scale) properties, whose values can be less or greater than others, the questions are constructed differently. In that case, the question takes the form "Is ${propertyName} of ${object} less than/greater than/equal to ${value}", with the comparison formulation chosen based on the used comparison operator.

The answer options for this type of question are "Yes" or "No"; explanations are generated similarly to the previous type of questions: it is enough to show the student the correct value of the property in question in order to show why their answer was incorrect. It should be noted that inequality operator (!=) as well as non-strict comparisons (>= and <=) do not produce their own formulations in the question (in order to reduce the question's complexity), but are rather treated as the inversion of another operator. So, rather than asking, "Is it true that the associativity of ${X} isn't ${value}?", the system asks, "Is it true that the associativity of ${X} is ${value}?", and then inverts the student's answer.

Another type of comparison recognized by the system is the comparison between the values of the same property of different objects, which have the form '<object1>.<property> <operator> <object2>.<property>' for the regular (boolean-typed) comparisons and 'compare(<object1>.<property>, <object2>. <property>)' for three-way (greater, equal, or less) comparisons

(for example, 'X.precedence == Y.precedence' and 'compare(X.precedence, Y.precedence)' respectively). Depending on the property's type, the answer options are constructed differently. If the property allows for less/greater comparisons, the system constructs the question of the form of "Compare ${propertyName} of ${object1} and ${object2}", with placeholder values being filled as it was described before, and answer options are "${propertyName} is greater for ${object1}", "${propertyName} is greater for ${object2}", and "They are equal". If the property type only allows for equality comparisons, the question generated is "Is ${propertyName} of ${object1} equal to that of ${object2}?" with answer options "Yes." or "No.", with explanations being generated similarly to the previous two types of questions.

Expressions that require assessing the object's class ('<object>.class' and '<object> is <class>') are technically separate, but operate very similarly to the property-related expressions described above (the object's class may be thought of as a property of it), so the questions and explanations are generated by a similar method. For them, the question template "What is ${obj}?" and the statement template "${obj} is ${class}" are used. The answer options are constructed from subclasses of the class that was used to define the variable holding the object.

Another kind of questions the system recognizes is the question about the existence of a certain relationship between objects. The expressions in this case have the form '<subject>->relationship>(<objects>)' (For example, 'Y->isLeftOf(X)'). This type of questions has similar text to the comparison of a property to a constant: the statement template is defined for the relationship checked (for example, "${subj} is to the left of ${obj}") and then the question is generated using the same "Is it true that ${statement}?" template, with answers and explanations being constructed in the same manner.

The last question type we identified is a check if an object matching a certain set of criteria exists. The expression structure in this case is '[not] exists <Var> {<boolean criteria>}'. The Question Nodes containing such expressions are similar to the Action Nodes for finding the object that matches those criteria, except that for Question Nodes, the object itself does not matter in the long term and so should not be remembered. This means that we can reuse the method of generating descriptions for Action Nodes to create an object description and use the general template "Is there any ${objectDescription}?". The answers here are once again "Yes" and "No"; the explanation are generated like "That's incorrect, because the ${object}, matches all the criteria".

Introducing those distinct question types allowed us to specialize Node Questions generated by the system, which led to using low-level templates which can be reused in several questions each. While we discussed this method with respect to Question Nodes only, it should be noted that this approach can be utilized in other nodes that contain expressions—for example, Loop Nodes that iterate over all the objects matching certain criteria can use the same method of generating descriptions as the Action Nodes and existence-checking Question Nodes.

4 Results

The proposed approach allows to replace a lot of repeated text in the descriptions of the nodes of Thought Process Trees with a smaller set of shorter templates assigned to the domain entities. That can considerably reduce the effort required to enable the system to generate all the necessary questions and explanations for a subject domain. We used the Thought Process Tree for the order of expression evaluation to evaluate the gains of the proposed method.

Out of 237 textual templates that are required for the question generation of that tree, 172 correspond to the nodes that contain expressions and can benefit from our approach. Those templates were replaced by 54 much smaller ones, assigned to individual domain entities like properties and relationships, which reduced the number of required templates by more than three times. The templates themselves also became smaller (see Table 1).

The remaining 65 templates were not reduced by this approach because they correspond to the nodes related to the control structures of Thought Process Tree—specifically Branching Nodes and their branches. There was no Loop nodes in the that tree so they are not represented in the table; those nodes also are not covered by our method. Optimizing natural-language message generation for Branching and Loop nodes requires further work.

By assigning templates to domain entities like object properties and relationships, we also reduced the conceptual load on the domain expert because it is easier to create lists of domain entities and assign them all of the necessary information (including templates, now) than it is to go through the entire Thought Process Tree to create the templates for each node.

Table 1. Improvements made to the amount and size of the templates.

	before			after		
	total templates	avg. words per template	total words	total templates	avg. words per template	total words
action nodes	38	13.7	521	54	5.5	297
question nodes	134	12.6	1681			
branching nodes	65	15.2	985	65	15.2	985
total	237	13.4	3187	119	10.8	1282

5 Discussion

One of the important questions to discuss is the generalizability of the proposed method. It was initially created to lower the workload of generating pedagogical questions and relevant explanations for subject domains described by Thought Process Trees. However, the basic patterns of natural languages, utilized in the proposed method, can be used in other contexts.

For example, the Thought Process Language model (see [15]) lends itself well to such an integration. TPL already employs templates connected to formal language constructs for the generation of natural-language textual explanations;

however, the approach is not described in detail, and it seems to have similar limitations to the first version of Thought Process Tree natural-language generation, that is, the rigidity of templates and their inability to substitute names of domain-specific entities. As such, TPL-based systems can also benefit from adapting the proposed approach to lower the workload of creating templates and allow for question-based dialogue (currently, it only supports explanatory monologue).

Other systems can also benefit from that approach. For example, the question system in Jeliot 3 [14], in which the questions provided to the students are manually entered by teachers, can be improved using that method. Jeliot uses Java code as both the model and the subject of study, so the automatic question generation can be implemented there by assigning templates to Java expressions and classes (matching node expressions and domain-specific entities in our work, respectively).

Systems using the Knowledge Construction Dialogues framework [1,5,10] can also benefit from the reduced workload that our method provides because they rely heavily on the domain expert to provide both formulations and structure of the dialogue. However, those systems do not use any kind of formal model to describe the process by which the questions are asked; the templates must be not only created but also used by the question authors manually. The question of applying the proposed method to other systems requires further research.

6 Conclusion

In this study, we proposed a method to reduce the workload of creating natural-language templates for generating pedagogical questions, answer options for them and explanations of wrong answers required to construct an ITS capable of having a question-based dialogue with the student. The previous approach required specifying natural language templates for each node of a Thought Process Tree describing the problem-solving reasoning separately, which resulted in the domain expert needing to write many similar texts.

We proposed a method that allows attributing the text templates to domain elements like object classes, properties and their relationships, and generating descriptions based on the expressions contained in the nodes. By recognizing the patterns within these expressions, we were able to classify nodes based on the natural-language patterns required to describe them and use that classification for question generation. The placeholders inside the templates are substituted with the descriptions of the domain elements used in the expression.

That allowed us to significantly reduce both the number of templates and the average template length, making the system of templates more modular to allow for template reuse, while still maintaining the possibility for the expert to create more nuanced, higher-level templates if they so choose.

There are several ways this approach can be further improved. The directions of further research include identifying more expression patterns to describe; choosing the appropriate language pattern for question formulation based on the

question type and property (relationship) description (e.g., if the main word in the description is a noun or a verb) and so on. It is also important to extend this approach to the structural nodes of Thought Process Trees: Branching Nodes and Loop Nodes.

References

1. Albacete, P., Jordan, P., Katz, S.: Is a dialogue-based tutoring system that emulates helpful co-constructed relations during human tutoring effective? In: Conati, C., Heffernan, N., Mitrovic, A., Verdejo, M.F. (eds.) AIED 2015. LNCS (LNAI), vol. 9112, pp. 3–12. Springer, Cham (2015). https://doi.org/10.1007/978-3-319-19773-9_1
2. Aleven, V., McLaren, B.M., Sewall, J., Koedinger, K.R.: The cognitive tutor authoring tools (CTAT): preliminary evaluation of efficiency gains. In: Ikeda, M., Ashley, K.D., Chan, T.-W. (eds.) ITS 2006. LNCS, vol. 4053, pp. 61–70. Springer, Heidelberg (2006). https://doi.org/10.1007/11774303_7
3. Anderson, R.C., Biddle, W.B.: On asking people questions about what they are reading. In: Bower, G.H. (ed.) Psychology of Learning and Motivation, vol. 9, pp. 89–132. Academic Press (1975). https://doi.org/10.1016/S0079-7421(08)60269-8
4. Belland, B.R.: Scaffolding: definition, current debates, and future directions. In: Spector, J.M., Merrill, M.D., Elen, J., Bishop, M.J. (eds.) Handbook of Research on Educational Communications and Technology, pp. 505–518. Springer, New York (2014). https://doi.org/10.1007/978-1-4614-3185-5_39
5. Freedman, R., Rosé, C.P., Ringenberg, M.A., VanLehn, K.: ITS tools for natural language dialogue: a domain-independent parser and planner. In: Gauthier, G., Frasson, C., VanLehn, K. (eds.) ITS 2000. LNCS, vol. 1839, pp. 433–442. Springer, Heidelberg (2000). https://doi.org/10.1007/3-540-45108-0_47
6. Ge, X., Land, S.: Scaffolding students' problem-solving processes in an ill-structured task using question prompts and peer interactions. Educ. Technol. Res. Dev. **51**, 21–38 (2003). https://doi.org/10.1007/BF02504515
7. Gruppen, L., Irby, D.M., Durning, S.J., Maggio, L.A.: Interventions designed to improve the learning environment in the health professions: a scoping review. MedEdPublish **7**, 211 (2018). https://doi.org/10.15694/mep.2018.0000211.1
8. Hughes, J.: The deskilling of teaching and the case for intelligent tutoring systems. J. Ethics Emerg. Technol. **31**(2), 1–16 (2021). https://doi.org/10.55613/jeet.v31i2.90
9. Koedinger, K., Anderson, J., Hadley, W., Mark, M.: Intelligent tutoring goes to school in the big city. Int. J. Artif. Intell. Educ. **8**, 30–43 (1997)
10. Lane, H.C., VanLehn, K.: Teaching the tacit knowledge of programming to novices with natural language tutoring. Comput. Sci. Educ. **15**(3), 183–201 (2005). https://doi.org/10.1080/08993400500224286
11. Le, N.-T., Kojiri, T., Pinkwart, N.: Automatic question generation for educational applications – the state of art. In: van Do, T., Thi, H.A.L., Nguyen, N.T. (eds.) Advanced Computational Methods for Knowledge Engineering. AISC, vol. 282, pp. 325–338. Springer, Cham (2014). https://doi.org/10.1007/978-3-319-06569-4_24
12. Mazidi, K., Tarau, P.: Automatic question generation: from NLU to NLG. In: Micarelli, A., Stamper, J., Panourgia, K. (eds.) ITS 2016. LNCS, vol. 9684, pp. 23–33. Springer, Cham (2016). https://doi.org/10.1007/978-3-319-39583-8_3

13. Moreno, A., Myller, N., Sutinen, E., Ben-Ari, M.: Visualizing programs with jeliot 3. In: Proceedings of the Working Conference on Advanced Visual Interfaces, AVI 2004, pp. 373–376. Association for Computing Machinery, New York (2004). https://doi.org/10.1145/989863.989928
14. Myller, N.: Automatic generation of prediction questions during program visualization. Electron. Notes Theor. Comput. Sci. **178**, 43–49 (2007). https://doi.org/10.1016/j.entcs.2007.01.034
15. O'Rourke, E., Andersen, E., Gulwani, S., Popović, Z.: A framework for automatically generating interactive instructional scaffolding. In: Proceedings of the 33rd Annual ACM Conference on Human Factors in Computing Systems, CHI 2015, pp. 1545–1554. Association for Computing Machinery, New York (2015). https://doi.org/10.1145/2702123.2702580
16. Peverly, S.T., Wood, R.: The effects of adjunct questions and feedback on improving the reading comprehension skills of learning-disabled adolescents. Contemp. Educ. Psychol. **26**(1), 25–43 (2001). https://doi.org/10.1006/ceps.1999.1025
17. Rothkopf, E.Z.: Learning from written instructive materials: an exploration of the control of inspection behavior by test-like events. Am. Educ. Res. J. **3**(4), 241–249 (1966). https://doi.org/10.3102/00028312003004241
18. Shah, R., Shah, D., Kurup, L.: Automatic question generation for intelligent tutoring systems. In: 2017 2nd International Conference on Communication Systems, Computing and IT Applications (CSCITA), pp. 127–132 (2017). https://doi.org/10.1109/CSCITA.2017.8066538
19. Sychev, O., Gumerov, M.: Generating pedagogical questions to help students learn. In: Frasson, C., Mylonas, P., Troussas, C. (eds.) Augmented Intelligence and Intelligent Tutoring Systems, pp. 195–208. Springer, Cham (2023). https://doi.org/10.1007/978-3-031-32883-1_17
20. Sychev., O., Penskoy., N., Terekhov., G.: Using software reasoning to determine domain-law violations and provide explanatory feedback: expressions tutor example. In: Proceedings of the 14th International Conference on Computer Supported Education, vol. 1: CSEDU, pp. 116–123. INSTICC, SciTePress (2022). https://doi.org/10.5220/0011070100003182
21. Uglev, V., Sychev, O.: Synthesizing didactic explanatory texts in intelligent tutoring systems based on the information in cognitive maps. In: Augmented Intelligence and Intelligent Tutoring Systems, pp. 233–246. Springer, Cham (2023). https://doi.org/10.1007/978-3-031-32883-1_20
22. VanLehn, K., Graesser, A.C., Jackson, G.T., Jordan, P., Olney, A., Rosé, C.P.: When are tutorial dialogues more effective than reading? Cogn. Sci. **31**(1), 3–62 (2007). https://doi.org/10.1080/03640210709336984
23. Wise, A.F.: Designing pedagogical interventions to support student use of learning analytics. In: Proceedings of the Fourth International Conference on Learning Analytics and Knowledge, LAK 2014, pp. 203–211. Association for Computing Machinery, New York (2014). https://doi.org/10.1145/2567574.2567588

Cyber Intelligence and Applications (CIA 2024)

An Android Malware Multi-class Classification Explained Through Genetic Programming

Gianni D'Angelo, Francesco Palmieri, and Antonio Robustelli(✉)

Department of Computer Science, University of Salerno, Fisciano, Italy
{giadangelo,fpalmieri,arobustelli}@unisa.it

Abstract. The interest in applying Artificial Intelligence algorithms within security contexts is rapidly growing, particularly for the tasks related to malware detection and classification. Over the last decade, numerous Machine Learning (ML) and Deep Learning (DL)-based techniques have been proposed to address the growth of malicious applications, focusing on utilizing features derived from dynamic malware analysis. However, these approaches are often considered black boxes due to their limited ability to explain the results they produce. On the contrary, this study seeks to develop a new model for identifying malware families in an interpretable manner. The methodology employs Genetic Programming to construct a multi-class classifier characterized by a mathematical formula expressing the relationship between dynamic features and the considered malware families. Experimental results, based on Android applications from Unisa Malware Dataset (UMD), showcase the effectiveness of our approach in achieving comparable average scores to the most famous Machine Learning techniques.

Keywords: Android Malware · Explainable Classification · Genetic Programming · Artificial Intelligence · API-Calls

1 Introduction

Due to their popularity, Android OS-based devices have attracted billions of end-users around the World, becoming one of the main targets for malware threats. Indeed, as highlighted by famous cybersecurity companies, unprotected devices (e.g. smartphones, tablets, smart TVs, and wearable devices) represent one of the principal targets on which to perform several malicious activities, such as stealing sensitive information and launching cyberattacks. For instance, according to the last McAfee Mobile Threat Reports [25,26], cyber-criminals increased the effectiveness of their activities with the support of a wide variety of methods, such as back-doors and fake cryptocurrencies. Consequently, the number of malicious applications has drastically increased, reaching 40 million in 2020 and growing by at least 4 million yearly.

© The Author(s), under exclusive license to Springer Nature Switzerland AG 2024
O. Gervasi et al. (Eds.): ICCSA 2024 Workshops, LNCS 14816, pp. 53–70, 2024.
https://doi.org/10.1007/978-3-031-65223-3_4

Therefore, on the basis of these outcomes [30], the interest in Artificial Intelligence algorithms has rapidly grown, especially for detection and classification purposes. As is known, in the last decade, many Machine Learning (ML) and Deep Learning (DL)-based techniques have been proposed to counteract the exponential growth of malicious applications by leveraging features coming from both static and dynamic analysis [23,24,32]. In detail, static-based approaches can extract relevant features and signatures without executing applications but, instead, by performing several reverse engineering operations [29,34].

However, such static approaches can be strongly affected by obfuscation tools. Also, they become ineffective against most existing malware capable of evading pattern-matching detection mechanisms, namely metamorphic and polymorphic ones [18]. For this reason, dynamic analysis-based solutions are widely employed to analyze the behavior of an application during its execution and collect different features, such as system parameters and API-Calls [10]. Moreover, in order to capture more significant and relevant insights, dynamic features have been leveraged to face malware detection as corresponding image classification tasks [6,28]. For instance, D'Angelo et al. [4] proposed a sparse matrix representation of API-Calls sequences. More precisely, they demonstrated the effectiveness of the proposed API-Images by obtaining an average accuracy of 95% in performing a binary classification task.

Nevertheless, similar to other mainstream AI methodologies, Deep Learning (DL)-based approaches tend to lack transparency because they do not reveal the underlying processes behind the provided outputs. For this reason, the issue of interpretability has become increasingly significant, giving rise to two emerging research areas: Explainable Artificial Intelligence (XAI) [8] and Interpretable Machine Learning (IML) [28]. In this context, Genetic Programming (GP) stands out as a promising solution for XAI, offering the unique ability to 'explain' outputs by providing a mathematical formula. As a result, GP has proven effective in numerous application domains, with a particular focus on health care [2,7]. Of course, GP has also been employed to face several malware classification tasks [17], but a multi-class model has yet to be proposed in the literature.

In this work, intending to improve the explainability of malware classification, we propose a GP-based model capable of spotting different malware families using dynamic features. To this end, we employ Genetic Programming to provide a mathematical formula expressing the relationship between the previously mentioned API-Images and predicted families. More specifically, we combine the derived formula with the threshold concept in order to gain a powerful multi-class classifier.

The main contributions of this work can be summarized as follows:

1. A malware multi-class classifier, which combines GP with the threshold concept, is proposed and compared with the most famous ML-based techniques.
2. A mathematical formula describing the relationship between API-Images and predicted families is provided to improve the explainability behind the classification process.

The remainder of the paper is organized as follows. Section 2 will present the related works on malware classification. Section 3 will report the background concepts related to the proposed approach, namely the API-Images and the symbolic regression process. Then, Sect. 4 will describe the proposed GP-based classifier by including the threshold concept. Finally, Sect. 5 will report the experimental results, while Sect. 6 will show the conclusions and future work.

2 Related Works

Nowadays, many detection frameworks and methodologies based on static and dynamic analysis have been proposed [23,24,32] to counter the continuous diffusion of malware. In detail, static-based approaches can extract useful features (e.g. signatures) without executing the analyzed applications. To this end, such approaches disassemble the applications by performing several reverse engineering operations. For instance, Zhang et al. [34] proposed a semantic-based approach using dependency graphs created from the application code. Instead, Onwuzurike et al. [29] presented MaMaDROID, a malware detection system that finds the sequences of methods potentially invoked and maps them to their corresponding packages and classes.

However, static approaches can be strongly affected by obfuscation tools. Also, they become ineffective against most existing malware capable of evading pattern-matching detection mechanisms, namely metamorphic and polymorphic ones [18]. Therefore, in order to overcome these issues, several dynamic analysis-based solutions have been proposed to analyze the behavior of an application and consider several related aspects, such as parameter monitoring and API-Calls tracing [10,13]. For instance, Kolosnjaji et al. [19] leveraged the capability of Deep Neural Networks (DNNs) to analyze the sequence of system calls extracted during the app's execution. To accomplish this, they combined convolutional and recurrent layers by obtaining an average accuracy of 89.0% on 10 Android malware families. Instead, Ficco [12] analyzed the effectiveness of several Machine Learning (ML)-based classifiers in spotting benign and malicious applications using Markov chains. To this end, they arranged API-Call sequences as a graph summarizing the execution flow. The experimental results, obtained by collecting 22K benign and 24K malware applications, have shown an average accuracy of 89%. Next, D'Angelo et al. [3,5] have improved this Markov chains-based approach by employing associative rules (i.e. pairs of API-Calls) as corresponding nodes in the related graphs. The achieved results, derived by considering a federated scenario with non-Independent and Identically Distributed (non-IID) data, have proven the effectiveness of the proposed approach in classifying several malware families with an average accuracy of 99%.

Moreover, in order to capture more significant and relevant insights, dynamic features have been leveraged to face malware detection as corresponding image classification tasks [6,28]. For instance, Abderrahmane et al. [1] proposed a CNN to perform the malware analysis by considering a matrix representation of system calls. The obtained results, with the aid of an unbalanced dataset, have shown

an average accuracy of 93.3%. Next, D'Angelo et al. [4] have improved this representation technique by considering the API-Calls sequences. More precisely, they demonstrated the effectiveness of their approach, called API-Images, by obtaining an average accuracy of 95% in performing a binary classification task through Sparse Autoencoders (SAEs).

Nevertheless, despite the satisfactory accuracy demonstrated in these studies, the proposed methodologies often lack the transparency needed to comprehend the processes generating the provided outputs. For this reason, recent advances in AI have shifted their focus towards models falling under the Explainable Artificial Intelligence (XAI) category. A promising avenue in implementing XAI is Genetic Programming (GP), known for its ability to provide a mathematical formula explaining the rationale behind a given output. Consequently, GP has proven effective in several application domains, with a particular emphasis on healthcare [2,7]. Of course, GP has also been employed to face several malware classification tasks [17], but a multi-class model has yet to be proposed in the literature. In detail, Le et al. [22] employed GP as a pure binary malware classifier. The experimental results, derived from 800 malicious and 1600 benign applications, have shown an average accuracy of 93%. Instead, Harahsheh et al. [16] proposed a GP-based feature section technique. To this end, they analyzed the effectiveness of this approach by considering different famous classifiers and other feature selection techniques. The best experimental results, achieved by the Random Forest algorithm, have shown an average accuracy of 97%.

Therefore, with the aim to enhance the explainability of malware classification, this study combines the effectiveness of Genetic Programming with a multi-class threshold concept to establish an explainable correlation between API-Images and several Android malware families.

3 Background

This Section briefly describes the preliminary concepts employed for our classification purposes. For this reason, we recall the definition of API-Images and the related workflow. Then, we report some information about the Symbolic Regression (SR), which represents the core activity performed by GP.

3.1 API-Images

API-Images are a set of sparse matrices proposed by D'Angelo et al. [4], whose peculiarity is to represent the dynamic behavior of analyzed applications. In detail, given a sequence of API-Calls, an API-Image can be built through the following two main steps:

1. Identification of each API-Call with a unique ID.
2. Matrix creation through consecutive pairs of API-Calls.

The first step can be accomplished using a dictionary in which a numeric ID is assigned to each API-Call. Then, from the traced API-Calls sequence, every

two consecutive calls can be used as coordinates to build the related API-Image matrix. Hence, each pair of API-Calls is employed to draw a fixed point in the API-Image. For instance, let a_1, a_2, and a_3 be three APIs where a_2 is called after a_1 and a_3 is called after a_2. On the basis of the described process, we can consider only two pairs of coordinates, $P1 = (a_1, a_2)$ and $P2 = (a_2, a_3)$, respectively. Also, since an application may invoke different times the same API-Calls sequence, some pairs can occur more than once. This situation can be managed through different colour scales (e.g. RGB or Gray-scale) in which each colour represents a frequency. Figure 1 summarizes the workflow to generate an API-Image.

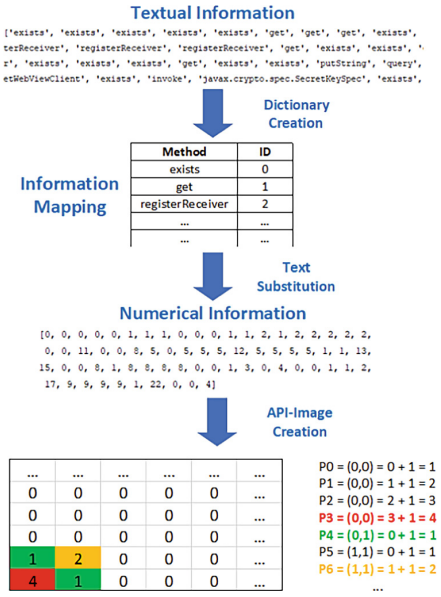

Fig. 1. The workflow to obtain an API-Image [15].

3.2 Symbolic Regression in Genetic Programming

Symbolic Regression (SR) is a well-established method for uncovering the optimal mathematical expression that best fits a multivariate dataset. The core rationale behind adopting SR lies in its ability to produce an interpretable model, which diverges from classic AI approaches operating as black boxes. In the last decades, SR has witnessed increased utilization through the Evolutionary Algorithms (EAs) [9,11]. These algorithms, inspired by Darwinian Theory, excel in generating a set of candidate solutions. Each solution represents a population, with its members also known as individuals. Consequently, the primary objective of an EA is to iteratively navigate through populations to identify the best individual or the optimal solution.

The concept of applying Symbolic Regression (SR) through Evolutionary Algorithms (EAs) was introduced by John Koza, who employed a Genetic Algorithm (GA) [27] in a methodology known as Genetic Programming (GP) [21]. Similar to EAs, GP involves multiple individuals forming a population. In detail, each individual corresponds to a mathematical function represented by a tree structure where leaves represent operands, while other nodes represent mathematical operations. The effectiveness of each individual, computed across all dataset entries, undergoes evaluation through a fitness function that measures the error between the expected outcome and the predicted one.

4 The Employed GP-Based Classifier

As previously mentioned, this work aims to provide an explainable malware classification. To this end, we employ Genetic Programming to derive a mathematical formula describing the relationship between API-Images and the considered malware families. Indeed, differently from other mainstream AI methodologies, Genetic Programming provides an explainable, transparent, and intuitive solution, making the reasoning behind the model's decisions more accessible. Moreover, although Genetic Programming has been employed to face several malware classification tasks [17], no effective multi-class models have been proposed in the literature. Therefore, leveraging the API-Images' capabilities in representing the dynamic behavior of applications, this Section shows how to implement the mathematical formula derived by GP as an effective multi-class classifier. In detail, to better appreciate the provided formulation, we first describe how to build the classifier to face a binary classification task. Next, we extend the provided formulation for a multi-class scenario.

Accordingly, let X^n be the set of one-dimensional API-Images and let C be the set of corresponding output classes, the proposed GP-based classifier aims to provide a function $f^* : X^n \rightarrow C$, which represent the best mathematical formula describing the relationship between input/output pairs of a training dataset S. Notice that $S = (X^n \cup C)$, that is any item of S includes input parameters $(x_i \in X^n)$ and its corresponding class $(c_i \in C)$.

For a binary classification task, the problem to solve can be formally defined as follows:

$$f^* = arg\ min_{f \in F}\ \ \{\mathcal{D}(f(x_i), c_i)\}\ \ \forall (x_i, c_i) \in S \tag{1}$$

where F is the set of all admissible functions, c_i is the ground truth (i.e., the considered malware family), and $\mathcal{D}$ is a distance metric expressing the discrepancy between the predicted and expected outcomes, which can be defined as follows:

$$\mathcal{D} = \frac{1}{|S|} \sum_{(x_i, c_i) \in S} P(x_i, c_i) \tag{2}$$

where

$$P(x_i, c_i) = \begin{cases} 1, f(x_i) = c_i \\ 0, f(x_i) \neq c_i \end{cases} \tag{3}$$

Nevertheless, since the GP-derived mathematical formula yields numerical outputs, certain assumptions are necessary for implementing the classifier effectively. First, the expected output values must be changed into two class values (e.g. 0 and 1). This approach enables GP to discover a formula that fits all numeric inputs to the corresponding output values.

Second, since for an arbitrary input vector x_i the resulting output may not precisely correspond to the expected output class, the concept of a threshold is frequently employed to overcome this issue. More specifically, for a given formula, f, the associated threshold, T_f, is determined as the point of maximum separation among the predicted outcomes of f^* across the entire testing dataset. In detail, a threshold value discretizes the search space into two distinct areas, each representing a specific class. Next, the classification of an input sample is determined by assessing the area in which the provided output falls.

Generally, the selection of the threshold value aims to maximize specific evaluation metrics, such as F-Score or AUC (See Eqs. 10 and 11 below). As expressed in Eq. 4, for a given input vector x_i, if the outcome of the formula $f^*(x_i)$ greater than T_{f^*}, the vector belongs to Class 1; otherwise, it belongs to Class 0.

$$Class = \begin{cases} 1, f^*(x_i) > T_{f^*} \\ 0, f^*(x_i) \leq T_{f^*} \end{cases} \tag{4}$$

Once the definition of the binary classifier is provided, we can derive the related multi-class one by extending the assumptions discussed above with m classes ($m > 2$). To this end, the concept of multiple threshold values is employed. More specifically, let m be the number of classes belonging to C and let $\mathcal{T} = \{T^1_{f^*}, T^2_{f^*}, ..., T^{m-1}_{f^*}\}$ be the set of derived threshold values, then the outcome provided by f^* can be assigned to the related class as follows:

$$Class = \begin{cases} c_{m-1}, f^*(x_i) > T^{m-1}_{f^*} \\ \vdots \\ c_1, T^1_{f^*} < f^*(x_i) \leq T^2_{f^*} \\ c_0, f^*(x_i) \leq T^1_{f^*} \end{cases} \tag{5}$$

5 Experimental Results

This Section aims to demonstrate the effectiveness of the GP-based classifier in recognizing malware categories starting from API-Images. To accomplish this,

we first perform a preliminary study to analyze the capabilities of the most notable ML-based techniques in spotting several malware families. Then, we prove the effectiveness of Genetic Programming by comparing its results with those derived from the preliminary study. Finally, in order to explain the correlation between API-Images and the given category, we provide the mathematical formula describing the employed classifier. All the experiments were conducted by using a MacBook Pro equipped with an Apple M1 CPU and 16 GB of unified memory.

5.1 Dataset and Pre-processing

The dataset used in the following experiments was derived by the Unisa Malware Dataset (UMD) [15]. In detail, we considered 1403 malware applications belonging to 4 notable Android families: Anydown (Class 0), BaseBridge (Class 1), FakeDoc (Class 2), and Opfake (Class 3).

First, we performed an Exploratory Data Analysis (EDA) [20] to accurately study the malware distribution in relationship to the considered classes. As shown in Table 1, the following analysis has counted 326 applications for Anydown, 313 for BaseBridge, 149 for FakeDoc, and 615 for Opfake.

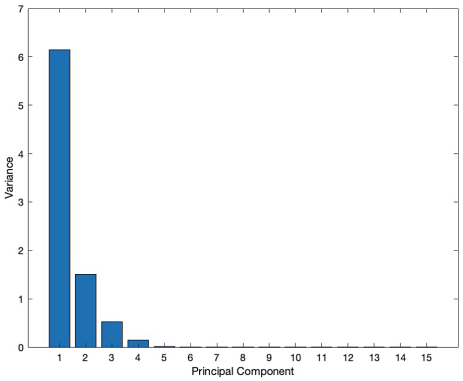

Fig. 2. The distribution of principal components according to their eigenvalues.

Next, by following the workflow shown in Fig. 1, we transformed each sequence of API-Calls into a corresponding API-Image (70×70). For the sake of clarity, since no image classification task is faced, we did not consider a particular colour scale. Instead, due to the unbalanced nature of the employed dataset, we scaled each API-Image for the total number of applications belonging to the related family. Then, we arranged API-Images in a corresponding one-dimensional space of 4900 features.

However, due to the high dimensions of the resulting vectors, we performed an additional dimensionality reduction step by using the Principal Compo-

nent Analysis (PCA) [14]. Hence, we mapped each flattened image in a one-dimensional space of 10 features by also applying a subsequent data standardization with $\mu = 0$ and $\sigma = 1$. In detail, to better choose the output dimensions, we considered the rank of principal components according to their eigenvalues (See Fig. 2). Notice that we conducted the entire data pre-processing phase using several dedicated Python scripts on the whole dataset.

Finally, as shown in Table 1, we have split the resulting dataset with the 70/30 criterion. Therefore, for each family, we employed the 70% for training and the remaining 30% for testing.

Table 1. An overview of the employed dataset splitted with the 70/30 criterion.

	Training	Testing	Total
Anydown	228	98	326
BaseBridge	218	95	313
Fakedoc	104	45	149
Opfake	431	184	615
Total	981	422	1403

5.2 Evaluation Metrics

To appreciate the classification quality of the employed models, we used the following evaluation metrics derived from the confusion matrix for a multi-class classifier: Accuracy (Acc.), Sensitivity (Sens.), Specificity (Spec.), Precision (Prec.), F-Score (F-Mea.), and Area Under the ROC Curve (AUC).

$$Accuracy = \frac{TP + TN}{TP + TN + FP + FN} \tag{6}$$

$$Sensitivity = \frac{TP}{TP + FN} \tag{7}$$

$$Specificity = \frac{TN}{TN + FP} \tag{8}$$

$$Precision = \frac{TP}{TP + FP} \tag{9}$$

$$F - Score = \frac{2 * Sens * Prec}{Sens + Prec} \tag{10}$$

$$AUC = \frac{Sens + Spec}{2} \tag{11}$$

For each category, TPs (True Positives) refer to the applications correctly classified, while TNs (True Negatives) refer to the applications correctly identified in another category. Instead, FPs (False Positives) are the applications

mistakenly identified as the considered category, while FNs (False Negatives) are the applications mistakenly identified in another category. Also, to provide a global perspective of the employed models, the average performance values (Avg.) among all the considered malware classes have been derived.

5.3 Preliminary Results

To compare the effectiveness of the proposed classifier, we have first analyzed the capabilities of the most notable ML-based techniques in classifying the considered malware families. To this end, we used some famous algorithms provided by WEKA [33], namely Naive Bayes (NB) classifier, Logistic Regression (LOG), Multi-Layer Perceptron classifier (MLP), Support Vector Machine (SMO), J48 Decision Trees (J48), and Random Forest (RF) algorithm. Tables 2, 3, 4, 5, 6, and 7 report the testing results related to each ML-based technique, respectively. Instead, Table 8 compares the average (Avg.) results.

Table 2. Results achieved by Naive Bayes classifier (NB).

	Acc.	Sens.	Spec.	Prec.	F-Mea.	AUC
Anydown	0.9521	0.9540	0.9516	0.8469	0.8973	0.9528
BaseB	0.9175	0.8861	0.9249	0.7368	0.8046	0.9055
FakeDoc	0.9869	1.0000	0.9852	0.9000	0.9474	0.9926
Opfake	0.9265	0.9783	0.8839	0.8738	0.9231	0.9311
Avg.	0.9458	0.9546	0.9364	0.8394	0.8931	0.9455

Table 3. Results achieved by Logistic Regression (LOG).

	Acc.	Sens.	Spec.	Prec.	F-Mea.	AUC
Anydown	0.9855	0.9894	0.9844	0.9490	0.9688	0.9869
BaseB	0.9714	0.9053	0.9908	0.9663	0.9348	0.9480
FakeDoc	1.0000	1.0000	1.0000	1.0000	1.0000	1.0000
Opfake	0.9761	0.9485	1.0000	1.0000	0.9735	0.9742
Avg	0.9833	0.9608	0.9938	0.9788	0.9693	0.9773

As shown in Table 8, the Random Forest (RF) algorithm, the Logistic regression (LOG), and Decision Trees (J48) achieved the best results with a 98% average accuracy. In detail, they outperformed Multi-Layer Perceptron (MLP) by 1%, Naive Bayes (NB) by 4%, and Support Vector Machine (SMO) by 5%, respectively. Furthermore, it is also possible to appreciate the peculiarity of such models to have a discrete number of false positives and false negatives. This, in

Table 4. Results achieved by Multi-Layer Perceptron classifier (MLP).

	Acc.	Sens.	Spec.	Prec.	F-Mea.	AUC
Anydown	0.9733	0.9307	0.9871	0.9592	0.9447	0.9589
BaseB	0.9548	0.9750	0.9500	0.8211	0.8914	0.9625
FakeDoc	1.0000	1.0000	1.0000	1.0000	1.0000	1.0000
Opfake	0.9709	0.9388	1.0000	1.0000	0.9684	0.9694
Avg.	0.9748	0.9611	0.9843	0.9451	0.9511	0.9727

Table 5. Results achieved by Support Vector Machine (SMO).

	Acc.	Sens.	Spec.	Prec.	F-Mea.	AUC
Anydown	0.9510	0.9877	0.9414	0.8163	0.8939	0.9645
BaseB	0.9134	1.0000	0.8983	0.6316	0.7742	0.9491
FakeDoc	1.0000	1.0000	1.0000	1.0000	1.0000	1.0000
Opfake	0.8765	0.7797	1.0000	1.0000	0.8762	0.8898
Avg.	0.9352	0.9418	0.9599	0.8620	0.8861	0.9509

Table 6. Results achieved by J48 Decision Trees (J48).

	Acc.	Sens.	Spec.	Prec.	F-Mea.	AUC
Anydown	0.9808	0.9588	0.9875	0.9588	0.9588	0.9731
BaseB	0.9737	0.9468	0.9815	0.9368	0.9418	0.9642
FakeDoc	0.9976	1.0000	0.9973	0.9778	0.9888	0.9986
Opfake	0.9855	0.9785	0.9912	0.9891	0.9838	0.9849
Avg.	0.9844	0.9710	0.9894	0.9656	0.9683	0.9802

Table 7. Results achieved by Random Forest algorithm (RF).

	Acc.	Sens.	Spec.	Prec.	F-Mea.	AUC
Anydown	0.9881	0.9697	0.9938	0.9796	0.9746	0.9817
BaseB	0.9834	0.9889	0.9819	0.9368	0.9622	0.9854
FakeDoc	1.0000	1.0000	1.0000	1.0000	1.0000	1.0000
Opfake	0.9857	0.9684	1.0000	1.0000	0.9840	0.9842
Avg.	0.9893	0.9818	0.9939	0.9791	0.9802	0.9878

fact, is highlighted by the obtained F-Score values, which range from 88% to 98%.

However, as discussed in Sect. 2, the considered ML-based techniques do not explain why they generate a particular result (i.e., the predicted class) [2]. Consequently, in order to improve the model explainability, we investigated the

Table 8. A summarize of the average results of the most notable ML-based techniques powered by WEKA tool.

	Acc.	Sens.	Spec.	Prec.	F-Mea.	AUC
RF	0.9893	0.9818	0.9939	0.9791	0.9802	0.9878
LOG	0.9833	0.9608	0.9938	0.9788	0.9693	0.9773
J48	0.9844	0.9710	0.9894	0.9656	0.9683	0.9802
MLP	0.9748	0.9611	0.9843	0.9451	0.9511	0.9727
NB	0.9458	0.9546	0.9364	0.8394	0.8931	0.9455
SMO	0.9352	0.9418	0.9599	0.8620	0.8861	0.9509

effectiveness of a GP-based classifier in correlating the considered API-Images with the given output (i.e., the prediction of a class for an arbitrary malware application).

5.4 GP-Based Classifier and Results

To implement the proposed GP-based classifier, we used a MATLAB library for symbolic data mining, namely GPTIPS (Genetic Programming Toolbox for the Identification of Physical Systems) [31]. It is a variant of the GP approach that employs the Multi-Gene-based Genetic Programming (MGGP) algorithm to derive the mathematical formula. In detail, MGGP performs the symbolic scaling regression, whose peculiarity is capturing the behavior of individuals more effectively than the classic SR discussed in Sect. 3.

Therefore, in our experiments, we implemented the GP-classifier by varying different hyper-parameters. For the sake of clarity, only the set-up that provided the best results is shown below:

- pop_size: the dimension of considered population = 100;
- $runs$: the number of algorithm iterations = 100;
- num_gen: the number of generations at each iteration = 35;
- $tournament.size$: the size of tournament selection criteria = 9;
- max_depth: the max depth of solution trees = 11;
- $bias$: the range of bias values $[-10; 10]$;
- $functions$: the considered arithmetic operators $[\times, -, +, /, sqrt, exp]$.

Table 9 reports the results obtained by the GP-based classifier on the whole testing set, while Table 10 compares average results with those derived from the preliminary study (i.e., the ML-based techniques provided by WEKA).

Table 9. Results achieved by GP-based classifier.

	Acc.	Sens.	Spec.	Prec.	F-Mea.	AUC
Anydown	0.9579	0.9765	0.9530	0.8469	0.9071	0.9647
BaseB	0.9281	0.8495	0.9506	0.8316	0.8404	0.9000
FakeDoc	0.9847	0.9333	0.9914	0.9333	0.9333	0.9624
Opfake	0.9579	0.9196	0.9951	0.9946	0.9556	0.9574
Avg.	0.9572	0.9197	0.9725	0.9016	0.9091	0.9461

Table 10. Comparison among the GP classifier and ML-based techniques.

	Acc.	Sens.	Spec.	Prec.	F-Mea.	AUC
RF	0.9893	0.9818	0.9939	0.9791	0.9802	0.9878
LOG	0.9833	0.9608	0.9938	0.9788	0.9693	0.9773
J48	0.9844	0.9710	0.9894	0.9656	0.9683	0.9802
MLP	0.9748	0.9611	0.9843	0.9451	0.9511	0.9727
GP	0.9572	0.9197	0.9725	0.9016	0.9091	0.9461
NB	0.9458	0.9546	0.9364	0.8394	0.8931	0.9455
SMO	0.9352	0.9418	0.9599	0.8620	0.8861	0.9509

As shown in Table 10, all the metrics achieved comparable scores with those derived by ML-based techniques provided by WEKA. In detail, with an average accuracy of 95%, the employed GP-based classifier obtained a 1% more on Naive Bayes and a 2% on Support Vector Machine (SMO). On the contrary, our approach has achieved a 2% less on the Multi-Layer Perceptron (MLP) and a 3% on Decision Trees (J48) and Random Forest (RF) algorithm. Consequently, this confirms the effectiveness of the GP-based classifier in spotting multiple malware families.

5.5 Formula Extraction and Explainability

Despite the confirmed effectiveness of the GP-based classifier in the preceding experiments, notice that our proposal distinguishes itself for its ability to present a mathematical formula expressing the connection between API-Images and the given category. To this end, we derived f^* by running the MGGP algorithm on the whole training dataset.

The outcome is represented by the following equations:

$$f^* = Z_1 + Z_2 + Z_3 \tag{12}$$

$$Z_1 = 0.3431 \cdot x_3 + 0.3431 \cdot x_4 + 0.02946 \cdot x_5 + 0.1568 \cdot x_6 \tag{13}$$

$$Z_2 = -0.07404 \cdot x_9 - x_4 \cdot e^{exp(exp(x_4) - (3 \cdot x_5 - 2 \cdot x_3 + exp(x_4))^4)} \cdot 0.6738 \tag{14}$$

$$Z_3 = \frac{0.07404 \cdot x_1}{2 \cdot x_3 - 3 \cdot x_5} + 0.8997 \tag{15}$$

Next, as shown in Fig. 3 and with reference to Table 4, we considered three threshold values ($T_{f^*} = 0.74$, 1.47, and 2.45) to distinguish the malware families provided by the testing dataset, that are: Anydown - Class 0, BaseBridge - Class 1, FakeDoc - Class 2, and Opfake - Class 3.

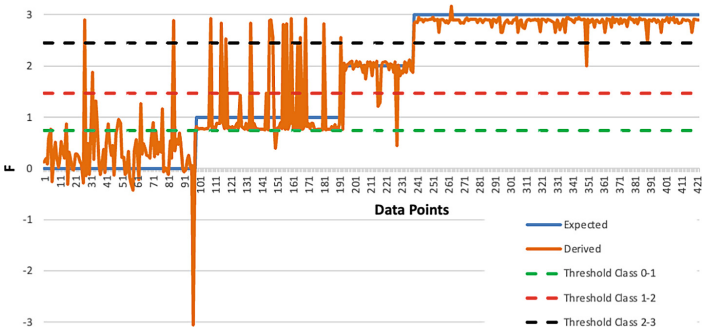

Fig. 3. Predicted vs expected classes. The threshold values are also depicted.

More formally, this means that we adapted the definition provided by Eq. 5 for the considered malware families as follows:

$$Class = \begin{cases} 3, f^*(x_i) > T^3_{f^*} \\ 2, T^2_{f^*} < f^*(x_i) \leq T^3_{f^*} \\ 1, T^1_{f^*} < f^*(x_i) \leq T^2_{f^*} \\ 0, f^*(x_i) \leq T^1_{f^*} \end{cases} \tag{16}$$

with $T^1_{f^*} = 0.74$, $T^2_{f^*} = 1.47$, and $T^3_{f^*} = 2.45$.

As depicted, the derived formula is given by the sum of three functions, namely Z_1, Z_2, and Z_3. Although the interpretation of this formula is not trivial, we highlight some helpful considerations to foster a better comprehension of the correlation between the API-Images and the predicted malware families.

Firstly, the selection of 6 out of 10 features (x_i) demonstrates that the adopted PCA decomposition has provided an effective dimensionality reduction of input images. As previously remarked, this step is fundamental to overcoming bias situations arising from the flattening process of API-Images.

Second, with reference to Fig. 3 and Table 9, it is possible to appreciate how the employed formula has correctly classified most malware applications by obtaining an accuracy score between 92% and 98%.

Finally, regarding the presence of false positives and false negatives, it is also possible to appreciate how the derived formula limits the number of applications incorrectly classified. Indeed, for 3 families out of 4, the derived formula has achieved an F-Score between 90% and 95%. Whereas, only for BaseBridge (Class 1), the number of both false positives (16) and false negatives (14) is a little bit

high. Nevertheless, such values do not adversely affect the overall validity of the provided formula and, thus, of this proposal.

Therefore, from these considerations, we can state that the derived formula can effectively explain how malware applications belong to a specific family. Consequently, its employment could offer more targeted solutions capable of mathematically justifying their results instead of performing only a simple classification task.

6 Conclusions and Future Work

In this paper, we proposed a Genetic Programming (GP)-based model to classify malware families in an explainable way. More precisely, since classic Machine Learning and Deep Learning-based approaches do not provide any information about how they generate the related outputs, we employed Genetic Programming to provide a mathematical formula expressing the relationship between malware applications and the corresponding family. To this end, we first considered a famous feature representation technique, named API-Images, to effectively arrange the dynamic behavior of applications. Then, we have shown the validity of the proposed multi-class classifier by using multiple thresholds to turn the given predictions into corresponding classes. Experimental results, based on 4 Android malware families representative of the Unisa Malware Dataset (UMD), have shown comparable scores with those derived by the most famous Machine Learning techniques. Finally, we derived the mathematical formula expressing the relationship between API-Images and the given outcomes to provide an understandable interpretation of the employed classifier.

Therefore, on the basis of the achieved outcomes, we would like to employ the GP-based approach to spot new malware families, such as those not only related to Android OS. Moreover, we will investigate the effectiveness of GP in classifying malware applications by considering static and Run-time features, which represent two highly considered parameters in malware analysis. All of this could offer several benefits for both end-users and developers, such as more targeted solutions, faster detection and mitigation, and reduction of caused damages.

Acknowledgments. This work was partially supported by project SERICS (PE00000014) under the NRRP MUR program funded by the EU - NGEU.

Author contributions. Gianni D'Angelo: Supervision, Methodology, Reviewing, and Editing.
Francesco Palmieri: Supervision, Methodology, Reviewing, and Editing
Antonio Robustelli: Conceptualization, Investigation, Software, and Writing.

Conflict of interest. The authors declare that they have no conflict of interest.

Informed Consent. Informed consent was obtained from all individual participants included in the study.

Ethical Approval. This article does not contain any studies with human participants or animals performed by any of the authors.

References

1. Abderrahmane, A., Adnane, G., Yacine, C., Khireddine, G.: Android malware detection based on system calls analysis and cnn classification. In: 2019 IEEE Wireless Communications and Networking Conference Workshop (WCNCW), pp. 1–6 (2019). https://doi.org/10.1109/WCNCW.2019.8902627
2. D'Angelo, G., Della-Morte, D., Pastore, D., Donadel, G., De Stefano, A., Palmieri, F.: Identifying patterns in multiple biomarkers to diagnose diabetic foot using an explainable genetic programming-based approach. Future Gener. Comput. Syst. **140**, 138–150 (2023). https://doi.org/10.1016/j.future.2022.10.019. https://www.sciencedirect.com/science/article/pii/S0167739X2200334X
3. D'Angelo, G., Farsimadan, E., Ficco, M., Palmieri, F., Robustelli, A.: Privacy-preserving malware detection in android-based iot devices through federated markov chains. Future Gener. Comput. Syst. **148**, 93–105 (2023). https://doi.org/10.1016/j.future.2023.05.021. https://www.sciencedirect.com/science/article/pii/S0167739X23002054
4. D'Angelo, G., Ficco, M., Palmieri, F.: Malware detection in mobile environments based on autoencoders and api-images. J. Parallel Distrib. Comput. **137**, 26–33 (2020). https://doi.org/10.1016/j.jpdc.2019.11.001. https://www.sciencedirect.com/science/article/pii/S0743731519302436
5. D'Angelo, G., Ficco, M., Palmieri, F.: Association rule-based malware classification using common subsequences of api calls. Appl. Soft Comput. **105**, 107234 (2021). https://doi.org/10.1016/j.asoc.2021.107234. https://www.sciencedirect.com/science/article/pii/S1568494621001575
6. D'Angelo, G., Palmieri, F., Robustelli, A.: Effectiveness of video-classification in android malware detection through API-streams and CNN-LSTM autoencoders. In: You, I., Kim, H., Youn, T.-Y., Palmieri, F., Kotenko, I. (eds.) MobiSec 2021. CCIS, vol. 1544, pp. 171–194. Springer, Singapore (2022). https://doi.org/10.1007/978-981-16-9576-6_13
7. D'Angelo, G., Scoppettuolo, M.N., Cammarota, A.L., Rosati, A., Palmieri, F.: A genetic programming-based approach for classifying pancreatic adenocarcinoma: the SICED experience. Soft Comput. **26**(19), 10063–10074 (2022). https://doi.org/10.1007/s00500-022-07383-3
8. Došilović, F.K., Brčić, M., Hlupić, N.: Explainable artificial intelligence: a survey. In: 2018 41st International Convention on Information and Communication Technology, Electronics and Microelectronics (MIPRO), pp. 0210–0215 (2018). https://doi.org/10.23919/MIPRO.2018.8400040
9. D'Angelo, G., Palmieri, F.: A co-evolutionary genetic algorithm for robust and balanced controller placement in software-defined networks. J. Netw. Comput. Appl. **212**(C) (2023). https://doi.org/10.1016/j.jnca.2023.103583
10. Egele, M., Scholte, T., Kirda, E., Kruegel, C.: A survey on automated dynamic malware-analysis techniques and tools. ACM Comput. Surv. **44**(2) (2008). https://doi.org/10.1145/2089125.2089126
11. Elia, S., et al.: A machine learning evolutionary algorithm-based formula to assess tumor markers and predict lung cancer in cytologically negative pleural effusions. Soft Comput. **24**(10), 7281–7293 (2019). https://doi.org/10.1007/s00500-019-04344-1
12. Ficco, M.: Detecting IoT malware by Markov chain behavioral models. In: 2019 IEEE International Conference on Cloud Engineering (IC2E), pp. 229–234 (2019)

13. Ficco, M.: Malware analysis by combining multiple detectors and observation windows. IEEE Trans. Comput. **71**(6), 1276–1290 (2022). https://doi.org/10.1109/TC.2021.3082002
14. F.R.S., K.P.: Liii. on lines and planes of closest fit to systems of points in space. Lond. Edinburgh Dublin Phil. Maga. J. Sci. **2**(11), 559–572 (1901). https://doi.org/10.1080/14786440109462720
15. Gianni D'Angelo, Francesco Palmieri, A.R., Castiglione, A.: Effective classification of android malware families through dynamic features and neural networks. Connect. Sci. **33**(3), 786–801 (2021). https://doi.org/10.1080/09540091.2021.1889977
16. Harahsheh, H., Shraideh, M., Sharaeh, S.: Performance of malware detection classifier using genetic programming in feature selection. Informatica **45**(4) (2021). https://doi.org/10.31449/inf.v45i4.3819
17. Heba Harahsheh, Mohammad Alshraideh, S.A.S., Al-Sayyed, R.: Improving classification performance for malware detection using genetic programming feature selection techniques. J. Appl. Secur. Res. **18**(3), 627–647 (2023). https://doi.org/10.1080/19361610.2022.2067459
18. Hosmer, C.: Polymorphic and metamorphic malware - black hat briefings. https://www.blackhat.com/presentations/bh-usa-08/Hosmer/BH_US_08_Hosmer_Polymorphic_Malware.pdf
19. Kolosnjaji, B., Zarras, A., Webster, G., Eckert, C.: Deep learning for classification of malware system call sequences. In: Kang, B.H., Bai, Q. (eds.) AI 2016. LNCS (LNAI), vol. 9992, pp. 137–149. Springer, Cham (2016). https://doi.org/10.1007/978-3-319-50127-7_11
20. Komorowski, M., Marshall, D.C., Salciccioli, J.D., Crutain, Y.: Exploratory data analysis. In: Secondary Analysis of Electronic Health Records, pp. 185–203. Springer, Cham (2016). https://doi.org/10.1007/978-3-319-43742-2_15
21. Koza, J.: Genetic programming as a means for programming computers by natural selection. Stat. Comput. **4**(2) (1994). https://doi.org/10.1007/bf00175355
22. Le, T.A., Chu, T.H., Nguyen, Q.U., Nguyen, X.H.: Malware detection using genetic programming. In: the 2014 Seventh IEEE Symposium on Computational Intelligence for Security and Defense Applications (CISDA), pp. 1–6 (2014). https://doi.org/10.1109/CISDA.2014.7035623
23. Marra, A.L., Martinelli, F., Mercaldo, F., Saracino, A., Sheikhalishahi, M.: D-bridemaid: a distributed framework for collaborative and dynamic analysis of android malware. J. Wirel. Mobile Netw. Ubiq. Comput. Depend. Appl. (JoWUA) **11**(3), 1–28 (2020)
24. Martín, A., Rodríguez-Fernández, V., Camacho, D.: Candyman: classifying android malware families by modelling dynamic traces with Markov chains. Eng. Appl. Artif. Intell. **74**, 121–133 (2018). https://doi.org/10.1016/j.engappai.2018.06.006. https://www.sciencedirect.com/science/article/pii/S0952197618301374
25. McAfee: Mcafee 2022 consumer mobile threat report. https://www.mcafee.com/blogs/mobile-security/mcafee-2022-consumer-mobile-threat-report/. Accessed 24 Jan 2022
26. McAfee: Mcafee mobile threat report 2021. https://www.mcafee.com/content/dam/global/infographics/McAfeeMobileThreatReport2021.pdf. Accessed 24 Jan 2024
27. Mitchell, M.: An Introduction to Genetic Algorithms. The MIT Press, Cambridge (1998). https://doi.org/10.7551/mitpress/3927.001.0001

28. Molnar, C., Casalicchio, G., Bischl, B.: Interpretable machine learning – a brief history, state-of-the-art and challenges. In: Koprinska, I., et al. (eds.) ECML PKDD 2020. CCIS, vol. 1323, pp. 417–431. Springer, Cham (2020). https://doi.org/10.1007/978-3-030-65965-3_28
29. Onwuzurike, L., Mariconti, E., Andriotis, P., Cristofaro, E.D., Ross, G., Stringhini, G.: Mamadroid: detecting android malware by building markov chains of behavioral models (extended version). ACM Trans. Priv. Secur. **22**(2) (2019). https://doi.org/10.1145/3313391
30. Potha, N., Kouliaridis, V., Kambourakis, G.: An extrinsic random-based ensemble approach for android malware detection. Connect. Sci. **33**(4), 1077–1093 (2021). https://doi.org/10.1080/09540091.2020.1853056
31. Searson, D.P.: GPTIPS 2: an open-source software platform for symbolic data mining. In: Gandomi, A.H., Alavi, A.H., Ryan, C. (eds.) Handbook of Genetic Programming Applications, pp. 551–573. Springer, Cham (2015). https://doi.org/10.1007/978-3-319-20883-1_22
32. Taheri, L., Kadir, A.F.A., Lashkari, A.H.: Extensible android malware detection and family classification using network-flows and api-calls. In: 2019 International Carnahan Conference on Security Technology (ICCST), pp. 1–8 (2019). https://doi.org/10.1109/CCST.2019.8888430
33. Witten, I.H., Frank, E., Hall, M.A., Pal, C.J.: Data Mining, Fourth Edition: Practical Machine Learning Tools and Techniques, 4th edn. Morgan Kaufmann Publishers Inc., San Francisco (2016)
34. Zhang, M., Duan, Y., Yin, H., Zhao, Z.: Semantics-aware android malware classification using weighted contextual api dependency graphs. In: Proceedings of the 2014 ACM SIGSAC Conference on Computer and Communications Security, CCS 2014, pp. 1105–1116. Association for Computing Machinery, New York (2014). https://doi.org/10.1145/2660267.2660359



TinyIDS - An IoT Intrusion Detection System by Tiny Machine Learning

Pietro Fusco(✉), Gennaro Pio Rimoli, and Massimo Ficco

Università degli Studi di Salerno, Via Giovanni Paolo II, 132 - 84084 Fisciano, SA, Italy
{pfusco,grimoli,mficco}@unisa.it

Abstract. The use of Internet of Things (IoT) devices in sectors, such as healthcare, automotive, and industrial automation, has increased the risk of attacks against critical assets. Machine learning techniques may be utilized to identify malicious behaviors, but they often require dedicated, energy-intensive, and expensive devices, which may not be deployable in IoT infrastructures. Furthermore, privacy constraints, security policies, and latency constraints could limit the sending of sensitive data to powerful remote servers. To address this issue, the emerging field of TinyML offers a solution for implementing machine learning algorithms directly on resource-constrained devices. Therefore, this article presents the implementation of an intrusion detector, named TinyIDS, which exploits the Tiny machine learning techniques. The detector can be deployed on resource-constrained IoT devices to detect attacks against sensor networks, as well as malicious behaviors of compromised smart objects. On-board training has been exploited to train and analyze data locally without having to transfer sensitive data to remote or untrusted cloud services. The solution has been tested on common MCU-based devices and ToN_IoT datasets.

Keywords: TinyML · On-Board Training · IDS · Security · Intrusion Detection · MCU · Microcontroller

1 Introduction

The widespread diffusion of consumer electronics in every context of our daily lives, including healthcare, transport, industrial automation, military, etc., has ushered in a new era, which transcends individual functionality, making it an integrated element of a more complex interconnected Internet of Things (IoT) ecosystem [1]. Despite the great potential, their utilization in the context in which sensitive data are managed makes them prone to cyber intrusion due to the lack of robust security measures implementation. Several studies described potential attacks on the different layers of an IoT system, highlighting the risks that a vulnerability in IoT devices could pose [2–4]. Such vulnerabilities may result in the theft of sensitive data, as well as be exploited to cause system malfunctions.

© The Author(s), under exclusive license to Springer Nature Switzerland AG 2024
O. Gervasi et al. (Eds.): ICCSA 2024 Workshops, LNCS 14816, pp. 71–82, 2024.
https://doi.org/10.1007/978-3-031-65223-3_5

Centralized Machine Learning (ML) based security detection mechanisms may not be suitable solutions for such contexts, in which strict security and privacy policies are required, as they could demand sensitive data to be transferred and processed in remote and untruest servers. For example, in healthcare applications, smart monitoring sensors worn by the patients should be able to read and process private data (such as heartbeat, blood pressure, and sugar level) and notify alerts directly to the interested party (*e.g.*, if the values are symptomatic of some ongoing pathology), without sending data to a cloud service. Moreover, there are application contexts in which may be necessary to deploy smart devices in areas with poor or no Internet access (*e.g.*, along drinking water pipes), as well as provide low-latency and low-energy consumption (*e.g.*, Drone of Things).

Tiny machine learning (TinyML) emerges as a pivotal technology to process ML algorithms on low-cost devices [5]. Deploying TinyML algorithms on devices that are the source of data or nearby can significantly improve privacy, security data protection regulations, and achieve low latency with comparable accuracy.

This paper presents an ML-based implementation of a Tiny Intrusion Detection System (TinyIDS) to be installed on commercial resource-constrained Microcontroller Units (MCUs) based devices. TinyIDS can be used to detect security anomalies within a network of IoT objects, with one of them assuming the role of intrusion detector. Specifically, two kinds of intrusion detector models could be implemented: rule-based and machine learning-based. Rule-based IDS uses parameters such as signatures, message content, protocols, logs, etc. to detect threats. On the other hand, a machine learning-based model detects anomalous behaviors and dynamically adapts to new threats, making them more efficient compared to traditional methods. In this paper, we focused on the latter approach. Moreover, on-board training has been adopted to avoid transferring sensitive data to remote cloud services and improve security and privacy. An extension of Genann C library implemented in our previous work has been used [6].

TinyIDS can be used to detect attacks against a sensor network or malicious behaviors of smart objects (*e.g.*, the anomalous behavior of a compromised drone within a swarm). The device chosen as a detector can be either a peer node in the network (*e.g.*, the sink node), or the most powerful device in terms of energy, memory, and computational resources (*e.g.*, the leader drone within the swarm).

An experimental campaign has been carried out, deploying the implemented detector on common MCU-based devices, including ESP32, ESP8266, and Arduino Portenta H7. ToN_IoT datasets have been used for performance evaluation. It includes heterogeneous IoT data sources collected from telemetry and industrial sensors [7], along with several attack traces. Experimental results have shown that the proposed solution archives about 85% of accuracy.

The paper is structured as follows: Sect. 2 describes the used dataset and the current state of the art. Dataset pre-processing is presented in Sect. 3. Section 4 presents the implementation of the proposed solution. The solution evaluation is shown in Sect. 5. Finally, potential future work based on the results obtained is outlined in Sect. 6.

2 Background and Related Work

2.1 TON_IoT Dataset

The TON_IoT dataset was generated in 2019, and it was based on a testbed environment at the Cyber Range and IoT Labs at the University of New South Wales (UNSW) Canberra, Australia[1] The experimental setup specified in [7] includes physical and simulated connected devices. The name of the dataset "TON_IoT" refers to its content and provenance: telemetry data, operating system data, and network data from the IoT/IIoT testbed. Three layers of virtualized switches and routers were integrated into the testbed:

- Cloud layer (virtualized): Contains a Message Queuing Telemetry Transport (MQTT) broker.
- Fog layer (virtualized): Contains the monitored vulnerable hosts and attacker machines. It includes a Node-RED [8] server that simulates 6 out of 7 sensor sources.
- Edge layer (physical): Contains the physical devices, from which an ESP8266 weather station acts as the 7th sensor data source. Other devices in the edge layer are two smartphones, a smart TV, and the NSX VMware server emulating virtualized layers.

As an objective to acquire the specifications of IoT and IIoT systems, this paper aims to focus on the IoT telemetry part of this dataset. TON_IoT telemetry dataset makes available the sensor readings as registered by a Node-RED server, delivered through the MQTT protocol via the MQTT broker in the Cloud layer. This part of the data is provided for any sensors as a comma-separated values (CSV) file. Network capture and processing data from operating systems on the targeted virtual machines, which will not be used in this paper, are also part of the dataset.

There is a high degree of heterogeneity in the dataset. To gain a better awareness of its content, a closer look at its characteristics can help. Specifically, the data falls into these classes:

- IoT telemetry data (*i.e.*, IoT/IIoT sensor measurements, which will be used for the scope of this paper);
- Linux host data;
- Windows host data.

Additionally, basic specifications for security events are available. The dataset also makes available basic statistics on the number of records in each class. The TON_IoT dataset comprises a hierarchical structure where are included the following directories:

- *Raw datasets*: IoT/IIoT datasets were logged in log and CSV files, where more than 10 IoT and IIoT sensors, such as weather and Modbus sensors, were used to capture their telemetry data;

[1] UNSW - Canberra: https://www.unsw.adfa.edu.au.

- *Processed datasets*: To produce standard features and labels, the four datasets that were previously included in these directories have been filtered (to be used on any platform, the whole dataset has been processed and filtered in CSV format);
- *Train_Test_datasets*: Samples of the four datasets in CSV format that were selected for evaluating the fidelity and efficiency of new cyber security application-based AI and machine learning algorithms are included in this folder.

As previously described, the telemetry data come from 7 physical and simulated sensors. Table 1 shows a summary of the sensors and their outputs. There are 17 features from seven different sensors in both the Processed Dataset and Train_TEST_Dataset dataset, as well as a time stamp. A binary label field has been added to each data record, (0 means normal operation, and 1 indicates an attack). In addition, what event occurs is indicated by the *type* field.: *i.e.*, if label = 0, *normal* event occurs, otherwise it indicates attacks, such as *backdoor*, *DDoS*, *injection*, *password*, *ransomware*, *scanning*, or *XSS*.

Table 1. Train_Test_datasets sensors ranges.

Sensor	Measure	Values
Fridge	Fridge temperature	[1.0; 14.0]
	Temp condition	{'high', 'low'}
Garage Door	Door state	{'open', 'closed' }
	Sphone signal	{'true', 'false', 0, 1 }
GPS Tracker	Latitude	[0.00; 550.00]
	Longitude	[10.00; 556.00]
Modbus	FC1 Read Input Register	$\mathbb{N} \cap [0; 65535]$
	FC2 Read Discrete Value	$\mathbb{N} \cap [0; 65535]$
	FC3 Read Holding Register	$\mathbb{N} \cap [0; 65535]$
	FC4 Read Coil	$\mathbb{N} \cap [0; 65535]$
Motion Light	Motion status	0, 1
	Light status	{'on', 'off'}
Thermostat	Current temperature	[25.00; 35.00]
	Thermostat status	{0, 1}
Weather	Temperature	[20.00; 50.00]
	Pressure	[–12.00; 12.50]
	Humidity	[0.20; 100.00]

2.2 Related Work

Anomaly detection and analysis of unexpected states in IoT devices is a critical research area for various domains, including assisted living, automated operations in industries, and healthcare [9,10]. Several anomaly detection techniques have been proposed to identify abnormalities, outliers, and specific events, by exploiting both time-series and non-temporal data from various domains that can be applied in IoT-specific scenarios [11].

The use of Machine Learning (ML) techniques to create Intrusion Detection Systems is a widely discussed topic in the literature [12–16]. The typical approach involves a thorough analysis of the dataset to identify functional dependencies. Subsequently, the dataset is preprocessed to extract features before applying an artificial intelligence (AI) model. The datasets used in the process are constructed using physical and virtual devices that communicate over various network configurations, including peer-to-peer and client-server setups, such as web and cloud services, or client-broker setups, such as MQTT servers, Node-Red, and others. These datasets are specifically designed for IoT applications.

All of the previously cited documents rely on the use of energy-consuming terminals to perform the role of IDS. However, a more interesting alternative is the possibility of utilizing IoT devices that are already integrated into the system or dedicated IoT devices for this purpose. These devices are significantly more energy-efficient. Efforts in this direction are still in development in the literature. Tekin et *al*. [17] discussed the timing, consumption, and accuracy of various AI models based on algorithms, such as Logistic Regression, Random Forest, K-Nearest Neighbor, Decision Tree, Naive Bayes, or Multi-Layer Perceptron. However, it does not provide a clear definition of the structure of each model and the memory used, making replication of the results challenging. The findings indicate the possibility of a hybrid training approach that combines network and edge computing. However, the challenge of weight sharing needs to be addressed [4].

3 Dataset Processing

To detect attacks against an IoT system, as well as malicious behavior of the monitored smart objects, the TinyIDS exploits sensor readings provided by the observed IoT devices (*e.g.*, telemetry data transmitted by drones) or data directly observed in the field (*e.g.*, the change of path by a compromised drone). Therefore, to evaluate the presented solution TON_IoT Dataset has been exploited [7]. The data processing starts converting the seven IoT datasets into just one big dataset consisting of all readings of all sensors. The procedure consists of a few subsequential steps:

– *Concatenation*: Takes the source CSV files from seven sensors as input and outputs a merge of the records into a single DataFrame object [18] whose columns contain all features.

- *Assembling*: Takes a data frame object and collapses the rows which are of identical timestamps, only taking account of the last one, to reduce the number of records and create the corresponding DataFrame object.
- *Division*: Takes as input a series of samples and outputs a series divided into blocks of the given size. As a general rule, this process intends to exploit the development of sensor measurements over time and therefore should preserve as much temporal continuity as possible. As in every valid machine learning application, training and test datasets must be disjoint. The TON_IoT dataset does not yet contain separate training and test sets, so it is broken down into pieces of a parameterizable dimension. It is more likely that a clear picture of system development and attack patterns will be obtained if the number of subsequent measurements contained in a single piece of data is higher.
- *Splitting*: Specifies two separate datasets, training and test sets, composed of records from these blocks, which are the blocks of packaged rows that were created in the previous step as input. The splitting step decides whether a segment of the assembled dataset records will be part of the training or the testing dataset. A random seed is assigned for reproducing the uniform distribution given the percentage driving the partitioning.
- *Attribution*: Gets a series of records and provides the same records, which are appropriately modified by filling in the missing values. The sensors in the Train_Test_datasets have different sampling and periods of working. To maintain the maximum extent of detection, it is necessary to keep attention on all measurements that have at least one sensor transmitting. When a sensor does not output any data, "missing values" can be found.

It is worth noting that the step *division* explained above may be better understood taking into consideration the Fig. 1.

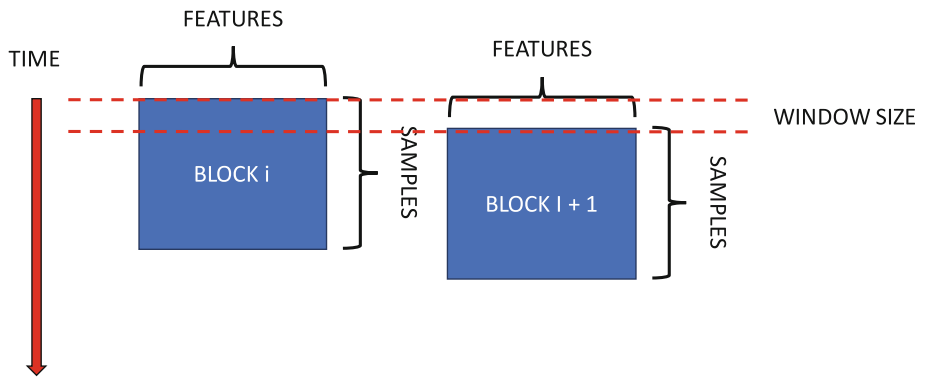

Fig. 1. Dataset blocks.

It is important to note that each block, either included in the training dataset or test dataset, contains more than one sample. To allow time-based learning and

to make the detection system more robust for the measurement of floods, the *division* step is performed. In subsequent steps, a fixed number of records for machine learning will be used to support training based on the past state. The machine can take into account the system's past state of affairs. The selection of the fixed number of records for machine learning supports an analysis based on past states in later phases. The previous state of the system can therefore be taken into account by the machine.

4 Model Implementation

The implementation of the neural network is based on the multilayer perceptron (MLP), also known as a feedforward network. It consists of 510 input neurons, which correspond to a sliding window of 30-time instants, 32 neurons for a 32-layer of fully connected neurons with a nonlinear activation function, represented by the RELU function in our case, and finally, 8 output neurons. These output neurons allow for the identification of either the normal state or the 7 possible threats.

The network was trained using the technique proposed in article [6], which utilizes the Genann library. This C library has been optimized for microcontrollers (including Arduino, Raspberry, and Espressif boards) to perform on-board training and inference. Moreover, it has been updated using float data type instead of double in order to reduce memory usage without compromising the performance of the model [19]. Moreover, the library has been improved with proper metrics (which can be stored in a CSV file) to assess the effectiveness of the newral network. Finally, it supports the export and import of the model's weights for a possible federated learning implementation.

This library allows for the selection of network weights based on the intended device usage context. The weights can be deployed from a previously trained model on more powerful machines or trained live directly on the device. However, this article uses a hybrid approach where the network is pre-trained on a significant dataset and then fine-tuned through on-board training. The training procedure pseudocode is shown in Algorithm 1. It consists of an initial part where all the weights of the neural are initialized to random values. After, it is possible to find out two nested loops, the outer loop goes through the epochs until the last epoch is reached. The inner loop is broken down by the batches of training data collected. It is necessary to step in a different direction from the cost curve of the whole training data set, so as to reduce loss function. Therefore, the gradient approach is sometimes referred to as a batch descent.

By using a dataset with millions of data points, that is not uncommon in many applications for machine learning, in such scenarios carrying out *Batch Gradient Descent* (BGD) can be pretty high in terms of computational costs because every time the algorithm steps up to the Global Minimum, it requires a reevaluation of your entire training database. The *Stochastic Gradient Descent* (SGD) is considered a valid alternative to the BGD algorithm. Rather than update the weights according to the number of errors that have accumulated in all training examples for N, x_i:

$$\nabla \mathcal{L}_i = \sum_{i=1}^{N} \big[y_i - y_{pred}(x_i) \big] x_i,$$

$$\theta_i^{k+1} \leftarrow \theta_i^k - \eta \nabla \mathcal{L}_i.$$

SGD corrects the weights for each training example in a gradual way. Although SGD may be considered an approximation of the gradient descent, as a result of increasing frequency of weight changes, it usually approaches convergence much more quickly.

The Mini-Batch Learning (MBL) algorithm may be considered a point of equilibrium between BGD and SGD algorithms. The application of BGD to a smaller portion of the original training data, *e.g.*, n training examples at a time, can explain MBL. The advantage of minibatches compared to BGD is that convergence can be achieved more quickly due to a higher frequency of weight changes.

Algorithm 1. Training procedure.

Initialization of all weights of neural network;
$\theta \leftarrow \mathbb{R}$ ▷ ML weights are initialized with floating point
for $epoch = 1, 2, \ldots, MAX_EPOCHS$ **do**
  for $batch_data = 1, 2, \ldots, N$ **do**
    FEEDFORWARD PASS
    $\hat{y} \leftarrow model(\mathbf{x}_{batch}, \theta^{epoch})$
    BACKWARD PASS
    $\forall \theta_i : \nabla \mathcal{L}_i \leftarrow \frac{\partial \mathcal{L}}{\partial \theta_i}$
    $\theta_i^{batch} \leftarrow \theta_i^{batch-1} - \eta \nabla \mathcal{L}_i$
  end for
end for

The GitHub project of an implementation of the TinyIDS is available at: *https* : *//github.com/iotresearchunisa/TinyIDS*.

5 Measurements and Results

Following the creation of the model, the experimental phase was carried out on ESP8266, ESP32, and Arduino Portenta H7 devices. The PlatformIO development platform was used to compile the code. It is an integrated development environment (IDE) that provides all the necessary libraries to create code for embedded products [20]. After compilation, the platform performed static code analysis and provided the amount of memory required to run the program.

Table 2 presents the results for ESP32 and Arduino Portenta H7 devices, but not for the ESP8266. The ESP8266 was unable to accommodate all network nodes due to its limited memory capacity of only 32kb of RAM.

Table 2. Memory consumption measurement (PlatformIO building tools).

DEVICES	Memory consumption (kb)
ESP32	114.492
Arduino Portenta H7	157.304

To avoid any interference with the algorithm, a benchmarking station was used, which consisted of an Arduino UNO R3 and an INA219 sensor capable of measuring voltage, power, and current. The benchmarking station provides data in batches to the device under analysis and measures the execution time and current required to perform a single training or inference step. The connection between the benchmarking station and the device under analysis was established via serial communication. Table 3 presents the average of the results obtained.

Table 3. Time and electric current measurement.

Devices	Training		Inference	
	Time (ms)	Current (mA)	Time (ms)	Current (mA)
ESP8266	Failed			
ESP32	2832	71.16	2482	71.23
Arduino Portenta H7	362	216.15	351	223.60

Lastly, a consideration can be made about the accuracy and loss results shown in Figs. 2 and 3 respectively. As it is possible to note, the accuracy curve reaches the convergence quite rapidly. The most important thing is that the curve is completely free from oscillations. Analogously, also in the loss curve oscillations are absent. As the final result, the neural network model provided an accuracy on the test dataset of 84.03

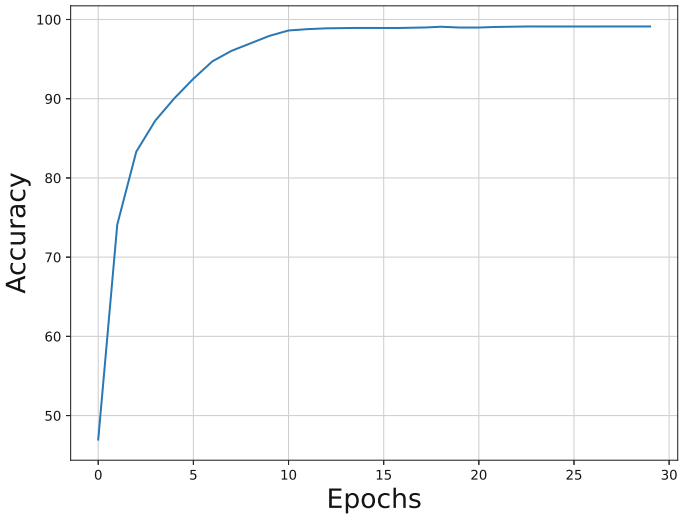

Fig. 2. Training accuracy.

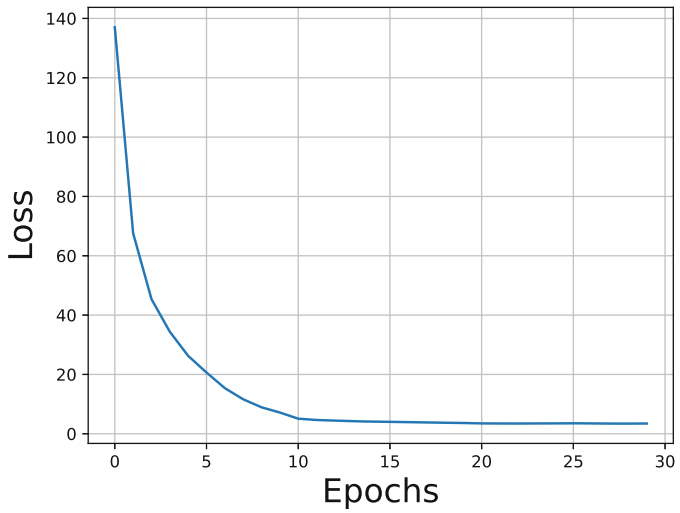

Fig. 3. Training loss.

6 Conclusion

In this paper, an IDS based on Tiny deep learning model is proposed to detect attacks against IoT systems. The presented analysis is performed by using a feedforward network as intrusion detection implementation, which performs its task on the MCU with a limited availability of resources, and the TON_IoT dataset for performance evaluation.

In future works, it is planned to produce a new dataset generated by the physical implementation of more complex and realistic IoT scenarios, as well as increase the detection accuracy of the model by the generated datasets, and the use of the Federated Learning paradigm.

Acknowledgments. The work is part of the research activities realized within the projects Federated Learning for Generative Emulation of Advanced Persistent Threats (FLEGREA), CUP. E53D23007950001, Bando PRIN 2022, as well as SERICS (PE00000014) under the NRRP MUR program funded by the EU - NGEU.

References

1. Akram, J., Anaissi, A., Othman, W., Alabdulatif, A., Akram, A.: Dronessl: self-supervised multimodal anomaly detection in internet of drone things. IEEE Trans. Consum. Electron. **70**, 4287–4298 (2024)
2. Pietrantuono, R., Ficco, M., Palmieri, F.: Survivability analysis of IoT systems under resource exhausting attacks. IEEE Trans. Inf. Forensics Secur. **18**, 3277–3288 (2023)
3. Gerodimos, A., Maglaras, L., Ferrag, M.A., Ayres, N., Kantzavelou, I.: IoT: communication protocols and security threats. Internet Things Cyber-Phys. Syst. **3**, 1–13 (2023)
4. Pietrantuono, R., Ficco, M., Palmieri, F.: Testing the resilience of MEC-based IoT applications against resource exhaustion attacks. IEEE Trans. Depend. Secure Comput. **21**(2), 804–818 (2024)
5. Abadade, Y., Temouden, A., Bamoumen, H., Benamar, N., Chtouki, Y., Hafid, A.S.: A comprehensive survey on tinyml. IEEE Access **11**, 96892–96922 (2023)
6. Ficco, M., Guerriero, A., Milite, E., Palmieri, F., Pietrantuono, R., Russo, S.: Federated learning for IoT devices: enhancing TinyML with on-board training. Inf. Fusion **104**, 102189 (2024)
7. Alsaedi, A., Moustafa, N., Tari, Z., Mahmood, A., Anwar, A.: TON_IoT telemetry dataset: a new generation dataset of IoT and IIoT for data-driven intrusion detection systems. IEEE Access **8**, 165130–165150 (2020)
8. Node-RED, a Browser-based flow editing. https://nodered.org. Accessed Sept 2023
9. Chatterjee, A., Ahmed, B.S.: IoT anomaly detection methods and applications: a survey. Internet Things **19**, 100568 (2022)
10. Ukil, A., Bandyoapdhyay, S., Puri, C., Pal, A.: IoT healthcare analytics: the importance of anomaly detection. In: Proceedings of the IEEE 30th International Conference on Advanced Information Networking and Applications (AINA), pp. 994–997 (2016)
11. Fahim, M., Sillitti, A.: Anomaly detection, analysis and prediction techniques in iot environment: a systematic literature review. IEEE Access **7**, 81664–81681 (2019)

12. Smiliotopoulos, C., Kambourakis, G., Kolias, C.: Detecting lateral movement: a systematic survey. Heliyon **10**(4), 1–24 (2024)
13. Kodyš, M., Lu, Z., Fok, K.W., Thing, V.L.L.: Intrusion detection in internet of things using convolutional neural networks. In: 2021 in Proceedings of the 18th International Conference on Privacy, Security and Trust (PST), pp. 1–10 (2021)
14. Altunay, H.C., Albayrak, Z.: A hybrid CNN+ LSTM-based intrusion detection system for industrial IoT networks. Eng. Sci. Technol. Int. J. **38**, 101322 (2023)
15. Thein, T.T., Shiraishi, Y., Morii, M.: Personalized federated learning-based intrusion detection system: poisoning attack and defense. Future Gener. Comput. Syst. **153**, 182–192 (2024)
16. Mahadevappa, P., Murugesan, R.K., Al-Amri, R., Thabit, R., Al-Ghushami, A.H., Alkawsi, G.: A secure edge computing model using machine learning and IDS to detect and isolate intruders. MethodsX **12**, 102597 (2024)
17. Tekin, N., Acar, A., Aris, A., Uluagac, A.S., Gungor, V.C.: Energy consumption of on-device machine learning models for IoT intrusion detection. Internet Things **21**, 100670 (2023)
18. Pandas, a flexible data analysis and manipulation library for Python. https://github.com/pandas-dev/pandas. Accessed Oct 2023
19. Nadalini, D., Rusci, M., Benini, L., Conti, F.: Reduced precision floating-point optimization for Deep Neural Network On-Device Learning on microcontrollers. Future Gener. Comput. Syst. **149**, 212–226 (2023)
20. PlatformIO IDE, a toolset for embedded C/C++ development. https://platformio.org/. Accessed Nov 2023

A General Study on the Malware Propagation Models in Wireless Sensor Networks

Eslam Farsimadan(✉), Leila Moradi, and Francesco Palmieri

Department of Computer Science, University of Salerno, Fisciano 84084, Italy
{efarsimadan,lmoradi,fpalmieri}@unisa.it

Abstract. The propagation of malware in wireless sensor networks has recently garnered significant attention from researchers as a pressing issue. Wireless sensor networks consist of sensor nodes interconnected in a decentralized and distributed manner via wireless connectivity. Malware attacks can raise the energy consumption of wireless sensor network sensor nodes. The propagation of the infection initiates from a single infected node and utilizes neighboring nodes to increase throughout the entirety of the wireless sensor network. Hence, a comprehensive knowledge of spreading malware patterns in wireless sensor networks is advantageous. This paper examines the current models to analyze malware propagation in wireless sensor networks. This study presents a comprehensive overview of the strategies developed over the past decade. Equation-based epidemic models are observed to accurately represent the critical characteristics of wireless sensor networks and the spread of malware within them. The vulnerability of wireless sensor networks to malware attacks poses a significant challenge due to the limited defense capabilities of sensors. Consequently, the propagation of malware within these networks concerns the security community. This study examines the most crucial and up-to-date global epidemic models to explain network malware propagation.

Keywords: Wireless sensor networks · Malware propagation · Epidemic models · Basic reproductive number · Stability analysis

1 Introduction

Wireless Sensor Networks (WSNs) provide an instrument to connect the physical infrastructure with information and communication technologies [1]. WSNs have been extensively utilized for several innovative applications, including patient health care monitoring, military surveillance, and chemical or biological threats detection, including environmental monitoring, tracking, and targeting [2]. An essential concern in WSNs is the presence of several forms of security threats [3,4]. These networks operate in situations that are widely spread out and have limited resources. WSNs can be targeted by several types of attacks, including

© The Author(s), under exclusive license to Springer Nature Switzerland AG 2024
O. Gervasi et al. (Eds.): ICCSA 2024 Workshops, LNCS 14816, pp. 83–99, 2024.
https://doi.org/10.1007/978-3-031-65223-3_6

denial of service attacks, worms, Sybil attacks, and other forms of malicious code. Moreover, with the extensive use of computer networks, the Internet, and WSNs, investigating attacks and malware detection, classification, and propagation models in these systems has become of great importance [5–7].

Malware creates one of the most significant problems in the contemporary society. The increasing number of malware is directly correlated with the rise in internet usage during this era, necessitating a substantial enhancement in computer security systems. Malicious software, also known as malware, is the product of several viruses designed to engage in harmful activities, such as stealing information or conducting scans. The primary objective of the malware is to inflict extensive damage to information and resources or to obtain unauthorized access to the network. Furthermore, it is defined as a category of computer software specifically created to harm the functionality of a legitimate user's device through various ways [8]. These dangers are pervasive in terms of their prevalence and the level of sophistication of the programs and viruses involved. The researchers proposed a range of remedies to safeguard against malware infections. Malware poses a significant challenge for contemporary internet users. The increase in malware attacks significantly threatens sensitive data and valuable computing resources. Hence, it is imperative to analyze the virus propagation model. Malware is an abbreviation for harmful software.

Malware has a significant impact on the growth and progress of organizations. Malware specifically targets internet-based apps. The Internet has become a fundamental and necessary part of our daily lives in the modern world. Over the past few years, there has been a significant rise in the prevalence of malware propagation in WSNs, and numerous study findings have been published on this topic by [9–11]. The security of WSNs is crucial due to the potentially sensitive nature of the data acquired by the sensor nodes [9]. Moreover, the majority of sensor devices can function in unsafe environments. WSNs are at risk from attacks, eavesdropping, and malware attacks that can disrupt their regular functioning [4,12] or perhaps cause their destruction [13]. According to [14], the propagation of malware has a more significant impact on WSNs than on the Internet.

Malware attacks provide serious security concerns for WSNs. The strategy of interleaving work and sleep schedules, high density, low communication range, power consumption (limited energy), and node topology all lead to the susceptibility to malware spreading. Based on the information provided, there are three distinct characteristics of the process of malicious software propagation in a WSN that are not present in other types of networks [15,16], as are listed following:

– Malware on a network, such as an Internet host, attempts to propagate itself by doing random scans of other hosts' IP addresses to infect them. As opposed to this, malware within a WSN node has the ability to propagate across its neighbors, allowing them to speak with the node directly.

– The malware on an active node can propagate to adjacent active nodes, but it does not infect inactive nodes. Furthermore, while a node is dormant, it cannot spread any malware to other nodes.
– Once the nodes' energy runs out, they transition into non-functional nodes that are no longer susceptible to infection and do not contribute to malware propagation in a WSN. When a dead node is infected with malware, it promptly vanishes from the network.

In order to investigate the propagation of malware in WSNs, researchers initially focused on traditional techniques of malware propagation observed on the Internet. The epidemic models have also been expanded to include this particular case [10]. The majority of mathematical models that address the dynamics of malware propagation in WSNs include systems of Ordinary Differential Equations (ODEs) (refer to [17,18]). The model presented in [19], which is based on a delayed ODE system and assumes that all network sensors are identical, is interesting.

The structure of this paper is as follows: The description and properties of WSNs are provided in Sect. 2. Section 3 focuses on the categorization of malware. The global models for malware spreading in WSN were recently proposed and are explained in Sect. 4. An example of one of the models described in Sect. 4 is selected to analyze the stability and basic reproductive number in Sect. 5. The conclusion is finally presented in Sect. 6.

2 Description of WSNs

A WSN is a set of networked microsensors dispersed in various locations without specified positions. Furthermore, in the absence of a particular configuration, it is near the phenomenon being assessed or situated within it. Each node is a sensor device that can autonomously arrange itself and is designed to observe and regulate physical phenomena. These phenomena include sensing various variables such as temperature, humidity, sound, vibration, pressure, pollutants, etc. The sensor node can gather data from its immediate environment and transmit it to the sink node, also known as the base station. In addition, they can analyze the collected data, retain it, and transmit it to other devices. While WSNs were initially developed and utilized for military applications like surveillance in conflict zones, their usage has now expanded to various other domains such as smart grids, smart water networks, intelligent transportation, smart homes, intelligent agriculture, and e-health [13,20,21]). The subsequent phases outline the implementation of a WSN:

– Placing: The sensors are put in the area that will be monitored (the sensor field). This placement could be random (the sensors are dropped from the air at random) or predictable (the sensors are placed in exact places already planned).
– Wake up and identify: Each sensor gets awake and identifies other sensors nearby.

– Connection: Using a predetermined topology (linear, star, tree, mesh, etc.), the sensor nodes are arranged into a connected network.
– Transmission: To send the gathered data, connecting paths that take the network consideration are calculated.

Fig. 1 illustrates the structure of the WSNs. The configuration of a WSN is determined by the specific applications it is designed for and is deployed in various types of terrain, including challenging conditions, to facilitate monitoring activities. WSNs have numerous applications, including military operations on battlefields, detecting fires in forests, and monitoring desert areas. The sensor network operates in a decentralized manner and utilizes wireless connections for the exchange of information. Malicious individuals and marketers take advantage of the weaknesses in the software and focus on a specific point of entry to deliver harmful software or worms into a WSN. When a WSN node becomes infected, it spreads gradually throughout the network by moving through neighboring nodes. Energy shortage is a significant issue in sensor networks. A malware assault reduces the energy of sensor nodes, causing a slowdown in the operation of the sensor network and an increase in network traffic. Researchers have discovered that biological worms spread is comparable to software-generated worms. Research on the security of WSNs related to malware assaults is currently a crucial area of study. To examine the dynamics of malware spreading in WSN, several researchers [22–26] have utilized epidemic modeling.
The characteristics of WSNs vary based on whether they are employed in indus-

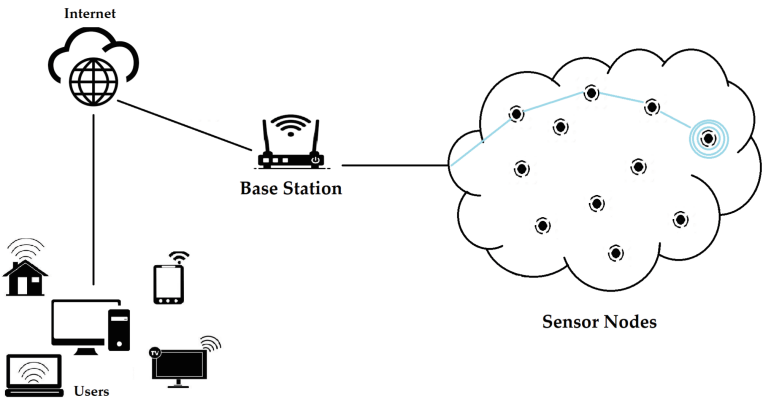

Fig. 1. Basic scheme of a WSNs

trial or conventional networks. In the first case, since all sensors are essential for the functioning of a plant, a malfunctioning node must be substituted. Conversely, in conventional networks, individual nodes have the potential to experience power loss or destruction. However, the network as a whole will remain operational. Since WSNs are inherently self-restoration capable, in the case of a

node loss, the network will find alternative paths for data packets to be transmitted. Therefore, the network will survive as a unified entity. Sensor nodes typically spend significant time in sleep mode due to their low power consumption.

3 Malware Classification

Categorizing malware is a challenging procedure. Software that allows illegal manipulation of a system is considered malicious. Malware exists in several forms and categories. To clarify, the malware makes the network temporarily inaccessible, resulting in significant harm or problems, and interrupts regular social or economic activities. The subsequent list presents prevalent categories of malware:

- **Virus:** A program reproduces by embedding its code into other programs for its advantage. Transmission of an infection can occur between machines and applications.
- **Worms:** Malicious software that replicates itself to damage and erase computer data and files. Worms can also encrypt data or transmit spam email messages. Unlike viruses, worms move themselves within their enclosures.
- **Trojan horse:** Trojan horses, posing as genuine software, engage in unauthorized and undesired activities. Trojans enable attackers to enter a fully operational computer and extract sensitive user data, including passwords and secret banking information.
- **Spyware:** Spyware is a computer software that constantly monitors and tracks user behavior. Without their awareness, the system clandestinely gathers user information, including frequently accessed online pages and payment card details, and transfers this data to the attackers.
- **Rootkit:** A rootkit program is a set of malicious software designed to infiltrate a computer network and grant unauthorized access to various types of malware within the system.
- **Ransomware:** Ransomware is a substantial threat to internet business and industry. Ransomware takes control of computers by encrypting data, disabling some applications, and allowing them to use operating systems only when their demands are met. The inquiries typically pertain to monetary funds. After making a financial payment, it is not guaranteed to restore power.
- **Adware:** Adware is a malware designed to continuously display advertisements on your computer. It is commonly bundled with free downloadable applications and software, such as free-to-play games.
- **Botnet:** Malicious software controls several devices, including computers, cell phones, and IoT devices. Then, they have been infected with malware and are under the control of a cybercriminal. A botnet is frequently employed to conduct denial-of-service attacks or spam operations. They can prevent unauthorized attacks on the system, distribute unsolicited emails, and steal information. Many users are often unaware that their infrastructure has been compromised by malware and is being used as part of a botnet.

- **Cookies:** Cookies are text documents that store data on the user's computer for a certain period. Internet browsers use them and are generally harmless; however, they can become dangerous when utilized by certain spyware.
- **Sniffers:** The software detects and tracks the organization's traffic. They explore different parcel fields and collect data to organize the virus attack.
- **Keyloggers:** The software detects and tracks the organization's traffic. It explores different parcel fields and collects data to organize the virus attack.
- **Spam:** Junk messages are another name for spam. These identical messages are generated and sent to multiple recipients simultaneously, consuming significant data bandwidth and slowing the system.

4 Global Models for Malware Propagation in WSN

Global models do not consider the unique features of particular devices or their specific interactions within local interactions. Therefore, they are expected to be evenly distributed and connected and have similar characteristics and behaviors. In our research, we delve into the complexity of the model variables, which are time-dependent and represent the number of devices in specific compartments. The interactions between these variables and parameters, which govern the system's dynamic behavior, are typically described by systems of ODEs. These equations, by capturing the temporal variability, allow us to determine how the observed characteristics change over time, despite not explicitly representing the interconnected actions of the devices in the model.

This section examines several epidemic models related to the spread of malware in WSNs. Various epidemic models have been employed to investigate malware propagation in WSNs. Kermack and Mckendrick [27] created the notion of epidemic modeling to analyze the transmission of infection among individuals. Academics employ this notion in diverse fields, such as social networks, computer networks, the Internet of Things, and WSN. The majority of malware propagation models, such as SI, SIR, SIRD, SEIRD, SEIVR, SILRD, etc., are based on and derived from the classical SIR model [10,18,28–36]. A mathematical model is constructed by making simplified assumptions about a significant problem, such as malware or network concerns. The assumptions are associated with the respective malware, network outages, and hacking incidents. WSN epidemic models aim to analyze the factors involved in transmitting harmful objects from a single node to the entire system. The malware propagation models in WSN consider various states of nodes, which are listed in Table 1. The number of sensor nodes in a WSN at any given time t is categorized into different states of nodes based on their condition. The number of nodes in any model is denoted as $N(t)$ that is eual to sumation of states of nodes for $t \geq 0$.

The researchers investigated the influence of secondary immunity on the spread of malware in WSNs. Generally, the basic reproductive number can be defined as the overall number of secondary infections induced by a single infectious device in a network where everyone is vulnerable. Therefore, the fundamental factor determining the system's evolution is a basic reproductive number

Table 1. Represent variables for epidemic models in WSN.

Subclasses of nodes	signify
S(t)	**Susceptible:** The sensor nodes currently remain unaffected by malware infections. However, they lack protection against attacks in WSNs
I(t)	**Infectious:** The sensor nodes in WSNs have been targeted by malware, which has the power to infect other susceptible nodes
V(t)	**Vaccinated:** The sensor nodes that are vaccinated are considered part of the vaccinated state
R(t)	**Recovered:** The sensor nodes were infected with malware and successfully disinfected by antivirus software
E(t)	**Exposed:** The sensor nodes have been infected with malware. However, they are not currently capable of infecting other nearby sensor nodes. Over time, these nodes become infected and spread malware in WSN
D(t)	**Dead:** The sensor nodes that have lost their energy can not communicate with other nodes, so they can not spread malware in a WSN

denoted as R_0. This coefficient is the most crucial threshold in the field of epidemiology. To examine the propagation patterns of the virus in WSN, the value of R_0 was calculated. It was determined that if $R_0 < 1$, the malware will cease to exist in WSNs. Conversely, if $R_0 > 1$, the number of infected nodes will continue to increase, and the malware will propagate across the entire WSN. Moreover, this parameter is crucial in analyzing the qualitative dynamics of the system of ordinary differential equations. Suppose $R_0 < 1$. In that case, the steady state without malware (the equilibrium point of the system when there are no infected devices) will be both locally and globally asymptotically stable. Otherwise, if $R_0 > 1$, the steady state of the malware epidemic (the point at which the number of infectious devices remains constant throughout time) will be locally and globally asymptotically stable.

4.1 SI Model

As proposed in [28–30], the SI model describes worm propagation behavior in WSNs. Several differential equations were used in the model's structure, and simulation results confirmed its validity. The authors attempted to ascertain the

fundamental elements of the network and the epidemic that hindered the dissemination of WSNs. The SI model is suggested for understanding the dynamics of worm propagation on the Internet [28–30]. According to the SI model, a host can be in one of two states: susceptible or infectious. The current state of a host infected by internet worms is called an infectious state. The susceptible state refers to the current condition of a worm that has not infected a host. This model delineates the attributes of malware propagation on the Internet. Figure 2 depicts the transitional condition of the sensor node, as mentioned in [28–30].

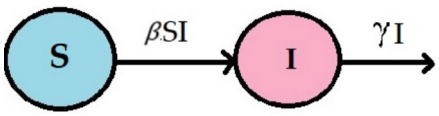

Fig. 2. Transition state diagram of the SI model [30,31]

The SI model is formalized as follows:

$$\begin{cases} \frac{dS}{dt} = -\beta SI, \\ \frac{dI}{dt} = \beta SI - \gamma I. \end{cases} \tag{1}$$

These nodes is categorized into two distinct states. The parameters used in model formulation are defined in Table 2.

Table 2. Present parameters for SI model

Parameters	Description
β	Rate of susceptible node become infected
γ	Rate of infected node become recovered

The SI model does not consider cases where specific hosts may be destroyed due to heavy infection by Internet worms. Furthermore, it does not account for situations where the host may have immunity to the same class of worms eradicated from that host. Therefore, the SI model needs to be revised to depict the worm propagation process on the Internet accurately.

4.2 SIR Model

The SIR model is an expanded version of the SI model, commonly used to analyze the spread of malware over the internet. Nevertheless, the SI and SIR models are not explicitly designed for WNSs. Therefore, these models cannot facilitate

the spread of malware while considering the energy consumption of nodes in WSNs. The SIR model expands the SI model by incorporating the presence of infectious hosts who are immunized, isolated, or dead while assuming that all susceptible hosts remain active indefinitely. Nevertheless, any individual node inside a WSN can become inactive due to its energy consumption. Rozenberg proposed the SIR Model, which concentrates on the spread of malware on WSN. The conventional global epidemic model typically assumes a population of N(t) identical sensor nodes that are uniformly and randomly dispersed. This SIR epidemic model classifies the population into three categories: susceptible S(t), infected I(t), and removed R(t) individuals. This case involves the SIR model, a type of epidemic model proposed in [30,31]. The model can be accurately solved on different kinds of networks. The SIR model assumes that all the sensitive sensor nodes will operate indefinitely, without considering any sleep and work schedule interweaving [30,31]. Figure 3 depicts the transitional condition of the sensor node, as referenced in [30,31].

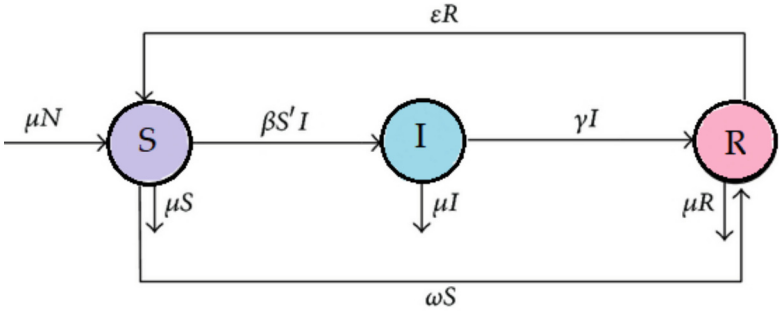

Fig. 3. Transition state diagram of the SIR model [30,31]

$$\begin{cases} \dfrac{dS}{dt} = \mu N - \xi SI - (\mu + \omega)S + \varepsilon R, \\ \dfrac{dI}{dt} = \xi SI - (\mu + \gamma)I, \\ \dfrac{dR}{dt} = \omega\, S + \gamma\, I - (\mu + \varepsilon)\, R, \end{cases} \tag{2}$$

where $\xi = \frac{\pi r^2}{L^2}\beta$. The number of sensor nodes in a WSN at any given time t is categorized into three distinct states: S(t), I(t), and R(t). The parameters employed in model formulation are described in Table 3.

Table 3. Present parameters for SIR model

Parameters	Description
β	Rate of susceptible node become infected
γ	Rate of infected node become recovered

4.3 SIRD Model

The Susceptible-Infectious-Recovered-Dead (SIRD) model was introduced in [31] for analyzing the dynamics of worm propagation in WSN. The SIRD model improved the SIR model by introducing the idea of the dead state of nodes in WSNs. It presented a novel model to evaluate the dynamics of worm propagation in WSNs. The SIRD model is derived from epidemic theory and comprises a set of differential equations. It can accurately represent the spread of worms in WSNs while considering the energy consumption of the network nodes. In the SIRD paradigm, susceptible sensor nodes become infected upon contact with the malware, and the infected nodes are restored to their original state after the malware is identified and eliminated. Conversely, specific devices restored to working order can again be susceptible if they lose resistance due to the antivirus software. Figure 4 illustrates the transition relationships between the states of the nodes.

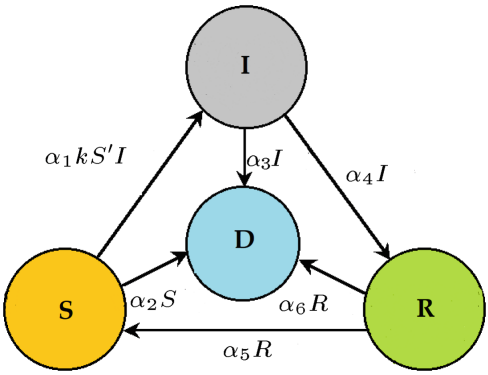

Fig. 4. Transition state diagram of the SIRD model [31]

$$\begin{cases} \dfrac{dS}{dt} = \dfrac{\alpha^2}{q^2}\alpha_1 k\, SI - \alpha_3 I - \alpha_4 I, \\ \dfrac{dE}{dt} = \alpha_5 R - \frac{\alpha^2}{q^2}\alpha_1 k\, SI - \alpha_2 S, \\ \dfrac{dI}{dt} = \alpha_4 I - \alpha_5 R - \alpha_6 R, \\ \dfrac{dR}{dt} = \alpha_2 S + \alpha_3 I + \alpha_6 R. \end{cases} \tag{3}$$

The number of sensor nodes in a WSN at any given time t is categorized into four individuals based on their current condition: S(t), I(t), R(t), and D(t). Table 4 lists the parameters employed in model formulation.

Table 4. Present parameters for SIRD model

Parameters	Description
k	The average number of malware residing in an infectious node
α_1	Rate of susceptible node become infected
α_2	Rate of susceptible node become dead
α_3	Rate of infected node become dead
α_4	Rate of infected node become recovered
α_5	Rate of recovered node become susceptible
α_6	Rate of recovered node become dead

4.4 SEIRD Model

The researchers in [32] introduced a Susceptible-Exposed-Infectious-Recovered-Dead (SEIRD) model established by epidemic theory. This model examined the spread of malware and developed strategies to control its propagation. The SEIRD model includes a system of differential equations that describe the relationship between various states of sensor nodes. The impact of early malware detection in WSN is elucidated by the revealed status in [32]. Early detection benefits in managing the spread of malware. Figure 5 depicts the transitional state of the sensor node.

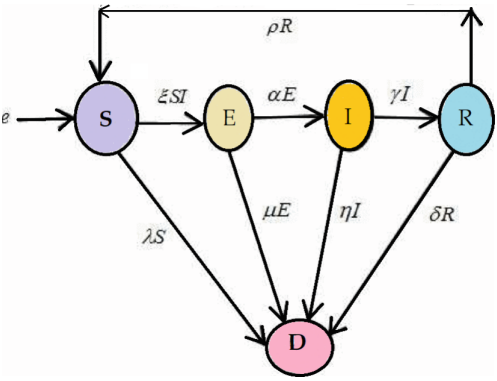

Fig. 5. Transition state diagram of the SEIRD model [32]

$$\begin{cases} \dfrac{dS}{dt} = e - \xi SI - \lambda S + \rho R, \\ \dfrac{dE}{dt} = \xi SI - (\mu + \alpha)E, \\ \dfrac{dI}{dt} = \alpha\, E - (\gamma + \eta)I, \\ \dfrac{dR}{dt} = \gamma\, I - (\delta + \rho)\, R, \\ \dfrac{dD}{dt} = \delta\, S + \mu\, E + \eta\, I + \delta\, R, \end{cases} \tag{4}$$

where $\xi = \frac{q^2}{L^2}\beta K$ and e is the constant rate at which new sensor nodes enter WSN. This proposed model includes five states: S(t), E(t), I(t), R(t), and D(t). The parameters used in model formulation are defined in Table 5.

Table 5. Present parameters for SEIRD model

Parameters	Description
K	The average number of malware present in each infected nodes
λ	Rate of Dead nodes
α	Rate of exposed node become infected
μ	Rate of exposed node become dead
γ	Recovery rate of infected node
η	Dead rate of infected node
ρ	Rate of recovered node become susceptible
δ	Rate of recovered node become dead

4.5 SEIVR Model

Therefore, a defense mechanism is necessary for protecting the WSN from malware attacks. To accomplish this goal, the authors in [33] introduced the Susceptible-Exposed-Infectious-Vaccinated-Recovered (SEIVR) model. The SEIVR model, based on epidemic theory, contains fractional differential equations. The SEIVR model considers two distinct infectious states of the sensor nodes. The states referred to are the "exposed state sensor node" and the "Infectious state sensor node." Malware transfers crucial data from one active sensor node to another in a WSN network. The suggested model provided a method to detect transitions of sensor nodes from a susceptible state to an infected state. This detection offers an opportunity to include additional methods for managing the sensor nodes and stabilizing WSNs under different situations. The SEIVR model investigated the dynamics of worm propagation in WSNs, with its transition state diagram depicted in Fig. 6. A set of differential equations is used to analyze the transmission dynamics of malware and the changing state of sensor nodes. The set of equations are expressed in the following form:

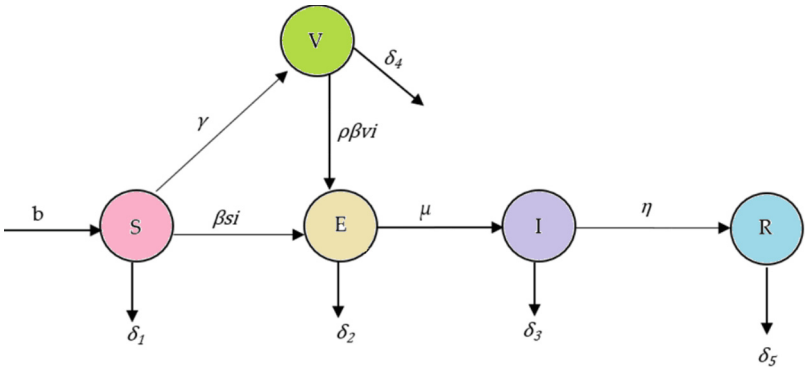

Fig. 6. Transition state diagram of the SEIVR model [33]

$$\begin{cases} \dfrac{dS}{dt} = b - \beta SI - (\sigma_1 + \lambda)S, \\ \dfrac{dE}{dt} = \beta SI + \rho\beta VI - (\sigma_2 + \eta)E, \\ \dfrac{dI}{dt} = \mu E - (\sigma_3 + \eta)I, \\ \dfrac{dV}{dt} = \lambda S - \rho\beta VI - \sigma_4 V, \\ \dfrac{dR}{dt} = \eta I - \sigma_5 R. \end{cases} \tag{5}$$

The total number of sensor nodes in a WSN at any given time t is categorized into five distinct states: $S(t)$, $V(t)$, $E(t)$, $I(t)$, and $R(t)$. The parameters used in model formulation are defined and explained in Table 6.

Table 6. Present parameters for SEIVR model

Parameters	Description
b	Susceptible rate
β	Vaccinated rate
μ	Rate of exposed node become infected
ρ	Rate of effectiveness vaccination
η	Recovery rate of Infected node
σ_1	Mortality rate of susceptible nodes
σ_2	Mortality rate of exposed nodes
σ_3	Mortality rate of infected nodes
σ_4	Mortality rate of vaccinated nodes
σ_5	Mortality rate of recovered nodes

5 Selected Example of One of the Models

In this section, a specific model example is chosen for analyzing stability and R_0 to evaluate the system. This section examines the SEIRD model described in [32] that relates to the spread of malware in WSN. The simulation findings are depicted in Figs. 7 and 8, representing the state of several categories of users in a WSN over time t. These categories include S, E, I, R, and D individuals.

- **Case 1**: Consider $L = 600, e = 0.38, K = 5, \alpha = 0.02, \beta = 0.03,\ \rho = 0.13, \lambda = 0.00005, \mu = 0.0004, \gamma = 0.07, q = 10, \eta = 0.006, \delta = 0.0004$. For $t = 0$, the values of $(S(0), E(0), I(0), R(0), D(0)) = (10000, 1, 1, 0, 0)$ respectively. In this case, $R_0 = 4.084967$. As Fig. 7 illustrates, malware continues to exist on the network if $R0 > 1$. Additionally, Fig. 7 shows that at first, the number of sensor nodes rises to a maximum value, decreases, and stabilizes as time passes. Other sensor network parameters similarly affect the maximum number of sensor nodes in the corresponding states. It discovered that the number of dead nodes rises linearly as sensor nodes' energy runs out.
- **Case 2**: Consider $L = 600, e = 0.3, K = 4, \alpha = 0.02, \beta = 0.03,\ \rho = 0.13, \lambda = 0.00005, \mu = 0.0004, \gamma = 0.07, q = 10, \eta = 0.006, \delta = 0.0004$. For $t = 0$ the values of $(S(0), E(0), I(0), R(0), D(0)) = (10000, 1, 1, 0, 0)$ respectively. As shown in Fig. 8, the number of sensor nodes in various stages varies over time. It is discovered that, at first, node state changes occur pretty slowly. Nevertheless, as time passes and reaches its maximum value, the number of nodes in the exposed, infected, and recovery states begins to decrease and eventually reaches zero. Figure 8 illustrates how, as sensor nodes' energy runs out, the number of dead nodes rises linearly while susceptible nodes are stable. In this case, $R_0 = 0.951837$. It has been noted that the virus gets eliminated from the WSN if $R0 < 1$. Therefore, in worm-free equilibrium, the system will be asymptotically stable.

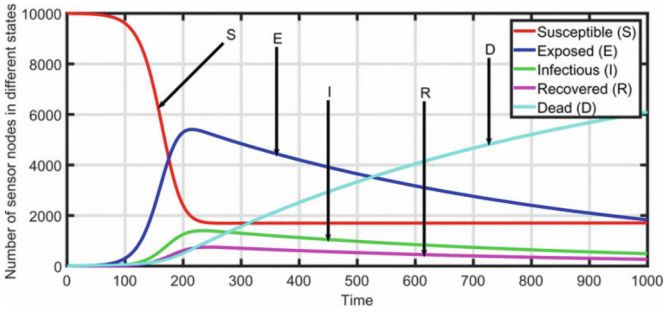

Fig. 7. The status of users in WSN when $R_0 > 1$ (case1) [32].

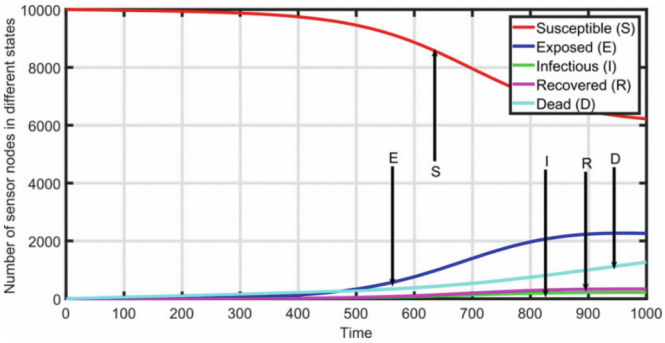

Fig. 8. The status of users in WSN when $R_0 < 1$ (case2) [32].

6 Conclusion

This work has provided an overview of the latest developments in research relative to malware propagation in WSN. This study analyzes epidemic models for the propagation of malware in WSNs. The majority of these systems are demonstrated to be based on ODE systems. As a result, neither individual characteristics nor the local interactions among the network parts are considered. Malware harms user computer systems by illegally acquiring personal and confidential information and compromising or turning off our security mechanisms. This study discussed the strategies that security researchers use to address these threats. The survey article explained several propagation techniques. This research analyzes the present status of global models used to simulate malware propagation in WSNs. Several models for WSNs have enhanced existing models of malware spread on the Internet by restricting the range of worm dissemination. Despite abundant studies and findings, numerous tasks still need to be accomplished.

Acknowledgements. This work was partially supported by project SERICS (PE00000014) under the NRRP MUR program funded by the EU - NGEU.

References

1. Khan, S., Pathan, A.S.K., Alrajeh, N.A.: Wireless Sensor Networks: Current Status and Future Trends. CRC Press, Boca Raton (2013)
2. Akyildiz, I.F., Su, W., Sankarasubramaniam, Y., Cayirci, E.: Wireless sensor networks: a survey. Comput. Netw. **38**, 393–422 (2002)
3. Pathan, A.S.K., Lee, H.W., Hong, C.S.: Security in wireless sensor networks: issues and challenges. In: Proceedings of the 8th IEEE ICACT, vol. 2, pp. 1043–1048 (2006)
4. Perrig, A., Stankovic, J., Wagner, D.: Security in wireless sensor networks. Commun. ACM **47**, 53–57 (2004)

5. D'Angelo, G., Farsimadan, E., Ficco, M., Palmieri, F., Robustelli, A. Privacy-preserving malware detection in Android-based IoT devices through federated Markov chains. Future Gener. Comput. Syst. **148**, 93–105 (2023). https://doi.org/10.1016/j.future.2023.05.021
6. D'Angelo, G., Ficco, M., Palmieri, F.: Association rule-based malware classification using common subsequences of API calls. Appl. Soft Comput. **105**, 107234 (2021). https://doi.org/10.1016/j.asoc.2021.107234
7. D'Angelo, G., Farsimadan, E., Palmieri, F.: Recurrence plots-based network attack classification using CNN-autoencoders. In: Gervasi, O., et al. (eds.) ICCSA 2023. LNCS, vol. 14105, pp. 191–209. Springer, Heidelberg (2023). https://doi.org/10.1007/978-3-031-37108-0_13
8. Abu-Zaideh, S., Snober, M.A., Al-Haija, Q.A.: Smart boosted model for behavior-based malware analysis and detection. In: Joby, P.P., Balas, V.E., Palanisamy, R. (eds.) IoT Based Control Networks and Intelligent Systems. Lecture Notes in Networks and Systems, vol. 528, pp. 803–813. Springer, Singapore (2023). https://doi.org/10.1007/978-981-19-5845-8_58
9. Conti, M.: Secure Wireless Sensor Networks: Threats and Solutions. AIS, vol. 65. Springer, New York (2015). https://doi.org/10.1007/978-1-4939-3460-7
10. Feng, L., Song, L., Zhao, Q., Wang, H.: Modeling and stability analysis of worm propagation in wireless sensor network. Math. Prob. Eng. **2015**, Article ID 129598, 8 (2015). https://doi.org/10.1155/2015/129598
11. Hu, J., Song, Y.: The model of malware propagation in wireless sensor networks with regional detection mechanism. Commun. Comput. Inf. Sci. **501**, 651–662 (2015)
12. Sen, J.: A survey on wireless sensor network security. Int. J. Commun. Netw. Inf. Secur. **1**, 55–78 (2009)
13. Yang, Y., Zhu, S., Cao, G.: Improving sensor network immunity under worm attacks: a software diversity approach. In: Proceedings of ACM International Symposium on Mobile Ad Hoc Networking and Computing, pp. 149–158 (2008)
14. Guo, W., Zhai, L., Guo, L., Shi, J.: Worm propagation control based on spatial correlation in wireless sensor network. In: Wang, H., Zou, L., Huang, G., He, J., Pang, C., Zhang, H.L., Zhao, D., Yi, Z. (eds.) APWeb 2012. LNCS, vol. 7234, pp. 68–77. Springer, Heidelberg (2012). https://doi.org/10.1007/978-3-642-29426-6_10
15. Shengjun, W., Junhua, C.: Modeling the spread of worm epidemics in wireless sensor networks. In: 5th International Conference on Networking and Mobile Computing in Wireless Communications, pp. 1–4 (2009)
16. Queiruga-Dios, A., Hernández Encinas, A., Martín-Vaquero, J., Hernández Encinas, L.: Malware propagation models in wireless sensor networks: a review. In: Graña, M., López-Guede, J.M., Etxaniz, O., Herrero, Á., Quintián, H., Corchado, E. (eds.) SOCO/CISIS/ICEUTE -2016. AISC, vol. 527, pp. 648–657. Springer, Cham (2017). https://doi.org/10.1007/978-3-319-47364-2_63
17. De, P., Das, S.K.: Epidemic Models, Algorithms, and Protocols in Wireless Sensor and Ad Hoc Networks. Wiley, New York (2008)
18. Shen, S., Li, H., Han, R., et al.: Differential game-based strategies for preventing malware propagation in wireless sensor networks. IEEE Trans. Inf. Forensic Secur. **9**(11), 1962–1973 (2014)
19. Zhu, L., Zhao, H.: Dynamical analysis and optimal control for a malware propagation model in an information network. Neurocomputing **149**, 1370–1386 (2015)
20. Fadel, E., et al.: A survey on wireless sensor networks for smart grid. Comput. Commun. **71**(1), 22–33 (2015)

21. Ojha, T., Misra, S., Raghuwanshi, N.S.: Wireless sensor networks for agriculture: the state-of-the-art in practice and future challenges. Comput. Electron. Agric. **118**, 66–84 (2015)
22. De, P., Liu, Y., Das, S.K.: An epidemic theoretic framework for vulnerability analysis of broadcast protocols in wireless sensor networks. IEEE Trans. Mob. Comput. **8**(3), 413–425 (2009)
23. De, P., Liu, Y., Das, S.K.: Deployment-aware modeling of node compromise spread in wireless sensor networks using epidemic theory. ACM Trans. Sensor Netw. **5**(3), 1–33 (2009)
24. Mishra, B.K., Keshri, N.: Mathematical model on the transmission of worms in Wireless Sensor Network. Appl. Math. Model. **37**(6), 4103–4111 (2013)
25. Ojha, R.P., Sanyal, G., Srivastava, P.K.: Pre-vaccination and quarantine approach for defense against worms propagation of malicious objects in wireless sensor networks. Int. J. Inf. Syst. Model. Des. (IJISMD) **9**(1), 01–20 (2018)
26. Haghighi, M.S., Wen, S., Xiang, Y., Quinn, B., Zhou, W.: On the race of worms and patches: modeling the spread of information in wireless sensor networks. IEEE Trans. Inf. Forensics Secur. **11**(12), 2854–2865 (2016)
27. Kermack, W.O., McKendrick, A.G.: A contribution to the mathematical theory of epidemics. Proc. R. Soc. London **115**, 700 (1927)
28. Khayam, S.A., Radha, H.: Using signal processing techniques to model worm propagation over wireless sensor networks. IEEE Signal Process. Maga. **23**(2), 164–169 (2006)
29. Zou, C.C., Towsley, D., Gong, W.: Modeling and simulation study of the propagation and defense of internet e-mail worms. IEEE Trans. Depend. Secure Comput. **4**, 105–118 (2007)
30. Kim, J., Radhakrishnan, S., Dhall, S.K.: Measurement and analysis of worm propagation on Internet network topology. In: Proceedings of IEEE International Conference on Computer Communications and Networks, Chicago, Illinois, USA, pp. 495–500 (2004)
31. Xiaoming, W., Yingshu, L.: An improved SIR model for analyzing the dynamics of worm propagation in wireless sensor networks. Chin. J. Electron. **18**(1), 8–12 (2009)
32. Biswal, S.R., Swain, S.K.: Model for study of malware propagation dynamics in wireless sensor network. In: 3rd International Conference on Trends in Electronics and Informatics (ICOEI), Tirunelveli, India, pp. 647–653 (2019). https://doi.org/10.1109/ICOEI.2019.8862736.
33. Srivastava, V., et al.: Generalized defensive modeling of malware propagation in WSNs using Atangana-Baleanu-Caputo (ABC) fractional derivative. IEEE Access **11**, 49042–49058 (2023). https://doi.org/10.1109/ACCESS.2023.3276351
34. Zhou, H., Shen, S., Liu, J.: Malware propagation model in wireless sensor networks under attack-defense confrontation. Comput. Commun. **162**, 51–58 (2020). https://doi.org/10.1016/J.COMCOM.2020.08.009
35. Shen, S., Zhou, H., Feng, S., Liu, J., Zhang, H., Cao, Q.: An epidemiology-based model for disclosing dynamics of malware propagation in heterogeneous and mobile WSNs. IEEE Access **8**, 43876–43887 (2020). https://doi.org/10.1109/ACCESS.2020.2977966
36. Zhang, H., Yang, S., Wu, G., Shen, S., Cao, Q.: Steady-state availability evaluation for heterogeneous edge computing-enabled WSNs with malware infections. Mobile Inf. Syst. **2022**, 1–16 (2022). https://doi.org/10.1155/2022/4743605



Comparative Analysis of AI-Based Methods for Enhancing Cybersecurity Monitoring Systems

Federica Uccello[1(✉)], Marek Pawlicki[2], Salvatore D'Antonio[1], Rafał Kozik[2], and Michał Choraś[2]

[1] University of Naples 'Parthenope' Centro Direzionale, Isola C4, 80133 Napoli, Italy
federica.uccello@assegnista.uniparthenope.it, salvatore.dantonio@uniparthenope.it

[2] Bydgoszcz University of Science and Technology,, PBS Bydgoszcz, Poland
chorasm@pbs.edu.pl

Abstract. Traditional security monitoring systems may struggle with detecting advanced and novel cyber threats, especially as cyberattacks are becoming more sophisticated. As a consequence, there is a growing need for advanced techniques to improve defense mechanisms. Among these, Artificial Intelligence (AI) has emerged as a promising solution. The paper explores the growing popularity of AI technologies in cybersecurity and investigates three distinct methodologies aimed at improving attack detection criteria within security monitoring systems. The first methodology is based on the extraction and analysis of correlation indexes between features and target variables, enabling the identification of recurring patterns indicative of anomalies. Secondly, Association Rule Mining (ARM) is utilized to identify hidden patterns and relationships between features, leading to more accurate detection criteria. Lastly, explainable AI (xAI) is leveraged to mine advanced rules, as well as increase the transparency of the model, enabling security analysts to understand the decision-making process behind threat detection. Through a comparative analysis, the efficacy of each method is evaluated in terms of detection accuracy, precision, recall, and F1-score. Promising experimental results demonstrate the potential of AI-driven approaches to enhance the capabilities of security monitoring systems, providing organizations with a new layer of protection against an evolving threat landscape.

Keywords: Explainable Artificial Intelligence · Association Rule Mining · Rule-Based SIEM · Attack Detection

1 Introduction

Cybersecurity has become one of the most important fields in today's digital landscape, as the recent technological advancement has pushed virtually any system to move towards an Information Technology (IT) paradigm, where data has become one of the most critical assets. Together with multiple benefits, this

© The Author(s), under exclusive license to Springer Nature Switzerland AG 2024
O. Gervasi et al. (Eds.): ICCSA 2024 Workshops, LNCS 14816, pp. 100–112, 2024.
https://doi.org/10.1007/978-3-031-65223-3_7

revolution has brought increasingly sophisticated cyber-actors [1] and cyber-threats [2], which can lead to disastrous consequences, as underlined by the European Commission in the European Data Strategy [3].

Therefore, enabling rapid attack detection remains a priority, and tools like Security Information and Event Management (SIEM) and Intrusion Detection Systems (IDS) stand as well-established solutions within a comprehensive monitoring and threat protection strategy [4].

However, attackers continuously evolve tactics to exploit vulnerabilities in digital systems [5]. The ever growing evolution of attack techniques require constant effort in enhancing traditional security monitoring, which often struggle to keep up with the changing requirements [6–8]. To respond to these concerns, there has been an increasing interest in featuring Artificial Intelligence (AI) and Machine Learning (ML) techniques to enhance defense mechanisms [9].

The present work seeks to investigate and compare three distinct methodologies aimed at enhancing attack detection criteria within security monitoring systems. The major contribution of the paper include:

- Usage of Correlation Index Analysis, Association Rule Mining (ARM), and Explainable AI (xAI) to mine advanced correlation criteria for SIEM.
- Testing of the mined correlation rules to discriminate Malicious and Benign network traffic.
- Evaluation of the rules in terms of Precision, Recall, F1-score and Accuracy.
- Comparison between the three different approaches, based on the experimental results.

The remainder of the paper is organised as follows: Sect. 2 overviews the related work. Section 3 presents the methods employed, including the SIEM and the AI techniques involved. Section 4 details the proposed methodology for advanced rules extraction, while Sect. 5 showcases the experimental setup and the results, comparing the performance of the different methods. The results are discussed in higher detail in Sect. 6. Finally, Sect. 7 concludes the paper.

2 Related Work

Recent advancements in ML, ARM, xAI have shown promise in augmenting security measures. Various studies have explored the application of these techniques in cybersecurity, highlighting their potential to improve threat detection accuracy and efficiency.

In particular, the enhancement of SIEM through ML and AI has been subject of various research [10–12], with the main goals to robust security measures and provide optimization. The concept of hybrid IDS has also been explored in various domains [13,14], including the Internet of Things (IoT) [15,16]. The potential of ML-enabled Network Intrusion Detection System (NIDS) is also explored in [17].

ARM is a data mining technique that allows to uncover hidden relationships within dataset's features. The literature shows several applications of ARM as

a toolkit for the enhancement of cyber incident detection. As an instance, the integration of associative rules in SIEM systems is investigated in [18]. The work shows an approach incorporating fuzzy sets theory and data mining techniques to construct associative rules based on an analysis of cyber incidents. Sequential rule mining is featured in [19] to analyse intrusion detection alerts, with the goal to reduce the amount of alerts received by security personnel. Similarly, [20] addresses the issue of false positive alerts in IDS using Modified Frequent Pattern (MFP-Tree) with the K-means algorithm to detect a range of attacks. In [21], a method for mining association rules from logs to identify intrusion behavior in cloud platforms is introduced.

Within AI, xAI methods aim to provide human-understandable explanations of ML models, to improve model transparency, robustness, and user trust. The usage of xAI in security has been discussed, among the others, in [22,23], where it is employed to enhance IDS with a focus on transparency. Trust management in IDS is the main concern of [24], where the need for transparency in ML models utilized in the cybersecurity domain is discussed. Therefore, the usage of xAI techniques such as decision tree algorithms, is proposed to enhance trust in IDS. Boosting detection accuracy and maintaining data integrity is the core focus of [25], where an evaluation within various intrusion scenarios is presented. The work aims at identifying key network features contributing to intrusion. The detection of attacks based on xAI has been also studied in [26]. The work leverages autoencoders and xAI to identify the most influential features for attack detection. Then, individual thresholds are set for such features to support attack detection.

With respect to the literature, the present work seeks to enhance traditional SIEM systems by the exploration and comparison of three AI techniques to mine advanced and highly accurate correlation criteria. The proposed methodology has the advantage of being versatile and suitable for various application domains, as it can be generalised and employed within wider scopes.

3 Innovative Methods for Improving SIEM

This section provides an overview of the SIEM system and AI techniques employed throughout the research.

3.1 Security Information and Event Management

Within the present work, SIEM systems serve as the base framework for the development and testing of the proposed hybrid SIEM, enhanced through the definition of AI-powered detection criteria. In general, SIEM systems consist of essential modules and key functionalities that can be schematized as follows:

– Data collection agent: this module is composed by one or more probes in charge of gathering data from heterogeneous sources. IDS can also be a used as a part of this set. If needed, this module can be connected to another one dedicated to parsing and normalization.

- Event correlation engine: this component acts as a kernel for the SIEM, as it correlates the data collected and raises alerts in case of anomalies.
- Historical Database/Log storage: an essential module for the storage of relevant data.
- User Interface: this module is usually connected to the storage one, and it can be used for monitoring and reporting. It can include dashboards to display information in user friendly way.

Event correlation is a crucial functionality and, traditionally, it follows a rule-based logic, consisting in identifying patterns or sequence that might be symptoms of potential threats. The correlation rules are typically crafted based on domain knowledge, known attack patterns, and heuristic analysis. However, this process of defining rules can lead to inaccurate criteria, especially when dealing with advanced and novel threats. This work extends the SIEM presented in the authors' previous research [27], with the goal to address such limitations. The SIEM was fed with simulated traffic, generated based on the considered datasets (Sect. 5), and the various correlation rules defined through AI techniques were tested and evaluated as shown in the following sections.

3.2 Correlation Index Analysis

The first approach for the generation of SIEM rules was the simplest one, based on Correlation Index Analysis. The goal was to identify the most relevant features associated with malicious behavior within the considered datasets and uncover patterns and relationships between various dataset features and the target label.

To perform the analysis, the correlation index between each dataset feature and the target label was calculated, focusing on malicious samples. The feature with the highest correlation index was selected for inclusion in the correlation rules, due to its strong association with Malicious behavior. Following the analysis, the correlation logic was defined by defining individual thresholds for the most correlated features.

3.3 Association Rule Mining

Subsequently to the previous approach, ARM was used to mine more advanced discrimination criteria. The purpose of ARM is to discover hidden patterns and relationships within datasets, and its application to the present research focused on the APRIORI algorithm [28].

APRIORI is a well-known algorithm for association rule discovery: it was applied to the preprocessed datasets to mine relationships between multiple features. In comparison to the Correlation Index Analysis approach, the APRIORI derived rules provide more detailed insights into the behaviors and patterns associated with network traffic, in particular with anomalous one.

3.4 Explainable Artificial Intelligence

The third method for the generation of discrimination criteria was xAI. In the literature, the most well-known xAI approaches include feature importance, rule-based explanations, and counterfactual explanation. These methods can help professionals understand how ML models are making decisions, as well as identifying potential biases in the models and supporting debugging problems that could arise. In addition, xAI can be employed to identify the most important features for the model's predictions.

Within the present experiment, multiple methods and criteria to build rules were considered. Ultimately, enhanced rules were mined through SHapley Additive exPlanations (SHAP) [29] and ANCHORS [30]. In the next section, all the aforementioned methods for rule extraction are formalized and detailed.

4 Proposed Approach for SIEM Rules Definition

The entire selection of AI techniques for rule definition were preceded by common initial steps.

At first, appropriate network traffic datasets D_1 and D_2 were selected (Sect. 5). To ensure quality and suitability of the datasets, and consistency among them, essential data preprocessing steps were conducted: this included handling missing values, removing duplicates, and addressing class imbalance issues. To formalize the following approach, let $X = x_1 , ... , x_n$ represent the set of features in the generic dataset D_i, and let $y = \{Malicious, Benign\}$ be the corresponding labels. The aim is to identify a set of x_{rule} and use them to build discrimination criteria between Malicious and Benign samples. Table 1 and Table 2 provide a short definition of the features involved in the definition of the set of rules for D_1 and D_2, respectively.

Table 1. D_1 Features selected for the definition of detection rules.

Feature	Description
Bwd Packet Length Mean	It stands for the mean packet length observed in the backward direction (from destination to source) in the flow. It provides direction-specific insights.
Fwd Packet Length Mean	It represents the average length of packets in the forward direction (from source to destination) in the flow.
Destination Port	This feature indicates the port number used by the destination in the network flow. It can help identifying specific services or applications involved in the communication.
Total Backward Packets	This feature represent the total number of packets transmitted in the backward direction during the flow.
Flow Duration	It refers to the time duration of a network flow

Table 2. D_2 Features selected for the definition of detection rules.

Feature	Description
Source Rate	It denotes the rate at which data packets are transmitted from the source.
Protocol	This feature specifies the communication protocol utilized in the network. It is useful for identifying different types of network traffic.
Source Loss	It indicates the percentage of data packets lost during transmission from the source. Monitoring source loss helps in assessing network reliability and identifying potential issues.
Destination Loss	The percentage of data packets lost during transmission to the destination.
TCP RTT	The TCP connection setup round-trip time

4.1 Rules Derived Through Correlation Index Analysis

As explained previously, linear correlation analysis has been performed between the dataset features and the target label, referred to as malicious samples. Let C be the correlation index and x_i be the ith feature in the dataset. The linear correlation analysis selects the feature x_i with the highest correlation index, as shown in Eq. 1:

$$j = argmax_i(C(f_i, target_{label})) \tag{1}$$

After the analysis, the features with the highest correlation index were selected and used for the creation of the correlation rules. The present method led to the creation of the rules formalized in Eq. 2 and Eq. 3, which were the best one defined using this method. In the equations, $BPLengthMean$ denotes the mean packet length observed in the backward direction, while $SrcRate$ represents the source packets per second. The criteria for the definition of the thresholds are explained in Sect. 5.

$$y_{corr} = \begin{cases} Malicious\ if\ BPLengthMean \geq T_{BPLengthMean} \\ Benign \qquad\qquad\qquad otherwise \end{cases} \tag{2}$$

$$y_{corr} = \begin{cases} Malicious\ if\ SrcRate \geq T_{SrcRate} \\ Benign \qquad\qquad\qquad otherwise \end{cases} \tag{3}$$

4.2 Rules Derived Through Association Rule Mining

To mine more advanced correlation rule, the APRIORI algorithm was applied to the datasets. As a result, the criteria shown in Eq. 4 and Eq. 5 were the best

one defined using this method. In the equations, $FPLengthMean$ denotes the mean packet length observed in the forward direction, while $DstRate$ represents the destination packets per second.

$$y_{arm} = \begin{cases} Malicious\ if\ BPLengthMean \geq TM_1 \times FPLengthMean \\ Benign \qquad\qquad otherwise \end{cases} \tag{4}$$

$$y_{arm} = \begin{cases} Malicious\ if\ SrcRate > TM_2 * DstRate \\ Benign \qquad\qquad otherwise \end{cases} \tag{5}$$

4.3 Rules Derived Through Explainable Artificial Intelligence

The third and last method involved the usage of xAI techniques to define more complex detection rules. The criteria shown in Eq. 6 and Eq. 7 were the best ones defined using this method. In Eq. 6, $DestPort$ denotes the destination port, $TotBWDP$ the total number of backward packets, and $FlowDuration$ the time duration of network flow. mean packet length observed in the forward direction, while $DstRate$ represents the destination packets per second. In Eq. 7, $Protot$ denotes the network protocol, $SrcLoss$ and $DstLoss$ the Source/Destination packets respectively that are re transmitted and/or dropped, while $TcpRtt$ indicates the TCP connection setup round-trip time.

$$y_{xAI} = \begin{cases} Benign \quad if \quad DestPort \in Whitelist \\ Malicious\ if \quad TotBWDP \leq T_{TPL} \\ \qquad\qquad\qquad or \\ \qquad\qquad FlowDuration > T_{FlowDuration} \\ Benign \qquad\qquad otherwise \end{cases} \tag{6}$$

$$y_{xAI} = \begin{cases} Benign \quad if \quad Proto \in Whitelist \\ Malicious\ if\ SrcLoss > DstLoss \\ \qquad\qquad\qquad or \\ \qquad\qquad TcpRtt < \epsilon \\ Benign \qquad\qquad otherwise \end{cases} \tag{7}$$

In the next section, the experiment setup and the performance evaluations for the three methods are detailed.

5 Experimental Setup and Results

5.1 Datasets

Within the present experiments, two datasets have been employed. The fist one is the CICIDS2017 [31], a well-recognised benchmark dataset designed for evaluating IDS against sophisticated and evolving network attacks. The choice of this dataset was motivated by its careful addressing of the flaws of other datasets,

which might suffer from outdated information, lack of diversity and anonymization of critical data. In addition, the methodology was tested using a more recent and specialised dataset, the WUSTL-IIOT-2021 [32], meant to emulate real-world industrial systems.

Essential data preprocessing steps were conducted to ensure the quality and suitability of the datasets. This included handling missing values, removing duplicates, and addressing class imbalance issues by selecting an equal number of Benign and Malicious samples for each dataset. For dimensionality reduction, the SelectKBest feature selection method from the scikit-learn library was employed. SelectKBest utilizes univariate statistical tests, such as ANOVA F-value, to identify the most relevant features for the analysis. Afterwards, the datasets were employed to simulate real-time network traffic to feed to the SIEM, once the last column representing the label was removed. Then, the SIEM rules were employed to label the simulated traffic as Benign or Malicious, and the performance of the detection was evaluated by comparison with the ground truth.

5.2 Parameter Settings

During the process to define correlation rules, the threshold values and parameters were derived from the statistical properties of the selected features and the discovered criteria.

In Eq. 2 and Eq. 3, the thresholds $T_{BPLengthMean}$ and $T_{SrcRate}$ have been set equal to the mean value of the selected feature for all the samples of the original dataset.

To define a suitable value for the TM_1 and TM_2 parameters shown in Eqs. 4 and 5, multiple approaches have been considered. Ultimately, the optimal value for TM_1 has been obtained by calculating the average $BPLengthMean$ to $FPLengthMean$ ratio for Malicious instances. Similarly, TM_2 has been set equal to the average $SrcRate$ to $DstRate$ ratio for Malicious instances.

In Eq. 6), the thresholds T_{TPL} ans $T_{FlowDuration}$ were calculated using the same logic employed for $T_{BPLengthMean}$ and $T_{SrcRate}$. The $Whitelist$ and $Blacklist$ have been derived checking the exclusive values of $DestinationPort$ for Benign and Malicious labels, respectively. The $Whitelist$ parameter from Eq. 7 has been derived using a similar criteria, but considering the $Prot$ feature instead. Finally, the ϵ parameter is defined as shown below (Eq. 8):

$$\epsilon \rightarrow 0 \tag{8}$$

This value has been selected as threshold for the $TcpRtt$ feature, as it has been observed that this feature was close to zero, on average, for Malicious samples only.

5.3 Results

The following tables show a summary of the classification report based on Precision (9), Recall (10), F1-Score (11), and Accuracy (12). In the following equations, for the sake of brevity, True Positive (TP), True Negative (TN), False Positive (FP) and False Negative (FN) are denoted using the acronyms.

$$\text{Precision} = \frac{\text{TP}}{\text{TP} + \text{FP}} \tag{9}$$

$$\text{Recall} = \frac{\text{TP}}{\text{TP} + \text{FN}} \tag{10}$$

$$\text{F1 Score} = 2 \times \frac{\text{Precision} \times \text{Recall}}{\text{Precision} + \text{Recall}} \tag{11}$$

$$\text{Accuracy} = \frac{\text{Number of Correct Predictions}}{\text{Total Number of Predictions}} \tag{12}$$

Table 3. Performance report of SIEM rules derived through Correlation Index Analysis.

Correlation Rules	Precision		Recall		F1-score		Accuracy
	Benign	Malicious	Benign	Malicious	Benign	Malicious	
Equation 2	0.73	0.98	0.98	0.63	**0.84**	0.76	**0.77**
Equation 3	0.62	**0.99**	**0.99**	0.49	0.77	0.57	0.70

Table 4. Performance report for SIEM rules derived through ARM.

Correlation Rules	Precision		Recall		F1-score		Accuracy
	Benign	Malicious	Benign	Malicious	Benign	Malicious	
Equation 4	**1**	0.99	0.99	**1**	**0.99**	**0.99**	**0.99**
Equation 5	0.90	0.98	0.98	0.90	0.94	0.94	0.94

Table 5. Performance report for SIEM rules derived through xAI.

Correlation Rules	Precision		Recall		F1-score		Accuracy
	Benign	Malicious	Benign	Malicious	Benign	Malicious	
Equation 6	**1**	0.96	0.96	**1**	0.98	0.98	0.98
Equation 7	**1**	0.99	0.99	**1**	**0.99**	**0.99**	**0.99**

6 Discussion

As shown in the Tables, the different rules implemented present varying degrees of performance. Table 3 suggest a potential trade-off between precision and recall in the SIEM rules derived though simple Correlation Index Analysis. The performance metrics of the both rules, while providing a baseline for correlation, reveal the need for further refinement, as denoted by the Accuracy values.

The ARM approach, as depicted in Table 4, demonstrates a significant advancement in the system's discriminatory power. ARM allows to discover association rules that significantly contribute to the identification of Malicious traffic. In particular, Eq. 4 exhibits high Precision, Recall, F1-Score, and Accuracy, indicating a near-perfect performance in distinguishing between Benign and Malicious instances The effectiveness of ARM rules can be attributed to their ability to capture intricate relationships and dependencies within the network traffic data. The discovered patterns empower the intrusion detection system to make more informed decisions, leading to a substantial improvement in its overall performance.

The xAI approach, represented in Table 5, offers a unique perspective on correlation rules. The interpretability of the rules derived through xAI techniques enhances the system's transparency and facilitates a deeper understanding of the decision-making process. Both Eq. 6 and Eq. 7 showcase near-perfect Precision, Recall, F1-Score, and Accuracy. Additionally. Both xAI rules show balance between Precision and Recall, highlighting the superior potential of xAI techniques in comparison to the previous approaches. the xAI rules provide human-understandable insights into the features and patterns contributing to the decision-making process.

The comparison of the three approaches reveals a progressive refinement in the system's performance. The SIEM rules derived through correlation analysis provide a baseline, while the ARM and xAI approaches contribute advanced correlation rules that significantly enhance the system's ability to discern between Benign and Malicious traffic.

7 Conclusion

The paper explores the application of AI techniques in enhancing attack detection within security monitoring systems. Three distinct methodologies were investigated: Correlation Index Analysis, ARM, and xAI. Each method was employed to derive correlation rules aimed at improving the discrimination between Benign and Malicious network traffic within a rule-based SIEM system.

Through a comparative analysis of the experimental results, it was observed that each approach brings a different perspective in enhancing the capabilities of security monitoring systems. The Correlation Index Analysis method provides a straightforward approach to identifying correlation between features and target labels. While it offers a baseline for correlation rules, its performance may be limited in capturing complex relationships within the data.

On the other hand, ARM enables the discovery of intricate patterns and dependencies within the dataset, leading to more accurate and robust correlation rules. The ARM-derived rules exhibited significant improvement in detection

accuracy, precision, recall, and F1-score compared to Correlation Index Analysis. However, its application might not be as straightforward as the previous one, and it might be more challenging to apply to complex scenarios. Finally, xAI techniques offer human-understandable insights into the decision-making process of the model. The xAI-derived rules demonstrated near-perfect performance metrics, highlighting the superior potential of xAI techniques in enhancing attack detection criteria. Similarly to the ARM approach, this method might also bring challenges with the perspective of more intricate scenarios. Future research directions may involve further exploration of advanced AI techniques and their integration into security monitoring systems, as well as the development of hybrid approaches combining multiple methodologies to enhance detection accuracy and efficiency even further. Additionally, the scalability and real-time implementation of these techniques in large-scale environments might be worth of further investigation for practical deployment within actual systems.

Acknowledgment. This research has received funding from the European Union's Horizon 2020 Research and Innovation Programme under Grant Agreement No 101020560 CyberSEAS, and from the Industrial Cyber Shield (ICS) No C83C22001460001 project funded by INAIL. The content of this publication reflects the opinion of its authors and does not, in any way, represent opinions of the funders. The European Commission and INAIL are not responsible for any use that may be made of the information that this publication contains.

References

1. Pawlicka, A., Choraś, M., Pawlicki, M.: The stray sheep of cyberspace aka the actors who claim they break the law for the greater good. Pers. Ubiquit. Comput. **25**(5), 843–852 (2021)
2. Kozik, R., Choraś, M.: Current cyber security threats and challenges in critical infrastructures protection. In: 2013 Second International Conference on Informatics & Applications (ICIA), pp. 93–97 (2013)
3. E. Commission, A european strategy for data.' https://digital-strategy.ec.europa.eu/en/policies/strategy-data
4. Younus, Z., Alanezi, M.: A survey on network security monitoring: tools and functionalities. Mustansiriyah J. Pure Appli. Sci. **1**(2), 55–86 (2023)
5. Pawlicki, M., Pawlicka, A., Kozik, R., Choraś, M.: The survey and meta-analysis of the attacks, transgressions, countermeasures and security aspects common to the cloud, edge and iot.Neurocomputing, 126533 (2023)
6. Duo, W., Zhou, M., Abusorrah, A.: A survey of cyber attacks on cyber physical systems: recent advances and challenges. IEEE/CAA J. Automatica Sinica **9**(5), 784–800 (2022)
7. Li, Y., Liu, Q.: A comprehensive review study of cyber-attacks and cyber security; emerging trends and recent developments. Energy Rep. **7**, 8176–8186 (2021)
8. Guembe, B., Azeta, A., Misra, S., Osamor, V.C., Fernandez-Sanz, L., Pospelova, V.: The emerging threat of ai-driven cyber attacks: a review. Appl. Artif. Intell. **36**(1), 2037254 (2022)
9. Zhang, Z., et al.: Artificial intelligence in cyber security: research advances, challenges, and opportunities. Artifi. Intell. Rev., 1–25 (2022)

10. Ban, T., Takahashi, T., Ndichu, S., Inoue, D.: Breaking alert fatigue: Ai-assisted siem framework for effective incident response. Appl. Sci. **13**(11), 6610 (2023)
11. Radoglou-Grammatikis, P.: Securecyber: an sdn-enabled siem for enhanced cybersecurity in the industrial internet of things. IEEE COMSOC MMTC Commun. - Front. **18**(2), 2023 (2023)
12. Alturkistani, H., El-Affendi, M.A.: Optimizing cybersecurity incident response decisions using deep reinforcement learning. Inter. J. Electr. Comput. Eng. **12**(6), 6768 (2022)
13. Al, S., Dener, M.: Stl-hdl: a new hybrid network intrusion detection system for imbalanced dataset on big data environment. Comput. Sec. **110**, 102435 (2021)
14. Kim, T., Pak, W.: Real-time network intrusion detection using deferred decision and hybrid classifier. Futur. Gener. Comput. Syst. **132**, 51–66 (2022)
15. Smys, S., Basar, A., Wang, H., et al.: Hybrid intrusion detection system for internet of things (iot). J. ISMAC **2**(04), 190–199 (2020)
16. Narayana Rao, K., Venkata Rao, K., Prasad Reddy, P.V.G.D.: A hybrid intrusion detection system based on sparse autoencoder and deep neural network. Computer Commun. **180**, 77–88 (2021)
17. Kim, T., Pak, W.: Robust network intrusion detection system based on machine-learning with early classification. IEEE Access **10**, 10754–10767 (2022)
18. Subach, I., Mykytiuk, A.: Methodology of formation of fuzzy associative rules with weighted attributes from siem database for detection of cyber incidents in special information and communication systems. Inform. Technol. Sec. **11**(1), 20 (2023)
19. Husák, M., Bajtoš, T., Kašpar, J., Bou-Harb, E., Čeleda, P.: Predictive cyber situational awareness and personalized blacklisting: a sequential rule mining approach. ACM Trans. Manag. Inform. Syst. (TMIS) **11**(4), 1–16 (2020)
20. Sivanantham, S., Mohanraj, V., Suresh, Y., Senthilkumar, J.: Association rule mining frequent-pattern-based intrusion detection in network. Comput. Syst. Sci. Eng. **44**(2) (2023)
21. Lou, P., Lu, G., Jiang, X., Xiao, Z., Hu, J., Yan, J.: Cyber intrusion detection through association rule mining on multi-source logs. Appl. Intell. **51**, 4043–4057 (2021)
22. Patil, S., et al.: Explainable artificial intelligence for intrusion detection system. Electronics **11**(19), 3079 (2022)
23. Zhou, Q., Li, R., Xu, L., Nallanathan, A., Yang, J., Fu, A.: Towards explainable meta-learning for ddos detection,' arXiv preprint arXiv:2204.02255(2022)
24. Mahbooba, B., Timilsina, M., Sahal, R., Serrano, M.: Explainable artificial intelligence (xai) to enhance trust management in intrusion detection systems using decision tree model. Complexity **2021**, 1–11 (2021)
25. Karna, S.K., Paudel, P., Saud, R., Bhandari, M.: Explainable prediction of features contributing to intrusion detection using ml algorithms and lime
26. Kalutharage, C.S., Liu, X., Chrysoulas, C., Pitropakis, N., Papadopoulos, P.: Explainable ai-based ddos attack identification method for iot networks. Computers **12**(2), 32 (2023)
27. Coppolino, L., et al.: Detection of radio frequency interference in satellite ground segments. In: 2023 IEEE International Conference on Cyber Security and Resilience (CSR), pp. 648–653 (2023)
28. Hegland, M.: The apriori algorithm–a tutorial. Math. Comput. Imaging Sci. Inform. Process. 209–262 (2007)
29. Bowen, D., Ungar, L.: Generalized shap: Generating multiple types of explanations in machine learning, arXiv preprint arXiv:2006.07155 (2020)

30. Ribeiro, M.T., Singh, S., Guestrin, C.: Anchors: high-precision model-agnostic explanations. In: Proceedings of the AAAI Conference on Artificial Intelligence, vol. 32 (2018)
31. Sharafaldin, I., Lashkari, A.H., Ghorbani, A.A.: Toward generating a new intrusion detection dataset and intrusion traffic characterization. ICISSp **1**, 108–116 (2018)
32. Zolanvari, M., Teixeira, M.A., Gupta, L., Khan, K.M., Jain, R.: WUSTL-IIOT-2021 Dataset for IIoT Cybersecurity Research (October 2021). http://www.cse.wustl.edu/~jain/iiot2/index.html

A Predictive Model for Phishing Attacks on Mobile Intelligent Agent Systems

Mashako D. Manyama and Okuthe P. Kogeda(✉)

School of Mathematics, Statistics, and Computer Science, University of KwaZulu-Natal, Westville Campus, Durban 4000, Republic of South Africa
KogedaO@ukzn.ac.za

Abstract. Phishing attacks continue to evolve with time and the attackers are always ahead of the existing mitigation plans. The more technology advances, the more sophisticated phishing attacks become. As more people rely on technology to conduct their online businesses, the need for secure Mobile Intelligent Agents (MIAs) systems becomes higher. MIAs are software that execute functions or duties such as managing electronic mail, gathering, and sending out information on behalf of an online user. MIAs play a vital role in carrying out electronic commerce activities whether from business-to-customer, customer-to-customer, or business-to-business. In this paper, we use Decision Tree (DT) to accurately predict the status of a Uniform Resource Locator (URL) and flag those predicted to be phishing. The DT algorithm extract URL features such as the domain name, URL length, host name, page ranking, etc., and feeds them into the model which then makes status prediction. The extracted features are then filtered into the model to improve its future predictions. The proposed model has a prediction accuracy of 91.3% and it is also cost effective as well as easy to use. The other benefit of the proposed solution is its capability to flag phishing URL and prevent a user from launching the web browser thereby protecting their personal information from being stolen by criminals.

Keywords: Agent · Algorithm · Artificial intelligence · Cyber-security · Decision tree · e-commerce · m-commerce · Mobile intelligent agent · Predictive · Prevention · Phishing

1 Introduction

In 2024, the worldwide retail e-commerce sales are estimated to exceed $6.3 trillion (US dollars), and the figure is expected to continue to grow in the coming years [1]. As of 2023, online marketplaces accounted for the largest share of online purchases worldwide. Globally, e-commerce market share accounts for 20.1% of the total retail sales [1]. One of the most contributing factors in the e-commerce growth is the unprecedented usage of mobile devices whereby smartphones account for nearly 80 percent of all retail websites visits worldwide [1]. The usage of mobile devices makes the mobile commerce (m-commerce) much easier for the online customers and it is particularly popular in Asia, with countries like China and South Korea generating more than two-third of their total online sales via mobile devices [1].

© The Author(s), under exclusive license to Springer Nature Switzerland AG 2024
O. Gervasi et al. (Eds.): ICCSA 2024 Workshops, LNCS 14816, pp. 113–128, 2024.
https://doi.org/10.1007/978-3-031-65223-3_8

The research work conducted by [2] reported a potential massive growth opportunity in the digital commerce sector over the next few years particularly in Sub-Saharan Africa whereby the number of Internet users is expected to grow. Such growth is driven mainly by a high number of mobile device users, rising consumer confidence in online transactions, and the expansion of brick-and-mortar retailers into the online sphere by adopting a multi-channel approach [2]. Although the Sub-Saharan Africa (SSA) is the smallest e-commerce region, however, it shows a very strong growth potentials especially since after COVID-19 pandemic that made people to change their shopping behaviour [2].

E-commerce transactions take place using the Internet, which often present an opportunity for online scammers who are always ready to try their luck on unsuspecting e-commerce customers [3, 4]. When performing online transactions, the customers often expose a large amount of their personal information to the merchant or service provider using the Internet, which as a result exposes them to many cyber security attacks. For this reason, a high level of confidentiality and authenticity between the e-commerce stakeholders is always expected [5, 6]. The concept of security and privacy continues to get an enormous amount of attention from the commercial sector since it has got a potential to determine the success of the m-commerce as a new way of shopping [7, 8].

One of the most common cyber security risks to the growth of the m-commerce is phishing attacks aimed at the Mobile Intelligent Agents (MIAs) [9] used to carry out the online business activities on behalf of both the customer and the merchant [10]. The mobile intelligent agents dispatched by the user onto the Internet are the ones interacting with the online shopping system [11], and it is at this moment that they become vulnerable to phishing attacks whilst roaming the Internet [12]. Phishing is a type of cyber-attack used by online scammers to target internet users mainly the e-commerce users with an intention of acquiring personal confidential information through deception [13, 14]. This type of attack involves tracking the potential target by sending spam emails or instant messages with the intention of leading them to a fraudulent website wherein their confidential personal information gets stolen [15]. For example, a phisher may deceive the victim by representing themselves as a particular well-known organization or online shopping outlet despite having no knowledge of the recipient or victim at all [16].

Online businesses across the world continue to be flooded with phishing attacks targeting their employees that are often ill-prepared and under-equipped to process or take necessary actions against such threats [17]. In [18] it is also reported that worldwide organizations are at a higher risk of data breaches with an average monetary loss of over $4.45 million (US dollars) per organization per year. The phishing report [19] titled "Phishing Activities Trends Report 4th Quarter 2022" by an organization called Anti-Phishing Working Group (APWG) reported that the number of global phishing attacks grew slightly in fourth quarter of the year 2022. The organisation observed a total number of 1,350,037 phishing attacks in the fourth quarter from a previous total of 1,270,833 phishing attacks in third quarter of the same year which is a new record high and was the worst quarter that APWG has ever observed.

In this study, we designed and developed a Phishing Predictive Model (PPM) that is used to verify the legitimacy of a URL before launching it on the web browser. We used

the Decision Tree algorithm to train and test our model. To input the URL, we used a mobile application developed in Python and integrated with the decision tree predictive algorithm to return the URL status to the user. Depending on the URL prediction results, the mobile application then allows the user to either launch the verified legitimate URL on the web browser or gets blocked from launching a web browser of a suspected phishing URL. The user is also able to download a list of previously predicted URLs stored in the database.

The rest of this article is structured as follows: Sect. 2 outlines the related work by discussing existing phishing solutions, Sect. 3 outlines the methodology we followed, Sect. 4 present the testing results and evaluation, and lastly Sect. 5 presents the conclusion of the study.

2 Related Works

Various studies have been conducted in the past to investigate ways to prevent phishing attacks aimed at MIA systems. The existing models focus on phishing attacks prediction with some focusing on the Internet in general, online banking, and some on e-commerce systems. As a result, phishing attacks on MIA systems remain one of the most critical areas in cyber security.

There are still other kinds of phishing attacks that not even the security services of various protocols such as Hypertext Transfer Protocol Secure (HTTPS) or Secure Sockets Layer (SSL) are able to prevent [20]. To overcome these security limitations, [20] proposed a phishing detection model which is based on machine learning classifiers and evaluated using different performance metrics. Their phishing detection model is made up of two phases namely, Classification Phase and Phishing Detection Phase. The classification phase's objective is to accurately detect the phishing websites from normal URLs to the phishing URLs. The objective of the feature selection module is to be able to extract all the valid and necessary features so that the classifier can accurately detect the phishing URLs from the attributes as given by the feature selection component. The objective of the phishing detection phase is to detect the legitimate URLs from the phishing URLs given a list of attributes extracted by the feature extraction module during the classification phase. The authors in [20] made use of the five-machine learning algorithms namely, Decision Tree (DT), K-Nearest Neighbour (KNN), Logistics Regression (LR), Random Forest (RF) and Support Vector Machine (SVM) to compare the URL status predictability. The RF algorithm recorded a better phishing detection accuracy of 91.4% as compared to the rest of the other four machine learning algorithms. The similarity between their model and ours is that we both used Decision Tree and our model with an accuracy of 91.30% is closer to their best performing model.

Another study in [21] developed a model to detect phishing websites using the machine learning approach. In their study, they made use of machine learning algorithms such as Random Forest, Decision Tree, Neural Network, and Linear Model to classify data into either phishing or legitimate. The model was able to identify and predict phishing websites from legitimate websites by extracting some unique features from the websites. The dataset used was collected from Miller Smiles archives, PhishTank archive as well as from Google searching operators. The dataset consisted of a total of 2,456

websites and 30 features. The values of attributes used were in the form of integers −1, 0, and 1, whereby the −1 represents phishing, the integer 0 denotes suspicious and the integer 1 denotes legitimate. First, the dataset was processed to ensure data was matured into a desired format before it was split into two datasets by applying the 70% training data and 30% testing data rule. The experiment was carried out using the RStudio installed on Windows 10 after which the four machine learning algorithms (Random Forest, Decision Tree, Neural Network, and Linear Model) were applied on the dataset. The results from the machine learning algorithms were compared in terms of accuracy, True Positive Rate (TPR), True Negative Rate (TNR), Precision, F-Measure, and Error Rate. The RF algorithm recorded the highest prediction accuracy of 95.7% as compared to the other three algorithms. The similarity between their model and ours is that we both used Decision Tree although our model recorded an accuracy of 91.30% which is a bit lower than their best performing model.

The researchers in [22] developed a preventative scheme that uses a specified set of rules on URL behaviour to determine the status of a website based on frequency analysis of extracted phishing features from PhishTank URL data. Support Vector Machine (SVM) was then used to increase the detection power of unknown or suspicious patterns on the URL. After a careful and extensive analysis of comparing the phishing URLs against legitimate URLs, certain heuristics categories were formulated under which classifications were made. Each heuristic category associated with a unique filter was used to formulate detection rules using various combinations of unique filters [22].

In addition, each filter was then mapped with a certain value using the SVM learning system. Each URL is then represented using a vector with either true or false after the identification of all the lexicals in the URL to indicate if it is a phishing or a legitimate URL. The schemes worked according to expectation on smartphones considering that they were also lightweight and taking the memory of the device into account. Although their research was mainly on phishing detection, it is somewhat like ours because it focuses on mobile agents.

The research study in [23] focused on phishing detection using a virtual similarity-based scheme with filtering approaches. The visual schemes compare the visual appearance of suspicious websites with the corresponding legitimate website using various parameters. In their study, they classified the visual similarity-based approaches into HTML Document Object Model (DOM) tree, Cascading Style Sheet (CSS) similarity, pixel-based model, visual feature model, visual perception model, and hybrid model. Three of these models namely, the DOM Tree model, CSS model, and Hybrid model stood out as the best phishing detection approaches since they turn to cover most of what the models are intended to do.

The DOM tree detection model compared the DOM tree websites of suspicious webpage with the legitimate one. The comparison was done to identify the usage of the same personal information (i.e., same username, password, etc.) on multiple websites before issuing warning flag activities on the second website as a suspicious attack. The CSS similarity approach was also effective due to its ability to depict the formatting of a document and set-up the visual appearance of a webpage written in HTML, XHTML, and XML. The authors in [23] used the CSS approach to detect any suspicious-looking features such as fonts, colours, page layout, etc., on any webpage. A combination of

various features from the webpage were analysed by the model by making use of the hybrid approach. The disadvantage of the DOM tree model is that it only compares the new websites with the previously visited websites unlike our model which still analyses the extracted features from any given URL to predict its legitimacy.

The researchers in [24] proposed a Bayesian model to determine the similarity threshold between suspicious websites and legitimate ones. The model is based on visual features such as webpage layout, logos, images, forms, font, background colour, and textual features such as stop words e.g., a, an, the, that, etc. Their model used a naïve Bayes rules-based text classifier to extract texts from the webpage as well as the Earth Mover's Distance (EMD) based image classifier to deal with pixel-level contents after the webpage has been transformed into an image. They used the Bayesian approach during offline training to set the appropriate threshold.

Lastly, they [24] used a Bayesian-based algorithm to aggregate the results from the image and the text classifiers. The model was effective since it presented the researcher with a text classifier using the naïve Bayes rule for phishing detection and its ability to combine the classified results from the text and image classifiers. Although not entirely like our model, we take a step further during our model by not only detecting phishing attacks, but we also prevent the user from accessing any suspicious phishing URL that has been flagged by our model.

The research study in [25] used the artificial neural networks (ANNs), support vector machines (SVMs), decision tree (DTs), and random forest (RF) techniques to develop four phishing detection models for investigating the efficiency of using machine learning to detect phishing domains. They used the uniform resource locators' (URL's) Unified Customer Interface (UCI) phishing domains dataset as a benchmark to evaluate their models. Upon comparing the phishing detection capabilities of the four models, the random forest technique was found to be the most effective algorithm which outperformed the other three techniques.

The authors in [26] proposed the use of Ensemble Learning Methods such as random forest (RF) algorithm and extreme gradient boosting (XBOOST) algorithm for efficient and accurate phishing website detection based on its URL. When comparing the prediction accuracy of the two algorithms, they found that the XBOOST algorithm had the best phishing website detection accuracy of 93.7% whilst the RF had a prediction accuracy of 91.1%.

The researchers in [27] used the Light Gradient Boosting Machine (LightGBM) and URL features such as the domain name to develop a machine-learning-based algorithm that can detect phishing websites and maintain the security of smart systems. They made use of the domain name features due to its capability for multiple domain-name generation algorithms that remain constant. Their model was first used to extract features of the domain name of any given website, including character-level features and other information on the domain name. The extracted features were then filtered to improve the model's accuracy and subsequently used for classification. They [27] found that the detection model which integrates two types of features for training, significantly outperforms the model that uses only a single type of feature.

In this study, we developed a machine learning algorithm using the decision tree (DT) to predict the status of a URL and flag all the suspicious phishing URLs. The developed

phishing prediction and prevention model specifically focuses on MIA systems with a focus on the m-commerce and Internet banking systems as first discussed in [28]. We based our research study on the groundwork that was done in [29] to determine the similarity threshold between the suspicious websites and the legitimate ones as it was first done by researchers in [24]. We make use of the Content-Based Filtering (CBF), Blacklisting, and Whitelisting detection model as first discussed in [30].

3 Methodology

The framework of our model starts with sourcing of URLs dataset from the PhishTank Database. The overall model framework and its various components is shown in Fig. 1.

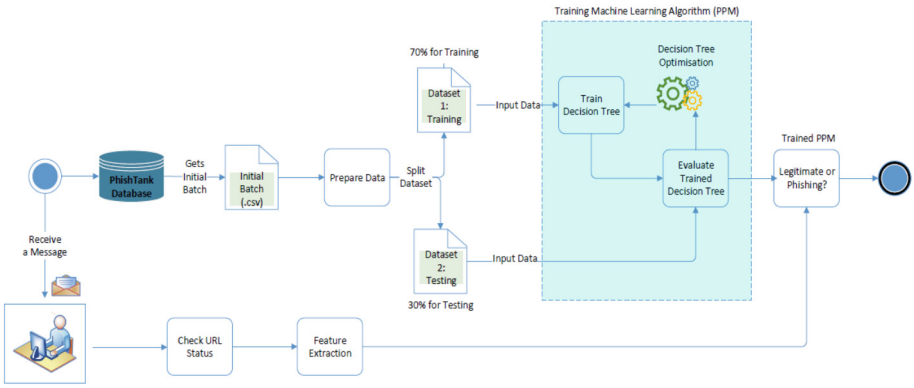

Fig. 1. Phishing Predictive Model (PPM) Framework

Step 1: Dataset Sourcing - the dataset used to train and test the model is sourced from a publicly accessible database on Mendeley website [6]. The dataset was already categorized into phishing and legitimate URLs by the time we sourced it.

Step 2: Dataset Processing - the dataset processing components involves splitting the sourced data into two datasets whereby, one dataset is for training and the other dataset is for testing the trained model. We applied the 70:30 rule to split data into 70% training dataset and 30% testing dataset.

Step 3: Feature Extraction **-** we used Power BI Desktop to extract and explore various data features. Various features were compared with the expected URL status to determine the correlation of such features against the output. This step gave us an indication as to which feature has an influence in predicting URL status and to what extent is the level of influence.

Step 4: Feature Selection **-** during this step, we remove all those features that are relatively discrete and have no correlation between them. We conducted the correlation analysis which is carried out to identify features that either have a strong positive or negative relationship between themselves. Such features cannot be used as inputs when training the machine learning decision tree algorithm.

Step 5: Train PPM **-** the selected features from Step 4 are then used to train the machine learning algorithm component of the PPM. The output of this step is a trained PPM which is later used to predict legitimacy status of any given URL. Once the PPM is fully trained and optimized, it is then integrated with a mobile application that was developed in Python and can predict the status of any given URL.

Step 6: Evaluate PPM **-** the experimental results of the trained and optimized PPM were then analyzed. To determine if the developed model meets the expected objectives, the model was then compared with other available solutions implemented by other researchers.

4 Results and Discussion

4.1 Experimental Hardware and Software Tools

The hardware tools used to implement the PPM model included 8 GB RAM and a 2.40 GHz Processor. The software tools used consists of Windows 10 Pro Operating System and a 64-bit Operating System, Python 3.10, SQL Server version 2019, and Power BI Desktop version 2.117.984.

4.2 Experimental Dataset

The dataset consists of 11,430 URLs obtained from Mendeley database [6]. The data is a consolidated list of known phishing and non-phishing URLs as reported by known industry expert systems such as PhishTank.org and Kaggle.com which are more trusted and reliable. The dataset consists of 87 extracted features and contains exactly 50% phishing and 50% legitimate URLs. The explored data was split into two datasets, namely training dataset and testing dataset. The training dataset consists of labelled data that was used to train the PPM whereas the testing dataset was used to evaluate the PPM. The dataset partitioning is diagrammatically shown in Fig. 2.

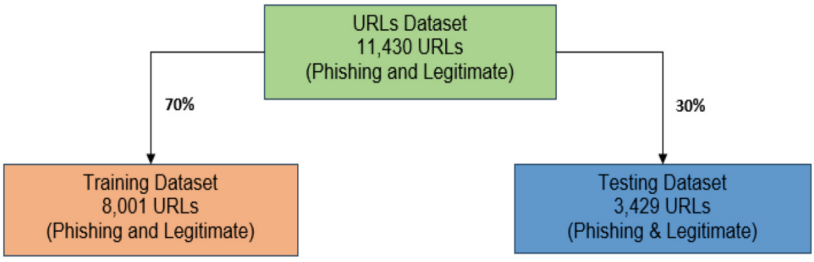

Fig. 2. Dataset Partition

4.3 PPM Performance Indicators

Performance indicators are used to assess the learning of an algorithm, to determine the effectiveness of an algorithm based on metrics using the test datasets. To measure the performance of the PPM, we measured the *accuracy, precision, recall, F-score, Mean Absolute Error (MAE), Mean Squared Error (MSE), and the Root Mean Squared Error (RMSE).* Of the measured indicators, accuracy (as given by Eq. (1)), precision (as given by Eq. (2)), recall (as given by Eq. (3)), and the F-score (as given by Eq. (4)) are the only four indicators used to calculate the confusion matrix:

$$Accuracy(A) = \frac{(TP + TN)}{TP + TN + FP + FN} \tag{1}$$

$$Precision(P) = \frac{TP}{TP + FP} \tag{2}$$

$$Recall(R) = \frac{TP}{TP + FN} \tag{3}$$

$$F1 = \frac{2TP}{2TP + FP + FN} \tag{4}$$

where *TP* represents the URLs that are predicted to be phishing and are indeed found to be phishing, *FP* represents the URLs that are predicted to be phishing while they are legitimate, *TN* represents the URLs that are predicted to be legitimate while they are indeed found to be legitimate, *FN* represents the URLs that are predicted to be legitimate while they are phishing.

The other indicators are measured as follows:

Mean Absolute Error(*MAE*), in the context of machine learning computes the impact or magnitude of the differences between the predicated URL statuses and the actual URL statuses. *MAE* is calculated by Eq. (5) as follows:

$$MAE = \frac{1}{n}\sum_{i=0}^{n-1}|y_i - x_i| \tag{5}$$

where Σ represents the summation value, $y_i$represents the actual URL statuses for the ith observation, $x_i$represents the predicated URL statuses for the ith observation, and $n$represent the number of observations in a dataset.

Mean Squared Error(*MSE*), measures the average squared error between the actual URLs statuses and the predicted URLs statuses. Since PPM is trained to predict the phishing URLs with minimum error, The *Mean Squared Error*(*MSE*) is calculated by Eq. (6):

$$MSE = \frac{\sum_{t\epsilon T}(t_{u,i} - p_{u,i})^2}{\|T\|} \tag{6}$$

where T represent the number of observations in a dataset, $t_{u,i}$ represents the actual URL status, and $p_{u,i}$ represents the predicted URL status.

The last indicator is called *Root Mean Squared Error*(*RMSE*, which is the square root of the *MSE* and is used to plot the difference between the predicted URLs statuses and the actual URLs statuses. The *RMSE* is calculated by Eq. (7):

$$RMSE = \sqrt{\frac{\sum_{t \epsilon T} (t_{u,i} - p_{u,i})^2}{\|T\|}} \tag{7}$$

where T represent the number of observations in a dataset, $t_{u,i}$ represents the actual URL status, and $p_{u,i}$ represents the predicted URL status.

4.4 Experimental Results

The developed mobile application is built to accept a valid URL from a user through a text box field where it can either be typed in or pasted on. Once a valid URL has been captured, the user would then click on the 'Search' button. The welcome page showing both the download and the search buttons is shown in Fig. 3.



Fig. 3. PPM Welcome Page

The PPM is able to save valid URL whose status was verified by the model. The user is also able to download a list of stored URLs from the database, which then automatically get saved on the user's local download folder as shown by the confirmation messgae in Fig. 4.

The mobile application validates each URL that has been received to ensure that only valid URLs, which conform to a certain criteria are accepted. The URL validation message is shown in Fig. 5.

Each URL searched through the mobile app evokes the algorithm component of the PPM system, which then makes URL status predictions. For any URL that is predicted to be 'Not Secure' or phishing, the system then blocks the user from launching the web page of such a URL address and the only option the user has is to exit the status result screen as shown in Fig. 6.

The model is also able to successfully predict a legitimate URL. Once a URL has been predicted to be secure, the user is able to launch the web page by clicking on the 'OPEN URL' button. Alternatlively, the user may opt to exit the confirmiation screen by clicking on the 'EXIT' button. The screen that allows the user to launch the web page or exit confirmation screen is shown in Fig. 7.

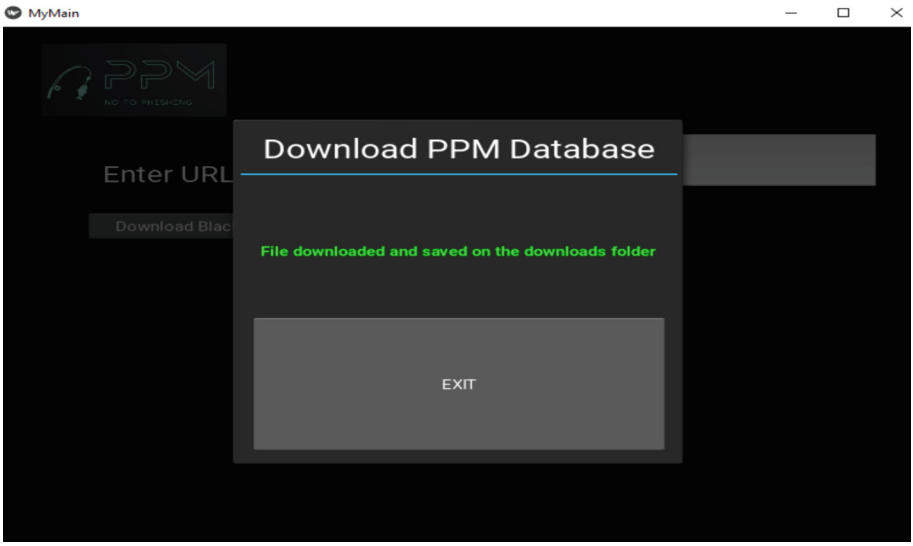

Fig. 4. Downloading URL List

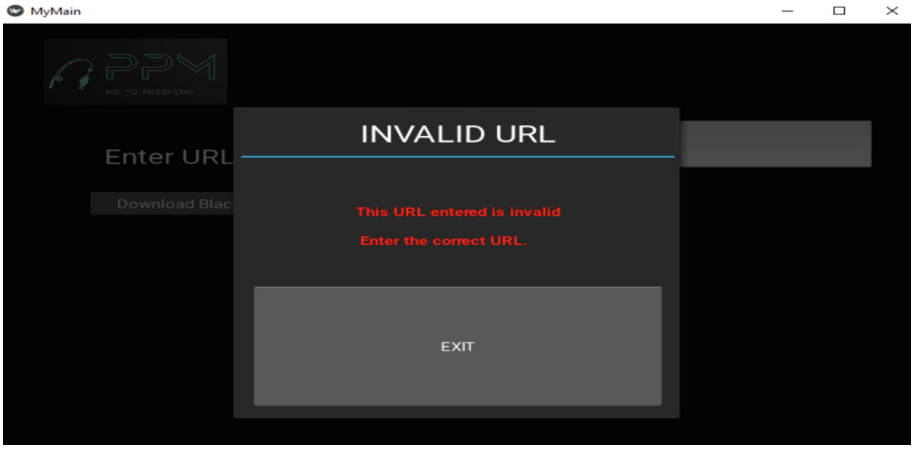

Fig. 5. URL Validation

4.5 Evaluation of PPM

We employed an experimental approach using three different PPMs based on the Decision Tree technique. We then computed the performance matrices of each DT classifier to get their True Positive Ratio (TPR) and True Negative Ratio (TNR) values as shown in Table 1.

To evaluate the performance of the proposed model, we computed their performance indicators, and the results are shown in Table 2.

The comparison results between the three classifiers are shown in Fig. 8.

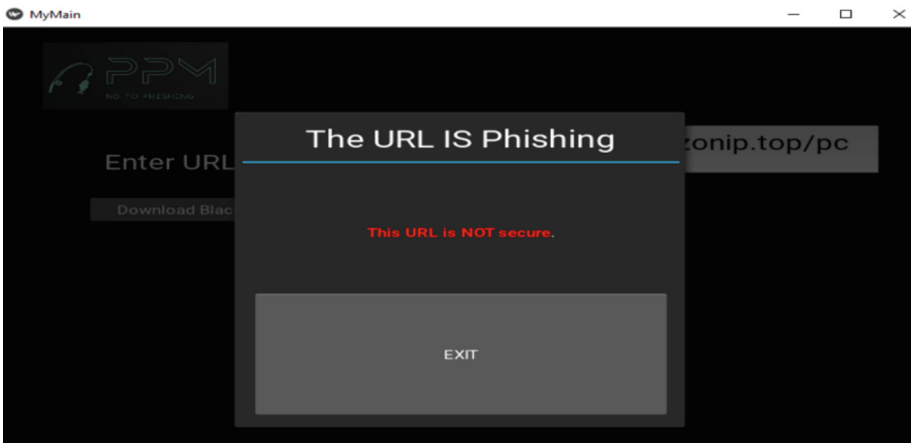

Fig. 6. Predicted Phishing URL

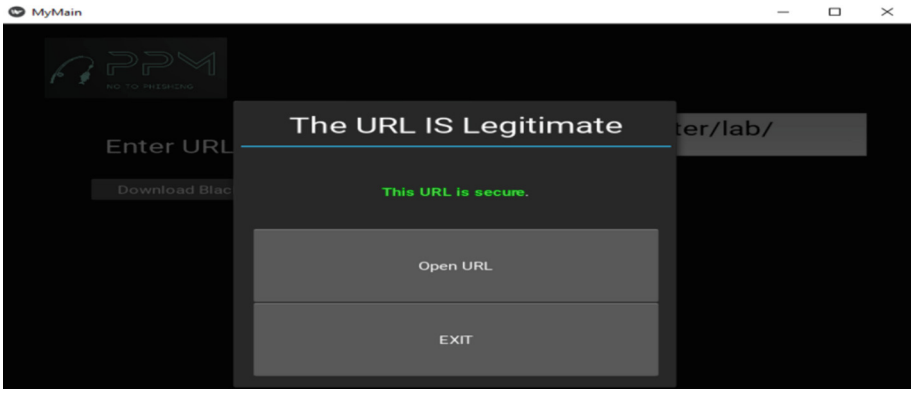

Fig. 7. Predicted Legitimate URL

Selecting the Best PPM: The best PPM is a model that can generalize the testing data very well. The best PPM was selected not only based on its prediction accuracy, but also considering that each of the classifiers used a different set of parameters as shown in Table 1. Based on the PPMs' performance results in Table 2, it would appear as though PPM2 is the best model when looking at its prediction accuracy of 93.2%, and the MSE of 6.8%. However, PPM2 was trained to its full depth which resulted in overfitting of the training data. That means the model would have a higher prediction accuracy during training but have a lower accuracy during testing. To overcome the overfitting effect of the training data, PPM3 was selected as the best model with a prediction accuracy of 91.3%, and the MSE of 8.7%. This is because PPM3 was able to generalize both the training and the testing datasets. Unlike the PPM2 that was trained to its full depth using all features, PPM3 was trained using only the important features and its decision tree was also pruned which made the model to have closer prediction outcomes between training

Table 1. Comparison of DT Classifiers

DT Classifiers	Parameters	TPR	TNR
PPM1	Criterion = gini, Splitter = best, Max_depth = None, min_samples_split = 2, min_samples_leaf = 1, and 87 Features	0.9278	0.9322
PPM2	Criterion = gini, Splitter = best, Max_depth = None, min_samples_split = 2, min_samples_leaf = 1, and 87 Important Features only	0.9278	0.9363
PPM3	Criterion = gini, Splitter = best, Max_depth = 5, min_samples_split = 2, min_samples_leaf = 5, and 50 Important Features only	0.9115	0.9135

Table 2. Evaluation of Phishing Prevention Model (PPM) Results in (%)

Performance Indicator	PPM1	PPM2	PPM3
Accuracy	93.1	93.2	91.3
Precision	93.3	93.7	91.4
Recall	93.0	92.8	91.2
F1-Score	93.1	93.3	91.3
MAE	6.9	6.8	8.7
MSE	6.9	6.8	8.7
RMSE	36.4	26	29.6

and testing. The accuracy scores for both training and testing in five folds for PPM3 shows closer scores between the training and the testing results as shown in Fig. 9.

The comparison between the actual and the predicted URLs statuses for PPM3 classifier is shown in Fig. 10. The graph shows how closely the model was able to make the correct prediction in comparison to the given actual outcome. Wherever the predicted values matched the actual values, only the orange line for the predicted value is visible on the graph as shown in Fig. 10.

Evaluating the Best PPM: The best selected DT classifier, which is PPM3, was then evaluated against existing solutions from studies carried out by other researchers. The evaluation criteria focused on the dataset type that was used by each research study, the machine learning algorithm, the accuracy of the developed model, and lastly the mean squared error. Table 3 shows the comparison between PPM3 and other models developed by other researchers. The researcher's name is listed under the first column called approaches. The dataset used differs from one research to another.

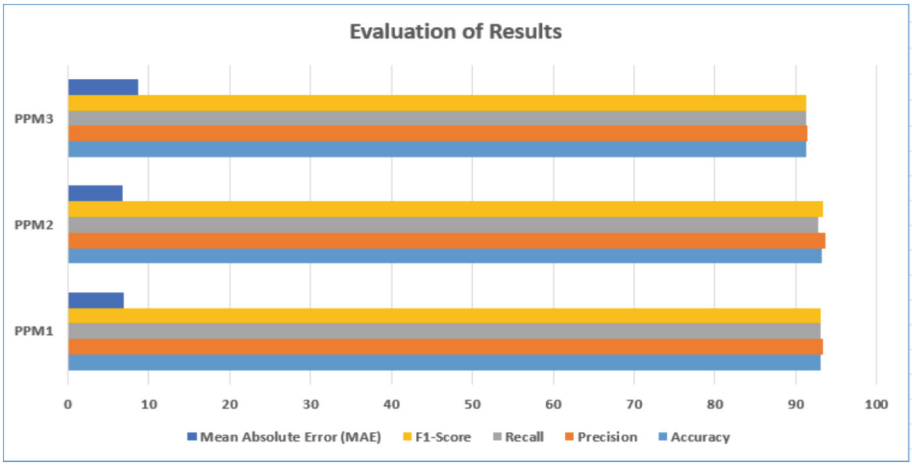

Fig. 8. DT Classifiers Comparison

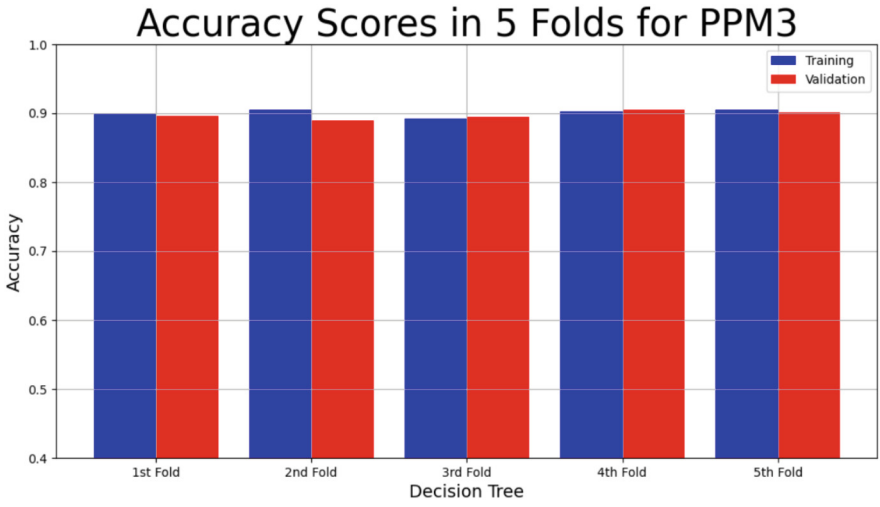

Fig. 9. Accuracy Scores for PPM3

Although PPM3 was selected as our best model amongst the three DT classifiers however, the model developed by [25] stands out as the best approach with an accuracy of 97.3% and error rate of 2.7%. This is because they used 10-fold cross-validation approach to locate a greater performance accuracy dataset amongst the artificial neural network (ANNs), support vector machines (SVMs), decision trees (DTs), and random forest (RF) techniques whilst we used 5-fold cross validation approach and only focused on one machine learning algorithm which is the decision tree (DT). The other reason is because they used URL's UCI phishing domains as their dataset whilst we used the entire URL details which consist of 87 features. Amongst the six researchers we compared our

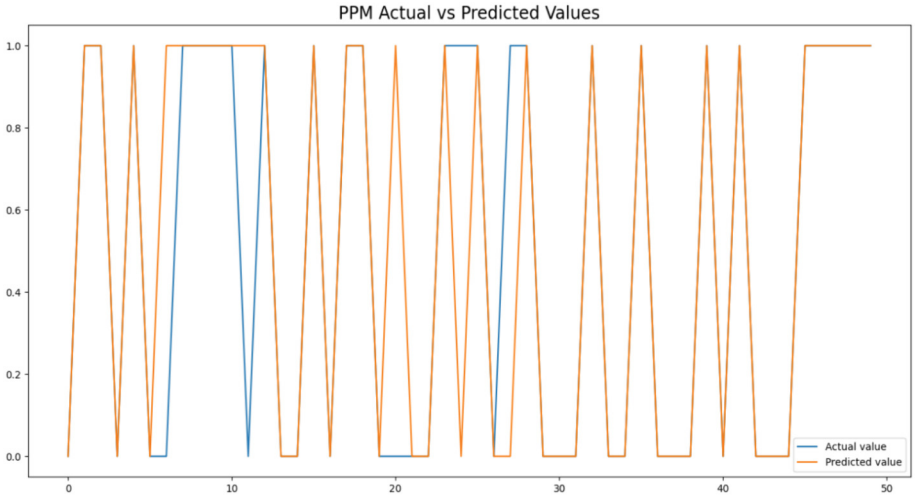

Fig. 10. Actual vs Predicted Values

model with, it is only [20] that our model comes closer to with an accuracy of 91.4% and an error rate of 8.6%. As a result, our study can be improved in the future by employing other machine learning algorithms together with the decision tree and evaluate their prediction results before selecting the best performing model and also by using 10-fold cross-validation as it was done by [25].

Table 3. Comparison of Proposed Model and Other Approaches

Approaches	Dataset Type	Machine Learning Algorithm	Accuracy	MSE
Alnemari and Alshammari [25]	URLs	ANN, SVM, DT, and RF	97.30%	2.70%
Orunsolu et al. [22]	URLs	SVM	96.60%	3.40%
Jalal and Naaz [21]	URLs	DT, RF, NN, and LM	95.70%	4.30%
Zhou et al. [27]	Websites	LightGBM	94.70%	5.30%
Dharani et al. [26]	URLs	RF, and XGBoost	93.70%	6.30%
Naresh et al. [20]	URLs	KNN, LR, RF, and SVM	91.40%	8.60%
Our Model (PPM3)	URLs	DT	91.30%	8.70%

5 Conclusion

In this paper, we designed and developed a predictive model for phishing attacks on MIA systems. The predictive model takes URLs as input and applies the machine learning algorithm to predict the authenticity of a URL and flags any suspicious phishing URL. The machine learning algorithm used is the Decision Tree. The developed model is an online mobile application developed in Python and SQL Server database. The users of the PPM solution can verify the legitimacy of any given URL before launching it on the web browser and can also download a list of previously predicted URLs with their statuses from the database. The developed model helps protect MIA system users from falling victims of phishing attacks and make them aware of already flagged URLs before launching them on the web browser. In this study, the decision tree machine learning algorithm was adopted, and the results were evaluated against other existing phishing algorithms. The developed predictive model can predict URL status with an accuracy of 91.3% and a mean squared error of 8.7%.

Acknowledgments. This research is undertaken in the department of computer science at the University of KwaZulu-Natal (UKZN). The authors would like to extend their special gratitude to the sponsors and the leadership of all the institutions who made it possible to carry out this research.

References

1. Statista, eCommerce Worldwide – Statistics and Facts. https://www.statista.com/topics/871/online-shopping/#editorsPicks. Accessed 28 April 2023
2. Visa Navigate, eCommerce Developments Across Sub Saharan Africa. https://navigate.visa.com/cemea/data-and-insights/sub-saharan-africas-ecommerce-potential/. Accessed 3 March 2023
3. Accounting Learning, eCommerce: What are Intelligent Agents? https://accountlearning.com/what-are-intelligent-agents-features-importance-advantages/. Accessed 8 June 2023
4. Patil, P.: Study on E-commerce security issues and solutions. Int. J. Comput. Sci. Mob. Comput. **6**(1), 100–102 (2017)
5. Niranjanamurthy, M., Chahar, D.: The study of e-commerce security issues and solutions. Int. J. Adv. Res. Comput. Commun. Eng. **2**(7), 1–12 (2013)
6. Mendeley Data: Web Page Phishing Detection. https://data.mendeley.com/datasets/c2gw7fy2j4/3. Accessed 20 July 2023
7. Pivk, A., Gams, M.: Intelligent agents in E-commerce. Electrotechn. Rev. **67**, 251–260 (2000)
8. CISCO, Email Security: What is phishing? https://www.cisco.com/c/en/us/products/security/email-security/what-is-phishing.html. Accessed 13 April 2018
9. Kogeda, O.P., Agbinya, J.I.: Proactive cellular network faults prediction through mobile intelligent agent technology. In: The Proceedings of the 2nd International Conference on Wireless Broadband and Ultra-Wideband Communications, pp. 27–30. Sydney, Australia (2007). ISBN: 978-0-7695-2846-5
10. Banday, M.T., Qadri, J.A.: Phishing - a growing threat to e-commerce, ISSN: 0972–8384, **12**(2), 76–83 (2007)
11. Jansen, W.A.: Intrusion detection with mobile agents. In: Proceeding of the Canadian Information Technology Security. Symposium, pp. 1–14. IPC Science and Technology Press, Ottawa, CA (2000)

12. Goel, D., Jain, A.K.: Mobile phishing attacks and defense mechanisms: state of art and open research challenges. Comput. Secur. **73**(1), 519–544 (2018)
13. Amro, B.: Mobile agent systems, recent security threats, and counter measures. Int. J. Comput. Sci. Issues **11**(2), 146–151 (2014)
14. Cui, Q., Jourdan, G.-V., Bochmann, G. V., Couturier, R., Onut.: Tracking phishing attacks over time. In: Proceedings of the 26th International Conference on World Wide Web. International World Wide Web Conferences Steering Committee, pp. 667–676. Republic and Canton of Geneva, Switzerland (2017)
15. Kumar, A., Roy, S.S., Saxena, S., Rawat, S.S.: Phishing Detection by determining reliability factor using rough set theory. In: Proceedings of International Conference on IEEE, pp. 236–240. Machine Intelligence and Research Advancement, Katra, India (2013)
16. Zhari, C., Hachicha, H., Ghedira, K.: Agent's security during communication in mobile system. Procedia Comput. Scie. **60**(2015), 17–26 (2015)
17. ITWeb. 2017. Phishing Response Trends Phishing response trends | ITWeb. Accessed 29 July 2018
18. The Ponemon Institute, Cost of Data Breach Study. https://www.ponemon.org/research/ponemon-library/security/2017-cost-of-data-breach-study-united-states.html. Accessed 28 July 2018
19. APWG, 4Q 2022 Phishing Activities Trends Report. https://docs.apwg.org/reports/apwg_trends_report_q4_2022. Accessed 15 August 2018
20. Naresh, K.D., et al.: Detection of phishing websites using an efficient machine learning framework. Int J. Eng. Res. Technol. **9**(5), 1–5 (2020)
21. Jalal, K., Naaz, S.: Detection of phishing websites using machine learning approach. In: Proceedings of International Conference on Sustainable Computing in Science, Technology and Management, pp. 1774–1781. Elsevier SSRN, New Delhi, India (2019)
22. Orunsolu, A.A., Alaran, M.A., Adebayo, A.A., Kareem, S.O., Oke, A.: A lightweight anti-phishing technique for mobile phone. Acta Informatica Pragensia, Prague Univ. of Econ. Bus. **6**(2), 114–123 (2017)
23. Gupta, B.B., Jain, A.K.: Phishing detection: analysis of visual similarity based approaches. Secur. Commun. Networks **2017**(4), 1–20 (2017)
24. Zhang, Y., Hong, I., Cranor, L.J.: Cantina: A content-based approach to detecting phishing websites. In: Proceedings of the 16th International World Wide Web, pp. 639–648. Association for Computing Machinery, New York (NY), United States (2007)
25. Alnemari, S., Alshammari, M.: Detecting phishing domains using machine learning. Appl. Sci. **13**(8), 4649 (2023)
26. Dharani, M., Soumya, B., Kimaya, G., Amarsinh, V., Dhanashri, B.: Detection of phishing websites using ensemble machine learning approach. In: ITM WE of Conferences 40, ICACC (03012), pp. 1–5 (2021)
27. Zhou, J.; Cui, H.; Li, X.; Yang, W., Wu, X.: A novel phishing website detection model based on LightGBM and domain name features. Symmetry **15**(1), 180 (2023)
28. Dong, H.L., Kim, H., Na, S.Y.: Prevention schemes against phishing attacks on internet banking systems. Int. J. Adv. Soft Comput. Appl. **6**(1), 1–15 (2014)
29. Padma, U.R., Sarannia, A.: Prevention model for phishing attacks in web applications using linkguard algorithm. Int. J. Innov. Res. Comput. Commun. Eng. **2**(1), 2889–2896 (2014)
30. Shahriar, H., Klintic, T., Clincy, V.: Mobile phishing attacks and mitigation techniques. J. Inf. Secur. **6**(3), 206–212 (2015)

Computational Methods, Statistics and Industrial Mathematics (CMSIM 2024)

Metabolic Cost of Load Carriage in a Special Forces Team – A Non-parametric Approach

Rui Lucena[1], Nuno Almeida[1], and Paula Simões[2(✉)]

[1] Military Academy Research Center - Military University Institute (CINAMIL) and MRLab-Military Readiness Lab-Portugal and CIPER – Faculdade de Motricidade Humana, Universidade de Lisboa, Lisbon, Portugal
{rui.lucena,almeida.nrc}@academiamilitar.pt

[2] Military Academy Research Center - Military University Institute (CINAMIL) and NOVA MATH - Center for Mathematics and Applications, NOVA University of Lisbon, Lisbon, Portugal
paula.simoes@academiamilitar.pt

Abstract. Military missions are often comprised of heavy load carriage whilst marching in difficult terrains. Furthermore, the ability of carrying a load is a fundamental requirement for successful missions and safety in these populations. The aim of the present study was to quantify the metabolic cost of load carriage in a Portuguese special forces team. Ten active-duty military personnel of a special forces team performed a graded protocol of until exhaustion on a treadmill in a thermoneutral environment in two different conditions: Unloaded and Fully loaded for combat. Using non-parametric statistical methods for hypothesis testing development, considering the Wilcoxon Test to compare two groups and Kruskal-Wallis test for analysing the differences by step in the different variables, with multiple pairwise comparisons, the study is performed in two main phases. First, considering the Unloaded and Fully loaded groups, it was analysed if it provided different results of peak oxygen uptake, heart rate and blood Lactate. Second, taking into account that higher differences were detected across categories (steps), we are interested in conducting an analysis which enables the definition of the ventilatory threshold and peak oxygen uptake for each condition. The fully loaded for combat condition showed higher values of oxygen consumption and heart rate in all steps of the exercise when compared to the unloaded condition. Peak oxygen uptake and heart rate were significantly different between the two conditions. This study enables to enhance our understanding of the metabolic cost of load carriage, in a special forces team, and its impact in military readiness.

Keywords: Metabolic Cost · Military · Load Carriage · Non-parametric tests · Multiple Pairwise Comparisons

1 Introduction

Military missions are often comprised of heavy load carriage whilst marching in difficult terrains. Despite the fact that the load carried by soldiers has been increasing throughout history [1], the ability of carrying a load is a fundamental requirement for successful missions and safety in these populations to this day [2].

© The Author(s), under exclusive license to Springer Nature Switzerland AG 2024
O. Gervasi et al. (Eds.): ICCSA 2024 Workshops, LNCS 14816, pp. 131–143, 2024.
https://doi.org/10.1007/978-3-031-65223-3_9

Military assignments require not only a high level of technical competence, but also substantial physical demands for their performance. Thus, the physical performance of military personnel is not limited to the execution of military tasks, but also maintain their ability to execute them for prolonged periods, with the aim of consistent performance [3].

In the current battlefield scenarios, there is a growing trend towards conflicts in the urban environment, where the physical demands are significantly different. Combat in an urban environment is characterized by its asymmetrical nature, the unpredictability of confrontations and the fact that it is a constantly changing environment. Unlike conventional combat where both the terrain and the enemy are properly framed and defined this scenario requires a capacity for rapid response, agility, and resilience to face the challenges inherent to a dynamic and unpredictable system [4].

Therefore, the ability to carry a load is fundamental requirement in military settings and varies according to function and mission. This fact means that individuals rely on their personal mobility to transport the convenient equipment to the mission [5]. Additionally, the location of the load (upper body, hip, etc.) can affect walking efficiency, energy cost, subjective comfort and the biomechanics of the individual [5–7]. The prediction and evaluation of the metabolic cost of load carriage has been studied both in the laboratory [2, 8] and in operational settings [5–7], leading to the idea that the high physiological costs of carrying a load enhance the possibility of personal injury compromising health and safety and even mission success [2].

Logically with an increased metabolic cost comes increased physiological markers [1]. Although the relevance of cardiorespiratory parameters has shown relevant results [2, 8, 9], other studies have been more conservative regarding the usage of such parameters [10].

The Maximal Oxygen Uptake ($VO_{2máx}$) has been shown to reflect the individual maximal rate of energy expenditure and to be related with athletic performance [11]. Additionally the Lactate Threshold (LT) and the associated changes in gas changes reported by the Ventilatory Threshold (VT) have also been related to endurance performance [11–13]. In addiction the LT has been referred to be the exercise intensity where blood lactate concentration increases above resting levels [14].

Taking this into account, no previous studies were found that address both the Peak Oxygen Uptake (VO_{2peak}) and ventilatory parameters relation with different loading conditions in a special forces team in the Portuguese Army.

Thus, the purpose of this study was to measure and compare different physiological parameters such as VO_{2peak} and ventilation parameters associated with the LT and the between different loading conditions in a special forces team of the Portuguese Army.

This work is organized as follows: Sect. 2 describes the objectives and methods of this study regarding: soldiers conditions characterization, the protocol and derived variables and lastly the statistical methods. Section 3 refers to the analysis and discussion of the main results. The main conclusions and final remarks are described in Sect. 4.

2 Objectives and Methods

This research focuses on quantifying the metabolic cost of load carriage in a Portuguese special forces team. A graded protocol until exhaustion on a treadmill in a thermoneutral environment in two different conditions: Unloaded and Fully loaded for combat was performed.

A sample consisted of ten soldiers from the Portuguese Army's Commandos Battalion, who was undergoing preparation for their 13th deployment to the Central African Republic's theatre of operations.

All the participants were free from any injury or pain prior to the performance testing. After receiving a thorough explanation of the protocol, all gave their written informed consent to the study. The experimental protocol, the gas analysis and the blood analysis are described in detail below.

Considering the VO_{2peak} and the HR, BL concentration and rating of perceived exertion (RPE) as metabolic variables, for the Unload and Fully Loaded Groups, the aim is to analyse and compare whether there are significant differences in both conditions, assessing their impact on different metabolic capacities. Such an approach enables the definition of the VT and VO_{2peak} for each condition.

2.1 Soldiers' Conditions Characterization: Unloaded and Fully Loaded for Combat

Regarding collective material, the Assault Pack MIL-TEC backpacks were used, equipped with extra ammunition, offensive grenades and flashbang grenades, planning material, water, stretchers, first aid kit; Benelli Super Nova or Franchi SPAS-15 shotguns and the Grenade Launcher (LG) 40mm FN40GL-S Mk2.

Regarding weaponry, military personnel were equipped according to their specific combat role. All snipers are equipped with the Glock 17 Gen 5 FS pistol with two additional cartridges, the normal Snipers are equipped with the FN SCAR-L assault rifle with eight additional cartridges, the LMG Sniper with the FN Minimi 5,56 Mk ML plus eight ribbons, and the Special Sniper with the FN SCAR-H with Trijicon VCOG optical sight, eight more chargers. The personal protective equipment used includes the OPS-CORE helmet, the THOR ballistic vest and the THOR Anti-Fragmentation belt.

The total sum of the weight carried by the military in this study ranged between 25 kg and 35 kg, taking into account that this variation was due to the function performed by the soldier.

2.2 Experimental Protocol

All participants performed a graded protocol of until exhaustion on a treadmill TR1000 BM (BH Fitness; EXERCYCLE, S.L., Spain) in a thermoneutral environment in two different conditions: Unloaded and Fully loaded for combat. Previous to the incremental test the subjects performed a standardized warm-up consisting of 8 to 10 min of light running followed by active rest, followed by a 5-min rest. All tests were within at least 2 h after the subject's last meal. All subjects were asked to avoid the consumption of coffee and alcohol and physical activity (training) 24 h before the test.

The protocol consisted of a maximal continuous incremental exercise of two-minute steps the gradient was increased every second minute by 2° up to a gradient of 8°. Thereafter, the gradient of 8° was maintained and the walking speed was increased by 1 km/h every second min until the subjects were not able or willing to continue the test. VO_{2peak} and maximal aerobic velocity (MAV) were determined. VT with corresponding heart rate (HR) and speed were also determined. VO_{2peak} was considered when the athlete reached volitional exhaustion, was unable to maintain the required speed or was unable to sustain the given speed for at least one minute in the last stage. The VT was calculated by v-slope method (i.e., disproportioned increase in carbon dioxide uptake relative to oxygen uptake) [15].

2.3 Gas Analysis - Oxygen Consumption

Respiratory data were collected breath-by-breath using a PNOE metabolic cart which operates on a mode that continuously measures volume and determines expired gas concentrations simultaneously. The measurements of oxygen consumption are made by via an open-circuit indirect calorimetry technique by assessing pulmonary gas exchange at the mouth and the nose. The metabolic cart is comprised of an electrochemical O_2 analyzer and an infrared CO_2 analyzer.

Breath-by-breath oxygen uptake values were averaged over 5 s with peak oxygen uptake taken as the highest 30 s oxygen uptake value. HR was measured throughout the test (Polar H10, Kempele, Finland).

2.4 Blood Analysis

Blood samples were collected from the earlobe of the participants using a Lactate Pro 2 (AKRAY Europe-Netherlands). Prior to the collection the site was cleaned in order to remove any sweat or blood.

2.5 Statistical Methodology

The data was analyzed using various descriptive statistical methods, implemented using IBM SPSS Statistics 28 software. Statistical Inference techniques and probability models were considered to evaluate the metabolic capacities of soldiers and understand the impact that load can have in reducing maximal exercise tolerance.

Point estimation, interval estimation and implementation of various hypothesis tests for the parameters of interest (median value) are considered, taking into account the enunciated problem, with a significance level of 5% [16].

Resorting to non-parametric statistical methods for hypothesis testing development, considering the Wilcoxon test and also using the Kruskal-Wallis test, with multiple pairwise comparisons, the study is performed [16].

Considering the Unloaded and Fully loaded groups, it was analysed if it provided different results of VO_{2peak}, HR and BL. The differences were also analysed considering the Unloaded and Fully loaded groups by step in the different variables.

3 Results Analysis and Discussion

The ten active-duty military personnel of a special forces team that constitute our sample are all male. These elite special forces team is specially trained for executing high-risk combat missions such as: direct combat, special reconnaissance, etc. All members had undergone intensive training in varied environments.

The participants were between 21 and 31 years old with an average of 24,7 years and a standard deviation (SD) of 3,5 years. Weight was between 68,8 kg and 96,8 kg, with an average of 77,12 kg and a SD of 8,5 kg; The height of the militaries ranged from 164 cm and 188 cm with an average of 175,8 cm and a SD of 7,88 cm. In terms of Body mass index, lies between 21,8 and 27,4 with an average of 25 kg/m^2 and a SD of 1,81 kg/m^2. Table 1 summarizes the mentioned main statistics.

Table 1. Table captions should be placed above the tables.

Statistics	Weight (Kg)	Height (cm)	Age (years)	Body mass index (kg/m^2)
Mean	77,1	175,8	24,7	24,9
Median	76,5	176,5	23,5	24,9
Std. Deviation	8,5	7,8	3,4	1,8
Range	28,6	24	10	5,6
Minimum	68,2	164	21	21,8
Maximum	96,8	188	31	27,4

3.1 Peak Oxygen Uptake

The VO_{2peak} by step is represented in Fig. 1 considering the two conditions, unloaded and fully loaded. It turns out that the VO_{2peak} was gradually higher in the Unloaded condition when comparing the two conditions. Furthermore, the oxygen consumption throughout the test was also higher in all steps of the exercise protocol (Fig. 1).

According to the study objective, and taking into account the null hypothesis, H0: The medians are the same across categories of Equipment, the Unloaded and Fully loaded groups, are compared in terms of VO_{2peak}. Resorting to Wilcoxon test, the null is rejected (p-value $< 0{,}001$), therefore significant different results of VO_{2peak} are provided depending on the equipment category (Fig. 2).

3.1.1 Peak Oxygen Uptake – Steps in Unload Group

Considering the non-parametric statistical test for the null hypotheses H0: The median value of the VO_{2peak} is the same across **categories (steps)** in **Unload** Group; this one is rejected (p-value $< 0{,}01$), and when we go through the pairwise comparisons between **categories (steps)** stands out that the steps 4 to 12 are significantly different from step 1 ($0{,}001 < p$-value $< 0{,}046$); steps 6 to 12 are significantly different from step 2, step 3

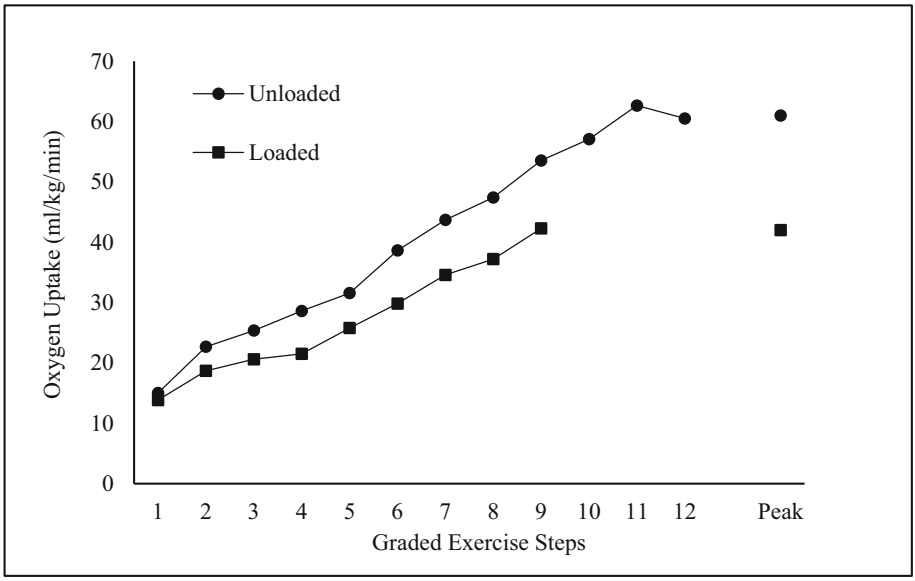

Fig. 1. Oxygen uptake during the graded exercise protocol in both conditions

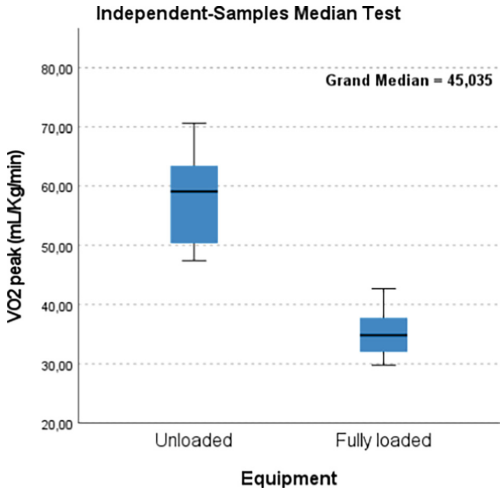

Fig. 2. Boxplot relative to VO_{2peak} across categories of Equipment.

and from step 4 (0,001 < p-value < 0,040); steps 8 to 12 are significantly different from step 5 (0,001 < p-value < 0,014), and steps 9 to 12 are significantly different from step 6 (0,001 < p-value < 0,032) (Fig. 3).

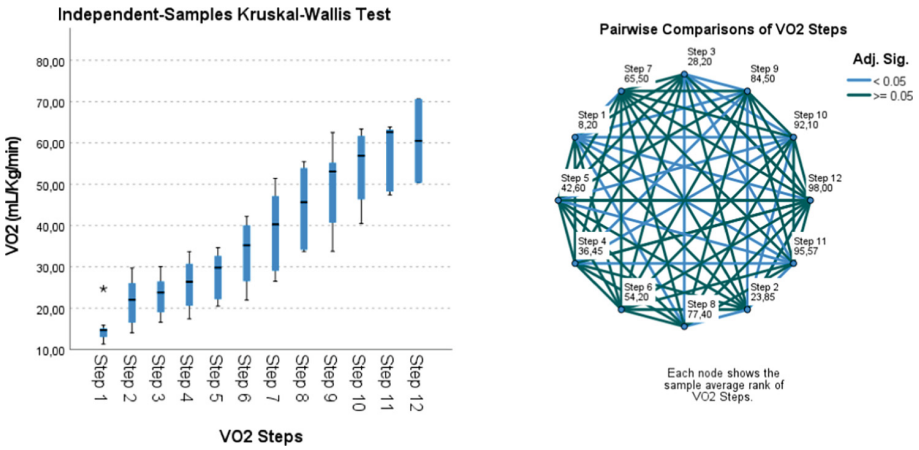

Fig. 3. Boxplot relative to VO_{2peak} across categories (steps) in Unload Group (left) and pairwise comparisons between steps (right).

3.1.2 Peak Oxygen Uptake – Steps in Load Group

Performing the non-parametric statistical test across **categories (steps)** in **Load** Group, for the null hypotheses H0: The median value of the VO_{2peak} is the same across **categories (steps),** is also rejected (p-value $< 0{,}01$), and when we carry out comparisons between **categories (steps)** stands out that the steps 4 to 9 are significantly different from step 1 ($0{,}001 < p\text{-value} < 0{,}016$), steps 5 to 9 are significantly different from step 2 ($0{,}001 < p\text{-value} < 0{,}007$), steps 6 to 9 are significantly different from step 3 and from step 4 ($0{,}001 < p\text{-value} < 0{,}002$), and step 7 are significantly different from step 5 (p-value $= 0{,}04$) (Fig. 4).

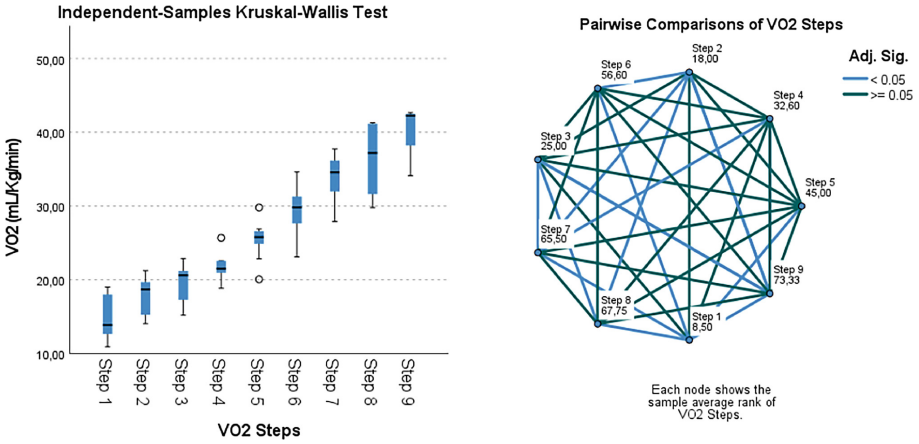

Fig. 4. Boxplot relative to VO_{2peak} across categories (steps) in Load Group (left) and pairwise comparisons between steps (right).

3.2 Heart Rate During Treadmill Exercise

The HR during treadmill exercise by step is represented in Fig. 5 considering the two conditions, unloaded and fully loaded. It turns out the Maximal Heart Rate was reached 3 steps earlier in the Loaded condition.

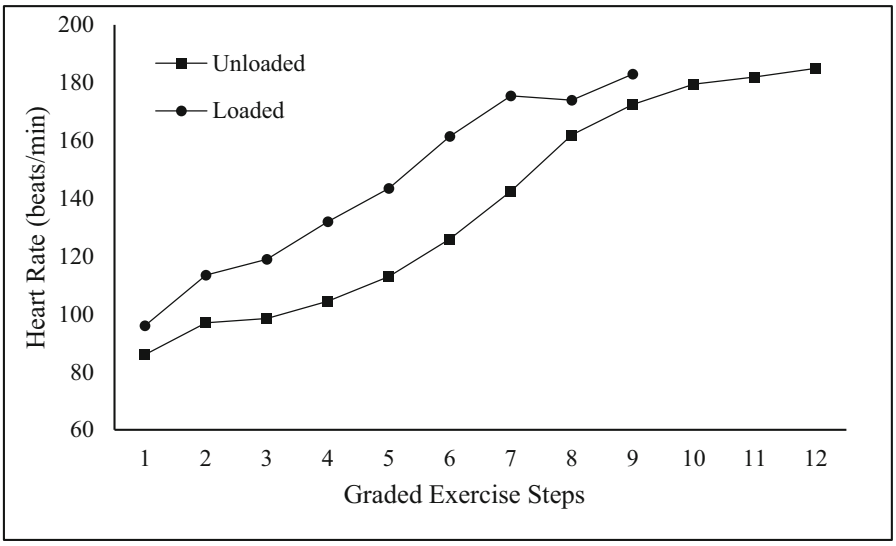

Fig. 5. Heart Rate during the graded exercise protocol in both conditions**.**

Following the aim of the investigation for the second metabolic variable under analysis, and taking into account the null hypothesis, H0: The medians are the same across categories of Equipment, the Unloaded and Fully loaded groups, are compared in terms of HR, in each common step during the graded exercise protocol. When the Wilcoxon test is applied, the null is rejected from step 2 (inclusive) (0,011 < p-value < 0,029), therefore from this level significant different results of heart rate are provided depending on the equipment category.

3.2.1 Heart Rate During Treadmill Exercise – Steps in Unload Group

For the null hypotheses H0: The median value of the HR is the same across **categories (steps)** in **Unload** Group, when going through the non-parametric statistical test, the hypothesis is rejected (p-value < 0,01), and when we go through the pairwise comparisons between **categories (steps)** stands out that the steps 5 to 12 are significantly different from step 1 (0,001 < p-value < 0,043), steps 6 to 12 are significantly different from step 2 (0,001 < p-value < 0,025), steps 7 to 12 are significantly different from step 3 and from step 4 (0,001 < p-value < 0,035), steps 8 to 12 are significantly different from step 5 (0,001 < p-value < 0,003), steps 9 to 12 are significantly different from step 6 (0,001 < p-value < 0,032), steps 10 and 11 are significantly different from step 7 (0.04 < p-value < 0,045) (Fig. 6).

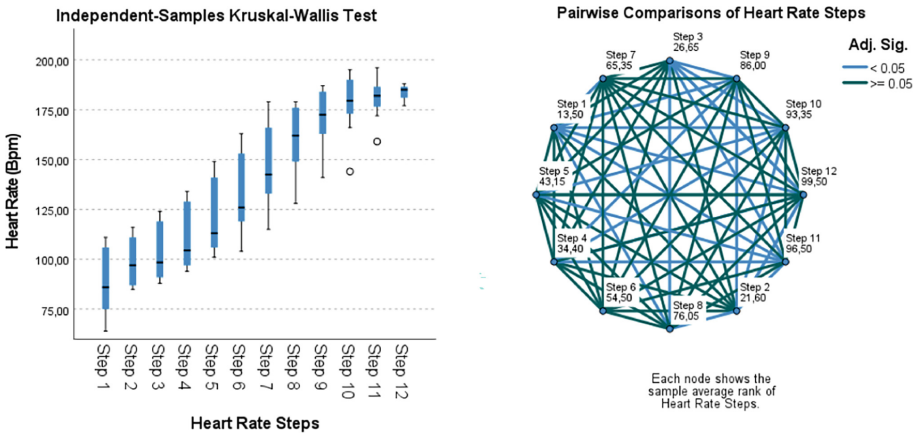

Fig. 6. Boxplot relative to Heart rate across categories (steps) in Unload Group (left) and pairwise comparisons between steps (right).

3.2.2 Heart Rate During Treadmill Exercise – Steps in Load Group

The Kruskal-Wallis non-parametric statistical test applied between **categories (steps)** in **Load** Group, for the null hypotheses H0: The median value of the HR is the same across **categories (steps),** is also rejected (p-value $<$ 0,01), and when we take effect comparisons between **categories (steps)** stands out that the steps 4 to 9 are significantly different from step 1 (0,001 $<$ p-value $<$ 0,049), steps 3 to 9 are significantly different from step 2 (0,001 $<$ p-value $<$ 0,007), steps 6 to 9 are significantly different from step 3 (0,004 $<$ p-value $<$ 0,021), and steps 7 and 9 are significantly different from step 4 (0,012 $<$ p-value $<$ 0,023) (Fig. 7).

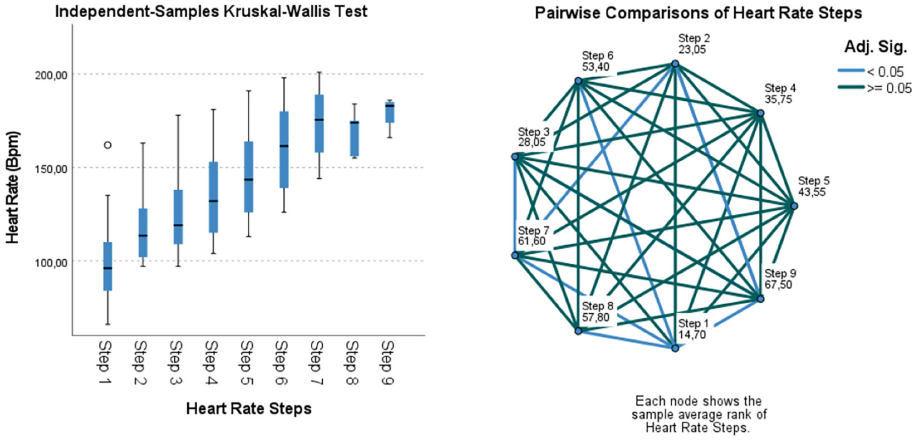

Fig. 7. Boxplot relative to Heart rate across categories (steps) in Load Group (left) and pairwise comparisons between steps (right).

3.3 Blood Lactate (mmol/l)

The step at which the blood lactate increases above resting levels is identical, the peak value for BL concentration for the Unloaded Condition occurs three steps prior to the Loaded Condition (Fig. 8).

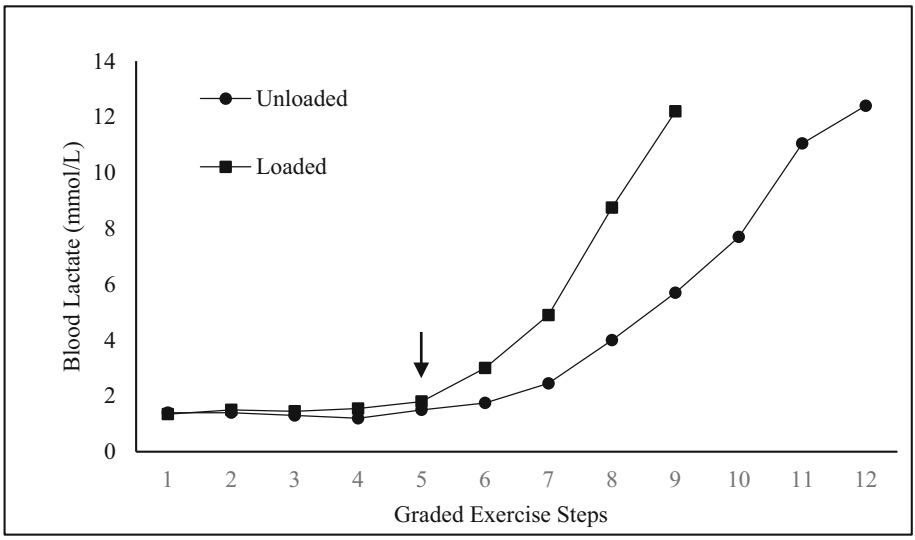

Fig. 8. Blood lactate concentration during the graded exercise protocol in both conditions (The vertical arrow represents the Lactate Threshold for both conditions).

From the perspective of the metabolic variable aimed at measuring BL concentration and given the null hypothesis, H0: The medians are the same across categories of Equipment, the Unloaded and Fully loaded groups, in each common step during the graded exercise protocol, through the Wilcoxon test, H0 is rejected from step 7 (0,007 $<$ *p*-value $<$ 0,001), and so significant differences emerged between the two groups in respect of blood lactate, from this level upwards.

3.3.1 Blood Lactate (mmol/l) – Steps in Unload Group

Considering the non-parametric statistical test for the null hypotheses H0: The median value of the BL is the same across **categories (steps)** in **Unload** Group; this one is rejected (*p*-value $<$ 0,000), and when we go through the pairwise comparisons between **categories (steps)** stands out that the steps 7 to 12 are significantly different from step 3 and from step 4 (0,024 $<$ *p*-value $<$ 0,001), the steps 8 to 12 are significantly different from step 6 and step 7 (0,017 $<$ *p*-value $<$ 0,001) (Fig. 9).

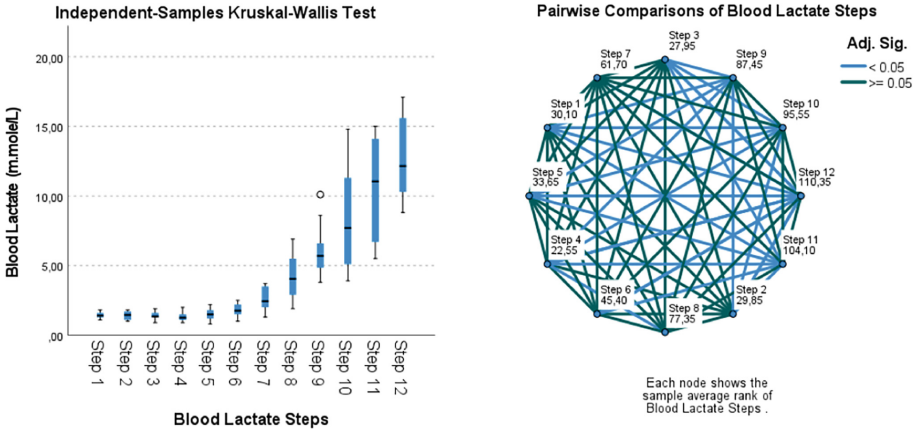

Fig. 9. Boxplot relative to Blood Lactate across categories (steps) in Unload Group (left) and pairwise comparisons between steps (right).

3.3.2 Blood Lactate (mmol/l) – Steps in Load Group

The Kruskal-Wallis non-parametric statistical test applied between **categories (steps)** in **Load** Group, for the null hypotheses H0: The median value of the BL is the same across **categories (steps),** is also rejected (p-value $< 0{,}001$), and when we take effect comparisons between **categories (steps)** stands out that the steps 7 to 9 are significantly different from step 1 to step 4 ($0{,}001 < p$-value $< 0{,}02$), steps 8 and 9 are significantly different from step 5 ($0{,}001 < p$-value $< 0{,}038$) (Fig. 10).

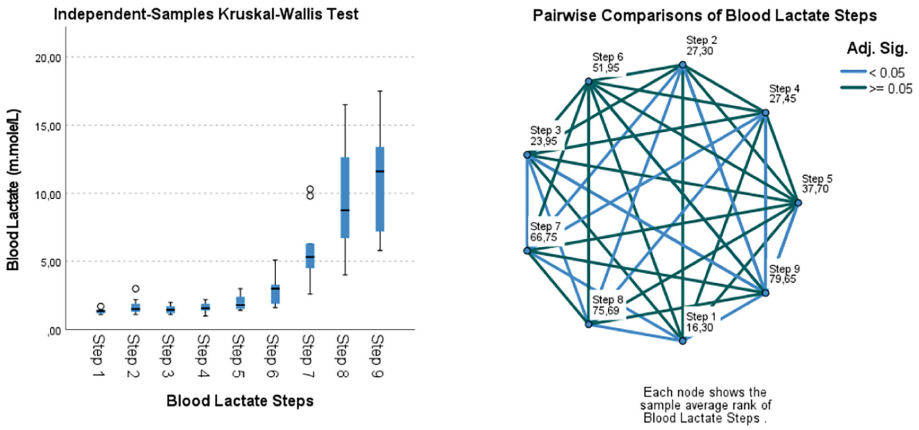

Fig. 10. Boxplot relative to Blood Lactate across categories (steps) in Load Group (left) and pairwise comparisons between steps (right).

4 Conclusions and Final Remarks

Changes in exercise tolerance caused by thoracic load carriage have been reported previously by several authors [9, 17, 18]. Although some authors have found no significant differences neither in VO_{2peak} nor in cardiorespiratory parameters (as long as the load is not excessive), thoracic load carriage may alter cardiopulmonary function [17].

This lends support to the possibility that cardiopulmonary function limits exercise with load carriage, but the point of work intolerance is perhaps reached earlier and at lower external work rates. According to Taylor [1] perhaps this (homeostatic) failure affects primarily less critical functions (hence the increased BL and HR) aiming to preserve pulmonary function.

This study was conducted with the aim of creating, implementing and analysing a suitably designed protocol, in order to quantify the metabolic cost of load carriage in a Portuguese special forces team combined with identification of differences in important metabolic variables in two conditions, Load vs Unload.

First, considering the Unloaded and Fully loaded groups, it was analysed if it provided different results of VO_{2peak}, HR and BL. It is important to emphasise that VO_{2peak} is significantly different between the two conditions, Load vs. Unload, but this difference is just registered in the metabolic variables related to HR and BL from a specific level. More specifically, from step 2 in heart rate, and from step 7 in BL.

Second, taking into account that higher differences were detected across categories (steps), when considering the conditions groups separately, an analysis is performed, which enables the definition of the VT, VO_{2peak} and BL threshold for each condition. Pairwise comparisons between steps are characterized and related to the physiological thresholds.

The RPE, another important metabolic variable, which was documented in the course of the protocol implemented, for the Unload and Fully Loaded Groups remains pending and will be considered in future analysis.

However, the conducted work up until now is considered to be a valuable contribution to the scientific community in the field of Human Performance, in comprehension the influence of load carriage on Portuguese special forces team performance, in particular and, on military missions' performance, in general. This study enables to enhance our understanding of the metabolic cost of load carriage, in a special forces team, and its impact in military readiness.

Acknowledgments. This work was funded by national funds through the project SmartVest, an Army Research and Development project of the Military Academy Research Center and the Military Readiness Lab.

Disclosure of Interests. The authors have no competing interests to declare that are relevant to the content of this article.

References

1. Taylor, N., Peoples, G., Petersen, S.: Load carriage, human performance, and employment standards 1. **147**(June), 131–47 (2016)
2. Ricciardi, R., Deuster, P., Talbot, L.: Metabolic demands of body armor on physical performance in simulated conditions. Mil. Med. **173**(9), 817–824 (2008)
3. Larsson, J., Dencker, M., Olsson, M., Bremander, A.: Development and application of a questionnaire to self-rate physical work demands for ground combat soldiers. Appl. Ergon. **1**(83), 103002 (2020)
4. Medby, J., Glenn, R.: Challenges posed by urbanized terrain. Str. Smart Intell. Prep. Battlef. Urban Oper. 25–38 (2022)
5. Knapik, J.: Load Carriage in Military Operations. Rev Lit Arts Am [Internet] (2010). http://oai.dtic.mil/oai/oai?verb=getRecord&metadataPrefix=html&identifier=ADA330082
6. Majumdar, D., Pal, M., Majumdar, D.: Effects of military load carriage on kinematics of gait. Ergonomics **53**(6), 782–791 (2010)
7. Attwells, R., Birrell, S., Hooper, R., Mansfield, N.: Influence of carrying heavy loads on soldiers' posture, movements and gait. Ergonomics **49**(14), 1527–1537 (2006)
8. Grenier, J., Millet, G., Peyrot, N., Samozino, P., Oullion, R., Messonnier, L., et al.: Effects of extreme-duration heavy load carriage on neuromuscular function and locomotion: a military-based study. PLoS One **7**(8) (2012)
9. Louhevaara, V., Ilmarinen, R., Griefahn, B., Künemund, C., Mäkinen, H.: Maximal physical work performance with European standard based fire-protective clothing system and equipment in relation to individual characteristics. Eur. J. Appl. Physiol. Occup. Physiol. **71**(2–3), 223–229 (1995)
10. Notley, S., Fullagar, H., Lee, D., Matsuda-Nakamura, M., Peoples, G., Taylor, N.: Revisiting ventilatory and cardiovascular predictions of whole-body metabolic rate. J. Occup. Environ. Med. **56**(2), 214–223 (2014)
11. Jones, A., Carter, H.: The effect of endurance training on parameters of aerobic fitness. Sport Med. **29**, 373–386 (2000)
12. Carter, H., Jones, A., Doust, J.: Effect of 6 weeks of endurance training on the lactate minimum speed. J. Sports Sci. **17**(12), 957–967 (1999)
13. Tanaka, K., Matsuura, Y., Matsuzaka, A., Hirakoba, K., Kumagai, S., Sun, S., et al.: A longitudinal assessment of anaerobic threshold and distance-running performance. Med. Sci. Sports Exerc. **16**(3), 278–282 (1984)
14. Pallarés, J., Morán-Navarro, R., Ortega, J., Fernández-Elías, V., Mora-Rodriguez, R.: Validity and reliability of ventilatory and blood lactate thresholds in well-trained cyclists. PLoS ONE **11**(9), e0163389 (2016)
15. Beaver, W., Wasserman, K., Whipp, B.: A new method for detecting anaerobic threshold by gas exchange. J. Appl. Physiol. **60**(6), 2020–2027 (1986)
16. Berger, R., Casella, G.: Statistical inference. Duxbury (2001)
17. Peoples, G., Lee, D., Notley, S., Taylor, N.: The effects of thoracic load carriage on maximal ambulatory work tolerance and acceptable work durations. Eur. J. Appl. Physiol. **116**, 635–646 (2016)
18. Phillips, D., Stickland, M., Petersen, S.: Ventilatory responses to prolonged exercise with heavy load carriage. Eur. J. Appl. Physiol. **116**, 19–27 (2016)

Performance Evaluation of Information Systems in Portuguese Municipalities

Domingos Martinho[1](✉), Inês Góis[1], Pedro Sobreiro[2], and António Pratas[1]

[1] ISLA Santarém, Rua Teixeira Guedes, 31, 2000-029 Santarém, Portugal
domingos.martinho@islasantarem.pt
[2] Instituto Politécnico de Santarém, Santarem, Portugal

Abstract. The success of organizations increasingly depends on the performance of their information systems, and public bodies are no exception. If the service provided to all of us, as citizens, depends on this performance, then it is essential that we can evaluate it. This research evaluates the performance of information systems in the Portuguese municipalities, applying the DeLone and McLean model, which is based on the perceptions of the systems' users. The research is based on a self-administered questionnaire to a representative sample of Portuguese municipalities employees. The six dimensions of the model were: system quality, information quality, service quality, utilization, user satisfaction and impacts. A seventh dimension - demographics - and its relationship with the original model were also analyzed. The results show that DeLone and McLean model is suitable for the Portuguese municipalities context, and it was concluded that the system quality and information quality dimensions have a major effect on user satisfaction and intention to use/use, respectively. It was also found that the user satisfaction dimension has a strong effect, and the intention to use/use dimension has a moderate effect on Impacts. These results provide relevant information for decision-making related to the evolution of information systems in Portuguese municipalities, showing the importance of investing in the systems quality and the quality of the information produced.

Keywords: DeLone and McLean · Information system · Information quality · Intention to use/use · Portuguese municipalities · Service quality · System quality · User satisfaction

1 Introduction

The new Information and Communication Technologies (ICT) are evolving rapidly and today play a fundamental role in the macro sectors of the economy, politics, society, and organisation [1].

In this context of digital revolution, the concept of e-government has emerged: a new management approach, in the case of public administration, which involves ICT [2], linking citizens, companies, public services and public bodies, generating administrative benefits such as improved public services, management efficiency, ethical behavior and transparency [3, 4].

© The Author(s), under exclusive license to Springer Nature Switzerland AG 2024
O. Gervasi et al. (Eds.): ICCSA 2024 Workshops, LNCS 14816, pp. 144–161, 2024.
https://doi.org/10.1007/978-3-031-65223-3_10

Although this evolution has been underway for three decades, little is known about the concrete results of its action in public administration. Knowing the impact of Information Systems (IS) is extremely important, since the overall performance of an organisation depends heavily on the performance of it IS, and the case of the public administration is no exception [5].

However, it is difficult to measure the performance of the public administration's IS, because we must not forget that a large part of the objectives and value creation in the public administration are intangible [4]. Among the many entities that the Portuguese public administration covers, it is at the local level (municipalities) that there is the greatest proximity to the citizen, which is why it is important to assess the performance of the information systems used.

The aim of this study is to assess the performance of IS in Portuguese municipalities by applying a widely validated model - the DeLone and McLean model [6]. This model makes it possible to evaluate IS based on the perspectives of its users, in this case municipalities employees, across all their activities and hierarchical levels [7, 8].

2 Literature Review and Research Framework

In this point we will focus the most important aspects of the study: (1) the context of application - Portuguese municipalities; (2) the techniques and metrics to performance assessment of information systems and (3) the application of the DeLone and McLean model to public administration.

2.1 Portuguese Municipalities

The Portuguese municipalities refers to local authorities (territorially based legal entities with their own representative bodies that aim to pursue the interests of their respective populations). Specifically, a local authority is made up of a Municipality and the respective Parish Councils. These entities are more complex from a management point of view than most organizations, and they also have customers to satisfy - citizens and local businesses - who evaluate the services provided and act on their opinion during municipal elections [9]. These customers are increasingly demanding in terms of the response from public services, as they are used to a certain quality and speed in the service provided by the private sector [10, 11].

In order to increase citizens' trust, thus influencing their assessment of local government management and consequently their voting decision, local authorities are increasingly adopting e-government [12], with the aim of making more innovative use of ICT, particularly networked platforms and the Internet, to provide citizens and businesses with more convenient access to information and services, improving the quality of services and providing greater opportunities for participation in democratic institutions and processes [13]. Thus, an e-government system consists of a single, integrated and networked electronic platform, which allows communication between the public administration, citizens, and organizations [14].

It is intended that local authorities use ICT so that they can be directly involved in decision-making processes [15]. In this way, the adoption of local e-government (e-government at local level) offers local authorities the opportunity to simultaneously

improve public services, management efficiency, openness to citizens (transparency), ethical conduct and professionalism, citizen confidence and the general well-being of the population [4].

2.2 Performance Assessment of Information Systems

To measure and evaluate the return on their investments, business organizations often rely on the financial indicator return on investment (ROI). However, it has already been demonstrated in other studies that this indicator is not appropriate for determining the effectiveness and efficiency of IS, as this is a complex, multidimensional task, and dependent on multiple and multidisciplinary criteria [16].

Nevertheless, and considering that the performance of the IS determines the individual performance of its users and, consequently, the overall performance of the organization, it is of the utmost importance that the investment in the IS is sustainable, and its return is countable [17–19].

It turns out that these impacts are difficult to measure given their intangible nature, such as the improvement in the quality of public services, efficiency in management, openness to citizens (transparency), ethical conduct and professionalism, citizen trust or the general well-being of the population [4].

As an aggravating factor, in the case of municipalities administration, investments dedicated to IS often come into direct competition with the amounts invested in issues of profound social importance such as social housing, employment or economic development of the region [20].

A performance assessment model is therefore needed for ISs that calculates the performance of their hardware, software, networking, data quality, but also the achievement of the organization's objectives as a whole [21].

2.3 DeLone and Mclean Model and Public Administration

The DeLone and McLean [6] information systems success model is one of the most widely used and well-regarded models for evaluating the success of information systems (IS). The model has been applied in a variety of contexts, including the public sector, where it has been used to assess the success of a wide range of IS initiatives. This model evaluates the performance of an IS through statistical analysis from the perspective of the system's users and includes six dimensions:

- System quality (SyQ): This dimension refers to the quality of the IS itself, including its ease of use, reliability, and performance.
- Information quality (IQ): This dimension refers to the quality of the information provided by the IS, including its accuracy, completeness, and relevance.
- Service quality (SeQ): This dimension refers to the quality of the support and assistance that users receive from the organization responsible for the information system (IS).
- User satisfaction (US): This dimension refers to the level of satisfaction that users have with the IS.

- Intention to use/Use (U): This dimension refers to the extent to which the IS is used by users.
- Impacts (I): This dimension refers to the ultimate consequences of using an information system within an organization. It encompasses the broader organizational, individual, and societal benefits that result from IS implementation and usage.

Although the DeLone and McLean [6] model has been widely validated when it comes to IS success evaluation, there are studies that focus on public sector and/or on local public administration.

All six factors in the model were considered in evaluating the performance of the newly implemented IS in three public hospitals in Korea [22]. The indicators analyzed were adapted to the hospital context, and the model confirmed that the three quality factors have a significant influence on user satisfaction and that this has a very strong influence on the benefits/impacts for the organization. They also conclude that both system quality and information quality are significant for the intention to use/use factor, but service quality did not show the same relationship, which was associated by researchers with the fact that the implementation was conducted recently [22].

The model was also used to evaluate the performance of a system (governmental IS) in one state in India [21]. This study focuses especially on understanding the effect of exogenous variables on user satisfaction and intention to use/use. There is a strong effect of information quality on intention to use/use. Similarly, there is an effect of the service quality and information quality dimensions on user satisfaction [21].

The e-government system in the Republic of Serbia was studied [8] using the DeLone and McLean [6] model, with employees of the local public administration. In this study, the demographic data of the respondents associated with the intention to use/use dimension were considered as an extra dimension. The results show that all three dimensions of quality (system quality, information quality and service quality) had a positive impact on intention to use/use, and that only service quality had a significant effect on user satisfaction. Intention to use/use had a positive and direct effect on user satisfaction. The intention to use/use and user satisfaction are significant in predicting benefits/impacts [8].

A study carried out in three organizations in the public sector in Belgium [23] to verify its explanatory power for the public sector, shows that the model demonstrates suitability. The researchers concluded that system quality, information quality and service quality have a medium effect on user satisfaction, and user satisfaction is strongly correlated with impacts [23].

Another adaptation of the model was put into practice in evaluating the performance of the Iraqi e-government system [24]. The results shows that dimensions system quality, service quality and information quality have a significant effect on intention to use /use and user satisfaction. It can also be seen that user satisfaction has a strong effect on impacts, while intention to use/use has an insignificant effect on impacts [24].

In a study targeting end users in all public-sector organizations in Kuwait, researchers [25] concluded that information quality has a significant positive effect on intention to use/use and user satisfaction. Intention to use/use did not have a significant effect on IS success, while information quality is more important for maintaining and enhancing IS use.

The DeLone and McLean [6] model was used in Tunisia to evaluate the model of e-government success from the perspective of government employees [26]. The results show that intention to use/use and user satisfaction positively affect impacts. The study also found that government employees' use and of e-government systems had a direct positive impact on intention to use/use and user satisfaction.

The model was also used to evaluate the performance of the IS used for human resources management in the public sector in Morocco [27]. The quality of information, the quality of the system, the quality of service, the use, the user satisfaction, and impacts are the main factors that influence the success of the IS. Finally, it was concluded that intention to use/use and user satisfaction dimensions has a strong effect on impacts [27].

2.4 Research Framework Hypotheses

The possibilities of correlation between the dimensions of the DeLone and McLean [6] model (Fig. 1) which was analyzed in this investigation, are the following:

- Hypothesis 1 (H1): SyQ positively affects U.
- Hypothesis 2 (H2): SyQ positively affects US.
- Hypothesis 3 (H3): IQ positively affects U.
- Hypothesis 4 (H4): IQ positively affects US.
- Hypothesis 5 (H5): SeQ positively affects U.
- Hypothesis 6 (H6): SeQ positively affects US.
- Hypothesis 7 (H7): US positively affects U.
- Hypothesis 8 (H8): U positively affects I.
- Hypothesis 9 (H9): US positively affects I.
- Hypothesis 10 (H10): D positively affects U.
- Hypothesis 11 (H11): D positively affects US.

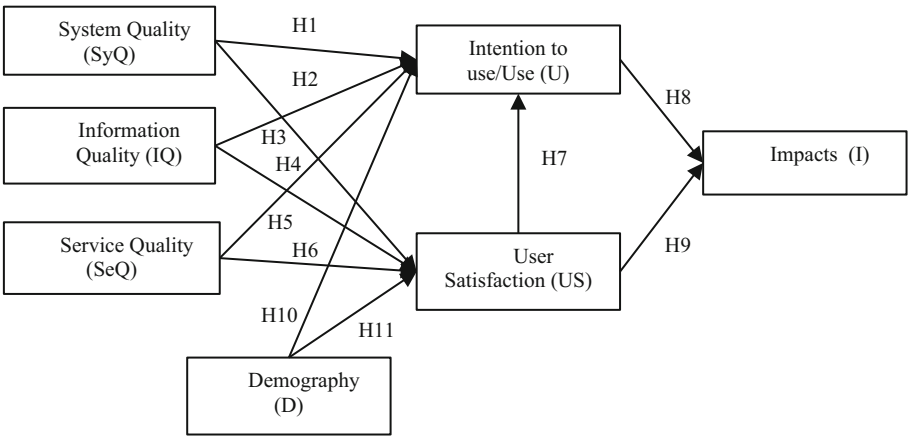

Fig. 1. DeLone and McLean Model [6] adapted.

3 Research Methodology

3.1 Participants and Data Collection

The participants (n = 1.310) where Portuguese municipalities employees, which in 2022 would represent a total of 137.205 employees [28], that were invited to participate in the questionnaire. The link to questionnaire was sent to everyone through e-mail message, along with an introduction about the research objectives.

For large populations, as the population increases, the sample size also increases, but at a decreasing rate, and remains relatively constant after 380 cases, with a margin of error of 5% and a precision of 95% [29]. We can therefore consider that, even though a convenience sampling method was used, the sample is sufficiently representative of the population.

3.2 Local Public Administration Employees Personal Information/Demographic Data

The questionnaire opened with a section dedicated to characterizing the respondents. This section corresponds to the demographic dimension (D) added to the model. The aim of this adaptation to the model was to understand whether the socio-demographic characteristics of Portuguese municipalities employees influenced their level of satisfaction as IS users, as well as their intention to use [8, 30]. The demographic characteristics considered relevant to the study were those that were thought to have the greatest significance in terms of the interaction between a worker and the IS available for carrying out their duties in the local authority.

The percentage of women respondents was 47 %, while men accounted for 53.0 % of the sample. Age stratification showed that 3.9 % of the employees were up to 29 years old, 13.8 % between 30 and 39, 41.0 % between 40 and 49, 32.4 % between 50 and 59 and 8.9 % aged 60 or over. In terms of academic qualifications, 1.5 % of the participants had primary education, 34.7 % had secondary education and 63.8 % had higher education. In terms of their position in the municipality, 9.2 % were operational assistants, 33.4 % technical assistants, 49.5 % senior technicians and 7.8 % hold political or senior positions (Fig. 2).

3.3 Survey Instrument and Structure

Considering the research developed on the conceptual model and considering the specific characteristics of the object under study – IS of the Portuguese municipalities – measurement indicators were defined for each of the six dimensions of the model (Table 1).

3.4 Pilot Study for the Questionnaire

Even knowing that the conceptual model [6] has already been validated numerous times, it is necessary to consider the (previously predicted) disparities in terms of educational qualifications and vocabulary used among the questionnaire participants.

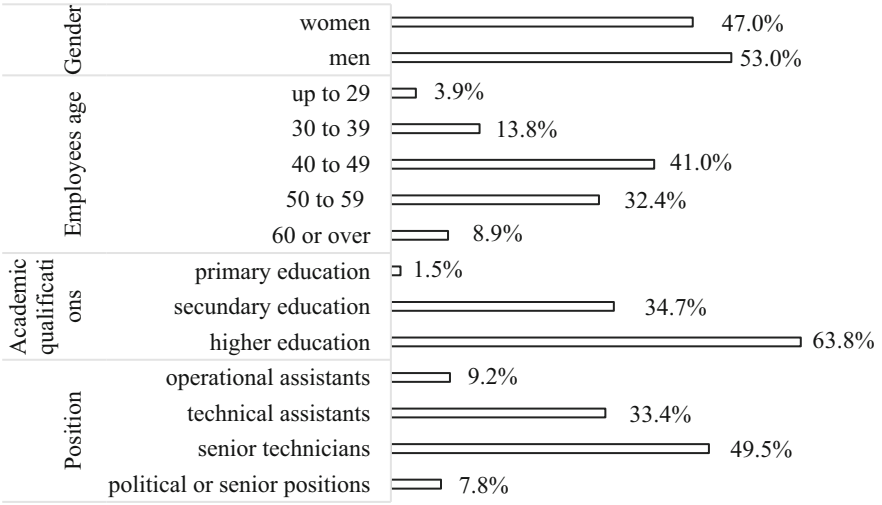

Fig. 2. Characterization of respondents (sample)

Table 1. Measurement Indicators.

Constructs	Items	Variable	Sources
System Quality (SyQ)	Pleasantness Intuition Functionality Celerity Integration	SyQ1 SyQ2 SyQ3 SyQ4 SyQ5	[6–8]
Information Quality (IQ)	Precision Update Trust	IQ1 IQ2 IQ3	[6–8]
Service Quality (SeQ)	Readiness Guarantee Empathy	SeQ1 SeQ2 SeQ3	[6–8, 30]
Intention to use/Use (U)	Dependency Frequency Duration Intention	U1 U2 U3 U4	[6–8]
User Satisfaction (US)	Satisfaction Expectation	US1 US2	[6–8]
Demography (D)	Age Gender Education Position	D1 D2 D3 D4	[8, 30]
Impacts (I)	Utility Efficiency Efficiency Control	I1 I2 I3 I4	[[6–8, 31]

Furthermore, it was necessary to conduct a linguistic adaptation, both in terms of translation in relation to the original model (and respective measurement indicators), and in relation to the context under study and respective target audience.

The method selected was the one in which most researchers place their trust: the Cronbach's Alpha internal reliability estimation technique [32]. This test is considered crucial when dealing with Likert scales [33].

The questionnaire was evaluated on an initial sample of twenty-one respondents, all of them employees of the Portuguese municipalities, selected by convenience.

An alpha value greater than 0.9 was obtained (Table 2), considering the excellent internal consistency reliability of the questionnaire [34].

Table 2. Cronbach's alpha value for pilot study.

Cronbach's alpha	Number of Items
0.928	21

3.5 SPSS and SmartPLS

SPSS Statistics v29 software [35] was used to analyze the demographic data, while SmartPLS 4 software [36] was used to estimate the PLS-SEM models. This tool can handle non-normal data, exploratory research for the same effect size and model complexity, and focus on prediction [37, 38].

3.6 Adjustment Quality for the PLS-SEM Model

The reference values for assessing the quality of the fit of the PLS-SEM model, as suggested in other studies [36–39, 41] were as follows:

- Loadings. Path loads must be above 0.70. The indicator should be discarded if the value is between 0.4 and 0.7 and if removing it improves composite reliability [37–39].
- Variance inflation factor (VIF). Indicates multicollinearity. VIF values should be <5 [38–40].
- Cronbach's Alpha (CA) and Composite Reliability (CR). They evaluate the reliability and internal consistency of the measuring instrument. Values >0.70 are satisfactory [36–39].
- Average variance extracted (AVE). Evaluates the portion of the variance of endogenous variables explained by the structural model. Results above the cutoff point >0.67 "substantial"; >0.33 "moderate"; >0.19 "weak" [37–39].
- R-square. Results with cutoffs 0.67, 0.33 and 0.19 are "substantial", "moderate" and "weak", respectively [37–39].
- Predictive validity (Q-square) or Stone-Geisser Indicator. Establishes the predictive relevance of endogenous constructs. Q-square >0 is good. [39, 41].
- Discriminant validity (DV). Fornell-Larcker criterium. The square roots of the AVEs must be greater than the correlations of the constructs [38, 42].

- F-square (Choen Indicator). Indicates the size of the effect. Values >0.35, >0.15, >0.02 and <0.02 are considered "strong", "moderate", "weak", "non-existent" respectively [37–39].

3.7 Model Adjustment

Analysis of the loadings of each of the factors (items) showed that there existed four items that has a value lower than 0.7. Following the protocol foreseen in these situations, the four variables that presented values lower than 0.7 were removed from the model and a new specification test was conducted. In this specification all weights of variable were greater than 0.7 and composite reliability improved. This meaning that the model has good adjustment characteristics. (Table 3).

Table 3. Adjustment quality for the SEM model.

Constructs	Items	Loadings	VIF	CA	CR	AVE	R-square	Q-square
SyQ	SyQ1	0.864	2.695	0.886	0.888	0.744	–	–
	SyQ2	0.873	2.814					
	SyQ3	0.874	2438					
	SyQ4	0.840	2.197					
IQ	IQ1	0.818	1.534	0.779	0.782	0.693	–	–
	IQ2	0.858	1.701					
	IQ3	0.821	1.628					
SeQ	SeQ1	0.834	1.733	0.809	0.812	0.724	–	–
	SeQ2	0.877	1.939					
	SeQ3	0.841	1.692					
D	D3	0.920	2.081	0.838	0.853	0.860	–	–
	D4	0.934	2.081					
U	U1	0.863	2.074	0.810	0.824	0.637	0.399	0.392
	U3	0.847	2.191					
	U4	0.824	1.496					
US	US1	0.950	2.791	0.890	0.890	0.901	0.685	0.682
	US2	0.948	2.791					
I	I1	0.917	3.603	0.914	0.914	0.795	0.683	0.632
	I2	0.888	2.978					
	I3	0.866	2.347					
	I4	0.893	2.892					

The values of VIF (<5), CA (> 0.70), CR (> 0.70), AVE (>0.67 "substantial" or >0.33 "moderate"), R-square (>0.67 "substantial" or >0.33 "moderate") and Q-square (> 0) presented in Table 3, show that the model has well-fitting conditions.

The discriminating validity (DV) results presents the highest value on the main diagonal, which means that the square roots of the AVEs its greater than the correlations of the constructs (Table 4).

Table 4. Discriminating Validity (Fornell – Larcker criterion).

	D	I	IQ	SeQ	SyQ	U	US
D	0,927						
I	–0,017	0,891					
IQ	0,002	0,736	0,833				
SeQ	0,042	0,611	0,631	0,851			
SyQ	–0,067	0,730	0,732	0,532	0,863		
U	0,067	0,616	0,601	0,515	0,488	0,798	
US	–0,068	0,782	0,707	0,610	0,788	0,489	0,949

The F-square Indicator values show that the effect of the user satisfaction (US) and intention to use/use (U) dimensions on impacts (I) are strong > 0.35 and moderate > 0.15, respectively. The effect of system quality (SyQ) dimension on user satisfaction (US) is strong > 0.35. All remaining effects are low (between 0.02 and 0.15) (Table 5).

Table 5. F-square (Choen Indicator).

Causal Relations	Coefficient Analyses
Demography (D) -> Intention to use/Use (U)	0,002
Demography (D) -> User Satisfaction (US)	0,006
Information Quality (IQ) -> Intention to use/Use (U)	0,083
Information Quality (IQ) -> User Satisfaction (US)	0,028
Intention to use/Use (U) -> Impacts (I)	0,221
Intention to use/Use (U) -> User Satisfaction (US)	0,006
Service Quality (SeQ) -> Intention to use/Use (U)	0,048
Service Quality (SeQ) -> User Satisfaction (US)	0,070
System Quality (SyQ) -> Intention to use/Use (U)	0,009
System Quality (SyQ) -> User Satisfaction (US)	0,413
User Satisfaction _(US) -> Impacts (I)	0,901

4 Results

The results of the test of the adjusted model, conducted using the bootstrapping algorithm so that the relationship between exogenous variables and endogenous variables can be obtained taking moderation into account, were as follows (Fig. 3):

- The system quality (SyQ) dimension has a weak effect on the intention to use/use (U) dimension (0.108) and a strong effect on the user satisfaction (US) dimension (0.538).
- The information quality (IQ) dimension has a strong effect on the intention to use/use (U) dimension (0.365) and a moderate effect on the user satisfaction (US) dimension (0.157).
- The service quality (SeQ) dimension has a moderate effect on both the intention to use/use (U) dimension (0.225) and the user satisfaction (US) dimension (0.197).
- The intention to use/use (U) dimension has a moderate effect (0.309) on the impacts (I) dimension.
- The intention to use/use (U) dimension has a weak effect on the user satisfaction (US) dimension (0.056).
- The user satisfaction (US) dimension has a strong effect on the impacts (I) dimension (0.624).
- The demography (D) dimension has a weak effect on the intention to use/use (U) dimension (0.034) and a zero effect on user satisfaction (US) (-0.043).

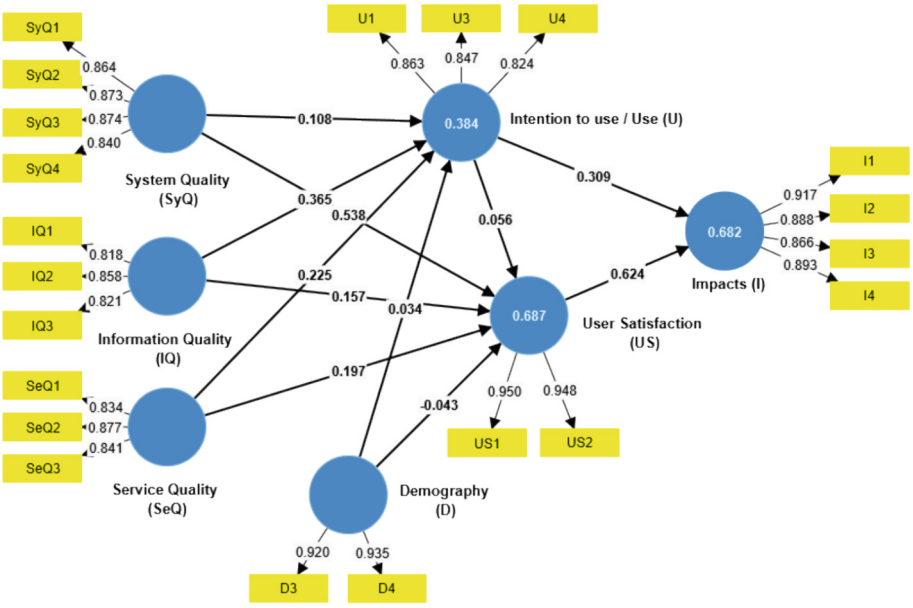

Fig. 3. Partial least square structure model (inner path coefficients and outer weights).

4.1 Specific Indirect Effects

The system quality (SyQ) has a significant indirect effect on user satisfaction (US), which in turn influences impacts (I) (0.335). The service quality (SeQ), through the intention to use/use, and service quality (SeQ), through the user satisfaction (US), have a significant indirect effect on impact (I) (Table 6).

Table 6. Specific Indirect Effects

Causal Relations	Coefficient Analyses
Demography (D) -> Intention to use/Use (U) -> Impacts (I)	0,011
Demography (D) -> Intention to use/Use (U) -> User Satisfaction (US) -> Impacts (I)	0,001
Intention to use/Use (U) -> User Satisfaction (US) -> Impacts (I)	0,035
Demography (D) -> User Satisfaction (US) -> Impacts (I)	−0,027
Information Quality (IQ) - > Intention to use/Use (U) -> Impacts (I)	0,113
Information Quality IQ) -> Intention to use/Use (U) -> User Satisfaction (US) -> Impacts (I)	0,013
Intention to use/Use (U) -> User Satisfaction (US) -> Impacts (I)	0,035
Information Quality (IQ) -> User Satisfaction (US) -> Impacts (I)	0,098
Intention to use/Use (U) - > User Satisfaction (US) -> Impacts (I)	0,035
Service Quality (SeQ) -> Intention to use/Use (U) -> Impacts (I)	0,070
Service Quality (SeQ) -> Intention to use/Use (U) -> User Satisfaction (US) -> Impacts (I)	0,008
Intention to use/Use (U) -> User Satisfaction (US) -> Impacts (I)	0,035
Service Quality (SeQ) -> User Satisfaction (US) -> Impacts (I)	0,123
System Quality (SyQ) -> Intention to use/Use (U) -> Impacts (I)	0,033
System Quality (SyQ) -> Intention to use/Use (U) -> User Satisfaction (US) -> Impacts (I)	0,004
Intention to use/Use (U) -> User Satisfaction (US) -> Impacts (I)	0,035
System Quality (SyQ) -> User Satisfaction (US) -> Impacts (I)	0,335

4.2 Results of Formulated Hypotheses

The results show that only one of the initially predicted correlations was found to be non-existent (H11): demography (D) has no effect on the user satisfaction (US) dimension. On the other hand, demography (D) has an effect (albeit weak, of 0.056) on intention to use/use (U) (Table 7).

The system quality (SyQ) has a greater influence on user satisfaction (US) than on the intention to use/use (U) of the system itself by employees. Information quality (IQ) has a

positive effect on intention to use/use (U) (strong) and user satisfaction (US) (moderate). Service quality (SeQ) has a moderate effect on user satisfaction (US) and intention to use/use (U).

Intention to use/use (U) and user satisfaction (US) dimensions are interdependent, linked, the correlation between these variables is only weak (0.056). Regarding the impacts (I) dimension, intention to use/use (U) exerts influence (moderate), but it is user satisfaction (US) that demonstrates the greatest effect (strong).

The factor that most influences the size of the impacts (I) is user satisfaction (US), which in turn is influenced by the quality of the system (SyQ).

Table 7. Results of Formulated Hypotheses

Hypothesis	Path Coefficients	Results	Effect
H1: SyQ positively affects U	0.108	Confirmed	Weak
H2: SyQ positively affects US	0.538	Confirmed	Strong
H3: IQ positively affects U	0.365	Confirmed	Strong
H4: IQ positively affects US	0.157	Confirmed	Moderate
H5: SeQ positively affects U	0.224	Confirmed	Moderate
H6: SeQ positively affects US	0.197	Confirmed	Moderate
H7: U positively affects US	0.056	Confirmed	Weak
H8: U positively affects I	0.309	Confirmed	Moderate
H9: US positively affects I	0.624	Confirmed	Strong
H10: D positively affects U	0.034	Confirmed	Weak
H11: D positively affects US	−0.043	Not confirmed	Non-existent

5 Results Discussion

The results show the suitability of applying DeLone and McLean [6] model in the context of Portuguese municipalities. The model proved to be adequate for the purpose of the research and only one of the correlations predicted in the model proved to be non-existent (H11): demographics (D) has no effect on the dimension of user satisfaction (US). On the other hand, demography (D) has an effect (weak, of 0.064) on use (U). This result, although weak, differs from that obtained by (Stefanovic et al. [8], which did not find any correlation between these two variables.

The empirical results demonstrate that system quality (SyQ) has a greater influence on user satisfaction (US) that is, Portuguese municipalities employees. This conclusion confirms the results obtained by similar studies [21–24]. It is also verified that the system quality has a weak influence on the intention to use/use (U). Considering the strong effect of system quality (SyQ) on user satisfaction (US), it seems that when the IS of the Portuguese municipalities is easy to use and dependable, employees are likely to feel more motivated and provide better services to citizens.

The study conclude that information quality (IQ) has a positive effect on intention to use/use (U) dimension (strong) and user satisfaction (US) (moderate). The effect on user satisfaction (US) is confirmed in other studies [21–25], while the effect of information quality (IQ) on intention to use/use (U) is like others [8, 21, 22, 24, 25]. The results obtained in this investigation mean that when the information available on IS is accurate, up-to-date, and relevant, Portuguese municipalities employees are more likely to use it, with the possibility of a positive impact on the services provided to citizens.

The service quality (SeQ) has a moderate effect on user satisfaction (US) and intention to use/use (U). This conclusion is confirmed by previous studies [8] but differs from other studies in which only the effect of service quality (SeQ) on user satisfaction (US) [21–23] or intention to use/use (U) [24] is confirmed. These results suggest that when Portuguese municipalities employees have quality of the support and assistance from the IS organisation, they are more likely to get involved and eventually contribute to a better service for citizens.

The intention to use/use (U) dimension exerts influence (moderate) on impacts (I) which is confirmed by previous studies [8, 26] while the study of Attar and Mazouz [27] conclude that the effect is strong and other studies do not confirm this effect [24, 25]. This conclusion shows that there is a probability of the intention to use/use (U) the IS in the future will have an impact on the success of the service provided to citizens.

The findings showed that user satisfaction (US) has the greatest effect (strong) on impacts (I). All the studies analyzed show the effect of user satisfaction (US) on impacts (I), and in most of these studies the conclusion is that, as in this study, there is a strong effect [8, 21–24, 27]. It should be noted that the factor that most influences the impacts (I) dimension is user satisfaction (US), which is influenced by system quality (SyQ) (although other correlations also occur) [43]. The results suggest that Portuguese municipalities should not only focus on systems quality; rather, but they should also continuously improve service quality and information quality to improve user satisfaction and eventually reach full the potential of IS performance. Finally, the results shows that the investment in the quality of the IS will have an impact on user satisfaction with which employees perform their tasks and thus constitute a contribution to improving the service that they provide to citizens.

6 Limitations

It is important to mention the limitations that this study faced related to the lack of data on the reality on which the study was intended to be conducted. Data on the number of Portuguese municipalities employees and their distribution by gender were obtained, but it was not possible to obtain data regarding other demographic aspects. Although the sample was considered representative, it was feared the lack of rigor in relation to the general panorama of the population about the distribution of the variables of the area of activity and the district, so it was decided not to carry out the analysis for these cases, avoiding. Thus, the deviations that could result from inter-municipal diversity and from the fact that many Portuguese municipalities did not participate in this survey. This issue was also addressed in a study of Sirsat and Sirsat [21]. In this study, the authors considered that the administrative and implementation diversity of IS that was felt between regions could have distorted the obtained results.

7 Conclusions

The present study adapted the success of DeLone and McLean [6] model, to evaluate the IS of Portuguese municipalities. The most relevant conclusions of the study are extremely important for decision-makers in the Portuguese municipalities as they reveal that employees express a high degree of satisfaction user satisfaction (US)) in relation to the IS they use. It is also concluded that the technical specificities of the system quality (SyQ) have a preponderant effect on satisfaction of employees and information quality (IQ) as a significant effect on intention to use/use (U).

The obtained results suggest that Portuguese municipalities managers should: (1) ensure that the information provided by the system is accurate, relevant, and accessible; (2) make the system easy to use and flexible; (3) provide effective user support; (4) ensure that users are satisfied with the systems.

By following these recommendations, managers can improve the effectiveness of the IS of Portuguese municipalities and provide a better quality of service to citizens.

To further this investigation, it would be interesting to evaluate the performance of the IS for each municipality individually, using this same conceptual model, with the aim of eliminating the limitation detected in terms of administrative and geographic diversity [21].

This model could also be applied within other public sector entities such as justice, health, education, etc. There is also another perspective that was not evaluated in this investigation, but which could be a source of relevant information in this context: the citizen's perspective.

References

1. Roztocki, N., Weistroffer, H.R.: Information and communication technology in transition economies: an assessment of research trends. Inf. Technol. Dev. **21**(3), 330–364 (2015). https://doi.org/10.1080/02681102.2014.891498
2. Bonsón, E., Torres, L., Royo, S., Flores, F.: Local e-government 2.0: Social media and corporate transparency in municipalities. Govern. Inform. Quar. 123–132 (2018). https://doi.org/10.1016/j.giq.2011.10.001
3. Heeks, R.: Understanding e-governance for development. i-Government Working Paper Series. Institute for Development Policy and Management, pp. 1–25 (2019)
4. Twizeyimana, J.D., Andersson, A.: The public value of E-Government–a literature review. Gov. Inf. Q. **36**(2), 167–178 (2019). https://doi.org/10.1016/j.giq.2019.01.001
5. Aydiner, A.S., Tatoglu, E., Bayraktar, E., Zaim, S.: Information system capabilities and firm performance: opening the black box through decision-making performance and business-process performance. Int. J. Inf. Manage. **47**, 168–182 (2019). https://doi.org/10.1016/j.ijinfomgt.2018.12.015
6. DeLone, W.H., McLean, E.R.: The DeLone and McLean model of information systems success: a ten-year update. J. Manag. Inf. Syst. **19**(4), 9–30 (2003). https://doi.org/10.1080/07421222.2003.11045748
7. Petter, S., DeLone, W., McLean, E.: Measuring information systems success: models, dimensions, measures, and interrelationships. Eur. J. Inf. Syst. **17**(3), 236–263 (2008). https://doi.org/10.1057/ejis.2008.15

8. Stefanovic, D., Marjanovic, U., Delić, M., Culibrk, D., Lalic, B.: Assessing the success of e-government systems: an employee perspective. Inform. Manage. **53**(6), 717–726 (2016). https://doi.org/10.1016/j.im.2016.02.007
9. Ralha, J.: Da Gestão, em Autarquias – Para Melhorar as Competências em Gestão, dos Eleitos, pp. 23–33. Edições Sílabo, Lda, Lisboa (2018). ISBN:978-972-618-942-8
10. Torres, L., Pina, V., Acerete, B.: E-government developments on delivering public services among EU cities. Gov. Inf. Q. **22**(2), 217–238 (2005). https://doi.org/10.1016/j.giq.2005.02.004
11. Pérez-Morote, R., Pontones-Rosa, C., Núñez-Chicharro, M.: The effects of e-government evaluation, trust and the digital divide in the levels of e-government use in European countries. Technol. Forecast. Soc. Change **154**, 119973 (2020). https://doi.org/10.1016/j.techfore.2020.119973
12. Tolbert, C.J., Mossberger, K.: The effects of E-government on trust and confidence in government. Public Adm. Rev. **66**(3), 354–369 (2006). https://doi.org/10.1111/j.1540-6210.2006.00594.x
13. Fang, Z.: E-government in digital era: concept, practice, and development. Int. J. Comput. Internet Manage. **10**(2), 1–22 (2002)
14. West, D.M.: E-government and the transformation of service delivery and citizen attitudes. Public Admin. Rev. **64**(1), 15–27 (2004). http://www.jstor.org/stable/3542623. Accessed 8 Jan 2024
15. Welch, E.W., Hinnant, C.C., Moon, M.J.: Linking citizen satisfaction with e-government and trust in government. J. Public Admin. Res. Theory **15**(3), 371–391 (2005). https://doi.org/10.1093/jopart/mui021
16. Botchkarev, A., Andru, P., Chiong, R.: A return on investment as a metric for evaluating information systems: taxonomy and application. Interdiscipl. J. Inform. Knowl. Manage. **6**, 245–269 (2011). https://doi.org/10.28945/1535
17. Monk, E.F., Wagner, B.J.: Concepts in enterprise resource planning. Course Technology, Boston (2013)
18. Nevo, S., Wade, M.R.: The formation and value of IT-enabled resources: antecedents and consequences of synergistic relationships. MIS Quar. 163–183 (2010). https://doi.org/10.2307/20721419
19. Irani, Z., Abril, R.M., Weerakkody, V., Omar, A., Sivarajah, U.: The Impacts of legacy systems on digital transformation in European public administration: Lesson learned from a multi case analysis. Govern. Inform. Quar. **40.1**, 101784 (2023). https://doi.org/10.1016/j.giq.2022.101784
20. Gouveia, L.B.; Ranito, J.: Sistemas de Informação de Apoio à Gestão. Inovação e Governação nas Autarquias VII. SPI – Sociedade Portuguesa de Inovação, Porto (2004). ISBN:972 8589 43 3
21. Sirsat, S.S., Sirsat, M.S.: A validation of the DeLone and McLean model on the educational information system of the Maharashtra State (India). Int. J. Educ. Learn. Syst. **2016**(1), 9–18 (2016)
22. Cho, K.W., Bae, S.K., Ryu, J.H., Kim, K.N., An, C.H., Chae, Y.M.: Performance evaluation of public hospital information systems by the information system success model. Healthcare Inform. Res. **21**(1), 43–48 (2015). https://doi.org/10.4258/hir.2015.21.1.43
23. Van Cauter, L., Verlet, D., Snoeck, M., Crompvoets, J.: The explanatory power of the Delone & McLean model in the public sector: a mixed method test. Inform. Polity **22**(1), 41–55 (2017). https://doi.org/10.3233/IP-170404
24. Al-Sulami, Z.A., Hashim, H.S.: Measuring the success of e-government systems: applying the success model of the Delone and Mclean information system. J. Theor. Appl. Inf. Technol. **96**(22), 7654–7670 (2018)

25. Rouibah, K., Dihani, A., Al-Qirim, N.: Critical success factors affecting information system satisfaction in public sector organizations: a perspective on the mediating role of information quality. J. Global Inform. Manage. **28**(3), 77–98 (2020). https://doi.org/10.4018/JGIM.2020070105
26. Mellouli, M., Bouaziz, F., Bentahar, O.: E-government success assessment from a public value perspective. Int. Rev. Public Admin. **25**(3), 153–174 (2020). https://doi.org/10.1080/12294659.2020.1799517
27. Attar, A., Mazouz, Y.: Evaluation of human resources information system success in public sector. Int. J. Innov. Appl. Stud. **34**(1), 81–90 (2021)
28. DGAEP. Booletim estatístico do emprego público (BOEP) (2021). https://www.dgaep.gov.pt/index.cfm?OBJID=C0F56E62-5381-4271-B010-37ECE5B31017. Accessed on 25 July 2023
29. Krejcie, R.V., Morgan, D.W.: Determining sample size for research activities. Educ. Psychol. Measur. **30**(3), 607–610 (1970). https://doi.org/10.1177/001316447003000308
30. Jiang, J., Klein, G.: User evaluation of information systems: By system typology. IEEE Trans. Syst. Man Cybern. **29**(1), 111–116 (1999). https://doi.org/10.1109/3468.736366
31. Torkzadeha, G., Doll, W.: The development of a tool for measuring the perceived impact of information technology on work. Omega, Int. J. Mgmt. Sci. **27**, 327–339 (1999). https://doi.org/10.1016/S0305-0483(98)00049-8
32. Marôco, J., Garcia-Marques, T.: Qual a fiabilidade do alfa de Cronbach? Questões antigas e soluções modernas? Laboratório de psicologia, pp. 65–90 (2006). https://doi.org/10.14417/LP.763
33. Gliem, J.A., Gliem, R.R.: Calculating, interpreting, and reporting Cronbach's alpha reliability coefficient for Likert-type scales. In: Midwest Research-to-Practice Conference in Adult, Continuing, and Community Education, pp. 82–88. Ohio State University, Ohio, EUA (2003)
34. George, D., Mallery, P.: IBM SPSS statistics 26 step by step: a simple guide and reference. Routledge, United Kingdom (2019). https://doi.org/10.4324/9780429056765
35. Marôco, J.: Análise Estatística com o SPSS Statistics. ReportNumber, Lda, Pêro Pinheiro, Portugal (2021). ISBN:9789899676374
36. Ringle, C.M., Wende, S., Becker, J.-M.: SmartPLS 4. SmartPLS: GmbH, Oststeinbek (2022). http://www.smartpls.com
37. Hair, J.F., Jr., Sarstedt, M., Hopkins, L., Kuppelwieser, V.G.: Partial least squares structural equation modeling (PLS-SEM), a emerging tool in business research. Eur. Bus. Rev. **26**, 106–121 (2014). https://doi.org/10.1108/EBR-10-2013-0128
38. Hou, H.-Y., Lo, Y.-L., Lee, C.-F.: Predicting network behavior model of E-learning partner program in PLS-SEM. Appl. Sci. **10**, 4656 (2020). https://doi.org/10.3390/app10134656
39. Martinho, D., Sobreiro, P., Vardasca, R.: Teaching sentiment in emergency online learning—a conceptual model. Educ. Sci. **11**, 53 (2021). https://doi.org/10.3390/educsci11020053
40. Marôco, J.: Análise de Equações Estruturais; ReportNumber, Lisboa, Portugal (20100. ISBN 9789899676336

41. Tenenhaus, M., Vinzi, V.E., Chatelin, Y.M., Lauro, C.: PLS path modeling. Comput. Stat. Data Anal. **48**(1), 159–205 (2005). https://doi.org/10.1016/j.csda.2004.03.005
42. Radomir, L., Moisescu, O.I.: Discriminant validity of the customer-based corporate reputation scale: some causes for concern. J. Prod. Brand Manage. **29**(4), 457–469 (2020). https://doi.org/10.1108/JPBM-11-2018-2115
43. Al-Kofahi, M.K., Hassan, H., Mohamad, R., Intan, T.P., Com, M.P.: Information systems success model: a review of literature. Int. J. Innov. Creat. Change **12**(8) (2020)



Portuguese Service Electricity Continuity Indicators: Municipality Code and Quality Service Zones Evaluation – 2014 to 2022

Marina A. P. Andrade[1,2(✉)] and M. Filomena Teodoro[3,4]

[1] ISCTE, University Institute of Lisbon, Av. das Forças Armadas, 1649-026 Lisbon, Portugal
marina.andrade@iscte-iul.pt
[2] ISTAR-ISCTE - Information Sciences, Technologies and Architecture Research Cente, Lisbon, Portugal
[3] CINAV, Center of Naval Research, Portuguese Naval Academy, Military Universitary Institute, 2810-001 Almada, Portugal
[4] CEMAT - Center for Computational and Stochastic Mathematics, Instituto Superior Técnico, Lisbon University, 1048-001 Lisbon, Portugal

Abstract. The possibility of supply disturbances could be detrimental to some customers. Such as in some industries, where these types of disruptions can represent a serious cost. Productivity and competitiveness in manufacturing and service industries increasingly depend on the quality of electricity supply and are also dependent on the good efficiency of continuity indicators. After initially monitoring its indicators in 2001, Portugal introduced a continuity of supply incentive regime in 2003. Since the introduction of the regime, indicators have consistently improved over the years, which pressures a constant improvement of the service related to client satisfaction. Frequency and duration of continuity service indicators are here considered to study the quality of service in Portugal's mainland in the period of 2014 up to 2022. Here a two–way analysis of variance (ANOVA) was performed aiming to evaluate the existence of differences between two factors: quality service regulation (QSR) zones and municipality code. The results point to the need to seek a more accurate analysis for each of the variables that represent continuity indicators. Even so, it was possible to identify differences in the medium and low voltage indicators regarding the two factors, as well as the existence of differences in the mean values in each factor.

Keywords: electricity continuity service · Interruption Frequency Index · Interruption Duration Index · two–way ANOVA

Supported by: The first author, this work was partially supported by Fundação para a Ciência e a Tecnologia, I.P. (FCT) [ISTAR Projects: UIDB/04466/2020 and UIDP/04466/2020]. The second was supported by Portuguese funds through the Center of Naval Research (CINAV), Naval Academy, Portugal and The Portuguese Foundation for Science and Technology (FCT), through the Center for Computational and Stochastic Mathematics (CEMAT), University of Lisbon, Portugal, project UIDB/Multi/04621/2020, DOI: (https://doi.org/10.54499/UIDB/04621/2020).

© The Author(s), under exclusive license to Springer Nature Switzerland AG 2024
O. Gervasi et al. (Eds.): ICCSA 2024 Workshops, LNCS 14816, pp. 162–176, 2024.
https://doi.org/10.1007/978-3-031-65223-3_11

1 Introduction

E–Redes is the main operator of the electricity distribution network in mainland Portugal of high, medium, and low voltage networks, connecting more than 6M customers. The company's objectives are to guarantee the supply of electricity to all consumers, with quality, safety, and efficiency; promote the development of the distribution network that supports the energy transition; ensure, in an impartial manner, the availability of services to market agents; maintain the distribution network and guarantee the security of supply; ensure compliance with quality standards; provide services to consumers, traders and other agents in the electricity sector, among others. In this sense, it presents itself as a trusted brand close to consumers, ensuring a quality service focused on the customer. The distribution network operator must determine, in each calendar year and for all delivery points, the number of interruptions and the total duration of interruptions, in minutes, which allows for defining, evaluating, monitoring, and adjusting service quality standards. The context of service quality standards to be observed by the distribution network operator may vary according to the service quality zones. To apply the Quality Service Regulation (QSR) in mainland Portugal, the following classification of service quality zones is defined: Zone A: district capitals and locations with more than 25 000 customers; Zone B: locations with the number of customers between 2 500 and 25 000; and Zone C: the remaining locations.

Low voltage connection is typically intended for residential customers, stores, offices, and small businesses. Within the low voltage connection, it may be chosen between a normal low voltage connection (NLV), for contracted powers equal to or less than 41.4 kVA, and a special low voltage connection (SLV), for contracted powers greater than 41.4 kVA. 4 kVA. The medium voltage connection is aimed more at companies with energy needs greater than 200 kVA, such as the automotive, metallurgical, or hotel industries. The high voltage connection is intended for companies typically with installed powers greater than 10 MVA, supplied at a voltage level of 60 kV. Here will be considered the medium voltage connection and low voltage connection, which we believe covers a large part of the business sector in mainland Portugal and private customers.

In November 2022, E–Redes launched the Open Data Portal[1] to share relevant data from its activity, to also contribute to *"the transparency of its activity data in the community, serve as a catalyst for the country's energy transition"* This initiative thus seeks to *"serve as a catalyst for the energy transition and design of smart cities; promote product or service innovation by extending data analytics to community members, such as the Scientific Community; strengthen interactions with the community and encourage the co-creation of value with Local Authorities, Energy Agencies, the research community, etc."*.

The E–Redes "explore" tab allows access to all datasets organized by categories - Consumption and Energy; Electrical network; Electric Mobility; Renewables and Operation and Quality of Service. It is part of this category - Operation

[1] https://e-redes.opendatasoft.com.

and Service Quality - that this work focuses on. The topic is vast, covering the number of low voltage consumption sites with remote readings; active power outages; scheduled power outages; number of remote service orders carried out; number of low voltage consumption sites with collection of load diagrams; network connections; and service continuity indicators by municipality. Here we are interested in studying a subset of data on service continuity indicators per municipality, as already mentioned for medium and low voltage, it is intended to study the System Average Interruption Frequency Index (SAIFI), and the System Average Interruption Duration Index (SAIDI), both indexes are commonly used as a reliability index by electric power utilities. SAIFI refers to the average number of interruptions that a customer would experience and SAIDI is the average outage duration for each customer served.

Service Continuity expressed by the number and duration of electricity supply interruptions is a technical aspect of service quality. Continuity of service characterizes and evaluates situations in which there is an interruption in the supply of electrical energy to the delivery points of a network, whether customers or connections to other networks. Service continuity indicators are general when they refer to the entire system, a group of customers, or a geographic area. The indicators are individual when referring to each of the delivery points.

For electric utilities, ensuring high continuity of service is crucial to maintaining customer trust and complying with government regulations. Frequent or prolonged outages can cause significant inconvenience to customers, negatively impact productivity in commercial and industrial environments, and even pose public safety risks in certain cases. Electricity companies frequently monitor and seek to improve service continuity through investments in infrastructure, preventive maintenance, use of advanced monitoring technologies, and quick response to network failures. This aims to minimize outages and ensure a reliable supply of electricity to all consumers. In summary, service continuity is an essential technical measure of service quality in an electrical utility, assessing the consistency and reliability of energy supply over time and playing a crucial role in customer satisfaction and the efficient functioning of modern society. Additionally to the assessment carried out by E-Redes, the energy services regulatory entity (ERSE) annually assesses the technical quality of the service provided, where the continuity of the service is an item of interest. This procedure also results from the need to fulfill the regulations of the Council of European Energy Regulators, similar to other European countries. Apart from this study, we are not aware of his topic being studied in Portugal.

In this work, we consider medium voltage, (mt), and low voltage, (bt), networks in mainland Portugal for which individual indicator limits are defined annually that must not be exceeded, per year and customer. These standards are grouped by quality of service regulation zone - QSR zone - and refer to long accidental interruptions (more than 3 min). Customers are entitled to automatic compensation whenever there is non-compliance with the standards of individual quality indicators relating to service continuity established, in each case. Consistent with this, the distributor monitors and seeks the best standards for

their product/service, which we will address in this work. Thus, this paper is divided into four sections. Following this introduction in Sect. 2, the methodology is exposed. Section 3 presents the data and the results of the data analysis, and in Sect. 4 a discussion of the results accompanied by possible future work is presented.

2 Methodology

2.1 ANOVA Two–Way

ANOVA stands for analysis of variance and tests for differences in the effects of independent variables on a dependent variable. A two–way ANOVA test is a statistical test used to determine the effect of two nominal predictor variables on a continuous outcome variable. The ANOVA test is the first step in identifying if factors influence the outcomes of interest, to evaluate how variables affect each other. The ANOVA test group's differences by comparing the means of each group and includes the distribution of variance between multiple origins. Used for subjects, test groups, between groups, and within groups [1,4,7]. A two–way ANOVA was considered to evaluate the impact of quality service regulation (QSR) zone, Factor A, and municipality code, Factor B, on the continuous variables' outcomes - SAIFI and SAIDI measures - both in medium and low voltage connection which result in four measurements, i.e., four different variables. Being the continuous variables - SAIFI and SAIDI - the dependent variables and the nominal variables of each factor the independent variables.

The two–way ANOVA model, replicated four times, i.e., for each combination between variable (SAIFI and SAIDI) medium and low voltage (mt and bt), may be written as

$$Y_{ijr} = \mu + \alpha_i + \beta_j + \gamma_{ij} + \varepsilon_{ijr} \tag{1}$$

with Y_{ijr} the dependent variable measurement, α_i the effect of QSR Zone, β_j the effect of municipality code, γ_{ij} the interaction between factors, and μ and ε_{ijr}, the global mean and the error, respectively, with ε_{ijr} normally distributed with zero mean and standard deviation σ.

If interactions are not significant, then the model and interpretations are simpler, in that case, the effects of the two factors may be analyzed separately. Such a model is said to be "additive" because the effects of the factors sum.

The interaction test hypotheses are

- H_0 : There is no interaction between the two factors, i.e., all terms $\gamma_{ij} = 0$.
- *vs.*
- H_A : There is interaction between the two factors, i.e., at least one $\gamma_{ij} \neq 0$.

It is important to note that if an interaction is found to be important so the main effect tests may not be very interesting in an interaction model.

Factor Effects Model (Without Interactions): The Main Effects Model is

$$Y_{ijr} = \mu + \alpha_i + \beta_j + \varepsilon_{ijr} \tag{2}$$

where

- Y_{ijr} is the rth observation on $ijth$ treatment, where $0 \leq r \leq n$, and n is the size of the sample drawn from each treatment (here it is considered a balanced design);
- α_i is the differential effect of the ith level of factor A on the mean response (the mean of the dependent variable), with $\sum_i \alpha_i = 0$;
- β_j is the differential effect of the jth level of factor B on the mean response (the mean of the dependent variable) with $\sum_j \beta_j = 0$;
- ε_{ijr} is the error, assumed to be iid normally distributed with zero mean and standard deviation σ.

The α_i and β_j are called the "main effects" of factors A and B, respectively, to distinguish them from interactions, that is, effects of the levels on the mean response simply add.

As for the one–way ANOVA also the two–way ANOVA requires that the assumptions of normality and homogeneity of variance are met.

Testing the Two Main Effects. The hypotheses that are of interest to evaluate concerning the two main effects are:

Main effect test for factor A:

- H_0 : There are no differences in means across levels of factor A in population, given factor B is in the model, i.e., all terms $\alpha_i = 0$, in the additive model.
- *vs.*
- H_A : There are some differences in means across levels of factor A in population, given factor B is in the model, i.e., at least one $\alpha_i \neq 0$, in the additive model.

Main effect test for B:

- H_0 : There are no differences in means across levels of factor B in population, given factor A is in the model, i.e., all terms $\beta_j = 0$, in the additive model.
- *vs.*
- H_A : There are some differences in means across levels of factor B in population, given factor A is in the model, i.e., at least one $\beta_j \neq 0$, in the additive model.

If the null hypothesis is rejected, then further analysis is performed to explore where the individual differences are [8].

The ANOVA analysis assumes that the underlying data distribution is the normal distribution, the variance is the same in the population, and the observations are independent [4,7].

3 Data and Data Analysis

In this work service continuity indicators, SAIFI, concerning the frequency, and SAIDI, concerning the duration, of interruptions (accidental + foreseen) for medium voltage (mt) and low voltage (bt) indicators by quality service regulation (QSR) and municipality codes for 9 years, from 2014 up to 2022 were registered. The information made available by E-REDES establishes an approximation to the values taken from the system and is based on the moment it is collected. The available information may be subject to successive changes and updates since it is a result of the dynamic measures from the connection points, the electricity distribution network, and the consumption and production values themselves.

In the E–Redes Portal the data organization follows the QSR zones (Zone A, Zone B and Zone C) and presents also a category Municipality concerning the values for the municipality center as a separate category. Concerning the municipality code are available 35 codes thus having 35 categories for this factor.

3.1 Descriptive Measures

The data here considered, concerns the frequency of the interruptions and also the duration of the interruptions, for both the medium and low voltage, therefore the analysis is divided for the SAIFI and SAIDI variables, in each voltage, separated.

Along the nine years of observed values were collected 140 observations per year. As mentioned data are observed and presented, for each year, in two different categories of interest: the four categories of QSR Zone – Municipality, Zone A, Zone B, and Zone C – and the municipality code – in 35 different codes, i.e., the 35 categories of factor municipality code. Thus, one can count for each of the QSR Zone a total of around 315 observation measurements, and for the municipality codes a total of around 36 observation measurements.

SAIFI Medium and Low Voltage

Below are presented the descriptive statistics for both variables, SAIFI medium (mt) and low (bt) voltage, in Table 1, and the graphical representations, violin graphs in Fig. 1 and box-plot representations in Fig. 2:

Table 1. SAIFI mt and SAIFI bt descriptive statistics.

QSR Zone	SAIFI mt					SAIFI bt				
	Sum	Mean	St.d.	Min.	Max.	Sum	Mean	St.d.	Min.	Max.
Municipality	272.23	0.867	0.829	0.0	6.997	308.30	0.979	1.230	0.0	7.66
Zone A	244.61	0.774	0.793	0.0	3.907	267.31	0.846	0.822	0.0	4.882
Zone B	311.80	0.989	0.642	0.0	4.010	340.72	1.082	0.705	0.0	5.000
Zone C	259.06	0.825	0.759	0.0	3.291	283.75	0.904	0.814	0.0	4.865

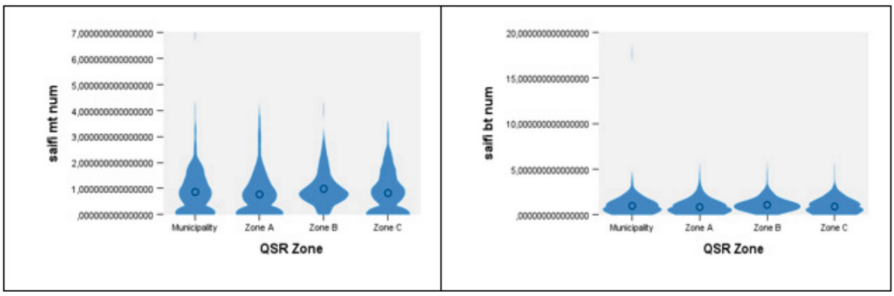

Fig. 1. SAIFI mt and SAIFI bt Violin graphs, by QSR zone

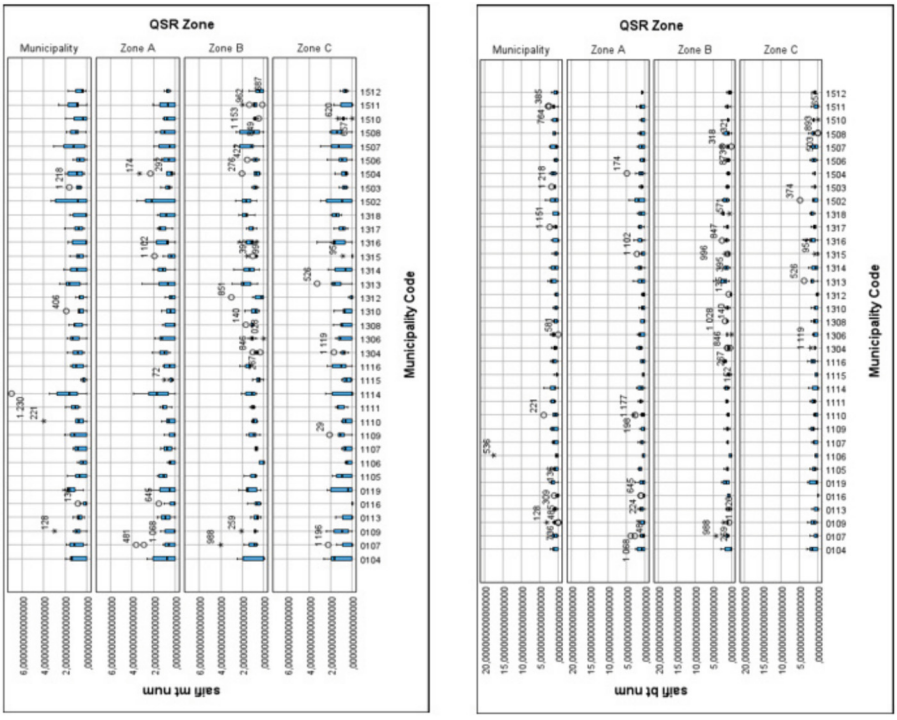

Fig. 2. SAIFI mt and SAIFI bt Boxplot graphs, by municipality code and QSR zone

SAIDI Medium and Low Voltage

Below are presented the descriptive statistics for both variables in Table 2, and the graphical representations, violin graphs in Fig. 3 for the SAIDI variables concerning medium and low voltage observed measurements.

Table 2. SAIDI mt and SAIDI bt descriptive statistics.

QSR Zone	SAIDI mt					SAIDI bt				
	Sum	Mean	St.d.	Min.	Max.	Sum	Mean	St.d.	Min.	Max.
Municipality	12219.9	38.8	37.9	0.0	233.7	14918.8	47.4	53.6	0.0	643.1
Zone A	11217.9	35.4	37.8	0.0	241.7	14292.5	45.3	66.2	0.0	932.9
Zone B	14640.3	46.5	34.4	0.0	307.1	17040.6	45.2	66.2	0.0	931.6
Zone C	12186.5	38.8	38.3	0.0	204.6	14903.3	47.5	47.6	0.0	324.9

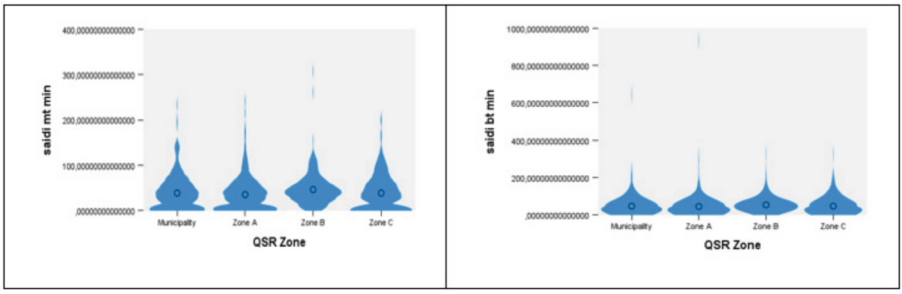

Fig. 3. SAIDI mt and SAIDI bt Violin graphs, by QSR zone

As one may observe there are some pattern similarities with SAIFI graph representations, either for the medium and the low voltage measurements. The box-plot representations concerning the QSR Zone and municipality code exhibit a similar pattern and therefore are not presented here.

For the duration of the interruption, both in medium and low voltage, it is possible to observe larger values for the standard deviation. Thus, below are presented the histograms of each variable across the four QSR zones, Fig. 4 where may be observed the asymmetry of the data that will influence the fulfillment of the required assumptions.

The descriptive analysis of data for medium and low voltage measurements, whether about the frequency with which they occur or their duration, in the categories of interest makes it possible to identify the existence of discordant observations. In the descriptive analysis, it was identified the presence of outliers, both moderate and even extreme, in those observations. This is certainly also influencing the variability in the data and conditioning the analysis as the confidence in the results.

An identical descriptive analysis to the one presented was also carried out per year. Apart from the existence of discordant observations, each year, the importance of comparatively analyzing the data obtained by year was not identified.

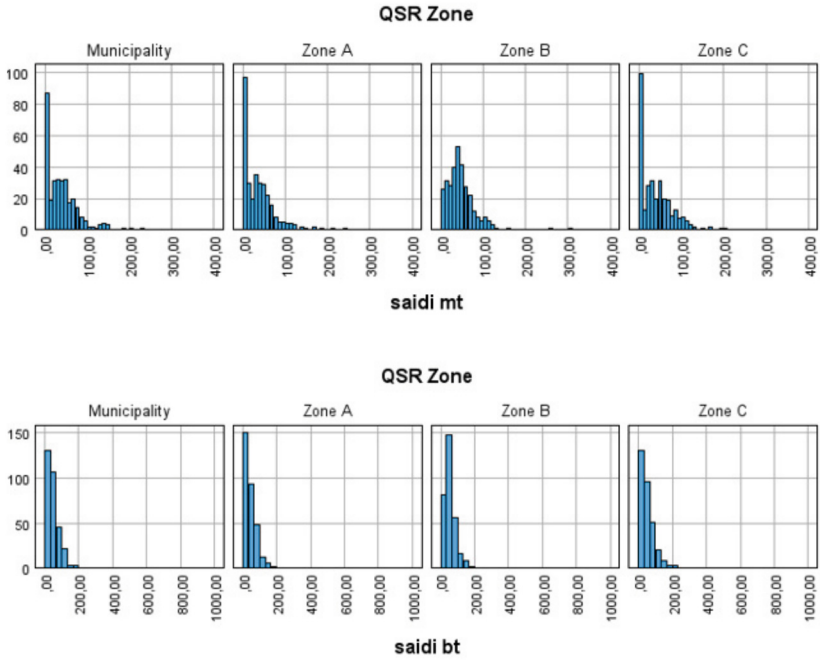

Fig. 4. SAIDI mt and SAIDI bt histogram graphs, by QSR zone

3.2 Model Analysis

After the descriptive analysis mentioned above, we are interested in evaluating whether the average values of the observations, frequency, and duration both at medium and low voltage, are identical in both factors - the categorical variables - or if there is at least one different value, in each case.

For this purpose, a two-factor analysis of variance, Sect. 2.1, was considered for the four mentioned variables starting to test, in each case, the possibility of interaction between the factors QSR Zone and municipality code.

Below, in Table 3 are presented the results of the two-way ANOVA for the variable SAIFI mt (medium voltage), i.e., if the model is the one referred to in Eq. 1. If the interaction is not relevant one can proceed to the Main Effects Model, i.e., to consider the additive model as mentioned in Eq. 2.

The ANOVA table analyzes the total variation by decomposing the sum of squares, (SS), into components that add to the total. The table also presents the degrees of freedom, (df), and add up for the corrected model + error = corrected total. The null hypothesis for the interaction F–statistic is that there is an additive relationship between the two categorical variables in their effects on the outcome variable.

Table 3. SAIFI mt – Tests of Between–Subjects Effects with interactions.

Source	Sum of Squares	df	Mean Square	F	Sig.
Corrected Model	175.406	139	1.262	2.536	< 0.001
Municipality Code	100.854	34	2.966	5.962	< 0.001
QSR Zone	6.872	3	2.291	4.604	0.003
Mun. Code*QSR Zone	54.826	102	0.538	1.080	0.283
Error	557.238	1120	0.498		
Corrected Total	732.644	1259			

The interaction line in the table presents an F–statistic 1.080 and a significance of 0.283 in the test. The test significance is also named the p-value of the test, as will be referred to in what follows. In this work the significance level of interest is 0.05, meaning that the values of the test below the test are significant and values above the test are not significant. It can be concluded that the interaction test is not significant, there is no evidence to reject the additive model, and the conclusion is that QSR zones are the same for the different municipality codes, and vice-versa. Therefore it is appropriate to re-run the ANOVA with an additive model.

Considering the limitation of written space, the tests of between-subjects effects are omitted and referred to only, and in each case, the F–statistics and p-values for the remaining variables concerning testing the factor's interaction. The obtained values are: for variable SAIFI bt, the F–statistic is 1.059 and the respective p-value 0.331; for variable SAIDI mt the F–statistic is 1.143 and a p-value of 0.165; and for variable SAIDI bt the F–statistic observed is 0.891 with a p-value of 0.770.

Since the p-values for the four variables under study are greater than 0.05 the interactions are not significant, and the model to adopt is the additive model. Therefore, it is appropriate to re-run the ANOVA two–way with a different means model, i.e., with an additive model presented in Eq. 2.

Additive Model (Without Interactions)

As before, in what follows are presented the results for variable SAIFI mt, Table 4 and the remaining results are just discussed. It is then important to test the two main effects to proceed with the analysis. Table 4 exhibits the results for SAIFI mt, and as it can be observed, at a significant level of 0.05 both factors affect SAIFI mt. The square root of the mean square of the error, $\left(\sqrt{0.501} = 0.708\right)$ indicates that the residual (within-group) variance is about 0.708.

Table 4. SAIFI mt – Tests of Between–Subjects Effect, without interactions.

Source	Sum of Squares	df	Mean Square	F	Sig.
Corrected Model	120.580	37	3.259	6.506	< 0.001
Municipality Code	112.556	34	3.310	6.609	< 0.001
QSR Zone	6.856	3	2.285	4.563	0.003
Error	612.064	1222	0.501		
Corrected Total	732.644	1259			

The estimated means table for each factor allows us to directly check the existence of differences in different municipality codes and also in the different QSR zones. Here is only presented the estimated means for the QSR zones, Table 5, easily to check since this factor has four levels (the municipality code factor has 35 different codes).

Table 5. SAIFI mt – Marginal Means Estimates.

QSR Zone	Mean	Std. Error	95% Confidence	Interval
			Lower Bound	Upper Bound
Municipality	0.870	0.040	0.791	0.949
Zone A	0.788	0.040	0.709	0.868
Zone B	0.982	0.040	0.904	1.061
Zone C	0.816	0.040	0.737	0.895

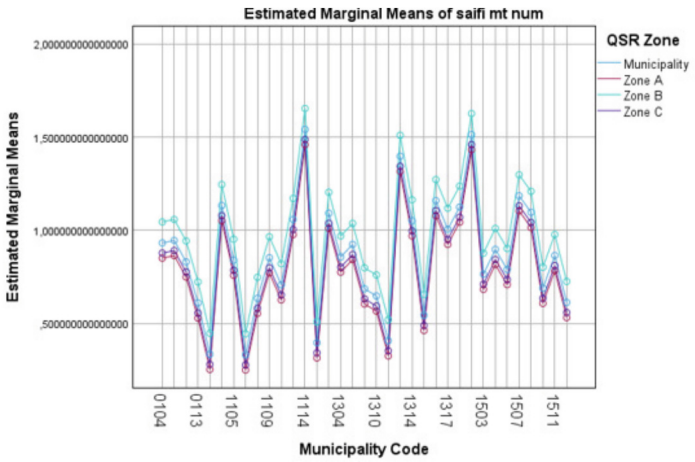

Fig. 5. SAIDI mt profile plots for the two factors.

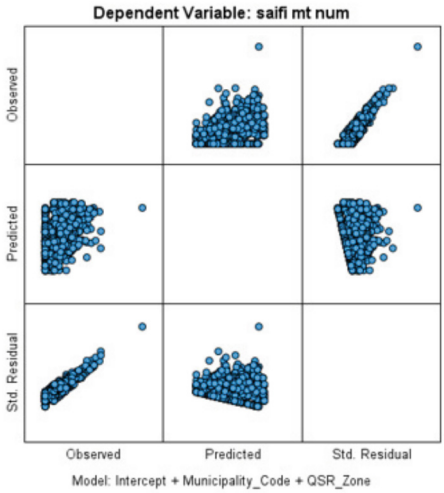

Fig. 6. SAIDI mt residuals plot.

As it can be observed the estimated mean for Zone B is higher than the remaining ones. This fact allows us to consider two different homogeneous subsets, one formed with the municipality, Zone A and Zone C leaving Zone B separated; or another possibility a homogeneous subset with Zone A and Zone C and a homogeneous subset with the municipality and Zone C.

In the figure below, Fig. 5, it is possible to observe the profile plots of both factors, for variable SAIFI mt. the graph shows a very similar profile for all QSR zones although the Municipality is always higher. This is interesting and it is important to determine if it is important or not, as well as its meaning.

In Fig. 6, are presented the residuals plots for variable SAIFI mt.

Table 6, summarizes the information for the remaining variables subject to the same analysis. A brief analysis of the table shows that the two factors are significant for the variables SAIFI bt and SAIDI mt, even though the respective MSE presents large differences. For factor Municipality the formed homogeneous subsets are six varying between 16 municipality codes up to 27 municipality codes, not shown here resulting of the limitation of written space. For SAIDI bt only the municipality code is a significant factor.

A test is only meaningful if the assumptions of the test we are performing are reasonably well met. Therefore, it is important to check the assumptions involved in the model construction so that one can rely on the inferences that follow. Similarly, models cannot perfectly capture the fundamental realities of nature. That is why it is common to say, “All models are wrong, but some are useful”. And for that, it takes some experience to evaluate how far an assumption can be distorted before reasoning stops. Thus, if the normality assumption is significantly violated, if the equal variance assumption is moderately violated,

Table 6. Estimates.

	SAIFI bt	SAIDI mt	SAIDI bt
Mun. Code p-value	< 0.001	< 0.001	< 0.001
QSR Zone p-value	0.012	0.002	0.191
Error $\sqrt{\text{MSE}}$	0.884	34.83	50.59
Homogeneous subsets for QSR Zone	{A, C and Mun.} *vs* {B} or {B, C and Mun.} *vs* {A}	{A, C and Mun.} *vs* {B}	all

or if the independent error assumption is slightly violated the obtained results and the model use are compromised.

During the descriptive analysis of the variables, the existence of several discordant observations was noted, which led to difficulties being foreseen both about the normality of the data and the homogeneity of variability within the groups, as was confirmed. The homogeneity of variances is not verified and the residuals are not all independent for the four variables.

3.3 Some Remarks

Simultaneous confidence intervals [8] were not created due to the inadequacy of the model. The one–way ANOVA test was conducted for variable SAIDI bt which does not perform differently, being the heteroscedasticity slightly accentuated, i.e., $\sqrt{\text{MSE}} = 50.63$.

Given the above, non-parametric tests were also carried out [2,9], highlighting the differences postulated at the beginning of the work. Considering the observed violation of the assumptions of the additive ANOVA model, even with large samples, a non-parametric approach was considered. Hence, either for QSR zone or municipality code as group variables, the equality of medians across the groups was tested using the Kruskal-Wallis H test. This exposes that a new methodological approach is necessary, eventually correcting the discordant observations and rerunning the analysis.

For each variable, the data sets exhibit an equal number of observations in each category on both factors, that is, the groups are balanced, and in all cases, with more than 30 observations. Still, it is important have present the violation of assumptions. Therefore, it is important to consider a new analysis with variable transformation to at least minimize the effect of outliers. As several values of zero are observed, the most appropriate transformation seems to be the transformation of the square root to stabilize the variability of the data. At the same time, evaluate outlier observations and evaluate the impact of these observations on the analysis and what information these observations relate to. This can give us new insights into what to do next and is thought to future work.

4 Conclusion

The continuity of the electrical service is one of the important quality elements for both the consumer and the electrical energy supplier, in this case, the quality of technical service [11,12]. This quality of technical service is measured by the number of interruptions as well as the duration of these interruptions in the service provided [10].

The regulation of service continuity considers the set of installations with equal characteristics related to the quality of service. In this way, three different service quality zones are defined, the division of which results from distinguishing the zones by population density. In this work, the center of the municipality is still considered a QSR zone. Naturally, locations with a higher density of customers have more demanding quality levels. This is why the QSR zone was considered a factor of interest, except for variable SAIDI bt.

In this work, general continuity indicators were studied, namely the frequency and duration of service interruptions, and it is clear the need to improve and refine this study. However, differences were identified in the average values of the variables of interest - SAIFI and SAIDI - also noticing the distinction between medium and low voltage indicators, which allows a new perspective on what to evaluate of these indicators in the future as mentioned.

It is easy to recognize that maintaining an electrical network in continuous service is neither technically nor economically viable. Therefore, it is important to evaluate and outline measures that allow mitigating the interruption of continuity indicators, and consequently to improve consumer satisfaction standards.

This may be central to identifying the specificity and difficulties assessed in the indicators and trying to detect how to correct them. Here, characteristics or factors to consider were highlighted, making clear the need for a more refined and targeted analysis for each of the variables that represent the continuity indicators that we intend to address in future work.

References

1. Bewick, V., Cheek, L., Ball, J.: Statistics review 9: analysis of variance. Crit. Care **7**, 451–459 (2004)
2. Bewick, V., Cheek, L., Ball, J.: Statistics review 10: further nonparametric method. Crit. Care **8**(3), 196–199 (2004)
3. Manual de Procedimentos da Qualidade de Serviço dos setores elétrico e gás. Entidade Reguladora dos Serviços Energéticos (2023)
4. Montgomery, D.C.: Design and Analysis of Experiments, 5th edn. Wiley, New York (2001)
5. Morgado, L., Teodoro, L., Perdocoulis, T.: Manual de Métodos Estatísticos em Ciências Biomédicas. Universidade de Trás os Montes e Alto Douro (UTAD, Vila Real). Série Didáctica Ciências Aplicadas, 400 (2010). ISBN 978-972-669-018-2
6. Regulação da Energia – Legislação Essencial. Entidade Reguladora dos Serviços Energéticos (2024)
7. Seltman, H.J.: Experimental Design and Analysis. https://www.stat.cmu.edu/~hseltman/309/Book/Book.pdf

8. Scheffé, H.A.: The Analysis of Variance. Willey, New York (1959)
9. Sprent, P., Smeeton, N.C.: Applied Nonparametric Statistical Methods. Chapman & Hall/CRC, London (2001)
10. Towards Voltage Quality Regulation in Europe – an ERGER conclusions paper. European Regulators' Group for Electricity and Gas (2007)
11. 4th Benchmarking Report on Quality of Electricity Supply 2008. Council of European Energy Regulators ASBL (2008)
12. 7th Benchmarking Report on the Quality of Electricity and Gas Supply. Council of European Energy regulators (CEER) and the Energy Community Regulatory Board (ECRB) (2022)

Spatial and Multivariate Statistics in Assessing Water Quality in the North Sea

Christopher Ody[1], M. Rosário Ramos[1,3], and E. Carolino[2(✉)]

[1] Universidade Aberta, Lisbon, Portugal
mariar.ramos@uab.pt
[2] H&TRC- Health and Technology Research Center, ESTeSL- Escola Superior de Tecnologia da Saúde, Instituto Politécnico de Lisboa, Lisbon, Portugal
etcarolino@estesl.ipl.pt
[3] CEAUL - Centro de Estatística e Aplicações, Faculdade de Ciências, Universidade de Lisboa, Lisbon, Portugal

Abstract. The Southern North Sea region plays a vital role for both the economy and society of the surrounding countries. Analyzing the quality of your water is a critical process that involves an assessment of physical, chemical, and biological parameters, essential to guarantee environmental sustainability and the health of local communities and marine ecosystems. Using Multivariate and Spatial Statistics methods, this study seeks to identify spatial patterns and autocorrelations to assess water quality in that region. The data set used was taken on a scientific cruise carried out in December 2020 aboard the RV Meteor vessel, led by a team of German researchers. The raw data went through pretreatment guided by the Data Quality Control protocol of SeaDataNet, an international oceanography project aimed at making European maritime data available. Spike and gradient tests were performed, in addition to data standardization and imputation through inverse distance weighting interpolation. For a better understanding of the scientific area, the data were aggregated by zones for certain analyses, and were sometimes considered globally. An exploratory spatial data analysis (ESDA) was carried out in order to summarize its main characteristics. A reduction in the dimensionality of the original data was carried out through principal component analysis as an auxiliary tool for spatial analysis. The Spatial autocorrelation is analyzed by calculating global and local Moran's I Statistics. The outcomes indicate a significant spatial autocorrelation for all variables considered in the freshwater areas and a notable range flattening of the variables in the open sea areas, which possibly caused the lack of significant spatial autocorrelation in those areas.

Keywords: Exploratory spatial data analysis · North Sea · Principal components · Spatial correlation · Water quality

1 Background and Motivation

The North Sea is a vital region for many countries, including Germany, the Netherlands, Denmark and the United Kingdom. It is a crucial center for trade,

© The Author(s), under exclusive license to Springer Nature Switzerland AG 2024
O. Gervasi et al. (Eds.): ICCSA 2024 Workshops, LNCS 14816, pp. 177–193, 2024.
https://doi.org/10.1007/978-3-031-65223-3_12

fishing and energy production, significantly involved in the German economy and the economies of other neighboring North Sea countries. The region's importance has led to extensive scientific exploration, with researchers studying the area's unique ecosystem and the impact of human activities on the environment.

Water analysis is essential as it provides information about the quality of North Sea water, nutrient levels and the possible presence of pollutants. Recent studies show that North Sea water quality has improved over the past few decades, thanks to efforts to reduce pollution and improve wastewater treatment. [4,8] showed that changes in carbon dioxide (CO2) and pH are influenced by circulation patterns, Atlantic inflow, local climate conditions and water mass properties components. They also demonstrated nutrient changes influenced by circulation patterns, and changes in oxygen concentration, especially near the sea floor, influenced by respiration of organic matter, decomposition of organic matter, lack of oxygen supply, and temperature. Studies on salinity and temperature, among other variables, are frequently carried out in the North Sea area. For example, the study carried out on the oceanographic event known as "Great Salinity Anomaly" (GSA). During the 1960s and 1970s, a significant change in salinity patterns was detected on the surface of the North Atlantic Ocean, particularly in the North Sea and Norwegian Sea regions. This change was characterized by a large accumulation of fresh water on the ocean surface, resulting in a sharp decrease in water salinity, as a consequence of the accelerated melting of sea ice and glaciers caused by climate change [2] and more recently [5]. Monitoring seawater quality helps identify and mitigate environmental threats, ensuring the preservation of marine resources, the prevention of environmental disasters and the support of sustainable economic practices, essential for the well-being of coastal communities and conservation of marine ecosystems. Statistical geospatial knowledge of water analysis variables in the North Sea is still motivated by a number of critical reasons, including those mentioned above. In addition to monitoring water quality for public health and the sustainability of marine life, the constant monitoring of these variables assesses the impacts of climate change and human activity in the region, such as pollution and the exploitation of natural resources. They also provide essential data for making informed political and economic decisions aimed at the environmental sustainability and economic development of the region [8,10]. The TRAM project (Tracing origin and distribution of geogenic and anthropogenic dissolved and particulate critical high-technology metals in the southern North Sea), led by Dr. Andrea Koschinsky from Jacobs College in Germany, was a research cruise, the RV Meteor, which took place in 2020 and aimed to study anthropogenic inputs of emerging critical metallic contaminants, from the German rivers Elbe, Weser and Sem to the ocean (TRAM, 2024). On its trip, the work area comprised the estuaries of these rivers, from the freshwater end member to the seawater end member along the salinity gradient, as well as the dispersion of the plume along the prevailing currents, mostly in heading east.

This work aims to use multivariate and geospatial statistical techniques to obtain indicators that allow qualifying the variables obtained from RV Meteor

and looking for patterns of similarity between them in the studied area. To this end, spatial data sets of different variables were analyzed in an attempt to locate specific patterns and characterize the oceanographic profile in the region.

This paper is structured as follows: Sect. 2 provides a description of the material and methods used. In Sect. 3, the results of the exploratory spatial data analysis as well as the application of Principal Components Analysis to data of the North Sea to dimension reduction and spatial correlation analysis with Moran test. Conclusions and some remarks are presented in Sect. 4.

2 Material and Methods

2.1 Study Area and Data Sources

Data is from TRAM project which aims to study anthropogenic inputs of emerging critical metallic contaminants, such as rare earth elements, Sc, Ga, Ge, Pt, Zr, Ti, Mo and V, from the German rivers Elbe, Weser and Sem to the ocean. The scientific cruise *RV Meteor* collected data during a week of december 2020, based on two autonomous thermosalinography systems (thermosalinograph - TSG), named TSG1 and TSG2, consisting of the use of the TSG model SBE21 together with an SBE38 thermometer. The systems worked independently of each other throughout the cruise, ensuring cross-validation of data and redundancy in collection. Observations were taken every 5 s at TSG1 and 10 s at TSG2. In the data not yet processed from the sensors, averages of the minute-by-minute measurements were taken, discarding values that exceed 2 times the value of the standard deviation. Finally, the group chose the TSG1 dataset to publish the results, with salinity and temperature values being very close for both sensors as demonstrated in the time series in Fig. 1. For specific technical details of the sensors and data quality control steps, see the full data processing report provided by the research team [9], which was used as a reference for pre-processing data in the present study.

Although the previous study [9] only considered salinity and temperature data, the characterization of the area proposed by the present study considered the value of the other variables taken in each observation by the same sensor. The raw TSG1 data was then made available by the team for 11 variables (Table 1), including date and time of the observation and coordinates (latitude and longitude). The variables calculated from the absorptions at wavelengths can be seen in the spectrum in Fig. 2.

The analyzed data set was divided into three zones so that the waters in each zone had the potential to show different profiles in the studied variables. For this, the official German division presented in Fig. 3 (Maritime Borders of the Federal Republic of Germany, 2019) was used. The considered zones were Internal Waters (IW) - referring to fresh waters and nearby slopes, Territorial Sea (TS) - being the German part of the North Sea, which covers around 22km of the coast, and North Sea (NS) - being international waters. It is expected that each zone will present differences in at least some variables, such as salinity and temperature. It is also necessary to mention that the zones are not being considered as areas

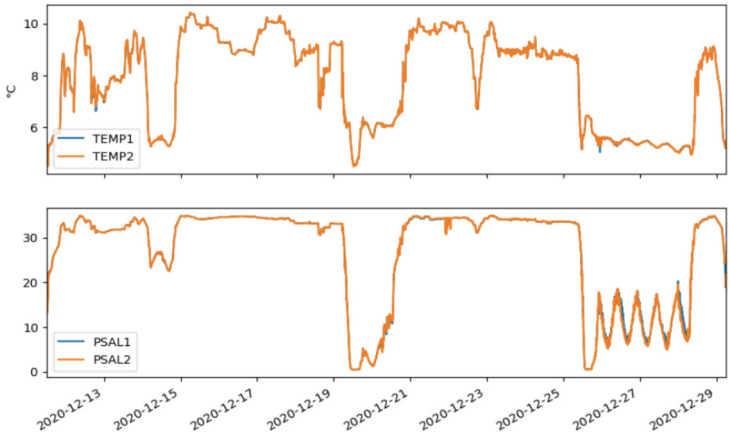

Fig. 1. Time series of Temperature (TEMP1, TEMP2) and Salinity (PSAL1, PSAL2) measured by two sensors TSG1 and TSG2 respectively.

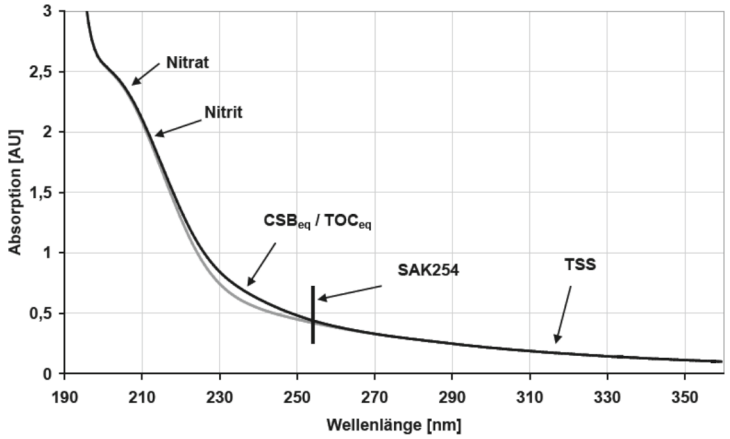

Fig. 2. Absorption Regions of the Different Calculated Variables (TriOS GmbH, 2017).
Note: CSBeq - Chemical Oxigen Demand; TOCeq - Total Organic Carbon; SAK254 - Specific Absorption of Carbon at 254 nm; TSS - Total Suspended solids.

(polygons) in spatial statistics tests, but are only being analyzed separately through the points collected within each region. Figure 3 also shows the cruise route during the considered period, represented by the gray dotted line, as well as points in each region colored according to their location.

To make the data suitable for subsequent analysis, pre-processing was carried out following the SeaDataNet Data Quality Control protocol [6], which will be described in the next topic.

Table 1. Description of water quality variables under study.

Variable	Acronym	Measurement unit	Observations
Salinity		PSU (Practical Salinity Units)	Estimated within the interior of the TSG based on conductivity and interior temperature; external temperature, measured by the SBE38 thermometer
Temperature	TempExtern	°C	
Nitrate	N.NO3	mg/L	Concentration of nitrate ions (NO3-) in the water sample. Nitrate analysis is important because high levels of this ion in water can indicate pollution or contamination, which can have harmful effects on aquatic ecosystems and pose risks to human health (World Heath Organization, 2016)
Dissolved Organic Carbon	DOCeq	mg/L	Assess the quality of water
Absorption at each wavelength (210 nm, 254 nm and 360 nm)	Abs210, Abs254, Abs360	AU (Absorption Units)	
Specific Absorption of Carbon at 254nm	SAC254	AU (Absorption Units)	Useful indicator of organic water quality and can be used to estimate the amount of natural organic matter, including humic and fulvic acids, present in the water sample

2.2 Pre-processing: Data Validation and Imputation

The raw data contained around 17 thousand observations that were obtained over a period of 7 d, and the first step of pre-processing was to evaluate whether there were missing data. As the focus of the expedition was only on salinity and temperature data, it was possible that the other variables could be incomplete. The variables N.NO3, DOCeq and Abs210 were the most compromised, with around 31.27%, 28.93% and 22.85% of missing data. Most of these missing spots in the spectroscopy were found between Glückstadt and Wedel, on the River Elbe, near Hamburg. The points with missing values for N.NO3 reading were removed, thus having around 0.78% of the DOCeq points missing and 10.8% of the Abs210 points.

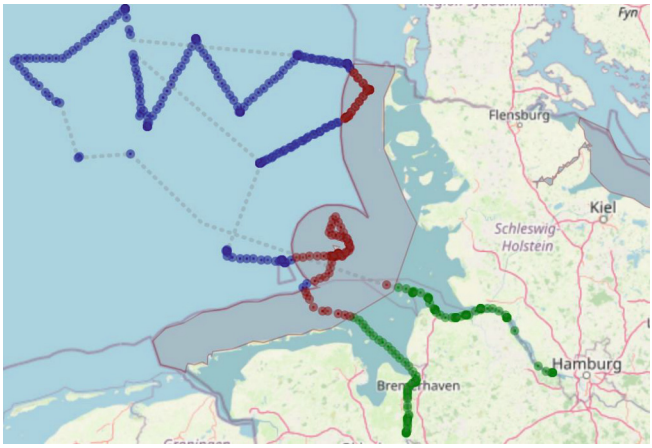

Fig. 3. Zones: Internal Waters (Green), Territorial Sea (Red) and North Sea (blue). (Color figure online)

For the remaining incomplete points, spatial interpolation of the data was carried out. The method chosen for spatial interpolation was inverse distance weighting (IDW). In this method, values at unsampled locations are estimated as the weighted average of values at the rest of the locations with weights inversely proportional to the distance between the unsampled and sampled locations. The calculation is carried out through $\hat{Z}(s_0) = \sum_{i=1}^{n} Z(S_i) w_i$, where $\hat{Z}(s_0)$ is the predicted value at (s_0), n is the number of sampled locations (about 7700, depending on the variable), $Z(S_i)$ is the value at location (S_i) [7]. The weights, w_i, are given by $w_i = \frac{d_i^{-\beta}}{\sum_{i=1}^{n} d_i^{-\beta}}$, being d_i the distance between locations s_i and s_0 and β the power of distance d_i which determines the degree to which closer distances are preferred over more distant locations. In this study was considered $\beta = 1$.

The next pre-processing step was analyzing data consistency in relation to sequential measurements, that is, the differences between sequential measurements, where one measurement is quite different from adjacent ones, presenting a peak in magnitude and gradient. This treatment is guided by SeaDataNet's Data Quality Control Procedures [6].To test the magnitude between sequential measurements the Spike test was performed [11].

2.3 Exploratory Spatial Data Analysis

In the analysis of spatial processes, the interaction between heterogeneity and spatial dependence presents significant challenges in the specification of spatial models, making the specification process time-consuming and error-prone, potentially leading to inappropriate models. An effective tool for defining such models is Exploratory Spatial Data Analysis (ESDA), which is essential to better understand the data before modeling. This preliminary approach helps ensure

more accurate modeling, following the recommended practice of exploring the data before proceeding with more sophisticated analyzes [1].

2.4 Spatial Autocorrelation: Moran's *I*

Spatial autocorrelation gives us an idea of the degree to which a set of features tends to be clustered together or evenly dispersed over the Earth's surface. Global Moran's I is evaluated by measuring the covariance between attributes at each place and near sites toward the overall mean. If both neighboring values are above or below the mean (similar high-high - HH - or low-low - LL - values), the product is positive, reflecting the presence of a similar spatial autocorrelation. Otherwise, the product of the two mean deviations will be negative (unrelated high-low - HL - and low-high - LH - values), indicating a non-positive situation. In a certain way, this index is the modified Pearson coefficient for a single variable. Global Moran I is given by $I = \frac{N}{W} \times \frac{\sum_i \sum_j w_{ij}(x_i - \bar{x})(x_j - \bar{x})}{\sum_i (x_i - \bar{x})^2}$,where N is the number of spatial observations, x_i and x_j are the values of variable in locations i and j, $\bar{x}$ is the mean, w_{ij} is the ij-th element of the spatial weight matrix and W is the sum of spatial weights. To calculate W the inverse distance of nearest neighbors method was considered, $w_{ij}(k) = \begin{cases} 0, & if \quad i = j \\ \frac{1}{d_{ij}}, & if\ d_{ij} \leq d_i \\ 0, & if\ d_{ij} > d_i \end{cases}$, where d_{ij} is the distance between the point and the nearest neighbor according to a cutoff distance $d_i(k)$[7][12]. The distance d_{ij} was determined based on the great circle distance, which represents the minimum distance between two points on a path on the spherical surface [11]. This distance is calculated by $d_{ij} = Rcos^{-1}\left[sen\theta_i sen\theta_j + cos\theta_i \theta_j cos\left(k_i - k_j\right)\right]$. Where R is the radius of the Earth around the Equator (6378Km); θ and k are the latitude and longitude, respectively. To test the significance of Global Moran's I under the null hypothesis of no spatial autocorrelation, the statistic is given by $z = \frac{I - E(I)}{Var(I)^{1/2}}$, where $E[I] = \frac{-1}{n-1}$, $Var[I] = \frac{n^2(n-1)S_1 - n(n-1)S_2 - 2S_0^2}{(n+1)(n-1)^2 S_0^2}$, $S_0 = \sum_{i \neq j} w_{ij}$, $S_1 = \frac{1}{2}\sum_{i \neq j}(w_{ij} + w_{ji})^2$ and $S_2 = \sum_k \left(\sum_j w_{kj} + \sum_i w_{ik}\right)^2$. This statistic follows asymptotically a standard normal distribution for a sufficiently large number of regions. Since there are only three regions in this study, an alternative approach to judge significance was used, namely Monte Carlo randomization.

The local Moran I is calculated when there is interest in evaluating the local similarity between the value of each area (region) and that of neighboring areas. Local Indicators of Spatial Association (LISA), such as Local Moran's I is a decomposition of Global Moran I into a set of local statistics, given by $I_i = \frac{n(x_i - \bar{x})}{\sum_j (x_j - \bar{x})^2} \sum_j w_{ij}\left(x_i - \bar{x}\right)$.

2.5 Principal Components Analysis (PCA)

The central idea of PCA is dimensionality reduction for a data set that consists of a considerable number p of correlated variables, while seeking to retain as

much variability in data as possible. The original set is transformed into a set of new p variables, the Principal Components (PC), after obtaining the eigenvalues and eigenvectors of the covariance matrix [3]. The i-th PC is the weighted linear combination of the original variables associated with the i-th eigenvector of the covariance matrix, and is given by $Y_i = a_{i1}X_1 + a_{i2}X_2 + ... + a_{ip}X_p$, where a_{ij} are the elements of the i-th eigenvector, also called loadings, which describe how much each variable contributes to a particular principal component. Large loadings (positive or negative) indicate that a particular variable strongly relates to a particular principal component. The sign of a loading indicates whether a variable and a principal component are positively or negatively correlated. The coefficients $a_{ij}, i, j = 1, ...p$ are chosen to satisfy three requirements: **i)** variance of component 1 (PC_1) is large as possible, e.g. $Var\,[PC_1] \geq Var\,[PC_2] \geq ... \geq Var\,[PC_p]$; **ii)** the principal components are uncorrelated; **iii)** for any principal component $a_{i1}^2 + a_{i2}^2 + ... + a_{ip}^2 = 1$.

In the present study, considering the high number of variables and different measurement scales, PCA was applied on the correlation matrix after standardization of data. The components were extracted forcing independence using the Varimax rotation with Kaiser normalization to ensure orthogonality. To evaluate the quality of the PCA, the Kaiser-Meyer-Olkin statistic (KMO), Bartlett test for sphericity (uncorrelated variables) and square of the cosine ($\cos^2$) of the variables were used:

- $KMO = \frac{\sum\sum_{j\neq k} r_{jk}^2}{\sum\sum_{j\neq k} r_{jk}^2 + \sum\sum_{j\neq k} p_{jk}^2}$, where r_{jk} is the simple correlation coefficient between variables X_j and X_k and p_{jk} is the partial correlation coefficient between X_j and X_k, given the other X_s variables. KMO varies between 0 and 1, and higher values indicate a better PCA fit to the data.

- Bartlett statistic $\chi^2 = -\left[(n-1) - \frac{2p+5}{6}\right] ln\,|R|$, that follows a χ^2 distribution, with $\frac{p(p-1)}{2}$ degrees of freedom, where n is the sample dimension, p is the number of variables and $|R|$ is the correlation's matrix determinant.

- $cos_{ij}^2 = \frac{a_{ij}^2}{\sum_{k=1}^{p} a_{jk}^2}$, where a represents the observation's score, i represents the component, j represents the variable and p is the number of components [3]. cos_{ij}^2, varies in $[0; 1]$ and higher values indicate that component i retains a high proportion of the variance of the variable j.

Keiser's criterion was used to decide how many PC to retain, that is the components for which the eigenvalue is above 1.

3 Results

3.1 ESDA

Preliminary analysis through histograms for all variables after standardization made it possible to obtain a representation of distributions for comparison purposes. A similar pattern is observed between the TS and NS zones, with the greatest variability occurring the IW zone (Fig. 4). Once the presence of outliers was detected in all variables, Box-Cox transformations were performed to normalize the data for the remaining analyses.

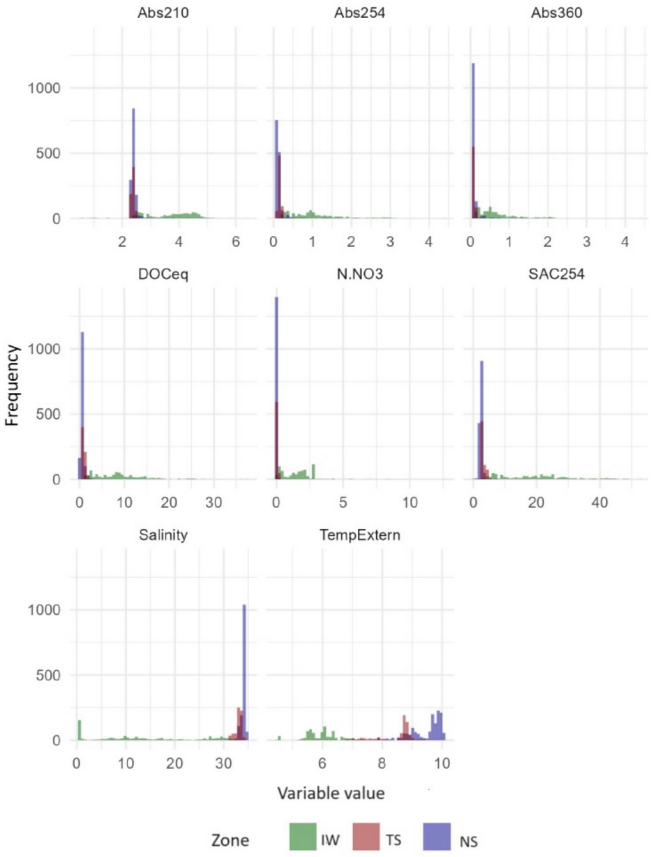

Fig. 4. Histograms for all variables by zone: IW-Internal waters, TS-Territorial Sea, NS-North Sea

In the analysis by zones, we noticed that temperature and salinity have a moderate correlation in IW, but significantly strong for the other two regions. This may occur because both vary differently as one moves towards the North

Sea, or they may also have different variation in waters further away from the sea, entering to the mainland. They still present a negative correlation varying from moderate to strong intensity for all other variables. N.NO3 and Abs210 have a correlation of similar magnitude with the other variables, and moderate between them. The absorption variables showed a strongly positive correlation between them, which may be influenced by the turbidity of the water (TriOS GmbH, 2017) (Fig. 5).

The NS region showed weak and/or non-statistically significant correlations for some pairs of variables. This result can be explained by the compression of the data in that area. N.NO3, DOCeq and SAC are considerably compressed and in their small variation no linear correlation between them is observed. Still in the NS, Salinity and TempExtern present a strong positive correlation for this area, demonstrating a linear correlation significantly stronger than in the IW area. The global correlogram indicated that, when considering the complete set of data, the variables present a strong correlation with each other (Fig. 5).

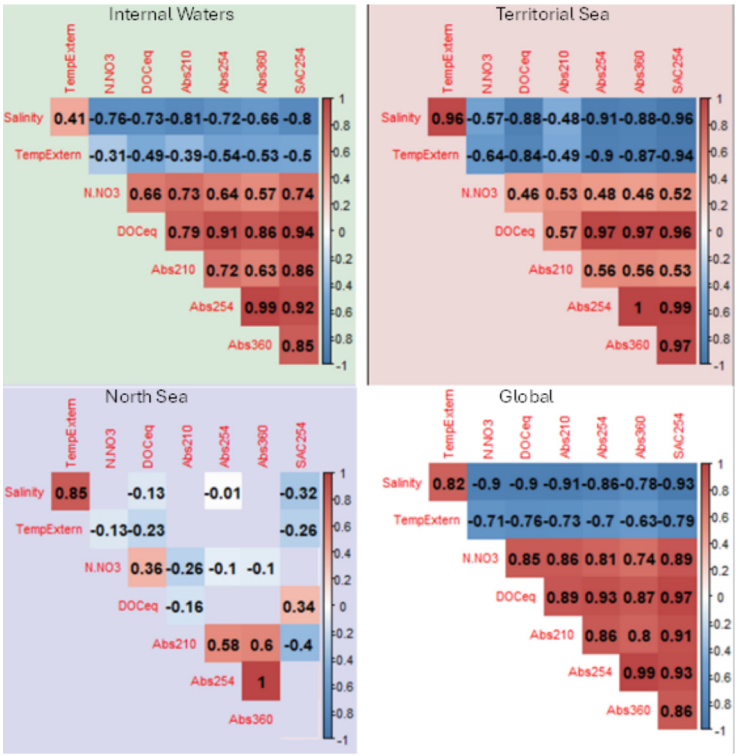

Fig. 5. Correlogram by Zone and Global.

From this initial analysis of the global data, we can then conclude that we mainly have two groups of variables that strongly positively correlate with each

other: the group with Salinity and External Temperature (TempExtern) and the group with all other variables. We also see that between these two groups there is a strongly negative correlation.

After analyzing the correlograms, it was observed that the variables had a high correlation structure that PCA can explore.

3.2 PCA: By Region and Globally

In the IW zone, the loadings demonstrate that no variable or group of variables is mostly loaded in PC1, although it contributes around 74.5% of the total variability of the original data. In PC2, the loading of the TempExtern (0.7) stands out, followed by N.NO3 (0.45). The first two PCs together represent 85% of the variability of the original variables. In the TS zone, loadings on PC1 demonstrate similar behavior to IW. PC2 represent more effectively the variables N.NO3 (0.7) and Abs210 (0.6). The first two components preserve 90% of the variability of the original variables in that zone. In NS zone, the components extracted reflects also the correlogram analysis. It was seen that most of the variables did not present a significantly strong linear correlation and it is known that this characteristic reduces the effectiveness of PCA. In this case, the % of the variance explained is now more distributed between the two chosen components and the total variability explained was around 60%. (Fig. 6).

	Internal Water		Territorial Sea		North Sea	
	PC1	PC2	PC1	PC2	PC1	PC2
Salinity	-0.3526	-0.2834	-0.3772	0.11432	0.20344	-0.4937
TempExtern	-0.2371	0.71746	-0.3759	0.01752	0.30041	-0.4558
N.NO3	0.32304	0.44178	0.24799	0.70834	-0.1808	0.13156
DOCeq	0.38411	-0.0428	0.37805	-0.1823	-0.0476	0.40351
Abs210	0.35595	0.30206	0.25221	0.5962	0.48835	0.01666
Abs254	0.38692	-0.1942	0.38763	-0.1816	0.53044	0.31932
Abs360	0.36518	-0.2789	0.38144	-0.1862	0.54275	0.29665
SAC254	0.39722	0.0338	0.39066	-0.1689	-0.1378	0.42204

	Internal Water		Territorial Sea		North Sea	
	PC1	PC2	PC1	PC2	PC1	PC2
Variance	5.964	0.843	6.353	0.852	2.613	2.17
% of Variance	74.545	10.542	79.408	10.644	32.664	27.119
Cumulative % of Variance	74.545	**85.087**	79.408	**90.052**	32.664	**59.784**

Fig. 6. Heatmap - PCA Loadings and explained variance by Zone.

Regarding to the global, PC1 presents the same separation of variables found in the correlogram. This strong correlation also justifies the large portion of the variability explained in the first PC, 86.4%. PC2 was characterized by the variables TempExtern, Abs254 and Abs360, but this represented only 5.9% of the percentage of the total variance (Fig. 7).

	Global	
	PC1	PC2
Salinity	-0.3631	0.2442
TempExtern	-0.3122	0.65956
N.NO3	0.34589	-0.1737
DOCeq	0.36757	0.09276
Abs210	0.35708	-0.0467
Abs254	0.36301	0.39596
Abs360	0.34225	0.55452
SAC254	0.37355	0.01002

	Global	
	PC1	PC2
Variance	6.912	0.47
% of Variance	86.402	5.876
Cumulative % of Variance	86.402	**92.278**

Fig. 7. Heatmap - PCA Loadings and explained variance for global region.

In Fig. 8, the biplot of IW and TS show the negative correlations of Salinity and TempExtern with the other variables. In both graphs (IW and TS), is also observed that most of the variables were close to the PC1 axis. The cos^2 values indicated by the colors of the vectors illustrates the adequacy of only 2 components. The NS zone biplot emphasized that the 2 components do not correctly represent the variability of N.NO3, DOCeq and SAC254 data. The magnitude of their vectors was smaller and consequently the cos^2 values were low. The biplot of the Global clearly demonstrated the strong linear correlations between the variables. The vectors presented are located around the PC1 axis, confirming their efficiency in representing the variability of the original data, with little loss of this information (86%). The cos^2 values support this result, having values around 0.9 for most variables.

3.3 Global and Local Moran's $I-$statistic

To define the weight matrix, the arrangement chosen established a temporal spacing of 60 min and $k = 5$ neighbors, as shown in Fig. . Such an arrangement with 49 points allowed broad coverage of the navigated area, avoiding dense agglomerations of points in a single region, at the same time that connections are made without leaving 'islands'. Due to the number of points, the computational load of calculating the weight matrix was not extremely onerous in terms of time and machine consumption. Furthermore, consider a large number of close neighbors can bias the results towards more uniform predictions due to the potential dilution effect that may occur between the many points, reducing local sensitivity. The arrangement obtained is represented in Fig. 9.

Considering the weight matrix, the Moran index was calculated and results are presented in Table 2. All I values represented positive spatial autocorrelation. Taking into account that the p-values were lower than 0.05, the hypothesis of negative spatial autocorrelation or absence of autocorrelation is rejected, and therefore it is concluded that the data provide evidence for the existence of positive spatial autocorrelation.

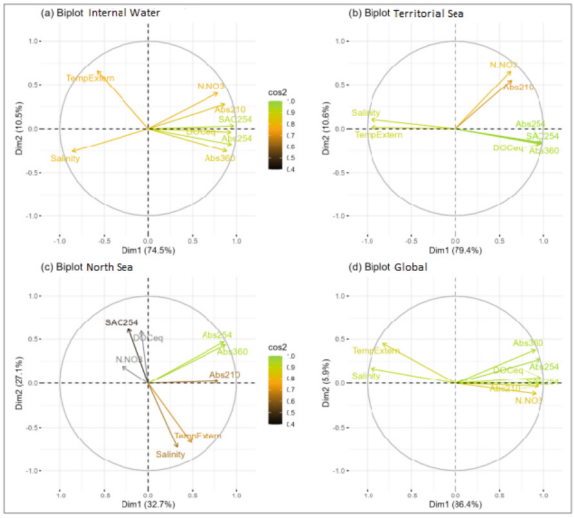

Fig. 8. Biplot by zone and global with $\cos^2$.

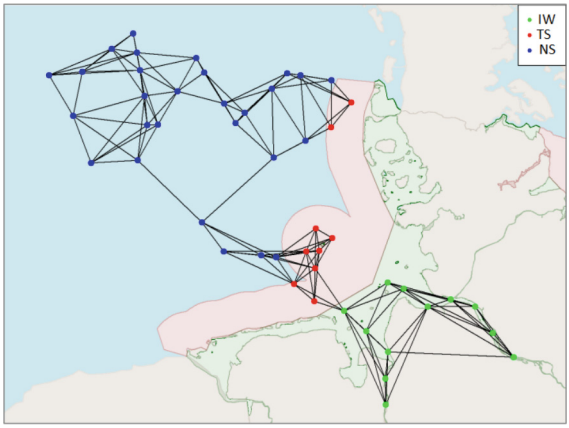

Fig. 9. Arrangement to calculate the Weight Matrix, W.

The variable with the highest value was TempExtern which, according to histograms of the variable distributions by zone (Fig. 4), indicated a gradual increase towards the NS zone. The second highest value was Salinity which, had an increase in the same direction. However, the variability in this variable is large for the TS and NS zones, remaining reasonably constant. Therefore, the variation of these two variables is constant and increasing towards the MN zone. The reduced number of extreme values observed for these two variables is also a potential factor that contributes to a more prominent spatial autocorrelation. For

Table 2. Moran's I per variable and for PC1 and PC2.

	Moran's I	z-score	p-value
Salinity	0.65463	7.2445	2.17E-13
TempExtern	0.80615	8.5925	4.25E-18
N.NO3	0.50486	5.7203	5.32E-09
DOCeq	0.39864	4.9059	4.65E-07
Abs210	0.36964	4.1697	1.52E-05
Abs254	0.45485	5.3906	3.51E-08
Abs360	0.42591	4.9868	3.07E-07
SAC254	0.41866	5.0087	2.74E-07
PC1	0.55069	6.3064	1.43E-10
PC2	0.57698	6.4722	4.83E-11

the remaining variables from the original data set, Moran's I reveals moderate values (Fig. 10).

Taking PC1 and PC2, a moderate value of Global Moran's I for both was observed (Table 2). As these variables represent the variability of the data set as a whole, it is interesting to see that their values were intermediate to the values of the other variables. The data set, as a whole, presents a significant spatial correlation, especially considering the results of PC1 due to its high loading of originals data variability. Thus, the use of PCs in this analysis helps in the interpretation of the joint result of the spatial autocorrelation of the variables studied, indicating that, when considered together, they are not only strongly correlated (see Fig. 5), but they also present positive spatial autocorrelation.

Next, the local Moran I (LISA) values were analyzed. Remember that the objective of LISA is to indicate statistically significant spatial clusters for each variable. From the analysis of the results presented in Fig. , there is an absence of significant spatial autocorrelation in the TS and NS zones for most variables. It was also found that observations from the IW zone showed positive spatial autocorrelation for most variables. This profile was reflected in PC1, a component that explained most of the variability in the original data in the PCA test.

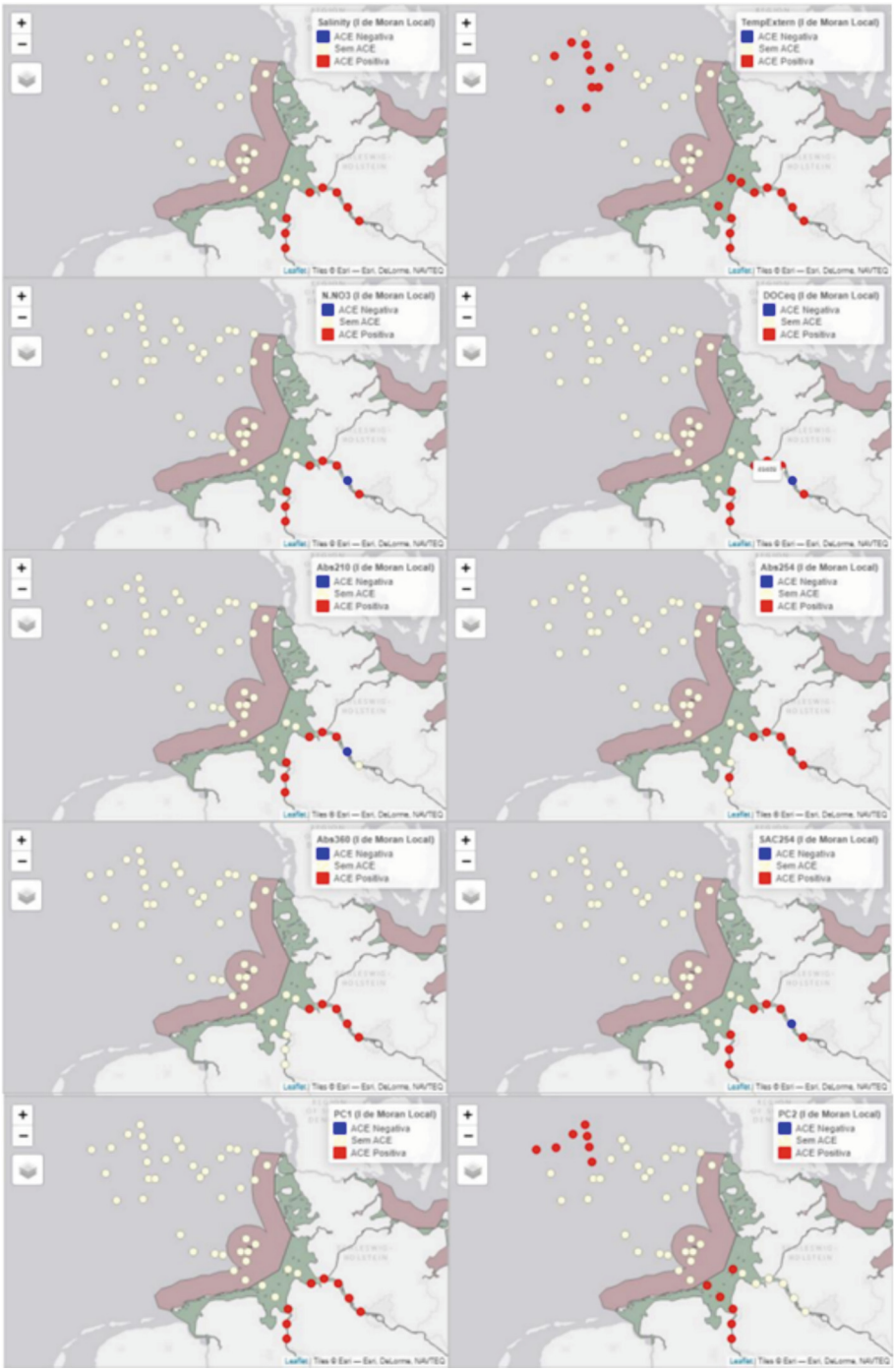

Fig. 10. Local Moran's I for all variables and principal components PC1 and PC2. Blue dots represent Negative spatial autocorrelation, white dots are no spatial autocorrelation and red dots are positive spatial autocorrelation. (Color figure online)

4 Comments and Concluding Remarks

Exploratory Spatial Data Analysis made by zone revealed that most of the variables were flattened into a small range in the Territorial Sea and North Sea (south) zones. Salinity and External temperature differed from the other variables but were similar to each other. The Internal Waters zone shown the greatest variance for all the variables. ESDA also indicated a possible spatial autocorrelation from the Internal Waters in direction to North Sea. As such, spatial autocorrelations under global Moran's I indicate that they are mostly located in the Internal Waters. LL clusters were found for Salinity and External temperature in the Internal Waters region while HH clusters were found in the same zone for the other original variables. PCA resume data into two principal components. PC1 point to clusters similar to the original variables as a whole and PC2 similar to External Temperature. The same point was determined as a LH spatial outlier for 4 variables, indicating that there may be a variation of interest in that zone, as there is a drop in the value of some of the variables in relation to their near neighbors.

This study has some limitations, such as the data collection method. Data was collected during the voyage along the cruise route. Thus, there aren't simultaneous observations at the different points, which potentially influenced the results, due to tides and/or other local maritime and meteorological dynamics. Another limitation concerns the period of data collection, which is too short to apply more robust spatio-temporal methods that would be convenient for understanding the changes in the variables considered over a more significant period. Seasonal imbalances in the region, such as the aforementioned Great Salinity Anomaly, could take a considerable amount of time to be realized, perhaps years, if not decades.

In the future, it is intended to obtain data from the same region for a longer period and different seasons which will allow to confirm, or not, the spatial autocorrelation found, identify seasonal effects, and ultimately implement spatial or even spatio-temporal modelling.

Acknowledgments. This work is partially financed by national funds through FCT-Fundação para a Ciência e a Tecnologia under the projects:
UIDP/05608/2020. DOI 10.54499/UIDP/05608/2020
(https://doi.org/10.54499/UIDP/05608/2020),
UIDB/05608/2020. DOI 10.54499/UIDB/05608/2020
(https://doi.org/10.54499/UIDB/05608/2020) and
UIDB/00006/2020. DOI: 10.54499/UIDB/00006/2020
(https://doi.org/10.54499/UIDB/00006/2020).

The authors thank the three referees for their constructive comments and valuable suggestions, which led to improvements to this work and will contribute to future work. The authors thank to Dr. Andrea Koschin from Jacobs College in Germany, coordinator of the TRAM project who provided the data.

References

1. Anselin, L.: Spatial Econometrics: Methods and Models. Studies in Operational Regional Science. Springer Netherlands (1988). https://books.google.pt/books?id=3dPIXClv4YYC
2. Belkin, I.M., Levitus, S., Antonov, J., Malmberg, S.A.: "Great salinity anomalies" in the north atlantic. Prog. Oceanogr. **41**(1), 1–68 (1998)
3. Hair, J., Babin, B., Black, W., Anderson, R.: Multivariate data analysis. Cengage (2019). https://books.google.pt/books?id=0R9ZswEACAAJ
4. Huthnance, J., et al.: Recent change—North Sea. In: Quante, M., Colijn, F. (eds.) North Sea Region Climate Change Assessment. RCS, pp. 85–136. Springer, Cham (2016). https://doi.org/10.1007/978-3-319-39745-0_3
5. Kim, W.M., Yeager, S., Danabasoglu, G.: Revisiting the causal connection between the great salinityanomaly of the 1970s and the shutdown of labrador sea deep convection. J. Climate **34**(2), 675 – 696 (2021). https://doi.org/10.1175/JCLI-D-20-0327.1, https://journals.ametsoc.org/view/journals/clim/34/2/JCLI-D-20-0327.1.xml
6. Management, P.E.I.F.O..M.D.: Seadatanet.data quality control (2019). https://www.seadatanet.org/Standards/Data-Quality-Control, (Accessed 22 Mar 2023)
7. Moraga, P.: Spatial Statistics for Data Science: Theory and Practice with R. Chapman & Hall/CRC Data Science Series (2023)
8. Quante, M., Colijns, F.: North Sea Region Climate Change Assessment. Springer International Publishing (2016)
9. Schlundt, M.: Continuous thermosalinograph oceanography along rv meteor cruise m169-data processing report (2021). https://doi.org/10.1594/PANGAEA.938474
10. Walday, M., Kroglund, T.: The north sea. European Environ. Agency **32** (2008)
11. Wong, A., Keeley, R., Carval, T., Team, A.D.M.: Argo quality control manual for ctd and trajectory data (2024). https://doi.org/10.13155/33951
12. Zhou, X., Lin, H.: Spatial Weights Matrix. Encyclopedia of GIS. Springer, Boston (2008)



Enhancement of Database Access Performance by Improving Data Consistency in a Non-relational Database System (NoSQL)

Adam A. E. Alflahi[1], Mohammed A. Y. Mohammed[2], and Abdallah Alsammani[3](✉)

[1] Department of Computer Science and Mathematics, Bahri University, Khartoum, Sudan
[2] Department of Mathematics and Statistics, Georgia State University, Atlanta, GA, USA
[3] Department of Mathematics, Jacksonville University, Jacksonville, FL, USA
aalsamm@ju.edu

Abstract. This study aims to improve data consistency in NoSQL databases, which traditionally follow BASE properties instead of the strong consistency guaranteed by ACID principles in RDBMS. We have developed a four-stage server-side model specifically for MongoDB to achieve this. Our model addresses transaction management, separation of read and write transactions, assessment of transaction readiness, and transaction execution using a specialized locking algorithm. We tested our model using the Yahoo Cloud Services Benchmark (YCSB), particularly for update-heavy workloads (A, B, and F). Our model showed significant improvements, with the average throughput, read, and update latencies improving to 2864.726 ms, 32806.275 ms, and 51845.629 ms, respectively, as compared to the baseline metrics of 2914.110 ms, 26510.930 ms, and 32457.662 ms. These results demonstrate that our proposed model effectively enhances consistency in document-based NoSQL databases like MongoDB and other NoSQL database variants, including key-value, graph, and wide-column stores.

Keywords: NoSQL · BASE · RDBMS · ACID · MongoDB · YCSB · benchmark · transaction management · database consistency

1 Introduction

In today's digital era, data storage techniques have had to evolve with the exponential growth of data and its diversified nature. Conventional databases, which are highly structured and rely on the ACID properties (Atomicity, Consistency, Isolation, Durability) to ensure data accuracy and reliability, often struggle when dealing with voluminous and varied data. As a result, NoSQL databases have emerged, which prioritize flexibility, scalability, and speed. NoSQL, which stands for "Not Only Structure Query Language," offers an alternative to the rigid structures of traditional relational databases.

There are four main categories in which NoSQL databases are classified: Graph Stores, Document Stores, Key-Value Stores, and Wide Column Stores. Graph Stores utilize graph structures, such as nodes and edges, to store data. Document Stores use BSON

© The Author(s), under exclusive license to Springer Nature Switzerland AG 2024
O. Gervasi et al. (Eds.): ICCSA 2024 Workshops, LNCS 14816, pp. 194–205, 2024.
https://doi.org/10.1007/978-3-031-65223-3_13

(Binary JSON) documents to store data. Key-value stores use unique key-value pairs for data storage, while Wide Column Stores utilize columns as their primary data storage. These categories significantly improve database design and offer greater flexibility and scalability than traditional relational databases.

The evolution of data storage and retrieval methodologies has undergone a significant transition from traditional relational databases to NoSQL systems. This shift has been primarily influenced by the ability of NoSQL systems to accommodate the vast and diverse nature of Web 2.0 data [1]. However, these systems deviate from the relational model's foundational consistency measures [2]. While NoSQL databases promise advantages like scalability and flexibility, they introduce challenges in ensuring data consistency, especially in commercial cloud storage [1]. Vogels laid the foundation by discussing the concept of eventual consistency, wherein updates might not be instantaneous but are guaranteed over time [3]. This idea was further extended by researchers who explored flexible update mechanisms for weakly consistent replication, creating a bridge between strict consistency and high availability [4]. Parallel efforts in this arena have seen González-Aparicio et al. designing transaction processes that focus on user applications [5] and Lotfy et al. suggesting a middle layer to support ACID properties traditionally absent in NoSQL systems [6]. Taking a broader perspective, systems like "Megastore" [7] and "CloudTPS" [8] have emerged to offer scalable, consistent storage solutions in distributed environments. The narrative was further enriched by solutions like "Granola," aiming at low overhead in transaction coordination [9], and "ElasTraS," envisioning elasticity in cloud transaction storage [10]. Amidst these developments, a focus on specific tools and their transaction capabilities has flourished, such as exploring MongoDB's scalable transactions [11]. Innovative solutions like policy-based access control for consistency [12] and multilevel transaction models for distributed systems [13] have showcased the depth and breadth of research in reconciling scalability with data consistency.

Efforts to improve consistency in NoSQL databases have been a focus of recent research, given these databases often trade off strong consistency for scalability [14, 15]. Various locking mechanisms have been studied to maintain data consistency in NoSQL systems [16–18]. Alternative consistency models, like Causal Consistency, have also been explored to balance performance and consistency [16, 19]. Tools like the Yahoo Cloud Serving Benchmark (YCSB) are the standard for evaluating database performance [20]. Consequently, enhancing consistency in scalable NoSQL databases remains an active area of research.

This paper explores the challenges of NoSQL databases, focusing on the trade-offs between scalability and consistency. While NoSQL databases have revolutionized how data is stored and managed, they often operate on the BASE properties, which can compromise the strong consistency offered by traditional RDBMSs and their ACID properties. To bridge this gap, we introduce a server-side model segmented into four pivotal stages to enhance database consistency. Our model's efficacy is empirically examined using the YCSB benchmark, targeting workloads that underscore update operations. After implementing our proposed algorithm, our findings show significant improvements in average throughput and read and update timings. Our research demonstrates a promising advancement in achieving enhanced consistency for NoSQL databases.

We are optimistic about the potential applicability of our model across various NoSQL platforms, including key-value, graph, and wide-column stores, thereby pushing the boundaries of what these databases can offer regarding data reliability.

2 Methods

Based on the insights we gathered from our extensive literature review, we created a customized framework that effectively addresses the identified challenges and gaps. We carefully integrated its components to ensure a cohesive structure and designed it to blend the selected tools' functionalities seamlessly. The architecture we developed is scalable and adaptable to potential future modifications.

2.1 Tools Employed

MongoDB Database. MongoDB is a well-known NoSQL database that is famous for its document-oriented structure. It stores data in flexible, JSON-like documents. This format enables fields to vary from document to document and permits data structure changes over time. As a result, MongoDB is highly adaptable and efficient for handling large volumes and diverse data types.

One of MongoDB's major strengths is its scalability, which is achieved through features like sharding and replication. Sharding distributes data across multiple machines, while replication ensures data availability and reliability. MongoDB's performance is further enhanced by indexing, which allows for faster data retrieval. Additionally, MongoDB has a rich query language that supports complex searches and aggregations.

MongoDB plays a crucial role in storing data and managing user transactions with robust security measures in our framework. The database operates on the principles of BASE (Basically Available, Soft state, Eventual consistency), which prioritizes availability and partition tolerance. Yet, it still allows configurable consistency levels to meet various application needs.

To optimize our use of MongoDB, we have meticulously designed the schema and managed transactions to enhance consistency without sacrificing performance. We fine-tuned the consistency settings and leveraged MongoDB's built-in features like write concerns, read preferences and atomic operations. By doing so, we ensure that our system performs efficiently, maintains high data integrity, and meets our applications' consistency requirements.

Performance Benchmarking with YCSB. We utilized the Yahoo Cloud Serving Benchmark (YCSB) to evaluate the efficacy and robustness of our proposed solution. YCSB is a well-known benchmarking tool in the industry that provides a comprehensive suite of tests to measure performance across different real-world scenarios. Our assessment with YCSB covered multiple dimensions of performance analysis, including latency, throughput, and scalability across diverse data workloads. The data generated from these benchmarks helped identify and quantify the efficiency enhancements our framework offers during different phases of data processing.

The results obtained from these benchmarks demonstrated significant improvements in processing speeds and response times, as well as our system's ability to scale effectively under increased loads. This rigorous benchmarking process has enabled us to fine-tune our solution, ensure it meets industry standards, and effectively address practical user demands.

Programming Environment. We chose Java as the programming language for our proposed model. Java is an object-oriented language widely used and appreciated for its versatility, platform independence, and robust library ecosystem. We chose Java for its cross-platform capabilities, which are particularly useful in ensuring consistent performance across different operating systems - a crucial factor for deploying enterprise-level applications. Additionally, Java is compatible with various tools and frameworks, such as MongoDB for NoSQL database interactions and YCSB (Yahoo! Cloud Serving Benchmark) for performance benchmarking. This integration capability allows our model to leverage existing technologies while maintaining scalability and high performance.

We adhered to recognized design patterns and industry best practices throughout the development process. This approach not only facilitated a more maintainable codebase but also enhanced our model's overall efficiency and reliability. By adopting these strategies, we aimed to create a solution that meets current technical demands and is adaptable to future advancements and requirements.

3 Results

We evaluated our proposed algorithm's performance on multi-document transactions in MongoDB using the YCSB benchmark standards. Specifically, we focused on assessing the impact of our algorithm on workloads A, B, and F, with the primary goal of evaluating read/write consistency and its effect on multi-document performance in MongoDB. Our algorithm was integrated into the YCSB framework for this purpose.

To accomplish our goal, we added a lock() class to the YCSB benchmark. This class temporarily locks a MongoDB document accessed by the initial client's transaction. Once the transaction is complete, it calls the commit() method. If the transaction is not finalized within a predetermined timeframe, the abort() method is invoked, and the transaction is rolled back. After this, the document is unlocked, allowing other clients to access it.

We conducted experiments on a dataset of 10,000 operations and records to assess the performance of a proposed algorithm across different client configurations. The configurations included one, five, ten, and fifteen clients. Each client operated independently, with varying levels of operations per millisecond. For instance, a single client executed 10,000 operations/ms, whereas fifteen clients performed 150,000 operations/ms.

We used a two-phase structure comprising loading and run phases to measure the performance. During the loading phase, data was loaded, and the run phase executed the data using the selected YCSB workloads. This methodology helped measure the throughput (ops/sec) and latency variations. We analyzed the consistency of the results in MongoDB after the YCSB workload executor processed both the data load and run.

We have provided graphical representations of our findings in accompanying figures that compare transaction operations across 1, 5, 10, and 15 clients, both pre/post

algorithm integration into the YCSB benchmark. Metrics were captured in time (milliseconds) and operations per second.

We evaluated the proposed algorithm using the YCSB benchmark, focusing on workloads A, B, and F. These benchmarks were selected to understand how the algorithm impacted throughput, average update latency, and average read latency.

3.1 Workload A (Update Heavy Workload)

This workload comprises a 50/50 mix of operations by default. Throughput: As shown in Fig. 1, throughput was significantly improved for 1 and 15 clients after applying our algorithm. However, due to possible data inconsistencies during ongoing operations, its effect was comparatively lesser on 5 and 10 clients.

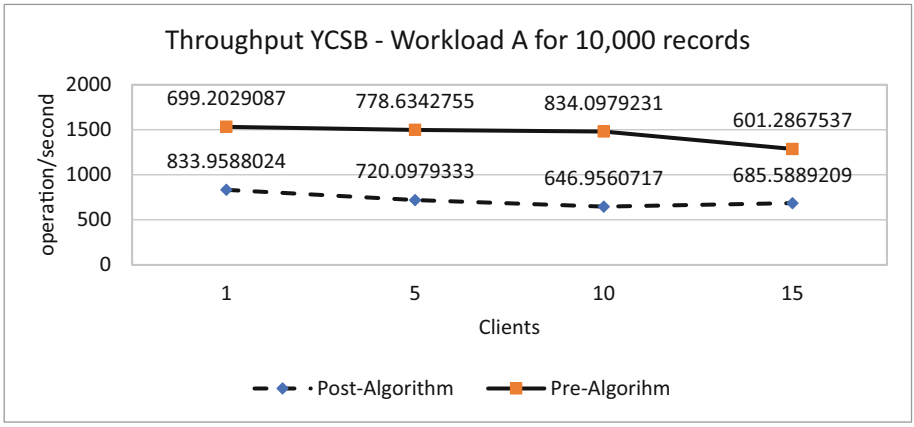

Fig. 1. Comparison of Throughput in YCSB Workload A for 10,000 Records Before and After Implementing the Proposed Algorithm.

Update Latency. As presented in Fig. 2, data across all clients showed strong consistency after applying the proposed algorithm.

Read Latency. Figure 3 displays the read latency results. Data in 5 and 10 clients showed high consistency, whereas 1 and 15 clients exhibited reduced consistency, which might be attributed to data conflicts when reading multiple operations concurrently. The proposed algorithm enhanced data consistency for Workload A, especially with concurrent transactions. However, the discrepancy in read transactions occasionally led to read failures during execution.

3.2 M Workload B (Read Mostly Workload)

This workload consists of a 95/5 read/write mix. Throughput: As evidenced in Fig. 4, the throughput was considerably higher for 1, 5, and 15 clients post-algorithm applications. However, the effect was least observed in the 10-client setup due to possible inconsistencies in write operations during execution.

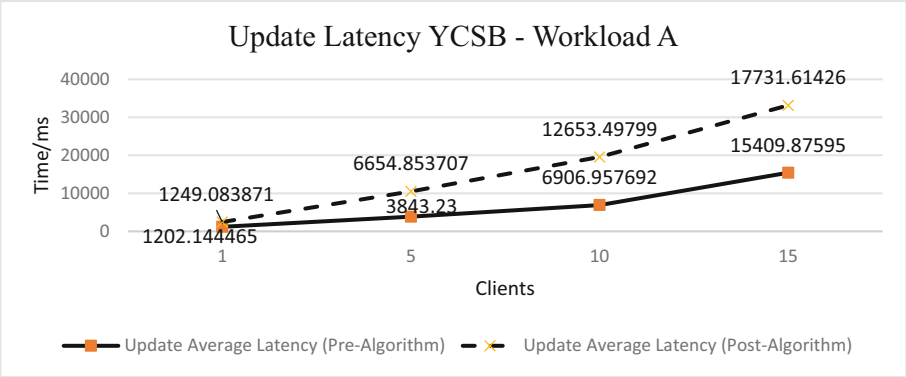

Fig. 2. Update Latency under Workload A - The graph illustrates the update latency measured at 3 ms, highlighting the system's efficiency in handling update-heavy operations within a NoSQL database environment.

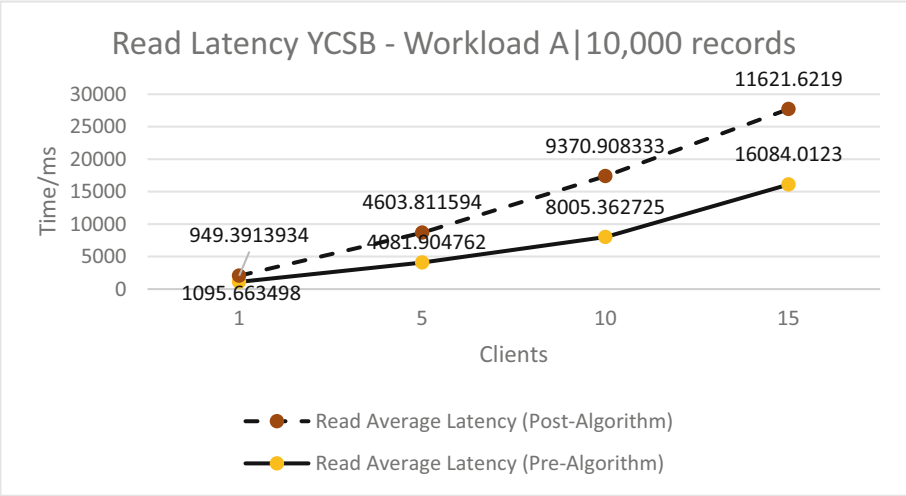

Fig. 3. Comparison of Read Latency for Workload A with 10,000 Records: Before and After Algorithm Implementation

Update and Read Latency. Both Figs. 5 and 6 suggest that our algorithm ensured strong data consistency across the board, with only the 10-client setup showing minor inconsistencies. This pattern is consistent with the algorithm's design, prioritizing strong workloads consistent with predominant read operations.

3.3 Workload F (Read, Modify, Write Workload)

Records are read and modified in this workload, and the changes are written back. Throughput: Fig. 7 highlights the algorithm's noticeable impact on 10 and 15 clients,

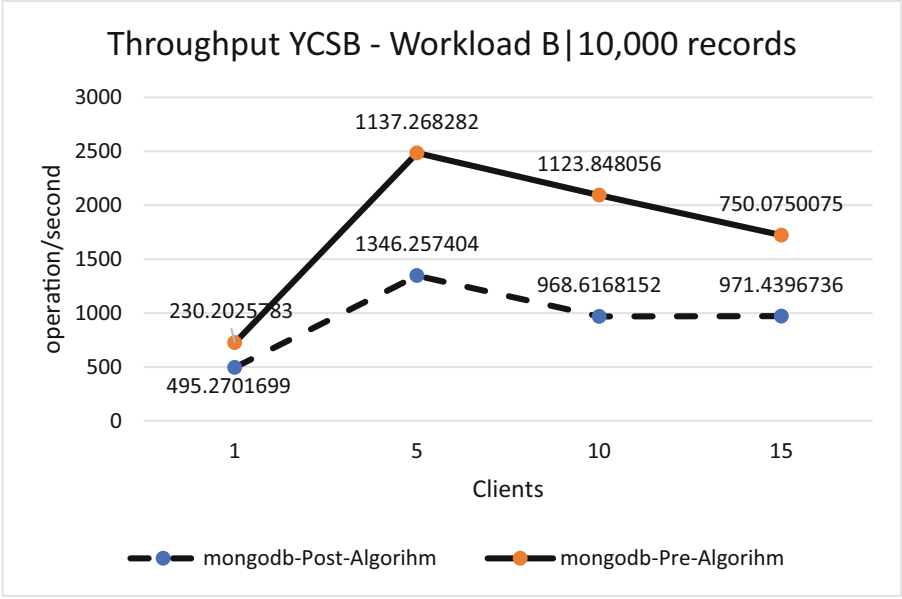

Fig. 4. Comparison of Throughput in YCSB Workload B for 10,000 Records Before and After Implementing the Proposed Algorithm. The graph illustrates the number of transactions per second for various client configurations (1, 5, 10, and 15 clients) both before and after the application of the algorithm. The aim is to highlight the algorithm's effectiveness in enhancing database throughput.

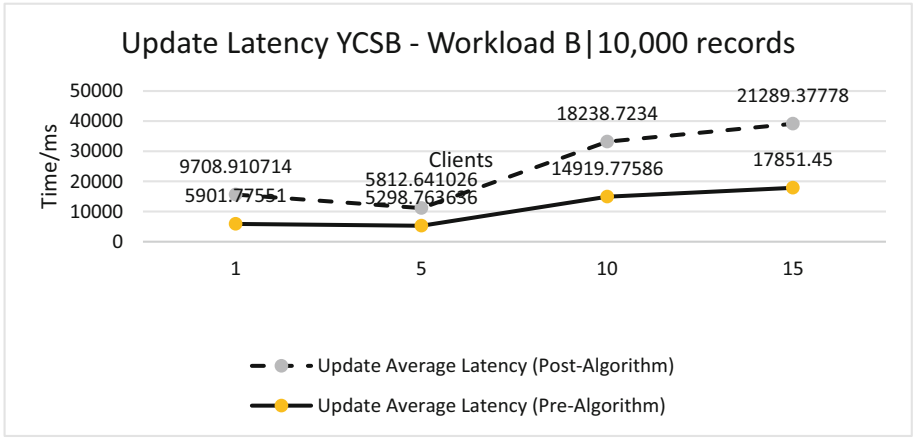

Fig. 5. Comparison of Update Latency in YCSB Workload B for 10,000 Records Before and After Implementing the Proposed Algorithm

with minimal effects on 1 and 5 clients. This could be due to inconsistencies during ongoing operations.

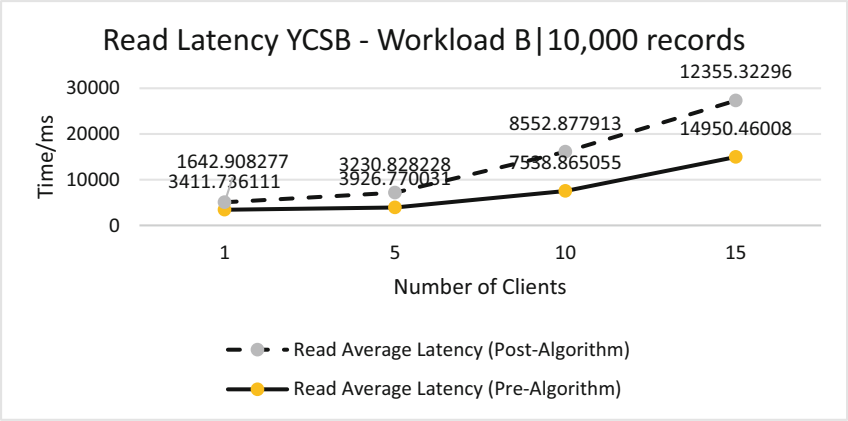

Fig. 6. Comparison of Read Latency for Workload B with 10,000 Records Before and After Implementing the Proposed Algorithm. This graph illustrates the variation in read latency among 1, 5, 10, and 15 clients, showcasing the impact of the algorithm on improving data consistency and transaction speed.

Update Latency. As depicted in Fig. 8, most client setups showed increased consistency in update latency post-algorithm application, except for the 5-client setup (Fig. 9).

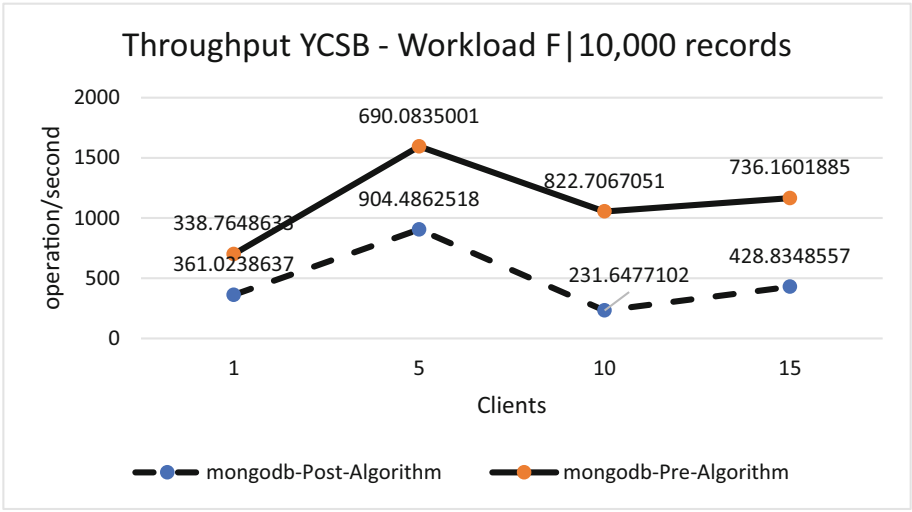

Fig. 7. Comparison of Throughput in YCSB Workload F with 10,000 Records, Before and After Implementing the Proposed Algorithm. The graph illustrates the increase in throughput across different client scenarios (1, 5, 10, 15 clients) after the algorithm's implementation, demonstrating its effectiveness in improving database performance.

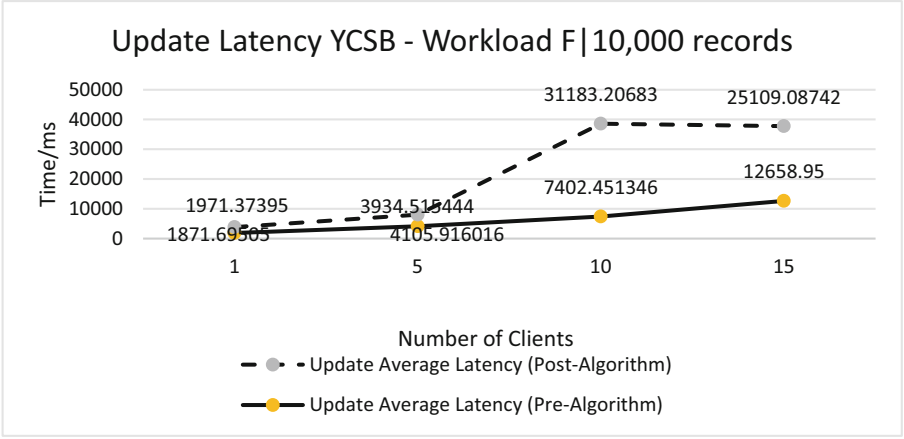

Fig. 8. Update Latency YCSB - Workload F for 10,000 Records (Pre-Algorithm): This graph shows baseline update latency across different client counts before implementing the proposed algorithm, serving to evaluate its effectiveness.

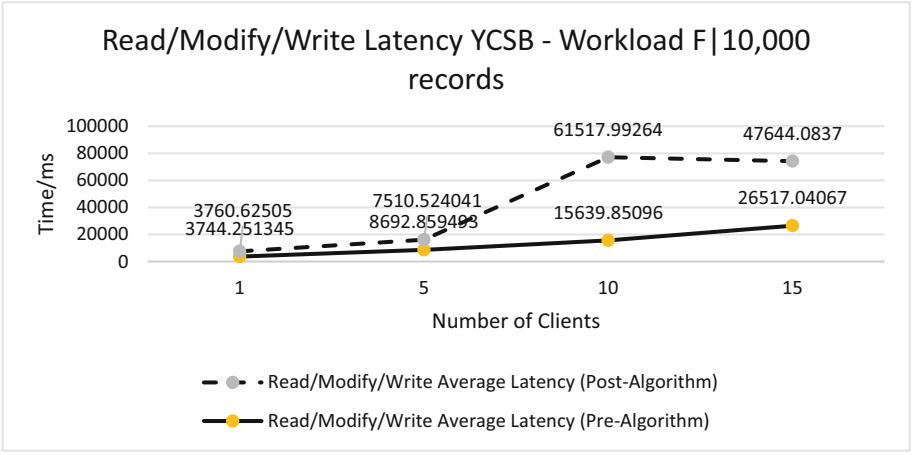

Fig. 9. Comparison of Read/Modify/Write Latency Before and After Algorithm Implementation for YCSB Workload F with 1000 Records.

Read Latency. In Fig. 10, the 10 and 15 client configurations demonstrated the algorithm's impact, with lesser effects on the 1 and 5 client configurations. For Workload F, our algorithm strengthened consistency in most tests, especially during update operations. However, read operations exhibited varying levels of consistency.

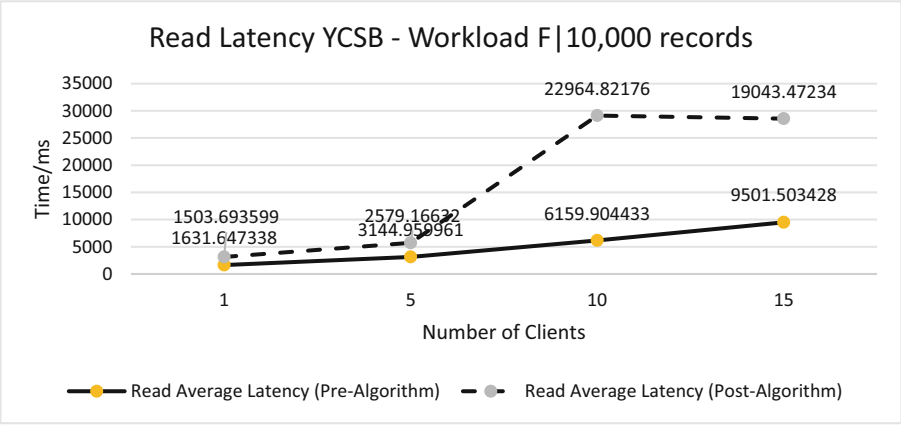

Fig. 10. Comparison of Read Latency for 10,000 Records in YCSB Workload F Before and After Algorithm Implementation.

Table 1. Table 2 Impact of the Proposed Algorithm on MongoDB Database Performance

Workloads	Throughput Latency AVG				Update Latency AVG				Read Latency AVG				Read/Modify/Write Latency AVG			
	Clients				Clients				Clients				Clients			
	1	5	10	15	1	5	10	15	1	5	10	15	1	5	10	15
Workload A	✔	✖	✖	✔	✔	✔	✔	✔	✖	✔	✔	✖	–	–	–	–
Workload B	✖	✔	✖	✔	✔	✔	✔	✔	✖	✖	✔	✖	–	–	–	–
Workload F	✔	✔	✖	✖	✔	✖	✔	✔	✖	✖	✔	✔	✔	✖	✔	✔

4 Discussion

This study has a clear and focused aim to critically assess the integration of our proposed algorithm within the YCSB (Yahoo! Cloud Serving Benchmark) framework, employing MongoDB as an exemplar of NoSQL databases. Our primary goal was to explore the algorithm's influence on data consistency amidst varying client loads. We employed Workloads A, B, and F from the YCSB to facilitate a detailed measurement and comparative analysis of several key performance metrics, including average latency, throughput, read latency, and update latency under diverse experimental setups.

The empirical results in Table 1 demonstrate that our algorithm significantly bolsters data consistency within MongoDB. This improvement is consistent across a broad spectrum of client operations, encompassing both reads and writes. Notably,

update operations exhibited substantial enhancements in consistency across most client configurations, validating the algorithm's effectiveness in achieving its intended goals.

However, the results reveal inconsistencies in specific client scenarios, potentially attributable to data inaccuracies during ongoing transactions. These observations call for a cautious interpretation of the data and underline the urgent need for additional empirical research, particularly in environments where data access and modification are concurrent. This research is crucial for data consistency in MongoDB and similar NoSQL databases.

5 Conclusion

In big data processing, NoSQL databases have become increasingly favored for their capacity to manage large datasets with notable performance and efficiency. However, maintaining data consistency during transaction processing is a pivotal challenge for these databases.

Our research team addressed this challenge by developing an algorithm designed to enhance data consistency during multi-transaction processes in MongoDB. The algorithm ensures that updates conducted within transactions are consistently reflected in subsequent transactions, bolstering overall data integrity.

To evaluate the effectiveness of our algorithm, we integrated it into the Yahoo! Cloud Serving Benchmark (YCSB) and conducted rigorous testing across various transactional scenarios. We assessed the algorithm's performance under diverse client configurations, employing 1, 5, 10, and 15 clients across workloads A, B, and F.

The results from our extensive testing indicate that the proposed algorithm substantially improves data consistency compared to baseline metrics, particularly in writing transactions (updates) across most client setups. Although some variability was observed in consistency levels for read transactions across different clients, these variations were considered acceptable since no modifications were made to the data during processing.

In summary, our study offers crucial insights into the efficacy of our algorithm as a strategic tool to address consistency challenges in NoSQL databases. By enhancing data consistency, our algorithm improves the performance and efficiency of NoSQL databases and sets the stage for further advancements in big data processing.

Conflict of Interest Statement. The authors confirm no conflicts of interest associated with this publication.

References

1. Wada, H., Fekete, A., Zhao, L., Lee, K., Liu, A.: Data Consistency Properties and the Trade-offs in Commercial Cloud Storages: the Consumers' Perspective"
2. Codd, E.F.: A relational model of data for large shared data banks. Commun. ACM **13**(6), 377–387 (1970). https://doi.org/10.1145/362384.362685
3. Vogels, W.: Eventually consistent. Commun. ACM **52**(1), 40–44 (2009). https://doi.org/10.1145/1435417.1435432

4. Petersen, K., Spreitzer, M.J., Terry, D.B., Theimer, M.M., Demers, A.J.: Flexible update propagation for weakly consistent replication. In: Proceedings of the Sixteenth ACM Symposium on Operating Systems Principles - SOSP 1997, pp. 288–301. ACM Press, Saint Malo, France (1997). https://doi.org/10.1145/268998.266711
5. González-Aparicio, M.T., Ogunyadeka, A., Younas, M., Tuya, J., Casado, R.: Transaction processing in consistency-aware user's applications deployed on NoSQL databases. Hum.-Centric Comput. Inform. Sci. **7**(1) (2017). https://doi.org/10.1186/s13673-017-0088-3
6. Lotfy, A.E., Saleh, A.I., El-Ghareeb, H.A., Ali, H.A.: A middle layer solution to support ACID properties for NoSQL databases. J. King Saud Univ. Comput. Inform. Sci. **28**(1), 133–145 (2016). https://doi.org/10.1016/j.jksuci.2015.05.003
7. Baker, J., Bond, C., Corbett, J.C., Furman, J., Khorlin, A., Larson, J.: Megastore: Providing Scalable, Highly Available Storage for Interactive Services
8. Wei, Z., Pierre, G., Chi, C.-H.: CloudTPS: scalable transactions for web applications in the cloud. IEEE Trans. Serv. Comput. **5**(4), 525–539 (2012). https://doi.org/10.1109/TSC.2011.18
9. Cowling, J., Liskov, B.: Granola: Low-Overhead Distributed Transaction Coordination
10. Das, S., Agrawal, D., Abbadi, A.E.: ElasTraS: An Elastic Transactional Data Store in the Cloud
11. Chaple, L., Ahirrao, D.S.: Scalable transactions using mongodb cloud data store (2005)
12. Wobber, T., Rodeheffer, T.L., Terry, D.B.: Policy-based access control for weakly consistent replication. In: Proceedings of the 5th European Conference on Computer Systems, pp. 293–306. ACM, Paris France (2010). https://doi.org/10.1145/1755913.1755943
13. Tripathi, A.: A transaction model with multilevel consistency for shared data in distributed groupware systems. In: 2016 IEEE 2nd International Conference on Collaboration and Internet Computing (CIC), pp. 236–245. IEEE, Pittsburgh, PA, USA (2016). https://doi.org/10.1109/CIC.2016.041
14. Ramzan, S., Bajwa, I.S., Kazmi, R., Amna: Challenges in NoSQL-based distributed data storage: a systematic literature review. Electronics **8**(5), 488 (2019). https://doi.org/10.3390/electronics8050488
15. Khan, W., Kumar, T., Zhang, C., Raj, K., Roy, A.M., Luo, B.: SQL and NoSQL database software architecture performance analysis and assessments—a systematic literature review. Big Data Cogn. Comput. **7**(2), 97 (2023). https://doi.org/10.3390/bdcc7020097
16. Alzaidi, M., Vagner, A.: Benchmarking Redis and HBase NoSQL databases using yahoo cloud service benchmarking tool. Ann. Math. Informaticae **56**, 1–9 (2022)
17. Vyas, K., Jat, P.: Study of consistency and performance trade-off in cassandra. In: Computer Science & Technology Trends, Academy and Industry Research Collaboration Center (AIRCC), pp. 61–77 (2022). https://doi.org/10.5121/csit.2022.121907
18. Tian, J., Yang, Q.: Horae: causal consistency model based on hot data governance. J. Supercomput. **78**(3), 4574–4599 (2022). https://doi.org/10.1007/s11227-021-04030-w
19. Ahmed, J., Karpenko, A., Tarasyuk, O., Gorbenko, A., Sheikh-Akbari, A.: Consistency issue and related trade-offs in distributed replicated systems and databases: a review. Radioelectron. Comput. Syst. (2), 171–179 (2023). https://doi.org/10.32620/reks.2023.2.14
20. Benchmarking cloud serving systems with YCSB | Proceedings of the 1st ACM symposium on Cloud computing. https://dl.acm.org/doi/abs/, https://doi.org/10.1145/1807128.1807152. Accessed 25 Aug 2023

Algorithm of Determining Errors of Gimballed Inertial Navigation System

Olha Sushchenko[1](✉), Yurii Bezkorovainyi[1], Oleksandr Solomentsev[1], Maksym Zaliskyi[1], Oleksii Holubnychyi[1], Ivan Ostroumov[1], Yuliya Averyanova[1], Viktoriia Ivannikova[1], Borys Kuznetsov[2], Ihor Bovdui[2], Tatyana Nikitina[3], Roman Voliansky[4], Kostiantyn Cherednichenko[1], and Olena Sokolova[1]

[1] National Aviation University, Liubomyra Huzara Avenue, 1, Kyiv 03058, Ukraine
sushoa@ukr.net
[2] Anatolii Pidhornyi Institute of Mechanical Engineering Problems of the National Academy of Sciences of Ukraine, Pozhars′koho Street, 2/10, Kharkiv 61046, Ukraine
[3] Educational Scientific Professional Pedagogical Institute Ukrainian Engineering Pedagogical Academy, University Street 16, Kharkiv 61003, Ukraine
[4] National Technical University of Ukraine "Igor Sikorsky Kyiv Polytechnic Institute", Beresteiskyi Avenue, 37, Kyiv 03056, Ukraine

Abstract. This paper deals with determining errors in gimballed inertial navigation systems. One of the aims of the study is to obtain expressions for transformations between different coordinate systems and expressions describing the system kinematics. The appropriate matrices of directing cosines have been obtained. The expressions for correction of reading of accelerometers taking into consideration rotation of the Earth, motion of the moving vehicle, and Coriolis acceleration have been obtained. Features of the considered system lie in the usage of the trajectory coordinate system as a basic navigation system contrary to the geographical reference frame and the usage of the two-axis gimballed platform. The structure chart and the necessary instrumentation of the researched system are represented. The equations for the determination of methodical errors for the inertial stabilization and inertial system have been obtained. The simulation of the basic errors of the studied system has been carried out. The obtained results of the simulation show the high accuracy of the researched system.

Keywords: Stabilization System · Moving Vehicle · Navigation Systems · Errors · Correction Expressions · Simulation

1 Introduction

The modern stage of the creation of moving vehicles requires improved techniques for the design of navigation systems, including course systems. For many vehicles, it is mandatory to use a course determination system based on gyroscopic devices [1–3]. If it is necessary to achieve high accuracy, systems with a gimballed platform should be

© The Author(s), under exclusive license to Springer Nature Switzerland AG 2024
O. Gervasi et al. (Eds.): ICCSA 2024 Workshops, LNCS 14816, pp. 206–218, 2024.
https://doi.org/10.1007/978-3-031-65223-3_14

used. Such a platform is mounted in a special suspension consisting of some frames and ensuring the possibility for angular motion in the inertial space. Dynamically adjusted gyroscopes and accelerometers could be used as sensing elements in such systems. One of the gyroscopes could be used as a vertical gyro reference, the other – as a directional gyroscope. The advantages of the chosen gyroscopes are the high stability of characteristics, low power consumption, low sensitivity to changing surrounding temperature, and small time of operation readiness. Accelerometers are used to correct gyroscopes to determine navigation parameters, namely speed and coordinates after appropriate double integration.

Requirements of high accuracy and mass and dimensions restrictions can be satisfied by the usage of a two-axis gyro-stabilized platform. Stabilization of the platform in the horizon plane is implemented by gyro vertical. In its turn, the gyro vertical is setting to the horizon plane by signals of accelerometers using the integral correction.

The application of the two-axis gyro-stabilized platform requires the usage of the trajectory reference frame. This is accompanied by complications algorithms of processing the primary navigation information.

The main objective of the paper is the assessment of errors in the gimballed platform stabilization. For this, the algorithm for determining errors and modelling stabilization processes have been carried out. The novelty of the approach lies in developing an algorithm for the determination of errors for gimballed inertial navigation systems operating in trajectory instead of the geographical reference frame.

The paper is organized as follows. In Sect. 2 we consider features of an inertial navigation system with a two-axis gimballed platform including basic kinematical relationships. The algorithm for determining errors of the studied system is in Sect. 3. The modelling results are given in Sect. 4.

2 Features of Inertial Navigation System with Two-Axis Gimballed Platform

Nowadays, gimballed inertial navigation systems are used in high-precision applications only. The main features of such systems are defined by the choice of the kinematic scheme. The choice of the kinematic scheme depends on many factors including accuracy and weight-dimension requirements. The usage of the stabilization and navigation system with a three-axis gimballed platform is the most widespread. However, such an approach requires significant mass and size costs. It is possible to improve these characteristics using a stabilization and navigation system based on a two-axis gyro-stabilized platform [4–6]. At the same time, additional hardware and algorithmic expenses arise. This is caused by the necessity to use an additional rotary device to ensure turns of the gyroscopic device. This gyroscopic unit performs the functions of the directional gyroscope [7–9]. The use of a two-axis platform also leads to the need to use a trajectory coordinate system. This leads to the complication of primary navigation information processing algorithms [10–12]. The position of the gyroscopic devices is controlled by the signals of the accelerometers. The stabilization motors ensure the coordination of the position of the platform with the horizon plane. This makes possible control of gyroscopes with dynamic adjustment using relatively small moments. Due to the use

of two-stage gimbals, the platform turns with the object in azimuth. Such peculiarity is connected with additional errors due to the change of object heading. For compensation, it is necessary to know the data about the linear velocity and course of the object. The choice of the kinematic scheme of this system depends on many factors, including accuracy and weight requirements [13].

To obtain kinematic ratios, the following coordinate systems must be used:

- trajectory $O'\zeta\eta\xi$ (the $O'\eta$ axis is pointed along the object's velocity vector, the $O'\zeta$ axis is normal to the horizontal plane, the $O'\xi$ axis is pointed perpendicularly to the $O'\eta$ axis and is in the horizontal plane);
- body-axis $Ox_0y_0z_0$ (the Oy_0 axis is pointed along the longitudinal axis of the object, the Oz_0 axis is normal to the horizontal plane, the Ox_0 s is located perpendicularly to the Oy0 axis and is located in the horizon plane);
- the platform's $Ox_py_pz_p$ (the Oy_p axis is pointed along the axis of the outer frame of the platform gimbals, the Oz_p axis is normal to the horizontal plane, the Ox_p axis is located perpendicularly to the y_p axis and is located in the horizontal plane);
- $Ox_ry_rz_r$ connected with the Rezal's axes of a dynamically adjusted gyroscope, which performs the functions of a vertical gyro reference.

The vector radius of the platform installation place concerning the center of mass of the object r_p determines the position of the origin of the coordinate systems. The relative angular location of the entered coordinate systems is given in Figs. 1 and 2.

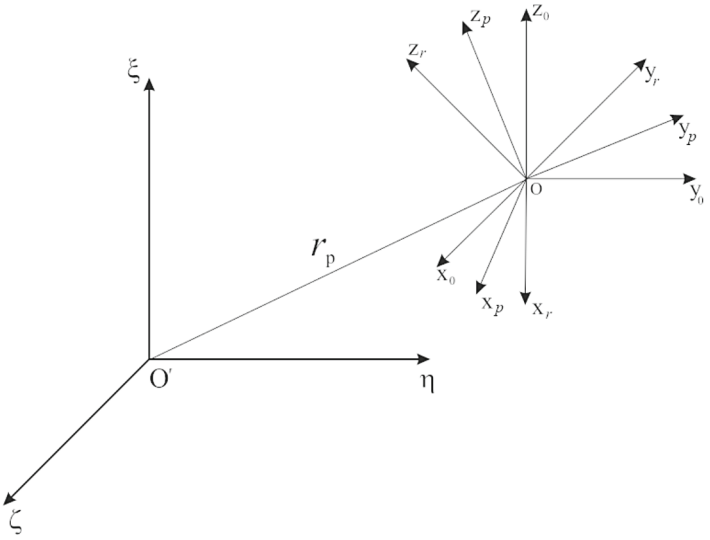

Fig. 1. The relative location of all the above mentioned systems of coordinates.

The scheme with a two-axis gimballed platform is presented in Fig. 3. Two gyroscopes with dynamic adjustment and two accelerometers are located on the platform.

The platform is stabilized in the horizontal plane by the data of the gyroscope, which performs the functions of a vertical gyro reference. The vertical gyro is brought

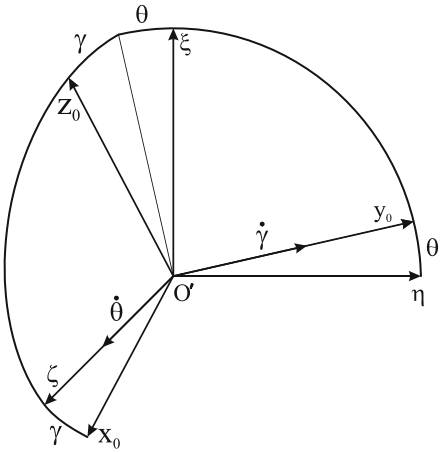

h

Fig. 2. The relative location of body-axes system and the platform's system of coordinates: $\alpha_p \beta_p$ are angles that define a location of the platform).

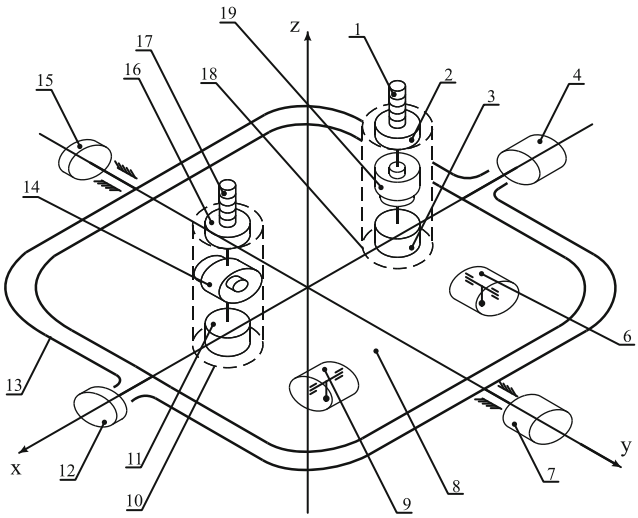

Fig. 3. The stabilization and navigation system using two-axes platform: x, y, z is the body-axes coordinate system; 15, 12, 16, 2 are angle-data sensors; 7, 4, 11, 3 are torque sensors; 13 is the outer gimbal; 1, 17 are shunts; 18, 10 are rotating units; 8 is the platform; 9, 6 are accelerometers; 14, 19 are dynamically adjusted gyroscopes

to the horizon plane by the signals of the corresponding accelerometers using integral correction. The directional gyroscope is installed on a separate rotary base. It should be noted that in the given scheme (Fig. 3), the vertical gyro reference is also installed on a rotating base. This is done to ensure checks of the directional gyroscope.

A feature of the considered system is the distribution of control functions. At the same time, the position of the main axis of the dynamically adjusted gyroscope is controlled by the signals of accelerometers. Stabilizing motors ensure the perpendicular position of the main axis relative to the stabilized platform. This position coincides with the orientation of the dynamically adjusted gyroscope rotor. Such a distribution of functions ensures the formation of comparatively few control moments in the torque sensors of the dynamically adjusted gyroscopes [13].

Another feature of the considered system is the use of a two-stage gyro-stabilized platform. At the same time, the platform rotates with the object in the azimuthal plane. On contrary to the standard version with a platform using three-axe gimbals, this ensures an invariant position of the axis of the outer frame of the platform to the North. This feature makes the system susceptible to perturbations due to changes in the course of the moving object, as well as the Earth's elliptical shape. To compensate for such perturbations, there is a need to use data about the linear velocity, as well as the course of the object and the rate of change of course.

When compiling a mathematical description of the researched system, it is necessary to apply a trajectory coordinate system. This greatly complicates the algorithms of the studied system in terms of its functionality. The system is close to an attitude and heading reference system and requires the formation of appropriate corrections by accelerometer signals [14, 15].

3 Algorithm of Determining Errors

We will assume that the gyro-stabilized platform repeats the movement of the Rezal axes of the vertical gyro reference with accuracy to the stabilization errors. At the same time, platform stabilization errors are determined by angles α_r, β_r. The equations of motion of the vertical gyro reference can be obtained on the basis of the precession equations of motion of gyroscopes with dynamic adjustment. They have the form [4, 6] as presented in the system (1))

$$\begin{cases} I\ddot{\alpha}_{\mathrm{r}} - H\dot{\beta}_r + c\alpha_r + d\dot{\alpha}_r - \frac{H}{T}\beta_r = H_1\omega_x + I\dot{\omega}_{\mathrm{y}} - k_i\int\limits_0^t W_y + M_y^b \\ I\ddot{\beta}_{\mathrm{r}} + H\dot{\alpha}_r + c\beta_r + d\dot{\beta}_r - \frac{H}{T}\alpha_r = -H_1\omega_y + I\dot{\omega}_x - k_i\int\limits_0^t W_x + M_x^b \end{cases}; \qquad (1)$$

where H is the kinetical moment; c is the gimbals remanent inflexibility; d is the subsidence ratio; T is the constant time of the gyroscope precession; $H_1 = H(1+s)$; $s = 1 \cdot 10^{-3}$; I is the equatorial moment of the gimbals frames and the gyroscope rotor; ω_x, ω_y are projections of the platform's angle velocity; $\dot{\omega}_x$, $\dot{\omega}_y$ are projections of angular accelerations of the platform; k_i is the factor of the integrating correction; W_x, W_y are projections of seeming acceleration of the platform onto the sensitivity axes of accelerometers; M_x^b, M_y^b are moments caused by perturbation actions. To ensure the condition of system stability, the coefficient of integral correction should be determined as $k_i = \frac{H_\perp}{R_M}$, where R_M is the basic radius of bending the surface of the Earth's ellipsoid in the meridian plane.

To determine the projections of the angle velocity of the platform, it is necessary to project the angle velocities of the initial trajectory coordinate system on the axis associated with the platform. To evaluate the errors of a virtually vertical line, it is expedient to define projections as functions of the angles α_r, β_r. These angles determine the location of the vertical gyroscope reference concerning the platform and represent platform stabilization errors. The angles α, β determine the location of the vertical gyroscope reference concerning the horizontal plane. They represent errors of the virtual vertical line [16–18].

The corresponding matrices of directing cosines between the trajectory coordinate system and the system of coordinates connected to the vertical gyro reference C_1 and between the coordinate system connected to the platform and the coordinate system connected to the vertical gyro reference C_2 have the forms, respectively, (2) and (3)

$$C_1 = \begin{bmatrix} \cos\alpha & 0 & -\sin\alpha \\ \sin\alpha \cdot \sin\beta & \cos\beta & \cos\alpha \cdot \sin\beta \\ \sin\alpha \cdot \cos\beta & -\sin\beta & \cos\alpha \cdot \cos\beta \end{bmatrix}; \tag{2}$$

$$C_2 = \begin{bmatrix} \cos\alpha_r & 0 & -\sin\alpha_r \\ \sin\alpha_r \cdot \sin\beta_r & \cos\beta_r & \cos\alpha_r \cdot \sin\beta_r \\ \sin\alpha_r \cdot \cos\beta_r & -\sin\beta_r & \cos\alpha_r \cdot \cos\beta_r \end{bmatrix}; \tag{3}$$

Considering the angles α_r, β_r, α, β to be small, after simplifications we obtain the matrix of directing cosines of the trajectory coordinate system and the coordinate system connected to the platform:

$$C_2C_1 = \begin{bmatrix} 1+\alpha\alpha_r\beta\beta_r+\alpha\alpha_r & \alpha_r\beta_r-\beta\alpha_r & -\alpha+\alpha_r\beta\beta_r+\alpha_r \\ \alpha\beta-\alpha\beta_r & 1+\beta\beta_r & \beta-\beta_r \\ -\alpha_r+\alpha\beta\beta_r+\alpha & \beta_r-\beta & \alpha\alpha_r+\beta\beta_r+1 \end{bmatrix} \approx$$

$$\approx \begin{bmatrix} 1 & 0 & -\alpha+\alpha_r \\ 0 & 1 & \beta-\beta_r \\ \alpha-\alpha_r & -\beta+\beta_r & 1 \end{bmatrix}. \tag{4}$$

Conformably, the projections of the angle velocity of the platform onto its axes based on expression (1) and matrices C_1, C_2 described by expressions (2)–(4) are determined as follows:

$$\begin{aligned} \omega_x &= \dot{\beta} - \dot{\beta}_r + \omega_\zeta - \omega_\xi(\alpha - \alpha_r); \\ \omega_y &= \dot{\alpha} - \dot{\alpha}_r + \omega_\eta + \omega_\xi(\beta - \beta_r); \end{aligned} \tag{5}$$

In Eqs. (5), ω_ζ, ω_η, ω_ξ represent the projections of the angler velocity of the trajectory coordinate system onto its axes, which concerning [7] have the form, respectively, (6) and (7)

$$\begin{cases} \omega_\zeta = -\frac{V_\eta \sin K + V_\zeta \cos K}{R_1}\sin K - \frac{V_\eta \cos K - V_\zeta \sin K}{R_M}\cos K - \Omega\cos\phi\sin K; \\ \omega_\eta = \frac{V_\eta \sin K + V_\zeta \cos K}{R_1}\cos K - \frac{V_\eta \cos K - V_\zeta \sin K}{R_M}\sin K + \Omega\cos\phi\cos K; \\ \omega_\xi = \frac{V_\eta \sin K + V_\zeta \cos K}{R_1} tg\phi - \dot{K} + \Omega\sin\phi; \end{cases} \tag{6}$$

where V_ζ, V_η, V_ξ are lateral, longitudinal, and vertical projections of the moving vehicle's velocity; K is the course of the moving vehicle; R_1 is the radius of bending of the terrestrial ellipsoid surface; Ω is the angle velocity of the daily rotation of the Earth; $\dot{K}$ is the angle velocity of changes of the course [19, 20].

Projections of the acceleration vector of the platform onto the axis of the coordinate system connected to the moving object are determined as follows [7, 8]

$$\begin{bmatrix} W_{x_0} \\ W_{y_0} \\ W_{z_0} \end{bmatrix} = \mathrm{C}_1 \begin{bmatrix} W_\zeta \\ W_\eta \\ W_\xi \end{bmatrix} + \begin{bmatrix} \dot{\omega}_{x_0} z_\mathrm{p} - \dot{\omega}_{z_0} y_\mathrm{p} \\ \dot{\omega}_{z_0} x_\mathrm{p} - \dot{\omega}_{x_0} z_\mathrm{p} \\ \dot{\omega}_{x_0} y_\mathrm{p} - \dot{\omega}_{y_0} x_\mathrm{p} \end{bmatrix} + \\ + \begin{bmatrix} \omega_{y_0}(\omega_{x_0} y_\mathrm{p} - \omega_{y_0} x_\mathrm{p}) - \omega_{z_0}(\omega_{z_0} x_\mathrm{p} - \omega_{x_0} z_\mathrm{p}) \\ \omega_{z_0}(\omega_{y_0} z_\mathrm{p} - \omega_{z_0} y_\mathrm{p}) - \omega_{x_0}(\omega_{x_0} y_\mathrm{p} - \omega_{y_0} x_\mathrm{p}) \\ \omega_{x_0}(\omega_{z_0} x_\mathrm{p} - \omega_{x_0} z_\mathrm{p}) - \omega_{y_0}(\omega_{y_0} z_\mathrm{p} - \omega_{z_0} y_\mathrm{p}) \end{bmatrix}; \tag{7}$$

where W_{x_0}, W_{y_0}, W_{z_0} represent projections of the susceptible acceleration of the platform onto the axes of the body-axis coordinate system; ω_{x_0}, ω_{y_0}, ω_{z_0} are projections of moving vehicle absolute angle velocity; x_p, y_p, z_p are coordinates of the platform, which define the place of location of the platform concerning the center of a mass of the moving vehicle.

The matrices of directing cosines between the coordinate system associated with the moving vehicle and the trajectory and platform coordinate systems C_3, C_4 have the form, respectively, (8), (9)

$$C_3 = \begin{bmatrix} \cos\gamma & \sin\theta \cdot \sin\gamma & -\cos\theta \cdot \sin\gamma \\ 0 & \cos\theta & \sin\theta \\ \sin\gamma & -\sin\theta \cdot \cos\gamma & \cos\theta \cdot \cos\gamma \end{bmatrix}; \tag{8}$$

$$C_4 = \begin{bmatrix} \cos\alpha_p & 0 & -\sin\alpha_p \\ \sin\alpha_p \cdot \sin\beta_p & \cos\beta_p & \cos\alpha_p \cdot \sin\beta_p \\ \sin\alpha_p \cdot \cos\beta_p & -\sin\beta_\pi & \cos\alpha_p \cdot \cos\beta_p \end{bmatrix}. \tag{9}$$

The projections of the object's absolute angular velocity on its axes are as follows

$$\begin{cases} \omega_{x_0} = (\omega_\zeta + \dot{\theta})\cos\gamma + \omega_\eta \sin\gamma \sin\theta - \omega_\xi \sin\gamma \cos\theta; \\ \omega_{y_0} = \dot{\gamma} + \omega_\eta \cos\theta + \omega_\xi \sin\theta; \\ \omega_{z_0} = (\omega_\zeta + \dot{\theta})\sin\gamma - \omega_\eta \cos\gamma \sin\theta + \omega_\xi \cos\gamma \cos\theta. \end{cases} \tag{10}$$

One of the most important points for determining errors in the inertial stabilization and navigation system is the necessity to determine corrections for calculating accelerations. These corrections are caused by the daily rotation of the Earth, the motion of a moving vehicle, and also Coriolis acceleration.

Taking into account the formulas (5)–(10) including matrices C_3, C_4, the expressions for determining the projections of the susceptible acceleration on the axes of the platform

could be calculated in the following way

$$\begin{gathered}
W_x = \cos\alpha_\pi\cos\gamma W_\zeta + \cos\alpha_\pi\sin\theta\sin\gamma W_\eta + \cos\alpha_\pi\sin\gamma W_\xi + \\
+\cos\alpha_\pi\dot{\omega}_{y_0}z_\mathrm{p} - \cos\alpha_\pi\dot{\omega}_{z_0}y_\mathrm{p} + \\
+\cos\alpha_\pi[\omega_{y_0}(\omega_{x_0}y_\mathrm{p} - \omega_{y_0}x_\mathrm{p}) - \omega_{z_0}(\omega_{z_0}x_\mathrm{p} - \omega_{x_0}z_\mathrm{p})] - \\
-\sin\alpha_\pi\sin\gamma W_\zeta + \sin\alpha_\pi\sin\theta\cos\gamma W_\eta - \sin\alpha_\pi\cos\theta\cos\gamma W_\xi - \\
-\sin\alpha_\pi(\dot{\omega}_{x_0}y_\mathrm{p} - \dot{\omega}_{y_0}x_\mathrm{p}) - \\
-\sin\alpha_\pi[\omega_{x_0}(\omega_{z_0}x_\mathrm{p} - \omega_{x_0}z_\mathrm{p}) - \omega_{y_0}(\omega_{y_0}z_\mathrm{p} - \omega_{z_0}y_\mathrm{p})]; \\
W_y = \sin\alpha_\pi\sin\beta_\pi\cos\gamma W_\zeta + \sin\alpha_\pi\sin\beta_\pi\sin\theta\sin\gamma W_\eta + \sin\alpha_\pi\sin\beta_\pi\sin\gamma W_\xi + \\
+\sin\alpha_\pi\sin\beta_\pi(\dot{\omega}_{y_0}z_\mathrm{p} - \dot{\omega}_{z_0}y_\mathrm{p}) + \\
+\sin\alpha_\pi\sin\beta_\pi[\omega_{y_0}(\omega_{x_0}y_\mathrm{p} - \omega_{y_0}x_\mathrm{p}) - \omega_{z_0}(\omega_{z_0}x_\mathrm{p} - \omega_{x_0}z_\mathrm{p})] + \\
+\cos\beta_\pi\cos\theta W_\eta + \cos\beta_\pi\sin\theta W_\xi + \\
+\cos\beta_\pi(\dot{\omega}_{z_0}x_\mathrm{p} - \dot{\omega}_{x_0}z_\mathrm{p}) + \\
+\cos\beta_\pi[\omega_{z_0}(\omega_{y_0}z_\mathrm{p} - \omega_{z_0}y_\mathrm{p}) - \omega_{x_0}(\omega_{x_0}y_\mathrm{p} - \omega_{y_0}x_\mathrm{p})] + \\
+\cos\alpha_\pi\sin\beta_\pi\sin\gamma W_\zeta - \cos\alpha_\pi\sin\beta_\pi\sin\theta\cos\gamma W_\eta + \cos\alpha_\pi\sin\beta_\pi\cos\theta\cos\gamma W_\xi + \\
+\cos\alpha_\pi\sin\beta_\pi(\dot{\omega}_{x_0}y_\mathrm{p} - \dot{\omega}_{y_0}x_\mathrm{p}) + \\
+\cos\alpha_\pi\sin\beta_\pi[\omega_{x_0}(\omega_{z_0}x_\mathrm{p} - \omega_{x_0}z_\mathrm{p}) - \omega_{y_0}(\omega_{y_0}z_\mathrm{p} - \omega_{z_0}y_\mathrm{p})]; \\
W_z = \sin\alpha_\pi\cos\beta_\pi\cos\gamma W_\zeta + \sin\alpha_\pi\cos\beta_\pi\sin\theta\sin\gamma W_\eta + \sin\alpha_\pi\cos\beta_\pi\sin\gamma W_\xi + \\
+\sin\alpha_\pi\cos\beta_\pi(\dot{\omega}_{y_0}z_\mathrm{p} - \dot{\omega}_{z_0}y_\mathrm{p}) + \\
+\sin\alpha_\pi\cos\beta_\pi[\omega_{y_0}(\omega_{x_0}y_\mathrm{p} - \omega_{y_0}x_\mathrm{p}) - \omega_{z_0}(\omega_{z_0}x_\mathrm{p} - \omega_{x_0}z_\mathrm{p})] - \\
-\sin\beta_\pi\cos\theta W_\eta - \sin\beta_\pi\sin\theta W_\xi - \\
-\sin\beta_\pi(\dot{\omega}_{z_0}x_\mathrm{p} - \dot{\omega}_{x_0}z_\mathrm{p}) - \\
-\sin\beta_\pi[\omega_{z_0}(\omega_{y_0}z_\mathrm{p} - \omega_{z_0}y_\mathrm{p}) - \omega_{x_0}(\omega_{x_0}y_\mathrm{p} - \omega_{y_0}x_\mathrm{p})] + \\
+\cos\alpha_\pi\cos\beta_\pi\sin\gamma W_\zeta - \cos\alpha_\pi\cos\beta_\pi\sin\theta\cos\gamma W_\eta + \cos\alpha_\pi\cos\beta_\pi\cos\theta\cos\gamma W_\xi + \\
+\cos\alpha_\pi\cos\beta_\pi(\dot{\omega}_{x_0}y_\mathrm{p} - \dot{\omega}_{y_0}x_\mathrm{p}) + \\
+\cos\alpha_\pi\cos\beta_\pi[\omega_{x_0}(\omega_{z_0}x_\mathrm{p} - \omega_{x_0}z_\mathrm{p}) - \omega_{y_0}(\omega_{y_0}z_\mathrm{p} - \omega_{z_0}y_\mathrm{p})];
\end{gathered} \tag{11}$$

In expressions (11), the projections of the acceleration of the object's centre of mass on the axis of the trajectory coordinate system have the form

$$\begin{gathered}
W_\zeta = \dot{V}_\zeta + V_\xi\omega_\eta - V_\eta\omega_\xi + V_\xi\Omega\cos\phi\cos K - V_\eta\Omega\sin\phi; \\
W_\eta = \dot{V}_\eta + V_\zeta\omega_\xi - V_\xi\omega_\zeta + V_\zeta\Omega\sin\phi + V_\xi\Omega\cos\phi\sin K; \\
W_\xi = \dot{V}_\xi + V_\eta\omega_\zeta - V_\zeta\omega_\eta - V_\eta\Omega\cos\phi\sin K - V_\zeta\Omega\cos\phi\cos K - g.
\end{gathered} \tag{12}$$

Equations (1), supplemented by formulas (5)–(12), describe a model of vertical gyroscope errors.

The equations of motion of the gyroscope, which performs the functions of a course-measuring instruments, are as follows:

$$\begin{cases}
I\ddot{\alpha}_K + H\dot{\beta}_K + c\alpha_K + d\dot{\alpha}_K + \frac{H}{T}\beta_K = -H_1\omega_{x_1} + M_{z_1}^b + M_{z_1}^{\text{y}\pi\text{p}}; \\
I\ddot{\beta}_K + H\dot{\alpha}_K - c\beta_K - d\dot{\beta}_K + \frac{H}{T}\alpha_K = H_1\omega_{z_1} - M_{x_1}^b - M_{x_1}^{\text{y}\pi\text{p}}.
\end{cases} \tag{13}$$

The expressions for determining the angular velocity projections of the rotary device of the heading gyroscope have the form as presented in (14)

$$\begin{cases}
\omega_{x_1} = \omega_x\cos(K_1 + \Delta K) + \omega_\text{y}\sin(K_1 + \Delta K); \\
\omega_{z_1} = \omega_z + \dot{K} + \Delta\dot{K}.
\end{cases} \tag{14}$$

Accordingly, the control moments can be defined as follows

$$\begin{cases} M_{z_1}^{\text{упр}} = \text{H}_1 k_z \cdot W_y / g + \text{H}_1 \omega_{x_1}^{\text{кор}}; \\ M_{x_1}^{\text{упр}} = \text{H}_1 k_x \cdot W_x / g + \text{H}_1 \omega_{z_1}^{\text{кор}}. \end{cases} \tag{15}$$

where k_x, k_z are transfer coefficients of control loops; W_x, W_y are accelerations; $\omega_{x_1}^{cor}$, $\omega_{z_1}^{cor}$ are correction speeds. In its turn, these speeds are defined by expressions

$$\begin{gathered} \omega_{x_1}^{cor} = \omega_\zeta \cos(K - K_1) + \omega_\eta \sin(K - K_1) = \\ = \left(-\frac{V_\eta \sin K + V_\zeta \cos K}{R_1} \sin K - \frac{V_\eta \cos K - V_\zeta \sin K}{R_M} \cos K - \Omega \cos\phi \sin K\right) \cos(K - K_1) + \\ + \left(\frac{V_\eta \sin K + V_\zeta \cos K}{R_1} \cos K - \frac{V_\eta \cos K - V_\zeta \sin K}{R_M} \sin K + \Omega \cos\phi \cos K\right) \sin(K - K_1); \\ \omega_{z_1}^{cor} = \frac{V_\eta \sin K + V_\zeta \cos K}{R_1} tg\phi - \dot{K} + \Omega \sin\phi. \end{gathered} \tag{16}$$

The equations of motion of the heading gyroscope (13), supplemented by expressions (14)–(16) represent the model of errors of the course measuring instrument.

4 Modelling Results

The main objective of modelling is obtaining assessments of the accuracy of stabilization and navigation processes. To achieve this goal, models of stabilization and navigation errors in the software MATLAB have been developed. More precisely, these models have been created using Simulink Toolbox. The results of determining errors of the inertial stabilization and navigation system in the form of transient processes for regular and irregular perturbations are presented in Figs. 4, 5, 6 and 7.

Simulation has been carried out for the gimballed inertial navigation system assigned for a marine vehicle. Simulation results are given in the form of transient processes with the aim of taking into consideration the dynamics of stabilization. Figures 4, and 5 show transient processes of stabilization by angles of the pitch and roll for regular perturbations.

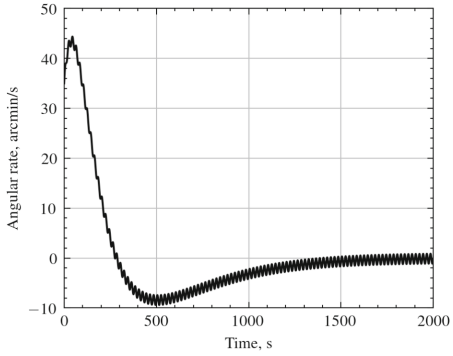

Fig. 4. The transient process of the error on the angle α for the regular perturbations.

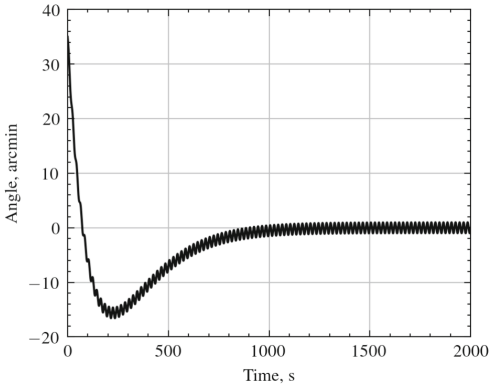

Fig. 5. The transient process of the error on the angle β for the regular perturbations.

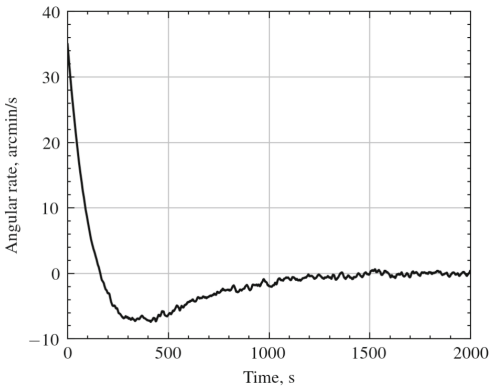

Fig. 6. The transient process of the error on the angle α for irregular perturbations.

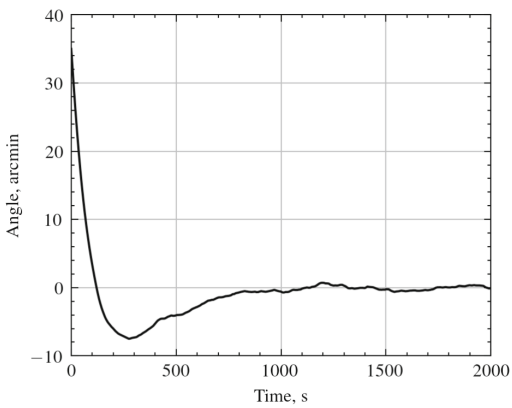

Fig. 7. The transient process of the error on the angle β for irregular perturbations.

Figures 6, and 7 present transient processes of stabilization by angles of the pitch and roll for irregular perturbations. Regular perturbations are given as harmonic signals with constant magnitude and frequency. Irregular perturbations are simulated based on known spectral densities of sea irregularities. Hence, both deterministic and stochastic factors are taken into consideration.

The represented results of the simulation show the high accuracy of the studied stabilization and navigation system. Magnitudes of stabilization errors do not exceed 1.5–2 arcmins and 3 arcmins for regular and irregular perturbations respectively.

5 Conclusions

The expressions for determining errors of the gimballed stabilization and navigation system are derived.

The important feature of the research is obtaining of expressions for determining phantom accelerations using basic concepts of the theoretical mechanics and directional cosines between the trajectory and body axes systems of coordinates. The obtained expressions ensure improving the accuracy of both stabilization and navigation processes. The complex conversions between different coordinate systems are defined in the form of directing cosines.

The novelty of the research lies in obtaining expressions based on using the trajectory coordinate system contrary to the well-known geographical coordinate system.

The expressions for correction of methodical errors for readings of accelerometers have been derived.

The obtained expressions for correction take into consideration the daily rotation of the Earth, the motion of the moving vehicle, and Coriolis acceleration.

The simulation of errors in the stabilization and navigation systems has been carried out. The simulation results prove the high accuracy of the studied system.

In future work, it is proposed to study errors of similar systems with a three-axis gimballed platform.

6 Discussion

The aim of the paper was to the research accuracy characteristics of the inertial navigation system with a two-axis gimballed platform. The research is based on the creation of models of stabilization and navigation system errors. The main result of the research is the creation of a model for determining errors in the precision navigation system with a two-axis gyro-stabilized platform. The developed model takes into consideration kinematical relationships and features of control in modes of gyroscopic vertical and course determination. The results of the research prove the possibility of the usage of the gimballed inertial navigation system in applications that require high precision of navigation and stabilization processes.

The obtained results can be useful for gimballed inertial navigation systems operated on moving vehicles of the wide class. In other words, obtained results could be spread on aerial and land moving vehicles. It should be noted that the accuracy of stabilization

leads to comfortable conditions of operation of inertial measuring instruments including gyroscopic devices and accelerometers.

In future work, it is proposed to apply this approach for systems, which combine navigation of moving objects and stabilization of payload mounted on these objects such as observation and measuring devices. Also, the creation of a full model including control features and the dynamics of moving objects is planned.

Acknowledgments. This work is partially supported by the Ministry of Education and Science of Ukraine under the projects “Development of an Integrated Flight Control System” (№ 0121U109490) and "Methods of Improving the Operational Efficiency of Telecommunication and Electronic Systems of Critical Infrastructure Facilities in Ukraine" (№ 0122U001804).

References

1. Osadchyi, S., Zozulia, V.: Synthesis of optimal multivariable robust systems of stochastic stabilization of moving objects. In: 5th International Conference Actual Problems of Unmanned Aerial Vehicles Developments (APUAVD), pp. 106–111. IEEE, Kyiv, Ukraine (2019). https://doi.org/10.1109/APUAVD47061.2019.8943861
2. Averyanova, Y., Larin, V., Kuzmenko, N., Ostroumov, I., Zaliskyi, M., Solomentsev, O., et al.: Turbulence detection and classification algorithm using data from AWR. In: IEEE 2nd Ukrainian Microwave Week (UkrMW), pp. 518–522. IEEE, Kyiv, Ukraine (2022). https://doi.org/10.1109/UkrMW58013.2022.10037172
3. Larin, V., Solomentsev, O., Zaliskyi, M., Shcherban, A., Averyanova, Y., Ostroumov, I., et al.: Prediction of the final discharge of the UAV battery based on fuzzy logic estimation of information and influencing parameters. In: 3rd KhPI Week on Advanced Technology, pp. 1–6. IEEE, Kharkiv, Ukraine (2022). https://doi.org/10.1109/KhPIWeek57572.2022.9916490
4. Qian, L., Guoping, X., Tian, W., Wang, J.: A novel hybrid EMD-based drift denoising method for a dynamically tuned gyroscope (DTG). Measurement **42**(6), 927–932 (2009). https://doi.org/10.1016/j.measurement.2009.01.017
5. Xia, D., Yu, C., Kong, L.: A micro dynamically tuned gyroscope with adjustable static capacitance. Sensors **13**(2), 2176–2195 (2013). https://doi.org/10.3390/s130202176
6. DTG Gyroscope: Exploring the Revolutionary Technology Behind It. https://gyroplacecl.com/dtg-gyroscope-exploring-the-revolutionary-technology-behind-it/
7. Yang, Q., Zhang, R., Li, H.: Economical high-low temperature and heading rotation test method for the evaluation and optimization of the temperature control system for high-precision platform inertial navigation systems. Sensors **18**(11), 3967 (2018). https://doi.org/10.3390/s18113967
8. Jia, R., Nandikolla, V.K., Haggart, G., Volk, C., Tazartes, D.: System performance of an inertially stabilized gimbal platform with friction, resonance, and vibration effects. J. Nonlinear Dyn. **2017**, 1–20 (2017). https://doi.org/10.1155/2017/6594861
9. Mukhina, M.P., Filyashkin, M.K.: Computer modeling of accuracy characteristics of strapdown inertial navigation system. Radio Electron. Comput. Sci. Control (4), 157–165 (2019). https://doi.org/10.15588/1607-3274-2019-4-15
10. Jekeli, C.: inertial navigation systems with geodetic applications. De Gruyter, Berlin, Boston (2023). https://doi.org/10.1515/9783110784329
11. Braasch, M.: Fundamentals of Inertial Navigation Systems and Aiding. London, IET (2022). https://doi.org/10.1049/SBRA550E

12. Wang, Y., Shkel, A.M.: pedestrian inertial navigation with self-contained aiding. IEEE Press with John Wiley & Sons (2021). ISBN-13: 978-1119699552
13. Sushchenko, O.A.: Features of control by two-axis gimbaled attitude and heading reference system. In: IEEE 3rd International Conference on Methods and Systems of Navigation and Motion Control (MSNMC), pp. 190–193. IEEE, Kyiv, Ukraine (2014). https://doi.org/10.1109/MSNMC.2014.6979766
14. Sushchenko, O., Goncharenko, A.: Design of robust systems for stabilization of unmanned aerial vehicle equipment. Int. J. Aerospace Eng. p. 6054081 (2016). https://doi.org/10.1155/2016/6054081
15. Sushchenko, O.A., Bezkorovainyi Y.M., Golitsyn, V.O.: Fault-tolerant inertial measuring instrument with neural network. In: 40th International Conference on Electronics and Nanotechnology (ELNANO), pp. 797–801. IEEE, Kyiv, Ukraine (2020). https://doi.org/10.1109/ELNANO50318.2020.9088779
16. Niu, S.S., Xiao, D.: Process control: engineering analyses and best practices. Springer, Cham (2022)
17. Passaro, V.M.N., Cuccovillo, A., Vaiani, L., De Carlo, M., Campanella, C.E.: Gyroscope technology and applications: a review in the industrial perspective. Sensors **17**(10), 2284 (2017). https://doi.org/10.3390/s17102284
18. Zerrik, El, H., Castillo, O.: Stabilization of Infinite Dimensional Systems. Springer, Cham (2021)
19. Voliansky, R.S., Sadovoi, A.V.: The transformation of linear dynamical object's equation to Brunovsky canonical form. In: IEEE 4th International Conference Actual Problems of Unmanned Aerial Vehicles Developments (APUAVD), pp. 196–199. Kyiv, Ukraine (2017) https://doi.org/10.1109/APUAVD.2017.8308808
20. Qi, W., Weiwei, Q., Lixin, W., Qiang, S.: Continuous self-calibration of platform inertial navigation system based on attitude quaternion model. IET Radar Sonar Navig. **13**, 1256–1263 (2019). https://doi.org/10.1049/iet-rsn.2018.5564

Crossover Design on the Bioequivalence of Pharmaceuticals - A Case of Study

M. Filomena Teodoro[1,2(✉)], Marina A. P. Andrade[3,4], and Teresa A. Oliveira[5,6]

[1] CINAV, Center of Naval Research, Naval Academy, Portuguese Navy, 2810–001 Almada, Portugal
mteodoro64@gmail.com
[2] CEMAT, Center for Computational and Stochastic Mathematics, Instituto Superior Técnico, Lisbon University, 1048–001 Lisboa, Portugal
maria.teodoro@tecnico.ulisboa.pt
[3] ISCTE, Instituto Universitário de Lisboa, Lisboa Portugal, 1649–026 Lisboa, Portugal
marina.andrade@iscte.pt
[4] ISTAR, Instituto Universitário de Lisboa, Lisboa Portugal, 1649–026 Lisboa, Portugal
[5] Departamento de Ciências e Tecnologia, Universidade Aberta, 1269–001 Lisboa, Portugal
Teresa.Oliveira@uab.pt
[6] CEAUL, Faculdade de Ciências, Universidade de Lisboa, 1649–014 Lisboa, Portugal

Abstract. This study performs experimental design and analysis of variance in assessing the bioequivalence of two treatments, which involves evaluating the efficacy of different treatments administered to two distinct cohorts of patients: the control group and the test group. In order to compare the control group that received the reference medication, with the test/treatment group that received the investigational drug, a crossover experimental design was employed. The respective analysis of variance was conducted, taking into consideration both intra-subject and inter-subject variability in formulating the probabilistic model. This included specifying tests to detect carryover effects and period effects. The practical implementation of the proposed model involved validating the hypothesis, revealing that the carry-over effect was found to be not significant, when assessed at the usual levels of significance (1% and 5%). In terms of the treatments, it was concluded that there was statistical significance, leading to the assertion that the studied pharmaceuticals were not bioequivalent.

Keywords: experimental design · clinical trials · analysis of variance · bio-equivalence · computational methods

1 Introduction

Clinical trials play a crucial role in advancing medical knowledge and improving patient outcomes in a myriad of scenarios. For instance in [1], a randomized trial

© The Author(s), under exclusive license to Springer Nature Switzerland AG 2024
O. Gervasi et al. (Eds.): ICCSA 2024 Workshops, LNCS 14816, pp. 219–234, 2024.
https://doi.org/10.1007/978-3-031-65223-3_15

is performed so a decision-making for patients with acute myocardial infarction can be taken; in [2], the care management of insomnia occurring simultaneously with sleep apnea is studied; the authors of [3] compare the effectiveness of virtual reality game to clinic based therapy for chronic non-specific low back pain; in [4], it is described the allocation of patients to in headache clinical trials randomization and in [5] the meticulous designing protocols for cancer clinical trials is presented.

The publication in [6], offers various techniques for patient allocation in clinical trials, while the subsequent work in [7] by the same author provides a comprehensive overview on designing, analyzing, and interpreting such data in a straightforward manner, complete with historical context, present-day relevance, and future outlook. Similar works can be found in [8], where Bayesian adaptive biased-coin designs with Gaussian response are described for clinical trials. Also, the authors of [9] made some interesting considerations about randomization-based inference. The author of [10] made restricted randomization designs in headache clinical trials and the authors of [4] proposed the randomization, stratification, and treatment matching to allocation of patients.

Some recent works proposed to improve the efficiency of the clinical trials. In [11], the authors propose a new algorithm gaining efficiency in randomized controlled trials. The authors of [12] explore some recent innovations in clinical trials where a single therapeutic treatment is tested on several patient populations, each of which forms a basket, using Bayesian hierarchical models. A qualitative study is developed by the authors of [13], where some randomization methods in clinical trials are compared and evaluated. The authors of [14] explore statistical tools focused in clinical pharmacology under the theme of bioequivalent trials.

The current research places emphasis into the realm of bioequivalence trials, specifically focusing on the comparison of two treatments. The manuscript is divided into five sections, beginning with an introduction that sets the stage for the subsequent analysis. Section 2 provides a comprehensive overview of the bioequivalence of treatments, while Sect. 3 delves into the methodology employed in the study. Moving on to Sect. 4, various empirical issues are addressed, starting with fundamental statistical techniques, then progressing to the assessment of data normality and finally to the computation and interpretation of the ANOVA table results. Section 5 offers detailed discussions and final remarks on the findings of the study.

2 Preliminaries

The main objective of this research endeavor is to ascertain the efficacy of the prescribed treatment in patients and to examine and evaluate any pertinent clinical reactions. Specifically, the study in question centers on a comparative analysis between a control group and an experimental group receiving the treatment. Despite involving a limited number of individuals, it is hoped that the findings of this study case may offer valuable insights to guide therapeutic decisions for individuals experiencing similar medical conditions.

In detail, the aim is to evaluate the existence or not of bioequivalence between a pharmaceutical-treatment (T) and a reference-control pharmaceutical (R). To prove the existence of bio-equivalence between these two groups it is not necessary to conclude that one is better than the other, just that it is not worse. In a first phase, the bioavailability of people taking the drug is measured. This action consists of recording the concentration in some fluid over time, after taking the treatment (and reference respectively) and constructing for both the concentration versus time graph. This is followed by the calculation of the pharmacokinetic parameters of interest, such as maximum concentration area under the curve (AUC) or others.

Knowing that the same individual must be subject to both the reference and to the treatment, the chosen design was a 2×2 crossover, given the importance of pairing. An even number of individuals were randomized into two groups. One of the groups received the reference pharmaceutical in the first period and, in the second period, the treatment. The second group received the treatment in the first period and the reference in the second period. The interval between the two periods of intake is supposed to be long enough to fade the effect of taking the first medication. This time interval is called washout (see Fig. 1) This type of design makes it possible to test whether there are reinforcement effects in the 2nd period, whether the treatments are different or whether any tests should be carried out on individuals.

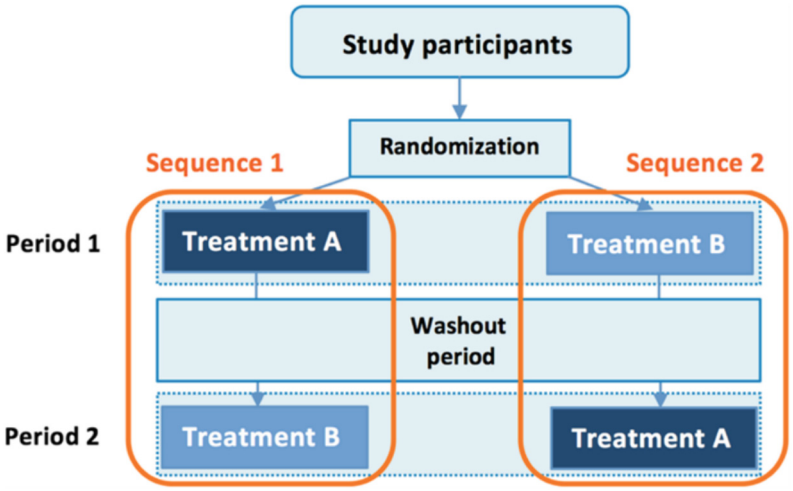

Fig. 1. Scheme of experimental design: 2×2 crossover. Source: [15].

To review some basic concepts of experimental design and analysis of variance [16–19] are recommended, among many others.

3 Theoretical Model

The statistical model used to determine bio-equivalence has as response variable Y_{ijk} a random variable (r.v.) whose observed value y_{ijk} corresponds to the ith individual, in the kth sequence of the jth period, with $k = 1 \ldots p$, $i = 1 \ldots n_k$, and $j = 1, \ldots, p$. In general, data is given in tabular form (1).

$$\begin{array}{c|cccc} & \textit{Period } 1 & \textit{Period}2 & \cdots & \textit{Period } \mathrm{p} \\ \hline \textit{Sequence } 1 & y_{111} \ldots y_{n_1 11} & y_{121} \ldots y_{n_1 21} & \cdots & y_{1p1} \ldots y_{n_1 p1} \\ \textit{Sequence } 2 & y_{112} \ldots y_{122} & y_{221} \ldots y_{n_2 22} & \cdots & y_{1p2} \ldots y_{n_2 p2} \\ \vdots & \vdots & \vdots & \vdots & \vdots \\ \textit{Sequence } \mathrm{g} & y_{11g} \ldots y_{n_g 1g} & y_{12g} \ldots y_{n_g 2g} & \cdots & y_{1pg} \ldots y_{n_g pg} \end{array} \tag{1}$$

The theoretical model is defined in Eq. (2).

$$Y_{ijk} = \mu + S_{ik} + P_j + F_{jk} + C_{jk} + \epsilon_{ijk}, \tag{2}$$

where

- μ is the global mean (or global effect);
- S_{ik} is the random effect of the $i-th$ individual at the $k-th$ sequence, $k = 1, \ldots, g,$ and $i = 1, \ldots, n_k$;
- P_j is the fixed effect of the $j-th$ period, $j = 1, \ldots, p$;
- F_{jk} is the fixed effect of the administered formulation at the $k-th$ sequence during the $j-th$ period (reference R or test T);
- C_{jk} is the carry-over first order fixed effect of the administered formulation at the $k-th$ sequence during the $j-1-th$ period;
- ϵ_{ijk} is the random error of Y_{ijk}.

The following restrictions are considered:

$\sum_j P_j = 0$, $\sum_{j,k} F_{jk} = 0$, $\sum_{j,k} C_{jk} = 0$ and , $C_{0k} = 0$ conducting to

- $p-1$ effects P_j linearly independents;
- $(p-1)(g-1)$ effects F_{jk} linearly independents;
- $(p-1)(g-1)$ effects C_{jk} linearly independents.

The hypotheses inherent to the model (2) are:

- The S_{ik} are independent and Gaussian

$$S_{ik} \cap N(0, \sigma_s^2).$$

- The ϵ_{ijk} are independent and Gaussian

$$\epsilon_{ijk} \cap N(0, \sigma_e^2).$$

- The $\{S_{ik}\}$ and $\{\epsilon_{ijk}\}$ are mutually independent.

Table 1. Scheme of experimental design: 2×2 crossover, $n_k = n_1 = n_2$, $p = 2$, $g = 2$.

	Period I	*Period* II
Sequence 1 (RT)	$y_{111} \dots y_{n_1 11}$	$y_{121} \dots y_{n_1 21}$
Sequence 2 (TR)	$y_{112} \dots y_{122}$	$y_{221} \dots y_{n_2 22}$

We can conclude that Y_{ijk} are r.v. independents and Gaussian. Also, we need to evaluate the variability due the subjects, namely, to compute the proportion of total variability explained by the individuals.

The σ_s estimate is used to explain the variability inter-subject, the σ_e estimate is used to explain the variability intra-subject.

Considering the design *crossover* 2×2, $n_k = n_1 = n_2$, $p = 2$, $g = 2$ then the scheme of date presented in tabular form 1 is reduced to the form displayed in Table 1.

If we consider the administration of the drug test in the first period of the first sequence, we obtain the definition of the effect F_{jk} and the effect C_{jk} respectively given by Eqs. (3) and (4), noting that the effect carryover only occurs during the second period.

$$C_{jk} = \begin{cases} C_R, & if\ k = 1, j = 2 \\ C_T, & if\ k = 2, j = 2 \end{cases} \tag{3}$$

$$\begin{array}{lll} \textit{Sequence} & \textit{Period I} \& & \textit{Period II} \\ 1\ (RT) & \mu_{11} = \mu + P_1 + F_R \& & \mu_{21} = \mu + P_2 + F_T + C_R \\ 2\ (TR) & \mu_{12} = \mu + P_1 + F_T \& & \mu_{11} = \mu + P_2 + F_R + C_T \end{array} \tag{4}$$

and

$$\begin{cases} P_1 + P_2 = 0 \\ C_R + C_T = 0 \\ F_R + F_T = 0 \end{cases} \tag{5}$$

The fixed effect that occur in each period and in each sequence is given by the expected value for each individual μ_{jk} (4) imposing (5).

In a study of bioequivalence between pharmaceuticals, it is usual to consider the non existence of the carryover effect. This fact can be achieved with a long period of washout, allowing to eliminate the residuals of the drug administration. In this situation, the model is reduced to formula (6)

$$Y_{ijk} = \mu + S_{ik} + P_j + F_{jk} + \epsilon_{ijk}. \tag{6}$$

In the case of the model (2), the basic objectives are to test if $P_1 = P_2$, $C_R = C_T$, $T_R = T_T$ and the variability of the residuals σ_s.

4 Analysis of Variance

The comparison of the bio-availabilities of the two formulations can be made using variance analysis for crossover trials, with the model residuals being analyzed using either inter-subject variability or intra-subject variability. Then, define the following sums of squares with the usual interpretation. The total sum of squares (SST) with $N-1$ degree of freedom (d.f.) is given by formula (7).

$$SST = \sum_{k=1}^{2}\sum_{j=1}^{2}\sum_{i=1}^{n_k}\left(y_{ijk} - \overline{y}\right)^2, \tag{7}$$

with $N = 2(n_1 + n_2)$.

After some calculations, we can find some decomposition's of interest. For example, if we add and subtract to each term of sum given by formula (7) the mean per individual $\overline{y}_{i.k}$

$$SST = \sum_{k=1}^{2}\sum_{j=1}^{2}\sum_{i=1}^{n_k}\left(y_{ijk} - \overline{y} + \overline{y}_{i.k} - \overline{y}_{i.k}\right)^2 \tag{8}$$

$$= \underbrace{\sum_{k=1}^{2}\sum_{j=1}^{2}\sum_{i=1}^{n_k}\left(y_{ijk} - \overline{y}_{i.k}\right)^2}_{\text{variability within the individuals}} \tag{9}$$

$$+ \underbrace{2\sum_{k=1}^{2}\sum_{i=1}^{n_k}\left(\overline{y}_{i.k} - \overline{y}\right)^2}_{\text{variability between the individuals relatively to global mean}}. \tag{10}$$

we get the equality given by formula (11) that provides a good way to analyse the individual variability.

$$SST = SS_{within} + SS_{between}. \tag{11}$$

Other decomposition's that evidence the other intended effects are those determined by the formulas (12) and (14).

$$SS_{between} = SS_{carry} + SS_{residual\ \ between}, \tag{12}$$

with

$$SS_{carry} = \frac{2n_1n_2}{n_1+n_2}\left[\left(\overline{y}_{.12} + \overline{y}_{.22}\right) - \left(\overline{y}_{.11} + \overline{y}_{.21}\right)\right]^2 \cap \chi^2_{[1]} \tag{13}$$

$$SS_{within} = SS_{pharmaceutical} + SS_{period} + SS_{residual\ \ within}, \tag{14}$$

with

$$SS_{pharmaceutical} = \frac{2n_1n_2}{n_1+n_2}\left[(\overline{y}_{.21}+\overline{y}_{.11})-(\overline{y}_{.22}+\overline{y}_{.12})\right]^2 \cap \chi^2_{[1]} \tag{15}$$

$$SS_{period} = \frac{2n_1n_2}{n_1+n_2}\left[(\overline{y}_{.21}+\overline{y}_{.11})-(\overline{y}_{.12}+\overline{y}_{.22})\right]^2 \cap \chi^2_{[1]} \tag{16}$$

The sum of the squares mean is defined as usual, the sum is divided by the number of degrees of freedom (df). All details are summarized in Table 2.

The last column of Table 2 concerns to the following significance tests:

- $$H_{0C} : C_T = C_R \text{ versus } H_{1C} : C_T \neq C_R.$$

  A rejection of H_{0C} means that there is no experimental evidence that the washout period is long enough. The process shall be ended. The following tests assume that there is no carryout effect.

- $$H_{0F} : F_T = F_R \text{ versus } H_{1F} : F_T \neq F_R.$$

  A rejection of H_{0F} means that there is experimental evidence that the pharmaceuticals have distinct effects, so there is no experimental evidence for bio-equivalence between them.

- $$H_{0\,s} : \sigma_s^2 = 0 \text{ versus } H_{1\,s} : \sigma_s^2 \neq 0.$$

  A rejection of H_{0s} means that there is experimental evidence that the individual effects are distinct effects, it means that the random factor S_{ik} is statistically significant.

- $$H_{0P} : P_1 = P_2 \text{ versus } H_{1P} : P_1 \neq P_2.$$

  A rejection of H_{0P} means that there is experimental evidence that the period has distinct effects.

Table 2. Anova Table.

Variation Source	Sum of Squares	Degree of Freedom	Mean Sum of Squares	F
	SS	DF	MS	
Between				
Carry-over	SS_{carry}	1	SS_{carry}	$F_c = \frac{MS_{carry}}{MS_{res,btween}}$
Residuals	$SS_{res,between}$	$n_1 + n_2 - 2$	$\frac{SS_{res,between}}{n_1+n_2-2}$	$F_s = \frac{MS_{res,between}}{MS_{res,within}}$
Within				
pharmaceutical	$SS_{pharmaceutical}$	1	$SS_{pharmaceutical}$	$F_F = \frac{MS_{pharmaceutical}}{MS_{res,within}}$
Period	SS_{period}	1	SS_{period}	$F_F = \frac{MS_{period}}{MS_{res,within}}$
Residuals	$SS_{res,within}$	$n_1 + n_2 - 2$	$\frac{MS_{res,within}}{n_1+n_2-2}$	
Total	SST	$2(n_1 + n_2) - 1$	$\frac{SST}{2(n_1+n_2)-1}$	

The F statistic to each of the specified tests is displayed in the Table 2, and has a distribution F of Snedcor whose degrees of freedom are the degree of freedom of the numerator and denominator respectively.

The critical region, for a level of significance α is given by

$$\begin{aligned} F_{C|H_{0C}} &> F_{(1,n_1+n_2-2,1-\alpha)}, \\ F_{F|H_{0F}} &> F_{(1,n_1+n_2-2,1-\alpha)}, \\ F_{s|H_{0s}} &> F_{(n_1+n_2-2,n_1+n_2-2,1-\alpha)}, \\ F_{P|H_{0P}} &> F_{(1,n_1+n_2-2,1-\alpha)}, \end{aligned}$$

respectively.

5 Descriptive Data Analysis and Validation Tests

All data were classified and quantified using the software Matlab. The studied variable Y is the area under the concentration curve registered along the time (AUC). The data illustration is displayed in Table 3. For the case under study, $n_k = 6,\ p = 2$ and $g = 2$.

The reduced data display can be observed in a histogram (see Fig. 2) and in a qq-plot (see Fig. 3).

In both figures there is not a strong visual evidence of data with non Gaussian behavior. However some bias, with heavier tails can be observed on left. In a preliminary phase, it is useful to perform some normality tests.

In a standart normal distribution, the measures of asymmetry and Kurtosis are, respectively, 0 and 3. The third and fourth sampling moments of the observations, duly normalized, are given by formulas (17) and (18),

$$\sqrt{b_1} = \frac{\sum (y_{ijk\ norm})^3}{N}, \tag{17}$$

$$b_2 = \frac{\sum (y_{ijk\ norm})^4}{N}, \quad N = 2(n_1 + n_2). \tag{18}$$

If normality occurs, the estimators $\sqrt{B_1}$ and B_2 must be centered with mean 0 and 3 respectively and are assymptoticaly Gaussian (19) (20),

$$\sqrt{B_1} \dot{\sim} N(6, \frac{6}{N}) \tag{19}$$

$$B_2 \dot{\sim}\ N(3, \frac{24}{N}). \tag{20}$$

Table 3. Area under the concentration curve registered along the time (AUC).

Sequence	Individual	Period I	Period II
RT	1	6934.5	6458
RT	2	5330.5	3108.1
RT	5	5848.3	7079.4
RT	7	8405.2	6455.3
RT	8	7403.5	7125.7
RT	9	7409.4	8427.7
TR	3	7762.2	9034.2
TR	4	8137.3	8107.3
TR	6	4998.1	6455.3
TR	10	8763.9	10406
TR	11	8430.4	9239.6
TR	12	5053.4	5696.3

Also, the following results (21) (22) can be established:

$$\frac{\sqrt{B_1}}{6/N} \dot{\sim} \chi^2_{(1)} \tag{21}$$

$$\frac{(B_2-3)^2}{24/N} \dot{\sim} \chi^2_{(1)} \tag{22}$$

Moreover, the statistic defined by $B = \frac{N}{6}B_1 + \frac{N}{24}(B_2-3)^2$, proposed by Bera and Jarque, under the hypothesis of normality and for large samples, has an asymptotic chi-square distribution with 2 degree of freedom [20].

It is important to remember that, in small samples, the measurements of asymmetry and Kurtosis can be significantly altered. The sample used in this work has 24 observations. Thus, there is the need of cautious with the results and their interpretation. Despite the sample bias being negative, the hypothesis that data are from a Gaussian population was not rejected. The values $\sqrt{b_1} = 0.3863$ and $b_2 = 2.8308$, led to test statistics values of, respectively,

$$\frac{\sqrt{b_1}}{6/N} = 0.5971,$$

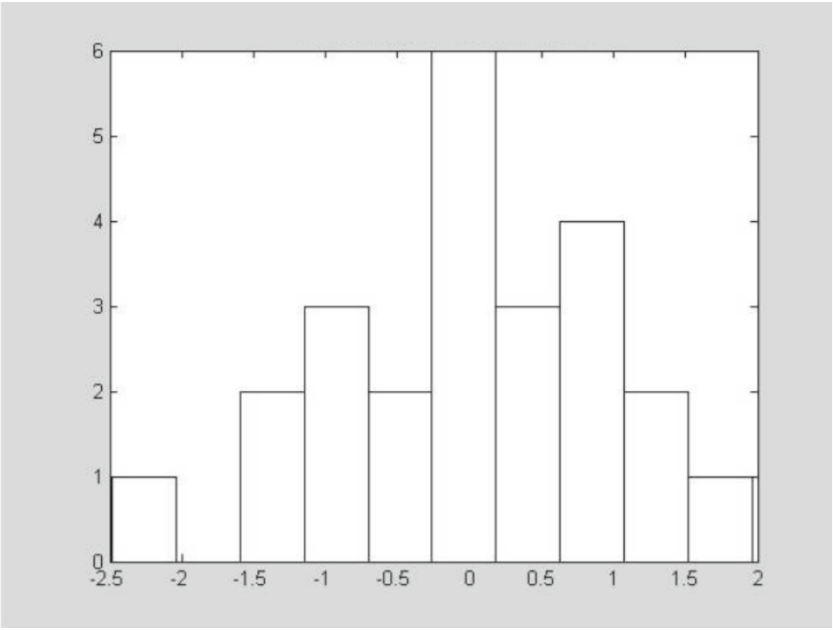

Fig. 2. Histogram of reduced AUC.

and

$$\frac{(b_2 - 3)^2}{24/N} = 0.0286.$$

Hence

$$b = 0.6257,$$

being clearly lower than the critical values obtained for a significance level of 5%, $\chi^2_{(0,95,1)} = 3.8415$, $\chi^2_{(0,95,1)} = 3.8415$, and $\chi^2_{(0,95,2)} = 5.9915$. The corresponding $p - values$ are 0.4397, 0.8656 and 0.7314, respectively, with evidence that the observations come from a normal population. Given the caution due to the small sample size, the results were confirmed by the non-parametric Kolmogorov Smnirnov test (KS), which compares the empirical distribution with the distribution of a reduced normal. The KS statistic conduced to $KS = 0.0880$. This value implies a $p - value = 0.9893$, so we do not have statistical evidence to reject the normality behavior hypothesis.

6 Empirical Application - Analysis of Variance

After some descriptive analysis and some validation tests, the computation to all values and complete the analysis of variance (ANOVA) table (see Table 4) were performed.

Table 4. ANOVA relatively to the area under the concentration curve registered along the time (AUC).

Variation Source	Sum of Squares	Degree of Freedom	Mean Sum of Squares	F	p-value
	SS	DF	MS		
Between	5.3031×10^7				
Carry-over	2.2937×10^7	1	2.2937×10^7	$F_c = 2.7593$	0.1277
Residuals	4.1563×10^7	10	4.1563×10^6	$F_s = 17.3563$	≈ 0
Within	8.8779×10^6				
Pharmaceutical	5.4721×10^6	1	5.4721×10^6	$F_F = 22.8511$	≈ 0
Period	1.0112×10^6	1	1.0112×10^6	$F_P = 4.2226$	0.0670
Residuals	2.3947×10^5	10	2.3947×10^4		
Total	6.1909×10^7	23			

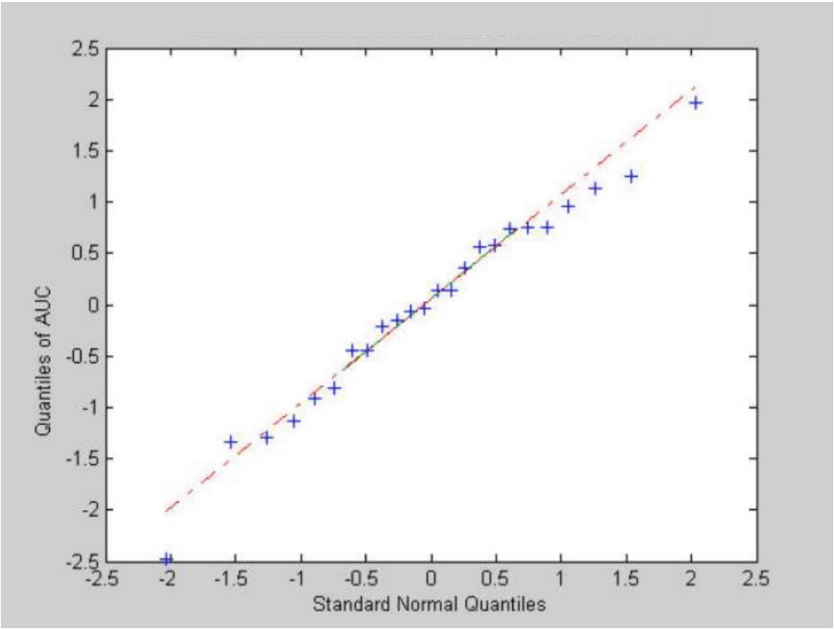

Fig. 3. Qq-plot of reduced AUC.

According to the $p - values$ displayed in last column (on right) of Table 4 the conclusion is that, relatively to each of the identified tests there are distinct decisions.

- For the test concerning the wash-out period,

$$H_{0C} : C_T = C_R \text{ versus } H_{1C} : C_T \neq C_R,$$

it was obtained $p - value = 0.1277$. There is not statistical evidence to reject H_{0C} for the usual values of the level of significance. This means that there is statistical evidence that the washout period is long enough. There is statistical evidence for usual levels of significance that there is no carry-out effect. The process shall continue.

- On what concerns the effects of the reference and the treatment,

$$H_{0F} : F_T = F_R \text{ versus } H_{1F} : F_T \neq F_R,$$

it was obtained $p - value \approx 0$. The rejection of H_{0F} for any value of significance level means that there is experimental evidence that both have distinct effects, so there is no experimental evidence for bio-equivalence between them.

- Relatively to the effects of the individuals,

$$H_{0\,s} : \sigma_s^2 = 0 \text{ versus } H_{1\,s} : \sigma_s^2 \neq 0,$$

it was obtained $p - value \approx 0$. A rejection of H_{0s} for any value of significance level means that there is an experimental evidence that the individual effects are distinct, implying that the random factor S_{ik} is statistically significant.
- The effects of the period are evaluated by the hypothesis

$$H_{0P} : P_1 = P_2 \text{ versus } H_{1P} : P_1 \neq P_2.$$

The $p - value = 0.0670$, thus, considering the significance level of 5% there is no statistical evidence to reject the null hypothesis. However, for the level of significance $6.7010\% < \alpha < 10\%$ there exists experimental evidence to reject H_{0P}, meaning that there exists experimental evidence that the period has distinct effects. In that case the authors recommend [21] for details on optimal crossover designs as well as [22] to perform a 2×2 crossover design.

7 Final Remarks

The main objective of the present manuscript was to identify if the treatment (test pharmaceutical) and the reference (reference pharmaceutical) were bioequivalent. To find a conclusion about it was necessary to verify some assumptions, such as the normality of the observed variable Y. It was verified that existed statistical evidence that data came from a Gaussian population. Also, there was not statistical evidence of the carryout effect existence, i.e., the washout period is long enough. The period effect was significant only for values of significance above 6.7010%. This fact validates the continuation of the execution of the remaining tests, concluding that there is no bioequivalence of the studied pharmaceuticals.

In future work, we intend to update the data base, in order get more data, and to explore it following a distinct battery of tests proposed on the book by the author in [7].

Acknowledgements. The first author was supported by Portuguese funds, by The Portuguese Foundation for Science and Technology (FCT), through the Center for Computational and Stochastic Mathematics (CEMAT), University of Lisbon, Portugal, project UIDB/Multi/04621/2020, DOI: (https://doi.org/10.54499/UIDB/04621/2020) and also by the Center of Naval Research (CINAV), Naval Academy, Portugal.

The second author was partially supported by Fundação para a Ciência e a Tecnologia, I.P. (FCT) [ISTAR Projects: UIDB/04466/2020 and UIDP/04466/2020].

The third author was supported by Portuguese funds, by The Portuguese Foundation for Science and Technology (FCT), through the project UIDB/Multi/00006/2020.

References

1. Branda, M.E., Kunneman, M., Meza-Contreras, A.I., et al.: Shared decision-making for patients hospitalized with acute myocardial infarction: A randomized trial. Patient Prefer. Adherence **16**, 1395–1404 (2022)
2. Eldridge-Smith, E.D., Manber, R., Tsai, S., et al.: Stepped care management of insomnia co-occurring with sleep apnea: the air study protocol. Trials **23**(1), 806 (2022)
3. Fatoye, F., Gebrye, T., Mbada, C.E., et al.: Cost effectiveness of virtual reality game compared to clinic based mckenzie extension therapy for chronic non-specific low back pain. Bulletin Géodesique **16**(6), 601–609 (2022)
4. Lipchik, G.L., Nicholson, R.A., Penzien, D.B.: Allocation of patients to conditions in headache clinical trials: randomization, stratification, and treatment matching. Headache **45**(5)(498), 419–428 (2005)
5. Brown, B.W.J.: Designing for cancer clinical trials: selection of prognostic factors. Cancer Treat. Rep. **64**(2–3), 499–502 (1980)
6. Pocock, S.J.: Allocation of patients to treatment in clinical trials. Biometrics **35**(1), 183–197 (1979)
7. Pocock, S.J.: Clinical Trials, 5th edn. e-book. Wiley, New Jersey (2013)
8. Atkinson, A.C., Biswas, A.: Bayesian adaptive biased-coin designs for Bayesian adaptive biased-coin designs for clinical trials with normal responses. Biometrics **61**(1), 118–125 (2005)
9. Gail, M.H., Mark, S.D., Carroll, R.J., et al.: On design considerations and randomization-based inference for community intervention trials. Stat. Med. **15**(11), 1069–1092 (1996)
10. Simon, R.: Restricted randomization designs in clinical trials. Biometrics **35**(2), 503–612 (1979)
11. Ling, S.X., Hobbs, B.P., Kaizer, A.M., Koopmeiners, J.S.: Calibrated dynamic borrowing using capping priors. J. Biopharm. Stat. **31**(6), 852–867 (2021)
12. Daniells, L., Mozgunov, P., Bedding, A., Jaki, T.: A comparison of Bayesian information borrowing methods in basket trials and a novel proposal of modified exchangeability-nonexchangeability method. Stat. Med. **42**(24), 4392–4417 (2023)
13. Bruce, C.L., Iflaifel, M., Montgomery, A., et al.: Choosing and evaluating randomisation methods in clinical trials: a qualitative study. Clin. Trial **25**(1), 199 (2024)
14. Patterson, S.D., B.J.: Bioequivalence and Statistics in Clinical Pharmacology. Chapman and Hall/CRC, New York (2017)
15. Zeng, L., Qureshi, R., et al.: A registration of phase 3 crossover trials on clinicaltrials.gov. Trials **21**(613) (2020)
16. Ross, S.M.: Introduction to Probability and Statistics for Engineers and Scientists, 6th edn. Academic Press, San Diego (2020)
17. Morgado, L., Teodoro, F., Perdocoulis, T.: Manual de Métodos Estatísticos em Ciências Biomédicas. Universidade de Trás os Montes e Alto Douro (UTAD, Vila Real. série Didáctica Ciências Aplicadas, 400 (2010). ISBN 978-972-669-018-2
18. Larsen, R., Marx, M.L.: Statistics, 5th edn. Prentice-Hall Inc. (2012)
19. Tamhane, A., Dunlop, D.: Statistics and Data Analysis. Prentice-Hall Inc., New Jersey (2000)

20. Thadewald, T., Büning, H.: Jarque-Bera test and its competitors for testing normality: A power comparison. Working Paper No.2004/9. Free University Berlin, School of Business & Economics, Berlin (2004). https://hdl.handle.net/10419/49919. Accessed 4 Apr 2024
21. Mausumi, B.and Dey, A.: Optimal Crossover Designs, pp. 1–19, 59–79, 168–172. World Scientific, Singapore (2009)
22. Rocco, B.: Review Various Methods to Perform Analysis of a 2 Treatment, 2 Period Crossover Study (2000)

Mathematical and Statistical Frameworks Fostering Advances in AI Systems and Computing

Teresa A. Oliveira[1,2(✉)] and Maria Filomena Teodoro[3,4]

[1] Departamento de Ciências e Tecnologia, Universidade Aberta, 1269-001 Lisbon, Portugal
[2] CEAUL, Faculdade de Ciências, Universidade de Lisboa, 1649-014 Lisbon, Portugal
Teresa.Oliveira@uab.pt
[3] CINAV, Center of Naval Research, Naval Academy, Portuguese Navy, 2810-001 Almada, Portugal
[4] CEMAT, Center for Computational and Stochastic Mathematics, Instituto Superior Técnico, Lisbon University, 1048-001 Lisbon, Portugal
maria.teodoro@tecnico.ulisboa.pt

Abstract. The rapid expansion of artificial intelligence (AI) areas and applications has become an everyday social reality and the development of computing methods and of technology, in order to accomplish for the respective needs, emerge as one of the biggest challenges of this century. However, a strong background in Mathematics and Statistical fundamentals is crucial to foster the robustness of AI Systems and to attain for the correspondent generalization capabilities. Thus, recognizing the importance and benefits of integrate multiple mathematical methodologies that can leverage the unique strengths of each to create synergistic effects, is here discussed. In the literature it is possible to find diverse connections of Mathematical and Statistical frameworks with AI Systems and Computing. For illustration: Algebra - can be used to manipulate data in high-dimensional spaces; Statistical Analysis - helps on providing confidence in decision-making; Linear Regression- can be used on data modelling and accuracy assessment; and Bayesian statistics - can be used in probabilistic programming for AI applications. This work particularly highlights the evolving role of Hadamard Matrices and Coding Theory, illustrating their synergy with AI Systems and Computing, and how such synergy is driving innovation in various fields and approaching the new reality of Quantic paradigms.

Keywords: computational mathematics · geometric modeling · incomplete block designs · combinatorial optimization · hadamard matrices · AI · quantum computing

1 Introduction

In 1956 John McCarthy coined originally the term Artificial Intelligence, defining it as the science and engineering of creating intelligent machines [1]. Within the ever-evolving landscape of technological progression, Artificial Intelligence (AI) emerges

© The Author(s), under exclusive license to Springer Nature Switzerland AG 2024
O. Gervasi et al. (Eds.): ICCSA 2024 Workshops, LNCS 14816, pp. 235–246, 2024.
https://doi.org/10.1007/978-3-031-65223-3_16

as a groundbreaking frontier and a paramount force driving innovation, namely by revolutionizing sectors, restructuring financial systems and, more than ever, reconfiguring human potential. The author of [2] mentions that the developments of AI and the life sciences are intertwined and that the ultimate goal of AI is to achieve human-like intelligence, as the human brain is capable of multi-tasking, learning with minimal supervision, and generalizing learned skills, all accomplished with high efficiency and low energy cost. However, besides all the beneath the veneer of AI remarkable utilities, resides a deep-seated dependence on the principles of mathematics.

From the genesis of algorithms to the intricate workings of neural networks [3–6], mathematics serves as the backbone that enables AI to interpret, infer, and evolve. In addition to the technical advantages of using a combination of multiple mathematical methodologies, there are also practical benefits to consider [7]. For example, by leveraging different approaches, researchers can gain a more holistic perspective on their research questions and explore different angles of analysis. This can lead to more robust findings and a deeper understanding of the underlying phenomena being studied. Furthermore, using a combination of methodologies can also help researchers to validate their results and ensure the robustness of their conclusions, adding an additional layer of credibility to their research. For example, some methodologies may be better suited for handling large data sets, while others may excel at capturing complex relationships within the data. On the other hand, while a statistical model may be able to provide precise estimates for certain parameters, a machine learning algorithm may be better at capturing nonlinear relationships within the data [8].

By understanding the unique strengths of each methodology, researchers can effectively leverage a combination of approaches to gain a more comprehensive understanding of the data and generate more accurate insights. For example, Hadamard matrices are mathematical structures that have properties suitable for error correction and data encryption. Hence, by integrating Hadamard matrices into AI systems, researchers can develop more robust and secure algorithms for data processing and analysis as in the case of cybersecurity, where Hadamard matrices can be used to encrypt sensitive data and protect it from unauthorized access [3,9–12].

This work is divided in five sections. An introduction starts the manuscript; in Sect. 2 some details about exploring connections of mathematical and Statistical frameworks with AI systems and computing are described. Some concepts about Hadamard matrices appear in Sect. 3. Also, the advantages of applying matrices in the most varied areas are highlighted in the Sect. 3. In Sect. 4 are debated the risks, questions and queries of AI in the quantum paradigm. Section 5 details the conclusions and displays some final remarks.

2 Exploring Connections of Mathematical and Statistical Frameworks with AI Systems and Computing

Algorithms are the essential components that drive the functionality of Artificial Intelligence, enabling machines to carry out specific tasks with precision and speed and likewise improving processes. By harnessing mathematical concepts, such as calculus and linear algebra, algorithms can efficiently process data, optimize workflows, and extract

meaningful patterns. For instance optimization algorithms, like gradient descent, work tirelessly to minimize errors and enhance the performance of AI models by iteratively adjusting their parameters. This particular method was originally presented in 1847 by Augustin-Louis Cauchy, but in 1907 Jacques Hadamard independently proposed and developed a similar one [7]. Through mathematical calculations, gradient descent adjusts the parameters of a model using weights, step by step and following the gradient of the cost function [4,6,8]. The gradient guides the algorithm to move weights in the direction of the steepest decrease in surface. As the process continues, it moves closer to a desired low point where predictions align more closely with the true data. Accordingly to IBM *"Gradient descent is an optimization algorithm which is commonly-used to train machine learning models and neural networks. It trains machine learning models by minimizing errors between predicted and actual results."* Still for gradient descent algorithm, the authors of [5] refer that *"This method involves adjusting the values of the parameters of the network to minimize the loss function over the course of many iterations. By repeating this process over and over again, the network will learn the weights needed to produce the optimal output for a given input."*

Statistical underpinnings illuminate the path forward in the realm of artificial intelligence, offering methodologies to extract patterns from data, estimating probabilities, and making rational decisions proposals amidst uncertainty. Statistical analysis is a powerful methodology for extracting valuable information from data and providing confidence in decision-making. Using probability theory, hypothesis testing, and inferential statistics, statisticians are able to quantify uncertainty, identify patterns, and draw meaningful conclusions from empirical data. Moreover, the essence of probability theory is exemplified in probabilistic graphical models, enabling the representation of complex dependencies between variables in AI domains like natural language processing and computer vision. By employing rigorous statistical and visualization techniques, analysts can assess the reliability of their findings, make informed decisions, and formulate data-driven strategies with a high degree of certainty.

Linear regression is a widely used statistical technique for modeling relationships between variables, assessing accuracy, and making predictions based on empirical data. By fitting a linear model to observed data points, researchers can estimate the strength and direction of relationships between variables, predict future outcomes, and evaluate the accuracy of their models. Linear regression is particularly useful in fields such as economics, finance, and social sciences [13,14], where understanding and predicting relationships between variables is critical for decision-making. Through the application of linear regression analysis, experts can uncover valuable insights, test hypotheses, and make informed decisions based on empirical evidence.

Bayesian statistics represents an innovative approach analyzing data and making predictions in a wide range of applications, including probabilistic programming for artificial intelligence (AI) systems. Using Bayesian inference, researchers can quantify uncertainty, update beliefs, and infer probabilities based on observed data. In the context of AI, Bayesian statistics can be used to build sophisticated models that encapsulate uncertainty, adapted to change environments, and make rational decisions in complex scenarios. Through the integration of Bayesian methods with AI technologies, develop-

ers can create more robust, adaptive, and intelligent systems capable of learning from data, making predictions, and solving complex problems. Through Bayesian inference, AI systems can refine beliefs based on new evidence, fostering adaptability and continuous learning.

Algebra is a fundamental mathematical tool that can be applied to manipulate data in high-dimensional spaces. In the realm of data analysis, algebraic techniques such as matrix operations, linear equations, and vector spaces play a crucial role in transforming raw data into meaningful insights. By applying algebraic principles, researchers can uncover patterns, relationships, and trends hidden within complex datasets, thereby facilitating the process of data interpretation and decision-making. The utilization of matrix operations, including multiplication and convolution, plays a crucial role in the transmission of signals throughout the layers of neural networks. This process enables the completion of complex tasks such as image recognition, language translation, and autonomous driving. Moreover, advanced concepts like eigenvectors and singular value decomposition serve to deconstruct and analyze a vast number of datasets in neural networks, heightening their efficacy and interpretability. By leveraging these mathematical tools, neural network architectures are able to efficiently navigate and process high-dimensional data for various applications [3,5,6,15].

Graph theory is a branch of discrete mathematics that finds ample utility in AI applications, particularly in optimization and network analysis. Graph algorithms like breadth-first search, Greedy Algorithm and Dijkstra's algorithm enable efficient traversal and path finding in complex networks, facilitating tasks such as route planning and resource allocation. Furthermore, optimization techniques - like integer programming and convex optimization - empower AI systems to maximize efficiency, allocate resources, and minimize costs across diverse domains, from logistics to finance. As artificial intelligence progresses, the respective connections with mathematics became increasingly important, paving the way for groundbreaking advancements in intelligence and automation [6,16].

Quantum Computation. Quantum computation, a revolutionary field that harnesses the principles of quantum mechanics to perform calculations exponentially faster than classical computers, is pushing the boundaries of what is possible in terms of artificial intelligence. Studies have shown that quantum computers have the potential to dramatically speed up tasks such as machine learning, optimization, and cryptography, leading to breakthroughs in AI research [17]. Further considerations will be presented in Sect. 4.

3 Hadamard Matrices: Connecting Past to Future in AI Applications

Hadamard matrices play a crucial role in various sectors, including quantum information, communication, networking, cryptography, biometrics and security, which make them a special bone in Artificial Intelligence. They are common in signal processing and coding applications. More information and examples can be seen in the books by Agaian [9] and by Horadam [18].

These matrices are key components in the formation of Hadamard configurations, a specialized block design from Experimental Design area that became a standard feature in everyday activities. It is then clear that, Hadamard matrices offer versatile solutions in numerous scenarios, namely through their adaptability showcased and their integration into advanced technologies and the popularity of QR codes [3,9,12,19]. They establish a very clear, and crucial bridge between mathematics, statistics and artificial intelligence by taking advantage of known classical methodologies, bringing it to current days and establishing their importance to recent and new scientific advances in the digital Era.

Consider the Hadamard's determinant theorem:

Theorem 1. *Let $\boldsymbol{X} = (x_{ij})$ be an $n \times n$ real matrix whose entries satisfy $|x_{ij}| \leq 1$, for all $i, j \in \mathbb{N}$. Then $|det(\boldsymbol{X})| \leq n^{n/2}$.*

These matrices were first considered as Hadamard determinants because the determinant of a Hadamard matrix satisfies equality in Hadamard's determinant theorem and so the equality holds if and only if **X** is a Hadamard matrix.

Definition 1. *Hadamard Matrix is an $n \times n$ matrix $\boldsymbol{H}$ with all entries ± 1 and $\boldsymbol{H}\boldsymbol{H}^T = nI_n$ is called a Hadamard matrix of order n, where C^T is the transpose of $\boldsymbol{H}$ and I_n is the identity matrix of order n.*

Important properties of Hadamard matrices are that:

1. The order of a Hadamard matrix is 1, 2 or $4n$, to n integer.
2. If the rows and columns of a Hadamard matrix are permuted, the matrix remains Hadamard.
3. If any row or column is multiplied by -1, the Hadamard property is retained.

A Hadamard matrix having the first row and first column containing only $+1$ entries is known as *normalized Hadamard Matrix*. Some details about Hadamard matrices can be found in [10,20–22]

The authors of [11] present examples of Hadamard matrices of order 2, 4 and 8, as it appears in Fig. 1.

The Hadamard conjecture proposes that a Hadamard matrix of order $4k$ exists for every natural k. Many orders of Hadamard matrices have already been constructed. Accordingly to the literature, Sylvester's construction and also Paley's work are the most famous methods to construct such kind of matrices [23,24]. In [25], the authors mention that it is well known that n must be 1, 2 or a multiple of 4 for a Hadamard matrix to exist, but was unknown at that time, whether Hadamard matrices exist for every n which is a multiple of 4.

Later on, [21] presented one Hadamard matrix of order 268 and Neil Sloan established the library of Hadamard matrices, which is available at http://neilsloane.com/hadamard/ [26]. The author of [16] established that the necessary condition for the existence of a Hadamard matrix $\mathbf{H}_n$, $n > 2$ is that $n \equiv 0(mod 4)$, but whether this necessary condition is sufficient as well it is not known either. Later on, Cameron presented Hadamard Matrices at http://designtheory.org/library/encyc/topics/had.pdf [27], in the Encyclopedia of Design Theory [28]. The [12] mentioned that Hadamard matrices have their existence confirmed to all permissible values of $n \leq 424$. In the meanwhile, bigger

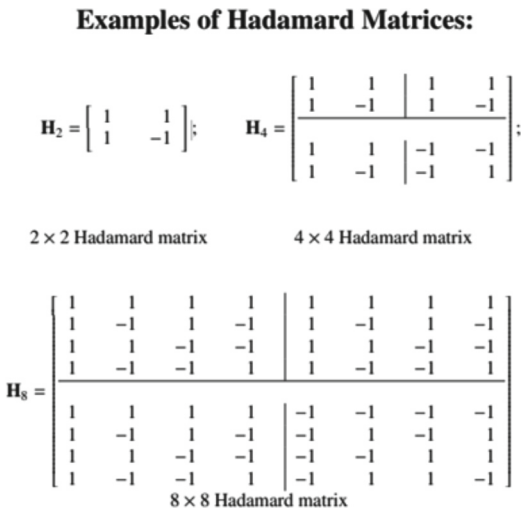

Fig. 1. Hadamard matrices of order 2, 4 and 8. Source [11].

Hadamard matrices were discovered, such as the one of order 428, which is available at http://neilsloane.com/hadamard/had.428.txt.

Research in the area of Hadamard matrices and their applications has steadily and rapidly grown, especially in this new century. The authors of [25] stated that in the area of Experimental Design, such matrices are particularly useful once they can be transformed to produce incomplete block designs, t-designs, Youden designs, orthogonal F-square designs, optimal saturated resolution III designs, optimal weighing designs, maximal sets of pairwise independent random variables with uniform measure, error correcting and detecting codes, Walsh functions, and other mathematical and statistical objects. Those authors also survey the existence of Hadamard matrices and many of their applications. Many other applications have emerged since then [1,3,9–11,15,18,25,29], and between a huge series of developments considering this matrices, the QR CODE from Coding Theory was selected for an example, thanks to the respective popularity and vast amount of real applications.

The QR Codes are 2-dimensional bar codes that can be easily read by a device capable of image capture, as is the case of most existing mobile phones. These codes can for example represent a file, an address for a web site (URL), a concert, a text, a GPS code, a phone number, an email, a contact or an SMS. QR codes have, as the base of their error correcting structure Hadamard matrices and there is a vast of number of links online for generating them, offering different features.

See, for example,

- a simple QR Code generator at https://www.qr-code-generator.com/;
- a dynamic QR code generator for the construction industry at https://www.flowcode.com/industry/construction;
- a QR Code for the Job Site at https://jobsitecodes.com/2023/11/06/using-qr-codes-on-the-job-site/;

- a QR Code for an event at https://www.qr-code-generator.com/solutions/event-qr-code/.

As an illustration, the QR Code for the 24th International Conference on Computational Science and Its Applications, ICCSA- 2024, was generated and is presented in Fig. 2.



Fig. 2. The QR Code for ICCSA 2024.

The mathematical properties jointly with the new technological advances allow simple figures to contain and transmit a huge amount of information. The mathematical properties that are intrinsic to these structures will allow great advances for error detection and correction, in huge amounts of information [12].

It is well known that in this digital Era, the paradigm of modern communications systems is heavily reliant on statistical techniques in order to recover information in the presence of noise and interferences and, moreover, to look for minimizing the risks of losing information. A historical note about AI can be found in [7]. Nowadays, AI is playing a critical role in revolutionizing experimental design by facilitating the automation of repetitive tasks, enabling real-time monitoring and control, and enhancing the overall efficiency of experimental processes. With the aid of AI technologies such as machine learning and deep learning, researchers can predict outcomes, optimize parameters, and identify trends in data with unprecedented accuracy and speed [4–6, 24].

The interdisciplinary mode of STAT-MATH-AI promotes taking advantage of joining strengths and provide to achieve the mentioned goals using the Hadamard matrices, which offer a very powerful and proper mathematical structure. This will not only accelerate the pace of scientific discovery but also opens up new opportunities for interdisciplinary collaboration and innovation in experimental design and AI [10].

4 AI in the Quantum Paradigm: Risks, Questions and Queries

Quantum computation presents an opportunity to catalyze AI innovation by leveraging the principles of quantum mechanics to execute computations at unparalleled velocities. Quantum algorithms, rooted in mathematical constructs such as superposition and entanglement, hold the promise of addressing intricate optimization challenges and simulating molecular configurations with unparalleled precision. The introduction of qubits and quantum computing represents a paradigm shift in the field of information processing. Unlike classical bits, which can only exist in a single state at a time, qubits

can be in a superposition of states, enabling the exploration of multiple states simultaneously. This feature allows for the development of quantum algorithms that can exploit the parallelism inherent in quantum systems to solve complex problems with a higher efficiency than classical algorithms.

A quantum computer can accommodate both analog and digital approaches, using qubits and, in the digital case, also relying on so-called quantum logical gates. Like bits, qubits can be in quantum states of 1 or 0, the difference being that qubits can assume a superposition of states 1 and 0, i.e., any linear combination of solutions is a solution. The fact that a set of bits does not admit a unique state, but rather a state function, represents a new paradigm that enables the creation of algorithms capable of handling multiple possible states simultaneously, and to solve problems in less time complexity, see [30]. This author mentions that the quantum state space can be described in terms of vectors and matrices or using a standard notation called bracket notation, also known as Dirac notation. This terminology arises from the fact that the inner product of two states is represented by a bracket $\|x>=|x>$, resulting a complex number. The external product of vectors $|x>$ and $y|$ is represented by $|x>|$ and can be represented by a matrix.

Accordingly with the Dirac's notation, during the processing of quantum information, the logical quantum state is a quantum superposition of the "base states" $|0>$ and $|1>$, with the quantum state $|0>$ always being converted to zero, just as $|1>$ is always converted to 1, in classical logic. Quantum operations must always be unitary, that is, leading to transformations that preserve $\sum E\,|\Psi_E|^2 = 1$ and are consequently reversible. For example, in Classical Computing, a set of two *bits* can admit the states 00, 01, 10 or 11, in Quantum Computing the state space includes a superposition of states $\Psi_{00}|00> + \Psi_{01}|01> + \Psi_{10}|10> + \Psi_{11}|11>$, where

$$|\Psi_{00}|^2 + |\Psi_{01}|^2 + |\Psi_{10}|^2 + |\Psi_{11}|^2 = 1,$$

with probability $|\Psi E|^2$ associated to the set in a certain state E.

The quantum phenomenon cannot be indifferent to all research considered for current binary systems (Fig. 3).

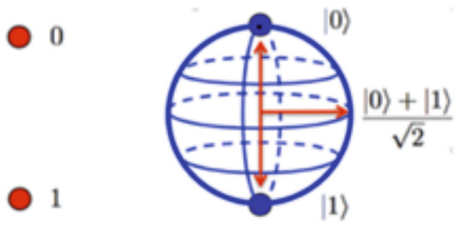

Fig. 3. Representation of bits (left side) and qubits (right side) [30]; inspired on [31].

It is possible that many developments of expansion and broadening of theories unknown to this new quantum context will be triggered. Experts predict that, among other things, the quantum revolution will allow the development of main issues like:

- ultra-precise sensors, envisioning a new era in medicine;
- new security systems based on Quantum Cryptography, which will be crucial for the protection of digital data of Web users;
- the evolution towards new forms of communication.
- More optimistic and future visionary researchers even consider the Quantum paradigm as the first step for tele-transportation.

Some interesting ideas can be found in [32] that presents a work about quantum risk analysis, comparing some traditional methods such as Monte Carlo with quantum computing. In [33] the authors conclude that recent work produced by quantum algorithms could act as the building blocks of machine learning programs, but the hardware and software challenges are still considerable. At [34], the authors claim that to understanding quantum machine learning requires rethinking generalization. In the same line, the author of [35] provides an explicit description of the reproducing kernel Hilbert space by embedding the Generalized Gaussian Radial Basis Function as an L2 measure that is used in the in the implementation of the analysis support vector machine. The empirical experiments described in the same work [35] suggest the possible future directions in terms of spectral decomposition of the Generalized Gaussian Radial Basis Functions.

5 Conclusions

The synergy between artificial intelligence and mathematics is becoming ever more essential as AI capabilities continue to progress, ushering in a new era of intelligence and automation. This symbiotic relationship is a testament to the synergistic potential inherent in their intersection and the fusion of mathematical principles with AI algorithms enables the creation of complex systems capable of processing vast amounts of data and deriving insights previously unimaginable. At the core of this symbiosis lies the foundational concepts of mathematics, providing the logical framework upon which AI systems operate. Whether through the application of algebra, statistical methods or optimization of neural networks, mathematics serves as the guiding force shaping the evolution of artificial intelligence.

Quantum computing stands out as a game-changing technology that can accelerate AI innovation by exploiting the principles of quantum mechanics to perform computations at unparalleled speeds. Quantum algorithms, grounded in mathematical concepts such as superposition and entanglement, have the potential to revolutionize AI by addressing complex optimization problems and enabling precise simulations. Quantum computation, is known as an emergent and revolutionary field that harnesses the principles of quantum mechanics to perform calculations exponentially faster than classical computers, is pushing the boundaries of what is possible in terms of artificial intelligence. Studies have shown that quantum computers have the potential to dramatically speed up tasks such as machine learning, optimization, and cryptography, leading to breakthroughs in AI research. The intersection of quantum computation and AI holds immense promise for unraveling the mysteries of the universe and unlocking new realms of innovation. Delving deeper into the intricate complexities of AI, the power

of mathematical abstraction becomes increasingly evident. The ability to distill complex problems into mathematical formulations not only enhances the efficiency of AI algorithms but also opens up new avenues of exploration and discovery.

Venturing into uncharted territories and being guided by the abstraction and the beauty of mathematical concepts, the horizon of possibilities in the field of artificial intelligence expands exponentially. The future of AI can be seen as a puzzle of human intellect and mathematical truths, where the ingenuity of the human mind is amplified and enhanced by the timeless principles of mathematics. Together, statistics, mathematics and AI will unlock new doors to innovation, revolutionizing industries, and transform the way of interacting with technology. In summary, considering the previous features, while navigating the quantum AI Era, requires a mindset shift towards embracing change, fostering innovation, and nurturing a symbiotic relationship between technology and humanity. By envisioning a future where quantum advancements amplify human capabilities, drive sustainability, and promote global cooperation, organizations and societies can pave the way for an equitable, sustainable, and prosperous future.

Acknowledgements. The first author was supported by Portuguese funds *The Portuguese Foundation for Science and Technology* (FCT), through the *project* UIDB/Multi/00006/2020.

The second author was supported by Portuguese funds *The Portuguese Foundation for Science and Technology* (FCT), through the *Center for Computational and Stochastic Mathematics* (CEMAT), University of Lisbon, Portugal, project UIDB/Multi/04621/2020, DOI: (https://doi.org/10.54499/UIDB/04621/2020) and through the *Center of Naval Research* (CINAV), Naval Academy, Portugal.

References

1. Malik, P., et al.: Overview of artificial intelligence in medicine. J. Family Med. Primary Care **8**, 2328 (2019)
2. Poo, M.M.: Towards brain-inspired artificial intelligence. Natl. Sci. Rev. **5**(6), 785 (2018)
3. Balonin, N.A., Petoukhov, S.V., Sergeev, M.B.: Matrices in improvement of systems of artificial intelligence and education of specialists. In: AIMEE 2017. AISC, vol. 658, pp. 39–52. Springer, Cham (2018). https://doi.org/10.1007/978-3-319-67349-3_4
4. Karabayir, I., et al.: A novel learning algorithm to optimize deep neural networks: evolved gradient direction optimizer (EVGO). IEEE Trans. Neural Netw. Learn. Syst. **32**, 685–694 (2020)
5. Mehmood, F., et al.: An efficient optimization technique for training deep neural networks. Mathematics **11**(6), 1360 (2023)
6. Weinan, E., et al.: A comparative analysis of optimization and generalization properties of two-layer neural network and random feature models under gradient descent dynamics. Sci. China Math. **63**, 1235–1258 (2020)
7. Haenlein, M., Kaplan, A.: A brief history of artificial intelligence: on the past, present, and future of artificial intelligence. Calif. Manag. Rev. **61**, 5–14 (2019)
8. Duchi, J., et al.: Adaptive subgradient methods for online learning and stochastic optimization. J. Mach. Learn. Res. **12**, 2121–2159 (2011)

9. Agaian, S.S.: Hadamard matrices and their applications. In: Dold, A., Eckmann, B. (eds.) LNM, vol. 1168. Springer, Cham (1985)
10. Banica, T.: Invitation to Hadamard matrices. ffhal-02317067v6f. HAL Open Science (2023). hAL Id: hal-02317067. https://hal.science/hal-02317067v6. Accessed 8 May 2024
11. Francisco, C., Oliveira, T., et al.: Hadamard matrices and links to information theory. In: Simos, T.E., et al. (eds.) Numerical Analysis and Applied Mathematics, ICNAAM 2014. AIP Conference Proceedings, vol. 1978, p. 460008. American Institute of Physics (2018)
12. Francisco, C., Oliveira, T.A., Oliveira, A., Carvalho, F.: Hadamard matrices on error detection and correction: useful links to BIBD. In: Ahmed, S.E., Carvalho, F., Puntanen, S. (eds.) IWMS 2016. CS, pp. 99–110. Springer, Cham (2019). https://doi.org/10.1007/978-3-030-17519-1_8
13. Hill, R.C., Griffiths, W.E., Lim, G.C.: Principles of Econometrics, 5th edn. Wiley, New York (2018)
14. Poston, D.L., Conde, E., Field, L.M.: Applied Regression Models in the Social Sciences. Cambridge University Press, Cambridge (2023)
15. Geramita, A.V., et al.: Orthogonal Designs: Quadratic Forms and Hadamard Matrices, 1st edn., Lecture Notes in Pure and Applied Mathematics, vol. 45. Dekker, M., New York-Basel (1979)
16. Hall, J.: Combinatorial Theory, 2nd edn. Wiley, New York (1986)
17. Mermin, N.: Quantum Computer Science: An Introduction, 1st edn. Cambridge University Press, Cambridge (2007)
18. Horadam, K.: Hadamard Matrices and Their Applications. Princeton University Press, Princeton (2007)
19. Francisco, C., Oliveira, T.: BIBD, Hadamard matrices and new technological devices: applications to QR codes. In: Simos, T.E., et al. (eds.) Numerical Analysis and Applied Mathematics, ICNAAM 2014. AIP Conference Proceedings, vol. 1648, p. 840004. American Institute of Physics (2015)
20. Osborn, J.H.: The Hadamard Maximal Determinant Problem. Honours thesis, University of Melbourne (2002). http://maths-people.anu.edu.au/osborn/publications/pubsall.html. Accessed 8 May 2024
21. Sawade, K.: A Hadamard matrix of order-268. Graphs Combinatorics **1**, 185–187 (1985)
22. Sopin, V.: Hadamard conjecture proof. ffhal-03693678f (2022). hAL Id: hal-03693678. https://hal.science/hal-03693678. Accessed 8 May 2024
23. Mitrouli, M.: Sylvester Hadamard matrices revisited. Special Matrices **2**, 120–124 (2014)
24. Paleyes, A., et al.: Challenges in deploying machine learning: a survey of case studies. ACM Comput. Surv. **55**, 1–29 (2022)
25. Hedayat, A., Wallis, W.D.: Hadamard matrices and their applications. Ann. Stat. **6**(6), 1184–1238 (1978)
26. Sloane, N.: A library of Hadamard matrices (2004). http://neilsloane.com/hadamard/. Accessed 7 May 2024
27. Cameron, J.: Hadamard matrices (2006). http://designtheory.org/library/encyc/topics/had.pdf. Accessed 7 May 2024
28. University of London: Encyclopedia of design theory (2004). https://webspace.maths.qmul.ac.uk/l.h.soicher/designtheory.org/library/encyc/. Accessed 7 May 2024
29. Haralambos, E., et al.: Applications of Hadamard matrices. J. Telecommun. Inf. Technol. **2**, 3–10 (2003)
30. Oliveira, T.A.: Provas de agregação: Lição- projecto unidade curricular e curriculum. Agregação, Universidade Aberta (2019). http://hdl.handle.net/10400.2/8888. Accessed 8 May 2024
31. A.D.R. Group: Quantum optics and quantum many-body systems (2011). https://qoqms.phys.strath.ac.uk/research_qc.html. Accessed 7 May 2024

32. Woerner, S., Egger, D.: Quantum risk analysis. NPJ Quantum Inf. **5**, Article no. 15 (2019)
33. Biamonte, J., et al.: Quantum machine learning. Nature **549**, 195–202 (2017)
34. Gil-Fuster, E., et al.: Understanding quantum machine learning also requires rethinking generalization. Nat. Commun. **15**, 2277 (2024)
35. Singh, H.: Application of generalized Gaussian radial basis function and its reproducing kernel theory. Mathematics **12**, 829 (2024)

Information Management's Influence on Telework Efficiency and Leadership: Perspectives from a Study in Portugal

Jaime Santos[1], João Farinha[1,2,3(✉)], Maria de Fátima Pina[1,4,5], and Rui Martins[1,6]

[1] ISLA - Santarém, Superior Institute of Management and Administration of Santarém, Rua Teixeira Guedes, 31, 2000-029 Santarém, Portugal
{joao.farinha,maria.pina,rui.martins}@islasantarem.pt
[2] CINTURS - University of Algarve, Faro, Portugal
[3] GOVCOPP - University of Aveiro, Aveiro, Portugal
[4] ISCTE - IUL, University Institute of Lisbon, Av. das Forças Armadas, 1649-026 Lisbon, Portugal
[5] ISR - UC, Institute of Systems and Robotics, Department of Electrical and Computer Engineering, University of Coimbra, Rua Silvio Lima - Pólo II, 3030-290 Coimbra, Portugal
[6] University of Beira Interior NECE - Research Unit, Covilhã, Portugal

Abstract. This paper investigates the impact of information management on telework effectiveness and the role of leadership in facilitating successful telework arrangements within the context of Portuguese organizations. Telework, enabled by advanced information and communication technologies (ICTs), has emerged as a significant alternative work arrangement, particularly in response to global events such as the COVID-19 pandemic. Leveraging data collected from Portuguese firms, this study employs qualitative and quantitative methods to analyze the relationship between information management practices, telework effectiveness, and the leadership strategies employed to support remote work. Findings suggest that effective information management is critical for enhancing telework effectiveness, with leadership playing a pivotal role in facilitating communication, collaboration, and employee well-being in a telework environment. The paper concludes with implications for practice and recommendations for organizations seeking to optimize telework arrangements amidst evolving workplace dynamics.

Keywords: Information management · Telework · Leadership · Remote work · Portugal

1 Introduction

Telework, defined as the practice of working remotely using ICTs, has gained considerable traction in recent years, driven by advancements in technology and

© The Author(s), under exclusive license to Springer Nature Switzerland AG 2024
O. Gervasi et al. (Eds.): ICCSA 2024 Workshops, LNCS 14816, pp. 247–265, 2024.
https://doi.org/10.1007/978-3-031-65223-3_17

changing attitudes towards work-life balance. In the wake of the COVID-19 pandemic, organizations worldwide have rapidly adopted telework arrangements to ensure business continuity and employee safety. Portugal, like many other countries, has witnessed a surge in telework adoption, necessitating a closer examination of its implications for organizational effectiveness, leadership practices, and information management.

This study investigates the impact of leadership styles in teleworking environments among employees in Portugal, recognizing the integral role of information management in facilitating successful remote work arrangements. Building upon the growing prevalence of telework, this research aims to explore the interplay between leadership strategies, information management practices, and organizational effectiveness within the Portuguese context. The evolving landscape of telework underscores the need for a holistic approach that integrates leadership, information management, and remote work dynamics to optimize teleworking environments and foster organizational resilience.

2 Literature Review

2.1 Telework and Its Implications for Organizational Effectiveness

Telework is one of the exceptional and somewhat atypical forms of working outside the previously habitual space, although it is gaining increasing prominence in the current economic and social paradigm, with a strong trend towards greater acceptance by workers and preference by organizations in general. With the relative ease with which companies and employees have adapted to new information and communication technologies, telework has been increasingly seen not only as a possibility for the continued performance of many functions but also as a new contractual form in which workers fulfill their obligations from any external point, whether in their own home (home office or home-based work) or in another location where an internet connection permits it [2].

The origin of the Portuguese word "teletrabalho" correspondent to the English word telework comes from the Greek expression "telou", which means "far from" or "at a distance", and the Latin word "tripaliare", which means "to work", resulting in the combination meaning "remote work". The nature of this work depends on the contractual typology agreed upon between employer and employee [7]. According to [8], the reason why we generally do not use the term "telecommuting", as used in the US, is because in the main European languages - Spanish, French, German, Italian, Portuguese - there is no term or expression equivalent to the English word "commuting", which means "going to and from work", hence the term "telecommuting". In this sense, the closest expression in our language would indeed be "telework".

Commonly, [2] shares the understanding that there are indeed some benefits for organizations, workers, and societies. However, there are also risks, particularly regarding the individualization of work, specifically the risk of professional, political, and social isolation by workers. Anker [1] suggests that organizations, on the other hand, seeks alternatives to optimize work in order to improve the

quality of life of workers, reducing the stress that existed when they returned from their usual workplace to their homes. Following this line of thought, [17] also agrees that workers can experience positive effects on health due to the reduction of stress, resulting in an improved balance between work and family. Further, it is crucial for a better quality of life and social sustainability when there is a more effective balance in the use of time between the worker's daily life and teleworking.

Regarding negative aspects, [5], in their analysis of public sector employees teleworking, concluded that those working from home show a more pronounced professional and less organizational isolation. These authors also mention that leadership styles in the hierarchy are not as suitable as in other teams and organizations due to their high degree of virtuality, as communication is less formal and hierarchical. It is worth noting that, based on the lack of personal contact and geographical dispersion, leaders also face greater difficulty in adopting traditionally used behaviors. DeVries [5] believes that, in teleworking, empathy and support from colleagues may no longer be available. Additionally, it may be necessary for workers (subordinates) to require greater monitoring from their respective leaders. From another perspective, despite public sector employees feeling good and committed to the employer when present in person, their sense of commitment may significantly decrease on days when they have to work from home.

2.2 Information Management in Telework Environments

In recent years, the landscape of work has evolved dramatically, with telework becoming increasingly prevalent, especially in response to technological advancements and global events such as the COVID-19 pandemic [15]. As organizations adapt to remote work arrangements, the management of information has become a critical aspect of ensuring productivity, collaboration, and data security in telework environments [13]. In telework environments, the efficient management of information is paramount to maintaining organizational cohesion and achieving strategic objectives. Caraiani [3] suggests that effective information management in telework settings requires a comprehensive understanding of the three fundamental levels of management: administration, management, and operations. Top managers, responsible for institutional management, must devise strategies to facilitate remote collaboration, establish clear communication channels, and ensure that remote workers have access to the necessary resources and support systems.

Middle managers play a crucial role in adapting organizational policies and strategies to the unique challenges of telework environments. They are tasked with coordinating remote teams, fostering a sense of belonging and accountability among teleworkers, and addressing any issues that may arise in the course of remote operations [3]. At the operational level, first-line managers oversee the day-to-day activities of remote workers, ensuring that tasks are completed efficiently and in line with organizational objectives. They must implement systems for monitoring and evaluating remote performance, provide remote workers

with the necessary training and support, and facilitate effective communication between remote teams [3].

Effective information management in telework environments also requires the implementation of appropriate technological solutions and security measures. Kuruzovich [12] emphasizes the importance of leveraging technology to enable remote collaboration, streamline workflows, and protect sensitive information from unauthorized access or data breaches. Moreover, ethical considerations, promoting a culture of trust, transparency, and accountability among remote workers, as well as addressing any ethical dilemmas or conflicts that may arise in the course of remote operations and cultural factors play a significant role in information management in telework environments.

In conclusion, information management in telework environments is a multifaceted process that requires careful planning, coordination, and adaptation to the unique challenges of remote work. By leveraging technology, fostering a culture of trust and transparency, and implementing appropriate security measures, organizations can effectively manage information in telework environments and ensure the success of remote operations.

2.3 Leadership Roles and Strategies in Facilitating Telework Effectiveness

In the context of contemporary organizational management, teamwork and leadership play pivotal roles in navigating the complexities of telework environments. Zamanov [19] asserts that effective team management within an organization involves coordinating and directing relationships among workers, with a focus on recognizing the value and relevance of each individual. This is particularly pertinent as organizations transition away from traditional hierarchical structures towards more collaborative and dynamic team-based approaches. Some authors distinguishes between mere groups of individuals and cohesive teams, emphasizing the importance of shared goals, complementary skills, and coordinated efforts in achieving common objectives. A key aspect of team dynamics, as highlighted, is the continuous exchange of feedback among team members. Leaders, therefore, must not only facilitate feedback mechanisms but also establish clear, achievable goals, conduct regular meetings to ensure alignment, and foster a supportive and inclusive team culture (see, for instance, [3]).

Furthermore, the composition of effective teams extends beyond innate characteristics to include behavioural competencies and technical skills. These authors delineate the defining characteristics of teams, emphasizing social interaction, shared goals, task interdependence, and integration within the broader organizational context. This interconnectedness underscores the importance of effective leadership in facilitating collaboration and coordination among team members. Leadership, as elucidated by [9], is a timeless concept that transcends historical epochs, encompassing the ability to influence and inspire individuals or groups towards common goals. It elaborates on the multifaceted nature of leadership, encompassing interpersonal attitudes and behaviors that shape

organizational culture and dynamics. Effective leadership involves not only influencing behaviors but also fostering a supportive and empowering environment conducive to individual and collective growth [3].

Despite the historical evolution of leadership theories, the significance of effective leadership in organizational success remains unequivocal. From trait-based theories to contemporary contingency and value-based approaches, leadership research continues to evolve, reflecting changing organizational landscapes and the complexities of human behavior. In the modern context, leadership extends beyond individual traits to encompass team dynamics and organizational effectiveness. Leaders must balance individual capabilities with collective performance, fostering collaboration, innovation, and resilience within their teams [6]. This requires emotional intelligence, empathy, and the ability to empower and motivate others towards shared objectives.

Ultimately, effective leadership in telework environments hinges on the ability to adapt to changing circumstances, foster collaboration, and empower individuals and teams to thrive in virtual settings. By embracing inclusive leadership practices, promoting open communication, and nurturing a culture of trust and accountability, leaders can facilitate telework effectiveness and drive organizational success [6]. These authors advance that effective leadership entails adopting behaviors that garner recognition and respect from subordinates, as this is pivotal to achieving desired outcomes. Emphasizing the importance of emotional intelligence, leaders must exert control over not only their own emotions but also those of their team members. By setting an example and delegating tasks while maintaining oversight, leaders can cultivate an environment of fairness and impartiality, thereby fostering team mobilization and achieving organizational success.

2.4 The Portuguese Context of Telework Adoption and Its Challenges

Coenen [4] highlights that while telework is often associated with working from home, its true definition pertains to task execution "outside the employer's premises", allowing for work to be conducted remotely with the aid of technology and communication equipment. Although commonly perceived as home-based work, telework encompasses diverse forms, including telecentres, satellite centres, and mobile telework, as described by [18]. According to [17], telecentres serve as shared resource centers where equipment, either owned or rented, is utilized by users from various companies. Similarly, satellite centers, located near users' residences, provide flexible spaces for remote collaboration, often adopting a coworking model. Coworking, involves work conducted outside the headquarters of the parent company, typically in its subsidiaries situated across different geographic locations but connected through ICT. This telework modality is predominantly adopted by large corporations in urban centers.

Mobile telework, as outlined by [17], involves work conducted from various locations using portable equipment such as laptops or mobile devices with wireless telecommunications capabilities [11]. In addition to geographical and phys-

ical distinctions, telework modalities encompass factors such as the proportion of work performed remotely, categorized as full-time, part-time, or ad hoc, as discussed by [17]. Furthermore, telework arrangements vary based on the employment relationship, with some individuals working exclusively for one employer from their residence while others, freelancers, may serve multiple clients, necessitating various employer relationships.

Additionally, telework may differ based on the timing of work, occurring during regular daytime hours, evenings, or weekends, serving as a means to compensate for tasks that cannot be completed during regular working hours as cited in [17].

2.5 Barriers to Telework Adoption

Despite its potential benefits, telework faces several barriers that hinder its adoption and effectiveness. Challenges include limited internet access, particularly in geographically remote areas, where telecommunication infrastructure may not meet the required standards. Additionally, organizational barriers such as limited access to company information through electronic devices and resistance to technological investments and cultural changes pose significant obstacles [19]. Other barriers include the necessity for physical presence in the workplace, computer illiteracy among employees, resistance to telework, reluctance of companies to invest in technology, concerns regarding loss of control over employees, and the desire to maintain a clear separation between personal and professional life.

Moreover, interpersonal interaction among colleagues may be limited, further complicating collaborative efforts. Given the demanding nature of telework, individuals must possess specific characteristics to succeed in this environment, such as self-motivation, proficiency in their work, independence, time management skills, comfort with solitude, reliability, and trustworthiness [17]. However, despite its potential, telework still faces challenges that necessitate further research, as findings regarding its impact remain inconclusive. While some studies suggest positive outcomes for teleworkers, others indicate potential drawbacks, such as decreased personal and familial satisfaction, highlighting the need for comprehensive investigations into telework's implications (see, e.g., [2]).

2.6 Research Question

Understanding the diverse modalities and inherent challenges of telework within the Portuguese context lays the foundation for investigating its efficiency in organizational settings. With telework encompassing various forms, including home-based, satellite centers, and mobile arrangements, it becomes crucial to explore how information management influences its efficacy. Moreover, organizational barriers such as limited access to company information, technological resistance, and concerns regarding control over employees highlight the need to assess the impact of information management on telework practices. Furthermore, examining leadership strategies in facilitating telework effectiveness becomes imperative,

considering the importance of leaders in fostering a conducive remote work environment. Therefore, the research question "How does information management influence the efficiency of telework practices and leadership strategies within Portuguese organizations?" emerges as a pivotal inquiry, aiming to uncover the interplay between information management, telework efficiency, and leadership approaches in the Portuguese organizational landscape.

3 Methodology

3.1 Data Collection

The research was conducted across mainland Portugal and the archipelagos of the Azores and Madeira, aiming to reach a broad spectrum of individuals regardless of their sector of activity or type of service. It was acknowledged from the outset that certain activities, such as repair workshops, assembly lines, construction, security, emergency services, and distribution, might not lend themselves to non-presential work. Therefore, the choice to distribute questionnaires via email was deemed the most suitable method considering the national scope and the number of individuals targeted. Overall, the contribution of respondents, varying in quantity, took shape thanks to their willingness to participate and, notably, the cooperation of many employers, which was crucial for the intended purposes.

Quantitative Approach: As previously mentioned, this study solely adopted a quantitative methodology. According to [6], this type of analysis tends to focus on how a variation in X may also cause a variation in Y, although the cause-and-effect relationship may not always be evident. To fulfil the objectives of this research, following the decision to employ a quantitative approach, a questionnaire was developed, encompassing the attributes and constructs under analysis, namely, the quality of life in telework, the interaction/relationship with boss/hierarchical superior in telework context, the perception of leadership style of boss/hierarchical superior towards oneself in telework, sociodemographic and professional data. The previous first three constructs were measured using fifteen questions with possible answers classified with a five points Likert scale. The last ones related with sociodemographic and professional data were of nominal type.

3.2 Sampling Strategy and Participant Demographics

The sample size calculation for this study was obtained using the software developed by [16], available online on the "Prática Clínica" webpage, resulting in 620 responses recorded for a minimum sample of 385 respondents, based on a 95% confidence interval and a 5% margin of error. Although a sample of 385 workers would have been sufficient according to the criteria defined in this software, a larger number was ultimately utilized, thereby enhancing the precision of the results obtained. The present survey targeted the entire active population working as employees in Portugal. According to data from Pordata (2023), based on the latest census in 2021, the total number of these workers was 3 435 002.

3.3 Data Analysis Techniques

Once the deadline for responses to the questionnaire was reached, the data were exported directly from Google Forms to Google Sheets, then transferred, saved, and processed in a Microsoft Excel file before being exported to IBM SPSS (Statistical Package for the Social Sciences) software for analysis. Statistical analysis was conducted to treat the data.

To characterize the sample, descriptive statistical techniques were employed, including vertical and horizontal bar charts, pie charts, absolute frequency tables (number of individuals) and relative frequency tables (percentages of individuals), mean, median, mode, standard deviation, maximums, and minimums. Quality assessment of the database was prioritized, and an anomalous situation of missing cases was identified. It was discovered that a line duplication occurred in the Microsoft Excel file, which had been created but interrupted midway, resulting in 621 respondents instead of the actual 620 received. This duplication, and particularly its inconsistency, was corrected, resulting in the accurate count of 620 received responses. Following [10], outliers were analyzed, and item sensitivity was studied using skewness coefficients ($|Sk| \leq 3$) and kurtosis ($|Ku| \leq 10$). The assumption of normality of items was verified. Otherwise, a severe violation of the normality assumption would be indicated.

To analyze the measures of Quality of life in telework, Interaction/relationship with boss/hierarchical superior in telework context, and Perception of leadership style of boss/hierarchical superior towards oneself in telework context, arithmetic means and standard deviations were calculated for each item of the 3 variables. The arithmetic mean (M) is the sum of all values in a given dataset divided by the number of elements in that dataset. The median (Md) is the smallest value of the variable up to which at least 50% of the observations accumulate. Considering each variable consists of an even number (620) of answers, which must be arranged in ascending or descending order beforehand, the median value for each of the 15 questions represents the central value of the dataset. Standard deviation (SD) is a measure that expresses the degree of dispersion of a dataset, indicating how uniform the data are. The closer the standard deviation is to 0 (zero), the more homogeneous the data are [14].

The Kaiser-Meyer-Olkin (KMO) statistic is calculated to verify the strength of partial correlation between the various variables under study, providing the adequacy of the input matrix. According to [14], KMO values close to 1.0 are considered ideal, while values below 0.5 are unacceptable. Most scholars argue that a KMO measure of at least 0.80 is good enough to start factor analysis. The Bartlett's Test of Sphericity is used to assess the null hypothesis that the correlation matrix reflects an identity matrix, implying that the variables are uncorrelated and thus unsuitable for factor analysis. However, to achieve an identity matrix, a significant test should assume minimum significance levels above 0.05. Factor Analysis using the Principal Components method, and Varimax with Kaiser Normalization as rotation method, was employed to determine the value of each construct. To validate the appropriateness of these data, the correlation coefficient was calculated using the KMO measure and Bartlett's

Test of Sphericity. Reference values for this scale, which serve as indicators of whether factor analysis is appropriate or not, may vary among authors. However, the most suitable fit in a factor analysis model should have a KMO value above 0.8. Based on [14] recommendations, values below 0.5 are unacceptable, between 0.5 and 0.6 are poor, between 0.6 and 0.7 are mediocre, between 0.7 and 0.8 are fair, between 0.8 and 0.9 are good, and between 0.9 and 1 are excellent.

In the field of Social Sciences, attempts are often made to measure phenomena that cannot be directly observed, referred to as constructs or latent variables. These variables are deduced mathematically from other variables that can be directly observed, i.e., that can be measured directly [14].

4 Findings

4.1 Impact of Information Management Practices on Telework Effectiveness

Understanding the demographics and professional backgrounds of respondents is crucial to discern the impact of information management practices on telework effectiveness. In terms of demographics, the sample of 620 respondents was predominantly female, comprising 71.77% (n = 445), which may be attributed to the pandemic's demands, where women often assumed primary caregiving responsibilities, potentially influencing their inclination towards telework. Regarding age distribution, a significant proportion (44.19%, n = 274) fell within the 41–50 age group, while those aged 16–30 represented only 8.39% (n = 52). Educational attainment revealed that 65.48% (n = 406) possessed a higher education degree, underscoring the sample's educational profile. Marital status data indicated that 65.65% (n = 407) of respondents were married. Household composition revealed diverse structures, with 31.13% (n = 193) having three-person households and 27.26% (n = 169) having four-person households, reflecting varying family dynamics among respondents. Professionally, the majority (76.61%, n = 475) worked in the public sector, predominantly in public administration (65.97%, n = 409). Regarding company size, 45.81% (n = 284) reported organizations with over 250 employees, highlighting the prevalence of larger establishments in the sample. Longevity in current employment varied, with 34.35% (n = 213) having over 20 years of service, while 26.94% (n = 167) had been with their current employer for less than 5 years. The majority (76.13%, n = 472) did not hold managerial positions. Telework practices showcased a significant adaptation during the pandemic, with 62.58% (n = 388) teleworking full-time. Preferences for telework arrangements revealed that 49.19% (n = 305) favoured a hybrid model, combining remote and in-person work, while 41.29% (n = 256) preferred working solely at the company's physical premises. Flexibility in working hours was notable, with 43.39% (n = 269) reporting flexible schedules.

In summary, it was possible to notice that the sample's composition reflects diverse demographic and professional backgrounds, with notable trends towards

telework adoption, particularly during the pandemic. Gender Disparity and Telework: the significant majority of female respondents (71.77%) suggests a potential gender disparity in telework participation, possibly influenced by caregiving responsibilities during the pandemic. This highlights the need for gender-inclusive telework policies to ensure equitable opportunities for all employees. Age Distribution and Telework Adoption: the higher proportion of respondents aged 41–50 (44.19%) compared to younger age groups indicates a greater propensity for telework adoption among mid-career professionals. This suggests that telework may be more prevalent among established professionals with greater flexibility in their roles. Educational Attainment and Telework Readiness: the majority of respondents (65.48%) holding a higher education degree may indicate a correlation between educational attainment and telework readiness ($r = 0.156,\ p < 0.001$). Higher-educated individuals may possess the skills and resources necessary for remote work, potentially impacting telework effectiveness and productivity. Company Size and Telework Implementation: the prevalence of respondents working in organizations with over 250 employees (45.81%) underscores the importance of organizational size in facilitating telework arrangements. Larger companies may have the resources and infrastructure to support remote work, impacting the scalability and effectiveness of telework initiatives.

Telework Preferences and Work Arrangements: the preference for a hybrid telework model (49.19%) suggests a growing demand for flexibility in work arrangements, allowing employees to balance remote and in-person work. This preference may impact organizational policies and infrastructure to accommodate hybrid work models effectively. Flexible Working Hours and Employee Satisfaction: the significant proportion of respondents (43.39%) reporting flexible working hours highlights the importance of autonomy and work-life balance in telework arrangements. Flexibility in working hours can positively impact employee satisfaction, productivity, and overall telework effectiveness. Managerial Positions and Telework Leadership: the majority of respondents (76.13%) not holding managerial positions may influence telework leadership and supervision practices. Effective telework leadership is crucial for fostering collaboration, communication, and accountability in remote teams, potentially impacting telework effectiveness and team performance. Overall, the analysis underscores the multifaceted nature of telework adoption and its implications for organizational policies, employee demographics, and work arrangements. Understanding these dynamics is essential for designing effective telework strategies that promote productivity, employee well-being, and organizational success.

In what follows, we present some results of the factor analysis that were performed. Factor analysis of the construct Quality of life in telework (15 items): KMO = 0.897, and the Bartlett's test of sphericity was highly significant ($\chi^2_{(105)} = 2903.97,\ p < 0.001$), confirming that the data were suitable for factor analysis. Four items with communalities lower than 0.5 were removed. This construct was found to be unidimensional, explaining 43.81% of the total variance, and the 11 items retained showed good internal consistency with a Cronbach's

alpha value of 0.868. Factor analysis of the construct Interaction/relationship with boss/hierarchical superior in telework context (15 items): KMO = 0.894, and a significant Bartlett's test of sphericity ($\chi^2_{(105)} = 3989.76,\ p < 0.001$). Two items with communalities lower than 0.5 were eliminated and 2 factors were retained, which together explain 58.27% of the total variance. The first factor, called Development, explains 39.67%, and the second, called Integration, 18.60% of the variance. The Cronbach's alpha reliability values obtained were, respectively, 0.899 and 0.684. Factor analysis of the construct Perception of leadership style of boss/hierarchical superior towards oneself in telework: KMO = 0.965, and a significant Bartlett's test of sphericity ($\chi^2_{(105)} = 8119.66,\ p < 0.001$). This construct was found to be unidimensional, explaining 63.69% of the total variance, and the 15 items showed good internal consistency with a Cronbach's alpha value of 0.94.

4.2 Leadership Strategies Conducive to Successful Telework Arrangements

The study provides valuable insights into the characteristics of the sample population participating in telework arrangements, which can be linked to leadership strategies conducive to successful telework arrangements as follows. Gender Disparity and Inclusive Leadership: the observation of a significant majority of female respondents engaging in telework highlights the importance of inclusive leadership strategies. Effective leaders must recognize and address potential gender disparities in telework participation by implementing policies that promote equal opportunities and support for all employees, irrespective of gender. Age Distribution and Leadership Adaptability: the higher representation of mid-career professionals in telework suggests the need for leadership adaptability to cater to diverse age groups. Leaders should tailor communication styles, performance management approaches, and support mechanisms to accommodate the preferences and needs of employees across different age demographics, ensuring successful telework implementation. Educational Attainment and Leadership Development: the correlation between higher educational attainment and telework readiness underscores the role of leadership development in facilitating remote work effectiveness. Leaders must invest in training and development initiatives to equip employees with the necessary skills, competencies, and technological proficiency required for successful telework arrangements. Company Size and Leadership Support: the prevalence of telework among employees in larger organizations highlights the importance of leadership support and organizational resources. Effective leaders in larger companies must provide strategic direction, allocate resources, and establish clear policies to enable seamless telework implementation, fostering a supportive work environment conducive to remote collaboration and productivity.

Telework Preferences and Transformational Leadership: the preference for hybrid telework models indicates the need for transformational leadership strategies that promote flexibility, innovation, and employee empowerment. Transformational leaders inspire trust, encourage autonomy, and facilitate continuous

adaptation to changing work arrangements, driving organizational resilience and agility in the face of uncertainty. Flexible Working Hours and Leadership Trust: the provision of flexible working hours underscores the significance of leadership trust in telework arrangements. Trustworthy leaders foster a culture of autonomy, accountability, and mutual respect, empowering employees to manage their time effectively and deliver results, regardless of physical location. Managerial Positions and Leadership Communication: the distribution of managerial positions among teleworkers emphasizes the importance of effective leadership communication. Leaders in telework environments must prioritize transparent communication, regular feedback, and active engagement to overcome challenges associated with remote supervision, ensuring clarity of expectations and alignment of goals across distributed teams. Overall, the study highlights the intersection between leadership strategies and the characteristics of the telework population, emphasizing the importance of inclusive, adaptable, supportive, and communicative leadership practices in facilitating successful telework arrangements.

4.3 Challenges and Opportunities Specific to the Portuguese Context

In the context of Portugal, the implementation of telework presents both challenges and opportunities that require careful consideration and effective leadership strategies to navigate successfully. Gender Disparity and Inclusive Leadership: a notable gender disparity in telework participation may reflect existing societal norms and caregiving responsibilities. Effective leadership should promote inclusive practices that address gender imbalances, ensuring equitable access to telework opportunities and support for all employees, regardless of gender. By fostering a culture of diversity and inclusion, leaders can harness the full potential of their workforce and promote gender equality in telework arrangements.

Age Distribution and Leadership Adaptability: Portugal's workforce comprises individuals spanning various age demographics, each with unique preferences and needs regarding telework. Leaders must adopt adaptable leadership styles that cater to diverse age groups, providing tailored support, training, and resources to accommodate employees at different stages of their careers. By embracing flexibility and embracing generational diversity, leaders can enhance employee engagement and productivity in telework environments. Educational Attainment and Leadership Development: disparities in educational attainment levels among teleworkers highlight the importance of leadership development initiatives. Effective leaders should invest in continuous learning opportunities, providing employees with the skills, knowledge, and technological proficiency required for successful telework. By prioritizing training and upskilling programs, leaders can empower their workforce to adapt to remote work challenges and drive organizational innovation and competitiveness.

Company Size and Leadership Support: in Portugal, organizations of varying sizes may face distinct challenges in implementing telework. Leaders in larger companies must provide strategic direction, allocate resources, and establish

clear policies to support telework initiatives effectively. Meanwhile, leaders in smaller enterprises may need to prioritize resource allocation and foster a supportive organizational culture conducive to remote collaboration and flexibility. By providing leadership support tailored to their organization's size and structure, leaders can mitigate barriers to telework adoption and promote organizational resilience. Telework Preferences and Transformational Leadership: the preference for hybrid telework models underscores the need for transformational leadership that promotes flexibility and innovation. Forward-thinking leaders should inspire trust, empower autonomy, and encourage continuous adaptation to changing work arrangements. By embracing transformational leadership principles, leaders can create an agile and adaptive organizational culture that maximizes the benefits of telework while fostering employee well-being and satisfaction.

Flexible Working Hours and Leadership Trust: flexible working hours require leaders to cultivate trust and accountability within their teams. Trustworthy leaders should foster open communication, provide clear expectations, and empower employees to manage their time effectively. By prioritizing transparency and mutual respect, leaders can build strong relationships with their remote teams, promoting collaboration, and driving performance in telework environments. Managerial Positions and Leadership Communication: effective leadership communication is essential for overcoming the challenges of remote supervision and fostering employee engagement. Leaders must leverage digital communication tools to facilitate regular feedback, provide guidance, and maintain team cohesion. By fostering a culture of open communication and collaboration, leaders can overcome barriers to remote supervision and ensure alignment of goals and objectives across distributed teams.

In conclusion, the Portuguese context presents unique challenges and opportunities for telework implementation, requiring leaders to adopt inclusive, adaptable, and communicative leadership strategies. By addressing gender disparities, embracing generational diversity, investing in leadership development, providing support tailored to organizational size, promoting flexibility and innovation, fostering trust and accountability, and prioritizing effective communication, leaders can navigate the complexities of telework and unlock its full potential for organizational success and employee well-being in Portugal.

5 Discussion

5.1 The Interplay Between Information Management, Telework Effectiveness, and Leadership

The interplay between information management, telework effectiveness, and leadership is multifaceted and dynamic, encompassing various challenges and opportunities within the Portuguese context. Gender disparities in telework participation underscore the importance of inclusive leadership strategies that promote gender equality and diversity. Age distribution highlights the need for adaptable leadership approaches that cater to the preferences and needs

of employees across different generations. Disparities in educational attainment underscore the significance of leadership development initiatives to equip teleworkers with the necessary skills and technological proficiency. Company size influences the leadership support required for successful telework implementation, with leaders needing to tailor their approaches to the organizational structure and resources available. Telework preferences, such as hybrid models, call for transformational leadership that fosters flexibility, innovation, and trust. Flexible working hours necessitate leadership that cultivates trust and accountability, while managerial positions require effective communication strategies to overcome the challenges of remote supervision. By addressing these aspects and adopting inclusive, adaptable, and communicative leadership strategies, organizations in Portugal can optimize the interplay between information management, telework effectiveness, and leadership to drive success and employee well-being in remote work environments.

5.2 Implications for Organizational Policy and Practice

The implications for organizational policy and practice stemming from the interplay between information management, telework effectiveness, and leadership are multifaceted and critical for the success of modern workplaces, particularly in the Portuguese context. Policy Development: organizations need to develop comprehensive telework policies that address various aspects of remote work, including communication protocols, performance expectations, data security measures, and employee well-being initiatives. These policies should be flexible enough to accommodate the diverse needs of employees while ensuring alignment with organizational goals and values. Technology Integration: to support effective telework, organizations must invest in and integrate appropriate technology infrastructure and digital tools. This includes cloud-based collaboration platforms, project management software, cybersecurity solutions, and remote access systems. Policies should outline guidelines for the use of these technologies and ensure compliance with data protection regulations.

Leadership Training: organizations should provide leadership training programs tailored to remote management. Leaders need to develop skills in virtual communication, team motivation, conflict resolution, and performance evaluation. Emphasis should be placed on fostering a supportive and inclusive work culture that transcends physical boundaries. Performance Evaluation: traditional performance evaluation methods may need to be adapted to suit remote work environments. Organizations should explore outcome-based performance metrics rather than relying solely on input-based measures. Regular feedback sessions and goal-setting exercises can help employees stay aligned with organizational objectives and track their progress effectively.

Employee Engagement: maintaining high levels of employee engagement in remote settings requires proactive efforts from organizational leaders. Regular virtual team meetings, social events, and recognition programs can help foster a sense of belonging and camaraderie among remote workers. Organizations should

also provide channels for employees to voice their concerns and feedback. Work-Life Balance: telework policies should promote work-life balance by establishing clear boundaries between work hours and personal time. Encouraging employees to take regular breaks, set realistic workloads, and disconnect after hours can help prevent burnout and improve overall well-being.

Data Security Measures: with the increase in remote work, organizations must priorities data security and privacy. This includes implementing robust cybersecurity protocols, encryption technologies, and access controls to protect sensitive information from cyber threats. Employee training on data security best practices is also essential to mitigate risks. Cultural Adaptation: organizations need to adapt their organizational culture to embrace remote work as a viable and sustainable model. This may involve fostering a culture of trust, autonomy, and accountability, where employees are empowered to manage their work independently. Leaders should lead by example and demonstrate a commitment to remote work practices.

5.3 Recommendations for Fostering Effective Telework Environments in Portugal

To foster effective, telework environments in Portugal, several recommendations can be proposed based on the interplay between information management, telework effectiveness, and leadership, as follows. Invest in Infrastructure: organizations should invest in robust technological infrastructure to support remote work, ensuring reliable access to digital tools and platforms for communication, collaboration, and information management. Promote Leadership Development: develop leadership programs focused on remote management skills, such as effective communication, team collaboration, and performance management in virtual settings. Leaders should be equipped with the necessary skills to motivate and support remote teams effectively. Implement Flexible Policies: establish flexible telework policies that accommodate diverse employee needs and preferences. Provide options for hybrid work arrangements, allowing employees to balance remote and on-site work based on their roles and responsibilities.

Enhance Digital Literacy: offer training programs to enhance employees' digital literacy skills, including proficiency in remote communication tools, cybersecurity practices, and information management techniques. Ensure that all employees have the necessary skills to navigate virtual work environments effectively. Prioritize Well-being: prioritize employee well-being by promoting work-life balance, setting clear boundaries between work and personal life, and offering mental health support resources. Encourage regular breaks, social interactions, and opportunities for physical activity to mitigate the challenges of remote work. Facilitate Communication: foster open and transparent communication channels between remote teams and leadership. Encourage regular check-ins, team meetings, and one-on-one discussions to maintain connection and alignment across the organization. Promote Collaboration: implement collaborative tools and platforms to facilitate teamwork, knowledge sharing, and project management in virtual environments. Encourage cross-functional collaboration and

team-building activities to foster a sense of belonging and camaraderie among remote employees. Ensure Data Security: prioritize data security and privacy measures to protect sensitive information in remote work settings. Implement robust cybersecurity protocols, data encryption techniques, and access controls to safeguard organizational data from potential threats and breaches.

Monitor Performance: establish clear performance metrics and goals for remote employees, regularly monitor progress, and provide constructive feedback and recognition for achievements. Implement performance management systems that focus on outcomes rather than hours worked to evaluate telework effectiveness. Adapt Organizational Culture: adapt the organizational culture to embrace remote work as a viable and sustainable model for the future. Promote a culture of trust, autonomy, and accountability, where employees feel empowered to take ownership of their work and contribute to the organization's success, regardless of their location. By implementing these recommendations, organizations in Portugal can create supportive and effective telework environments that enhance productivity, engagement, and overall organizational performance.

6 Conclusion

6.1 Summary of Key Findings

This study has shed light on the complex interplay between information management practices, telework effectiveness, and leadership strategies, particularly within the Portuguese context. Through an analysis of sociodemographic characteristics, professional profiles, and telework arrangements of respondents, several key findings have emerged. The sociodemographic characterization revealed a predominance of female respondents, with a significant proportion belonging to the age group of 41–50 years and holding higher education qualifications. Furthermore, a majority of respondents were married and had households with an average size of three people. From a professional standpoint, the majority of respondents were employed in the public sector, particularly in administrative roles. The duration of employment with their current employers varied, with a significant portion having more than 20 years of service. Additionally, most respondents did not hold managerial positions, and the prevalence of telework was evident, with a majority teleworking the entire week from their homes.

These findings underscore the importance of comprehensive telework policies, tailored leadership training programs, and robust technology infrastructure to support remote work initiatives. Organizations must also prioritize employee engagement, well-being, and data security to foster effective telework environments. Moving forward, it is essential for organizations in Portugal to adapt their policies and practices to accommodate the evolving nature of remote work. By embracing flexibility, technology, and inclusive leadership strategies, organizations can navigate the challenges and leverage the opportunities presented by telework to drive productivity, innovation, and organizational success.

6.2 Limitations and Avenues for Future Research

While this study provides valuable insights into the interplay between information management practices, telework effectiveness, and leadership strategies within the Portuguese context, some limitation existed: Given the extensive national scope of the population under investigation, obtaining consent from all employers proved challenging, particularly considering that the study was not centered in their geographical regions and not directly linked to the specific companies in question. The study's focus on Portugal also restricts generalizability, while overlooking organizational and managerial perspectives on telework. Future research should employ longitudinal and comparative approaches, incorporate objective metrics, and explore emerging technologies to address these limitations and foster effective telework environments globally.

6.3 Closing Remarks on the Significance of Information Management and Leadership in Enhancing Telework Effectiveness

In conclusion, this study underscores the pivotal role of information management and leadership in augmenting the effectiveness of telework arrangements, particularly within the unique context of Portugal. Through an extensive analysis of sociodemographic characteristics and professional profiles, it becomes evident that successful telework implementation hinges upon robust information management practices and adept leadership strategies. The findings highlight the intricate interplay between these factors and telework effectiveness, shedding light on the challenges and opportunities specific to the Portuguese landscape. As organizations navigate the evolving telework landscape, it is imperative for them to recognize the implications for policy and practice, integrating recommendations for fostering effective telework environments. Despite the limitations inherent in the study, such as the difficulty in obtaining consent from all employers within the national coverage, the insights gleaned pave the way for future research avenues. Moving forward, leveraging these insights can inform organizational policies and practices, ultimately driving towards more efficient and sustainable telework arrangements in Portugal and beyond.

Acknowledgements. The authors acknowledge the financial support of ISLA Santarém. The third author also acknowledge Fundação para a Ciência e a Tecnologia (FCT) and COMPETE 2020 program for financial support to project UIDB/00048/2020.

References

1. Anker, T.: At the boundary: post-COVID agenda for business and management research in Europe and beyond. Eur. Manag. J. **39**(2), 171–178 (2021). https://doi.org/10.1016/j.emj.2021.01.003
2. Blahopoulou, J., Ortiz-Bonnin, S., Montañez-Juan, M., Espinosa, G., García-Buades, M.: Telework satisfaction, wellbeing and performance in the digital era. Lessons learned during COVID-19 lockdown in Spain. Curr. Psychol. **41**(5), 2507–2520 (2022). https://doi.org/10.1007/s12144-022-02873-x
3. Caraiani, C., Lungu, C., Dascalu, C., Stoian, C.: The impact of telework on organisational performance, behaviour, and culture: evidence from business services industry based on employees' perceptions. Econ. Res.-Ekonomska Istraživanja **36**(2), 2142815 (2023). https://doi.org/10.1080/1331677X.2022.2142815
4. Coenen, M., Kok, R.: Workplace flexibility and new product development performance: the role of telework and flexible work schedules. Eur. Manag. J. **32**(4), 564–576 (2014). https://doi.org/10.1016/j.emj.2013.12.003
5. DeVries, H., Tummers, L., Bekkers, V.: The benefits of teleworking in the public sector: reality or rhetoric? Rev. Public Pers. Adm. **39**(4), 570–593 (2019). https://doi.org/10.1177/0734371X18760124
6. Farinha, J., Ascenso, L.: Telework as an element that leverages professional performance and family balance. In: Challenges for Human Resource management in the Covid-19 era, pp. 187–207 (2022). https://doi.org/10.4018/978-1-7998-9840-5.ch010
7. Golden, T.: Applying technology to work: toward a better understanding of telework. Organ. Manag. J. **6**(4), 241–250 (2009). https://doi.org/10.1057/omj.2009.33
8. Golden, T., Gajendran, R.: Unpacking the role of a telecommuter's job in their performance: examining job complexity, problem solving, interdependence, and social support. J. Bus. Psychol. **34**, 1–15 (2019). https://doi.org/10.1007/s10869-018-9530-4
9. Keles, N.: Leadership, Leadership Styles and Leadership in Public Administration Special of Turkish Customs Administrations (2022). https://doi.org/10.52848/ijls.1070904
10. Kline, R.: Principles and Practice of Structural Equation Modeling, 4th edn. The Guilford Press, New York (2016)
11. Korkeakunnas, T., Heiden, M., Lohela-Karlsson, M., Rambaree, K.: Managers' perceptions of telework in relation to work environment and performance. Sustainability **15**, 5845 (2023). https://doi.org/10.3390/su15075845
12. Kuruzovich, J., Paczkowski, W., Golden, T., Goodarzi, S., Venkatesh, V.: Telecommuting and job outcomes: a moderated mediation model of system use, software quality, and social exchange. Inf. Manag. **58**(3), 103431 (2021). https://doi.org/10.1016/j.im.2021.103431
13. Luo, B., Sun, T., Lin, C., Luo, D., Qin, G., Pan, J.: The human resource architecture model: a twenty-year review and future research directions. Int. J. Hum. Resour. Manag. 1–38 (2020). https://doi.org/10.1080/09585192.2020.1787486
14. Marôco, J.: Análise Estatística com o SPSS Statistics, 8th edn. ReportNumber (2021)
15. Rebelo, G., Almeida, A., Pedra, J.: Telework and work intensity: insights from an exploratory study in Portugal during the COVID-19 pandemic. Adm. Sci. **14**, 14 (2024). https://doi.org/10.3390/admsci14010014

16. Santos: Cálculo Amostral em Ciências Sociais. Prática Clínica (2017). https://praticaclinica.com.br/anexos/ccolaborativa-calculo-amostral/ccolaborativa-calculo-amostral.php
17. Tavares, F., Santos, E., Diogo, A., Ratten, V.: Teleworking in Portuguese communities during the COVID-19 pandemic. J. Enterp. Communities People Places Glob. Econ. **15**(3), 334–349 (2021). https://doi.org/10.1108/JEC-06-2020-0113
18. Van Looy, A.: How the COVID-19 pandemic can stimulate more radical business process improvements: using the metaphor of a tree. Knowl. Process Manag. **28**(2), 107–116 (2021). https://doi.org/10.1002/kpm.1659
19. Zamanov, S.: Team management. J. Manag. Sci. **10**(2), 11–14 (2020). https://doi.org/10.26524/jms.2020.2.3



The Fish Biology and Firms' Internationalisation: The Process Explained Through a Metaphor

Rui Martins[1,2(✉)], Maria de Fátima Pina[1,3,4], and João Farinha[1,5,6]

[1] ISLA - Santarém, Superior Institute of Management and Administration of Santarém, Rua Teixeira Guedes, 31, 2000-029 Santarém, Portugal
{rui.martins,maria.pina,joao.farinha}@islasantarem.pt
[2] University of Beira Interior NECE - Research Unit, Covilhã, Portugal
[3] ISCTE - IUL, University Institute of Lisbon, Av. das Forças Armadas, 1649-026 Lisbon, Portugal
[4] ISR - UC, Institute of Systems and Robotics, Department of Electrical and Computer Engineering, University of Coimbra, Rua Silvio Lima - Pólo II, 3030-290 Coimbra, Portugal
[5] CINTURS - University of Algarve, Faro, Portugal
[6] GOVCOPP - University of Aveiro, Aveiro, Portugal

Abstract. Globalisation has changed the way companies face the challenges of international markets, representing a path to expansion and sometimes survival in the context of global competitiveness. This paper investigates how companies face the stimuli of market expansion within the challenges of internationalisation, and aims to provide implications in barriers that have an impact on the business fabric, on planning and on companies' expectations in international markets. We incorporated two different studies into this work, where we proposed and tested a theoretical model. To this end, we included a quantitative survey made up of a sample of 406 managers of Portuguese companies, where we showed that the barriers are overcome with greater planning on the part of the companies and that the greater the planning on the part of the companies, the higher the expectations of a high financial return. The results shows that planning, barriers and expectations are central for managers and are decisive in motivating Portuguese companies to internationalise. Subsequently, we used a quantitative survey based on 100 questionnaires with CEOs of internationalised companies operating during Covid-19, which made it possible to outline a crucial diagnosis of the internationalisation process in the Covid-19 period. The results presented are based on the international development of companies, decision-making, strategy implementation, the impacts of the Covid-19 pandemic and the strategies used to reduce and mitigate these impacts in the post-Covid-19 period. In addition to other statistical analysis, confirmatory factor analysis within a structural equation modeling framework was performed.

Keywords: Barriers · Companies · Competitiveness · Innovation · Internationalisation · Stimuli · Sustainability

© The Author(s), under exclusive license to Springer Nature Switzerland AG 2024
O. Gervasi et al. (Eds.): ICCSA 2024 Workshops, LNCS 14816, pp. 266–283, 2024.
https://doi.org/10.1007/978-3-031-65223-3_18

1 Introdution

In the context of globalisation, where competition comes from developed economies as well as emerging ones, internationalisation is of paramount importance for innovation and technology, making companies increasingly competitive [4]. Companies must develop and leverage guidelines, as well as appropriate strategies, in order to maximise the company's performance, so a systematised strategy stimulates the entire internationalisation process [17]. However, at the management level, business decision-makers, in particular, should focus on strategic aspects, even in the early stages of company internationalisation, thus contributing to greater sustainability, which results in gains for the competitiveness of economies [9]. One of the most challenging areas for researchers is the need to develop and test new approaches based on the interpretative process of company internationalisation, without neglecting the various patterns that already exist [23].

The main aim of this study is to find out what stimuli and barriers companies face in the process of internationalisation, based on their development and, subsequently, their contribution to aligning and unifying the business trajectory that companies have to overcome in order to achieve success in international markets. The "fish biology" perspective proposes here a new theoretical lens for analysing and interpreting the internationalisation behaviour of companies in the 1st Covid-19 wave. Then we analyse how companies reinvented themselves to overcome the pandemic, explained using a metaphor, in which a pertinent gap emerges in the literature regarding the scarcity of studies on how companies circumvented the impacts of Covid-19 on international markets.

This metaphor is based on the assumption that we can draw an analogy between the process of internationalisation and the life cycle of fish, which are also of great economic importance as they enter the food chain as food for human beings. This article intends to serve several purposes for the literature on the internationalisation of companies. Firstly, it presents an overview of the paths taken by companies when approaching international markets, proposing a better understanding of the main factors that improve/affect company performance and the barriers they have to overcome, using the marine ecosystem as an existing analogy. As a second purpose, this study analyses the impacts and implications associated with the risk of internationalisation, focusing on the concern of entrepreneurs in the markets, our third purpose, which emphasises that the existing cooperation between companies and the government boosts competitiveness in international markets.

The paper is divided into seven sections, including the introduction. The next section presents the theoretical foundation and hypotheses on the subject in question. The Sect. 3 deals with research methodology. This is followed by the section of quantitative approaches and, finally, the last sections, containing the findings, conclusions, implications of the study and guidelines for future research.

2 Theoretical Foundation and Hypotheses

2.1 International Development

The international development of business activities is becoming a decisive instrument in business competitiveness being an entrepreneurial and innovative act, and the recognition of opportunities [7]. The path taken determines positive export effects, which result from the knowledge acquired by recruiting managers with previous international experience and the relationship with foreign buyers, which have a positive impact on export performance [14]. This is a fundamental lever for companies, as the business environment today is marked by greater complexity, competition and globalisation, through which they obtain very valuable resources to promote their products [11] and government policies that develop the economy, helping to create jobs and eradicate poverty through business development [29].

The dynamism of companies creates opportunities in international markets, as it benefits from business initiatives that improve and identify opportunities in international markets, encouraging the improvement of competitive advantages, thus minimising the possibility of these companies making fewer mistakes in the markets [19]. Processes triggered by impulses lead to contingent aspects without any prior plan and can cause barriers that are difficult to overcome, such as vulnerability to global financial crises [22].

Internationalisation can be the key to the survival and growth of companies [32]. The internationalisation of a company can help it to use a wider range of globally available resources, so it is essential to plan all activities [15]. In view of this, CEOs are constantly involved in the company's planning objectives [9], promoting complementary skills and planning to adapt their company's resources to what they will find in the destination country.

We can see that international development is generally influenced by expectations and barriers, which is why we launched hypothesis 1: companies' motivation to internationalise depends on barriers and expectations and the way in which planning is carried out.

2.2 Stimuli for International Development

The stimuli sought by companies in the search for better conditions of economic competitiveness and international expansion are outlined as one of the most important strategies (see, for instance, [6]). Success is thus determined by the ability to assimilate and use knowledge in accordance with market requirements, of which we can emphasise innovation and market orientation, which are relevant to their sustainability [28]. Some stimuli such as negotiating power, the number of distributors, the variety of distribution channels, the prestige of the company and brand awareness have a positive influence on companies' internationalisation strategies [8].

This rapid internationalisation can be seen as an early and global internationalisation strategy, with many companies internationalising by the end of their

first year in business and playing a significant role in driving economic growth [12]. Internationalisation is important for promoting growth and the long-term survival of companies, as it allows them to break away from the saturation of domestic markets, just like the brand, which plays a relevant role for companies [1]. Brand experiences are vital for developing brand loyalty and achieving sustainability in international business, contributing to customer loyalty and improving company performance and profits [24].

Public support agencies can mitigate financial barriers by helping companies to develop long-lasting relationships with venture capitalists and other commercial institutions, so it is imperative that governments boost international networking with public funding if they cannot circumvent or remove the financial barriers to internationalisation [3]. Hypothesis 2 will therefore allow us to identify the determining factors that entrepreneurs consider essential for the international development of their companies.

2.3 Barriers to International Development

There are certain companies that face international barriers and are unable to overcome them, such as an unexpected and sharp decrease in their involvement in international activities, which can inevitably culminate in disinvestment [25].

Paul et al. [27] refer to internal barriers that are called endogenous and external barriers called exogenous. Internal barriers include the cost of starting the internationalisation process, limited knowledge about international markets and their players, as well as limited financial resources [5]. External barriers to the internationalisation process inhibit companies, including, among others, the lack of government intervention to support companies, political changes, the capital market and low competition [21].

The barriers faced by entrepreneurs in the international development of their companies allow us to ascertain, in hypothesis 3, which are the greatest fears faced by entrepreneurs in the internationalisation of their companies. Based on the literature review explained above, the study proposes a theoretical model (Fig. 1) based on the research hypotheses.

3 Research Methodology

Two studies were designed and carried out to fulfil the proposed objective, as shown in Table 1. Study 1, based on 406 CEOs of firms active in international markets, identifies the fundamental premises for the internationalisation of companies, which will culminate in a theoretical model, carried out through a quantitative survey, which allows the research hypotheses to be tested, using IBM SPSS software and PLS-MEV.

In study 2, we carried out a quantitative survey based on 100 questionnaires with CEOs of firms operating in international markets during Covid-19 to delimit the stimuli and barriers in the impact of the Covid-19 pandemic, and how these companies envisioned the future, which will culminate in the visualisation of our

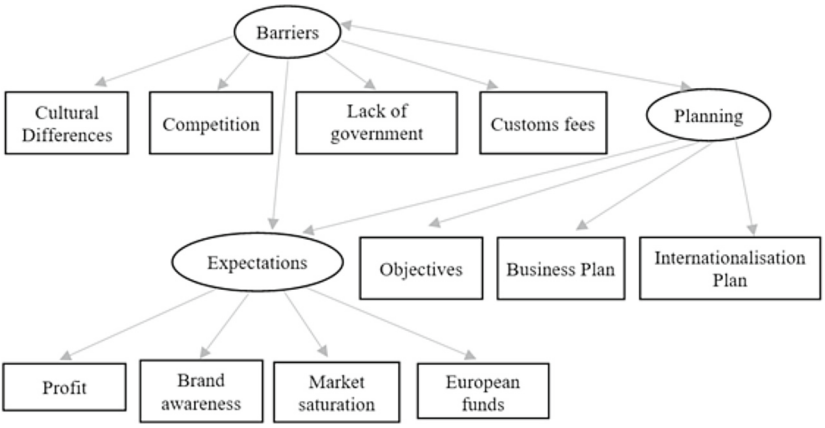

Fig. 1. Theoretical model.

fish, and will allow us to analyse all the stages of the internationalisation process of Portuguese companies.

3.1 Research Strategy

The lack of studies on the paths to success in international markets led us to build this research on a tripod of methodological foundations (Table 1).

Table 1. Methodological Tools.

Main Tools	Auxiliary and Complementary Instruments
Survey 1 406 CEOs of firms active in international markets, available on the AICEP-Portugal database (Google Forms submitted by email)	Secondary data Form: Confidential formal and informal documents, such as communications, memos, and internal reports Purpose: To support, combine, and/or inter-relate empirical findings
Survey 2 100 CEOs of firms operating in international markets during Covid-19, available on the AICEP-Portugal database (Google Forms submitted by email)	Secondary data Form: Confidential formal and informal documents, such as communications, memos, and internal reports Purpose: To support, combine, and/or inter-relate empirical findings

The first stage of the tripod of methodological foundations materialises the primary empirical tools used through a quantitative method research project

[30]. This configuration has made it possible to test complex relationships and to effectively and extensively explore the relationship between the motivation for the internationalisation of companies, which depends on overcoming barriers, and the way in which planning is carried out.

In this respect, the quantitative study 1 verified the mutually auxiliary roles of internationalisation and made it possible to draw up a theoretical model. Then the quantitative study 2 explored how the internationalisation of companies behaved in the Covid-19 and post-Covid-19 period, how barriers were overcome and the stimuli that came from this period.

4 Quantitative Research

The sample was compiled through a mixture of random and purposive selection. The random selection was obtained by means of a research questionnaire, used by [26], subsequently we used the Google forms platform and submitted it by email, along with a brief introduction to our research to a total of 7230 exporting companies, which are available on the AICEP-Portugal database and we received 406 duly validated responses, of which 138 were micro companies, 234 small and medium-sized companies and 34 large companies, distributed in the secondary sector in 52%, in the tertiary sector in 29.2% and in the primary sector corresponding to 18.8%. We divided the questionnaire into four topics: characterisation of the companies, approach to international markets, strategies used in these markets, opportunities and challenges, using a five-point Likert scale (1: Completely disagree; 5: Completely agree).

In study 2, data were obtained through a research questionnaire [2], to which we added the topic of Covid-19. This study was carried out in December 2021. We used the Google forms platform and submitted it by email, to a total of 2620 exporting companies, operating in international markets during Covid-19, which are available in the AICEP-Portugal database, having been received and validated, we identified our sample which corresponds to 100 responses, we then divided it into 4 topics of the questionnaire: barriers; opportunities; impact of the pandemic; future perspectives.

4.1 Results of Study 1

For the analyses presented, IBM SPSS software was used and the quantitative variables were analysed based on their respective values, while the variables measured on a Likert scale were analysed using the categories presented, presenting some relevant statistics, as discussed by [20], such as the mean (M) where on a scale of 1 to 5, a value higher than 3 is higher than its midpoint, the standard deviation (SD) which represents absolute dispersion, the coefficient of variation (CV) which illustrates relative dispersion and the minimum (Min) and maximum (Max) values observed (Table 2).

Further, observing Table 3, it is possible to notice that all the saturations of the variables measured in the respective dimensions are statistically significant ($p < 0.001$ or $p < 0.01$). For each dimension, the average factor saturations, internal consistency and composite reliability were calculated, as well as, the proportion of variance extracted.

Table 4 allows to observe that there is convergent validity for all the dimensions, as the factor saturations are high with average values above or close to the minimum required of 0.400, with the minimum value observed being 0.386, the factor saturations are also significant ($p < 0.001$ or $p < 0.01$). Further, the reliability of each construct is acceptable as the composite reliability values are always higher than the minimum required of 0.60, with the minimum value observed being 0.635, only the internal consistency shows two values lower than desirable, and the variance extracted is adequate for the planning dimension, although it is a little low for the expectations and barriers dimensions. The convergent validity of the measurement scale is also confirmed by the existence of positive and statistically significant saturations between all the dimensions.

Table 2. Entrepreneurs' Perceptions.

Question	N	M	SD	CV
9. The main reason that led the company to internationalise was to increase profits	406	3.72	1.08	29%
10. The main reason that led the company to internationalise was for greater brand recognition	406	3.52	1.18	34%
11. The main reason that led the company to internationalise was market saturation in the domestic market	406	3.52	1.18	33%
12. The main reason that led the company to internationalise was support from the European Union	406	1.78	1.03	58%
13. The main reason that led the company to internationalise was a partnership with another company	406	2.19	1.39	64%
14. The company has standardised rules for conducting international business	406	3.50	1.09	31%
15. The company has a business plan to address international markets	406	3.61	1.12	31%
16. The company defines a strategic plan for international markets	406	3.73	1.07	29%
17. The main challenge the company had to overcome to enter international business was cultural differences	406	2.58	1.15	44%
18. The main challenge the company had to overcome to enter international business was competition from SMEs and multinational companies	406	3.27	1.08	33%
19. The main challenge the company had to overcome to enter international business was lack of government support	406	3.07	1.24	40%
20. The main challenge the company had to overcome to enter international business was high customs duties	406	2.63	1.28	49%
21. International markets offer more opportunities to the company than domestic markets	406	3.99	1.02	26%

Measurement scale: 1 - Completely disagree; ... ; 5 - Completely agree.

Table 3. Model dimensions saturations, SEM results and convergent validity.

Dimension	Variable	Saturations Unstan.	Stan.	St. Error	t-test	**p**
Planning	Objectives	0.659	0.603	0.051	12.846	<0.001
	Business Plan	1.051	0.944	0.046	22.686	<0.001
	Internationalisation Plan	0.954	0.894	0.045	21.003	<0.001
Expectations	Profit	0.560	0.519	0.078	7.177	<0.001
	Brand Awareness	0.747	0.633	0.094	7.930	<0.001
	Market Saturation	0.220	0.187	0.078	2.814	0.005
	European Funds	0.210	0.204	0.068	3.085	0.002
Barriers	Cultural Differences	0.421	0.367	0.073	5.745	<0.001
	Competition	0.382	0.353	0.069	5.518	<0.001
	Lack of Government	0.758	0.611	0.084	9.012	<0.001
	Customs Fees	0.715	0.558	0.085	8.425	<0.001

The model uses the Maximum Likelihood Estimator method, which requires the data to fulfil the normality requirement. Fulfilling this requirement guarantees the validity of the model, although it is less relevant in large samples, as is the case here. Finally, to measure the quality of the adjustment, the reference values recommended are used.

Table 4. Criteria for validating model dimensions through convergent validity.

Dimension	Items	AFS	IC	CR	PVE
Planning	3	0.814	0.847	0.974	0.685
Expectations	4	0.386	0.389	0.635	0.187
Barriers	4	0.472	0.527	0.806	0.236

AFS-Average Factor Saturation; IC-Internal Consistency; CR-Composite Reliability; PVE-Proportion of Variance Extracted.

The fit indices used in Table 5 are justified by [16] who suggests tests that include the RMSEA, CFI, NFI, and Chi-square of the model, its degrees of freedom and the p-value. The authors [16] and [20] recommend the comparative fit index (CFI) and the root mean square error of approximation (RMSEA) as being the most widely used for assessing the fit of models. The measures indicate a good overall fit of the proposed model to the data collected, if we take into account the Chi-square/df (<5), and the other fit indices: RMSEA (RMSEA = 0.062 < 0.08), CFI (CFI = 0.931 > 0.90) and NFI (NFI = 0.894 > 0.80). With regard to the construct under study, the measurement model allows us to conclude that the items: i) are significant; ii) are consistent; iii) have convergent validity. In addition, the model has an adequate quality of fit. We can therefore conclude that the three dimensions studied can be used.

Table 5. Adjustment of the structural model.

$\chi^2/df(p)$	CFI	RMSEA	NFI
2.541 ($p < 0.001$)	0.931	0.062	0.894

CFI-Comparative fit index; RMSEA-Root mean square error of approximation; NFI-Normed of fit index.

The dimension with the highest score is Planning (M = 3.61), with an average value above the midpoint of the measurement scale; this is followed by Expectations (M = 3.14), with an average value slightly above the midpoint of the measurement scale; and then Barriers (M = 2.89), with an average value slightly below the midpoint of the measurement scale, as shown in the Table 6.

Table 6. Descriptive analysis of the dimensions of the model.

	N	M	DP	CV	Min	Max
Planning	406	3.61	0.96	26%	1.00	5.00
Expectations	406	3.14	0.67	21%	1.00	5.00
Barriers	406	2.89	0.77	27%	1.00	5.00

4.2 Results of Study 2

The study 2 questionnaires were compiled in five stages, identical to the research by [31], who explain that the assessment of trace elements in dam lake sediments is crucial for maintaining the health of the ecosystem.

In our study we will categorise the paths taken by companies, based on the five oceans that exist on the planet and the species of fish that live in them, to match the paths taken by companies in internationalisation and the respective results. Also, central to our study are the internationalisation pathways developed by companies, which is why we have identified the different stages, ups and downs of the waves, which contribute to international expansion, as shown in Fig. 2.

Stage 1: Start of International Expansion. The Pacific Ocean is of enormous economic importance, as it has great biodiversity and diverse minerals. It is strategically located in a nerve centre where decision-making is decisive for two of the world's superpowers, Japan and the United States of America.

For 30 CEOs, the paths taken at the start of expansion were the company's own initiative, 26 CEOs said they were based on their business network, 20 CEOs said that participation in trade fairs was decisive, 15 CEOs resorted to projects

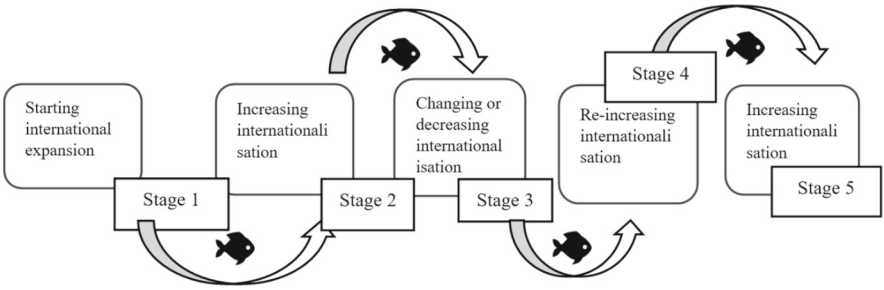

Fig. 2. Stages in the internationalisation of companies. Source: Authors.

with government support and 9 CEOs said it was a challenge from customers to the company. Also, based on decision-making, the reasons given for expanding into international markets were that for 57 CEOs growth was based on the search for new markets, for 32 CEOs the main reason was saturation of the domestic market and for 11 CEOs the decision to expand was a financial decision to achieve an increase in turnover in the future, as shown in Fig. 3.

However, this ocean also has adversities, such as the Pacific Ring of Fire, which is a region of the ocean where many earthquakes and volcanoes occur. The companies also list the main difficulties in approaching international markets and which cause them to maintain/decrease their internationalisation pathways, for 32 CEOs, the excess of legal bureaucracy in the host markets, for 30 the greatest difficulty was finding a network of credible partners, for 15 of them the greatest difficulty was affirming the brand and for 15 the greatest difficulty was competition in international markets, and 8 CEOs said that the lack of qualified labour was the main setback they experienced in international markets.

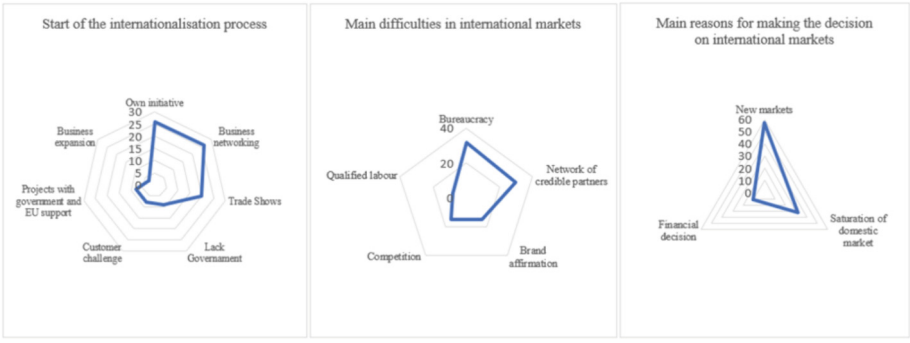

Fig. 3. Radar Charts - International expansion stage.

Stage 2: International Expansion. At this stage, we'll come across the second largest ocean in the world, called the Atlantic Ocean and associated with a titan from Greek mythology called "Atlas". It bathes several countries in the world and is located between three continents: America to the east and Europe and Africa to the west. These waters correspond to 20% of the earth's surface and are accelerated by their economic importance, causing the largest trade flows in the world. In the case of companies, the main accelerators for improving internationalisation are shown in Fig. 4. For 27 interviewees, stakeholders are decisive, for 20 CEOs government support is key, for 19 CEOs the support of clusters is decisive for improving results and for 14 CEOs the support of universities is fundamental, for 11 CEOs they say the dynamism driven by research centres, and the remaining 9 CEOs answered that it is banking. For 73 CEOs, the key to success in improving company results is based on the quality and differentiation of their products, 8 CEOs say that success is based on local partners who are decisive in exploring the pathways to internationalisation, 7 CEOs say that the key to success is based on innovation, another 6 CEOs say that skilled labour is the key and 6 CEOs say that financial stability is the key.

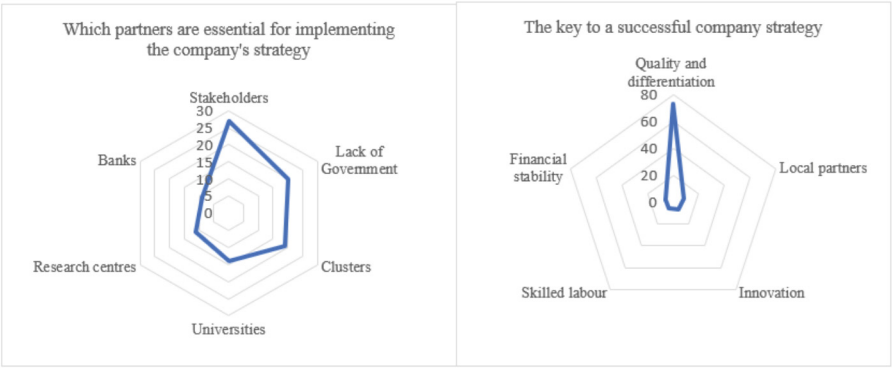

Fig. 4. Radar Charts - Growth in international expansion.

Stage 3: Retraction of International Expansion. The Indian Ocean is the third largest ocean on the planet and is also called the "Indian Sea", in reference to the East Indies, where ancient navigators set sail in search of spices and other products. Our study highlights the main impacts that entrepreneurs face in the internationalisation process in the context of Covid-19, which for 48 CEOs are the closure of international markets, for 42 CEOs they consider the significant drop in sales volume, 5 CEOs share uncertainty in the post-Covid-19 period as the main factor and for 5 CEOs they say that the main impact is the lack of being able to obtain raw materials, as shown in Fig. 5.

The main barriers in the internationalisation process for 29 CEOs were uncertainty in international markets, for 26 CEOs the biggest barrier was protectionism of local economies, for 20 CEOs they said that regaining market share was a determining factor, while for 12 CEOs the biggest barrier was cash flow difficulties and finally for 8 CEOs the lack of raw materials was adverse to activity in the post-Covid-19 period.

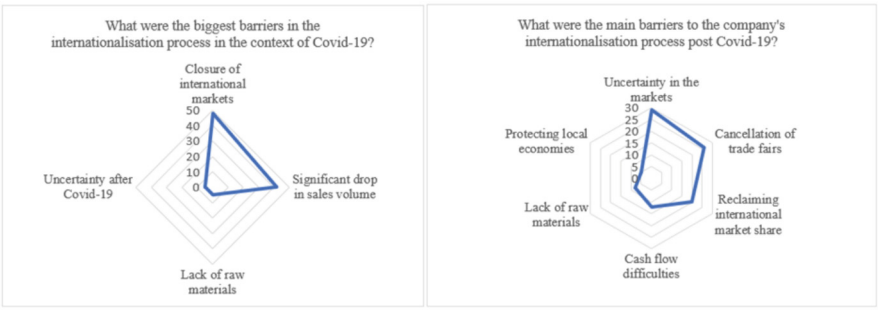

Fig. 5. Radar Charts - Slowdown in international expansion.

Stage 4: (Re)internationalisation. The Antarctic Ocean is the fourth largest ocean by surface area, and its discouraging points are radiation, cold water and the Antarctic winds. On the other hand, it is attractive at the point where the warmest water meets the coldest water, known as the Antarctic convergence. Also, 36 CEOs see the attractiveness of companies in the process of (re)/internationalisation to mitigate the current Covid-19 context, as they expect Portugal to be one of the first countries to emerge from this health crisis; for 32 CEOs, it will be an opportunity to launch new products, 21 CEOs said that using digital channels is the best option and finally 11 CEOs think that Portugal will improve its position in international markets, especially in the face of competition from countries such as Spain, Italy and China, which have been hit much harder by the Covid-19 pandemic, as shown in Fig. 6.

Stage 5: Internationalisation Growth. The world's fifth ocean is the Arctic, also known as the glacial Arctic Ocean, which surrounds the North Pole. It's an ocean that is home to around 400 species, as the climatic conditions in this place are truly extreme. Against this are the main expectations of entrepreneurs in the process of growing internationalisation in the post-Covid-19 period, which are for 31 CEOs to maintain the competitiveness they had before the arrival of Covid-19, for 19 CEOs the challenge is to survive the Covid-19 pandemic, for 19 CEOs customer loyalty is crucial and for 15 CEOs it is to maintain customer loyalty, 14 CEOs fear the bankruptcy of their customers and 12 CEOs the biggest challenge has been e-commerce, as shown in Fig. 6.



Fig. 6. Radar Charts - Opportunities and challenges for international expansion.

5 Discussion, Findings and Conceptualisation

The main objective of our study was to study the incentives and barriers to internationalisation. The quantitative study 1 revealed that planning, barriers and reasons are central to managers and are decisive in motivating Portuguese companies to internationalise. The article proposed hypotheses based on the literature review, the relationship that companies' motivation to internationalise depends on overcoming barriers and the way companies plan. Our results validate this hypothesis, establishing links between planning, barriers and expectations.

In hypothesis 2, we successfully validated that the variables observed in planning, which the managers highlighted as the main foundations of planning, were business plans, internationalisation plans and objectives, which allowed us to be in line with the research of [10], who consider this foundation to be decisive for companies and avoiding fruitless efforts when planning does not exist, as [13] point out, culminating in devastating risks and failure in international markets.

Risk-averse managers are also afraid of the barriers they have to overcome in the internationalisation process and, in line with our hypothesis 3, we validate that what most torments managers is the lack of government support, the cultural differences they will encounter in the destination countries, as well as the high competition and, finally, the high customs duties.

We then analysed the quantitative study 2 in the context of Covid-19, where the results presented are based on the international development of companies, decision-making, strategy implementation, the impacts of the Covid-19 pandemic and the strategies used to reduce and/or mitigate these impacts in the post-Covid-19 period. Internationalisation contributes to the better performance of companies at an early stage, but these internationalisation activities include both progress in the second stage and later setbacks in the third stage, in line with the research carried out by [18].

This failure in international business happens due to an unexpected decrease in involvement in international activities, divestment and is considered a natural part of a company's internationalisation process, as it includes setbacks [8]. Stage 4 shows the re-internationalisation of Portuguese companies in international markets, with expectations of improved sales in the current scenario.

Finally, stage 5 shows the CEOs' satisfactory expectations of a sharp increase in their sales volume in the post-Covid-19 period.

6 Typology and Contextualisation

Of the 24000 fish species evaluated, the whale shark is the largest fish in the world, also known scientifically as Rhincodon typus. However, this fish is not dangerous; it is a filter-feeding animal, just like the blue whale. It feeds on small organisms, such as crustaceans that form what is known as plankton, and its other favourite foods are some fish and molluscs, such as squid. The main areas of research into the internationalisation of companies allow us to visualise the development of our "whale shark" fish in Fig. 7.

Next to the tail is the beginning of the international expansion of companies and the barriers that can arise, then there are elements that can act as accelerators of international expansion and on the other hand there was the retraction caused by the Covid-19 pandemic, but companies reinvented themselves and saw opportunities, However, there were fears and expectations on the part of entrepreneurs to overcome this period, and government and European community support enabled them to overcome the challenges and rise up to achieve ambitious pillars for their companies and to improve the competitiveness of our economy in international markets.

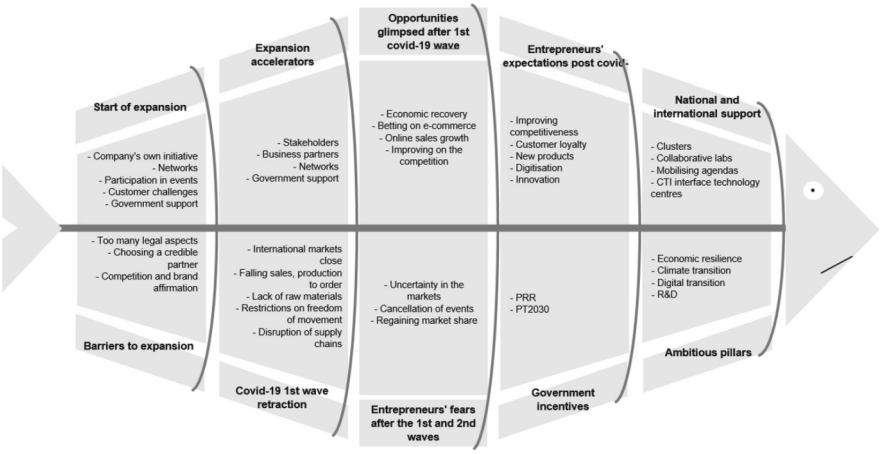

Fig. 7. Stages in the process of internationalising companies. Source: Authors.

7 Implications, Future Research and Conclusion

7.1 From Theoretical Implications to Executive Implementation

This study contributes to our understanding of the internationalisation of companies in a number of significant ways and how accumulated experiences shape

companies' decisions through this process. Firstly, we provide empirical evidence showing that planning, barriers and reasons are determining factors for entrepreneurs when they embark on international paths. Subsequently, we analysed that the start of the internationalisation process happens on the company's own initiative, in partnership, with challenges made by customers or with sectoral and governmental support, but there are barriers that arise, such as the excess of legal aspects, high competition and brand affirmation in international markets that plague our entrepreneurs.

The unprecedented pandemic situation has devastated and shaken the business world, causing businesspeople to have well-founded fears and inevitably contributing to the closure of international markets, cancellation of events, limitation of staff and loss of market share for companies. However, there were opportunities during this period for companies, such as the focus on digitalisation and e-commerce, thus enabling them to improve their position in the face of competition.

The companies that have opted for this route have achieved improved results and competitiveness, customer loyalty, improved innovation, new products and a winning bet on digitalisation and e-commerce, which has allowed them to be better equipped and face a brighter future. These national and international stimuli are boosted with the support of credible entities that support each business sector, through clusters, mobilising agendas, technology centres and collaborative laboratories that aim to promote and boost the RRP, which has the resilience of our economy, the improvement of the climate and digital transition as its desired pillars, based on the improvement of research and development that will culminate in the positioning of companies and our country that will reduce the existing asymmetries with other competing countries and aims to catapult the economic development of our companies.

Complementing the theoretical contribution of our study, our results suggest a number of practical implications, specifically addressing government support aimed at promoting an internationalisation strategy that brings together the various players and allows the national economy to position itself in the global market, stimulating economic growth, progressing towards the creation of skilled jobs and henceforth trying to obtain greater added value.

The support of government programmes is a key lever for companies to develop networks, through which they obtain valuable resources to promote their products, as well as support for the innovation of companies' processes and products. By focusing on the role of contextual factors, our study complements research investigating the aspects related to innovation and high-end technology necessary for internationalisation.

Our results indicate that the future development of company internationalisation depends on an articulated combination of stricter government regulation of target markets and financial support systems that encourage the purchase of high-end technology to promote company innovation. Without these support systems, the long-term survival of companies in competitive conditions will not be possible, thus jeopardising business strategies.

7.2 Conclusions, Limitations and Avenues for Further Research

In conclusion, internationalisation can create a high degree of uncertainty and destabilise companies' routines, requiring innovative and context-specific responses. Our study offers some guidelines on the internationalisation process. Specifically, our study demonstrates the importance of planning for companies to succeed in international markets. As is the case with all studies, there are limitations in this one too. These have to do with the small sample, which is unlikely to be representative of each sector of activity. It is therefore considered pertinent to extend the sample to a larger universe in order to achieve representativeness by sector. We can outline paths for future research and, given that the study is based only on Portuguese companies, we suggest a study with data from companies in other countries of origin, with which, from this research, they could provide other relevant information for researchers.

Acknowledgements. The authors acknowledge the financial support of ISLA Santarém. The second author also acknowledge Fundação para a Ciência e a Tecnologia (FCT) and COMPETE 2020 program for financial support to project UIDB/00048/2020.

References

1. Agostini, L., Filippini, R., Nosella, A.: Brand-building efforts and their association with SME sales performance. J. Small Bus. Manage. **53**(1), 161–173 (2015)
2. Ahimbisibwe, G., Ngoma, M., Nabatanzi-Muyimba, A., Kabagambe, L.: Entrepreneurial mindset and SME internationalisation in Uganda: the mediating role of international networking. Rev. Int. Bus. Strategy **33**(4), 669–690 (2023). https://doi.org/10.1108/RIBS-11-2021-0149
3. Baum, M., Schwens, C., Kabst, R.: International as opposed to domestic new venturing: the moderating role of perceived barriers to internationalisation. Int. Small Bus. J. **31**(5), 536–562 (2013). https://doi.org/10.1177/0266242611428343
4. Bianchi, C., Glavas, C., Mathews, S.: SME international performance in Latin America: the role of entrepreneurial and technological capabilities. J. Small Bus. Enterp. Dev. **24**(1), 176–195 (2017). https://doi.org/10.1108/JSBED-09-2016-0142
5. Cardoza, G., Fornes, G., Li, P., Xu, N., Xu, S.: China goes global: public policies' influence on small- and medium-sized enterprises' international expansion. Asia Pac. Bus. Rev. **21**(2), 188–210 (2015)
6. Casillas, J., Barbero, J., Sapienza, H.: Knowledge acquisition, learning, and the initial pace of internationalisation. Int. Bus. Rev. **24**(1), 102–114 (2015)
7. Chandra, Y., Styles, C., Wilkinson, I.: The recognition of first time international entrepreneurial opportunities: evidence from firms in knowledge-based industries. Int. Mark. Rev. **26**(1), 30–61 (2009)
8. Clavel San Emeterio, M., Juaneda-Ayensa, E., Fernández-Ortiz, R.: Influence of relationship networks on the internationalisation process: the moderating effect of born global. Heliyon **6**(1), e03148 (2020)
9. Cortellazzo, L., Bonesso, S., Gerli, F.: Entrepreneurs' behavioural competencies for internationalisation: exploratory insights from the Italian context. Int. J. Entrep. Behav. Res. (2020)

10. Dana, L., Grandinetti, R., Mason, M.: International entrepreneurship, export planning and export performance: evidence from a sample of winemaking SMEs. Int. J. Entrep. Small Bus. **29**(4), 602–626 (2016). https://doi.org/10.1504/IJESB.2016.079965
11. Gerschewski, S., Evers, N., Nguyen, A., Froese, F.: Trade shows and SME internationalisation: networking for performance. Manag. Int. Rev. **60**(4), 573–595 (2020)
12. Gerschewski, S., Lew, Y., Khan, Z., Park, B.: Post-entry performance of international new ventures: the mediating role of learning orientation. Int. Small Bus. J. **36**(7), 807–828 (2018)
13. Grandinetti, R., Mason, M.: Internationalisation modes other than exporting: the missing determinant of export performance. Eur. Bus. Rev. **24**(3), 236–254 (2012)
14. Haddoud, M., Jones, P., Newbery, R.: Export promotion programmes and SMEs' performance: exploring the network promotion role. J. Small Bus. Enterp. Dev. **24**(1), 68–87 (2017)
15. Kafouros, M., Buckley, P., Sharp, J., Wang, C.: The role of internationalisation in explaining innovation performance. Technovation **28**(1–2), 63–74 (2008). https://doi.org/10.1016/j.technovation.2007.07.009
16. Kline, R.: Principles and Practice of Structural Equation Modeling, 4th edn. The Guilford Press, New York (2016)
17. Knight, G., Moen, Ø., Madsen, T.: Antecedents to differentiation strategy in the exporting SME. Int. Bus. Rev. **29**(6), 101740 (2020)
18. Kriz, A., Welch, C.: Innovation and internationalisation processes of firms with new-to-the-world technologies. J. Int. Bus. Stud. **49**(4), 496–522 (2018). Palgrave Macmillan, Academy of International Business
19. Lu, J., Beamish, P.: The internationalisation and performance of SMEs. Strateg. Manag. J. **22**(6–7), 565–586 (2001). https://doi.org/10.1002/smj.184
20. Marôco, J.: Análise Estatística com o SPSS Statistics, 8th edn. ReportNumber (2021)
21. Martins, R., Farinha, L., Ferreira, J.: Analysing stimuli and barriers, failure and resilience in companies' internationalisation: a systematic and bibliometric review. Rev. Int. Bus. Strategy. (2021). https://doi.org/10.1108/ribs-07-2021-0103
22. Meliciani, V., Tchorek, G.: Internationalisation strategy, financial constraints and assets (in)tangibility. A study of euro area countries after the 2008 crisis. J. Int. Trade Econ. Dev. **28**(2), 161–188 (2019). https://doi.org/10.1080/09638199.2018.1514065
23. Morais, F., Ferreira, J.: SME internationalisation process: key issues and contributions, existing gaps and the future research agenda. Eur. Manag. J. **38**(1), 62–77 (2020)
24. Narooz, R., Child, J.: Networking responses to different levels of institutional void: a comparison of internationalising SMEs in Egypt and the UK. Int. Bus. Rev. **26**(4), 683–696 (2017). https://doi.org/10.1016/j.ibusrev.2016.12.008
25. Nummela, N., Saarenketo, S., Loane, S.: The dynamics of failure in international new ventures: a case study of Finnish and Irish software companies. Int. Small Bus. J. Res. Entrep. **34**(1), 51–69 (2016). https://doi.org/10.1177/0266242614539363
26. Paul, J.: Scope framework for SMEs: a new theoretical lens for success and internationalisation. Eur. Manag. J. **38**(2), 219–230 (2020)
27. Paul, A., Moktadir, M., Paul, S.: An innovative decision-making framework for evaluating transportation service providers based on sustainable criteria. Int. J. Prod. Res. **58**, 1–19 (2019)
28. Rastrollo-Horrillo, M., Martín-Armario, J.: Organisational barriers to nascent born-global growth: learning from the inside. J. Int. Entrep. **17**(3), 454–473 (2019)

29. Tob-Ogu, A., Kumar, N., Cullen, J.: ICT adoption in road freight transport in Nigeria - a case study of the petroleum downstream sector. Technol. Forecast. Soc. Chang. **131**, 240–252 (2018)
30. TrÇpczyński, P., Banalieva, E.: Institutional difference, organizational experience, and Foreign affiliate performance: evidence from Polish firms. J. World Bus. **51**(5), 826–842 (2016)
31. Varol, M., Ustaoğlu, F., Tokatlł, C.: Ecological risks and controlling factors of trace elements in sediments of dam lakes in the Black Sea Region (Turkey). Environ. Res. **205**, 112478 (2022)
32. Vuorio, A., Torkkeli, L., Sainio, L.: Service innovation and internationalisation in SMEs: antecedents and profitability outcomes. J. Int. Entrep. **18**(1), 92–123 (2020). https://doi.org/10.1007/s10843-019-00266-z

A New Probability Distribution: Theory, Simulation and Real Application

Nadia Hashim Al-Noor[1], Rafida M. Elobaid[2(✉)], and Suzan J. Obaiys[3]

[1] Department of Mathematics, College of Science, Mustansiriyah University, Baghdad, Iraq
nadialnoor@uomustansiriyah.edu.iq
[2] Faculty of Communication, Arts and Sciences, Canadian University Dubai, Dubai, United Arab Emirates
rafida@cud.ac.ae
[3] Deparoment of Computer System and Technology, Faculty of Computer Science and Information Technology, University of Malaya, 50603 Kuala Lumpur, Malaysia

Abstract. Developing and implementing innovative statistical distributions is an exciting field of study where different statistical models are established and proposed for data modeling in various sectors. The prime goal of this paper is to propose a novel probability distribution for analyzing real datasets. The new distribution is named the truncated Rayleigh odd Weibull Lomax (TROWL) distribution. Several statistical properties along with the entropy and reliability measures are derived. The maximum likelihood estimators of the unknown parameters are obtained. A simulation study is also provided. To illustrate the usefulness of TROWL distribution, a practical application is presented, where the comparison of the TROWL distribution is made with common competing probability models. Based on four information criterion quantities, it is observed that the new distribution is the best competing model for analyzing the considered real data.

Keywords: Lomax Distribution · Truncated Rayleigh Odd Weibull · Statistical Properties

1 Introduction

Lomax [1] pioneered the Lomax or Pareto II (shifted Pareto) distribution for modeling business failure data. This distribution is widely used in various domains, including income and wealth disparity, actuarial science, medical and biological sciences, engineering, and reliability modeling. The distributional features, estimates, and inference of the Lomax distribution are presented in many studies, see [2]. There are several approaches to characterizing the Lomax distribution. It is classified as a variant of the Pearson type VI distribution and a hybrid of the exponential and gamma distributions. This distribution has been proposed as a heavy-tailed alternative to the exponential, Weibull, and Gamma distributions. It is also connected to the Burr distribution family and, as a specific case, compound gamma distributions. The Lomax model, which belongs to the decreasing failure rate family, limits residual lives at advanced ages (see

© The Author(s), under exclusive license to Springer Nature Switzerland AG 2024
O. Gervasi et al. (Eds.): ICCSA 2024 Workshops, LNCS 14816, pp. 284–296, 2024.
https://doi.org/10.1007/978-3-031-65223-3_19

[2–4]). In recent years, there has been an increased interest in developing innovative generators for univariate continuous distributions. This entails adding one or more additional parameters to the existing distribution. These factors have been useful for investigating tail properties and improving the goodness-of-fit of the produced distribution. Several notable generator families can be found in [5–14]. The Lomax distribution has undergone substantial refining and extension to fit a wide range of situations and applications [15–18]. The main aim of this paper is to provide another version of extended Lomax distribution and to investigate several of its structural features. The novel distribution is proposed by adding two more parameters to the Lomax model. The rest of the paper is organized as follows. Section 2 contains the statistical methodology of the proposed distribution along with its cumulative distribution function (CDF), and probability density function (PDF). Section 3 discussed the distribution's essential statistical properties including reliability measures, linear form (expansion formula of the PDF), moments, moment-generating function, quantile function, and entropy. Further, estimates of the model's unknown parameters by maximum likelihood procedure are presented in Sect. 4 along with an empirical application. Section 5 provides a real application, while Sect. 6 offers some concluding remarks.

2 A New Model

In this section, the traditional Lomax is chosen as the baseline distribution to introduce a new member of the Truncated Rayleigh Odd Weibull-G (TROW − G) family proposed by Al-Noor and Sultan [19]. The CDF and PDF of the TROW − G with two parameters (scale parameter $\theta > 0$ and shape parameter $\beta > 0$) are given by

$$F(x;\theta,\beta,\psi) = \frac{1}{1-e^{-\theta/2}}\left(1-e^{-\frac{\theta}{2}\left(1-e^{-A^{\beta}}\right)^{2}}\right); A = \frac{G(x;\psi)}{\overline{G}(x;\psi)} \tag{1}$$

$$f(x;\theta,\beta,\psi) = \frac{\theta\beta g(x;\psi)G(x;\psi)^{\beta-1}}{\left(1-e^{-\theta/2}\right)\overline{G}(x;\psi)^{\beta+1}} e^{-A^{\beta}}\left(1-e^{-A^{\beta}}\right)e^{-\frac{\theta}{2}\left(1-e^{-A^{\beta}}\right)^{2}} \tag{2}$$

where $G(x;\psi)$ and $g(x;\psi)$ represent the CDF and PDF of any baseline distribution with vector parameter ψ and $\overline{G}(x;\psi) = 1 - G(x;\psi)$.

Consider the baseline CDF ($G(x;\psi)$) and PDF ($g(x;\psi)$) related to the two parameters "shape (α) and scale(δ)" Lomax distribution that is given by [16]

$$F(x;\alpha,\delta) = 1-(1+\delta x)^{-\alpha}\ ;\ x>0,\alpha,\delta>0 \tag{3}$$

$$f(x;\alpha,\delta) = \alpha\delta(1+\delta x)^{-(\alpha+1)}\ ;\ x>0,\alpha,\delta>0 \tag{4}$$

Substituting (3) and (4) in (1) and (2), with $A = \frac{G(x;\alpha,\delta)}{\overline{G}(x;\alpha,\delta)} = (1+\delta x)^{\alpha}-1$, the CDF and PDF of the new extended Lomax namely Truncated Rayleigh Odd Weibull Lomax (TROWL) with four parameters $(\theta,\beta,\alpha,\delta)$ are given by

$$F(x;\theta,\beta,\alpha,\delta) = \frac{1}{1-e^{-\theta/2}}\left(1-e^{-\frac{\theta}{2}\left(1-e^{-((1+\delta x)^{\alpha}-1)^{\beta}}\right)^{2}}\right); x>0,\theta,\beta,\alpha,\delta>0 \tag{5}$$

$$f(x;\theta,\beta,\alpha,\delta)=\frac{\theta\beta\alpha\delta}{\left(1-e^{-\theta/2}\right)}(1+\delta x)^{\alpha\beta-1}\left(1-(1+\delta x)^{-\alpha}\right)^{\beta-1}e^{-((1+\delta x)^{\alpha}-1)^{\beta}}$$
$$\left(1-e^{-((1+\delta x)^{\alpha}-1)^{\beta}}\right)e^{-\frac{\theta}{2}\left(1-e^{-((1+\delta x)^{\alpha}-1)^{\beta}}\right)^{2}} \tag{6}$$

Related to Fig. 1, the CDF's features are demonstrated in (a), and different PDF shapes are clearly shown in (b). As a result, it is noted that this new distribution is particularly suitable for modeling various positive data.

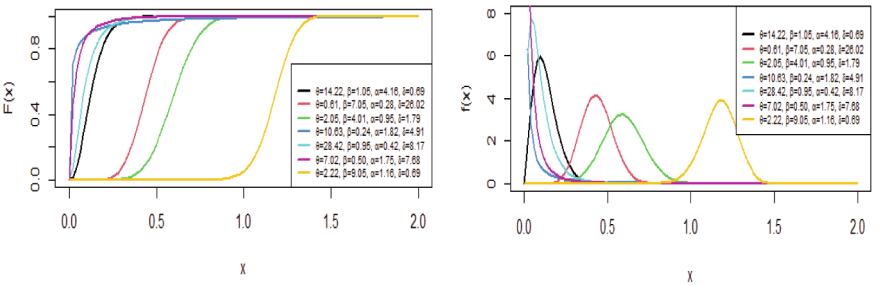

(a) (b)

Fig. 1. The TROWL (a) CDF (b) PDF plots with different parameter's values

3 Essential Statistical Properties

3.1 Reliability Measures

The reliability and hazard functions (RF and HF) are the most often used reliability measures in life data analysis and reliability engineering to assess a system's "component or item" operational performance. The forms of RF and HF of the TROWL are

$$R(x;\theta,\beta,\alpha,\delta)=1-F(x;\theta,\beta,\alpha,\delta)$$
$$=1-\frac{1}{1-e^{-\theta/2}}\left(1-e^{-\frac{\theta}{2}\left(1-e^{-((1+\delta x)^{\alpha}-1)^{\beta}}\right)^{2}}\right) \tag{7}$$

$$h(x;\theta,\beta,\alpha,\delta)=\frac{f(x;\theta,\beta,\alpha,\delta)}{R(x;\theta,\beta,\alpha,\delta)}$$
$$=\frac{\theta\beta\alpha\delta(1+\delta x)^{\alpha\beta-1}\left(1-(1+\delta x)^{-\alpha}\right)^{\beta-1}}{e^{-\frac{\theta}{2}\left(1-e^{-((1+\delta x)^{\alpha}-1)^{\beta}}\right)^{2}}-e^{-\frac{\theta}{2}}}\left(1-e^{-((1+\delta x)^{\alpha}-1)^{\beta}}\right)$$
$$e^{-((1+\delta x)^{\alpha}-1)^{\beta}-\frac{\theta}{2}\left(1-e^{-((1+\delta x)^{\alpha}-1)^{\beta}}\right)^{2}} \tag{8}$$

Related to Fig. 2, the reliability features are demonstrated in (a), and an aspect of the hazard function that can take on different shapes, such as increasing, decreasing, bathtub, skewed, J, and reversed-J, is shown in (b), indicating that the new distribution can be applied to analyze a variety of life data.

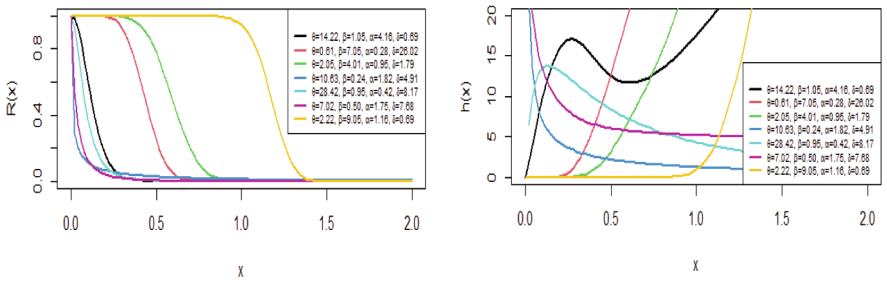

(a) (b)

Fig. 2. The TROWL (a) RF (b) HF plots with different parameter's values

3.2 Linear Form

The helpful expansion formula for PDF of the TROWL can be obtained using the following expansion formulas with some simple mathematical steps:

$(1-z)^a = \sum_{m=0}^{\infty}(-1)^m\binom{a}{m}z^m$; $\frac{1}{(1-z)^a} = \sum_{m=0}^{\infty}\binom{m+a-1}{m}z^m$ that valid for $|z| < 1, a > 0$; and $e^{-z} = \sum_{m=0}^{\infty}\frac{(-1)^m}{m!}z^m$. Thus, the PDF can be expanded to take the following form

$$f(x;\theta,\beta,\alpha,\delta)^E = \sum_{k,m=0}^{\infty}\xi_{(k,m)}\alpha\delta(1+\delta x)^{-(\alpha+1)}\left(1-(1+\delta x)^{-\alpha}\right)^{m+\beta(k+1)-1} \quad (9)$$

where

$$\xi_{(k,m)} = \frac{\theta\beta}{1-e^{-\frac{\theta}{2}}}\sum_{i,j=0}^{\infty}\frac{(-1)^{i+j+k}}{i!k!}(j+1)^k\binom{2i+1}{j}\left(\frac{\theta}{2}\right)^i\binom{m+\beta(k+1)}{m} \quad (10)$$

Further, the PDF in (9) can be expanded more by applying the Binomial expansion to be expressed as a linear representation of the baseline Lomax distribution, i.e.

$$\begin{aligned} f(x;\theta,\beta,\alpha,\delta)^E &= \sum_{k,m,s=0}^{\infty}\xi_{(k,m)}(-1)^s\binom{\beta(k+1)+m-1}{s}\alpha\delta(1+\delta x)^{-(\alpha(s+1)+1)} \\ &= \sum_{k,m,s=0}^{\infty}\xi_{(k,m)}\frac{(-1)^s}{s+1}\binom{\beta(k+1)+m-1}{s}\alpha(s+1)\delta(1+\delta x)^{-(\alpha(s+1)+1)} \\ &= \sum_{k,m,s=0}^{\infty}\xi_{(k,m)}\frac{(-1)^s}{s+1}\binom{\beta(k+1)+m-1}{s}g(x;\alpha(s+1),\delta)_L \end{aligned} \quad (11)$$

where $g(x;\alpha(s+1),\delta)_L$ represents the PDF of the traditional Lomax distribution with parameters $\alpha(s+1)$ and δ. That linear form plays an important role and will be used to obtain explicit expressions for the moments and moment generating function.

3.3 Moments and Moment Generating Function

The rth non-central moment can easily found regards linear form in (11)(11) as follows

$$E(X^r) = \sum_{k,m,s=0}^{\infty} \xi_{(k,m)} \frac{(-1)^s}{s+1} \binom{\beta(k+1)+m-1}{s} E(X^r)_{g(x;\alpha(s+1),\delta)_L}$$

where $E(X^r)_{g(x;\alpha(s+1),\delta)_L}$ represents the rth non-central moment of Lomax distribution with parameters $\alpha(s+1)$ and δ (see [16]). Therefore, the $r^{th}(r = 1,2,\ldots)$ moment of TROWL distribution for $\alpha(s+1) > r$ is given by

$$E(X^r) = \sum_{k,m,s=0}^{\infty} \xi_{(k,m)} \frac{(-1)^s}{s+1} \binom{\beta(k+1)+m-1}{s} \alpha(s+1)\delta^{-r} \frac{r!\Gamma(\alpha(s+1)-r)}{\Gamma(\alpha(s+1)+1)} \quad (12)$$

Based on (12), the moment generating function can be attained by applying its definition with the Maclaurin series as $\varphi_X(t) = E\left(e^{tX}\right) = \sum_{r=0}^{\infty} \frac{t^r}{r!} E(X^r)$, then

$$\varphi_X(t) = \sum_{k,m,s,r=0}^{\infty} \xi_{(k,m)} \frac{(-1)^s t^r}{s+1} \binom{\beta(k+1)+m-1}{s} \alpha(s+1)\delta^{-r} \frac{\Gamma(\alpha(s+1)-r)}{\Gamma(\alpha(s+1)+1)} \quad (13)$$

3.4 Quantile Function

The quantile function (QF), $Q(q)$ for $0 < q < 1$, is determined by solving the equation $F(Q(q)) = q$. Therefore, once calculating (5) for $Q(q)$ in terms of q yields the QF of the TROWL distribution as

$$Q(q) = x_q = \frac{1}{\delta}\left[\left(1 + \left\{-\ln\left(1 - \left(\frac{-2}{\theta}\ln\left(1 - \left(1 - e^{-\frac{\theta}{2}}\right)q\right)\right)^{\frac{1}{2}}\right)\right\}^{\frac{1}{\beta}}\right)^{\frac{1}{\alpha}} - 1\right] \quad (14)$$

The TROWL random variable can be generated from (14) by replacing q with U; where U denotes a standard Uniform random variable. The median can be gained easily with setting $q = \frac{1}{2}$. Other quantities, such as the inter-quantile range (IQR), skewness (Sk) and kurtosis (Ku) measures can be also computed by

$$IQR = Q\left(\frac{3}{4}\right) - Q\left(\frac{1}{4}\right); Sk. = \frac{Q\left(\frac{6}{8}\right) + Q\left(\frac{2}{8}\right) - 2Q\left(\frac{4}{8}\right)}{IQR}; Ku. = \frac{Q\left(\frac{7}{8}\right) - Q\left(\frac{5}{8}\right) + Q\left(\frac{3}{8}\right) - Q\left(\frac{1}{8}\right)}{IQR}.$$

3.5 Entropy

The entropy of a variable is a measure of variation in uncertainty that is commonly used in physics, tumor molecular imaging, and engineering. Shannon is discussed here due to its present applications, such as in simulations of laser dynamics and emergent events [20].

The Shannon entropy is specified by $S(X) = -E(ln(f(x))$. For more details about this entropy (see [11] and [20]). Recall (6), then

$$S(X) = -E(\ln(f(x;\theta,\beta,\alpha,\delta)) = \ln\left(\frac{1-e^{-\theta/2}}{\theta\beta\alpha\delta}\right) - (\alpha\beta-1)E(\ln(1+\delta x)) - (\beta-1)E\left(\ln\left(1-(1+\delta x)^{-\alpha}\right)\right) + E\left((1+\delta x)^{\alpha}-1\right)^{\beta} - E\left(\ln\left(1-e^{-((1+\delta x)^{\alpha}-1)^{\beta}}\right)\right) - \frac{\theta}{2}E\left(1-e^{-((1+\delta x)^{\alpha}-1)^{\beta}}\right)^{2} \quad (15)$$

The mathematical expectations can be calculated as follows:
Based on (9),

$$E(\ln(1+\delta x)) = \sum_{k,m=0}^{\infty} \xi_{(k,m)} \int_{0}^{\infty} \ln(1+\delta x)\,\alpha\delta\, e^{-(\alpha+1)\ln(1+\delta x)} \left(1-(1+\delta x)^{-\alpha}\right)^{m+\beta(k+1)-1} dx$$

Using the transformation $y = -(\alpha+1)\ln(1+\delta x)$ and then the expansion series $(1-z)^{a}$ with some mathematical simplification steps, the outcome is

$$E(\ln(1+\delta x)) = \sum_{k,m,s=0}^{\infty} \xi_{(k,m)} \frac{(-1)^{s}}{\alpha(s+1)^{2}} \binom{\beta(k+1)+m-1}{s} \quad (16)$$

Using series $\ln(1-z) = \sum_{m=1}^{\infty} \frac{1}{m} z^{m}$; $|z| < 1$ and the negative Binomial series, then

$$E\left(\ln\left(1-(1+\delta x)^{-\alpha}\right)\right) = \sum_{m=1}^{\infty}\sum_{r=0}^{\infty} \frac{(-1)^{r+1}}{m} \delta^{r} \binom{r+\alpha m-1}{r} E\left(X^{r}\right) \quad (17)$$

Using the Binomial series and expansion series $(1-z)^{a}$ with some mathematical simplification steps, then

$$E\left((1+\delta x)^{\alpha}-1\right)^{\beta} = \sum_{m,r=0}^{\infty} (-1)^{\beta-m} \delta^{r} \binom{\beta}{m} \binom{\alpha m}{r} E\left(X^{r}\right) \quad (18)$$

Using series $\ln(1-z)$, then

$$E\left(\ln\left(1-e^{-((1+\delta x)^{\alpha}-1)^{\beta}}\right)\right) = \sum_{m=1}^{\infty}\sum_{s=0}^{\infty} \frac{(-1)^{s+1}}{s!} m^{s-1} E\left((1+\delta x)^{\alpha}-1\right)^{\beta s} \quad (19)$$

$$E\left(1-e^{-((1+\delta x)^{\alpha}-1)^{\beta}}\right)^{2} = \sum_{m,s=0}^{\infty} \frac{(-1)^{s+m}}{s!} m^{s} E\left((1+\delta x)^{\alpha}-1\right)^{\beta s} \quad (20)$$

where $E((1+\delta x)^{\alpha}-1)^{\beta s}$ as in (18) (18) with βs instead of β, and $E(X^{r})$ as given in (12).

After substituting (16)–(20) in (15), the Shannon entropy of the TROWL is attained.

4 Estimation and Empirical Illustration

The maximum likelihood methodology is the most often used parameter estimate method due to its desirable features such as consistency, asymptotic efficiency, and invariance. Here, the maximum likelihood estimates (MLEs) of the unknown TROWL parameters are obtained and then investigated their performance via a simulation study.

Let $x_1, x_2, \ldots, x_n$ be a random sample of size n taken from the TROWL distribution with parameters $(\theta, \beta, \alpha, \delta)$. According to $f(\theta, \beta, \alpha, \delta)$ in (6), the likelihood and natural logarithm likelihood functions are given by

$$L = \prod_{i=1}^{n} \frac{\theta\beta\alpha\delta}{\left(1 - e^{-\theta/2}\right)} (1 + \delta x_i)^{\alpha\beta - 1} \left(1 - (1 + \delta x_i)^{-\alpha}\right)^{\beta - 1} e^{-((1+\delta x_i)^{\alpha} - 1)^{\beta}} \left(1 - e^{-((1+\delta x_i)^{\alpha} - 1)^{\beta}}\right) e^{-\frac{\theta}{2}\left(1 - e^{-((1+\delta x_i)^{\alpha} - 1)^{\beta}}\right)^2}$$

and

$$\begin{aligned} \ell = \ln(L) =& n \ln\left(\frac{\theta\beta\alpha\delta}{1 - e^{-\theta/2}}\right) + (\alpha\beta - 1) \sum_{i=1}^{n} \ln(1 + \delta x_i) \\ &+ (\beta - 1) \sum_{i=1}^{n} \ln\left(1 - (1 + \delta x_i)^{-\alpha}\right) - \sum_{i=1}^{n} \left((1 + \delta x_i)^{\alpha} - 1\right)^{\beta} \\ &+ \sum_{i=1}^{n} \ln\left(1 - e^{-((1+\delta x_i)^{\alpha} - 1)^{\beta}}\right) - \frac{\theta}{2} \sum_{i=1}^{n} \left(1 - e^{-((1+\delta x_i)^{\alpha} - 1)^{\beta}}\right)^2 \end{aligned}$$

To obtain the MLEs $\widehat{\theta}, \widehat{\beta}, \widehat{\alpha}$, and $\widehat{\delta}$, set the partial derivatives $\frac{\partial \ell}{\partial \theta}, \frac{\partial \ell}{\partial \beta}, \frac{\partial \ell}{\partial \alpha}, \frac{\partial \ell}{\partial \delta}$ to zero and solve numerically. After collecting the MLEs for the TROWL parameters, the next step is to conduct a simulation study to evaluate the estimate's performance. The empirical investigation is conducted with various combinations of parameter default settings and a 3000 i.i.d random sample created using formula (14) with $q = u$; $u \in U(0,1)$, and sample sizes $n = 15, 30, 60$, and 120. To quantify the performance of the MLEs of four parameters $(\Delta = \theta, \beta, \alpha, \delta)$, the mean square error (MSE) is used, where:

$MSE\left(\widehat{\Delta}\right) = \frac{1}{3000} \sum_{i=1}^{3000} \left(\widehat{\Delta}_i - \Delta\right)^2$. The simulation outcomes are offered in Tables 1 and 2. All numerical illustrations are made using the programming language R. From the empirical results, it is noted that as sample size increases, the MSE values seem to decrease as expected, demonstrating the consistency of the estimators.

Table 1. The MSE values of the parameters with $\theta = 0.8$

β	α	δ	n	$MSE\left(\hat{\theta}\right)$	$MSE\left(\hat{\beta}\right)$	$MSE(\hat{\alpha})$	$MSE\left(\hat{\delta}\right)$
0.8	0.8	0.8	15	0.15376	0.04660	0.08556	0.13058
			30	0.13982	0.02417	0.05873	0.10991
			60	0.11774	0.01410	0.03949	0.08264
			120	0.07146	0.00848	0.02328	0.05906
		3.8	15	2.54589	0.05636	0.04664	0.57484
			30	2.04800	0.02533	0.02507	0.48608
			60	1.56499	0.01299	0.01537	0.36576
			120	1.21595	0.00709	0.00968	0.25682
	3.8	0.8	15	2.54359	0.05585	1.03891	0.04524
			30	1.96029	0.02426	0.73120	0.02168
			60	1.53644	0.01253	0.45651	0.01415
			120	1.17183	0.00695	0.28833	0.00812
		3.8	15	4.77249	0.05847	1.51392	0.65831
			30	3.64465	0.02865	1.12342	0.47772
			60	2.40356	0.01453	0.58570	0.36005
			120	1.71234	0.00817	0.35195	0.24300
3.8	0.8	0.8	15	1.00856	0.67216	0.00455	0.00883
			30	0.95736	0.30337	0.00245	0.00512
			60	0.69499	0.14705	0.00143	0.00288
			120	0.56562	0.07244	0.00102	0.00222
		3.8	15	1.31644	0.73126	0.00244	0.10742
			30	1.21175	0.31548	0.00112	0.05771
			60	1.01482	0.15487	0.00064	0.03738
			120	0.81098	0.07549	0.00040	0.02300
	3.8	0.8	15	1.25079	0.82274	0.05770	0.00295
			30	1.16146	0.34628	0.03613	0.00163
			60	1.07692	0.16451	0.02338	0.00089
			120	0.97032	0.08258	0.01847	0.00066
		3.8	15	1.57937	0.88882	0.10691	0.10398
			30	1.55206	0.35128	0.06908	0.06453
			60	1.40266	0.17155	0.04836	0.04292
			120	1.08332	0.08965	0.03923	0.03283

Table 2. The MSE values of the parameters with $\theta = 3.8$

β	α	δ	n	$MSE\left(\hat{\theta}\right)$	$MSE\left(\hat{\beta}\right)$	$MSE\left(\hat{\alpha}\right)$	$MSE\left(\hat{\delta}\right)$
0.8	0.8	0.8	15	0.71852	0.05142	0.13726	0.20735
			30	0.53042	0.02325	0.07076	0.14500
			60	0.49501	0.01238	0.04169	0.10353
			120	0.40646	0.00754	0.02913	0.07431
		3.8	15	2.59504	0.04668	0.06750	1.02020
			30	2.16270	0.01871	0.03816	0.83027
			60	1.56751	0.00890	0.01811	0.64045
			120	1.44441	0.00496	0.01164	0.48159
	3.8	0.8	15	3.32293	0.04563	1.36966	0.05166
			30	2.33285	0.01866	1.11777	0.02744
			60	1.63680	0.00886	0.68167	0.01550
			120	1.24378	0.00430	0.41350	0.01032
		3.8	15	6.13892	0.04687	1.83802	0.86736
			30	4.39848	0.01992	1.39589	0.63768
			60	2.64507	0.00933	0.84043	0.46963
			120	1.79249	0.00486	0.51075	0.34381
3.8	0.8	0.8	15	0.90275	0.83419	0.00505	0.00923
			30	0.74397	0.32512	0.00253	0.00525
			60	0.61284	0.14825	0.00156	0.00325
			120	0.52579	0.07165	0.00113	0.00249
		3.8	15	1.14603	0.87652	0.00328	0.12181
			30	1.04420	0.34476	0.00110	0.05357
			60	0.92939	0.15582	0.00061	0.03218
			120	0.78274	0.07310	0.00036	0.02452
	3.8	0.8	15	1.07682	0.95370	0.07336	0.00355
			30	1.05458	0.37302	0.03491	0.00155
			60	0.87862	0.16460	0.02292	0.00085
			120	0.75269	0.07604	0.01579	0.00060
		3.8	15	1.73248	0.96797	0.11104	0.09848
			30	1.73136	0.36938	0.05497	0.05668
			60	1.58875	0.16517	0.03986	0.03819
			120	1.17608	0.07534	0.03401	0.02842

5 Real Application

The data represent a medical dataset that includes 42 values indicating deaths from leukemia, the most common type of cancer among children under the age of 15, as reported by the Iraqi Ministry of Health and Environment's Central Children's Teaching Hospital from January 1, 2021, to August 31, 2022 (for more details about the data, see [21]). These values are:

"264, 91, 21, 5, 2, 515, 33, 154, 17, 60, 65, 534, 1, 177, 15, 16, 562, 23, 4, 219, 22, 2, 431, 34, 485, 145, 29, 22, 180, 241, 25, 3, 158, 64, 111, 131, 5, 45, 17, 83, 258, 594".

Table 3 exhibits the data's basic descriptive statistics, indicating data to be right-skewed and leptokurtic. The proposed distribution's fitting behavior is compared with the baseline and extended Gompertz linked to different families: Beta-G [5], Kumaraswamy-G [7], Exponentiated Generalized-G [8], Weibull-G [9], and Gompertz-G [10] represented by BL, KuL, EGL, WL, and GoL, respectively. It is worth noting that the p-values of KS (Kolmogorov Smirnov) goodness of fit for the competitive distributions are significant (more than 0.05). Furthermore, the fitted competitive distributions are evaluated using four information criteria (IC). The mathematical forms of ICs (Akaike, Consistent Akaike, Bayesian, and Quinn and Hanan) are given with the sample size (n), number of the parameters (p), and the natural log-likelihood function assessed at ML estimates ($\hat{\ell}$) by:

$$AIC = -2\left(\hat{\ell} - p\right); CAIC = -2\left(\hat{\ell} - np/(n-p-1)\right); BIC = -2\hat{\ell} + p\ln(n);$$

and $HQIC = -2\left(\hat{\ell} - p\ln(\ln(n))\right)$. The lower value for these IC indicates a better model. Table 4 displays the computed MLE values for all models' unknown parameters. The IC results are presented in Table 5. The TROWL distribution has the lowest IC values compared to other competitive distributions, giving it the best fit for the data under consideration. Furthermore, the plots of the estimated PDFs and CDFs in Fig. 3 demonstrate TROWL's best fitting.

Table 3. Basic descriptive statistics for the dataset

No. of Observations	Mean	Median	Sk	Ku	IQR	Min	Max
42	139.6	62	1.49	1.10	172.8	1	594

Table 4. The MLE values for real data

Dist.	$\widehat{\theta}$	$\widehat{\beta}$	$\widehat{\alpha}$	$\widehat{\delta}$
TROWL	1.873245142	0.408337976	2.226987477	0.005220733
BL	15.16697169	17.41461274	0.089978350	23.49742675
KuL	0.778873302	5.107866512	0.393857533	0.003247987
EGL	1.525472892	0.720553488	1.525472857	0.003677375
WL	0.774736320	0.026015526	0.123750038	0.002238511
GoL	0.150395300	2.452011600	0.263685900	0.760978600
L	—	—	1.118514210	0.015501820

Table 5. The IC for fitting real data

Dist.	NLL	AIC	CAIC	BIC	HQIC
TROWL	244.2122	496.4244	497.5054	503.3750	498.9721
BL	248.0107	504.0213	505.1024	510.9720	506.5690
KuL	245.4805	498.9609	500.0420	505.9116	501.5086
EGL	245.4544	498.9088	499.9899	505.8595	501.4565
WL	245.4091	498.8182	499.8993	505.7689	501.3659
GoL	244.2726	496.5451	497.6262	503.4958	499.0928
L	246.7595	497.5189	497.8266	503.9943	498.9928

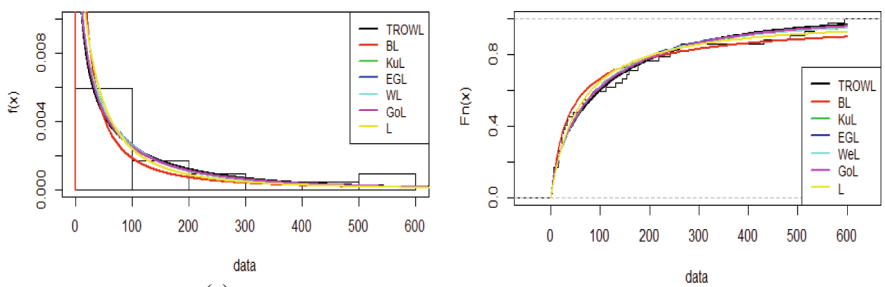

Fig. 3. The TROWL and competitive distributions (a) histogram (b) empirical CDF plots.

6 Conclusion

The Lomax distribution has been widely used in a variety of contexts. Although the Lomax distribution was originally designed to represent business failure data, it has since been utilized for dependability modeling and life testing. In contrast, the Lomax distribution has served as the basis for several generalizations and extensions. Here, a new extended Lomax distribution with four parameters, the Truncated Rayleigh Odd Weibull Lomax (TROWL), is introduced. Some important statistical functions and features are discussed, including the quantile function, linear representation, moments, moment-generating function, median, simulated data, reliability measures, and entropy. The maximum likelihood method is used to estimate the distribution parameter. The new distribution's abilities and flexibility are demonstrated through simulation and real-life applications. The estimators' performance is measured using mean square error. The simulation results demonstrated the flexibility and consistency of the maximum likelihood estimates, and for various information criteria, the real-life application results demonstrated that the proposed distribution outperformed other considered distributions for representing deaths from leukemia among children under the age of 15 in Iraq from January 1, 2021, to August 31, 2022. Because of this versatility, the TROWL distribution may be used in a larger range of applications. Furthermore, as an open subject for future research, various parameter estimate approaches such as moments, least squares, and Bayesian employing informative priors might be examined.

References

1. Lomax, K.S.: Business failures: another example of the analysis of failure data. J. Am. Stat. Assoc. **49**(268), 847–852 (1954)
2. Tahir, M.H., Gauss, M.C., Mansoorz, M., Zubair, M.: The Weibull-Lomax distribution: properties and applications. Hacettepe J. Math. Statist. **44**(2), 455–474 (2015)
3. Chahkandi, M., Ganjali, M.: On some lifetime distributions with decreasing failure rate. Comput. Stat. Data Anal. **53**, 4433–4440 (2009)
4. El-Din, M.M., Okasha, H.M., Al-Zahrani, B.: Empirical bayes estimators of reliability performances using progressive type-ii censoring from lomax model. J. Adv. Res Appl. Math. **5**(1), 74–83 (2013)
5. Eugene, N., Lee, C., Famoye, F.: Beta-normal distribution and its applications. Commun. Statist.-Theory Meth. **31**, 497–512 (2002)
6. Zografos, K., Balakrishnan, N.: On the families of beta-and gamma-generated generalized distribution and associated inference. Statist. Methodol. **6**, 344–362 (2009)
7. Cordeiro, G.M., de Castro, M.: A new family of generalized distributions. J. Stat. Comput. Simul. **81**, 883–893 (2011)
8. Cordeiro, G.M., Ortega, E.M.M., da Cunha, D.C.C.: The exponentiated generalized class of distributions. J. Data Sci. **11**, 1–27 (2013)
9. Bourguignon, M., Silva, R.B., Cordeiro, G.M.: The Weibull-G family of probability distributions. J. Data Sci. **12**(1), 53–68 (2014)
10. Alizadeh, M., Cordeiro, G.M., Pinho, L.G.B., Ghosh, I.: The Gompertz-G family of distributions. J. Statist. Theory Pract. **11**(1), 179–207 (2017)
11. Hesham, R., Jamal, F., Othman, S., Hamedani, G.G.: The transmuted Gompertz-G family of distributions: properties and applications. Tbilisi Math. J. **11**, 47–67 (2018)

12. Abid, S.H., Al-Noor, N.H., Boshi, M.A.A.: On the generalized inverse Weibull distribution. AIP Conf. Proc. **2086**, 030002 (2019)
13. Dey, S., Nassar, M., Kumar, D., Alzaatreh, A., Tahir, M.H.: A new lifetime distribution with decreasing and upside-down bathtub-shaped hazard rate. Statistica (Bologna) **4**, 399–426 (2019)
14. Mandouh, R.M., Mahmoud, M.R., Abdelatty, R.E.: A new (T-Xθ) family of distributions: properties, discretization and estimation with applications. Sci. Rep. **14**, 1–22 (2024)
15. Cordeiro, G.M., Ortega, E.M., Popovi´c, B.V., Pescim, R.R.: The Lomax generator of distributions: properties, minification process and regression model. Appl. Math. Comput. **247**, 465–486 (2014)
16. Shabbir, M., Riaz, A., Gull, H.: Rayleigh Lomax distribution. J. Middle East North Africa Sci. **4**(12), 1–4 (2018)
17. Hadi, H.H., Al-Noor N.H.: Truncated exponential Marshall Olkin Lomax distribution: properties, entropies, and applications. In: 6th Local Scientific Conference-3rd Scientific International, pp. 1–12. AIP Conference Proceedings 2414, 040054, Iraq (2023)
18. Al-Zahrani, B., Sagorb, H.: The Poisson-Lomax distribution. Revista Colombiana de Estadística **37**(1), 223–243 (2014)
19. Al-Noor, N.H., Sultan, A.J.: Truncated Rayleigh odd Weibull exponential distribution with application to COVID-19 data. In: Contemporary Information Technology and Mathematics (ICCITM). 8th International Conference, pp. 410–416. IEEE, Iraq (2022)
20. Guisado, J.L., Jiménez-Morales, F., Guerra, J.M.: Application of Shannon's entropy to classify emergent behaviors in a simulation of laser dynamics. Math. Comput. Model. **42**, 847–854 (2005)
21. Ghasaq, H.S., Hassan I.: Study of new exponential-Weibull distribution about children with Leukemia. pp. 1–12. AIP Conference Proceedings 3036, 040030, Iraq (2024)

Computational Optimization and Applications (COA 2024)

Digitalization of Restrictions for Assigning Workstations

Francisca Santos[1], Ana Ribeiro[2(✉)], and Carina Pimentel[1,3]

[1] Production and Systems Department, University of Minho, Braga, Portugal
[2] COMEGI, Lusiada University, Vila Nova Famalicão, Portugal
anacecidias@gmail.com
[3] ALGORITMI Research Centre/LASI, University of Minho, Braga, Portugal

Abstract. Industry 4.0 has made it possible to better integrate and streamline different stages of the production process mainly through the support of a collection of technologies. One of these technologies that might give businesses a competitive edge is digitalization, which can improve the effectiveness of corporate operations. This paper reports a research carried out in a Bosch factory, in the division responsible for Termotechnology, which designs, manufactures, and sells water and heating solutions for homes. Digitalizing the process related to operator allocation to workstations was the project's main goal. In order to do this, a platform was created to compile all the data required for assigning workers to workstations based on facts, increasing transparency in the process by informing platform users of each worker's degree of training and ergonomic restrictions. Another objective was to reduce the Full-Time Equivalent indicator. A pilot was run in one of the production lines of the factory to validate the developed platform. Lean tools and the action-research approach were used to address and accomplish the goals. Outsystems platform was used in the development of the application in addition to these tools. The outcomes showed that the operator allocation procedure using the new platform took less time overall, saving around 20 min per allocation. The division saw a decrease in assembly mistakes and rework, easier access to the information needed for allocation, and a shift in the allocation process from one based on empirical knowledge to one based on facts when this platform was implemented on the factory floor.

Keywords: Digitalization · Technologies · Industry 4.0 · Lean · Action-Research

1 Introduction

Beginning in the 20th century, the industrial sector was marked by a rapid growth and fundamental changes in the ways that goods or services are manufactured or delivered. These changes are not superficial or minor but rather deep and impactful, often involving the adoption of new technologies. In the 1990s, developed nations embarked on a technological revolution, integrating information and communication technologies into industrial processes. This integration required the development of methodologies to connect information systems effectively. At the industrial level, machine-to-machine communication is highly helpful for identifying production faults, facilitating continuous improvement, and simplifying information flows [1].

© The Author(s), under exclusive license to Springer Nature Switzerland AG 2024
O. Gervasi et al. (Eds.): ICCSA 2024 Workshops, LNCS 14816, pp. 299–312, 2024.
https://doi.org/10.1007/978-3-031-65223-3_20

The advancement of information technology enables industrial processes to reach new heights. This new development allows organizations to enhance the present environment and satisfy clients through new forms, employing new business models to create value and make cash for themselves [2].

The concept of "smart factories," which refers to manufacturing with cutting-edge technology like automation, artificial intelligence, and the Internet of Things (IoT), was introduced by Industry 4.0. This sector has elevated intelligent technology to the forefront of production. Furthermore, Industry 5.0 will promote more human-smart system collaboration. Therefore, it is crucial to understand the effects of past industrial revolutions that have occurred globally in order to comprehend how drastic changes affect industry. The fourth industrial revolution's innovations are upending industries and generating new opportunities for wealth creation. By exchanging knowledge, digital networks make the development and transportation of physical goods easier. Producing digital goods is quite cheap. Factory workers are already feeling the effects of Industry 4.0, and in order to continue to be important to their employers in the future, they will need to pick up new skills [3].

Lean 4.0 is a new iteration of Lean that has evolved as digitalization becomes the norm in this connected age. Combining Industry 4.0 technology with lean manufacturing concepts enables a thorough exploration of the advantages of both paradigms [1].

Production systems have undergone a major transformation thanks to Industry 4.0, which is defined by real-time integration in global value chains. Processes and procedures may be automated using Lean 4.0 to enable real-time analysis and intervention. Digital technologies are developing quickly, which is driving the creation of new industrial techniques to detect and eliminate waste [4].

Three key ideas come to light in this context: digitization, digital transformation, and digitalization. These concepts, while related, have distinct meanings depending on where an organization is in its digital journey. Converting manual readings to computerized ones is becoming more widespread in businesses, transferring information from analog to digital form through the process of digitization. There are several advantages to digital, including time savings, improved productivity, and higher-quality output [5].

Digital transformation involves a shift in company strategy and a customer-focused approach, which enables processes to be streamlined and automated to enhance business strategy and increase efficiency.

Digitalization is the process of using digitalization to enhance corporate processes and provide chances for value creation. It encompasses more than simply digital technology and data. Organizations have the ability to lower lead times, boost internal efficiency, connect value chains, and provide improved operational control. In the area of industrial manufacturing, digitalization has garnered more attention than digitization [6].

The Bosch group is one of those that relies on the most cutting-edge and inventive techniques, hoping to position itself as the market leader in innovation regarding both its goods and operations, given the technological competition felt amongst organizations.

In information technologies it is thought that smart working practices depend on utilizing state-of-the-art technology to support business intelligence, communication, and product and service delivery [7].

Industry 5.0 aims to combine technology with human creativity and intuition in order to create a more flexible and collaborative manufacturing environment. Cutting-edge technology like human-cooperative robotics, augmented and virtual reality, and real-time monitoring and feedback systems make this cooperation possible. This is in contrast to Industry 4.0, which integrates, for the past several years, manufacturers experimenting with integrating digital technologies such as IoT, cloud computing, automation algorithms, and software-as-a-service into their internal production processes [8, 9].

The benefits of Industry 5.0 include increased efficiency, improved quality assurance, sustainability, increased worker safety, increased consumer happiness, affordability, a competitive advantage, increased innovation, and good social impact [10].

Musculoskeletal diseases associated with the workplace that are caused by factors such as job performance and surroundings, or that worsen or prolong the illness, are known as work-related musculoskeletal disorders (WMSD). An evaluation of the data about WMSD was released in 1997 by the National Institute for Occupational Safety and Health. They concluded that among the job situations that may develop WMSD are routine overhead lifting of large things, everyday exposure to whole-body vibration, working with the neck in a chronic flexion position, and performing repetitive, forceful activities. Employers bear significant costs from musculoskeletal problems, including reduced productivity, absenteeism, and higher medical, disability, and worker's compensation expenses [11].

To solve the problem of human resource assignment, [12] highlights the use of optimization techniques. These optimization-based approaches help find the best combination of skills, availability, and costs for human resources. They aim to maximize efficiency and productivity by assigning the most appropriate professionals to the relevant tasks, considering time and cost constraints.

In addition [12] provides practical guidance for human resource management in projects, with a focus on efficient assignment of professionals. Through optimization techniques and continuous analysis, the aim is to achieve the best combination of skills, availability, and costs, ensuring project success and team efficiency.

2 Project Context and Diagnostic

This research emerged from a practical context due to the aim of the company to improve the operator's assignment to workstations, by developing a digital platform using low-code that compiles data about ergonomic limitations and skills of operators. It is a data-driven platform that enhances the decision-making process by showing detailed, relevant information with a user-friendly interface. The need comes from the increasing growth of Bosch, such as a new production line and, consequently, the hiring of new operators.

Furthermore, with the manual process, there is a high risk of assigning operators without the required training level for a given workstation, as well as of assigning operators with ergonomic limitations to an inadequate workstation, considering their ergonomic condition. It is important to understand that the risk is for both the client and the company.

Additionally, owing to the complexity of operations at the workstations, the diversity of workstations, and the usual rotation of operators, it was necessary to establish a

platform to manage them, addressing their specific needs. Associating the assignment based on facts enhances transparency in the process.

The aim of this study was to examine the potential benefits of digitalization for ordinary tasks. The overall goals were:

- Establish a platform that compiles all operator information;
- Assign operators based on data and facts;
- Provide high transparency regarding operator situations, including skills and ergonomic limitations;
- Boost productivity by allowing operators to be more flexible; and
- Decrease the capacity needed to plan and assign operators and the FTE (full-time equivalent) indicator.

It is anticipated that the creation of a digital platform will accomplish the following particular goals:

- Establish connections between operators and workstations;
- Deploy the operator assignment module on the manufacturing line;
- Test the platform in an actual working setting.

The following issues were noted:

- There is no binding assignment of operators, and they are not documented;
- Operators' assignment is not explicitly based on training level for a given job or ergonomic circumstances pertaining to the operator or workstations.

The research approach used to meet the project goals was action research. First, the research team met with the industrialization team of the boiler production line to ascertain the demands for digitalization before beginning to build the real project. The members of this team are in charge of industrial engineering, mechanical engineering, and times and methods measurement.

After that, a review of currently under-construction digital platforms was done, and it was found that the Skillinx platform was the most suitable to satisfy the demands and requirements of the industrialization team. The tool known as Skillinx was created by Bosch Terotechnology in Aveiro and is anticipated to be used in all departments and production lines inside the Aveiro factory, in addition to all other Bosch factories now in operation around the globe.

After that, a brainstorming session was held to decide which functions should be created in order to satisfy the list of prerequisites that had been previously established. The people in charge of building Skillinx and those in charge of digitalizing internal processes participated in this brainstorming session. A series of in-depth needs emerged from many brainstorming sessions and will be provided in the comprehensive project description.

Formalizing the criteria was followed by an analysis and diagnosis of the existing state of affairs. Since the operators' assignment team will be using the Skillinx platform in the future, negotiations with them were necessary at this point. Semi-structured interviews with the assigned point of contact in each of Bosch's value streams were used to diagnose the current state of affairs. Then, Outsystems low-code software was used to

construct the worker assignment to workstations and worker check-in modules that are components of the Skillinx platform.

After developing the two Skillinx platform modules, it was concluded that to evaluate the viability of the Skillinx platform and obtain reliable results, it would be better to implement it in a small production line that already has all the software required for the Skillinx platform. As a result, Skillinx was launched in the boiler production line, as a pilot project.

In order to determine whether additional recruits were required, each area manager needed to be able to view the availability of workers from other areas, their capabilities, and their ergonomic restrictions. Line managers' familiarity with the operators was the basis for the loaning. They would choose an operator for a certain task after reviewing the training records and being aware of the ergonomic constraints.

This project's development is necessary in light of the aforementioned considerations in order to reduce the possibility of placing operators at a workstation without the necessary training or ergonomic constraints.

3 Improvement Proposals

The platform that was chosen, called Skillinx, enables operators to integrate pertinent data models and data sourcing across various dimensions. This allows managers and manufacturing support teams to have a new management tool that will likely improve operator engagement and well-being, in addition to enhancing performance.

A multidisciplinary team's knowledge was considered when developing the requirements. During this time, it became clear that an ergonomic assessment was necessary, taking into account the tasks performed at the workstation and the limitations of the operators, given the heavy and large nature of the product that needed to be assembled. Process leaders, suggestions made it necessary to design a check-in procedure that guarantees flexibility across workstations. The assignment manager can see who is at the workstation thanks to the check-in system, and employees may be informed of any changes that may occur during the process, such as a reference change, thanks to flexibility.

3.1 Requirements

The team as a whole recommended the inclusion of the training requirement since it is necessary to have access to and stay up-to-date with all information pertaining to each employee's training and skills. The fulfillment of these conditions was created using the Outsystems low-code platform, which subsequently prompted the development of modules that were included in Bosch Aveiro's in-house platform, Skillinx.

Table 1 gives a summary of the compliance with these requirements.

A compilation of all the requirements used in the construction of the modules may be seen in Table 2. Note that the focus of this research is on the addition of new functionalities to the already existing Skillinx platform, namely regarding workers assignment to workstations and workers check-in.

Table 1. Requirements definition to digitalize the process.

Digitalization Requirement	Description
Training support	Due the line dimension (quantity of workers) and the fluctuation of associates it is important to digitalize this part
Ergonomics evaluation	Representation of ergonomic limitations per worker
Check-in	Tool that allows to map operations/workstations that each worker has already done and develop a matrix of competencies that support the rotation
Flexibility	To make it possible to make changes quickly and easily in the process, whether it is the Exchange of references or Exchange of tasks. This change should be easily perceived by workers

Table. 2. Requirements resume board.

Requirement	When used	Skillinx Status
Introduce data about lines and workstations of each work center	System startup	Functionality already providedin Skilinx (Augmanity)
Make ergonomic evaluation of each workstation (ergonomic profile)		Functionality already providedin Skilinx (Augmanity)
Define necessary skills per workstation		Functionality already providedin Skilinx (Augmanity)
Introduce workers data into the system (name, number, medical and ergonomic evalutation, and skills)		Functionality already providedin Skilinx (Augmanity)
Assign workers for each workstation, on each line	Previously Friday's	New: adjustments to the allocation of people to workstations
Workers begin to arrive, do the "Plant Check-in" and are directed to the respective work center/line/workstation	Monday's 05:45	New: Plant Check-in
Last minute absence management	Monday's 05:46	New: adjustments to the allocation of people to workstations
Workstation check-in - last validation that this worker was assign to this workstation	Monday's 05:47	Functionality already providedin Skilinx (Augmanity)
Update worker skills	"Master Data" Update	
Updating of the medical assessment or ergonomics evaluation		

The subsequent procedure for the future was conceived when the criteria were put into practice. The design of the future worker assignment process is shown in Fig. 1, and it has been defined by using the BPMN notation.

3.2 Skillinx

The development of the modules in Outsystems to integrate into Bosch's internal platform, Skillinx, consisted of the process of designing, programming, and configuring the

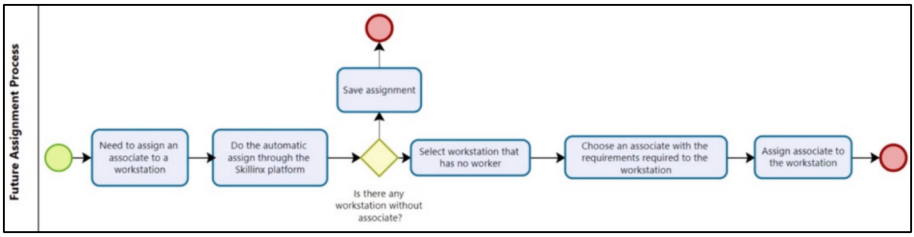

Fig. 1. New process: Future worker assignment.

platform according to the established requirements and objectives. On the other hand, the physical implementation of the Skillinx platform on the gas boiler production line aimed to ensure the proper functioning of the platform on the physical computers of the line. This involved hardware installation and integration with existing systems necessary for the platform to work correctly. These two phases, platform development and physical implementation, are interconnected processes and depend on each other to achieve a complete, functional and optimized solution.

There is information about the workstations and operators available on the newly created platform. The information that was accessible about the workstation included an ergonomic assessment of the workstations and a description of the necessary responsibilities and abilities.

The information that was accessible to operators included: endorsement; physical and psychological impairments; and completed training. The Skillinx platform further facilitates the scheduling and administration of absences. Therefore, two modules were made in order to gather the information mentioned: Worker Assignment and Check-in.

The two platforms, Outsystems and Skillinx, are described here in order to set the tools used in project development in perspective and the potential optimized results.

A software development methodology known as low-code helps programmers create apps with minimal human coding. With low-code, Outsystems programmers utilize a graphical language that is model-driven and has a drag-and-drop interface instead of typing code by hand, like in a traditional coding environment, to create software.

Skillinx is a cutting-edge, all-encompassing platform that integrates pertinent data models and sources from operators across multiple dimensions. Succinctly, Skillinx provides new tools to engage operators, provide them with personalized context assistance, and facilitate new procedures and interactive tools to enhance operator well-being. By utilizing modern digital technology to create a healthier and better industrial environment and by optimizing conventional human resource management techniques, these tools increase worker productivity.

Skillinx is an innovative holistic platform that integrates workers' relevant data models and data sources across multiple dimensions in order to provide managers and manufacturing support teams with new management tools that enable optimize worker well-being and engagement, among other things, which are likely to improve performance and attrition rates.

These tools increase human productivity by creating a better and healthier production environment using new digital technology and enhancing basic human resource management procedures.

Furthermore, Skillinx integrates non-structured data into a structure management decision platform, allowing for current situation analysis, future scenario planning, and assistance for both preventative and corrective measures. Skillinx also encourages workers to collaborate in decision-making and communicate more effectively using digital technologies.

Skillinx has six main modules, presented in Fig. 2.

The modules functionalities are:

- The workstation is responsible for ergonomic evaluation and digital work instructions;
- Skills Requirements (Workstation Level), Roles and Skills Definition, and Chemical Handling;
- Organizational modules are responsible for survey definition and communication management;
- Machine Interface is responsible for guaranteeing the software used to show the check-in modules in the machines;
- Worker skills is responsible for skills management, endorsement, and role definition required from operators;
- Worker physical evaluation is responsible for operator limitations regarding ergonomic evaluation and chemical intolerances.

The introduction of smart, connected, and autonomous digital and physical technologies such as IoT and robotics has had, and will continue to have, a significant impact on shop floor operations. As a result, in order to build action plans that clarify performance and HR well-being, we must first understand the technology underlying Industry 4.0 and how it impacts the work environment as well as the workers themselves.

3.3 Worker Assignment Module

The objective to developing this module was to facilitate the process of assignment of the workers to the workstations in a production line context. This module is intended to assist managers in managing their teams by enabling them to assign their workers to the multiple workstations of the lines they are responsible for. As already mentioned, this assignment is based on factual considerations such as ergonomic limitations and training conditions.

This module allows managers to assess which workers are most suitable for specific workstations, considering the skills level required to operate them, as well as the MARZC evaluation, a risk assessment methodology by corporal zone.

The left side of interface configuration developed in Outsystems can be seen in Fig. 3, and the right side in Fig. 4.

Regarding to the workers, it is possible to filter them according to area, sub-area, work center, line and shift or search by worker name. Once selected the filters for the working area, it is possible to filter the list of workers by those who have already been assigned to a workstation, therefore closing the gap for errors within the process of worker assignment. Also, it is possible to filter by those who have already done area

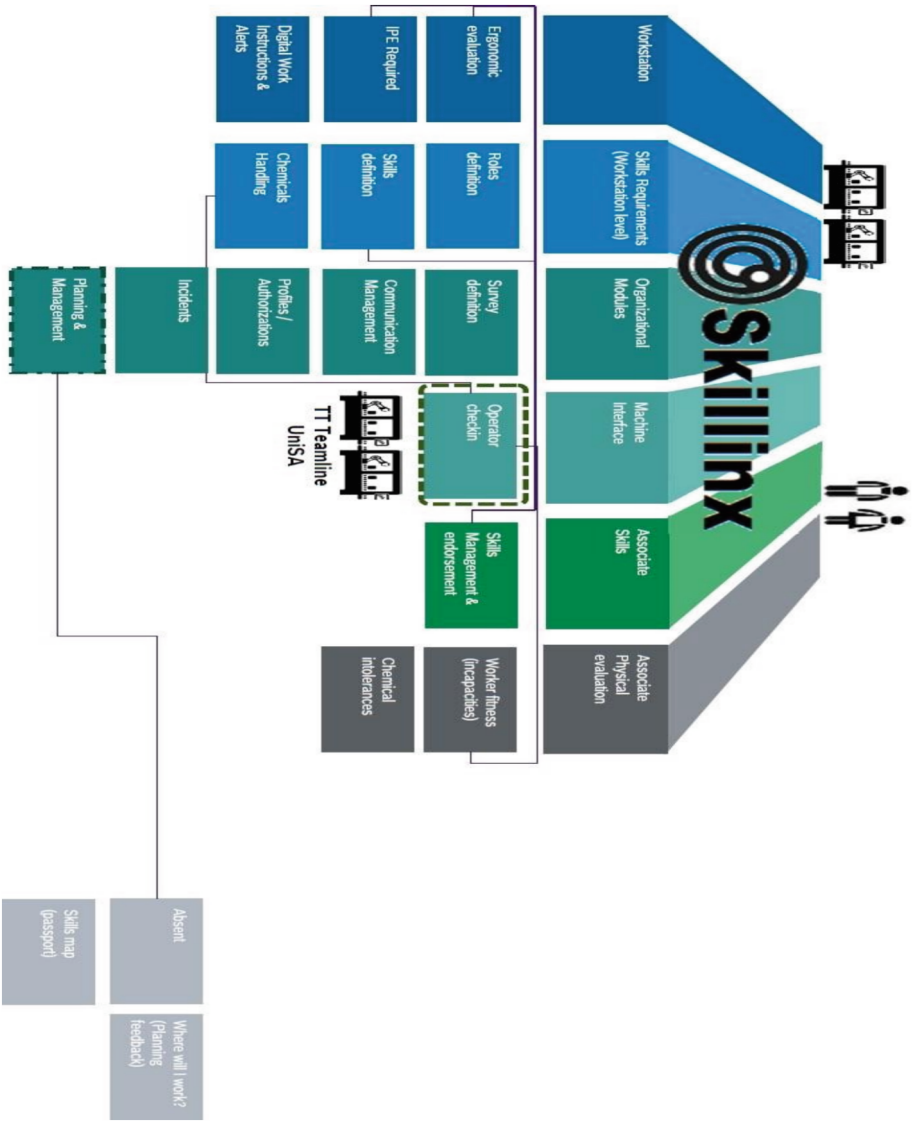

Fig. 2. The modules of Skillinx.

check-in and workstation check-in. The area check-in and workstation check-in modules allow workers to validate if they can work in that specific workstation. While the Area Check-in module was configured on a monitor at the entrance of the factory zone, the Workstation Check-in module was set up at each individual workstation. Figure 5 gives an example of the interface after filtering.

The fields "name" and "assigned workstation," which include the worker's name and the workstation to which they have been allocated by the person with responsibility, are

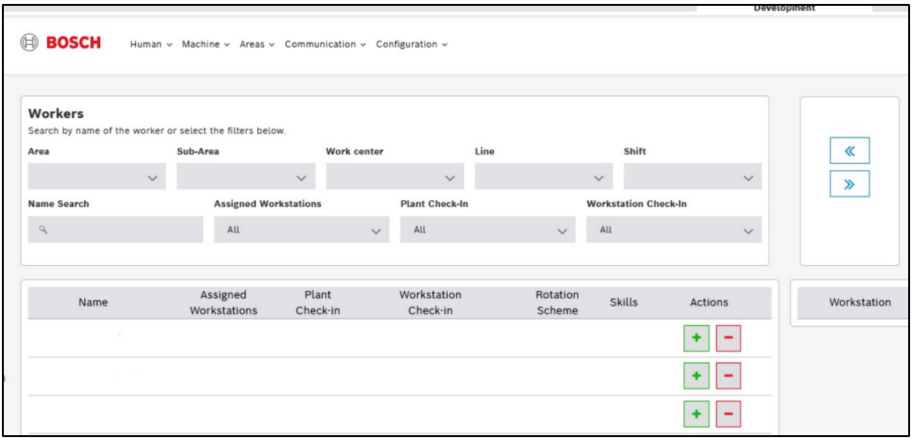

Fig. 3. Left side of the interface Worker Assignment window.

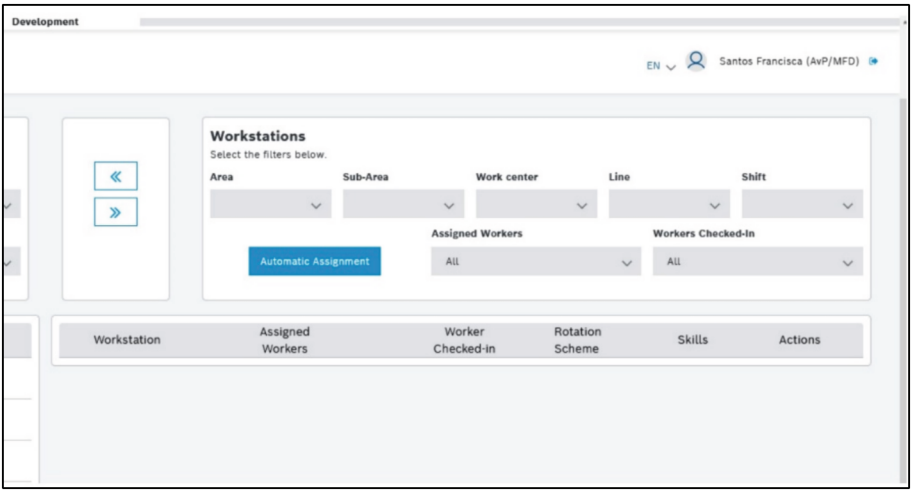

Fig. 4. Right side of the interface Worker Assignment window.

related to the workers. “Plant check-in,” which confirms if the employee has checked in before; “Workstation check-in” displays the workstation number, line number, and section number where the corresponding worker completed the check-in; Moreover, shading in either green or yellow has been used; The worker that checked in at a workstation where he/she wasn’t allocated previously is shown by the yellow shading; If the worker checks-in at the designated workstation, the result is shown in green coloring; “rotation scheme” refers to constraints related to ergonomics; When there are no restrictions, green coloring is used for a more readable indicator; When it comes to competencies, “skills” is represented by a green checkmark or a red cross, and “actions” is where the person responsible for the assignment can add or remove a worker from

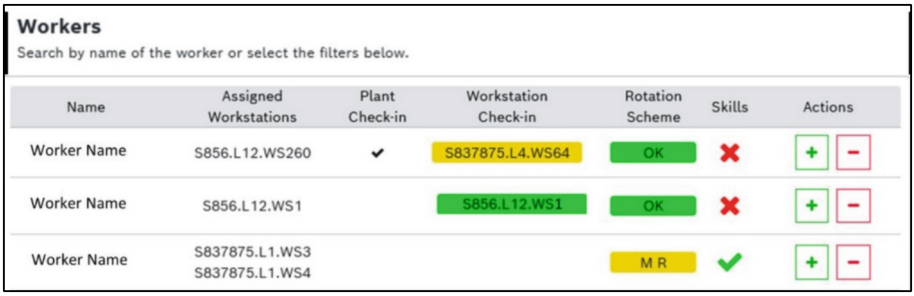

Fig. 5. Worker fields.

his/her workstation based on whether he/she is missing, by a square with a plus sign or a minus sign.

4 Main Results and Discussions

Following the implementation of the modules "Worker Assignment", "Area Check-In" and "Workstation Check-in", the Skillinx platform's Worker Assignment module has an intuitive user interface that makes it simple to understand and utilize and is prepared for integration, enabling communication with other databases, particularly the training data repository.

It has been possible to go from an empirically-based decision-making process to one that is data-driven to achieve as close as possible to an optimized assignment of the workers to the workstation. This involves making judgments about assignments based on ergonomic settings and actual training data. Improved transparency on the conditions of operators includes their abilities and ergonomic constraints. Also, a reduction in the necessary capacity, expressed in full-time equivalent (FTE) figures, for scheduling and allocating operators was achieved (Table 3).

Table 3. Key Performance Metrics

Performance metrics	Key Performance Indicator	Units	Current	Goal	area manager	team leader	shift supervisor
		Hours/ weekly	0.025	0.013	0.016	0.018	0.018

Because of the hold-up in getting performance indicator data, only the FTE metric was taken into consideration in order to meet the goals of efficiently managing labor capacity and maximizing operator assignment, since it is a metric that takes into consideration both full-time and part-time employees, aiding in hiring, restructuring, and downsizing decisions.

The data acquired during the research served as the foundation for calculating the FTE measure. Within a 40-h workweek, the present assignment procedure is anticipated to take one hour. Finding the number of FTEs that equal one hour was the aim, as one FTE is equivalent to forty hours per week. As a consequence, 0.025 FTE is equal to one hour. The outcomes were as follows: the area manager required around 40 min, equivalent to 0.016 FTE and both the team leader and shift supervisor used approximately 45 min, equivalent to 0.018 FTE each. The time required by each responsible party to utilize the Worker Assignment module was assessed three times, once for each assignment responsibility (e.g., area manager, shift supervisor, etc.), in order to track the metric, assess platform efficacy, and examine user-friendliness.

Furthermore, the assignment manager's experiential understanding of ergonomic limits was taken into account, even though the medical and ergonomics teams were still developing ergonomic limitation data.

In addition, an A3 problem-solving report was created to demonstrate the project's advancement throughout the whole organization, but by the time of the project, few outcomes were obtained.

5 Conclusions and Future Work

The large number of workers who needed to be assigned to their individual responsibilities made it necessary to create a platform that would optimize and fact-check the process, accounting for things like ergonomic settings and staff training. In response to these requirements, a platform was created that compiles all operator data into a single location and establishes an operator assignment procedure based on verifiable facts. This minimizes the time needed for scheduling and assigning operators while ensuring maximum transparency about skills and ergonomic restrictions.

The first step in achieving these goals was defining the conditions that the Skillinx platform had to meet. The Outsystems software was used to carry out the development of the work, following brainstorming meetings to determine the most important modules to create.

Thus, it can be said that the worker assignment module's implementation succeeded in achieving the goals of centralizing operator data and developing a fact-based assignment mechanism. The goal of guaranteeing openness in training and ergonomic constraints was accomplished by means of the worker assignment module and the workstation check-in module. These modules also resulted in a decrease in the amount of time needed for operator assignment and planning.

The creation of these modules encouraged accountability and trust among operators while also lessening the workload for those in charge of assignments. Inquiring about new product references and addressing difficulties related to ergonomic restrictions or necessary training can foster employee empowerment and dedication to their work.

In order to achieve the goal of calculating the amount of time spent on each assignment, three measurements were made, one for each operator assignment supervisor. The results showed that supervisors needed 43 min on average to do the work. After thorough investigation, it was evident that one of the main areas for improvement was cutting down on the amount of time needed to assign operators to workstations. Working together across departments during the project enabled shared decision-making and

helped to clarify the issues and challenges facing the weekly production line process at the moment.

Only the first phase of the first cycle was taken into consideration while applying the action research approach. Due to the limited time allotted for the project, it was not feasible to finish a second cycle, which precluded a thorough examination of the interaction cycles recommended by the approach. Installing the Skillinx platform required obtaining many software packages, which was a hindrance.

Future work may involve acquiring mobile devices that can support the Skillinx platform. This will provide assignment supervisors with more process flexibility and enable them to do the task from different locations within the plant, for example.

This experimental concept was validated through one production line, but it is expected that the entire facility, worldwide, would be added to the Skillinx platform. The goal of this platform is to compile all the information needed about the workers and production lines so that the plant manager and assignment supervisors may access it.

Acknowledgments. This work was supported by FCT - Fundação para a Ciência e Tecnologia, I.P. by project reference and DOI identifier <10.54499/UIDB/04005/2020 (https://doi.org/10.54499/UIDB/04005/2020)> and UIDB/00319/2020 (Algoritmi Research Unit).

Disclosure of Interests. The authors have no competing interests to declare that are relevant to the content of this article.

References

1. Naciri, L., Mouhib, Z., Gallab, M., Nali, M., Abbou, R., Kebe, A.: Lean and industry 4.0: A leading harmony. Procedia Computer Science, 200, 394–406 (2022)
2. Khan, A., Turowski, K.: A perspective on industry 4.0: from challenges to opportunities in production systems. IoTBD 2016 - Proceedings of the International Conference on Internet of Things and Big Data, pp. 441–448. SciTePress. Germany (2016)
3. Doyle-Kent, M., Kopacek, P.: Industry 5.0: Is the manufacturing industry on the cusp of a new revolution? In: Durakbasa, N.M., Güneş Gençyılmaz, M. (eds.) ISPR -2019. LNME, pp. 432–441. Springer, Cham (2020). https://doi.org/10.1007/978-3-030-31343-2_38
4. Mayr, A., et al.: Lean 4.0-A conceptual conjunction of lean management and Industry 4.0. Procedia CIRP **72**, 622–628 (2018)
5. Ritter, T., Pedersen, C.: Digitization capability and the digitalization of business models in business-to-business firms: past, present, and future. Indust. Market. Manage. **86**, 180–190 (2020)
6. Björkdahl, J.: Strategies for Digitalization in Manufacturing Firms. Calif. Manage. Rev. **62**(4), 17–36 (2020)
7. Lee, J., Bagheri, B., Kao, H.A.: A Cyber-Physical Systems architecture for Industry 4.0-based manufacturing systems. Manufac. Let. **3**, 18–23 (2015)
8. Jonek-Kowalska, I., Wolniak, R., Marinina, O., Ponomarenko, T.: Stakeholders, Sustainable Development Policies and the Coal Mining Industry. Perspectives from Europe and the Commonwealth of Independent States. 1st edn. Routledge, London (2022)
9. Wang, H., Lv, L., Li, X., Sun, C., Luo, G.: A safety management approach for Industry 5.0′s human-centered manufacturing based on digital twin. J. Manufac. Syst. **66**, 1–12 (2023)

10. Rachmawati, I., Multisari, W., Triyono, T., Simon, I.M., da Costa, A.: Prevalence of academic resilience of social science students in facing the industry 5.0 era. Int. J. Eval. Res. Educ. 676–683 (2021)
11. CDC - Centers for Disease Control and Prevention. Work-Related Musculoskeletal Disorders (WMSDs) Evaluation Measures _ Workplace Health Strategies by Condition _ Workplace Health Promotion. https://www.cdc.gov/workplacehealthpromotion/health-strategies/musculoskeletal-disorders/evaluation-measures/index.html. Accessed 2 Dec 2023
12. Kerzner, H.: Project management best practices: achieving global excellence, 4th edn. Wiley, New Jersey (2010)

A Firefighting Resource Dispatch Problem Optimization Using Metaheuristics

Marina A. Matos, Rui Gonçalves, Ana Maria A. C. Rocha(✉), Lino A. Costa, and Filipe Alvelos

ALGORITMI Research Centre/LASI, University of Minho, Campus de Gualtar, 4710-057 Braga, Portugal
mmatos@algoritmi.uminho.pt, {arocha,lac,falvelos}@dps.uminho.pt

Abstract. Forest fires are a growing concern in our planet, as they have been increasing in frequency and severity over the last few decades. It is therefore essential to manage firefighting in order to prevent and reduce the damage caused to life, the economy and ecosystems. This work deals with the forest firefighting resource dispatch problem using metaheuristics. It is essential to know when and which suppression resources should be sent to extinguish the ignitions. Note that the faster the resources act, the smaller the burned area. An adapted genetic algorithm and differential evolution algorithm are used to solve a firefighting resource dispatch problem aiming to find the optimal allocation of resources to ignitions, and at what instant of time each resource is assigned to each ignition, in order to minimize the total burned area. The two metaheuristics are applied to a set of 60 randomly generated instances, comprising 5, 7 and 10 resources to extinguish 20 or 30 ignitions. A statistical analysis of the results is used to compare the efficiency of the metaheuristics, where the GA shows more competitive results.

Keywords: Fire Suppression · Dispatch Problem · Genetic Algorithm · Differential Evolution Algorithm

1 Introduction

The increase in forest fires around the world has caused several negative aspects, such as deaths, pollution and damage to infrastructure, making it a very worrying factor for society and planet Earth. Therefore, it is crucial to implement forest fire management strategies, which involve preventing fires, anticipating their occurrence, identifying fire risk locations and applying necessary and effective

This work has been supported by FCT Fundação para a Ciência e Tecnologia within the R&D Units Project Scope UIDB/00319/2020 and PCIF/GRF/0141/2019: "O3F - An Optimization Framework to Reduce Forest Fire" and the PhD grant reference UI/BD/150936/2021.

© The Author(s), under exclusive license to Springer Nature Switzerland AG 2024
O. Gervasi et al. (Eds.): ICCSA 2024 Workshops, LNCS 14816, pp. 313–323, 2024.
https://doi.org/10.1007/978-3-031-65223-3_21

measures to reduce the damage caused by forest fires. In Europe, in 2021, more than 1500 km^2 of land burned, of which 1000 km^2 belong to protected areas in the European Union [15]. In 2017, there was a record number of forest fires in Portugal, caused by high temperatures and dry thunderstorms.

Firefighting is a very important area that has been studied in the literature. The number, skills and level of preparedness of firefighting teams are very important factors in fighting fires [1,9]. The better and faster the firefighting team performs, the less damage it causes. In the field of engineering, various optimization techniques have been used to tackle challenges related to fire suppression. The main objectives involve identifying the optimal trajectory and positioning for firefighting vehicles, determining the most efficient route and deciding on the amount and type of resources to be used [5]. A mathematical optimization model was developed in Zeferino et al. [17], aiming to find the best locations for different aircraft on the ground in order to maximize coverage of risk areas. This model was applied to a case study in Portugal. Mendes and Alvelos [12] focused on solving a fire suppression problem represented by a grid network and a fire ignition location. Their objective was to determine the optimal allocation of firefighting resources to minimize both the burned area and the use of resources as a secondary objective. They used a novel iterative local search metaheuristic and a mixed integer programming model, demonstrating the effectiveness of the metaheuristic in identifying optimal solutions.

The firefighting resource dispatch problem optimization involves selecting and allocating resources to a fire, as well as determining the appropriate time to dispatch them [2]. Genetic algorithms have been widely used to solve this type of problem, with the main objective of minimizing the burned area [7]. Matos et al. [11] studied a firefighting resource dispatch problem, involving the allocation of 7 resources (tank vehicles) to extinguish 20 ignitions, aiming to minimize the total burned area. However, in this modeling of the problem, it was not possible to refill the vehicles' tanks whenever they ran out of water. To solve the optimization task, they used a genetic algorithm adapted to this specific problem. In addition, a statistical analysis was carried out comparing different operators of the genetic algorithm, including crossover, mutation and selection, to determine which combination of operators produced the most favorable results. They found that the operators best suited to this type of problem were exponential crossover, polynomial mutation and tournament selection. The same problem was discussed in [10] where an adapted version of the differential evolution algorithm was used. In addition, a statistical analysis was carried out to evaluate its performance with different selection and crossover operators. The results suggested that the current-to-best selection and exponential crossover operators were the most effective for solving this problem.

In this work, a genetic algorithm (GA) and a differential evolution algorithm (DE) adapted and implemented in the *Python* language are applied to solve the firefighting resource dispatch problem. It should be noted that in this implementation, it is possible to refill the vehicles' water tanks (resources) whenever they run out of water, requiring a different representation of solutions by permutation,

adapted for the GA and DE algorithms, than that used in the previous works [10,11]. The main goal is to assign different resources of combat to various ignitions in order to minimize the total burned area. To compare the performance of the two algorithms, a set of 60 instances is randomly generated, comprising 5, 7 and 10 resources to extinguish 20 or 30 ignitions. In addition, a statistical analysis is performed to compare the results obtained by the two metaheuristics.

This paper is organized as follows. The problem is described in Sect. 2. Section 3 explains the permutation representation, and the steps of genetic algorithm and differential evolution algorithm. In Sect. 4 the details and results of the computational experiments, using GA and DE, are presented. Finally, the discussion and conclusions of this study and future work are stated in Sect. 5.

2 Problem Description

In this work, a firefighting resource dispatch problem is optimized, aiming the minimization of the total burned area.

In this problem, there may be a number of ignitions, which can be understood as several fronts of the same forest fire. In addition, there are a number of firefighting resources, which are based on forest firefighting land vehicles with water tanks, which can have different capacities.

At the beginning, all the firefighting resources (vehicles) are at the base (fire station) and their water tanks are at full capacity. Concerning the ignitions, they are all active (burning) and located in different places. The main idea is to allocate the vehicles to the ignitions, over various instants of time, in order to completely extinguish them.

Taking into consideration the location of the ignitions, travel times are calculated based on the Euclidean distance between each ignition and the base and between ignitions, satisfying the triangular inequality. The values of the burned area by each ignition at each instant of time are known. To do this, a different exponential growth model of the fire spread over time was applied to each ignition, resulting in different types of growth of the burned area. The water required to extinguish a given ignition over time is calculated using the values of the burned area at each instant of time, based on the perimeter of a circle.

It should be noted that each ignition can be extinguished only once (even taking more than one instant of time) and it may require more than one resource to extinguish it completely. On the other hand, each resource can only be allocated to one ignition at each instant of time.

In each instant of time, each resource is available to be assigned to one ignition or is traveling to the location of an ignition or is being refilled. When a resource is allocated to a particular ignition, it is extinguished instantly, if the resource has enough water in its tank. Whenever the water capacity of a resource is not sufficient to extinguish a given ignition, the ignition remains active an the resource refills in this ignition taking one instant of time.

3 Metaheuristics

In this paper, a genetic algorithm and a differential evolution algorithm are used. These metaheuristics are evolutionary and stochastic algorithms that are applied to optimization problems. Although they share some similarities, they have distinct features in their mechanisms and approaches.

3.1 Solution Representation by Permutation

The permutation representation is relevant for combinatorial problems. In this work, this type of representation allows to search for potential solutions to the problem of dispatching firefighting resources. Both metaheuristics work with a population of individuals (chromosomes for GA and vectors for DE) that is a permutation of the decision variables. This permutation is a unique sequence of integer values, ensuring that each firefighting resource can deal with several ignitions at different instants of time, i.e. the permutation indicates a specific order of priority for assigning resources to ignitions. The size of individual is determined by multiplying the number of resources by the number of ignitions and a parameter (m). This parameter defines the maximum number of times a resource can return to a given ignition, i.e., when a resource runs out of water, it refills at that ignition, and can go to that ignition up to m times, while the ignition is still active. For example, for a problem with 2 resources to extinguish 3 ignitions and with $m = 3$, an individual of size 18 ($2 \times 3 \times 3$) is required to represent a potential solution of the problem, as shown in Table 1. Thus, according to this individual, resource 1 goes first to ignition 2, then to ignition 1, then again to ignition 2, and so on, ending at ignition 2. Resource 2 starts its journey at ignition 1 and ends at ignition 2. As mentioned earlier, in this example, each resource can be sent to the same ignition up to 3 times ($m = 3$).

Table 1. Permutation representation (example)

Resource	R1									R2								
Decision Variables	13	4	10	6	14	16	8	15	9	1	12	17	5	3	18	2	7	11
Ignitions Order	I_2	I_1	I_2	I_1	I_3	I_3	I_1	I_3	I_2	I_1	I_3	I_3	I_2	I_1	I_3	I_1	I_2	I_2

3.2 Genetic Algorithm

Genetic algorithm is a metaheuristic inspired by the principles of biological evolution [6]. It was developed as a machine learning and optimization algorithm and applied to solve optimization problems with the aim of finding the best possible solution in complex search spaces. GA working comprises the following essential components, a population of individuals (chromosomes), a fitness

function, a selection mechanism and genetic operators such as crossover and mutation. The population is evolved until a given termination criterion [8].

In GA, potential solutions of the problem are represented as chromosomes made up of genes (a vector of elements). Genes encode various aspects of the solution, and genetic operators, such as crossover and mutation, act on these genes to produce offspring chromosomes. Algorithm 1 starts with a given population of NP individuals generated at random. Each individual is evaluated by a fitness function and the fittest individuals have higher probability of being selected to generate offspring. The selected individuals generate offspring by the operators of crossover and mutation. The offspring individuals are then evaluated. This cycle continues until some stopping criterion is reached.

Algorithm 1. Genetic Algorithm

```
1: Initialize population
2: Evaluate population
3: while stopping criterion is not met do
4:     Selection
5:     Crossover
6:     Mutation
7:     Evaluate population
8: end while
```

In this work, a tournament selection was adopted. The GA operators used in this work are the exponential crossover and the polynomial mutation. These choices are based on a previous work in which several different operators were tested for the problem of dispatching forest firefighting vehicles, and these were the ones that gave the best results [11].

In the tournament selection two or more parent chromosomes are randomly selected from population, and the one with the highest fitness function value is selected to generate offspring. In this work, a binary tournament selection was used. Thus, tournaments between two selected chromosomes are successively performed. Each chromosome of the population can only participate in a single tournament. Exponential crossover is applied to two parent individuals to generate two new offspring. An initial starting position is generated at random that guaranties that at least the offspring will differ from the parents in one position. Then, for the remaining positions of the parent individuals, a random number between 0 and 1 is generated; if it is less than the control parameter (CR, crossover rate), the parent genes are copied to the offspring; otherwise, the parent genes are swapped and then copied to the offspring individual [13,19]. The crossover rate determines the probability of crossover occurring [14]. Thus, the offspring vector u_i is componentwise computed either from the elements of first parent vector $x_{i,\cdot} = x_{i,j} = x_{i,1}, \ldots, x_{i,n}$ or the elements of the second parent vector $v_{i,\cdot} = v_{i,j} = v_{i,1}, \ldots, v_{i,n}$ ($i = \{1, \ldots, NP\}$, $j = \{1, \ldots, n\}$ and n is the dimension of the individual):

$$u_{i,j} = \begin{cases} v_{i,j}, \text{ if } \text{rand}_{i,j} \geq \text{CR} \text{ or } j = j_{\text{rand}} \\ x_{i,j}, \text{ otherwise} \end{cases}$$

where $\text{rand}_{i,j} \sim U(0,1)$ is a uniformly distributed random number which is generated for each j and $j_{\text{rand}} \in \{1, \ldots, n\}$ is a random integer used to ensure that $u_{i,\cdot} \neq x_{i,\cdot}$ in all cases.

In the polynomial operator, a polynomial probability distribution is used to generate a solution in the vicinity of a parent. The polynomial mutation employs a distribution parameter, η_m, which is typically set in the range between 20 and 100. This parameter plays a crucial role in controlling the spread effect of the mutation. The probability distribution, both to the left and right of a variable value, is adjusted so that values outside the specified interval $\left[x_j^L, x_j^U\right]$ can not be created by the mutation operator. A mutated individual $y_{i,\cdot}$ is created from the parent individual $x_{i,\cdot}$ by mutating each position $j \in \{1, \ldots, n\}$ of the parent individual, according to a polynomial distribution where $u \sim U(0,1)$ [4].

$$y_{i,j} = \begin{cases} x_{i,j} + \delta_L(x_{i,j} - x_j^L), & \delta_L = (2u)^{\frac{1}{1+\eta_m}} - 1 \quad \text{for } u \leq 0.5 \\ x_{i,j} + \delta_R(x_j^U - x_{i,j}), & \delta_R = 1 - (2(1-u))^{\frac{1}{1+\eta_m}} \quad \text{for } u > 0.5 \end{cases} \tag{1}$$

The termination criteria determines the end of the search. Possible termination conditions are related with the stagnation of the population where there is no further improvement in the value of the objective function, reaching the specified maximum number of iterations, or reaching a predetermined value of the objective function evaluations. If the stopping criterion is not met, the algorithm continues and repeats all steps again to generate a new generation.

3.3 Differential Evolution

Differential evolution is an evolutionary algorithm and was first introduced by Storn and Price in 1997 [16]. Since then, it has been widely adopted due to its simplicity and effectiveness in solving complex optimization problems [14]. The DE steps are presented in Algorithm 2, where NP is the population size, F is the mutation factor and CR is the crossover rate. DE has some similarities with GA, differing in the order of operators. It starts with a given population of individuals (vectors). The population evolves through mutation, crossover and finally selection. This evolution takes place while the stopping criterion has not been reached.

In DE, potential solutions of the problem are represented as vectors in the search space. DE uses mutation, crossover and selection operators. The operators define different variants of DE, which nomenclature is as follows: DE/Selection/1/Crossover. In this work, the variant chosen was DE/Current-to-best/1/Exponential, since it was the best variant for the dispatch problem, found in [10].

During the mutation phase, a new candidate is formed by adding a scaled differential term to an existing base vector (individual). A key factor influencing

Algorithm 2. Differential Evolution Algorithm

```
Initialize population
Evaluate population
while stopping criterion is not met do
    Mutation
    Crossover
    Evaluate population
    Selection
end while
```

this mutation process and subsequently the effectiveness of the algorithm is the mutation factor (F_1 and F_2), typically limited to a range of 0 to 2. This parameter plays a fundamental role in regulating the rate of evolution within the population, dictating the magnitude of the adjustment to the differential term. A higher value of F_1 and F_2 corresponds to a greater probability of breaking free from local optima, thus promoting the exploration of the solution space. The mutation in the variant DE/current-to-best/1 is defined by a mutant vector v_i computed by [18]

$$v_i = x_i + F_1 \left(x_{\text{best}} - x_i\right) + F_2 \left(x_{r_1} - x_{r_2}\right)$$

where x_i is the selected individual (i.e. $r_1 \neq r_2 \neq r_3 \neq i$) and F_1 and F_2 are real constants, $F_1, F_2 \in [0, 2]$.

In this work, an exponential crossover is used, as in GA. In DE, crossover involves combining mutant vectors with the candidate solutions present in current population. In other words, the algorithm combines two populations: the current one and the mutated one, and a new experimental population is created.

In the selection phase, a mechanism is used to select the individuals that will form the next generation. Based on their objective values, a comparison is made between the experimental and current individuals. The individuals with the lowest function value (when considering a minimization problem) are selected to form the next generation. Thus, the new target vector is obtained and its value is computed as follows:

$$x_i = \begin{cases} u_i, \text{ if } f(u_i) < f(x_i) \\ x_i, \text{otherwise} \end{cases}$$

where $f(u_i)$ is the objective function value of the trial vector and $f(x_i)$ is the objective value of the parent vector.

As with GA, the DE algorithm terminates when a predefined stopping criterion is reached. If the stopping criterion is not reached, the algorithm continues and repeats all the steps to generate a new generation.

4 Computational Experiments

In this section, the details used in the algorithms (GA and DE), the results obtained by them and finally a discussion of the results through statistical analysis will be presented.

4.1 Details

In this work, the GA and DE are adapted from the framework *pymoo*: Single-objective Optimization in Python [3]. The experiments were carried out on a PC 11th Gen Intel(R) Core(TM) i7-1165G7 @ 2.80GHz, 2803 Mhz, 4 Nucleus(s), 8 Processor(s) Logic(s), 16 Gb RAM. The code was implemented in *python* (version 3.9.35) using *VScode* (Version 1.87).

In order to test our approach, these metaheuristics are used for a set of 60 instances of the firefighting resource dispatch problem. These instances were randomly generated for 20 and 30 ignitions and 5, 7 and 10 resources, available at https://github.com/MarinaAMatos/Inst_Firefighting. For each pair of ignitions and resources, 10 instances are randomly generated. There are different types of resources (with predefined water tank capacities - 500 l, 1000 l, 1500 l, 2000 l and 3000 l - randomly assigned). The values of the burned area of each ignition at the initial instant of time are also randomly defined for each instance and range from 1 to 500 m^2. The water required to extinguish a given ignition is calculated using the perimeter of a circle, whose radius is obtained by multiplying the burned area by 10, which is the amount of water needed to extinguish 1 m of the ignition area.

The initial population size used was set at 200 and the maximum number of generations and the maximum number of function evaluations were 1000 and 100000, respectively, for the two metaheuristics. The m parameter chosen was 5, i.e. each resource is allowed to return up to 5 times to a given ignition when its water tank needs refilling. This value was chosen because it was considered sufficient to obtain feasible solutions, since the higher it is, the longer the algorithms will run. The operators exponential crossover, polynomial mutation and tournament selection were used in GA. For DE, the variant applied is "DE/current-to-best/1/exp", i.e. the exponential crossover, polynomial mutation and current-to-best selection operators were applied. The $CR = 0.3$, $F_1 = F_2 = 0.5$ and all the other parameters used were the default ones.

4.2 Results

The results obtained from GA are described below. It should be noted that in all instances the ignitions were all extinguished. For each number of ignitions, NI, and number of resources, NR, Table 2 shows the results obtained by GA and DE, taking into account the average values of the best values (GA_{best} and DE_{best}) and the average of the values (GA_{avg} and DE_{avg}) over 30 runs. Columns 4 to 9 show the average of the values obtained in the 10 instances for each pair of NI and NR. TBA_{avg} represents the average value of the total burned

area TBA, UW_{avg} is the average value of used water, $Time_{avg}$ is the average value of the instants of time required to extinguish all ignitions, PT_{avg} the average value of the processing time in seconds, nfe_{avg} the average value of the number of function evaluations, and $ngen_{avg}$ the average value of the number of generations. The values obtained for TBA_{avg}, UW_{avg} and $Time_{avg}$ in GA are lower than DE. In relation to the values of PT_{avg}, nfe_{avg} and $ngen_{avg}$, it was found that the solutions obtained by DE were smaller than those obtained by GA.

Table 2. Solution values for GA and DE

NI	NR		TBA_{avg}	UW_{avg}	$Time_{avg}$	PT_{avg}	nfe_{avg}	$ngen_{avg}$
20	**5**	GA_{best}	**5210.5**	10802.3	114.0	270.8	20500.0	103.5
		DE_{best}	5318.1	10929.0	130.0	254.6	18400.0	93.0
		GA_{avg}	**5273.2**	10876.3	124.4	219.3	17289.3	87.4
		DE_{avg}	5388.2	11008.6	146.6	201.5	15051.3	76.3
	7	GA_{best}	**5420.1**	11101.6	101.0	271.4	20060.0	101.3
		DE_{best}	5481.6	11170.9	108.0	257.1	19440.0	98.2
		GA_{avg}	**5455.8**	11145.3	104.5	224.4	16208.7	82.0
		DE_{avg}	5520.4	11216.4	116.3	184.1	13890.0	70.5
	10	GA_{best}	**5433.1**	11059.9	80.0	294.4	21780.0	109.9
		DE_{best}	5458.7	11096.8	84.0	250.2	18260.0	92.3
		GA_{avg}	**5450.9**	11082.9	80.2	196.9	13580.0	68.9
		DE_{avg}	5477.4	11114.6	86.4	167.5	11922.7	60.6
30	**5**	GA_{best}	**8042.3**	16654.6	185.0	535.9	39800.0	200.0
		DE_{best}	8606.1	17301.5	242.0	316.8	21300.0	107.5
		GA_{avg}	**8309.7**	16970.5	212.7	392.3	26726.0	134.6
		DE_{avg}	8909.0	17584.6	264.4	291.2	17812.7	90.1
	7	GA_{best}	**7812.3**	16319.4	139.0	662.3	38080.0	191.4
		DE_{best}	8110.2	16633.8	175.0	347.9	21420.0	108.1
		GA_{avg}	**7971.2**	16514.8	162.4	413.4	24499.3	123.5
		DE_{avg}	8264.7	16835.1	193.6	280.5	16858.7	85.3
	10	GA_{best}	**7326.9**	15843.1	107.0	583.7	33460.0	168.3
		DE_{best}	7469.4	16004.1	130.0	361.8	23120.0	116.6
		GA_{avg}	**7390.9**	15921.7	115.6	419.7	23416.7	118.1
		DE_{avg}	7531.5	16089.7	131.2	245.2	14426.0	73.1

Table 3 shows the statistical analysis of the TBA values between GA and DE for all instances. For the statistical analysis, a one-tailed paired sample t-student test was used, and in all tests, a significance level of 5% was considered. The table shows the solutions for all pairs of number of ignitions and number of

resources, where the p-values and the difference in the TBA value between the two metaheuristics are shown. It was observed significant differences between all the results, since the p-value is less than 0.05.

Table 3. Statistical analysis between GA and DE

NI	**20**			**30**		
NR	**5**	**7**	**10**	**5**	**7**	**10**
GA-DE (best)	–107.7	–61.5	–25.6	–563.8	–298.0	–142.5
GA-DE (avg)	–115.0	–64.6	–26.5	–599.3	–293.5	–140.6
p-value	<0.001					

5 Conclusions

Currently, fires have become an area of interest in the academic community, due to the numerous damages caused. Managing the use of forest firefighting resources is a crucial issue, and they need to be used more efficiently so that the fire can be controlled in a shorter period of time.

This paper presents a firefighting resource dispatch problem that aims to know which and when each resource goes to each ignition, in order to minimize the total burned area. To this end, the GA and DE metaheuristics were adapted to this problem and applied to 60 randomly generated instances with 5, 7 and 10 resources to extinguish 20 ignitions, and 5, 7 and 10 resources to fight 30 ignitions. It was concluded that GA is better in terms of minimizing the value of TBA when compared to DE. However, DE takes less time to find solutions, i.e. it has a shorter runtime than GA.

In future work, a forest firefighting resource dispatch problem using real data will be solved.

References

1. Attri, V., Dhiman, R., Sarvade, S.: A review on status, implications and recent trends of forest fire management. Arch. Agric. Environ. Sci. **5**(4), 592–602 (2020)
2. Bélanger, V., Lanzarone, E., Nicoletta, V., Ruiz, A., Soriano, P.: A recursive simulation-optimization framework for the ambulance location and dispatching problem. Eur. J. Oper. Res. **286**(2), 713–725 (2020)
3. Blank, J., Deb, K.: Pymoo: multi-objective optimization in python. IEEE Access **8**, 89497–89509 (2020)
4. Deb, K., Deb, D.: Analysing mutation schemes for real-parameter genetic algorithms. Int. J. Artif. Intell. Soft Comput. **4**(1), 1–28 (2014)
5. Granberg, T.A.: Optimized dispatch of fire and rescue resources. In: Computational Logistics: 13th International Conference, ICCL 2022, Barcelona, Spain, 21–23 September 2022, Proceedings, pp. 132–146. Springer, Heidelberg (2022). https://doi.org/10.1007/978-3-031-16579-5_10

6. Holland, J.H.: Adaptation in Natural and Artificial Systems. MIT Press, Cambridge (1975)
7. HomChaudhuri, B., Kumar, M., Cohen, K.: Genetic algorithm based simulation-optimization for fighting wildfires. Int. J. Comput. Methods **10**(06), 1350035 (2013)
8. Lambora, A., Gupta, K., Chopra, K.: Genetic algorithm- a literature review. In: 2019 International Conference on Machine Learning, Big Data, Cloud and Parallel Computing (COMITCon), pp. 380–384 (2019)
9. Martell, D.L.: A review of recent forest and wildland fire management decision support systems research. Curr. Forest. Rep. **1**(2), 128–137 (2015). https://doi.org/10.1007/s40725-015-0011-y
10. Matos, M.A., Gonçalves, R., Rocha, A.M.A., Costa, L.A., Alvelos, F.: Resource dispatch optimization for firefighting using a differential evolution algorithm. In: Pereira, A.I., Mendes, A., Fernandes, F.P., Pacheco, M.F., Coelho, J.P., Lima, J. (eds.) International Conference on Optimization, Learning Algorithms and Applications, pp. 63–77. Springer, Heidelberg (2024). https://doi.org/10.1007/978-3-031-53025-8_5
11. Matos, M.A., Rocha, A.M.A.C., Costa, L.A., Alvelos, F.: Resource dispatch optimization for firefighting based on genetic algorithm. In: Gervasi, O., et al. (eds.) ICCSA 2023. LNCS, pp. 437–453. Springer, Cham (2023). https://doi.org/10.1007/978-3-031-37108-0_28
12. Mendes, A.B., Alvelos, F.P.: Iterated local search for the placement of wildland fire suppression resources. Eur. J. Oper. Res. **304**(3), 887–900 (2023)
13. Meng, Z., Chen, Y.: Differential evolution with exponential crossover can be also competitive on numerical optimization. Appl. Soft Comput. **146**, 110750 (2023). https://doi.org/10.1016/j.asoc.2023.110750
14. Price, K.V.: Differential Evolution, pp. 187–214. Springer, Heidelberg (2013). https://doi.org/10.1007/978-3-642-30504-7_8
15. San-Miguel-Ayanz, J., et al.: Forest Fires in Europe, Middle East and North Africa 2021. No. EUR 31269 EN, Publications Office of the European Union, Luxembourg (2022). https://doi.org/10.2760/34094
16. Storn, R., Price, K.: Differential evolution-a simple and efficient heuristic for global optimization over continuous spaces. J. Global Optim. **11**, 341–359 (1997)
17. Zeferino, J.A.: Optimizing the location of aerial resources to combat wildfires: a case study of Portugal. Nat. Hazards **100**(3), 1195–1213 (2020)
18. Zeng, Z., Zhang, M., Chen, T., Hong, Z.: A new selection operator for differential evolution algorithm. Knowl.-Based Syst. **226**, 107150 (2021)
19. Zhao, S.Z., Suganthan, P.N.: Empirical investigations into the exponential crossover of differential evolutions. Swarm Evol. Comput. **9**, 27–36 (2013)



Robust Optimization for IMPT: Introducing and Comparing Different Automated Approaches

Joana Neves[1], Humberto Rocha[1,2(✉)], Brígida Ferreira[2,3], and Joana Dias[1,2]

[1] University of Coimbra, INESC-Coimbra, 3030-290 Coimbra, Portugal
{hrocha,joana}@fe.uc.pt
[2] University of Coimbra, CeBER, FEUC, 3004-512 Coimbra, Portugal
[3] University of Lisbon, IBEB, Faculty of Sciences, 1749-016 Lisbon, Portugal
bcferreira@fc.ul.pt

Abstract. Intensity-modulated proton therapy (IMPT) is a radiotherapy treatment modality that has proven to be able to properly irradiate tumors while preserving as much as possible normal tissues. However, it is extremely vulnerable to several different sources of uncertainties, which motivates the use of robust treatment planning optimization. In this work we describe a new approach for robust automated IMPT treatment optimization, based on a set of auxiliary structures that are shifted versions of each one of the volumes of interest (clinical target volume - CTV and organs-at-risk - OARs), and that are named *clones*. This approach is compared with the use of a pseudo-Planning Target Volume (PTV) and pseudo-planning OAR volumes built by the union of all the CTV and OAR *clones*, respectively. For proof-of-concept, the proposed methodologies were tested using five post-operative prostate cancer cases. The quality of the calculated treatment plans was assessed by Monte Carlo simulation. For IMPT treatment plan robust optimization, the new strategy based on the use of *clones* using shifts of 6 mm presented better results in terms of robustness when compared with the traditional PTV-based approach. Taking uncertainties into consideration during the planning process can be an option to overcome one of the major drawbacks of IMPT.

Keywords: automated treatment planning · inverse optimization · Monte Carlo simulation · radiotherapy · robust optimization

1 Introduction

Several therapeutic modalities can be used for the treatment of cancer, namely surgery, chemotherapy, radiotherapy, among others. Radiotherapy is prescribed to most patients, many times in combination with surgery or chemotherapy [1]. Radiotherapy emerges as a form of oncological treatment that uses ionizing

© The Author(s), under exclusive license to Springer Nature Switzerland AG 2024
O. Gervasi et al. (Eds.): ICCSA 2024 Workshops, LNCS 14816, pp. 324–340, 2024.
https://doi.org/10.1007/978-3-031-65223-3_22

radiation to damage tumor cells. The aim is to deliver the prescribed dose of radiation to the tumor while minimizing the risk of side effects to healthy organs [2]. It can be delivered for therapeutic or palliative purposes, in order to alleviate the symptoms of patients. Highly sophisticated radiation therapy techniques have emerged in the last decades with the potential to deliver more conformal and homogeneous doses to the target volume, while better sparing the surrounding healthy tissues [3–5]. Intensity-modulated proton therapy (IMPT) is one of these techniques [5]. The physical properties of protons enable dose distributions that are conformal and homogeneous to the target volume, and, simultaneously, deposit less dose in organs at risk. Proton beams deposit maximum energy in a very precise location, called the Bragg peak, which contributes to the delivery of a dose distribution conformal to the target volume while keeping a low dose in the normal tissues. Consequently, there is the potential for an increase in tumor control probability as well as a decrease in the risk of secondary effects that occur by using ionizing radiation. However, one of the major drawbacks of IMPT is its higher susceptibility to uncertainties, such as the range of proton beams or patient positioning [6]. Therefore, it is essential to assure that treatment plans are robust, meaning that they are clinically admissible even under different scenarios that can occur [7].

When the medical oncologist prescribes an IMPT treatment, a set of procedures are put in place. First, it is necessary to acquire medical images of the patient, usually a computed tomography scan (CT), where all the volumes of interest are delineated. These volumes represent the tumor (clinical target volume - CTV) and also all the organs that must be spared (Organs-at-risk - OARs). These medical images create a 3D discretization of the patient, with the smallest 3D-element called a voxel. Then the oncologist defines the medical prescription, that establishes a set of upper or lower limits to some dosimetric measures associated with each volume of interest. For CTVs these limits will make sure that the volume is properly irradiated. For OARs, upper limits to the deposited dose are usually considered, depending on the characteristics of the organs, trying to assure that all the organs keep their functionality. Then the treatment planner goes through a lengthy and complex trial-and-error process, calculating different treatment plans iteratively until one treatment plan is found that complies with all the constraints defined in the medical prescription. This process is usually known as inverse optimization treatment planning and it is based on the use of optimization models and algorithms. The planner changes some of the parameters of an optimization model, that is solved producing a new treatment plan. Most of the time this inverse optimization procedure is interpreted by the planner as a black box, with which the planner can only interact by changing some parameters, but without knowing what the underlying optimization model is or how the changes made will affect the quality of the calculated treatment plan. This is mainly due to the fact that the medical prescription defines a set of non-linear constraints: they establish dose-volume limits that are non-linearly related with the decision variables (treatment plan parameters). This trial-and-error procedure can be very time consuming, and the final result depends on the planner's experience [8,9]. Optimization has been playing

a decisive role in improving treatment planning optimization aiming to consistently ensure high-quality plans while releasing the treatment planner for other important tasks, e.g., quality assurance. The contribution of optimization can be seen in many different aspects of radiotherapy treatment planning, from the calculation of radiation intensities [10], to the selection of appropriate irradiation angles [11–17] also considering the multiobjective nature of this problem due to the conflicting objectives to consider: maximizing CTV irradiation and, at the same time, OAR sparing [18].

The quality of a treatment plan is assessed based on a visual analysis of the three-dimensional dose distribution, on the analysis of the dosimetric parameters for each volume of interest and on the analysis of dose-volume histograms (DVH). The DVH is a graphical representation of the dose as a function of the volume, where, for each structure, the percentage of cumulative volume that receives a certain dose of radiation is obtained. Treatments are usually fractionated, meaning that a fraction of the total dose is delivered on different days. For the treatment to be delivered, the patient is positioned and immobilized on the treatment table. A mechanical arm, gantry, which rotates around a central axis, allows the radiation beam to be directed towards the patient. The treatment table can also rotate allowing, together with the rotation of the gantry, the irradiation of the tumor in almost all directions, except those where a collision between the treatment table and the gantry may occur.

Whilst treatment planning is always a difficult task for every radiotherapy treatment modality considered, it is even more difficult for IMPT due to the unavoidable impact of uncertainty. In the existing literature there are two different methodologies that try to achieve robust IMPT treatment plans: the stochastic or probabilistic approach and the worst-case scenario approach [19–21]. In the stochastic approach, a set of scenarios is usually considered, each one associated with a given probability of occurrence. The treatment planning process is then guided by an objective function that calculates a given expected value over all the considered scenarios. A probabilistic approach has been developed by Wahl et al. [22,23], considering range and setup uncertainties as random variables. In the worst-case approach, the objective is to guarantee that the best possible treatment plan for the worst possible situation is calculated [20]. This can be accomplished either by looking at the voxel, for each one of the considered structures of interest, that is in the worst situation, or looking only at the structure that, as a whole, is the worst among all the existing structures. For instance, for a given organ-at-risk (OAR) or planning OAR volumes (PRV - created by considering a given margin around the OAR), only the voxel with the highest dose contributes to the value of the objective function whilst for a clinical target volume (CTV) or planning target volume (PTV - the CTV plus a given margin) only the voxel with the lowest dose is of interest [21]. Examples of the use of the worst-case scenario can be found in Liu et al. [24] and Zaghian et al. [25].

In this work, we propose and compare two automated robust IMPT optimization approaches. The process is automated by using fuzzy inference systems, a method that has been successfully applied to intensity-modulated radiotherapy

(IMRT) [8]. These approaches differ from one another in the way uncertainty is represented and explicitly taken into consideration in the optimization. Robustness was embedded in this automated procedure considering two different strategies. The first strategy considers the creation of additional structures for each one of the volumes of interest (both CTV and OARs), named *clones*. These new structures are a copy of the original ones, but placed in a different relative position considering shifts in the x, y and z axes. All these *clones* are then taken simultaneously into account during treatment plan optimization, as well as the original ones (the number of structures that must be taken into account during treatment planning is increased). The second strategy considers one single structure for each volume of interest that is built from the union of all the corresponding *clones*. This second strategy mimics what is usually done in clinical practice: uncertainty is considered by applying margins to the CTV, creating an enlarged structure called the Planning Target Volume (PTV), and to the OARs, creating Planning Organ at Risk Volumes (PRV). These two strategies were tested on five prostate cancer cases. As uncertainty should also be explicitly considered in the assessment of the quality of the treatment plans, Monte Carlo simulation is used as an assessment tool. The different sources of uncertainty are represented by random variables, and the effects of treatment fractionation were also taken into account.

2 Sources of Uncertainty in IMPT

Any source of uncertainty in radiotherapy treatments can lead to a loss in the quality of the treatment, namely by the difference that exists between what is being planned and what is being really delivered. In IMPT, the impact of existing uncertainties is even more pronounced than in other radiotherapy modalities due to the physical properties of the beams [21]. Uncertainties can be caused by systematic errors, which are always the same in every treatment fraction, or random errors, which vary between different fractions of the treatment [6]. The greatest advantage of IMPT resides in the precise location of the Bragg peak and the respective finite range of the proton beams, but these are also the main cause of its greater sensitivity to uncertainties [20,21].

The treatment plan is based on the planning CT, where the volumes of interest are delineated. The delineation of these volumes introduces uncertainties in this process, since it is possible that different physicians perform different delineations [26]. Due to the movements of the organs and the changes that may occur during the treatment (such as the patient's weight loss, for example), this planning medical image represents only one of the possible geometries of the patient on each day of treatment. Furthermore, the artifacts that may be present in the image can influence the calculation of the depth of the Bragg peak as well as tissue density information that is given by the medical image and that impacts the calculation of the proton stopping power (uncertainties in the conversion from Hounsfield units (HU) to proton stopping power) [27]. During each fraction, in addition to internal movements of the organs, there may

be deviations in the patient's positioning on the treatment table, in relation to the position adopted in the planning CT scan. Thus, during treatment delivery, there may be changes in the beam range and Bragg peak location compared to what was planned [27], leading to an increased difficulty in adequately irradiating the tumor volume, and a potential overdose of healthy tissues [6].

Another source of uncertainty is related with the Relative biological effectiveness (RBE). RBE is a relative measure of the damage done by a given type of radiation per unit of energy deposited in biological tissues, and it is usually assumed to be equal to 1.1 for protons. However, it is known that this value should not be constant, since it depends on different factors, like proton energy, number of treatment fractions, characteristics of the traversed tissues, among others [6]. RBE uncertainties will not be considered in the current work.

3 Material and Methods

3.1 Prostate Clinical Cases

The proposed approaches were tested on five patients with prostate cancer, in stage T_2 with the tumor only present in the prostate gland, who were previously subjected to surgery. In the computer tomography (CT) images, the target volumes included the prostate gland and the CTV while the organs-at-risk considered were the rectum, bladder, right and left femoral heads. Dose prescription for the CTV was 68 Gy(RBE) to be delivered in 34 fractions. Table 1 presents the dose prescription and tolerance doses for the structures considered. In all the patients there is a significant overlap between the rectum and the CTV. Evaluation of plan quality was made using conventional dosimetric measures such as the value of the near-minimum dose, D_{98}, and the near-maximum dose, D_2, for the CTV and the mean dose and/or D_2 for the organs-at-risk. D_{98} represents the dose that is being deposited in, at least, 98% of the volume. For instance, saying that $D_{98} \geq 68$ Gy(RBE) means that at least 98% of the volume has to receive at least 68 Gy(RBE).

In the present work the irradiation angles considered were the ones usually used in clinical practice: two coplanar lateral parallel-opposed beam angles [9]. RBE was considered equal to 1.1.

Table 1. Dose prescription for the treatment plans (Gy(RBE)).

CTV	Rectum	Bladder	Femoral heads	Body
$D_{98} \geq 68$ $D_2 \leq 72.8$	$D_2 \leq 72.1$	$D_{mean} \leq 50$ $D_{max} \leq 76$	$D_2 \leq 45$	$D_{max} \leq 82$

3.2 Automated Treatment Planning Optimization

There are many different models described in the literature that can be used for treatment planning optimization when irradiation angles are considered fixed. When beam angle optimization is not performed, then the treatment parameters that must be determined consider the intensity of the radiation that is delivered from each one of the irradiation directions (beams). In IMPT these intensities can be modulated, meaning that each irradiation direction can be discretized. Each beam is interpreted as being composed by a set of small beams, the scanning pencil beams (beamlets), whose terminal zone of the beam is called a spot, responsible for the deposition of the largest dose fraction in the tumor [28]. The intensities of all the beams are optimized simultaneously, so that their spots lead to the production of a uniform total dose distribution in the tumor volume [29].

In this work, an unconstrained optimization model with a quadratic objective function was used. This objective function penalizes all voxels that do not comply with established lower and/or upper bounds. This penalty is calculated as the square difference between the upper/lower limit and the delivered dose at a given iteration, allowing to obtain a convex and easy to optimize function. This means that, for an OAR, the function is penalized when the dose at a certain voxel exceeds the corresponding upper limit, for instance. For the CTV, it is necessary to penalize the function when the dose at a given voxel is lower than the lower bound or the dose exceeds the upper bound being considered.

The objective function used for this optimization is presented in Eq. 1. The number of beamlets is represented by N and D_{ij} represents the dose contribution of beamlet j to the voxel i, so $\sum_{j=1}^{N} D_{ij}w_j$ is the total dose received by the voxel i, considering that w_j is the intensity of beamlet j. The lower and upper bounds are defined by L_s and U_s, respectively, for each structure s belonging to S, the set of all structures. Finally, λ_s is the weight (importance) of structure s.

$$\begin{aligned} \min f = & \sum_{s\in S}\sum_{i\in s}\left[\lambda_s(L_s - \sum_{j=1}^{N} D_{ij}w_j)_+^2 + (\sum_{j=1}^{N} D_{ij}w_j - U_s)_+^2\right] \\ & \text{such that}, w_j \geq 0, j = 1, \ldots, N \end{aligned} \tag{1}$$

In clinical practice, the planner iteratively changes some parameters of this objective function (namely λ_s, L_s and U_s) using a software that is called treatment planning system. The dose bounds and weights associated to each volume of interest are changed until an admissible treatment plan is found. One way to automate this process is through fuzzy inference systems (FIS), that allow an algorithmic and mathematical representation of the reasoning made by human planners during this trial-and-error procedure. FIS allow a set of simple rules to be defined, each rule of the form: if the deviation from the prescribed/tolerance dose is small, the parameters only need to be slightly changed; if the deviation from the prescribed/tolerance dose is medium, then the algorithm will need to change the parameters mediumly; if the deviation from the prescribed/tolerance dose is high, the parameters should be significantly changed. The mathematical representation of natural language concepts, like "small" or "high" can be achieved by using fuzzy numbers. This approach has already been successfully

applied to photon-based radiotherapy treatment planning in the work of Dias et al. [8], and has now been adapted to proton treatment optimization. The greatest advantage of this procedure is the fact that no manual tuning of the model parameters is needed.

3.3 Robust IMPT Treatment Planning Optimization

Two different robust automated treatment planning optimization approaches are considered and compared. In the first one, for each existing clinical region of interest (ROI - that can either be CTV or OAR) outlined by the radiation oncologist, a set of auxiliary structures is created (a set of *clones*). Each *clone* corresponds to the original structure but in a different relative position, by shifting the structure along the x, y and z axes. Overall, fourteen *clones* were created for each structure: six by shifting the original structures in each direction $(\pm x, \pm y, \pm z)$ and the remaining ones were created considering shifts in all the possible diagonal combinations. These *clones* inherit all the dosimetric objectives of the original structures, and they are all simultaneously taken into consideration during the optimization procedure to guarantee that the medical prescription is fulfilled regardless of what may occur when position and beam range uncertainties are simultaneously accounted for. Two different shift lengths were considered: 3 mm and 6 mm designated as *clones* 3 mm and *clones* 6 mm, respectively.

The second approach considers what is usually done in clinical practice, where a PTV and PRV are created as enlarged versions of the CTV and OARs to account for uncertainties. For the two alternative strategies to be fairly compared, in this work these structures are created by the union of all the corresponding *clones*. We call these structures pseudo-PTV and pseudo-PRV, just to highlight the fact that they have not been delineated manually by the medical oncologist. If manually PTV and PRV were considered, differences in the results could be due to the delineation choices and not to the differences between the two approaches. In this second approach it is possible to consider pseudo-ROI 3 mm or pseudo-ROI 6 mm, resulting from the union of the *clones* 3 mm and *clones* 6 mm, respectively.

Therefore, two robust optimization approaches were implemented: one resorting to the creation of several additional structures, the *clones*, and another one creating only one structure for each ROI, the pseudo-ROI. Both approaches were tested considering two shift lengths: 3 mm and 6 mm.

The top image of Fig. 1 shows an example of some of the *clones* created in each direction alone $(+x, +y, +z)$, for every structure. Not all the *clones* are represented in the figure as it would be impossible to distinguish the different structures in the image. Figure 1(b) shows the pseudo-PTV and pseudo-PRVs considering 6 mm shifts, as well as the original structures (but only the Pseudo-ROI structures are taken into account in treatment plan optimization).

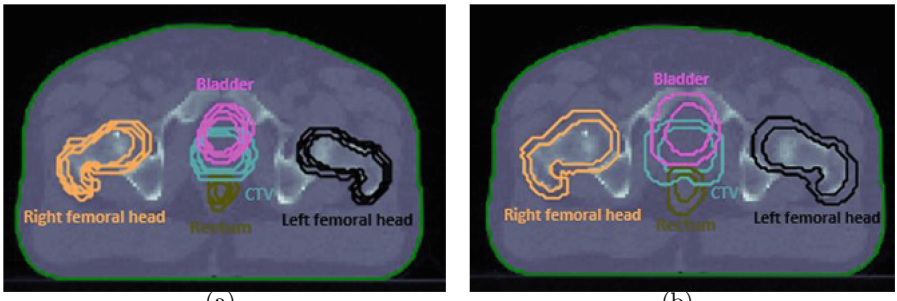

(a) (b)

Fig. 1. Representation of some of the *clones* created by applying a 6 mm shift from the structures outlined by the radiation oncologist in each direction $(+x, +y, +z)$ – 1(a) and representation of the original ROIs, as well as of the corresponding pseudo-PTV and pseudo-PRVs created from the union of all 6 mm-*clones* – 1(b).

3.4 IMPT Treatment Plan Quality Assessment

Any source of uncertainty that can arise during treatment delivery can lead to deviations between the planned and the delivered dose distribution. Thus, it is important to evaluate the resilience of each treatment plan against uncertainties. In this work, treatment plans were evaluated considering the impact of patient setup and beam range uncertainties. Monte Carlo simulation was used for this purpose, where setup and beam range uncertainties were represented by random variables following a normal distribution. In this evaluation, 100 scenarios were generated by simultaneously considering all the different sources of uncertainty, each scenario comprising 34 fractions to represent the whole treatment delivery time horizon. It is thus possible to consider both setup and random (daily) positioning errors.

Positioning uncertainties were simulated by shifting the isocenter position [30], following a normal distribution with mean of zero and a standard deviation of 2.5 mm. The positioning uncertainty considers both systematic and random errors. A random upscale or downscale was applied to the Hounsfield units of TC [20], following a normal distribution with mean value of zero and standard deviation of 1.75%. This is kept fixed for the 34 fractions. To avoid scenarios that are unlikely to occur, the maximum positioning deviation possible is 5 mm, whereas the maximum range upscale or downscale is 3.5% [25,28].

3.5 Computational Experiments Setting

The work was developed within the platform matRad, which is a radiotherapy treatment planning system developed at the German Center for Cancer Research (DKFZ) [31], programmed in MATLAB (version 2018b), for academic research. Computational tests were performed in an Intel 873 Xeon Silver 4116, 2.1 gigahertz, 12-core processor, 128 gigabyte 874 RAM.

Statistical analysis was done using the one-way ANOVA test to evaluate if there were statistical differences between the existing groups. A post-hoc Tuckey HSD test was done to confirm among which groups statistical differences occur.

4 Results

The main goal of this work was to investigate new strategies for automated robust treatment planning for IMPT. Two robust optimization approaches were applied to five prostate cancer patients. The fuzzy inference mechanism automated the FMO procedure and made it possible to achieve treatment plans complying with the defined tolerance doses and prescriptions for the defined ROI for every strategy described, i.e., the *clones* and the pseudo-ROI.

Monte Carlo simulation was used to assess the robustness of each treatment plan as well as the fulfillment of the prescribed and tolerance doses when uncertainty is explicitly considered. In this simulation, only the original structures of interest, impacted by the different sources of uncertainty, are taken into account for dose calculation.

The mean dosimetric values over the 100 scenarios were used to assess if the structure achieved or did not exceed, on average, the prescribed or tolerance dose, respectively. The standard deviation was used as a measure of robustness. The lower the standard deviation, the more robust the plan is, which means it presents a lower susceptibility to uncertainties.

For illustration purposes, the dose-volume histogram (DVH) for one of the patients in this study is presented in Fig. 2 for the plan obtained when optimization was based on the *clones* 6 mm and *clones* 3 mm strategies, for all the structures of interest, i.e., CTV, rectum, bladder, and femoral heads. The robustness of the treatment plan can be assessed by the band width of each set of curves. The narrower the set of curves the more robust the treatment plans are. For instance, the rectum is the structure where larger deviations occur, since it is the one with the widest curve group in both strategies. The curve obtained for CTV is narrower in the *clones* 6 mm strategy, compared with the *clones* 3 mm strategy, which means that there was a lower variability between the dose distributions of the CTV in the 100 simulated scenarios.

Figure 3 shows the histogram of the D_{98} values for the CTV obtained with Monte Carlo simulation for the optimization strategies implemented. The vertical dashed line indicates the prescription dose of the CTV, and thus the lowest dose value that is considered acceptable in the CTV for plan approval. This analysis is also very important because average values alone are not able to tell the whole story: for plan approval, the prescribed and tolerance doses should be met in all the generated scenarios. Monte Carlo simulation results show that, for all optimization strategies tested, the dose delivered to the CTV was equal or superior to 68 Gy(RBE) in every simulated scenario, except for the plan using *clones* 3 mm. For patient 0, the treatment plan did not achieve the prescribed dose in 12% of the scenarios (patient 0), and for other (patient 3) in 3% of the scenarios. So, the assurance of the satisfaction of the prescription under all generated scenarios was not guaranteed.

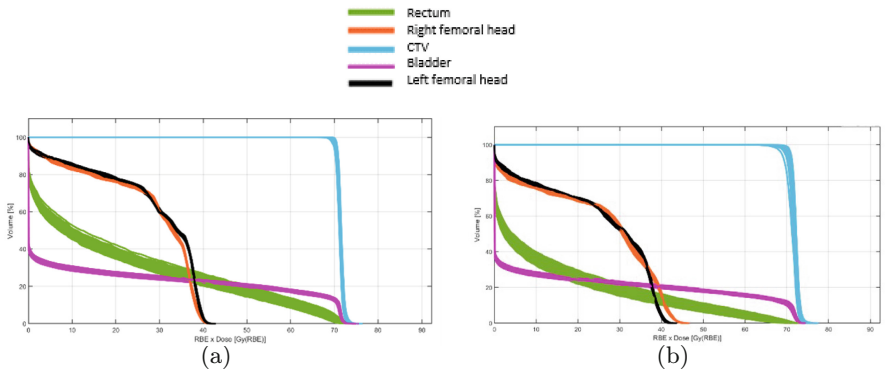

Fig. 2. DVH obtained for one patient for the 100 scenarios generated in the Monte Carlo simulation, for the strategy where *clones* were created with 6 mm shifts – 2(a) and with 3 mm shifts – 2(b) from the original structures.

Figure 4 presents a histogram with the values of D_2 for the rectum. The vertical dashed line represents the maximum dose that can be delivered to the rectum, i.e., the tolerance dose, showing that this tolerance was always respected. Furthermore, the average dose in the rectum is 5–10 Gy lower with the 3 mm shifts than with 6 mm. The bladder and right femoral head always fulfill the tolerance doses in the treatment plans calculated. Only the left femoral head exceeded the tolerance dose in the pseudo-ROI 3 mm strategy for one patient and in the pseudo-ROI 6 mm strategy in another patient.

Table 2 show the mean and standard deviation (SD) of the dosimetric parameters for the 100 scenarios simulated by Monte Carlo for each patient. The F value obtained from the ANOVA test and its p-value are also shown in Table 3, revealing that there are statistically significant differences between the four strategies.

Considering the results obtained when 3 mm shifts were used, the treatment plans obtained with the pseudo-ROI have a smaller SD than the treatment plans obtained with the *clones* 3 mm. Overall, the treatment plans obtained with the 6 mm shifted structures led to a reduction in the standard deviation comparing with the 3 mm shifts' strategies while adequate CTV coverage was achieved for every patient for the approach considering larger shifts.

For patient 0, the best CTV D_{98} value is obtained by the treatment plans *clones* 6 mm and Pseudo-ROI 3 mm, which present values that are not significantly different. Although better sparing of the rectum can be achieved, in average terms, with Pseudo-ROI 3 mm, this treatment plan is less robust since it presents a larger standard deviation value than the treatment plan based on the *clones* 6 mm strategy. A similar observation can be made regarding the right femoral head. *Clones* 6 mm present the best result for the left femoral head. For patient 1, the strategies based on the 6 mm shifts present better CTV D_{98} values, that are not significantly different between themselves. Comparing these two strategies, *clones* 6 mm present a statistically significant better OAR sparing. For

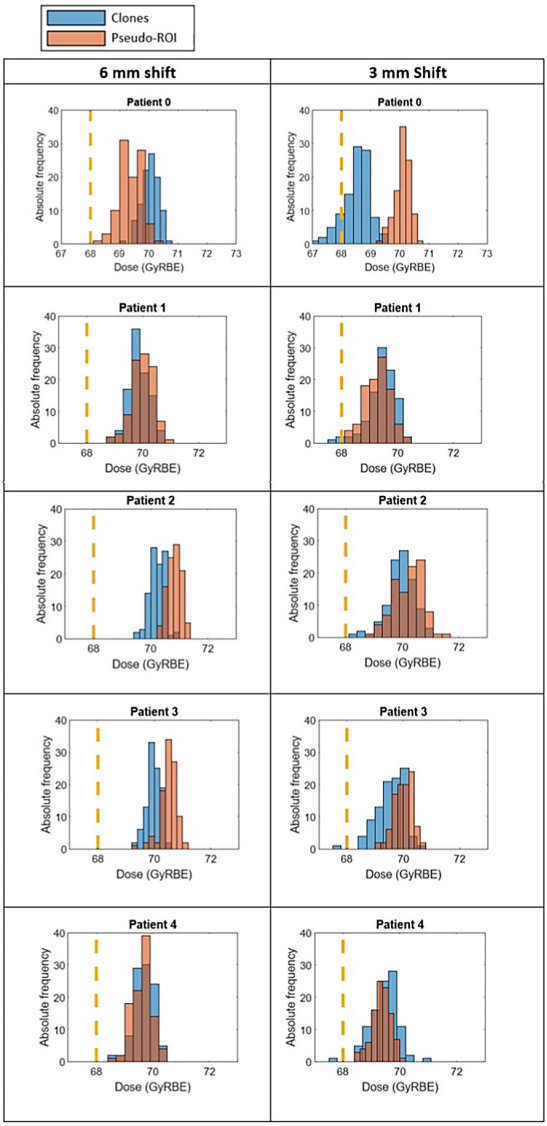

Fig. 3. Histograms of the D_{98} values for the CTV obtained with Monte Carlo simulation for the optimization strategies implemented.

patient 2, better CTV D_{98} value is obtained with the Pseudo-ROI 6 mm strategy, being the difference between this approach and the *clones* 6 mm of under 0.6 Gy. When looking at the OARs, *clones* 6 mm present much better dosimetric values, with differences, looking at the average values, of 5 Gy for femoral heads. The best CTV D_{98} value for patient 3 is also found with the Pseudo-ROI 6 mm

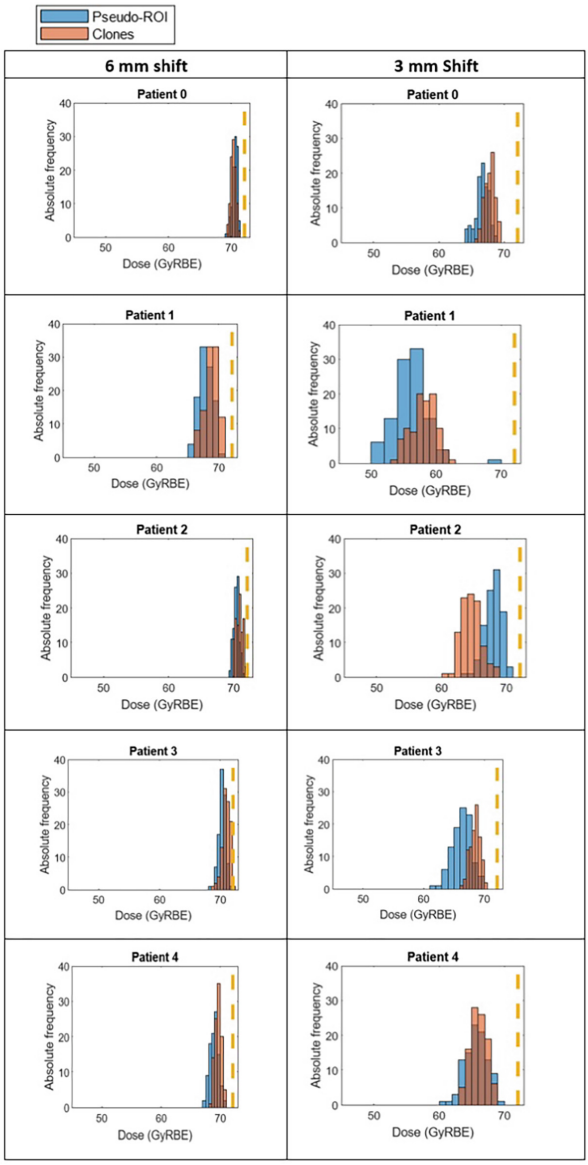

Fig. 4. Histograms of the D_2 values for the Rectum obtained with Monte Carlo simulation for the optimization strategies implemented.

strategy treatment plan but, once again, with differences considering average values of less than 0.6 Gy. *Clones* 6 mm treatment plan presents the lowest dose to the femoral heads. Pseudo-ROI 3 mm treatment plan presents a better value for rectum sparing, but at a cost of greater variability than with *clones* 6 mm.

Table 2. Mean and Standard Deviation (SD) obtained from Monte Carlo simulation, for 100 scenarios with 34 fractions, considering 3 mm and 6 mm shifts.

	3 mm shifts				6 mm shifts			
	Patient 0							
	Clones 3 mm		Pseudo-ROI 3 mm		Clones 6 mm		Pseudo-ROI 6 mm	
	Mean	SD	Mean	SD	Mean	SD	Mean	SD
D_{98} CTV	68.52^{a}	.46	70.09^{b}	.26	70.04^{b}	.29	69.38^{c}	.38
D_{mean} Bladder	11.31^{a}	.32	12.08^{b}	.31	13.61^{c}	.38	13.53^{c}	.33
D_2 rectum	66.66^{a}	.99	67.80^{b}	.78	70.56^{c}	.40	70.32^{c}	.38
D_2 right femoral head	41.09^{a}	.16	37.48^{b}	.30	39.55^{c}	.08	42.49^{d}	.08
D_2 left femoral head	41.66^{a}	.20	37.90^{b}	.21	39.92^{c}	.10	42.56^{d}	.08
	Patient 1							
	Clones 3 mm		Pseudo-ROI 3 mm		Clones 6 mm		Pseudo-ROI 6 mm	
	Mean	SD	Mean	SD	Mean	SD	Mean	SD
D_{98} CTV	69.43^{a}	.52	69.28^{a}	.47	69.84^{b}	.37	70.00^{b}	.39
D_{mean} Bladder	5.93^{a}	.30	5.75^{b}	.24	7.16^{c}	.32	8.50^{d}	.30
D_2 rectum	56.13^{a}	2.61	58.04^{b}	1.92	67.92^{c}	1.12	68.81^{d}	1.03
D_2 right femoral head	40.17^{a}	.19	39.94^{b}	.23	40.40^{c}	.29	41.13^{d}	.14
D_2 left femoral head	40.30^{a}	.29	41.38^{b}	.22	39.09^{c}	.15	42.43^{d}	.14
	Patient 2							
	Clones 3 mm		Pseudo-ROI 3 mm		Clones 6 mm		Pseudo-ROI 6 mm	
	Mean	SD	Mean	SD	Mean	SD	Mean	SD
D_{98} CTV	69.95^{a}	.50	70.21^{b}	.50	70.23^{b}	.26	70.82^{c}	.24
D_{mean} Bladder	24.94^{a}	.83	26.63^{b}	.81	30.17^{c}	.72	32.35^{d}	.66
D_2 rectum	67.98^{a}	1.29	64.58^{b}	1.51	70.44^{c}	.42	70.86^{d}	.50
D_2 right femoral head	40.96^{a}	.19	41.27^{b}	.18	39.15^{c}	.11	44.35^{d}	.23
D_2 left femoral head	41.89^{a}	.23	42.57^{b}	.34	39.45^{c}	.11	46.40^{d}	.13
	Patient 3							
	Clones 3 mm		Pseudo-ROI 3 mm		Clones 6 mm		Pseudo-ROI 6 mm	
	Mean	SD	Mean	SD	Mean	SD	Mean	SD
D_{98} CTV	69.57^{a}	.49	70.00^{b}	.32	69.97^{b}	.24	70.51^{c}	.29
D_{mean} Bladder	15.31^{a}	.29	16.42^{b}	.30	16.79^{c}	.29	17.78^{d}	.29
D_2 rectum	66.24^{a}	1.51	68.45^{b}	.83	70.32^{c}	.55	70.94^{d}	.61
D_2 right femoral head	43.21^{a}	.20	43.75^{b}	.09	39.83^{c}	.10	43.19^{a}	.20
D_2 left femoral head	40.60^{a}	.11	45.56^{b}	.08	40.16^{c}	.09	44.28^{d}	.12
	Patient 4							
	Clones 3 mm		Pseudo-ROI 3 mm		Clones 6 mm		Pseudo-ROI 6 mm	
	Mean	SD	Mean	SD	Mean	SD	Mean	SD
D_{98} CTV	69.45^{a}	.48	69.35^{a}	.33	69.68^{b}	.35	69.62^{b}	.35
D_{mean} Bladder	8.36^{a}	.55	9.53^{b}	.48	$11.47c$	.53	12.73^{d}	.68
D_2 rectum	65.69^{a}	1.72	66.16^{b}	1.22	68.97^{c}	.73	69.62^{d}	.54
D_2 right femoral head	37.54^{a}	.25	38.27^{b}	.22	39.97^{c}	.21	38.71^{d}	.18
D_2 left femoral head	36.38^{a}	.24	36.44^{a}	.32	40.29^{b}	.18	39.35^{c}	.25

Note: means with different letters are statistically different for $\alpha \leq 0.05$, considering post-hoc Tuckey HSD test. *** $p < .001$

Both *clones* 6 mm and Pseudo-ROI 6 mm present similar results regarding CTV D_{98} values for patient 4. *Clones* 6 mm spares better all the OARs but left femoral head, when compared with the Pseudo-ROI 6 mm plan.

Table 3. F values computed from the different plans calculated for each patient.

F value	Patient 0	Patient 1	Patient 2	Patient 3	Patient 4
D_{98} **CTV**	425.86***	59.27***	87.21***	121.87***	15.42***
D_{mean} **Bladder**	1125.90***	1852.61***	1959.41***	1216.47***	1185.13***
D_2 **rectum**	770.77***	1341.57***	760.36***	490.82***	294.31***
D_2 **right femoral head**	14497.24***	558.00***	13951.95***	19657.05***	2395.04***
D_2 **left femoral head**	16725.48***	4661.84***	16879.59***	67808.41***	7217.24***

Note: *** $p < .001$

5 Discussion

This paper presents and compares two different approaches for IMPT robust automated treatment plan optimization. The goal was to generate admissible treatment plans, with no human-planner intervention, guaranteeing that these plans were robust against uncertainties present in IMPT delivery, such as patient positioning and beam range. The treatment plans obtained by applying the automated fuzzy inference system optimization procedure made it possible to generate high quality plans in a totally automated way, even taking simultaneously into account a large number of structures, as it is the case with the approach based on the creation of *clones*.

Looking at the average values, and in the presence of setup and range uncertainties, the generated treatment plans can still fulfill the prescribed and tolerance doses. However, the aim was to assure that the treatment plans were admissible under all the generated scenarios and that the variability within the results was minimized. Thus, all treatment plans were assessed considering a set of 100 scenarios generated by Monte Carlo simulation.

This result is in accordance with what would be expected, but only possible thanks to the capability of the optimization method to automatically calculate treatment plans where all the restrictions (prescription and tolerance doses) are satisfied, either considering additional structures or one enlarged structure for each ROI. Actually, applying these shifts not only to the CTV but also to the OARs is crucial. If only the CTV structure was considered, then it would not be possible to properly spare the OARs when uncertainty is explicitly taken into account (actually, larger shifts would lead to worse results for the OARs).

It can be concluded that 6 mm margins increase the robustness of the treatment plans, in comparison with the 3 mm margins, guaranteeing proper CTV coverage whilst also sparing adequately OARs. Furthermore, with the treatment plans based on 6 mm shifts structures, target coverage was enhanced in comparison with the strategies using 3 mm shifts. The *clones* 3 mm strategy was the only one that did not guarantee target coverage in all the simulated scenarios. Although both strategies, i.e., the *clones* or the pseudo-ROI strategies, gave satisfactory results, some differences between them can be highlighted. The treatment plans obtained through the *clones* strategies were the ones better sparing the OARs, compared with the pseudo-ROI strategies. Actually, the *clones*

strategy with 6 mm shifts made it possible to guarantee proper target coverage while better sparing OARs in every simulated scenario.

Looking at the 6 mm shifts strategies, as target coverage was always achieved, OAR sparing and robustness of the treatment plans were the chosen features to assess which strategy performed better. The *clones* 6 mm strategy was more robust against the considered uncertainties, showing a lower standard deviation. So, these plans are less sensitive to uncertainties. Furthermore, the *clones* 6 mm delivered less dose to the OARs compared with the pseudo-ROI 6 mm. So, this strategy was able to guarantee that tolerance doses were always fulfilled. Hence, *clones* 6 mm is considered the strategy that performed best, showing a better compromise between dose prescription fulfillment and robustness.

Although these strategies were only implemented in a set of patients with prostate cancer, this study could be extended to other tumor sites. Proton radiotherapy is very sensitive to uncertainties, and even a small change in the patient's anatomy can have a large impact on the dose distribution. Consequently, a decrease in the plan's quality can occur. Hence, methods that guarantee delivery of the treatment plan to the patient as planned are crucial to further improve the success of the treatment. The strategies implemented in this study revealed that taking uncertainties into consideration during the planning process, namely considering additional auxiliary structures, led to a low variability in the dose distributions. Therefore, robust optimization algorithms can reduce the impact of uncertainties during treatment delivery.

6 Conclusion

One of the main disadvantages of Proton therapy treatment is the fact that this treatment modality is highly vulnerable to existing sources of uncertainty. This can lead to significant differences between the treatment that is planned and the treatment that is indeed delivered, with consequences in terms of the treatment outcome (probability of disease control and of occurrence of treatment induced complications). In this paper we show that explicitly taken uncertainty into account when optimizing treatment plans can improve the robustness of the treatment plans without increasing the workload of the human planners, since all the process can be totally automated. Robust optimization methods contribute to reducing the impact of setup and range uncertainties in the treatment plan for IMPT. Robust treatment plans were achieved with the four different strategies, i.e., the *clones* and pseudo-ROIs created with two different shift lengths. This conclusion can be reached since the fulfillment of the prescribed and tolerance doses was accomplished in almost every scenario (being the exception the *clones* 3 mm strategy). Most importantly, the robustness is assessed by the low standard deviations obtained, that reveal a low variability in the dose distributions. The difference between each one of the implemented strategies is related to compromises that exist among OAR sparing, tumor coverage and robustness. It was shown that the *clones* were better at guaranteeing these compromises compared to the pseudo-ROI's strategies.

It can be concluded that the *clones* 6 mm strategy can be a valuable alternative, assuring the automatic calculation of robust treatment plans that behave well under uncertainty. This strategy shows benefits when compared with the consideration of a single enlarged structure for each ROI (similar to the PTV/PVR approach). As the number of structures that are simultaneously considered increases significantly, this strategy is only feasible due to the possibility of using FIS to automate treatment planning optimization.

Acknowledgments. This work has been partly supported by the Fundação para a Ciëncia e a Tecnologia (FCT) under project grants UTA-EXPL/FMT/0079/2019, UIDB/00645/2020, UIDB/00308/2020 and UIDB/05037/2020 with DOI 10.54499/UIDB/05037/2020.

References

1. Evans, E., Staffurth, J.: Principles of cancer treatment by radiotherapy. Surg. Oxf. **36**, 111–116 (2018)
2. Shepard, D.M., Ferris, M.C., Olivera, G.H., Mackie, T.R.: Optimizing the delivery of radiation therapy to cancer patients. SIAM Rev. **41**, 721–744 (1999)
3. Brady, L.W., Heilmann, H.P., Molls, M.: New Technologies in Radiation Oncology. Springer, Heidelberg (2006). https://doi.org/10.1007/3-540-29999-8
4. Song, J., Shi, Z., Sun, B., Shi, L.: Treatment planning for volumetric-modulated arc therapy: Model and heuristic algorithms. IEEE Trans. Autom. Sci. Eng. **12**, 116–126 (2014)
5. Wang, F., Huang, Y.-L., Ju, F.: Simulation optimization gantry call-back control method for proton therapy systems. IEEE Trans. Autom. Sci. Eng. **20**, 1565–1576 (2022)
6. Mohan, R., Grosshans, D.: Proton therapy-present and future. Adv. Drug Deliv. Rev. **109**, 26–44 (2017)
7. ICRU, Prescibing, Recording and Reporting Proton-Beam Therapy (ICRU Report 78). J. ICRU (2007)
8. Dias, J., Rocha, H., Ventura, T., Ferreira, B., Lopes, M.C.: Automated fluence map optimization based on fuzzy inference systems. Med. Phys. **43**, 1083–1095 (2016)
9. Cao, W., et al.: Reflections on beam configuration optimization for intensity-modulated proton therapy. Phys. Med. Biol. **67**, 13TR01 (2022)
10. Rocha, H., Dias, J.M., Ferreira, B.C., Lopes, M.C.: Combinatorial optimization for an improved transition from fluence optimization to fluence delivery in IMRT treatment planning. Optimization **61**, 969–987 (2012)
11. Lim, G.J., Cao, W.: A two-phase method for selecting IMRT treatment beam angles: branch-and-Prune and local neighborhood search. Eur. J. Oper. Res. **217**, 609–618 (2012)
12. Bertsimas, D., Cacchiani, V., Craft, D., Nohadani, O.: A hybrid approach to beam angle optimization in intensity-modulated radiation therapy. Comput. Oper. Res. **40**, 2187–2197 (2013)
13. Rocha, H., Dias, J.M., Ferreira, B.C., Lopes, M.C.: Selection of intensity modulated radiation therapy treatment beam directions using radial basis functions within a pattern search methods framework. J. Glob. Optim. **57**, 1065–1089 (2013)

14. Dias, J., Rocha, H., Ferreira, B., Lopes, M.C.: A genetic algorithm with neural network fitness function evaluation for IMRT beam angle optimization. Cent. Eur. J. Oper. Res. **22**, 431–455 (2014)
15. Lim, G.J., Kardar, L., Cao, W.: A hybrid framework for optimizing beam angles in radiation therapy planning. Ann. Oper. Res. **217**, 357–383 (2014)
16. Rocha, H., Dias, J.M., Ventura, T., Ferreira, B.C., Lopes, M.C.: Beam angle optimization in IMRT: are we really optimizing what matters? Int. Trans. Oper. Res. **26**, 908–928 (2019)
17. Gutierrez, M., Cabrera-Guerrero, G., Lagos, C.: A Reduced Variable Neighbourhood Search for the Beam Angle Optimisation Problem. IEEE Trans. Emerg. Top. Comput. Intell. **7**, 1499–1510 (2023)
18. Chan, T.C., Craig, T., Lee, T., Sharpe, M.B.: Generalized inverse multiobjective optimization with application to cancer therapy. Oper. Res. **62**, 680–695 (2014)
19. Wedenberg, M., Beltran, C., Mairani, A., Alber, M.: Advanced treatment planning. Med. Phys. **45**, e1011–e1023 (2018)
20. Unkelbach, J., Paganetti, H.: Robust proton treatment planning: physical and biological optimization. Semin. Radiat. Oncol. **28**, 88–96 (2018)
21. McGowan, S.E., Burnet, N.G., Lomax, A.J.: Treatment planning optimisation in proton therapy. Br. J. Radiol. **86**, 20120288–20120288 (2013)
22. Wahl, N., Hennig, P., Wieser, H.P., Bangert, M.: Efficiency of analytical and sampling-based uncertainty propagation in intensity-modulated proton therapy. Phys. Med. Biol. **62**, 5790 (2017)
23. Wahl, N., Hennig, P., Wieser, H.-P., Bangert, M.: Analytical incorporation of fractionation effects in probabilistic treatment planning for intensity-modulated proton therapy. Med. Phys. **45**, 1317–1328 (2018)
24. Liu, W., et al.: Effectiveness of robust optimization in intensity-modulated proton therapy planning for head and neck cancers. Med. Phys. **40**, 051711 (2013)
25. Zaghian, M., Cao, W., Liu, W., Kardar, L., Randeniya, S., Mohan, R., Lim, G.: Comparison of linear and nonlinear programming approaches for "worst case dose" and "minmax" robust optimization of intensity-modulated proton therapy dose distributions. J. Appl. Clin. Med. Phys. **18**, 15–25 (2017)
26. Khoo, E.L., et al.: Prostate contouring variation: can it be fixed? Int. J. Radiat. Oncol. Biol. Phys. **82**, 1923–1929 (2012)
27. Unkelbach, J., et al.: Robust radiotherapy planning. Phys. Med. Biol. **63**, 22TR02 (2018)
28. Liu, W., Zhang, X., Li, Y., Mohan, R.: Robust optimization of intensity modulated proton therapy. Med. Phys. **39**, 1079–1091 (2012)
29. Mohan, R., Das, I.J., Ling, C.C.: Empowering intensity modulated proton therapy through physics and technology: an overview. Int. J. Radiat. Oncol. Biol. Phys. **99**, 304–316 (2017)
30. Fredriksson, A., Forsgren, A., Hardemark, B.: Minimax optimization for handling range and setup uncertainties in proton therapy. Med. Phys. **38**, 1672–1684 (2011)
31. Wieser, H.P., et al.: Development of the open-source dose calculation and optimization toolkit matRad. Med. Phys. **44**, 2556–2568 (2017)

Enhancing Medical Imaging Through Data Augmentation: A Review

Beatriz Teixeira[1], Gonçalo Pinto[1], Vitor Filipe[1,2], and Ana Teixeira[1,3(✉)]

[1] University of Trás-os-Montes e Alto Douro, Quinta de Prados, 5001-801 Vila Real, Portugal
{al73263,al74081}@alunos.utad.pt, {vfilipe,ateixeir}@utad.pt
[2] INESC TEC- INESC Technology and Science, 4200-465 Porto, Portugal
[3] Mathematics centre CMAT, Pole CMAT-UTAD, Vila Real, Portugal

Abstract. This article conducts a comprehensive review of the existing literature on data augmentation and data generation techniques within the context of medical image processing. Addressing the challenges associated with building sizable medical image datasets, including the rarity of certain medical conditions, patient privacy concerns, the need for expert labeling, and the associated expenses, this review focuses on methodologies aimed at enhancing the volume and diversity of available data. Special emphasis is placed on techniques such as data augmentation and data generation, with a particular interest in their application to medical image datasets. The objective is to provide a synthesis of current research, methodologies, and advancements in this domain, offering insights into the state-of-the-art practices and identifying potential avenues for future developments in medical image data augmentation.

Keywords: Data generation · Medical Image · Image Data Augmentation

1 Introduction

In supervised learning, where classification is one of the best-known tasks, the number of labeled examples available and the results are related: the greater the number of examples, the greater the prediction capacity of the classifiers generated. However, in real-life situations, having databases with a large number of labeled examples is not always an easy task, and is often costly. In order to overcome this problem, data augmentation (DA) approaches, based on computational techniques with the aim of increasing the number of labeled examples in a data set and improve the results obtained, can be used [1]. Data warping augmentations involve transforming existing images in a way that retains their labels. This includes geometric and color transformations, random erasing, adversarial training, and neural style transfer. Oversampling augmentations create synthetic instances and incorporate them into the training set. This encompasses techniques such as mixing images, feature space augmentations, and generative adversarial networks (GANs) (Fig. 1). Developing a generative AI model

© The Author(s), under exclusive license to Springer Nature Switzerland AG 2024
O. Gervasi et al. (Eds.): ICCSA 2024 Workshops, LNCS 14816, pp. 341–354, 2024.
https://doi.org/10.1007/978-3-031-65223-3_23

for image synthesis requires a deep understanding of machine learning ideas, including deep neural networks, loss functions and optimization strategies. Deep learning methods consist of mapping input data to output data using deep neural networks and optimization algorithms. These networks, with multiple layers of interconnected neurons, learn complex patterns by adjusting the weights of the connections during training. Optimization algorithms are used to minimize the cost function, allowing the neural network to improve mapping accuracy. The backpropagation process is key to calculating gradients and adjusting weights, making deep learning effective for a variety of applications, such as image recognition [2]. Creating large medical image datasets poses significant challenges, mainly due to the infrequency of certain diseases, privacy concerns related to patient data, the necessity for expert labeling, and the high costs and labor-intensive nature of medical imaging procedures. These difficulties have spurred extensive research into image data augmentation, with a particular focus on oversampling techniques using GANs. This research is driven by the practical need for effective medical image classification applications [3].



Fig. 1. A taxonomy of image data augmentations covered; for example, meta-learning using neural style transfer is covered by neural augmentation [3].

What's left of this article is organized as follows in Sect. 2, the Materials and Methods are introduced, in Sect. 3, is made an analysis of the articles found, and in Sect. 4, the results are discussed. In Subsect. 4.1, articles focused on general algorithms will be addressed, while in Subsect. 4.2, articles focused on a specific organ will be presented. Finally, in Sect. 5, the conclusion is presented.

2 Materials and Methods

A literature review was conducted to explore the application of data generation techniques in the realm of medical image analysis. The Scopus database, a comprehensive and multidisciplinary bibliographic resource spanning various academic domains, was used for the initial phase, which involved examining scientific works on the utilization of predictive models for medical image data generation. This examination employed keywords or abbreviations such as data generation and medical image. The complete search string used was (data AND & AND generation AND & AND medical AND & AND image). Subsequently, titles and abstracts were independently scrutinized based on predefined inclusion/exclusion criteria (Table 1).

Table 1. Article selection criteria.

Stage	Selection Criteria
Identification	Total number of articles initially found
Screening	Belong to the articles category
	Year of publication between 2020 and 2023
	Full access
	English language
Eligibility	Addressing medical imaging
	Approaching the field of engineering
Included	Relating to GANs
	Interface with medical imaging

Figure 2 shows the flow diagram of the work developed, which synthesizes the review/selection process performed. This methodology aimed to provide a comprehensive overview of the current research landscape and advancements in the domain of data generation in medical image analysis.

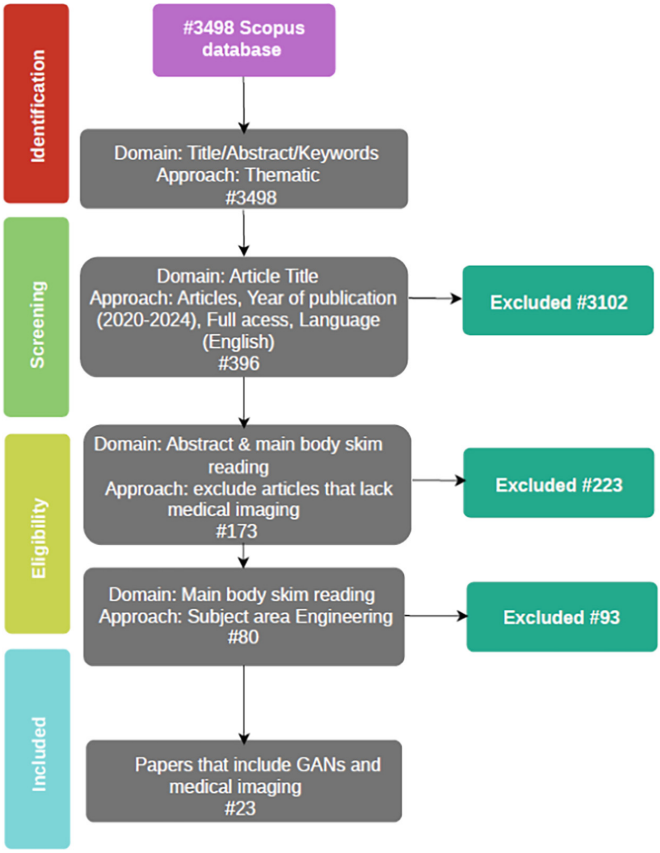

Fig. 2. PRISMA flow diagram

3 Quantitative Analysis of the Entries

During the 2020–2023 period, several authors have developed and written about techniques that make possible to generate larger databases; thus, allowing new artificial intelligence methods to obtain better classifications and, consequently, helping health professionals to make a more effective diagnosis. The following graph (Fig. 3) helps us to understand in which years the articles were written.

A graphic representation was meticulously drawn up showing the different countries of origin of each one of the analyzed articles (Fig. 4). The importance of collaborative efforts in scientific literature should be emphasized. Articles authored by several individuals bring a wide variety of perspectives and ideas to the table. As our graphic representation vividly illustrates, the amalgamation of diverse voices from different regions creates a mosaic of knowledge.

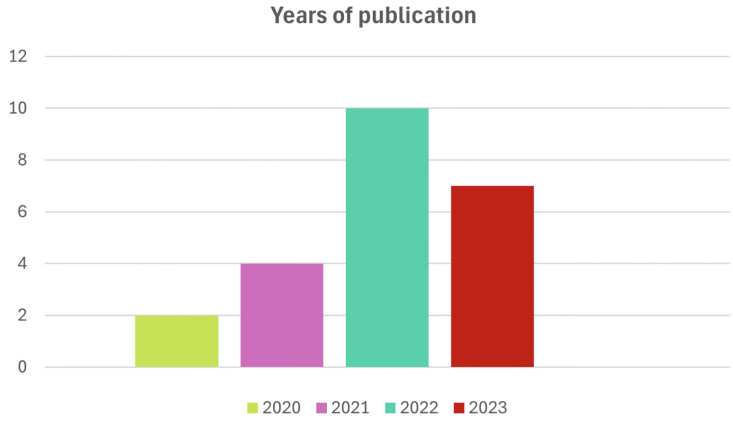

Fig. 3. Articles organized according to year of publication.

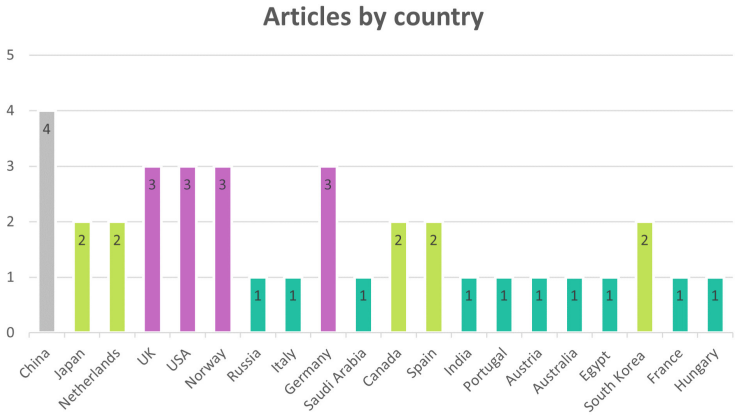

Fig. 4. Graphic of the number of articles by country.

4 Discussion

As the demand for more accurate diagnoses and personalized treatment plans grows, there is a need for advancements in the field. This work explores the application of data augmentation techniques to enhance medical imaging outcomes. The accurate interpretation of medical images, such as MRIs, CT scans, and X-rays, is fundamental to diagnostic accuracy. Discussing the critical role of medical imaging sets the stage for understanding the need for continuous improvement in this domain. Despite the advancements in technology, challenges persist in medical imaging, including limited datasets, class imbalance, and the need for diverse representations. Acknowledging these challenges highlights the necessity for innovative solutions. Delving into the specifics, the discussion outlines how data augmentation can be effectively applied to medical imaging datasets. Exam-

ples may include enhancing the robustness of neural networks trained for image recognition and segmentation tasks. By augmenting medical imaging data, the models are better equipped to generalize across diverse cases, leading to improved performance in real-world scenarios. This section emphasizes the impact on diagnostic accuracy and treatment planning. Of all the articles that have been analyzed, these are the ones that deal with the topic of image generation for medical analysis. Many of those that were discarded only focused on image classification techniques, which are not so relevant to this topic. The articles selected for the study apply data augmentation techniques to medical images of various regions of the human body, highlighting their specific applications and benefits. Part of the analyzed articles deal with algorithms aimed at specific organs of the human body, but the other part focus on general algorithms, that explain various techniques and how they can be applied to medical images. In this sequel and in order improve the clarity of the analysis, two subsections are introduced; in each one of them are explored just the works targeting the specified type of algorithms.

4.1 Articles Focusing on General Algorithms

The articles included in Table 2, focus on the creation and improvement of specific models, algorithms or techniques aimed at solving technical challenges in areas such as medical image processing and machine learning applied to health. These articles used techniques such as Few-shot semantic segmentation, which allows images to be segmented into different classes, even when there are only a small number of training examples available for each class. This is useful in scenarios where the collection of labeled data is limited or expensive. On the other hand, DCGAN is a generative neural network architecture designed to generate realistic images, taking advantage of deep convolutions to learn high-level representations. Finally, the articles listed in Table 3, stand out for their practical application in real clinical environments, including evaluating the performance of algorithms in conjunction with medical specialists and investigating the impact of these techniques on improving clinical results. These articles cover techniques such as GANs, which are a type of generative model made up of two neural networks, the generator and the discriminator, which are trained in adversarial fashion. The generator creates samples that mimic real samples, while the discriminator tries to distinguish between the generated and real samples. This competition leads to continuous improvements in the generator's generation abilities. And also a new end-to-end architecture that is designed to simplify and optimize the GAN training process, offering a more direct and efficient approach. By integrating all training steps into a single framework, this architecture reduces model complexity and improves computational efficiency.

4.2 Articles Focusing on Specific Organs

The articles in this section also use deep learning algorithms but focus on different organs. In Table 4 the successful implementation of data augmentation in

cardiac images is discussed, emphasizing its role in improving diagnostic accuracy and optimizing cardiac diagnostic processes. Next, in Table 5 the use of these techniques in brain imaging as approached, highlighting how data augmentation contributes to significant advances in the early detection of neurological disorders. Both articles deal with GAN-based techniques. In the context of lung imaging, in Table 6 the progress made with the application of data augmentation as highlighted, offering valuable insights for the early diagnosis of respiratory diseases. Exploring other anatomical regions, Table 7 focuses on the analysis of bowel images, emphasizing the gains provided by data augmentation in accurately identifying gastrointestinal conditions. In addition, in Table 8 advances in the analysis of eye images are focused, highlighting how data augmentation has contributed to a better understanding and showing of ophthalmic diseases. The

Table 2. Features of studies on model and technique development in medical image processing and machine learning for health.

Article	Author	Year	Country	Study aim
A dynamic few-shot learning framework for medical image stream mining based on self-training [4]	Zhengqiang Ye, and Wei Zhang	2023	China	Few-shot semantic segmentation (FSS) has been widely used in the field of information medicine and intelligent diagnosis. Due to the high cost of collecting medical data and protecting patient privacy, it is difficult to obtain labeled medical images. To address this issue, the authors propose a few-shot dynamic learning framework for medical semantic segmentation, which can fully utilize the characteristics of the newly collected/generated data stream. Experiment results show a significant performance gain in extracting medical data streams compared to the baseline method.
Empirical Analysis of Deep Convolutional Generative Adversarial Network for Ultrasound Image Synthesis [5]	Dheeraj Kumar, Mayuri A. Mehta, Indranath Chatterjee	2021	India and South Korea	In this article, is present an empirical analysis of the state-of-the-art Deep Convolutional Generative Adversarial Network (DCGAN) for the synthesis of ultrasound images. The results show that good quality synthetic ultrasound images are generated within 100 training epochs of the DCGAN. The quality of the synthetic ultrasound images is evaluated using Mean Squared Error (MSE), Peak Signal to Noise Ratio (PSNR) and Structural Similarity Index (SSIM).
Generating and Weighting Semantically Consistent Sample Pairs for Ultrasound Contrastive Learning [6]	Yixiong Chen, Chunhui Zhang, Chris H.Q. Ding, Li Liu	2022	China	This study presents a solution for the costly creation of large, well-crafted medical datasets by introducing a positive pair generation module and an automatic sample weighting module based on meta-learning. Experimental results across multiple computer-aided diagnosis tasks show that the proposed self-supervised method achieves state-of-the-art performance

Table 3. Characteristics of studies focusing on clinical applications and performance evaluation.

Article	Author	Year	Country	Study aim
Chronic Wound Image Augmentation and Assessment Using Semi-Supervised Progressive Multi-Granularity EfficientNet [7]	Ziyang Liu, Emmanuel Agu, Peder Pedersen, Clifford Lindsay, Bengisu Tulu, Diane Strong	2023	USA	This study utilizes semi-supervised learning to augment a small, unbalanced wound dataset with a secondary dataset and applies the augmented dataset for deep learning-based wound assessment. Employing progressive multi-granular training and a secondary corpus of 9870 unlabeled wound images, the study finds that generating synthetic wound images using Generative Adversarial Networks (GAN) does not improve wound assessment.
Hierarchical Amortized GAN for 3D High Resolution Medical Image Synthesis [8]	Li Sun, Junxiang Chen, Yanwu Xu, Mingming Gong, Ke Yu, Kayhan Batmanghelich	2022	USA and Australia	In this work, the authors propose a new end-to-end GAN architecture that can generate high-resolution 3D images. Experiments with 3D chest CT and brain MRI demonstrate that our approach surpasses the state of the art in image generation. The article also demonstrate clinical applications of the proposed model in data augmentation and the extraction of clinically relevant features.
Inverse Heat Dissipation Model for Medical Image Segmentation [9]	Yu Kashihara, Takashi Matsubara	2023	Japan	The diffusion model has achieved success in generating and editing high-quality images due to its ability to produce fine detail. Its superior generation capacity has the potential to facilitate more detailed segmentation. The proposed method involves generating a mask that gradually shrinks to fit the shape of the desired segmentation region. The results show that the proposed method outperforms existing methods and provides more detailed segmentation.
Learning From Limited and Imbalanced Medical Images With Finer Synthetic Images From GANs [10]	Xiaoli Qin, Francis M. Bui, Ha H. Nguyen, Zhu Han	2022	Canada, USA, South Korea	This article represents one of the first comprehensive investigations into the impact of synthetic image generation on classifier performance, elucidated empirically through a comparative analysis of a simple deep convolutional GAN with a more complex progressive GAN design. The results obtained show that the use of more detailed images synthesized by GANs with the proposed multiscale CNN achieved good classification performance, under a wide variety of operating conditions.
SSIS-Seg: Simulation-Supervised Image Synthesis for Surgical Instrument Segmentation [11]	Emanuele Colleoni, Dimitris Psychogyios, Beatrice Van Amsterdam, Francisco Vasconcelos, Danail Stoyanov	2022	UK	In this paper, is present a new method for generating surgical images that can fuse robotic instrument simulation and recent domain adaptation techniques to synthesize artificial surgical images for training surgical instrument segmentation models. The authors provide an extensive evaluation of our method in terms of segmentation performance, along with a validation study of image quality using evaluation metrics. In addition, was released a new segmentation dataset of real surgeries that will be shared for research purposes.
The Effectiveness of Data Augmentation for MatureWhite Blood Cell Image Classification in Deep Learning Selection of an Optimal Technique for Hematological Morphology Recognition [12]	Hiroyuki Nozaka, Kosuke Kamata, Kazufumi Yamagata	2023	Japan	The data augmentation method is known as a useful technique for generating a dataset with a large number of images from a set with a small number of images for supervised training in deep learning. However, a data augmentation method with low validity for image recognition was reported in a recent study on artificial intelligence (AI). This study aimed to clarify the optimal data augmentation method in deep learning model generation for white blood cell (WBC) recognition. Although data augmentation methods are often used to achieve high accuracy in the generation of AI with supervised training, the authors believe that it is necessary to select the optimal data augmentation method for the generation of medical AI based on the characteristics of medical images

Table 4. Characteristics of studies on data augmentation in cardiac images.

Article	Author	Year	Country	Study aim
A Domain Translation Framework With an Adversarial Denoising Diffusion Model to Generate Synthetic Datasets of Echocardiography Images [13]	Cristiana Tiago, Sten Roar Snare, Jurica Šprem, and Kristin McLeod	2023	Norway	Translation operations in the field of medical imaging are currently in high demand from researchers and clinicians. Among other capabilities, this task allows the generation of new medical images with a sufficiently high image quality, making them clinically relevant. The proposed framework is based on an adversarial Denoising Diffusion Model (DDM) to synthesize echocardiography images and perform domain translation. Unlike Generative Adversarial Networks (GANs), DDMs are capable of generating high quality image samples with great diversity. If a DDM is combined with a GAN, this ability to generate new data is completed with an even faster sampling time.
A Framework for Simulating Cardiac MR Images with Varying Anatomy and Contrast [14]	Sina Amirrajab, Yasmina Al Khalil, Cristian Lorenz, Jürgen Weese, Josien Pluim, Marcel Breeuwer	2023	Netherlands and Germany	One of the limiting factors for the development and adoption of new medical image analysis methods based on deep learning (DL) is the scarcity of labeled medical images. In this paper, was developed a flexible framework for simulating cardiac magnetic resonance (MR) images with varying anatomical and imaging characteristics, with the aim of creating a diverse virtual population. The proposed framework is optimized to generate a substantial number of cardiac MRI images with ground truth labels suitable for downstream supervised tasks. A database of virtual subjects is simulated and its usefulness in assisting a DL segmentation method is evaluated.
Development of anthropomorphic mathematical phantoms for simulations of clinical cases in diagnostic nuclear medicine [15]	Natalya Denisova, Marina Ondar, Hunor Kertesz, Thomas Beyer	2022	Russia and Austria	The aim was to propose a new generation of mathematically stylized phantoms with high levels of anatomical detail for the purposes of SPECT and PET simulations. Both phantoms produced realistic planar images, which closely mimic real clinical planar images. The images obtained in SPECT computer simulation of myocardial perfusion with a virtual patient (MMT) show the same errors and interpretation problems that exist in clinical routine. These phantoms can be used for clinical case simulations to help medical specialists understand the causes of artifacts and biases in PET and SPECT images.
Generating Synthetic Labeled Data from Existing Anatomical Models: An Example with Echocardiography Segmentation [16]	Andrew Gilbert, Maciej Marciniak, Cristobal Rodero, Pablo Lamata, Eigil Samset, Kristin McLeod	2021	UK and Norway	Instead of labeling images, in this paper was proposed an alternative approach where images are generated from existing high-quality annotations using generative adversarial networks (GANs). The authors demonstrate the approach by generating synthetic 2D echocardiography images for comparison with existing ultrasound segmentation datasets using deep learning. The results demonstrate that the images produced can be effectively used in place of real data for training. The proposed approach paves the way for the automatic generation of training data for many medical imaging tasks, as the same process can be applied to other segmentation or landmark detection tasks in any modality

articles present solutions for the automatic detection of diabetic retinopathy in retinal images. The application of these techniques to the analysis of chromosomal images is discussed in Table 9, where the potential of data augmentation in the presented genetic conditions and chromosomal disorders is emphasized. Skin image analysis is covered in Table 10, highlighting how data augmentation

Table 5. Characteristics of studies on data augmentation in brain imaging.

Article	Author	Year	Country	Study aim
A Transfer Deep Generative Adversarial Network Model to Synthetic Brain CT Generation from MR Images [17]	Yi Gu, Qiankun Zheng	2021	China	Medical imaging aims to convert existing medical images into one or more required medical images, reducing the time needed to diagnose samples and the exposure of the human body to radiation from multiple medical images. The model proposed in this article is called Dual3DPatchGAN and is based on transfer learning. This model does not require one-to-one paired data sets, offering a more flexible approach. It addresses the limitations of DualGAN by eliminating bar-shaped "shadows" in 3D images and allowing bidirectional conversion between the two types of medical images. The experimental results indicate that Dual3DPatchGAN is more suitable for generating medical images compared to other models, showing better quality in the images generated.
BrainGAN: Brain MRI Image Generation and Classification Framework Using GAN Architectures and CNN Models [18]	Halima Hamid N. Alrashedy, Atheer Fahad Almansour, Dina M. Ibrahim, Mohammad Ali A. Hammoudeh	2022	Saudi Arabia and Egypt	The lack of magnetic resonance images (MRI) of the brain makes it difficult to classify brain tumors using image-based classification. The solution to this challenge has been achieved by applying augmentation techniques based on Generative Adversarial Network (GAN). In this article, a framework, called BrainGAN, is proposed for generating and classifying MRI images of the brain using GAN architectures and deep learning models

Table 6. Characteristics of studies on data augmentation in respiratory imaging.

Article	Author	Year	Country	Study aim
CycleGAN Clinical Image Augmentation Based on Mask Self-Attention Mechanism [19]	Junzhuo Liu, Zhixiang Wang, Ye Zhang, Alberto Traverso, Andre Dekker, Zhen Zhang, Qiaosong Chen	2022	China and Netherlands	To overcome the lack and imbalance of data, this article was focused on generating and balancing data on radiation-induced pneumonia, an extremely rare disease with a low incidence. To deal with the aforementioned problems, the method used by previous researchers often involves using generative models to generate data to complement the sparse samples to achieve a balanced distribution of data samples. Among various generative models, CycleGAN is widely used in medical imaging due to its cyclic consistency to perform style migration without changing the basic content.
Synthesis of COVID-19 chest X-rays using unpaired image-to-image translation [20]	Hasib Zunair, A. Ben Hamza	2021	Canada	Motivated by the lack of publicly available datasets of chest X-rays of positive patients with coronavirus disease 2019 (COVID-19), the authors built the first open dataset of high-fidelity synthetic images of COVID-19 chest X-rays, using an unsupervised domain adaptation approach through class conditioning and adversarial training. In addition, the proposed data generation framework offers a viable solution for COVID-19 detection in particular and for medical image classification tasks in general

has promoted a more comprehensive and accurate analysis of dermatological diseases. Table 11 explores the opportunities in breast image analysis, demonstrating how data augmentation can play a crucial role in the early detection of breast and lung conditions.

Table 7. Characteristics of studies on data augmentation for gastrointestinal condition identification in bowel images.

Article	Author	Year	Country	Study aim
Data augmentation for computed tomography angiography via synthetic image generation and neural domain adaptation [21]	Malte Seemann, Lennart Bargsten, Alexander Schlaefer	2020	Germany	In the field of medical imaging, annotations are not only scarce, but also often not entirely reliable. To address both challenges, a two-step approach was developed to generate realistic synthetic CTA data for the purpose of data augmentation. The impact of synthetic data on lumen segmentation using convolutional neural networks (CNNs) is evaluated, and the resulting performances compared

Table 8. Characteristics of studies on data augmentation in eye image analysis.

Article	Author	Year	Country	Study aim
Data augmentation for improving proliferative diabetic retinopathy detection in eye fundus images [22]	Teresa Araújo, Guilherme Aresta, Luís Mendonça, Susana Penas, Carolina Maia, Ângela Carneiro, Ana Maria Mendonça, Aurélio Campilho	2020	Portugal	Public datasets labeled for diabetic retinopathy have a small representation of images of the most severe grades of the disease, and thus there is a lack of PDR cases to train diabetic retinopathy classification models. The authors propose a heuristic-based data augmentation scheme, which is based on the synthesis of neovessel (NV)-like structures, to compensate for the lack of PDR cases in labeled diabetic retinopathy datasets. The proposed algorithm for generating neovessels is based on general knowledge about the common location and shape of these structures.
Exudate Detection: Integrating Retinal-Based Affine Mapping and Design Flow Mechanism to Develop Lightweight Architecture [23]	Muhammad Hussain	2023	UK	This article presents an innovative solution to the critical challenges in the automatic detection of diabetic retinopathy using fundus images. To combat the scarcity of data, the authors investigated the process of modeling fundus images, proposing the "Retina-Based Affine Mapping" mechanism. This mechanism facilitated the generation of representative augmentations to model occurrences influenced by various internal and external factors during the acquisition of fundus images, diverging from the concept of previous work centered on generic augmentations focused mainly on data scaling and not on representation augmentation

Table 9. Characteristics of studies on data augmentation in chromosomal image analysis.

Article	Author	Year	Country	Study aim
Deep Anomaly Generation: An Image Translation Approach of Synthesizing Abnormal Banded Chromosome Images [24]	Lukas Uzolas, Javier Richo, Pierrick Coupé, Juan C. Sanmiguel, György Cserey	2022	Spain, France and Hungary	In the case of banded chromosome images, creating sufficiently large libraries is difficult for many pathologies due to the rarity of certain genetic diseases. Generative Adversarial Networks (GANs) have proved effective in generating synthetic images and expanding training data sets. In this work, the authors implemented a conditional GAN (cGAN) that allows the generation of realistic images of individual chromosomes following user-defined banding patterns

Table 10. Characteristics of studies on data augmentation in skin image analysis.

Article	Author	Year	Country	Study aim
Deep Convolutional Generative Adversarial Networks to Enhance Artificial Intelligence in Healthcare: A Skin Cancer Application [25]	Marco La Salvia, Emanuele Torti, Raquel Leon, Himar Fabelo, Samuel Ortega, Beatriz Martinez-Veja, Gustavo M. Callico, Francesco Leporati	2022	Italy, Spain and Norway	The lack of large data sets to train the models effectively limits the applications of DL in the medical field. Thus, its use with hyperspectral images is still at an early stage. The authors propose a generative adversarial deep convolutional network to generate synthetic hyperspectral images of epidermal lesions, aiming at skin cancer diagnosis and overcoming the challenges of small datasets to train DL architectures. Experimental results show the effectiveness of the proposed structure, capable of generating synthetic data to train DL classifiers

Table 11. Characteristics of studies on data augmentation in breast image analysis.

Article	Author	Year	Country	Study aim
GANs for generation of synthetic ultrasound images from small datasets [26]	Lennart Maack, Lennart Holstein, Alexander Schlaefer	2022	Germany	Generative adversarial networks (GAN) are capable of generating high-quality synthetic images. This paper investigates the capabilities of different state-of-the-art GAN architectures in generating realistic breast ultrasound images if only a small amount of training data is available. In conclusion, GANs can be successfully used to generate synthetic ultrasound images of high quality and diversity, improve the classification performance of CNNs and thus provide a benefit for computer-aided diagnosis

5 Conclusion

The integration of data augmentation techniques into the field of medical imaging marks a significant step forward in improving diagnostic accuracy and treatment efficacy. By overcoming challenges related to limited data sets and increasing model robustness through augmentation, we pave the way for a more versatile and reliable health imaging infrastructure.

This discussion highlights the fundamental role of augmented data in empowering machine learning models to discern subtle patterns, leading to better generalization across a range of clinical scenarios. However, it is important to recognize that traditional techniques, such as rotation, translation and brightness adjustments, also play an essential role in preparing datasets for model training.

When comparing traditional techniques with generative approaches such as GANs, it is important to consider the advantages and disadvantages of each. For example, while traditional techniques may be simpler to implement and interpret, GANs have the potential to generate more realistic and diverse data. However, GANs also face unique challenges, such as the difficulty in finding a balance point between the discriminator and the generator, which can lead to problems with convergence and the quality of the results.

Looking to the future, the synergy between medical imaging and data augmentation has enormous potential. The ongoing evolution of artificial intelligence

and machine learning in healthcare is set to redefine the boundaries of diagnostic accuracy. As we navigate this intersection, it is imperative to foster a collaborative approach, involving clinicians, researchers and technologists, to ensure that advances in medical imaging translate into tangible benefits for patient care and outcomes.

Acknowledgments. The research was partially financed by the Portuguese Funds through FCT (Fundação para a Ciência e a Tecnologia), within the Projects UIDB/00013/2020 and UIDP/00013/2020.

References

1. Luke, T., Geoff, N.: Improving deep learning using generic data augmentation. In: IEE SYMPOSIUM 2018, Bangalore, India, pp. 1542–1547 (2018). https://doi.org/10.1109/SSCI.2018.8628742
2. Tewari, A., et al.: State of the art on neural rendering. Comput. Graph. Forum **32**(2), 701–727 (2020)
3. Connor, S., Taghi, K.: A survey on image data augmentation for deep learning. J. Big Data **6**(1), 1–48 (2019)
4. Zhengqiang, Y., Wei, Z.: A dynamic few-shot learning framework for medical image stream mining based on self-training. EURASIP J. Adv. Signal Process. **2023**(1), 49 (2023)
5. Dheeraj, K., Mayuri A, M., Indranath, C.: Empirical analysis of deep convolutional generative adversarial network for ultrasound image synthesis. Open Biomed. Eng. J. **15**(1) (2021)
6. Yixiong, C., Chunhui, Z., Chris, H.Q.D., Li, L.: Generating and weighting semantically consistent sample pairs for ultrasound contrastive learning. IEEE Trans. Med. Imaging **42**, 1388–1400 (2022)
7. Ziyang, L. et al.: Chronic wound image augmentation and assessment using semi-supervised progressive multi-granularity EfficientNet. IEEE Open J. Eng. Med. Biol. 1–17 (2023) https://doi.org/10.1109/OJEMB.2023.3248307
8. Li, S., et al.: Hierarchical amortized GAN for 3D high resolution medical image synthesis. IEEE J. Biomed. Health Inf. **26**(8), 3966–3975 (2022)
9. Yu, K., Takashi, M.: Inverse heat dissipation model for medical image segmentation. IEICE Trans. Inf. Syst. **106**(11), 1930–1934 (2023)
10. Xiaoli, Q., et al.: Learning from limited and imbalanced medical images with finer synthetic images from GANs. IEEE Access **10**, 91663–91677 (2022)
11. Emanuele, C., Dimitris, P., et al.: SSIS-SEG: simulation-supervised image synthesis for surgical instrument segmentation. IEEE Trans. Med. Imaging **41**(11), 3074–3086 (2022)
12. Hiroyuki, N., Kosuke, K., Kazufumi, Y.: The effectiveness of data augmentation for mature white blood cell image classification in deep learning-selection of an optimal technique for hematological morphology recognition-. IEICE Trans. Inf. Syst. **106**(5), 707–714 (2023)
13. Cristiana, T., Sten, S., Jurica, S., Kristin, M.: A domain translation framework with an adversarial denoising diffusion model to generate synthetic datasets of echocardiography images. IEEE Access **11**, 17594–17602 (2023)
14. Sina, A., et al.: A framework for simulating cardiac MR images with varying anatomy and contrast. IEEE Trans. Med. Imaging **42**(3), 726–738 (2022)

15. Natalya, D., Marina, O., Hunor, K., Thomas, B.: Development of anthropomorphic mathematical phantoms for simulations of clinical cases in diagnostic nuclear medicine. Comput. Methods Biomech. Biomed. Eng. Imaging Visualizat. **11**(3), 433–441 (2023)
16. Andrew, G., et al.: Generating synthetic labeled data from existing anatomical models: an example with echocardiography segmentation. IEEE Trans. Med. Imaging **40**(10), 2783–2794 (2021)
17. Yi, G., Qiankun, Z.: A transfer deep generative adversarial network model to synthetic brain CT generation from MR images. Wirel. Commun. Mob. Comput. **2021**, 1–10 (2021)
18. Halima, H., et al.: BrainGAN: brain MRI image generation and classification framework using GAN architectures and CNN models. Sensors **22**(11), 4297 (2022)
19. Junzhuo, L., et al.: CycleGAN clinical image augmentation based on mask self-attention mechanism. IEEE Access **10**, 105942–105953 (2022)
20. Hasib, Z., A Ben, H.: Synthesis of COVID-19 chest X-rays using unpaired image-to-image translation. Social Netw. Anal. Mining **11**, 1–12 (2021)
21. Malte, S., Lennart, B., Alexander, S.: Data augmentation for computed tomography angiography via synthetic image generation and neural domain adaptation. De Gruyter (2020)
22. Teresa, A., et al.: Data augmentation for improving proliferative diabetic retinopathy detection in eye fundus images. IEEE Access **8**, 182462–182474 (2020)
23. Muhammad, H.: Exudate detection: integrating retinal-based affine mapping and design flow mechanism to develop lightweight architectures. IEEE Access **11**, 125185–125203 (2023)
24. Lukas, U., et al.: Deep convolutional generative adversarial networks to enhance artificial intelligence in healthcare: a skin cancer application. IEEE Access **10**, 59090–59098 (2022)
25. Marco, L.S., et al.: Deep convolutional generative adversarial networks to enhance artificial intelligence in healthcare: a skin cancer application. Sensors **22**(16), 16 (2022)
26. Lennart, M., Lennart, H., Alexander, S.: GANs for generation of synthetic ultrasound images from small datasets. Curr. Direct. Biomed. Eng. **8**(1), 17–20 (2022)

Unveiling Key Parameters: Time Windows and Travel Times in Capacitated Waste Collection

A. S. Silva[1,2,3,4,5(✉)], J. Lima[1,3], A. M. T. Silva[4,5], H. T. Gomes[2,3], and A. I. Pereira[1,3]

[1] Research Centre in Digitalization and Intelligent Robotics (CeDRI), Instituto Politécnico de Bragança, 5300-253 Bragança, Portugal
{adriano.santossilva,jllima,apereira}@ipb.pt
[2] Centro de Investigação de Montanha (CIMO), Instituto Politécnico de Bragança, 5300-253 Bragança, Portugal
htgomes@ipb.pt
[3] Laboratório Associado para a Sustentabilidade e Tecnologia em Regiões de Montanha (SusTEC), Instituto Politécnico de Bragança,, 5300-253 Bragança, Portugal
[4] Laboratory of Separation and Reaction Engineering - Laboratory of Catalysis and Materials (LSRE-LCM), Faculty of Engineering, University of Porto, Porto, Portugal
[5] ALiCE - Associate Laboratory in Chemical Engineering, Faculty of Engineering, University of Porto, Porto, Portugal
adrian@fe.up.pt

Abstract. Numerous studies in waste management propose solutions to the Waste Collection Problem, often focusing on constraints such as time windows and truck capacity. Travel times between points play a vital role in optimizing waste collection. However, the methods for determining them are frequently omitted. Another parameter that has a great influence on waste collection is the time window. Here, the impact of time windows and travel times on the capacitated waste collection problem with time windows solution was assessed for collecting three waste types. Surprisingly, travel times were found to have minimal influence on route optimization, while time windows significantly affected the algorithm's ability to identify the most efficient collection route. Addressing these considerations is crucial for practical application and improving the performance of waste collection algorithms in real-world contexts.

Keywords: Vehile Routing Problem · Metaheuristics · Recycling

1 Introduction

The 21st century is known as the information era, with significant developments and changes in how citizens consume goods worldwide [12]. Physical borders nowadays are being overcome by digitalization and globalization, with people

© The Author(s), under exclusive license to Springer Nature Switzerland AG 2024
O. Gervasi et al. (Eds.): ICCSA 2024 Workshops, LNCS 14816, pp. 355–369, 2024.
https://doi.org/10.1007/978-3-031-65223-3_24

having access to international markets and consuming more as a consequence of the great number of options and strong merchandising [18]. For instance, waste generation is one main sector impacted by increased consumption of goods [2]. High-income countries have some technologies to deal with their waste generation impacts, but low and middle-income countries are currently facing serious waste management problems [22]. The impact of the bad waste management system on human health and the environment is often neglected by authorities, leading to severe sanitation problems in developing countries [21]. In this scenario, sustainability has become paramount to guaranteeing a safe environment for future generations [19].

In our modern society, "sustainability" has become a word often heard in political speeches, companies praising their production system as sustainable, and other situations [11]. With such mention, the word starts losing its real impact in our lives, becoming so usual to be heard that it is neglected. Even in the literature, one can find a diverse number of studies evaluating the sustainability of a determined system. Still, the real definition of sustainability is neither presented nor differs according to the motivation. With this in mind, Moore *et al.* have published a study devoted to analyzing the real meaning of sustainability to guide future studies [9]. The authors analyzed 209 articles mentioning sustainability and enumerated the key concepts of sustainability "(i) after a defined period of time, (ii) a program, clinical intervention, and/or implementation strategies continue to be delivered and/or (iii) individual behavior change (*i.e.*, clinician, patient) is maintained; (iv) the program and individual behavior change may evolve or adapt while (v) continuing to produce benefits for individuals/systems". In other words, sustainability involves a concept that is not only based on respecting the economic, social and environmental pillars. It also involves an evolution of the initial proposal to follow and adapt according to the needs.

Sustainable solutions to waste management problems must consider future developments and ensure the initial proposed efficiency will keep the expected level. Several opportunities exist to explore optimization strategies in the municipal solid waste management system. The system is complex and divided into several steps, from discarding the waste on fixed dumpsters or household bins (depending on the system) to the final disposal [17]. In this system, waste collection is a task that consumes a considerable amount of resources and has a great impact on cities. Delayed garbage collection can cause health problems for humans by attracting wildlife, which in turn can spread diseases [16]. In most cases, the waste collection is carried out with pre-scheduled routes and collection days defined without optimization or even leaving the driver's decision [13]. The low amount of resources invested in this sector makes it difficult for the agencies in charge to improve the operations, leading to inefficiency in fuel expenses and increased operational costs. For instance, the collection cost can consume up to 60% of the company's budget [17]. In this regard, the sector could benefit from information and communication technologies to find feasible and cost-effective alternatives to improve their overall operation.

One of the possible alternatives to improve the waste collection operation is using algorithms to help decision-makers decide on the route to perform the waste collection [8]. The algorithm usually solves a problem modeled to represent the waste collection scenario. Several formulations have already been reported in the literature, most considering the waste collection problem as a vehicle routing problem with specific constraints related to the waste collection operation [8]. At first, the formulations were considering only distances to be optimized. However, increasing the formulation's similarity with real life has motivated researchers to include other objectives in their problems, such as environmental ones [1]. Despite the interesting solutions developed and presented in the literature, most studies are focused on modeling capacity as a constraint, ignoring other possible considerations in their formulation. For instance, time windows are extremely important when searching for optimization possibilities in route planning. When the authors consider time windows, it is unclear if travel times were calculated considering trucks traveling rather than regular cars. Additionally, time windows chosen to perform the task are not feasible (*i.e.* no lunch break or rest times).

In this context, the present paper is devoted to solving the Capacitated Waste Collection Problem with Time Windows (CWCPTW) using the finest metaheuristic algorithm available in Google OR-Tools, Guided Local Search (GLS) [14]. The solution was explored considering the simultaneous collection of the three waste types for the selective collection in Bragança, located in the northeast region of Portugal (paper, glass, and plastic waste). The influence of time windows and travel times were explored in the algorithm's performance to solve the problem. To do so, two time windows were selected: one considering only commercial hours and another considering commercial hours with lunch and rest breaks. Travel times were tested as obtained from Google Maps API and adjusted to the truck's travel times based on the literature [10]. The rest of the paper is organized to present the related literature in Sect. 2, the methodology used to carry out the work in Sect. 3, the results and discussion in Sect. 4, and the conclusion and future work in Sect. 5.

2 Literature Review

The nomenclature "waste collection problem" is not yet used in most papers dealing with the application of vehicle routing problems for waste collection. For this reason, to gather the most relevant literature for this study, papers with the keywords "vehicle routing problem", "waste," "time windows," and "capacity" were searched in the Web of Science search engine. The 135 papers found in this thematic were used to evaluate the current literature and developments and identify possible innovative research paths. The word cloud with the most used keywords amongst the published studies is shown in Fig. 1.

The word cloud is a fast way to analyze the field, observing the most common approaches to solve the waste collection problem under the desired constraints. For instance, several keywords refer to a specific algorithm or a class of algorithm, such as "genetic algorithm", "heuristic", and "metaheuristic". The next sections will briefly review the most recent formulations and algorithms.



Fig. 1. Word cloud of most relevant keywords amongst published studies. The size is proportional to the word count.

In general, Vehicle Routing Problems (VRP) are a family of problems devoted to finding the best solution to various logistic situations involving the assembly of delivery routes for trucks to serve all the customers with a given demand. In this family, capacity constraints are the most traditional, with the formulation of the Capacitated Vehicle Routing Problems well studied in the literature for a wide range of applications. Another constraint that is rather important to evaluate the viability of the solution in real scenarios is the time window. This constraint is often combined with capacity constraints to increase the complexity of the problem, arising the Capacitated Vehicle Routing Problem with Time Windows (CVRPTW). The VRP has already been explored for several real-life applications [15]; however, due to the great development of these problems in the waste collection strategy, a new variant of VRP, the Waste Collection Problems (WCP), arose in the literature. These problems are similar to the VRP family. Still, the variants have other considerations and concerns intrinsic to the waste collection task, such as right-turn constraints, obnoxious effects, multi-compartment trucks, residential waste, fixed station waste, and more- [8].

Similar to the VRP, in most WCP, the vehicles have a limited and fixed capacity and can be rather homogeneous or heterogeneous. Considering the different needs according to the collected waste type, the fleets are heterogeneous in most cases. The same objective of distance shortening is the objective in these problems, leading to the reduction of costs and emission of gases. Also, most studies explore the possibility of using the smallest number of vehicles to perform the waste collection task [6]. The main difference between VRP and WCP relies on the possibility of visiting the central depot multiple times on the latter due to the specificity of the waste collection task. The truck will only return to the central depot to park if the customers are all served or if some constraint would be violated by continuing the collection (*e.g.* time windows). The algorithms class used to solve these problems can range from linear programming to evolutionary algorithms [3,20]. The literature has reached the consensus that exploring exact solutions is not feasible due to the extremely high execution time faced in those

cases since the problem is classified as NP-hard, meaning the problem potentially takes exponential time to solve and has no known polynomial-time solution. In recent years, metaheuristic algorithms have effectively found acceptable solutions to WCP within a feasible execution time.

The formulations created in the waste collection problem are diverse and can include not only the waste collection but also the waste transference from one point to another (*i.e.*, taking the waste from the central depot to interested stakeholders). There is also several studies devoted to exploring the transportation of specific waste types. Zhang *et al.* [24], for example, studied the development of a search algorithm, Variable Neighborhood Search in that case, to solve the multi-cycle medical waste recycling problem. The authors explained that medical waste recycling is traditionally performed by collecting the waste at determined sites and returning it to the recycling site, which involves two main decision variables. The first is the service time in medical facilities, which will depend on the number of clients and the time windows available. The second important decision is to assign the vehicles to the routes for medical waste collection within a service time cycle. The authors classified medical facilities with coefficients 1 and 2 to optimize these tasks. Suppose the institution requires daily visits due to large medical waste production. In that case, the frequency is considered to be 2 as coefficient. In contrast, if the institution does not produce a large amount of medical waste, the frequency is 1, and collection can be performed any day of the cycle. In this scenario, the vehicle leaves the central depot to collect medical waste from the medical institutions and travels back to the central depot. The route is planned to collect all institutions with frequency 2 and the possible ones with frequency 1 if time windows are respected. The Variable Neighborhood Search algorithm proposed by the authors to solve the medical waste problem consists of two stages. The first stage involves building the initial solution using the Clarke-Wright algorithm. The second stage will improve the initial solution based on the variable neighborhood search algorithm combined with the simulated annealing algorithm. Combining two search strategies to improve the initial solution is the main feature of this paper, taking advantage of different search mechanisms to build a robust and optimized solution.

Another example of formulation for waste collection, including time windows, was presented by Zhang *et al.* [23]. In this paper, the authors have created a formulation called Collection Vehicle Routing Problem of the Garbage Facilities. The initial formulation is than transformed to another one, the Vehicle Routing Problem with Simultaneous Pickup and Delivery and Time Windows. Transforming the problem from the initial formulation to the last one was adopted as a strategy to decrease the computational complexity and find a feasible solution to the problem. The initial formulation includes a problem in which the garbage facility serves as the collection point, with sufficient empty containers. The waste collection trucks will collect the waste from residential areas and take it to the garbage facility. Once the containers in the garbage facility are loaded, the trucks can take them to the transfer station and return the empty containers to the garbage facility. The vehicles should return to the garbage facility and exchange

the empty container for a fully loaded one. Once the working day finishes, the vehicles must return to the yard (parking station). To transform the problem and decrease its computational complexity, the authors used dummy customers, such as those performed in other works dealing with VRP variant solutions [5]. Two dummy customer types are used: the first represents garbage facilities with different time windows and pickup tasks. The second is the dummy customer representing the transfer station, with time windows and delivery tasks. The strategy used by the authors converts the multiple trips for delivery and pickup into a circular path starting from the yard and eventually returning to it. The authors solved the problem using a parallel simulated annealing algorithm developed using mixed integer programming formulation.

There are more studies reported in the literature with different approaches to finding the optimal path to perform the waste collection task using time windows as a constraint. In most cases, the authors devote a significant amount of effort to increase the complexity of the problem but do not evaluate the feasibility of their solution based on realistic time windows or algorithm execution times. Time windows are created to improve the system's efficiency in finding optimal and cheapest paths, sometimes not considering the driver's needs to rest, considering only lunch breaks. Sometimes, the authors only validate their algorithm using datasets, not real locations, or even consider Euclidean distances between points to optimize routes. Furthermore, in most cases, there is little information on how the authors calculate the travel times between points, which is also crucial considering the time window constraint.

3 Methodology

This paper aims to evaluate the solution to the CWCPTW using GLS, the finest metaheuristic algorithm available in Google OR-Tools. The system studied here comprises 50 sets of 3 dumpsters each, used for the selective waste collection in the city of Bragança, located in the northeast region of Portugal. Dumpster locations were provided by the company in charge of MSWMS, Resíduos do Nordeste (see www.residuosdonordeste.pt). The route optimization was performed considering the daily waste level inside dumpsters and the number of trucks available to collect each waste type (provided by the company). The waste generation was modeled considering the approximate population density around the dumpster location, which is reported to influence waste generation significantly [4]. The time windows necessary to perform the waste collection task in this scenario were defined based on the working hours in Portugal (9 a.m. to 7 p.m.), considering lunch breaks as well (12 p.m. to 2 p.m.) and also resting hours (5 p.m. to 6 p.m.). Experiments with route optimization were also performed using a time window that consider only the working hours, with no lunch breaks or rest times. The service time in each dumpster was considered 3 min, based on information provided by the company. The routes were planned for the simultaneous collection of the three waste types. It is important to highlight that a determined truck will only collect one type of waste. The general representation of the work performed is illustrated in Fig. 2.

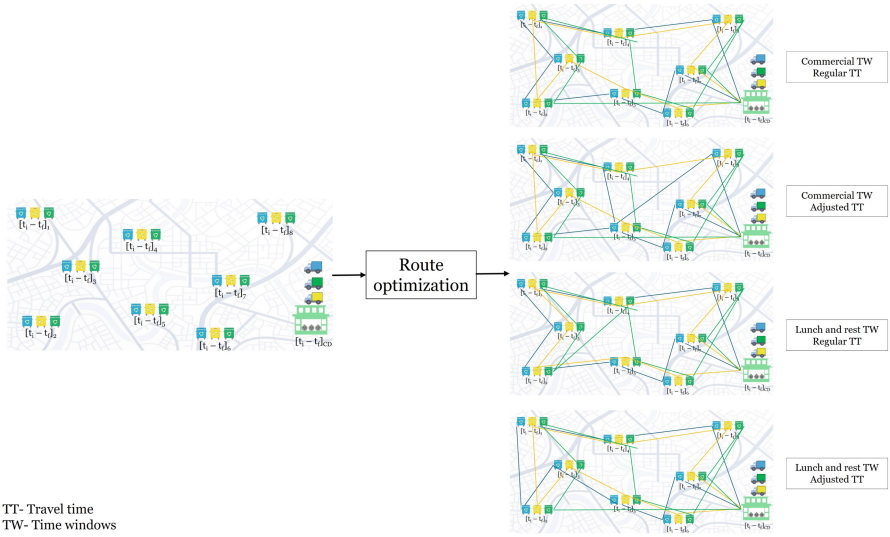

Fig. 2. Representation of the study performed. TW = Time Windows; TT = Travel Times.

3.1 Mathematical Formulation of the CWCPTW

The formulation for the CWCPTW is based on the traditional and recognized Capacitated Vehicle Routing Problem with Time Windows, which is a combinatorial optimization problem used to model several real-life situations in which a set of trucks needs to be used to serve customers for delivery or pick-up purposes. The problem can be summarized as finding the shortest path to serve a determined set of customers under two main constraints: the capacity of trucks and the time windows. The customers' demands are known, and all of them have a time window to be visited. The customers must be visited once by exactly one truck, and vehicles have a maximum capacity that cannot be exceeded.

The mathematical representation of the Capacitated Waste Collection Problem with Time Windows (CWCPTW) revolves around a complete graph, where V signifies the fleet of homogeneous waste collection vehicles with indices $1, 2, \ldots, k$, and C denotes the set of waste collection points. The graph comprises $n+1$ vertices, wherein vertex 0 represents the central waste disposal facility where trucks depart and arrive, and the waste collection points are labeled as $1, 2, 3, \ldots, n$. The CWCPTW entails various objectives, including the minimization of total travel time, the reduction in the number of waste collection vehicles employed, and the overall travel distance.

All edges originate and terminate at vertex 0, the central disposal facility. Each edge $(i, j) \in C_0$, in which $C_0 = C \in \{0\}$, is linked with a cost c_{ij} and a time duration t_{ij}, which may encompass the time spent on waste collection at point i, with the condition that $i \neq j$. The waste collection vehicles are constrained by a maximum capacity Q, and the waste collection points have associated waste

amounts d_i. These points must be visited within specified time windows $[a_i, b_i]$, where the vehicle must arrive at a waste collection point before b_i and after a_i. In cases where the latter condition is met, the vehicle must wait until a_i to execute the waste collection. The central disposal facility also imposes a time window $[a_0, b_0]$, mandating that waste collection vehicles do not depart before a_0 or arrive after b_0.

The parameters Q, a_i, b_i, d_i, c_{ij} are all non-negative integers, while the parameter t_{ij} is assumed to be a positive integer. It is further assumed that both c_{ij} and t_{ij} adhere to the triangular inequality. The formulation introduces two sets of decision variables, namely x_{ijk} and y_{ik}. For each arc (i, j), where $i \neq 0, j \neq 0, i \neq j$, and for each waste collection vehicle k, x_{ijk} is defined as 1 if the arc (i, j) is traversed by vehicle k in the optimal solution, and 0 otherwise. The additional decision variable, y_{ik}, pertains to each vehicle k and each waste collection point i, representing the time the waste collection vehicle k initiates the waste collection service at point i. If vehicle k does not commence service at waste collection point i, the decision variable y_{ijk} holds no significance. Assuming $x_ijk = 0$ for all waste collection vehicles, it is posited that $y_{ik} = 0$ for all k. The overarching objective of the problem is to design a set of routes, one for each waste collection vehicle, ensuring that each waste collection point is visited exactly once. All routes must commence and conclude at the central disposal facility (vertex 0), while adhering to specified time windows and capacity constraints. The formal mathematical formulation, drawing inspiration from the literature on the Capacitated Vehicle Routing Problem with Time Windows (CVRPTW) [7], is detailed as follows:

$$\text{Minimize} \sum_{k \in V} \sum_{i \in C_0} \sum_{j \in C_0} c_{ij} x_{ijk} \tag{1}$$

Subject to:

$$\sum_{i \in C_0} d_i \sum_{j \in C_0} x_{ijk} \leq Q, \forall k \in V \tag{2}$$

$$\sum_{k \in V} \sum_{j \in C_0} x_{ijk} = 1, \forall i \in C_0 \tag{3}$$

$$\sum_{j \in C} x_{0jk} = 1, \forall k \in V \tag{4}$$

$$\sum_{i \in C} x_{i0k} = 1, \forall k \in V \tag{5}$$

$$\sum_{i \in C} x_{ihk} - \sum_{j \in C} x_{hjk} = 0, \forall h \in C, \forall k \in V \tag{6}$$

$$a_i \leq y_{ik} \leq b_j, \forall i \in C_0, \forall k \in V \tag{7}$$

$$y_{ik} + t_{ij} - Q(1 - x_{ijk}) \leq y_{jk}, \forall i, j \in C_0, \forall k \in V \tag{8}$$

$$x_{ijk} \in \{0, 1\}, \forall i, j \in C_0, \forall k \in V \tag{9}$$

The constraint {2} states that waste collection vehicles cannot carry more waste load than their capacity, and constraint {3} guarantees that each waste collection point is visited exactly once. The next three constraints {4}, {5}, and {6} are related to the continuity of the route, ensuring that each vehicle leaves the central disposal facility, and leaves again after performing the waste collection service at a determined point, and arrives back at the central disposal facility. Constraint {7} ensures that time windows are respected, and constraint {8} states that a waste collection vehicle traversing from i to j cannot arrive at j before $y_{ijk} + t_{ij}$. Finally, constraints {9} are the integrality constraints for the decision variable x_{ijk}.

3.2 Waste Generation Model

The study does not focus on waste generation model validation. However, it requires the model to generate waste daily to assess its ability to find the shortest path for waste collection. Three types of waste generation-plastic, paper, and glass-were simulated in this study. Previous research indicates that demographic density around dumpsters affects waste generation levels in a Portuguese city. As described in prior work, waste level fluctuations for different waste types were calculated based on demographic factors derived from satellite images of dumpster surroundings [17]. The parameter ranges from 0 to 1, with low population density areas having values near 0 and high-density areas having higher values. It is calculated by dividing the area with construction sites by the area of a circle with a 300 m radius around the dumpster. The dumpsters set is denoted as $\{A\}$, and days set is $\{B\}$. Waste level ($L^T_{e,f}$, percentage) and volumetric amount (V^T) for waste type T in dumpster e on day f can be calculated using this equation:

$$L^T_{e,f} = d_e \cdot C_T \cdot \sigma \ + L^T_{e,f-1} \wedge V^T_{e,f} = L^T_{e,f} \cdot \frac{V_D}{100} \tag{10}$$

In which L^T is the waste level of waste type T on day f for dumpster e. The demographic factor for dumpster e is introduced in the equation as d_e, and C_T is a constant that represents the influence of demographic factor on waste type T generation. The parameter σ introduced waste levels' stochasticity and oscillated between $[1, 20]$. The waste level in the first day was determined using a normal distribution function that returns random values on the range defined as $[0, 70]$. The volumetric waste level for waste type T, V^T was determined by multiplying the waste level L^T by the total dumpster volume, V_D. The model presented here allows determining waste levels for all waste types studied: paper (waste type PA), plastic (waste type PL), and glass (waste type G). The dumpster locations are illustrated in Fig. 3 and were provided by the company in charge of the municipal solid waste management in the region studied.

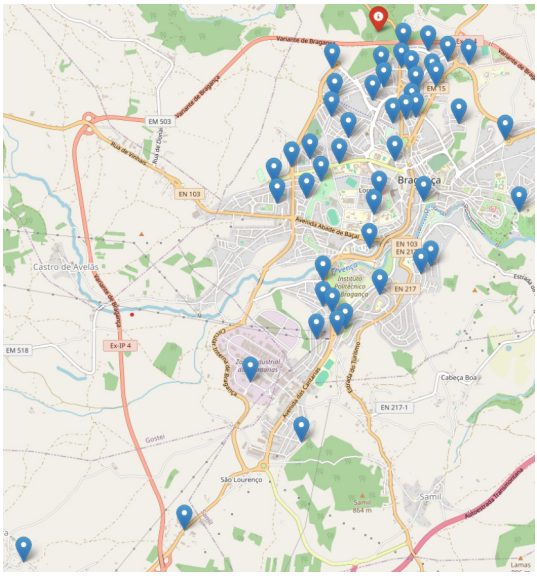

Fig. 3. Locations with three dumpsters (glass, paper, and plastic waste). The red location is the central depot. (Color figure online)

4 Results and Discussion

In this section, the results obtained for waste collection route optimization achieved using the Guided Local Search algorithm available in OR-Tools will be presented and discussed. The study was performed for 30 days, and the trucks used for the collection of the different waste types all have the same capacity ($Q = 16\,\mathrm{m}^3$). Following a similar dumpster/truck ratio as the real scenario, 3 trucks ($k = 3$) were considered per waste type for route optimization. The maximum capacity of waste that can be stored inside dumpsters is $TV = 2.5\,\mathrm{m}^3$.

The models used to simulate waste generation per type considered one parameter that has proven influence in waste generation, the demographic factor. There are different influences in waste generation per type using this parameter. The coefficients used to determine waste levels through days were $Cb = 9.52$, $Cy = 23.1$, and $Cg = 4.74$ for paper waste (blue dumpsters, Cb), plastic waste (yellow dumpsters, Cy), and plastic waste (green dumpsters, Cg), based on the literature [4].

The selection of dumpsters for collection on day i was performed based on the percentage level, using 90% as the threshold. The waste level used as a threshold here was proven to be the most effective according to previous waste collection studies. The problem was solved using the travel times gathered using Google Maps API, and a comparison was performed with a more realistic travel time obtained based on the paper published by Srinivas *et al.* [10], which presents a correlation between regular car and truck travel times.

4.1 Numerical Results

Four sets of results will be presented and compared in this section: one obtained with time windows in commercial hours only (9 a.m. to 7 p.m.) using regular travel times and truck-adjusted travel times, and another using more applicable time windows (9 a.m. to 12 p.m., 2 p.m. to 5 p.m., and 6 p.m. to 7 p.m.) in both travel time situations. The first time window is one example of what is often considered in most works exploring waste collection using time windows, and the second would be a more realistic time window that considers lunch breaks and rest times during the afternoon. The results obtained for the total time to perform the waste collection in the different scenarios studied are exhibited in Fig. 4.

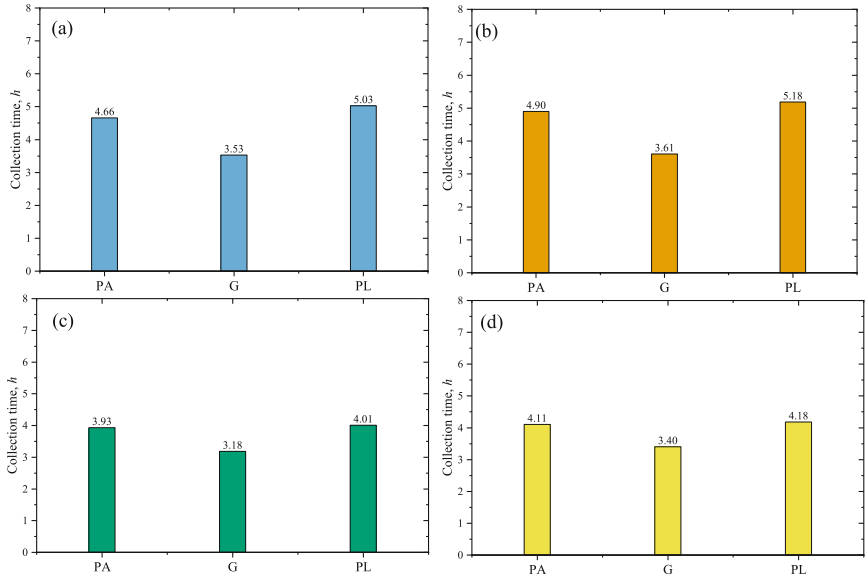

Fig. 4. Average daily time spent in collection task considering (a) working hours time windows and regular travel times, (b) working hours time windows and adapted travel time, (c) lunch break and rest hours time windows and regular travel times, and (d) lunch break and rest hours time windows and adapted travel times.

The results demonstrate that these parameters significantly influence hours spent during waste collection tasks. Comparing scenarios represented in Fig. 4a 4b reveals that regular travel times return smaller averages for daily waste collection tasks, which was expected considering that the adjusted travel times are more representative for trucks that are not as fast as cars. Nonetheless, the algorithm could still perform the route optimization using a more realistic travel time for the trucks, which is an important demonstration of the applicability in real scenarios. The time increase observed for all waste types was not the same,

which is a consequence of the difference in decision-making regarding the routes, once the algorithm had to follow different paths to respect all time windows.

Interestingly, the more realistic time windows scenario results reported in Fig. 4a and 4b returned average daily hours spent in waste collection tasks smaller than results obtained in wider time windows (0.75, 0.28, and 1.2 less time for paper, plastic, and glass waste collection in average). In other words, the algorithm's performance was improved by increasing the problem's difficulty, obliging the algorithm to improve route planning to respect all time windows. There is no report in the literature regarding the algorithm's performance in solving the waste collection problem using different time windows. The distance traveled also presented differences in the waste collection scenarios, and the average distance traveled per collection day is shown in Fig. 5.

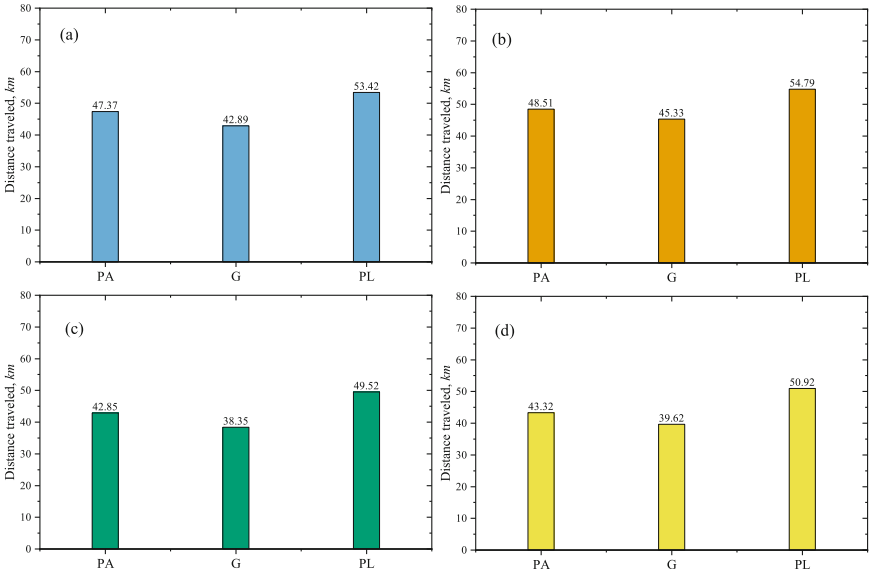

Fig. 5. Average daily distance traveled in collection task considering (a) working hours time windows and regular travel times, (b) working hours time windows and adapted travel time, (c) lunch break and rest hours time windows and regular travel times, and (d) lunch break and rest hours time windows and adapted travel times.

The results obtained for the average distance traveled in the different scenarios revealed a similar tendency as observed in the average daily time spent on waste collection tasks. Considering as the only difference the adjusted *vs* regular travel time, the difference was not so significant (*cf.* Fig. 5a *vs* 5b and Fig. 5c *vs* 5d). Comparing the different time windows and the same travel time (*cf.* Fig. 5a *vs* 5c and Fig. 5b *vs* 5d) revealed that the time windows are mainly influencing route planning. Specifically, the differences in distance traveled reached 4.9, 5.1, and 3.9 km for paper, plastic and glass waste collection on average. In

this case, the most restricted time windows resulted in better route planning using the GLS metaheuristic.

5 Conclusions and Future Work

In this paper, the influence of travel time and time windows on solving the CWCPTW using the GLS metaheuristic available in OR tools was assessed. The parameters evaluated are extremely important to validate the viability of implementing the solution in real scenarios. In most cases, the travel times used to solve the problems are acquired from external sources, and these sources often provide car travel times. Planning a truck route using the car's travel times might end up in future problems since the vehicles take considerably different times to travel the same route. Another important parameter is the time window to perform the waste collection task, often considered commercial hours. Here, a more realistic time window considering lunch and rest breaks was considered.

The scenarios were chosen to isolate the influence of one parameter and explore the algorithm's behavior upon changing the other parameter, keeping all the other parameters the same (*e.g.* number of trucks and demands). GLS algorithm revealed a small influence of travel times to solve this particular problem but a considerable influence of the time windows used. Interestingly, the most realistic and applicable time windows returned smaller average distance traveled to collect the waste and shorter times for all waste types studied.

Acknowledgments. This work was supported by national funds through FCT/MCTES (PIDDAC): CeDRI, UIDB/05757/2020 (DOI: 10.54499/UIDB/05757/2020) and UIDP/05757/2020 (DOI: 10.54499/UIDB/05757/2020); CIMO, UIDB/00690/2020 (DOI: 10.54499/UIDB/00690/2020) and UIDP/00690/2020 (DOI: 10.54499/UIDP/00690/2020); SusTEC, LA/P/0007/2020 (DOI: 10.54499/LA/P/0007/2020), LSRE-LCM, UIDB/50020/2020 (DOI: 10.54499/UIDB/50020/2020) and UIDP/50020/2020 (DOI: 10.54499/UIDP/50020/2020); and ALiCE, LA/P/0045/2020 (DOI: 10.54499/LA/P/0045/2020). Adriano Silva was supported by Doctoral Grant SFRH/BD/151346/2021 financed by the Portuguese Foundation for Science and Technology (FCT), and with funds from NORTE 2020, under MIT Portugal Program. The authors are grateful to Sociedade Ponto Verde for the financial support through the project "A digitalização como ferramenta para melhorar a sustentabilidade do processo de recolha seletiva".

References

1. Al-Dailami, A., et al.: Sustainable solid waste management in yemen: environmental, social aspects, and challenges. In: Biomass Conversion and Biorefinery, pp. 1–27 (2022). https://doi.org/10.1007/s13399-022-02871-w
2. Awino, F.B., Apitz, S.E.: Solid waste management in the context of the waste hierarchy and circular economy frameworks: an international critical review. Integr. Environ. Assess. Manag. **20**(1), 9–35 (2024). https://doi.org/10.1002/ieam.4774

3. Dündar, H., Ömürgönülşen, M., Soysal, M.: A review on sustainable urban vehicle routing. J. Clean. Prod. **285**, 125444 (2021). https://doi.org/10.1016/j.jclepro.2020.125444
4. Ferreira, J.A.O.: Optimização do Processo de Recolha de Resíduos: Desenvolvimento de Ferramentas de Investigação Operacional para o Problema de Orientação de Equipas com Multi-Restrições. Ph.D. thesis, Universidade do Minho (Portugal) (2015)
5. Ferrucci, F., Bock, S.: A general approach for controlling vehicle en-route diversions in dynamic vehicle routing problems. Transport. Res. Part B: Methodol. **77**, 76–87 (2015). https://doi.org/10.1016/j.trb.2015.03.003
6. Hannan, M., et al.: Solid waste collection optimization objectives, constraints, modeling approaches, and their challenges toward achieving sustainable development goals. J. Clean. Prod. **277**, 123557 (2020). https://doi.org/10.1016/j.jclepro.2020.123557
7. Kallehauge, B.: Formulations and exact algorithms for the vehicle routing problem with time windows. Comput. Oper. Res. **35**(7), 2307–2330 (2008). https://doi.org/10.1016/j.cor.2006.11.006
8. Liang, Y.C., Minanda, V., Gunawan, A.: Waste collection routing problem: a mini-review of recent heuristic approaches and applications. Waste Manag. Res. **40**(5), 519–537 (2022). https://doi.org/10.1177/0734242X211003975
9. Moore, J.E., Mascarenhas, A., Bain, J., Straus, S.E.: Developing a comprehensive definition of sustainability. Implement. Sci. **12**(1), 1–8 (2017). https://doi.org/10.1186/s13012-017-0637-1
10. Pulugurtha, S.S., Jain, R.N.: Passenger car equivalent travel time of a truck. Multimodal Transport. **1**(3), 100031 (2022). https://doi.org/10.1016/j.multra.2022.100031
11. Ruggerio, C.A.: Sustainability and sustainable development: a review of principles and definitions. Sci. Total Environ. **786**, 147481 (2021). https://doi.org/10.1016/j.scitotenv.2021.147481
12. Sassanelli, C., Rosa, P., Rocca, R., Terzi, S.: Circular economy performance assessment methods: a systematic literature review. J. Clean. Prod. **229**, 440–453 (2019). https://doi.org/10.1016/j.jclepro.2019.05.019
13. Silva, A.S., et al.: Dynamic urban solid waste management system for smart cities. In: Simos, D.E., Rasskazova, V.A., Archetti, F., Kotsireas, I.S., Pardalos, P.M. (eds.) LION 2022. LNCS, vol. 13621, pp. 178–190. Springer, Heidelberg (2022). https://doi.org/10.1007/978-3-031-24866-5_14
14. Silva, A.S., Lima, J., Pereira, A.I., Silva, A.M., Gomes, H.T.: Execution time experiments to solve capacitated vehicle routing problem. In: Gervasi, O., et al. (eds.) ICCSA 2023. LNCS, vol. 14111, pp. 273–289. Springer, Heidelberg (2023). https://doi.org/10.1007/978-3-031-37126-4_19
15. Silva, A.S., Lima, J., Silva, A.M.T., Gomes, H.T., Pereira, A.I.: Time-dependency of guided local search to solve the capacitated vehicle routing problem with time windows. In: Pereira, A.I., Mendes, A., Fernandes, F.P., Pacheco, M.F., Coelho, J.P., Lima, J. (eds.) OL2A 2023, vol. 1981, pp. 93–108. Springer, Cham (2024). https://doi.org/10.1007/978-3-031-53025-8_7
16. Silva, A.S., Pereira, A.I., Lima, J., Silva, A.M.T., Gomes, H.T.: Execution time as a key parameter in the waste collection problem. In: 2023 18th Iberian Conference on Information Systems and Technologies (CISTI), pp. 1–6 (2023). https://doi.org/10.23919/CISTI58278.2023.10211886
17. Silva, A.S., et al.: Capacitated waste collection problem solution using an open-source tool. Computers **12**(1) (2023). https://doi.org/10.3390/computers12010015

18. Sobol, K., Cleveland, M., Laroche, M.: Globalization, national identity, biculturalism and consumer behavior: a longitudinal study of Dutch consumers. J. Bus. Res. **82**, 340–353 (2018). https://doi.org/10.1016/j.jbusres.2016.02.044
19. Tanveer, M., Khan, S.A.R., Umar, M., Yu, Z., Sajid, M.J., Haq, I.U.: Waste management and green technology: future trends in circular economy leading towards environmental sustainability. Environ. Sci. Pollut. Res. **29**(53), 80161–80178 (2022). https://doi.org/10.1007/s11356-022-23238-8
20. Valenzuela, J., Alfaro, M., Fuertes, G., Vargas, M., Sáez-Navarrete, C.: Reverse logistics models for the collection of plastic waste: a literature review. Waste Manag. Res. **39**(9), 1116–1134 (2021). https://doi.org/10.1177/0734242X211003948
21. Vinti, G., et al.: Municipal solid waste management and adverse health outcomes: a systematic review. Int. J. Environ. Res. Public Health **18**(8) (2021). https://doi.org/10.3390/ijerph18084331
22. Williams, I.D., Phillips, J.: Leading the world: a review of household recycling in wales. Recycling **7**(4) (2022). https://doi.org/10.3390/recycling7040046
23. Zhang, S., Mu, D., Wang, C.: A solution for the full-load collection vehicle routing problem with multiple trips and demands: an application in Beijing. IEEE Access **8**, 89381–89394 (2020). https://doi.org/10.1109/ACCESS.2020.2993316
24. Zhang, W., Zeng, M., Guo, P., Wen, K.: Variable neighborhood search for multi-cycle medical waste recycling vehicle routing problem with time windows. Int. J. Environ. Res. Public Health **19**(19) (2022). https://doi.org/10.3390/ijerph191912887



Multi-objective Scheduling Optimization in Job Shop with Unrelated Parallel Machines Using NSGA-III

Francisco dos Santos[1,2(✉)], Lino Costa[1,3], and Leonilde Varela[1,3]

[1] ALGORITMI Research Centre/LASI, University of Minho, Braga, Portugal
francisco_dos_santos@outlook.pt
[2] Polytechnic Institute, Kimpa Vita University, Uíge, Angola
[3] Department of Production and Systems, University of Minho, Braga, Portugal
{lac,leonilde}@dps.uminho.pt

Abstract. Job shop scheduling problems are common in the engineering field. In spite of some approaches consider just the most important objective to optimize, several other conflicting criteria are also important. Multi-objective optimization algorithms can be used to solve these problems optimizing, simultaneously, two or more objectives. However, when the number of objectives increases, the problems become more challenging. This paper presents the results of the optimization of a set of job shop scheduling with unrelated parallel machines and sequence-dependent setup times, using the NSGA-III. Several instances with different sizes in terms of number of jobs and machines are considered. The goal is to assign jobs to machines in order to simultaneously minimize the maximum job completion time (makespan), the average job completion time and the standard deviation of the job completion time. These results are analysed and confirm the validity and highlight the advantages of this approach.

Keywords: Job shop scheduling problem · multi-objective optimization · evolutionary algorithms

1 Introduction

In general, Job Shop Scheduling (JSS) has played a fundamental role in manufacturing companies [20], as it maximizes efficiency while minimizing various costs, delivery time and cycle time, delays, among others [13]. Several studies have been carried out in order to analyse the impact of the job shop scheduling problem on manufacturing systems [1,14,19]. JSS problems with unrelated parallel machines aim to schedule N jobs that are available at initial time on M unrelated machines [9]. The goal is to find the feasible sequence of jobs in

This work has been supported by FCT - Fundação para a Ciência e Tecnologia within the R&D Units Project Scope: UIDB/00319/2020.

© The Author(s), under exclusive license to Springer Nature Switzerland AG 2024
O. Gervasi et al. (Eds.): ICCSA 2024 Workshops, LNCS 14816, pp. 370–382, 2024.
https://doi.org/10.1007/978-3-031-65223-3_25

each machine that minimizes simultaneously the objectives. Thus, JSS considers different machines with different sequences and processing times.

Most studies addressing JSS problems consider just the total production time (makespan) as the objective to minimize [2,12]. Therefore, these problems are solved using single objective optimization algorithms, often, based on metaheuristics [3,4]. Although, makespan being one of the main objectives to be minimized in the context of production, there are other objectives that can be simultaneously minimized, thus improving the optimization results [10,16]. It is important to maximize profits and balance workloads by minimizing different objectives such as the makespan, the average and standard deviation production times between machines. Therefore, it is required to use multi-objective optimization algorithms to solve this problem with more than two objectives. Multi-objective scheduling problems are common in industry and are considered complex because they involve different objectives to be optimized simultaneously as well as a combinatorial search space [17].

This paper presents a multi-objective optimization approach for the JSS problem, aiming to simultaneously minimize tree objectives: the total completion time of the jobs, the average completion time of the jobs and the standard deviation of the total completion time of the jobs. To solve this kind of problems, there are several multi-objective optimization algorithms studied and available in the literature [5], most of them based on evolutionary algorithms. In this work, the NSGA-III [7] was adopted, as it performs better when the number of objectives to be minimized is more than two [18]. NSGA-III is particularly suited to solve problems with many objectives allowing to obtain a good representation of the Pareto front since the search is oriented by a certain number of well distributed reference points [11,13]. Moreover, evolutionary algorithms are particularly suited to this kind of problems since they can tackle their combinatorial nature. In order to assess the performance of NSGA-III and compare it with other approaches, a set of small JSS instances are considered [3,4].

This paper is organized as follows. Section 2 briefly presents an overview on multi-objective optimization of JSS, describing the optimization problem and the multi-objective approach adopted in this work. In Sect. 3, the experimental results of NSGA-III are presented and discussed. In this section, the implementation details and parameters of NSGA-III are explained, as well as the analysis of its overall performance. Finally, Sect. 4 addresses the conclusion and future work.

2 Multi-objective Job Shop Scheduling

Job shop scheduling problems are common and have been studied for over 50 years with practical applications in industrial context. In particular, the unrelated parallel machine scheduling problem represents a challenge in job shop scheduling, involving the allocation of N jobs across M unrelated machines. Typically, the term span denotes the completion time of a machine, while makespan refers to the maximum completion time considering all machines [2]. While minimizing makespan is considered the main and single objective, other significant

and conflicting objectives, such as average and standard deviation of the completion times are important [19]. Consequently, JSS problems are inherently multi-objective optimization problems, reflecting the real-world complexity of real world scheduling problems prevalent in industrial settings. This complexity highlights the need for trade-off solutions that capture a balance among various objectives.

2.1 Problem Description

In JSS problems, there are N independent jobs that have to be processed in a set of M available machines. Each machine i can only execute one job j at each instant for $i \in \{1, \ldots, M\}$ and $j \in \{1, \ldots, N\}$. Moreover, all N jobs do not have any precedence restriction and preemption is not allowed, that is, the processing of any job in a machine cannot be interrupted.

The following nomenclature will be considered: $p_{i,j}$ is the processing time for job j on machine i, and $s_{i,j,k}$ is the setup time for job j after job k to be processed on machine i. The initial setup time for processing job j on machine i is denoted by $s_{i,j,0}$. The feasible sequence of all jobs assigned to machines is denoted by π. This vector includes all feasible subsequences π_i on each machine i. The total completion time of jobs for the feasible sequence π is represented by $c_i(\pi)$ for each machine i.

This work aims to find the sequence of jobs that simultaneously minimizes the makespan ($c_{max}(\pi)$), the average completion time ($\bar{c}(\pi)$) and the standard deviation of completion time ($c_\sigma(\pi)$). Mathematically, the objectives to be minimized can be expressed as follows:

$$c_{\max}(\pi) = \max_{i=1,\ldots,M}(c_i(\pi)) \tag{1}$$

$$\bar{c}(\pi) = \frac{1}{M}\sum_{i=1}^{M} c_i(\pi) \tag{2}$$

$$c_\sigma(\pi) = \sqrt{\frac{\sum_{i=1}^{M}(c_i(\pi) - \bar{c}(\pi))^2}{M}} \tag{3}$$

where $c_i(\pi) = \sum_{j\in\pi_i} p_{i,j} + \sum_{j\in\pi_i} s_{i,j,k}$ with k being the jobs that precedes jobs j in the subsequence π_i of the feasible sequence π. It should be noted that when the job j is the first job in the subsequence π_i, k is zero and therefore $s_{i,j,0}$ is the setup time.

Therefore, these multi-objective JSS optimization problem with three objectives can be mathematical formulated as follows:

$$\min \mathbf{F}(\pi) = (f_1(\pi), f_2(\pi), f_3(\pi))^T = (c_{\max}(\pi), \bar{c}(\pi), c_\sigma(\pi))^T \tag{4}$$

where π is a feasible sequence belonging to the feasible set Ω (the set of all possible permutations), and $\mathbf{F}(\pi)$ is the vector of objective functions defined in the objective space.

Since the objective space is a three-dimensional space, the comparison of solutions has to be based on the concept of Pareto dominance. Thus, for any two solutions $\pi_{\mathbf{a}}$ and $\pi_{\mathbf{b}}$ of the feasible set Ω, a solution $\pi_{\mathbf{a}}$ is said to dominate a solution $\pi_{\mathbf{b}}$ ($\pi_{\mathbf{a}} \prec \pi_{\mathbf{b}}$) if $\forall_{i\in\{1,2,3\}} : f_i(\pi_{\mathbf{a}}) \leq f_i(\pi_{\mathbf{b}}) \wedge \exists_{j\in\{1,2,3\}} : f_j(\pi_{\mathbf{a}}) < f_j(\pi_{\mathbf{b}})$.

In this sense, since solutions are compared with respect to different criteria, there is no longer a single optimal solution, and a set of incomparable optimal solutions exists, generally known as the Pareto optimal set. The images of these Pareto optimal solutions define a Pareto front in the objective space, that allows the perception of trade-offs. Thus, the Pareto front is useful to assist the decision making process and can be expressed by $\mathbf{PS} = \{\pi_{\mathbf{x}} \in \Omega \mid \nexists \pi_{\mathbf{y}} \in \Omega : \pi_{\mathbf{y}} \prec \pi_{\mathbf{x}}\}$.

2.2 Multi-objective Approach

Multi-objective optimization algorithms are developed to deal simultaneously with problems with two or more objective functions. The objective space is in general complex since, usually, criteria conflict each other in such a way that when one is improved degrades some of the others. The goal of any multi-objective optimization algorithm is to find a set of solutions that represent trade-off between the objectives [15]. From an algorithmic perspective, designing an efficient optimization techniques is not simple, in particular, when the number of objectives is large. More recently, several algorithms have been developed to be efficient in dealing with these complex optimization problems with a large number of objectives, known as many-objective optimization problems [6].

NSGA-III [13] is an example of an evolutionary algorithm that based on the well-known NSGA-II [8] was extended and modified to tackle many-objective optimization problems. NSGA-III maintains the diversity of solutions along the search by using a set of reference points. The reference points are scattered on a hyperplane with a dimension to the number of objectives of the problem. Selection is based on the distances to these reference set and constitutes the main difference from its ancestor NSGA-II. During the search, each individual of the population is associated to the reference point with the closest perpendicular distance. If two individuals are associated to the same point, the individual with the shortest distance is chosen. This promotes diversity in population and convergence toward the Pareto front. Genetic operators (such as crossover and mutation) are used to generate new offspring from parent individuals and are similar to the ones used by NSGA-II.

Some features of the evolutionary algorithms are adequate to tackle combinatorial problems, since constraints can be handled by permutation representations and genetic operators can be specifically designed for this kind of search spaces.

3 Experimental Results

In order to study the NSGA-III performance, test problems were taken from previous works [2–4]. In this study, instances of JSS problems with balanced processing and setup time for $M \in \{2, 4, 6, 8\}$, and $N \in \{9, 10, 11\}$ were used.

There are 15 different instances for each combination of M and N. The objectives were to minimize the makespan ($c_{max}(\pi)$), the average completion time ($\bar{c}(\pi)$) and the standard deviation of the completion time ($c_{\sigma}(\pi)$).

3.1 NSGA-III Implementation Details

The NSGA-III was used to solve the JSS optimization problem with three objectives. This algorithm was implemented in Python using the PYMOO framework [5]. A population size of 100 individuals was considered. The stopping criterion was based on the maximum number of generations and the period without improvement. The maximum number of generations was set at 10,000 and the period at 100 generations. Fourteen independent runs were made on the test problems because the algorithm used is stochastic.

Each chromosome of the population is a permutation of size $N + M - 1$ that expresses the feasible sequence of jobs on the machines, i.e., the sequence π. In the chromosome, genes larger than N are used to divide the chromosome into M subsequences (π_i) indicating the set of jobs and the corresponding order assigned to each machine i.

A binary tournament selection operator was used to select the chromosomes for being parents and generate offspring by the application of the genetic operators. The genetic operators were chosen to guarantee the feasibility of the solutions during the search: order-based crossover and inversion mutation. In the order-based crossover, the genes of two chromosomes are combined. So, two positions are generated at random and then the genes between those positions are swapped. The remaining empty positions are filled with the genes from the other parent, avoiding repeats. In the inversion mutation, two positions are generated at random and the genes between them are reversed.

3.2 Overall Analysis

The assessment of the performance of multi-objective optimization algorithms is not straightforward since it implies measuring its ability of convergence towards the Pareto optimal front as well as its ability to maintain diversity of solutions in objective space to facilitate the decision making process. So, in order to measure the performance of the NSGA-III, the hypervolume indicator (H) was used [21]. This measure allows to assess the algorithm performance both in terms of convergence to the Pareto front and diversity of the approximation along the Pareto front. All hypervolume indicator values were computed considering the reference point $(1000, 1000, 1000)^T$ and then standardized in order to belong to the interval $[0, 1]$. For a given problem, the higher the value of hypervolume, the best performance of the algorithm.

In Table 1, the statistics for the measured hypervolume for Pareto fronts obtained by NSGA-III for the 15 instances of the JSS problem for each combination of M and N are presented. For each instance of the JSS problem, 14 independent runs of NSGA-III were performed. Thus, for these 14 independent runs, the maximum (best) and mean hypervolume are computed and then the

respective average and standard deviation for each combination of M and N. The average number of non dominated solutions (#ND) obtained for the best hypervolume of each instance and the mean number of function evaluations (F_{eval}) are also provided. In this table, $AVG(H_{\text{mean}})$ and $SD(H_{\text{mean}})$ are the average and standard deviation of the mean hypervolume (maximum hypervolume), and $AVG(H_{\text{max}})$, $SD(H_{\text{max}})$ are the average and standard deviation of the best hypervolume, respectively.

From this table, it can be observed that for the same value of M, the mean and maximum hypervolume decrease consistently when the value of N increases. Moreover, for the same value of M, the standard deviations decreases as N increases. This behavior is expected since scheduling a larger number of jobs to the same number of machines tends to be a more difficult problem. On the other hand, the mean number of non dominated solutions in the Pareto fronts (#ND) seems to be independent of M and N. As expected, for the same M, the mean number of function evaluations (F_{eval}) grows with N due to the higher difficulty of the problems.

Table 1. Statistics for the average of mean and maximum hypervolume, number of non dominated solutions and objective function evaluations.

M	N	$AVG(H_{\text{mean}})$	$SD(H_{\text{mean}})$	$AVG(H_{\text{max}})$	$SD(H_{\text{max}})$	#ND	F_{eval}
2	9	0.1745	0.0156	0.1753	0.0154	7.8	14810.0
	10	0.1324	0.0144	0.1338	0.0145	4.3	17112.4
	11	0.0890	0.0120	0.0912	0.0120	7.0	17874.8
4	9	0.4655	0.0131	0.4688	0.0128	9.7	13798.6
	10	0.4348	0.0122	0.4390	0.0123	9.5	19267.6
	11	0.4092	0.0086	0.4174	0.0086	7.5	21959.8
6	9	0.6010	0.0112	0.6055	0.0116	10.7	19737.6
	10	0.5758	0.0087	0.5824	0.0080	9.3	22703.3
	11	0.5584	0.0063	0.5663	0.0068	7.3	25343.8
8	10	0.6350	0.0082	0.6406	0.0081	10.4	20049.0
	11	0.6158	0.0061	0.6222	0.0063	11.1	23621.4

In order to compare the performance of NSGA-III the data available on the Scheduling Research Virtual Center website[1] was used. This data provides information about the best makespan values known obtained by an improved Ant Colony Optimization (ACOII) [3] algorithm for the instances solved in this paper.

Table 2 presents, for each combination of M and N and each one of the 15 instances, the number of non dominated solutions found ($\#\text{ND}_{\text{total}}$) and the number of those solutions that have a makespan value equal or inferior to the best solution found by ACOII ($\#\text{ND}_{\leq c_{\max}}$). The last two columns of this table

[1] https://sites.wp.odu.edu/schedulingresearch/wp-content/uploads/sites/99/2016/01/Rm-Cmax-ACO-Arnaout-2014.xlsx.

indicate the number of instances in which $\#ND_{\leq c_{max}}$ is greater than 1 ($\#ND_{>1}$) and greater or equal than 1 ($\#ND_{\geq 1}$), respectively. All results presented in this table refer to the runs of NSGA-III with best hypervolume for each instance. The values of $\#ND_{>1}$ show that in the majority of the instances, more than one non dominated solution with the best value of makespan was found. This is important because it provides the decision maker with more than one alternative solution with the makespan value and differing on the average and standard deviation of the completion times in each machine. In addition, the values of $\#ND_{\geq 1}$ stress the advantage of using this approach since in the majority of the instances solutions with the best known makespan value were found. There are some instances in which NSGA-III was not able to find solutions with the best makespan value. However, NSGA-III found solutions close to those. Moreover, it should be noted that the results presented in this table were obtained with a number of function evaluations significantly inferior to the one used for ACOII [2,3]. Furthermore, NSGA-III was able to find a solution for the instance 3 of the combination $M = 2$ and $N = 11$ (signed in the table with *). This solution corresponds to the sequence $\pi =< \pi_1, \pi_2 >$ where $\pi_1 = [9, 10, 5, 4, 8, 6]$ and $\pi_2 = [3, 7, 11, 2, 1]$. The total completion times are $c_1(\pi) = 735$ and $c_2(\pi) = 738$, and therefore $c_{max}(\pi) = 738$, $\bar{c}(\pi) = 736.5$, and $c_\sigma(\pi) = 1.5$. For this instance 3, the best solution reported before has a makespan of 742 [3].

Table 2. Performance comparison of NSGA-III with the improved ant colony optimization (ACOII) algorithm.

M	N	Instance	1	2	3	4	5	6	7	8	9	10	11	12	13	14	15	$\#ND_{>1}$	$\#ND_{\geq 1}$
2	9	$\#ND_{total}$	8	10	4	8	7	7	10	7	10	6	9	3	10	7	11		
		$\#ND_{\leq c_{max}}$	6	7	2	3	3	3	4	5	10	2	7	2	8	2	7	15	15
	10	$\#ND_{total}$	5	3	4	6	2	4	4	7	4	7	2	3	5	4	4		
		$\#ND_{\leq c_{max}}$	1	2	1	1	1	3	1	1	1	6	1	2	1	0	1	4	14
	11	$\#ND_{total}$	5	5	6	9	7	9	3	6	6	8	5	11	6	8	11		
		$\#ND_{\leq c_{max}}$	3	1	4*	3	1	7	1	2	0	4	2	9	1	8	11	10	14
4	9	$\#ND_{total}$	12	9	10	10	12	8	8	9	12	10	8	6	11	11	9		
		$\#ND_{\leq c_{max}}$	4	4	3	3	2	7	4	5	2	5	2	5	4	2	4	15	15
	10	$\#ND_{total}$	7	5	11	16	17	7	4	4	11	9	11	14	10	10	7		
		$\#ND_{\leq c_{max}}$	5	2	2	2	1	3	0	2	7	2	2	4	3	3	4	13	14
	11	$\#ND_{total}$	6	8	7	8	8	6	7	7	7	9	11	7	7	8	7		
		$\#ND_{\leq c_{max}}$	2	0	0	2	2	1	0	1	0	1	0	0	1	0	1	3	8
6	9	$\#ND_{total}$	13	7	8	7	7	11	5	11	13	16	24	11	8	7	12		
		$\#ND_{\leq c_{max}}$	3	2	3	1	3	1	2	2	1	1	1	0	5	2	4	9	14
	10	$\#ND_{total}$	5	8	7	11	14	13	13	10	5	11	10	7	8	11	7		
		$\#ND_{\leq c_{max}}$	2	1	0	0	0	0	1	1	1	2	0	0	0	2	1	3	8
	11	$\#ND_{total}$	7	7	7	6	6	10	8	4	7	10	9	8	8	5	7		
		$\#ND_{\leq c_{max}}$	0	1	0	1	1	0	0	2	1	0		0	2	0	0	2	6
8	10	$\#ND_{total}$	8	8	10	10	8	20	14	8	6	12	14	10	9	12	7		
		$\#ND_{\leq c_{max}}$	4	4	2	3	3	4	1	0	2	3	2	1	4	2	2	12	14
	11	$\#ND_{total}$	11	14	13	4	13	10	12	16	6	10	16	10	9	13	10		
		$\#ND_{\leq c_{max}}$	1	3	4	2	3	1	3	2	0	0	0	4	4	1	3	8	12

3.3 Analysis of the Results of an Instance

In Fig. 1, the approximation to the Pareto optimal front obtained for the minimization of the makespan ($c_{\max}$), the average completion time ($\bar{c}$) and the standard deviation of the completion times (c_σ) for 4 machines and 9 jobs (instance 8) is depicted. In this figure, the makespan ($c_{\max}$) is represented in X-axis, the average completion time ($\bar{c}$) in the Y-axis, and the standard deviation of the completion times (c_σ) is represented by the size of the points.

For this instance, 9 different non dominated solutions were obtained by NSGA-III to approximate the Pareto optimal front. The trade-off represented by those solutions in terms of the 3 objectives can be clearly visualized in this 2D plot. This figure also includes the pay-off table indicating the values of the objectives for each solution. It can seen that there are 5 solutions with the best value of makespan ($c_{\max} = 328$) but with different values of the other objectives. These solutions are of great interest for the decision maker.

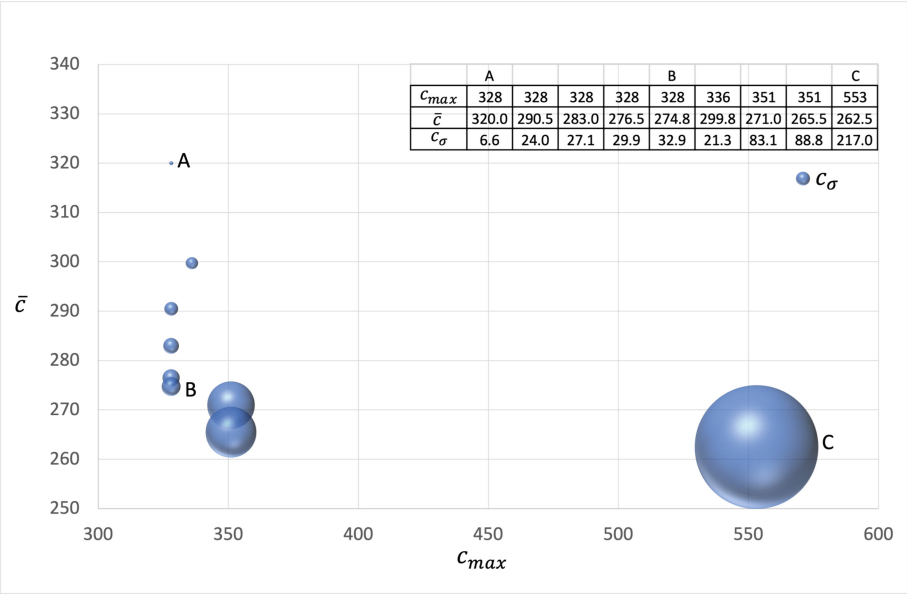

Fig. 1. Representation of the approximation to the Pareto optimal front for the minimization of makespan, the average completion time and the standard deviation of completion times for 4 machines and 9 jobs (instance 8).

Taking into account this approximation to the Pareto optimal front, 3 solutions (solutions A, B and C) were chosen as representative solutions to be analysed with more detail:

– Solution A is the solution with the best value of $c_{\max}$ and c_σ, and the worst value of $\bar{c}$;

- Solution B is the solution with the best value of $c_{\max}$, and intermediate values of $\bar{c}$ and c_σ;
- Solution C is the solution with the worst value of $c_{\max}$ and c_σ, and the best value of $\bar{c}$.

Solutions A and C are extreme solutions located on the upper-left and lower-right extremes of the Pareto front, respectively. Solution B is located on the elbow of the Pareto front and seems to be a good trade-off between the objectives.

It should be noted that if the 3 objectives were not considered as objectives to be minimized simultaneously, some important solutions would not be found. The following scenarios illustrate the importance of considering these 3 objectives for JSS problems:

- Scenario 1 - minimization of $c_{\max}$: any of the 5 solutions with $c_{\max} = 328$ could be found;
- Scenario 2 - minimization of $c_{\max}$ and $\bar{c}$, simultaneously: only solution B, solution C, and the two solutions between them could be found;
- Scenario 3 - minimization of $c_{\max}$ and c_σ: only solution A, solution C, and the 2 solutions between solution B and solution C could be found.

In Scenario 1, it is not guaranteed to find the solutions A and C that are good trade-offs. In Scenario 2, it is impossible to find solution A that is an interesting solution. Finally, Scenario 3 does not allow to find solution B. Thus, it is clear the importance of considering the 3 objectives, simultaneously.

In order to analyse solutions A, B and C, the data regarding instance 8 for $M = 4$ and $N = 9$ follows. The processing times $p_{i,j}$ of the job j on machine i are given in the following matrix:

$$p = \begin{pmatrix} 57\ 53\ 77\ 65\ 78\ 73\ 74\ 52\ 86 \\ 97\ 85\ 81\ 97\ 66\ 64\ 69\ 65\ 99 \\ 60\ 78\ 51\ 91\ 58\ 97\ 53\ 58\ 52 \\ 73\ 55\ 92\ 54\ 56\ 79\ 68\ 89\ 82 \end{pmatrix}.$$

The setup times $s_{i,j,k}$ to process job j after job k are given on matrices s_1, s_2, s_3, and s_4 for machines m_1, m_2, m_3, and m_4, respectively:

$$s_1 = \begin{pmatrix} 71\ 83\ 79\ 62\ 99\ 71\ 58\ 59\ 87 \\ 64\ 98\ 78\ 62\ 57\ 52\ 58\ 68\ 51 \\ 71\ 59\ 84\ 96\ 93\ 87\ 72\ 65\ 77 \\ 56\ 68\ 63\ 72\ 62\ 63\ 98\ 90\ 94 \\ 53\ 84\ 91\ 72\ 52\ 70\ 90\ 51\ 77 \\ 66\ 75\ 87\ 53\ 84\ 77\ 86\ 77\ 76 \\ 78\ 71\ 96\ 88\ 60\ 90\ 65\ 59\ 59 \\ 80\ 82\ 99\ 53\ 73\ 89\ 80\ 96\ 81 \\ 99\ 85\ 97\ 66\ 58\ 57\ 95\ 73\ 98 \end{pmatrix} \quad s_2 = \begin{pmatrix} 83\ 82\ 98\ 84\ 76\ 68\ 89\ 58\ 66 \\ 72\ 51\ 81\ 50\ 75\ 60\ 66\ 63\ 64 \\ 82\ 97\ 60\ 63\ 66\ 60\ 89\ 85\ 83 \\ 95\ 85\ 93\ 64\ 92\ 84\ 53\ 95\ 63 \\ 52\ 60\ 61\ 94\ 66\ 99\ 90\ 51\ 93 \\ 85\ 96\ 67\ 79\ 54\ 73\ 92\ 88\ 77 \\ 50\ 68\ 52\ 72\ 84\ 59\ 55\ 59\ 79 \\ 68\ 78\ 55\ 93\ 51\ 77\ 55\ 87\ 51 \\ 60\ 65\ 69\ 62\ 96\ 80\ 64\ 93\ 63 \end{pmatrix}.$$

$$s_3 = \begin{pmatrix} 60 & 55 & 59 & 81 & 87 & 61 & 68 & 95 & 73 \\ 67 & 99 & 96 & 53 & 93 & 79 & 69 & 90 & 60 \\ 81 & 73 & 58 & 77 & 77 & 90 & 55 & 58 & 80 \\ 51 & 77 & 70 & 85 & 65 & 56 & 56 & 71 & 59 \\ 52 & 59 & 54 & 78 & 82 & 50 & 74 & 59 & 96 \\ 78 & 88 & 75 & 70 & 70 & 54 & 85 & 73 & 64 \\ 89 & 76 & 94 & 97 & 95 & 77 & 52 & 90 & 59 \\ 57 & 50 & 93 & 86 & 77 & 63 & 97 & 51 & 62 \\ 52 & 63 & 92 & 85 & 61 & 64 & 72 & 99 & 56 \end{pmatrix} \quad s_4 = \begin{pmatrix} 50 & 90 & 68 & 77 & 85 & 67 & 85 & 80 & 86 \\ 98 & 97 & 53 & 96 & 50 & 88 & 71 & 79 & 98 \\ 98 & 74 & 90 & 53 & 53 & 89 & 71 & 53 & 63 \\ 62 & 95 & 77 & 63 & 99 & 89 & 69 & 95 & 69 \\ 53 & 67 & 83 & 81 & 86 & 81 & 86 & 84 & 56 \\ 82 & 81 & 91 & 68 & 70 & 77 & 65 & 99 & 66 \\ 87 & 93 & 67 & 97 & 88 & 55 & 63 & 70 & 68 \\ 71 & 99 & 62 & 60 & 59 & 82 & 70 & 54 & 91 \\ 76 & 89 & 94 & 75 & 78 & 79 & 60 & 80 & 87 \end{pmatrix}.$$

In the diagonal of the matrices s_1, s_2, s_3 and s_4, the setup time to process job j at the initial instant on machines ($s_{i,j,0}$) are given.

For illustration purposes, Fig. 2 to Fig. 4 represent solutions A, B and C for instance 8 with 4 machines (m_1, m_2, m_3, and m_4) and 9 jobs (n_1, n_2, n_3, n_4, n_5, n_6, n_7, n_8, and n_9). In these figures, grey boxes represent the jobs. Additionally, the processing times and setup times are also indicated below the grey boxes and before the jobs, respectively.

Figure 2 represents the solution A. This solution corresponds to the sequence $\pi =< \pi_1, \pi_2, \pi_3, \pi_4 >$ where $\pi_1 = [8, 6]$, $\pi_2 = [4, 5]$, $\pi_3 = [3, 7, 9]$, $\pi_4 = [2, 1]$. The total completion times are $c_1(\pi) = 310$, $c_2(\pi) = 319$, $c_3(\pi) = 328$ and $c_4(\pi) = 323$, and therefore $c_{\max}(\pi) = 328$, $\bar{c}(\pi) = 320$, and $c_\sigma(\pi) = 6.6$. This solution is very good in terms of the makespan and since the standard deviation of the completion times is very low, the workload distribution is very balanced between machines. However, this solution is the worst in terms the average completion time.

In Fig. 3, solution B is represented. This solution corresponds to the sequence $\pi =< \pi_1, \pi_2, \pi_3, \pi_4 >$ where $\pi_1 = [1, 8]$, $\pi_2 = [2, 6]$, $\pi_3 = [3, 7, 9]$, $\pi_4 = [4, 5]$. The total completion times are $c_1(\pi) = 239$, $c_2(\pi) = 260$, $c_3(\pi) = 328$ and $c_4(\pi) = 272$, and therefore $c_{\max}(\pi) = 328$, $\bar{c}(\pi) = 274.8$, and $c_\sigma(\pi) = 32.9$. This solution B has the same makespan value of solution A. However, it is clear that the workload is not so well-distributed between the machines. When compared to solution A, the average completion time is significantly inferior.

In Fig. 4, the solution C is shown. This solution corresponds to the sequence $\pi =< \pi_1, \pi_2, \pi_3, \pi_4 >$ where $\pi_1 = [\,]$, $\pi_2 = [2, 6, 5]$, $\pi_3 = [8, 9, 1, 3, 7]$, $\pi_4 = [4]$. The total completion times are $c_1(\pi) = 0$, $c_2(\pi) = 380$, $c_3(\pi) = 553$ and $c_4(\pi) = 117$, and therefore $c_{\max}(\pi) = 553$, $\bar{c}(\pi) = 262.5$, and $c_\sigma(\pi) = 217.0$. In this solution, no jobs are assigned to machine m_1 and the workload is clearly unbalanced. In spite of being the solution with the lowest average completion time, this solution does not represent a good scheduling of the jobs.

Overall, solution A and solution B seem to be good trade-offs. Note that solution A and solution B share some similar features. For instance, the subsequence π_3 is the same for both solutions, meaning that the assignment of jobs on machine m_3 is the same. Thus, choosing between them depends on the preferences of the decision maker.

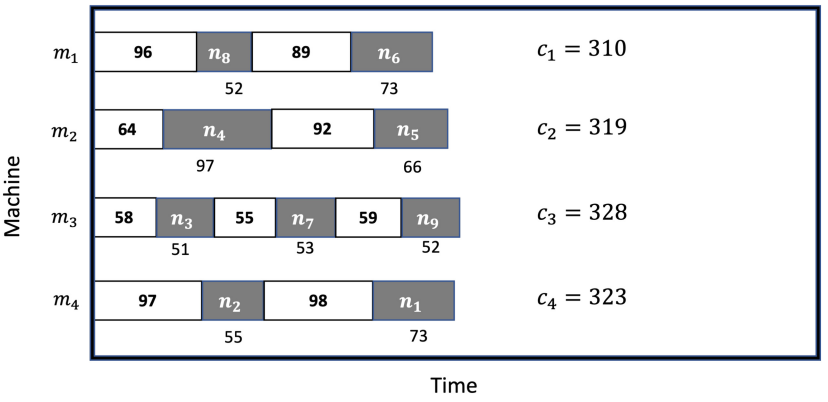

Fig. 2. Representation of solution A with 4 machines and 9 jobs (instance 8).

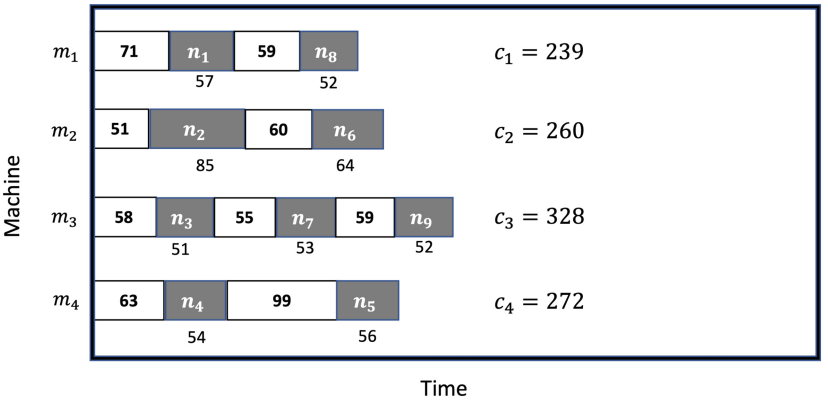

Fig. 3. Representation of solution B with 4 machines and 9 jobs (instance 8).

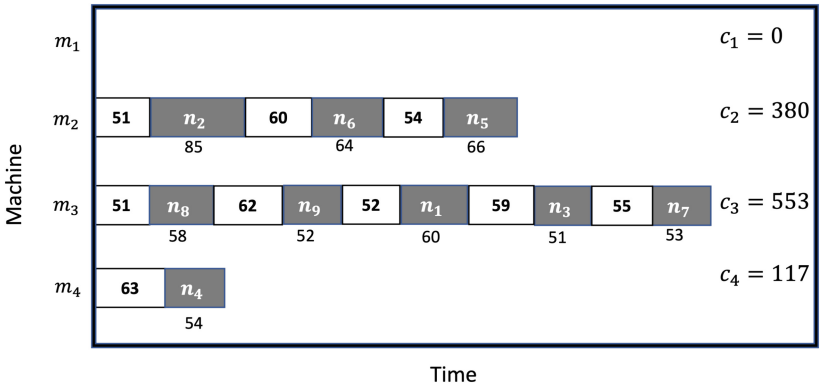

Fig. 4. Representation of solution C with 4 machines and 9 jobs (instance 8).

4 Conclusions and Future Work

In this paper, several instances of JSS problems on unrelated parallel machines with sequence-dependent setup times were solved as multi-objective optimization problems using NSGA-III. The makespan ($c_{\max}$), the average completion time ($\bar{c}$) and the standard deviation of the completion times were the objectives considered. In this work, 15 instances of JSS problems with balanced processing and setup times for M machines ($M \in \{2, 4, 6, 8\}$), and N jobs ($N \in \{9, 10, 11\}$) were used.

The hypervolume indicator was used to analyse the overall NSGA-III performance. These results indicate a good performance of NSGA-III to find approximations to the Pareto optimal set of JSS problems. The performance of NSGA-III was also compared with an improved Ant Colony Optimization (ACOII). These results demonstrate the advantage of using this approach since in the majority of the instances solutions with the best known makespan value were found. For some instances, the NSGA-III was not able to find solutions with the best makespan value, but solutions very close to those were found. However, it should be noted that in this work the number of function evaluations was significantly inferior to other approaches. Moreover, NSGA-III was able to find a solution for an instance that is better than the best solution reported before.

The analysis of some representative solutions from the approximation to the Pareto optimal set allows to confirm the validity and usefulness of this multi-objective optimization approach. Thus, the results also stress the importance of considering these three objectives, simultaneously. Also, the representation of the approximation to the Pareto optimal front highlights the trade-offs facilitating the decision making process.

Future work will include solving problems with more objectives and higher dimension, and to extend this approach to the distributed job shop problem. The performance of NSGA-III with other genetic operators for permutation representations will be also studied.

References

1. Abdelmaguid, T.F.: Representations in genetic algorithm for the job shop scheduling problem: a computational study. J. Softw. Eng. Appl. **3**(12), 1155 (2010)
2. Antunes, A.R., Matos, M.A., Rocha, A.M.A., Costa, L.A., Varela, L.R.: A statistical comparison of metaheuristics for unrelated parallel machine scheduling problems with setup times. Mathematics **10**(14), 2431 (2022)
3. Arnaout, J.P., Musa, R., Rabadi, G.: A two-stage Ant Colony optimization algorithm to minimize the makespan on unrelated parallel machines-Part II: enhancements and experimentations. J. Intell. Manuf. **25**, 43–53 (2014)
4. Arnaout, J.P., Rabadi, G., Musa, R.: A two-stage ant colony optimization algorithm to minimize the makespan on unrelated parallel machines with sequence-dependent setup times. J. Intell. Manuf. **21**, 693–701 (2010)
5. Blank, J., Deb, K.: Pymoo: multi-objective optimization in python. IEEE Access **8**, 89497–89509 (2020)

6. Chaudhari, P., Thakur, A.K., Kumar, R., Banerjee, N., Kumar, A.: Comparison of NSGA-III with NSGA-II for multi objective optimization of adiabatic styrene reactor. Mater. Today Proc. **57**, 1509–1514 (2022)
7. Deb, K., Jain, H.: An evolutionary many-objective optimization algorithm using reference-point-based nondominated sorting approach, Part I: solving problems with box constraints. IEEE Trans. Evol. Comput. **18**(4), 577–601 (2014)
8. Deb, K., Pratap, A., Agarwal, S., Meyarivan, T.: A fast and elitist multiobjective genetic algorithm: NSGA-II. IEEE Trans. Evol. Comput. **6**(2), 182–197 (2002)
9. Feldman, A.: Scheduling algorithms and systems. Columbia University (1999)
10. González-Neira, E.M., et al.: Robust solutions in multi-objective stochastic permutation flow shop problem. Comput. Ind. Eng. **137**, 106026 (2019)
11. Ibrahim, A., Rahnamayan, S., Martin, M.V., Deb, K.: EliteNSGA-III: an improved evolutionary many-objective optimization algorithm. In: 2016 IEEE Congress on evolutionary computation (CEC), pp. 973–982. IEEE (2016)
12. Katoch, S., Chauhan, S.S., Kumar, V.: A review on genetic algorithm: past, present, and future. Multimedia Tools Appl. **80**, 8091–8126 (2021)
13. Khan, B., Hanoun, S., Johnstone, M., Lim, C.P., Creighton, D., Nahavandi, S.: Multi-objective job shop scheduling using i-NSGA-III. In: 2018 Annual IEEE International Systems Conference (SysCon), pp. 1–5. IEEE (2018)
14. Liaqait, R.A., Hamid, S., Warsi, S.S., Khalid, A.: A critical analysis of job shop scheduling in context of industry 4.0. Sustainability **13**(14), 7684 (2021)
15. Para, J., Del Ser, J., Nebro, A.J.: Energy-aware multi-objective job shop scheduling optimization with metaheuristics in manufacturing industries: a critical survey, results, and perspectives. Appl. Sci. **12**(3), 1491 (2022)
16. dos Santos, F., Costa, L., Varela, L.: Multi-objective optimization of the job shop scheduling problem on unrelated parallel machines with sequence-dependent setup times. In: Gervasi, O., et al. (eds.) International Conference on Computational Science and Its Applications, pp. 495–507. Springer, Cham (2023). https://doi.org/10.1007/978-3-031-37108-0_32
17. dos Santos, F., Costa, L.A., Varela, L.: A systematic literature review about multi-objective optimization for distributed manufacturing scheduling in the industry 4.0. In: Gervasi, O., Murgante, B., Misra, S., Rocha, A.M.A.C., Garau, C. (eds.) Computational Science and Its Applications–ICCSA 2022 Workshops: Malaga, Spain, 4–7 July 2022, Proceedings, Part II, pp. 157–173. Springer, Cham (2022). https://doi.org/10.1007/978-3-031-10562-3_12
18. dos Santos, F., Costa, L.A., Varela, L.: Performance comparison of NSGA-II and NSGA-III on bi-objective job shop scheduling problems. In: Pereira, A.I., Mendes, A., Fernandes, F.P., Pacheco, M.F., Coelho, J.P., Lima, J. (eds.) International Conference on Optimization, Learning Algorithms and Applications, pp. 531–543. Springer, Cham (2024). https://doi.org/10.1007/978-3-031-53025-8_36
19. Yenisey, M.M., Yagmahan, B.: Multi-objective permutation flow shop scheduling problem: literature review, classification and current trends. Omega **45**, 119–135 (2014)
20. Zhang, J., Ding, G., Zou, Y., Qin, S., Fu, J.: Review of job shop scheduling research and its new perspectives under industry 4.0. J. Intell. Manuf. **30**, 1809–1830 (2019)
21. Zitzler, E., Thiele, L., Laumanns, M., Fonseca, C.M., Grunert da Fonseca, V.: Performance assessment of multiobjective optimizers: an analysis and review. IEEE Trans. Evol. Comput. **7**(2), 117–132 (2003)

A Simulation-Based Optimization Approach to the Firefighting Resource Scheduling Problem

Emerson J. Paiva[1,2], Marina A. Matos[1], and Ana Maria A. C. Rocha[1(✉)]

[1] ALGORITMI Research Centre/LASI, University of Minho, Campus de Gualtar, 4710-057 Braga, Portugal
emersonpaiva@unifei.edu.br, mmatos@algoritmi.uminho.pt, arocha@dps.uminho.pt

[2] Federal University of Itajubá, Campus Itabira, Itabira, Brazil

Abstract. In recent years, the number of forest fires has increased significantly. The main factors behind these disasters are rising temperatures and population growth. Optimization and simulation have been widely applied to forest firefighting problems, making it possible to improve the effectiveness and speed of firefighting actions. This work presents a forest firefighting resource scheduling problem, where a single firefighting resource is fighting 10 ignitions. A Genetic Algorithm (GA) is used to find the near-optimal sequence of actions, taking into account the maximization of the total unburned area. The solution found by the GA is evaluated using a Discrete-Event Simulation model developed in FlexSim software, thus validating the solution. Then, a simulation-based optimization approach is developed, involving uncertainty in some parameters.

Keywords: Forest Fires · Scheduling Problem · Optimization · Discrete-Event Simulation

1 Introduction

Forest fires are uncontrolled phenomena that can spread rapidly if no containment measures are put in place. They have been increasing in recent years, due to the rise in the ambient temperature and the increase in the world population. This is why viable strategies are needed to combat forest fires. Optimization is one of the most applied techniques in forest firefighting problems, allowing improvements in the effectiveness and speed of firefighter actions. Every year, around 4 million square kilometers of land are burned worldwide [17,21]. In the last 7 years (2016–2023) there has been a large number of fires in the countries

This work has been supported by FCT Fundação para a Ciência e Tecnologia within the R&D Units Project Scope UIDB/00319/2020 and GEQProd (Grupo de Estudos em Qualidade e Produtividade), and the PhD grant reference UI/BD/150936/2021.

© The Author(s), under exclusive license to Springer Nature Switzerland AG 2024
O. Gervasi et al. (Eds.): ICCSA 2024 Workshops, LNCS 14816, pp. 383–396, 2024.
https://doi.org/10.1007/978-3-031-65223-3_26

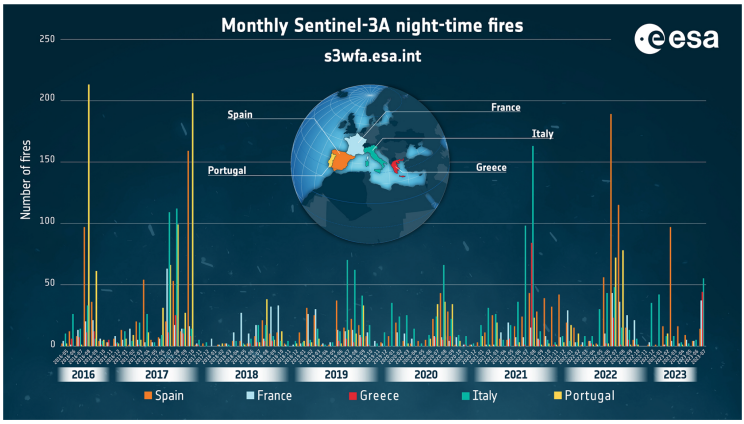

Fig. 1. Forest fires in 2016–2023 (https://www.esa.int/Space_in_Member_States/Portugal/Contagem_dos_incencios_florestais_no_mundo)

of Southern Europe: Spain, France, Greece, Italy and Portugal, as can be seen in Fig. 1. In 2016 and 2017, Portugal faced a large number of forest fires, both record years for the number of fires that occurred, where 2017 was the deadliest year in Portuguese history [1].

Firefighting is a very important field that has been studied in the literature. It is therefore necessary to find solutions to improve the fight against forest fires and, consequently, reduce the damage caused by them. Protecting and preventing fires is an important issue, and studies have been carried out to support the decisions of forest firefighting professionals (firefighters, civil protection, etc.). The characteristics of firefighting teams are defined as their number, their skills and their level of preparation, making them very important for the fight. The better and faster the firefighting team acts, the smaller the total burned area, which can save lives and reduce the impact on the ecosystem [2]. In order to manage forest fire suppression, it is necessary to know how many and which firefighting resources should be sent to each forest fire, to extinguish the fire as quickly as possible.

In engineering, optimization techniques have been applied to solve fire suppression problems, with the aim of finding the best trajectory and location for firefighting vehicles, obtaining the shortest route, determining the number and resources to send, among others. The work by Wu et al. [23] studied a forest firefighting vehicle scheduling problem. A multi-objective approach was applied to minimize the total time to extinguish the fire and the number of firefighting vehicles sent to the same fire. To do this, an integer programming model was developed, which is an improved and simplified version of an existing program. In addition, an exact dynamic programming algorithm and a fast, greedy heuristic method were applied to this problem. The effectiveness and efficiency of the proposed model and algorithms were confirmed using a real instance and randomly generated large reference instances.

A genetic algorithm (GA) is one of the most used metaheuristics to solve this type of problem, where several works have been presented using it in forest firefighting problems. HomChaudhuri et al. [12,13] used GA to minimize the total burned area, where homogeneous and heterogeneous meteorological conditions with uncertainty were considered. To deal with uncertainty, Monte-Carlo simulations were used, verifying the effectiveness of sending resources to combat complex forest fires in uncertain and dynamic conditions. There was a significant reduction in damage caused. In the work carried out by Matos et al. [16], the optimal scheduling of a forest firefighting resource to combat multiple ignitions was studied. The objective was to minimize the total burned area using GA in a problem with ten forest fire ignitions and one resource to extinguish these ignitions. Chan et al. [6] used the Firefly algorithm for a firefighting resource allocation problem. The algorithm used a combination of the maximum set coverage formulation and a new utility estimation technique, and used a knapsack formulation to calculate the allocation of resources. They found, with real data, that the strategy used achieved up to 80–90% performance of the optimal solution, even with a small number of drones. This strategy proved to be efficient in dealing with a dynamically changing environment and uncertainty.

This study focuses on the forest firefighting scheduling problem. The aim is to assign 1 forest firefighting resource to fight 10 ignitions. In a previous study [16], an adapted GA was used to maximize the total unburned area of the ignitions and find the near-optimal sequence of actions. In this work, the solution found by the GA is then tested in a Discrete Event Simulation model developed in the FlexSim software. A simulation-based optimization approach is then developed, involving uncertainty in some parameters, to validate the solution.

This paper is organized as follows. The simulation based approach is described in Sect. 2, where a Genetic Algorithm and Simulation technique are briefly presented. The description of the problem to be solved is shown in Sect. 3. The simulation model is described in Sect. 4 and the results are shown in Sect. 5, where a statistical analysis of the results is also presented. Finally, the conclusions of this study and future work are exposed in Sect. 6.

2 Simulation-Based Optimization Approach

In this section, the theories concerning the optimization algorithm and simulation techniques adopted in this work will be briefly presented. Starting with the description of Genetic Algorithm and Simulation, the criteria that led to the selection of the computational tool and the justification for the combined application of optimization and simulation as a way of validating the solutions obtained are addressed.

2.1 Optimization Technique

A Genetic Algorithm is a metaheuristic (optimization technique) inspired by the theory of species evolution, in which the fittest individual is the survivor of a

process based on biologically inspired operators such as mutation, crossover and selection [11]. The fittest individuals are those most likely to perpetuate their genetic characteristics. GA begins with the random generation of a population of potential solutions, called chromosomes, whose qualities are evaluated by the fitness function, and the selected chromosomes then undergo the process of evolution. Several generations are obtained in a cycle that is repeated until the stopping criterion is satisfied.

2.2 Simulation Tool

Simulation is an operational research technique in which a model is created by abstracting a real-world problem into mathematical or logical terms, converted into a computational system (a spreadsheet, a programming language, or specific software) to describe the behavior of a system over time [10,20].

According to Banks [3] and Robinson [19], simulation involves imitation of the operation of a real-world process or system. Banks emphasizes that simulation is an important method for solving various real-world problems. Forbus and Berleant [8] further explain that it is a simplified model of a particular real system, generated to investigate certain aspects of that system. Its application is justified by being a technique generally faster, easier, lower cost, and with minimal risks compared to real system experiments and observations. It can be a good option for analyzing the behavior of existing systems, testing new hypotheses, or even designing new systems, allowing managers to evaluate alternatives, test various scenarios, and generate predictions with reasonable approximations.

Law and Kelton [15] described a procedure to construct a simulation model. The construction of the computational representation of the model is one of the steps in this procedure. As important as constructing the computational model is choosing the appropriate computational tool. Nowadays, there are various computational tools available on the market for building simulation models and choosing one is not trivial. It depends on factors such as the type of application, type of simulation, and expected results, among other key factors. Rashidi in [18] proposed a ranking of simulation tools generated from the application of a hybrid approach between the Analytic Hierarchy Process, Feature Analysis, and Weighted Average Sum for thirteen key factors.

This work aims to use simulation to verify the dynamic behavior of the scheduling solution obtained by the GA application. In this context, it would be necessary to use a tool with good visual aspects, considering animations, user interfaces, and dynamic graphical elements during execution. Concerning the results, the tool selected should show a good internal coding level to allow the creation of specific tasks and user functions, good experimentation resources, and efficient input and output tools. Therefore, the *FlexSim* tool [9] is chosen, taking into account the key factors defined and the results of the studies by [7,18]. It is a computational tool capable of generating discrete event simulation models that feature, in terms of logistics, the *Geographic Information System (GIS)* module, which can manage road information, which is essential for the accuracy of the results of this work.

2.3 Simulation-Based Optimization Framework

Simulation and optimization are two strategies that are widely used in various engineering problems. Mathematical models have been applied combining those methodologies, thus initiating new scientific studies [5]. The problem of fire suppression has also been tackled with these strategies. Hu and Ntaimo [14] carried out a research into the simulation of forest fire propagation, the optimization of firefighting resources and the simulation of fire suppression techniques. They used a mixed integer stochastic programming model to generate firefighting resource dispatch plans and developed an agent-based discrete event simulation model to simulate fire suppression based on the generated dispatch plans. Experimental results indicated significant variations in fire suppression based on different firefighting tactics. The simulation of these tactics was important for validating dispatch plans based on optimization models. The article by Homchaudhuri et al. [12] shows the advancement of effective fireline construction strategies through resource allocation. The approach introduces a simulation and optimization technique using genetic algorithms and sophisticated forest fire propagation models. Given the uncertainties associated with weather conditions and the limited knowledge of vegetation and topographical factors, it is difficult to accurately predict forest fires. To solve this problem, Monte Carlo simulations have been used to devise robust strategies in uncertain circumstances. Through exhaustive simulations, the effectiveness of the proposed method is demonstrated in optimal allocation of resources to combat complex forest fires in dynamic and uncertain environments is demonstrated.

The strategy of applying optimization and simulation together was also adopted in this work. A code developed in *Python* for optimization using GA was connected to a simulation model developed in Discrete Event Simulation software. Figure 2 illustrates how optimization and simulation will interact to try to find the optimal result for the problem under investigation. Based on the input data, the optimizer identifies the best action scheduling for the firefighting team, using a Genetic Algorithm. The sequence obtained is then implemented in the simulator, which runs a certain number of replicas of the model, locating the best result among them. Based on this result, the input data is updated and resubmitted to the optimizer. The strategy is repeated until a stopping condition is met, identifying the sequence with the best performance at the end.

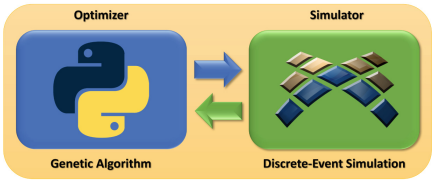

Fig. 2. Simulation-based optimization framework

3 Problem Description

This work presents a simulation-based optimization approach to determine the scheduling solution of one forest firefighting resource to combat several ignitions, under uncertainty of certain parameters. The initial data used and more details about the application of the GA to the scheduling problem can be found in [16].

The problem consists of determining the optimal schedule for a single resource (a firetruck which is based on forest firefighting land vehicle with water tank) to travel from its base to all the ignition points (which can be understood as several fronts of the same forest fire) and return to the base, in order to maximize the unburned area.

Figure 3 shows the selected study area, the fire ignitions, and routes generated from GIS that connect these locations.



Fig. 3. Fire locations on study area

At the center of the figure, in dark blue, is located the fire station, the locations of the ignitions that have requests for firefighting are marked in red square, and the numbers in the light blue circles indicate the fire ignitions. Marked in black can be seen the existing routes to attend to these locations. There are 11 interconnected locations: the fire station and the other 10 forest fire ignitions. The sum of the areas of the 10 forest fire ignitions corresponds to a total of 16124.78 ha.

4 Simulation Model

In this work, GA is implemented in the *python* (version 3.9.35) using *VScode* (Version 1.87), after being adapted from the *pymoo* framework: Single-objective Optimization in Python [4]. A permutation representation has been used to describe the scheduling solution. Under this representation, every chromosome comprises a unique sequence of integer values, each occurring only once. Consequently, each chromosome shows the sequence in which the firefighting resource will act to extinguish each ignition. Regarding the parameters used by GA, the population size was set to 20, and the GA default values for the maximum number of generations and the maximum number of function evaluations were 1000 and 100000, respectively. The GA operators used in this work were: tournament selection, order-based crossover and inverse mutation. Since GA is a stochastic algorithm, 30 independent runs were performed in order to statistically analyze its performance. The experiments were carried out on a PC 11th Gen Intel(R) Core(TM) i7-1165G7 @ 2.80 GHz, 2803 Mhz, 4 Nucleus(s), 8 Processor(s) Logic(s), 16 Gb RAM.

Firstly, a simulation model was created to observe the dynamic behavior of the proposed scheduling. The model considers the time spent between the necessary movements between each site, configured using the GIS module available in the FlexSim software. In order for the model to find the best route to follow, given the planned sequence of actions, each location was connected to the other 10 locations in the model. As a result, an origin-destination matrix is obtained, in which it is observed that certain paths have differences between outbound and inbound trips, some of them significant in terms of distance (km) and/or time (h). Table 1 presents the times, in hours, spent on travel between the 11 designated locations for investigation, where the number zero refers to the fire station.

Table 1. Travel time to each location

	0	1	2	3	4	5	6	7	8	9	10
0	0.00	0.99	0.78	0.28	0.21	1.69	0.19	0.28	0.33	0.63	0.39
1	0.99	0.00	0.42	1.04	0.95	1.29	1.13	1.22	1.28	1.48	1.33
2	0.78	0.42	0.00	0.91	0.82	1.52	0.97	1.06	1.07	1.27	1.17
3	0.28	1.04	0.91	0.00	0.10	1.71	0.35	0.43	0.56	0.85	0.54
4	0.21	0.95	0.82	0.11	0.00	1.62	0.32	0.41	0.49	0.78	0.52
5	1.69	1.29	1.51	1.71	1.62	0.00	1.80	1.89	1.97	2.26	2.00
6	0.20	1.12	0.96	0.35	0.31	1.79	0.00	0.20	0.41	0.71	0.32
7	0.29	1.21	1.05	0.43	0.40	1.88	0.21	0.00	0.53	0.82	0.19
8	0.33	1.28	1.08	0.56	0.49	1.97	0.41	0.53	0.00	0.54	0.53
9	0.61	1.47	1.27	0.85	0.78	2.26	0.71	0.80	0.55	0.00	0.85
10	0.40	1.32	1.16	0.54	0.51	1.99	0.32	0.19	0.53	0.85	0.00

Based on the results of the optimization procedure described in [16], a model was generated to adhere to the optimal planning: $FS \rightarrow F_5 \rightarrow F_9 \rightarrow F_1 \rightarrow F_{10} \rightarrow F_2 \rightarrow F_7 \rightarrow F_8 \rightarrow F_3 \rightarrow F_6 \rightarrow F_4$, where FS is the fire station and F_i is ignitions ($i = 1, ..., 10$). In other words, the vehicle departs towards the first defined location (Ignition 5, F_5). Upon arrival, the action time is timed according to Table 2. Then, the vehicle departs from this point towards the second location (Ignition 9, F_9), where the action time is also timed. And so on, until returning to the fire station, completing the scheduling.

Table 2. Defined firefighting times

	F_1	F_2	F_3	F_4	F_5	F_6	F_7	F_8	F_9	F_{10}
hours	0.2	1.8	1.4	1.0	1.4	0.2	0.1	0.6	0.8	1.2
seconds	720	6480	5040	3600	5040	720	360	2160	2880	4320

4.1 Model Verification and Validation

As mentioned earlier, simulation involves the construction of a computational model that mimics a process or system. When building this model, adaptations are necessary to reduce the complexity of the problem, increase its understanding, and expedite the obtaining of a solution, which should represent a reasonable approximation of reality. The process of verification and validation of a simulation model aims to identify the level of accuracy of the model. While verification is the process of ensuring that the computational model created exhibits sufficient accuracy, validation is the process of ensuring that the model is sufficiently accurate for the purpose for which it was constructed [19]. Sargent [22] described several techniques for the verification and validation of simulation models. Thus, comparison with other validated models is considered in this study, comparing the results obtained in the simulation model with empirical results from analytical models, for example.

In this context, Matos et al. [16] developed an optimization model that uses the GA to maximize the unburned area by generating a near-optimal scheduling of ignitions. Taking into account the comparison criterion presented by Sargent, based on the input data and results available in [16], a discrete event simulation model was generated to evaluate the described scenario, and the results were compared, as shown in Table 3. This table shows a divergence in the values for the burned area column. This is due to an error identified in the calculation of this area in the original work, which was corrected so as not to influence subsequent analyses. As observed, the results indicate a small error, as expected, in terms of total time, given the precision with which *FlexSim-GIS* handles geographical distances between the points of operation. Therefore, it was considered that the results of the simulated model were compatible with the analytical model, validating the simulation model. Therefore, based on a validated simulation model, experiments can be executed, as the results can be considered reliable.

Table 3. Validation by comparing models

	Unburned area (ha)	Burned area (ha)	Travel time (h)	Process time (h)	Total time (h)	Saved area
Matos et al.(2022) [16]	16029.38	95.4	11.88	8.70	20.58	0.9941
Matos et al.(2022) adj	15913.60	211.18	11.88	8.70	20.58	0.9869
Simulation Model	15937.29	187.49	10.79	8.70	19.49	0.9884
Error	0.57%	–	9.18%	–	5.30%	0.57%

4.2 Adding Uncertainty

From a validated simulation model, different scenarios can be tested, and experiments can be conducted. Thus, initially, uncertainty related to the time required to combat fire ignition points was incorporated into the model by replacing deterministic data with probability distributions. This procedure was named Experiment 1 (Exp. 1). Next, the travel time (journeys made between one ignition point and another) was also converted into probability distributions, as a way of increasing the robustness of the simulation model. This procedure was named Experiment 2 (Exp. 2). However, it is important to note that, for travel time, only travel delays were considered, as it is understood that there is no possibility of making journeys faster than defined in Table 1. Delays, in turn, characterize problems related to traffic (congestion or detours) or resource breakdowns.

Due to the lack of historical data, normal distributions of the combat and travel time were used, as shown in Table 4.

Table 4. Probability distribution for process and travel time

Location		F_1	F_2	F_3	F_4	F_5	F_6	F_7	F_8	F_9	F_{10}
Process time (h)	Mean	0.20	1.80	1.40	1.00	1.40	0.20	0.10	0.60	0.80	1.20
	S.Dev.	0.02	0.18	0.14	0.1	0.14	0.02	0.01	0.06	0.08	0.13
Travel time (h)	Mean	1.51	1.16	0.56	0.31	1.69	0.35	1.06	0.53	2.26	1.36
	S.Dev.	0.15	0.12	0.06	0.03	0.17	0.04	0.11	0.05	0.23	0.14

The combat and travel time are modelled by a probability distributions. An experimental design with 30 replications was executed, and the results were recorded. For each replication, the total time and the total unburned area were calculated. The total unburned area was calculated as described in [16].

Figure 4 displays the combat time variation for each ignition point in each experiment replication. Figure 5 presents a comparison between the total time and the area not burned, showing that there is no correlation between these two variables.

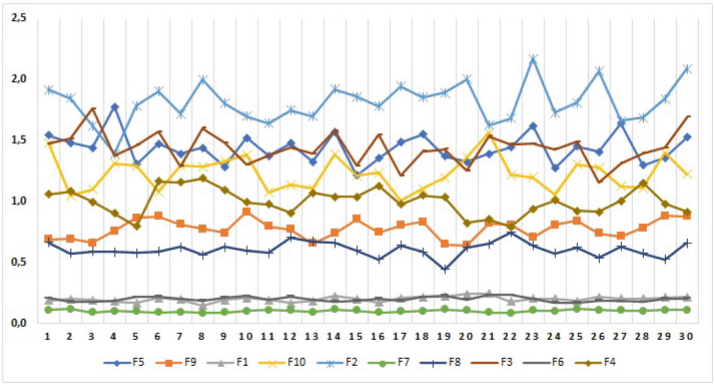

Fig. 4. Random process variation

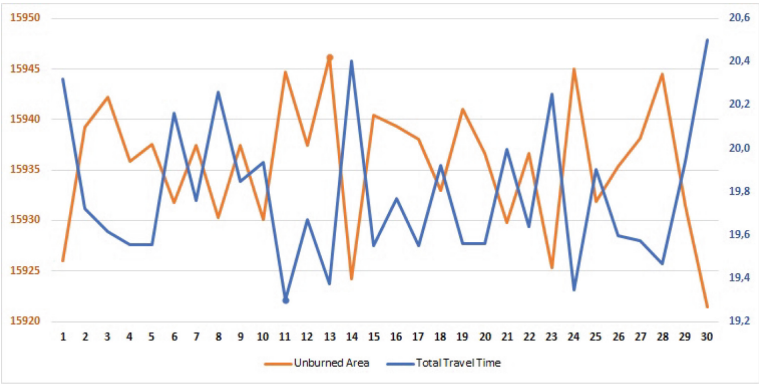

Fig. 5. Total time and unburned area results

5 Discussion of Results

Based on the experimental procedure described in Sect. 4, six simulation cycles (runs) were performed, to validate the solution presented by GA or find a new solution that maximizes the unburned area. It should be noted that the computational time required by GA was negligible for effective decision-making.

The first run was executed considering the schedule obtained by GA in [16], $FS \rightarrow F_5 \rightarrow F_9 \rightarrow F_1 \rightarrow F_{10} \rightarrow F_2 \rightarrow F_7 \rightarrow F_8 \rightarrow F_3 \rightarrow F_6 \rightarrow F_4$, in two stages. In the first stage, only the combat time was converted into probability distributions (Exp.1), based on the deterministic provided in [16]. In the second stage, in addition to combat time, travel time was also converted into probability distributions (Exp.2), taking into account the times described in the origin-destination matrix available in Table 1. At each stage, the simulation was run completely in all 30 runs, and the results were recorded for later analysis. Table 5 shows the average result, based on the unburned area of the 30 replicates in this

first simulation run, and the best result, which showed the largest unburned area among them.

Table 5. Results from experiments 1 and 2

		Unburned area (ha)	Burned area (ha)	Travel time (h)	Process time (h)	Total time (h)	Saved area (%)
Simulation Model		15937.29	187.49	10.79	8.70	19.49	98.84
Exp.1	Mean	15935.62	189.16	11.00	8.79	19.79	98.83
	Best	15946.20	178.58	11.00	8.38	19.38	98.89
Exp.2	Mean	15929.33	195.45	11.23	8.62	19.85	98.79
	Best	15947.32	177.46	10.96	8.00	18.96	98.90

Hypothesis tests were carried out for each result obtained. Considering the total travel time of Exp.1, there was a significant statistical difference, which suggests that there was an increase in performance when uncertainty was added to combat times. In terms of area burned, there was a decrease of 11.2% compared to the theoretical results. With Exp.2, there was a statistical difference between the averages, indicating a decrease of 7.5% in the burned area, based on the average result, and 16% based on the best result. The best result obtained in Exp.2 was adopted to continue the simulation-based optimization procedure.

In the following five runs, only Exp.2 (randomized combat and travel time) was considered, and analyses were carried out based only on the best result (maximum unburned area).

For a better understanding of the procedure used, Fig. 6 shows the flow of the simulation-based optimization process for the six planned experimental runs.

Once all six experimental runs had been carried out, the scheduling and respective results were recorded, as shown in Table 6. In this table, "Ref" identifies the result obtained from the model that disregards uncertainty in both combat time and travel time. It is important to note that in some runs the optimizer was unable to generate a different schedule to the previous one. This behavior may have occurred due to the random nature of the combat and travel processes that vary times for better or worse, generating a new OD matrix that is not significant in terms of optimization.

The results shown in Table 6 indicate statistical differences between each of the runs in relation to the result of the deterministic model. These differences represent the sensitivity of the simulation model to the presence of uncertainty in the variables of interest. However, the results confirm the scheduling initially determined by GA as the best possible result for the problem under investigation.

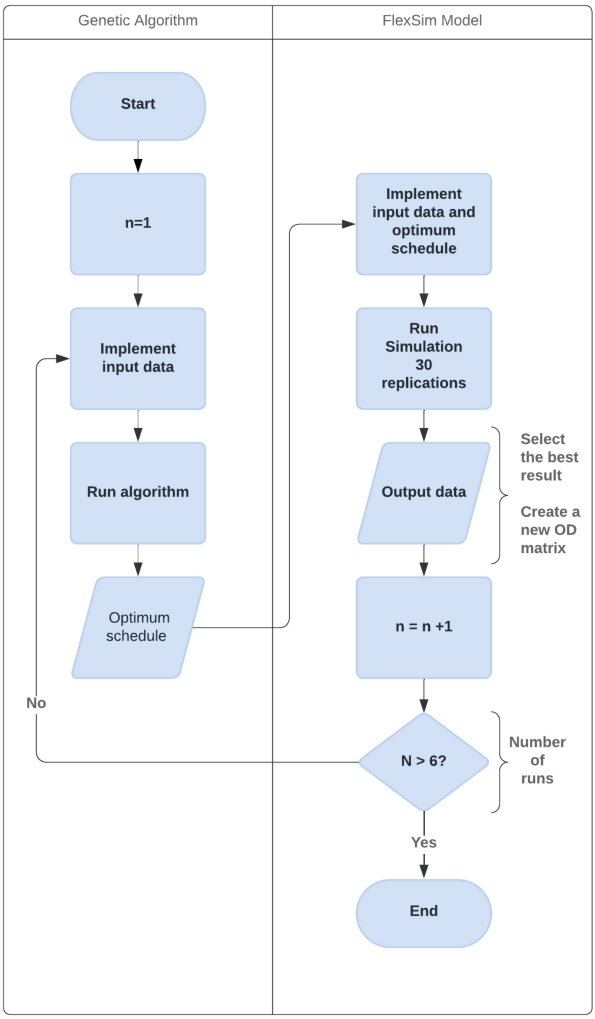

Fig. 6. Simulation-based optimization process flow

Table 6. Results of the experimental design

Runs	Scheduling	Unburned area (ha)	Travel time (h)	Process time (h)	Total time (h)	Saved area (%)
Ref	[5 9 1 10 2 7 8 3 6 4]	15937.29	10.79	8.70	19.49	98.84
1	[5 9 1 10 2 7 8 3 6 4]	15947.32	10.96	8.00	18.96	98.90
2	[5 9 2 10 1 3 8 4 7 6]	15925.71	10.87	8.26	19.13	98.77
3	[5 9 2 10 3 1 8 4 7 6]	15923.26	10.89	8.29	19.18	98.75
4	[5 9 2 10 3 1 8 4 7 6]	15921.37	11.10	8.24	19.34	98.74
5	[5 9 2 10 3 1 8 4 7 6]	15925.86	10.94	8.22	19.16	98.77
6	[5 3 2 10 9 1 8 4 7 6]	15939.69	10.32	8.25	18.57	98.85

6 Conclusions and Future Work

This work has highlighted the application of engineering in the search for solutions to problems that directly affect the quality of life of people and their environment and ecosystem. The occurrence of forest fires has increased in recent years and is essentially due to natural or human factors. Therefore, it is necessary to look for solutions that can manage fire suppression, such as optimizing firefighting actions.

In order to find a solution that would mitigate the impacts caused by this phenomenon, minimizing the total unburned area, a simulation-based optimization approach was used to properly plan the actions of one available resource to combat 10 ignitions. The solution was obtained by applying a Genetic Algorithm to the available data on the time and distance between the points of fire ignition and the combat time arbitrated for each. A simulation model was then built in FlexSim software, which was duly verified and validated. The model was prepared to take into account uncertainty in travel and combat time, and to interact with the optimizer, always trying to find a better solution to the problem. Once this model was in place, six experimental runs were carried out, which generated four different schedules. The results for the unburned area for the six runs were: 1) 98.90%; 2) 98.77%; 3) 98.75%; 4) 98.74%; 5) 98.77%; 6) 98.85%. As can be seen, the results did not deviate significantly from those presented by the model initially generated by GA (98.84%). Considering the uncertainty in travel time and process time, the original scheduling (run number 1) showed the most significant result, maximizing the unburned area.

For future work, we suggest investigating: a) The search for and insertion of real data, obtained from official websites; b) The inclusion of a greater number of resources; c) The inclusion of work shifts for the teams involved; d) Control of the volume of water used, with possible refilling at predetermined locations.

Acknowledgments. The authors would like to thank FlexSim Software Products, Inc. for supporting this research by providing a provisional educational license for the software, version 24.0.2.

References

1. Agbeshie, A.A., Abugre, S., Atta-Darkwa, T., Awuah, R.: A review of the effects of forest fire on soil properties. J. Forest. Res. **33**(5), 1419–1441 (2022)
2. Attri, V., Dhiman, R., Sarvade, S.: A review on status, implications and recent trends of forest fire management. Arch. Agric. Environ. Sci. **5**(4), 592–602 (2020)
3. Banks, J.: Handbook of Simulation: Principles, Methodology, Advances, Applications, and Practice. John Wiley & Sons, Hoboken (1998)
4. Blank, J., Deb, K.: Pymoo: multi-objective optimization in python. IEEE Access **8**, 89497–89509 (2020)
5. Bortz, M., Asprion, N.: Simulation and Optimization in Process Engineering: The Benefit of Mathematical Methods in Applications of the Chemical Industry. Elsevier, Amsterdam (2022)

6. Chan, H., Tran-Thanh, L., Viswanathan, V.: Fighting wildfires under uncertainty: a sequential resource allocation approach. In: Proceedings of the Twenty-Ninth International Conference on International Joint Conferences on Artificial Intelligence, pp. 4322–4329 (2021)
7. Dias, L.M., Vieira, A.A., Pereira, G.A., Oliveira, J.A.: Discrete simulation software ranking-a top list of the worldwide most popular and used tools. In: 2016 Winter Simulation Conference (WSC), pp. 1060–1071. IEEE (2016)
8. Forbus, J.J., Berleant, D.: Discrete-event simulation in healthcare settings: a review. Modelling **3**(4), 417–433 (2022)
9. Gelenbe, E., Guennouni, H.: Flexsim: a flexible manufacturing system simulator. Eur. J. Oper. Res. **53**(2), 149–165 (1991). https://doi.org/10.1016/0377-2217(91)90131-E
10. Hillier, F.S.: Introduction to Operations Research. McGrawHill, New York (2001)
11. Holland, J.H.: Adaptation in Natural and Artificial Systems. MIT Press, Cambridge (1975)
12. HomChaudhuri, B., Kumar, M., Cohen, K.: Genetic algorithm based simulation-optimization for fighting wildfires. Int. J. Comput. Methods **10**(06), 1350035 (2013)
13. HomChaudhuri, B., Zhao, S., Cohen, K., Kumar, M.: Generation of optimal fireline for fighting wildland fires using genetic algorithms. In: Dynamic Systems and Control Conference, vol. 48920, pp. 111–118 (2009)
14. Hu, X., Ntaimo, L.: Integrated simulation and optimization for wildfire containment. ACM Trans. Model. Comput. Simul. (TOMACS) **19**(4), 1–29 (2009)
15. Law, A.M., Kelton, W.D., Kelton, W.D.: Simulation Modeling and Analysis, vol. 3. Mcgraw-hill, New York (2007)
16. Matos, M.A., Rocha, A.M.A., Costa, L.A., Alvelos, F.: A genetic algorithm for forest firefighting optimization. In: Gervasi, O., Murgante, B., Misra, S., Rocha, A.M.A.C., Garau, C. (eds.) Computational Science and Its Applications–ICCSA 2022 Workshops, Malaga, Spain, 4–7 July 2022, Proceedings, Part II, pp. 55–67. Springer, Heidelberg (2022). https://doi.org/10.1007/978-3-031-10562-3_5
17. Naderpour, M., Rizeei, H.M., Khakzad, N., Pradhan, B.: Forest fire induced natech risk assessment: a survey of geospatial technologies. Reliabil. Eng. Syst. Saf. **191**, 106558 (2019)
18. Rashidi, Z.: Evaluation and ranking of discrete simulation tools. J. Electr. Comput. Eng. Innov. (JECEI) **4**(1), 69–84 (2016)
19. Robinson, S.: Simulation: The Practice of Model Development and Use. Bloomsbury Publishing, London (2014)
20. Romano, E., Iuliano, D.: A simulation/optimisation approach to support the resource allocation in service firms. Int. J. Procurement Manag. **11**(1), 53–75 (2018)
21. San-Miguel-Ayanz, J., et al.: Forest fires in Europe, Middle East and North Africa 2021 (KJ-NA-31-269-EN-N (online), KJ-NA-31-269-EN-C (print)) (2022). https://doi.org/10.2760/34094
22. Sargent, R.G.: Verification and validation of simulation models. In: Proceedings of the 2010 Winter Simulation Conference, pp. 166–183. IEEE (2010)
23. Wu, P., Chu, F., Che, A., Zhou, M.: Bi-objective scheduling of fire engines for fighting forest fires: new optimization approaches. IEEE Trans. Intell. Transp. Syst. **19**(4), 1140–1151 (2017)

On Polytopal Branch and Bound with Monotonicity

E. M. T. Hendrix[1(✉)], L. G. Casado[2], B. G.-Tóth[3], and F. Messine[4]

[1] Computer Architecture, Universidad de Málaga, 29080 Málaga, Spain
eligius@uma.es
[2] Informatics, Almería University, (CeiA3), Almería, Spain
leo@ual.es
[3] Informatics, University of Szeged, Szeged, Hungary
boglarka@inf.szte.hu
[4] LAPLACE, ENSEEIHT, University of Toulouse, Toulouse, France
frederic.messine@laplace.univ-tlse.fr

Abstract. In the field of Interval Arithmetic Branch and Bound (B&B) monotonicity detection and its use for dimension reduction and eliminations of partition sets has a long tradition. Recent investigation of extending ideas to simplicial B&B has shown that the relative success depends on the dimension of the simplex, i.e. the dimension of its affine hull. Linear constraints may provide a feasible area which is a polytope in a lower dimension due to equality constraints. We investigate the question how to deal with subsets defined by polytopes. We study how to construct a converging branch and bound, how to define bounds and how to refine and how to exploit monotonicity when bounds are provided by the interval hull.

Keywords: Global Optimization · polytope · branch and bound · interval

1 Introduction

Interval Arithmetic based branch and bound has a long tradition in monotonicity considerations to remove subsets, see [7,12]. The idea is that one can remove interior boxes where the function is monotone over the box and reduce the dimension with respect to a monotone component when a box facet is at the boundary of the search space. The idea to use the interval hull of a simplex to derive lower bounds has been discussed in [11]. We did not only extend this idea for deriving function bounds in [4,9], but we focused further on exploiting the derivative bounds of the interval hull to construct monotonicity tests in simplicial B&B [1,2].

This work has been funded by MCIN/AEI/10.13039/501100011033 and by "ERDF A way of making Europe", Grant PID2021-123278OB-I00 of the Spanish ministry of Science and Innovation.

© The Author(s), under exclusive license to Springer Nature Switzerland AG 2024
O. Gervasi et al. (Eds.): ICCSA 2024 Workshops, LNCS 14816, pp. 397–414, 2024.
https://doi.org/10.1007/978-3-031-65223-3_27

In recent numerical experiments comparing interval B&B which has quite some acceleration devices with simplicial B&B, we noticed that mainly for a feasible set which is on a lower dimensional hyperplane, simplicial B&B may provide some advantage in computation time [6]. We found that this is mainly due to handling linear constraints, as simple linear constraints actually define a polytope for a box region or simplicial feasible set. Our research question is whether it is possible to extend the analysis on lower bounding and monotonicity for a B&B defined by polytopal partition sets. We have several sub-questions. For instance, we would like to keep relatively "round" partition sets that fit well their interval hull to keep tight bounds on the derivatives. How can this be promoted and how can monotonicity be handled? How can we generate tight bounds?

To investigate these question, Sect. 2 introduces mathematical notation and Sect. 3 provides properties of monotonicity over polytopal sets. Moreover, we discuss some special cases together with LP and MIP models to find monotone directions. Section 4 describes a specifically designed algorithm. Section 5 investigates several ways to refine the polytopal subsets, while Sect. 6 summarises our findings.

2 Mathematical Notation

We consider the minimization of a continuously differentiable function $f : \mathbb{R}^d \rightarrow \mathbb{R}$, over a polytope P as feasible set. The 'polytope' as a convex hull of a finite number of points, is also called convex polytope in literature. Our main motivation is the use of linear equality constraints intersecting a box or simplex, which typically leads to polytope dimension $p \leq d$, i.e. in a lower dimensional space than that of the objective function f. The exact dimension of a polytope, like any subset of $\mathbb{R}^d$ is defined as the dimension of its affine hull: $\dim(P) := \dim(\text{aff}(P))$. Notice that also the concepts of relative interior $\text{rint}(P)$ and relative boundary apply. Let $P := \text{conv}(\mathcal{P})$ be defined by a set of q vectors that serve as vertices

$$\mathcal{P} := \{w_1, \ldots, w_q\} \subset \mathbb{R}^d.$$

We assume the vertices to be extreme points of P. The idea is to find or enclose all global minimum points of

$$\min f(x), x \in P. \tag{1}$$

Our experiments in [6] with interval B&B and simplicial B&B codes taught us that using partition sets based on simplices is more effective when the polytope dimension is low with respect to d, whereas partition sets based on boxes (intervals) can exploit better the acceleration devices developed for them when in fact $p = d$. Our main research question is whether we could simply use polytopal partition sets in a direct way. How can they be subdivided effectively and how can monotonicity over them be exploited?

In this concept, the partition set (subset) S is a polytope $S := \text{conv}(V)$, where $V := \{v_1, \ldots, v_m\} \subset \mathbb{R}^d$ is a set of extreme points of S. An interesting

aspect, is that the dimension $n := \dim(S)$ is not necessarily d. We will see why this is relevant. Notice that we can use the barycenter coordinates to describe partition set S:

$$S = \{x = \sum_j \lambda_j v_j, \lambda_j \geq 0, j = 1, \ldots, m, \sum_{j=1}^{m} \lambda_j = 1\} \tag{2}$$

and also its relative interior

$$\text{rint}(S) = \{x = \sum_j \lambda_j v_j, \lambda_j > 0, j = 1, \ldots, m, \sum_{j=1}^{m} \lambda_j = 1\}. \tag{3}$$

The centroid of S is given by $c := \frac{1}{m} \sum_{j=1}^{m} v_j$ and its interval hull $\square S := [\underline{x}, \overline{x}]$, where $\underline{x}_i := \min_{v \in V} v_i$ and $\overline{x}_i := \max_{v \in V} v_i$. In general for a polytope, the minimum is attained at one of its faces. The advantage of a polytopal branch and bound is that the faces of the feasible set are covered by the set of polytopal partition sets. This is not necessarily the case for interval based B&B and difficult to achieve for a simplicial B&B, if the polytope is not partitioned well into simplices.

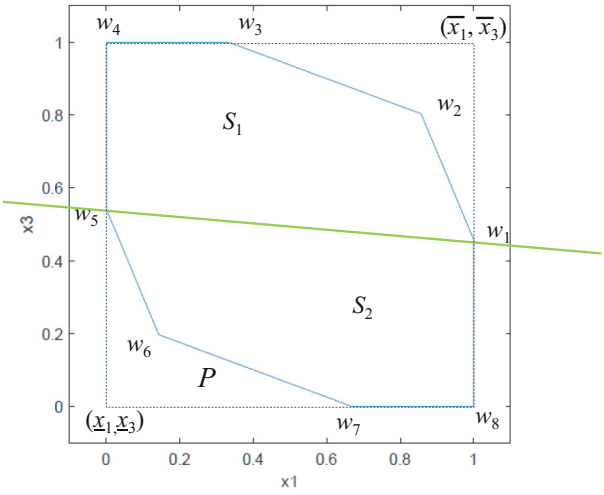

Fig. 1. 2D image from a 6 dimensional polytopal (octagon) feasible set with a partition into two polytopal subsets.

Example 1. Consider a 2-polytope in 6-dimensional space with 8 vertices $\mathcal{P}$ (an octagon) according to the vertex matrix

$$W := \begin{pmatrix} 1.00 & 0.86 & 0.33 & 0 & 0 & 0.14 & 0.67 & 1.00 \\ 0.67 & 1.00 & 1.00 & 0.86 & 0.33 & 0 & 0 & 0.14 \\ 0.46 & 0.80 & 1.00 & 1.00 & 0.54 & 0.20 & 0 & 0 \\ 1.00 & 1.00 & 0.54 & 0.20 & 0 & 0 & 0.46 & 0.80 \\ 0.31 & 0.58 & 0.89 & 1.00 & 0.69 & 0.42 & 0.11 & 0 \\ 0.11 & 0 & 0.31 & 0.58 & 0.89 & 1.00 & 0.69 & 0.42 \end{pmatrix}.$$

It may be clear from the data that the corresponding interval enclosure $\square P$ is given by $[\underline{x}, \overline{x}] = [0, 1]^6$ and the centroid by $c = 0.5(1, 1, 1, 1, 1, 1)^T$. The feasible set has been drawn in Fig. 1 in the coordinate plane x_1, x_3. For the illustration of the concept, we consider the quadratic objective $f(x) = \frac{1}{2}\|x - t\|_2^2$ with $t = (0.2, 0.8, 0.8, 0.3, 0.8, 0.8)^T$. This means that the minimum can be found in the relative interior of P. As we are dealing with a 2-polytope, the corresponding face graph [5] consists only of the vertices, edges and the complete feasible set as depicted in Fig. 2. For comparison reason, we also depicted the face graph of a 3D unit box in Fig. 5. There are several ways to partition the feasible set into polytopal subsets. We will discuss several options in this paper. For the example, we split P into S_1, S_2 by a hyperplane through the vertices w_1 and w_5. Later, we will discuss this choice.

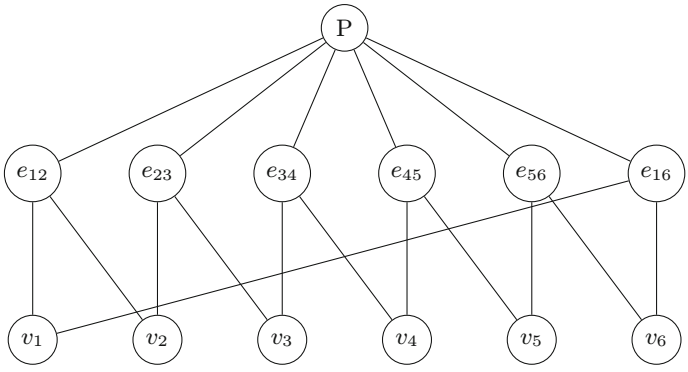

Fig. 2. Face graph of 2D polytopal feasible set

3 Mathematical Properties on Monotonicity

We first focus on mathematical properties with respect to polytopal subsets in Sect. 3.1 and then discuss several ways to find monotonic directions in Sect. 3.2.

3.1 Mathematical Properties on Monotonicity

Consider two points $x, y \in S, x \neq y$ that define a direction $r = x - y$ over polytope S.

Definition 1. *If* $\forall x \in S \ \frac{\partial}{\partial \mu} f(x + \mu r) > 0$ *for* $\mu = 0$*, direction* r *is called monotonically increasing. Monotonically decreasing and non-decreasing is defined similarly.*

As we consider continuously differentiable functions, the monotonicity can be written as $r^T \nabla f(x) > 0$, [8]. In a branch and bound context, we are mainly dealing with lower bound $\underline{r^T \nabla f(S)}$ and upper bound $\overline{r^T \nabla f(S)}$ over the subset S.

Although this is not a necessary consideration for the theoretical properties, in earlier studies we used the interval hull $\square S := [\underline{x}, \overline{x}]$ of the partition set S in order to exploit an enclosure G of the gradient $\nabla f(x) \in G := [\underline{G}, \overline{G}], \forall x \in S$, i.e. $[\underline{\nabla f(S)}, \overline{\nabla f(S)}] \subseteq G$. Interval vector G can be calculated by Interval Automatic Differentiation over the interval hull $\square S$ of subset S, see [13,14]. Considering directional vector r as the difference between two points in S, then the corresponding directional derivative $r^T \nabla f(x)$ is also included in the inner product

$$r^T G = \left[\underline{r^T G}, \overline{r^T G}\right] = \left[\sum_{i=1}^{d} \min\{r_i \underline{G}_i, r_i \overline{G}_i\}, \sum_{i=1}^{d} \max\{r_i \underline{G}_i, r_i \overline{G}_i\}\right]. \quad (4)$$

In [2], we focus on the question how to find monotonic directions in an efficient way in simplicial branch and bound.

The monotonicity is based on directional derivative bounds. This means that if $0 \notin [\underline{r^T \nabla f(S)}, \overline{r^T \nabla f(S)}]$, then r is a monotonic direction. The most generic impact is that, like for simplices [1], the interior of the polytopal partition set cannot contain an optimum.

Proposition 1. *Let* $S \subseteq P$ *be a partition set. If* $\exists\ x, y \in S$*, such that direction* $r = x - y$ *has corresponding directional derivative bounds* $0 \notin [\underline{r^T \nabla f(S)}, \overline{r^T \nabla f(S)}]$ *then* $\operatorname{rint}(S)$ *does not contain a global minimum point of* (1)*.*

Proof. Consider $z \in \operatorname{rint}(S)$. As z is in the relative interior, there exists a feasible direction r in which lower function values can be found, i.e. $\exists \varepsilon \in \mathbb{R}^+$ small enough, such that $z + \varepsilon r \in S$ and $f(z + \varepsilon r) < f(z)$. So z cannot be a minimum point of f. □

The elaboration for an algorithm depends on the choice of the direction r and the way to compute it.

Corollary 1. *Let* $S \subseteq P$ *be a partition set in a branch and bound algorithm. If the conditions of Proposition 1 apply and* $S \in \operatorname{rint}(P)$*, then* S *can be rejected.*

The argument is that the relative boundary of S may contain a global minimum point, but the same point is enclosed in the relative boundary of another partition set. The main consequence of Proposition 1 is that S can be replaced by the collection of its facets, which basically have a lower polytopal dimension and less vertices. This is mainly a theoretical observation. Keeping track of the facets of a polytope is a complex issue. One typical observation following Corollary 1 is the following.

Corollary 2. *Let F be a facet of $S \subseteq P$ in a branch and bound algorithm. If the conditions of Proposition 1 apply to F and $\mathrm{rint}(F) \subseteq \mathrm{rint}(P)$, then F can be rejected.*

The argument is that the relative boundary of F may contain a global minimum point, but the same point is enclosed in the relative boundary of another facet.

We now focus on the direction from a vertex of V pointing towards the relative interior, $r = y - v, v \in V$.

Proposition 2. *Let $S \subseteq P$ be partition set and $y \in \mathrm{rint}(S)$, such that for a vertex v of S, we have $\overline{(y-v)^T \nabla f(S)} < 0$. Then for all facets F of S which include vertex v, $\mathrm{rint}(F)$ cannot contain a global optimum point.*

Proof. Let $z \in \mathrm{rint}(F)$. The function value $f(z + \varepsilon r)$ is lower than $f(z)$ for $\varepsilon > 0$, because r is a decent direction as long as $z + \varepsilon r \in S$. This means, we have to show that $r = y - v$ is a feasible direction. For this, we should find a value for $\varepsilon \in \mathbb{R}^+$ small enough to show $z + \varepsilon(y - v) \in S$. Without loss of generality, number the vertices of S as $v_1, \ldots v_m$ with $v_1 = v$. Notice that F is a convex hull of a subset of those vertices. According to the definition of relative interior, we have that $y = \sum_1^m \mu_j v_j$ with $\mu_j > 0$. Let $z = \sum_1^m \lambda_j v_j$ with $\lambda_1 > 0$ be a point in the interior of a facet which contains v_1. This means that $x = z + \varepsilon r = (\lambda_1 + \varepsilon(\mu_1 - 1))v_1 + \sum_2^m (\lambda_j + \mu_j \varepsilon) v_j$ is a feasible point for $\varepsilon > \frac{\lambda_1}{1-\mu_1}$ with a function value $f(x)$ lower than in point z. So $z \in \mathrm{rint}(F)$ cannot be a minimum point of f. □

Corollary 3. *Let F be a facet of $S \subseteq P$ in a branch and bound algorithm including vertex v. If the conditions of Proposition 2 apply, then F can be rejected.*

The argument is that the relative boundary of F may contain a global minimum point, but the same point is enclosed in the relative boundary of another facet.

Example 2. For the illustration of the concept, consider the elements in Fig. 3. It shows a partition set S_2 with five vertices (re-)numbered as $v_1, \ldots, v_5$. If, for the orange direction $x - c$ we have $0 \notin [(x-c)^T \nabla f(S_2), \overline{(x-c)^T \nabla f(S_2)}]$, i.e. it is a monotonic direction, the interior of S_2 cannot contain an optimum. As pointed out by Corollary 2, the green faces need not be considered anymore. In [6], those are classified as non-border.

Now consider the direction $r = y - v_1$ and assume $\overline{(y-v)^T \nabla f(S_2)} < 0$ (blue arrow). We can not only conclude that vertex v_1 is not optimal, but according to Corollary 3, we can also leave out the facets $\mathrm{conv}(\{v_1, v_2\})$ and $\mathrm{conv}(\{v_1, v_5\})$ from consideration.

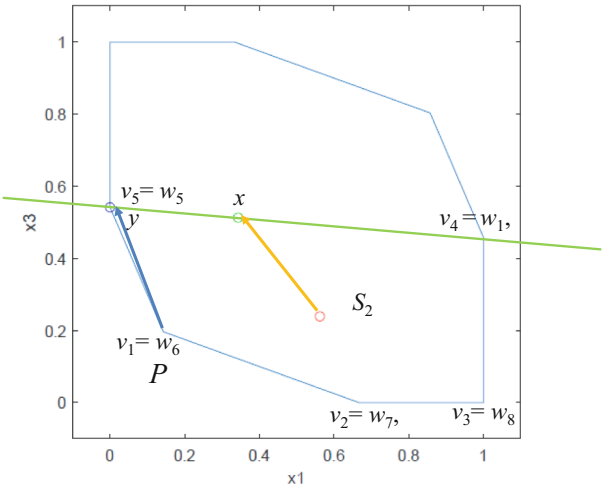

Fig. 3. 2D image from a 6 dimensional subset S_2 with renumbered vertices. The red dot is the centroid of S_2, the green dot the solution x of LP (6) and the blue dot the solution of LP (7) taking v_1 (w_6) as base. (Color figure online)

In the following section, we discuss a way to find the monotonic directions.

3.2 Finding Negative Directional Derivatives

We extend the earlier analysis of [3] for simplicial partition sets to polytopal partition sets. The analysis uses an enclosure G of the gradient based on interval enclosure $\square S$ of S. Notice again that the dimension d may be bigger than the polytopal dimension. This provides overestimation of $[\underline{\nabla f(S)}, \overline{\nabla f(S)}] \subset G$. A necessary, but not sufficient condition for the existence of a monotone direction is to have $0 \notin G$.

Example 3. Consider the 2-polytope in 6-dimensional introduced in Example 1. Due to the quadratic objective, the gradient $\nabla f(x) = (x - t)$ is linear. Bounds on the derivatives could be based on the 64 vertices of P, but also on the 8 vertices according to $\underline{\nabla f(P)}_i = \min_j(w_{ij} - t_i)$ and $\overline{\nabla f(P)}_i = \max_j(w_{ij} - t_i)$.

For the bound values we can write $[\underline{\nabla f(P)}, \overline{\nabla f(P)}]$ as the interval $[-0.2, 0.8] \times [-0.8, 0.2] \times [-0.8, 0.2] \times [-0.3, 0.7] \times [-0.8, 0.2] \times [-0.8, 0.2]$ which clearly includes 0. The idea is that partitioning leads to a tightening of the bounds. In our case, consider the partitioning in $S_1 := \text{conv}(\{w_1, w_2, w_3, w_4, w_5\})$ and $S_2 := \text{conv}(\{w_1, w_5, w_6, w_7, w_8\})$. This tightens $[\underline{\nabla f(S_1)}, \overline{\nabla f(S_1)}]$ towards $[-0.2, 0.8] \times [-0.5, 0.2] \times [-0.3, 0.2] \times [-0.3, 0.7] \times [-0.5, 0.2] \times [-0.8, 0.1]$ and $[\underline{\nabla f(S_2)}, \overline{\nabla f(S_2)}]$ is given by the interval $G :=$ $[-0.2, 0.8] \times [-0.8, -0.13] \times [-0.8, -0.26] \times [-0.3, 0.7] \times [-0.8, -0.1] \times [-0.7, 0.2]$ which does not include 0. This indicates, that f can be monotonic over S_2.

To prove that a monotonic direction exists, we need to find a direction $r = y - x$, with $x, y \in S$ corresponding to a negative upper bound of the directional derivative

$$0 > \overline{r^T G} = \sum_{i=1}^{d} \max\{r_i \underline{G}_i, r_i \overline{G}_i\}. \tag{5}$$

Finding such a direction can be done by looking for the steepest monotone direction $\min_r \overline{r^T G}$. Consider the terms $z_i = \min\{d_i \underline{G}_i, d_i \overline{G}_i\}$. This means we can write $\overline{r^T G} = \sum_{i=1}^{n} z_i$. If we fix one of the points $x \in S$ in $r = x - y$, then the term $z_i(y) = \max\{(x_i - y_i)\underline{G}_i, (x_i - y_i)\overline{G}_i\}$ is a convex function in x, as it is the maximum of two affine functions. Therefore, the upper bound on the directional derivative $\overline{g}(x) := \overline{(x-y)^T G}$ is a convex function being the sum of convex terms. We will show how an LP problem can be formulated to find a minimum of $\overline{g}(x)$.

Looking for the existence of a negative value of $\overline{r^T G}$ for some direction r, we can fix y to the centroid in the directional vector, i.e. $r = x - c$. The minimisation of convex piece-wise linear function $\overline{g}(x)$ over $x \in S$ can be formulated as the following LP problem.

$$\begin{aligned}
& \min \sum_{i=1}^{d} z_i \\
\text{s.t.} \quad & z_i \geq (x_i - c_i)\underline{G}_i, \ \ i = 1, \ldots, d \\
& z_i \geq (x_i - c_i)\overline{G}_i, \ \ i = 1, \ldots, d \\
& \sum_{j=1}^{m} \lambda_j = 1 \\
& y = \sum_{j=1}^{m} \lambda_j v_j \\
& \lambda_j \geq 0, j = 1, \ldots, m
\end{aligned} \tag{6}$$

If there is no monotone direction, then $x = c$ and $\sum_{i=1}^{d} z_i = 0$.

Example 4. Using the gradient enclosure G of subset S_2 we can now illustrate LP (6). We renumber the vertices $V_2 := \{v_1, v_2, v_3, v_4, v_5\}$. Given the gradient enclosure G and the centroid c of S_2, the result of LP (6) is a negative upper bound of $\sum_{i=1}^{d} z_i = -0.05$ for the vector $x = (0.34, 0.45, 0.51, 0.34, 0.56, 0.62)^T$ of which the components (x_1, x_3) are depicted as a point in Fig. 3. This means that f has been shown to be monotonic on S_2.

Following the line of reasoning of the example, according to Proposition 1, we can conclude that simplex S can be replaced by its facets after having shown a monotonic direction exists. Following Corollary 2, we can conclude for the example that the green facet (edge) between w_2 and v_5 can be rejected. This means for the example that S_2 can be replaced by its facets e_{18}, e_{78}, e_{67} and e_{56}. Figure 1 suggests that using Proposition 2, the edges which include w_7 and w_8

can also be removed as it seems that the direction $(x - c)$ is feasible. However, this is just a visual observation and not a mathematical rigorous proof. To show this mathematically, we have to find a feasible direction $r = y - v$ for which $\overline{r^T \nabla f(S_2)} < 0$ and have $y \in \text{rint}(S)$.

To answer the question whether such a direction exists, we can solve the following LP for a specific vertex v minimising the upper bound of a directional derivative. Consider now the re-ordered vertex set $V := \{v_1, v_2, \ldots, v_m\}$. Focusing on the direction $y - v_1$ with $y = \sum_{j=1}^{m} \lambda_j v_j$, we can demonstrate whether or not there is a (minimum) negative directional derivative by solving the LP

$$\begin{aligned} & \min \sum_{i=1}^{d} z_i \\ \text{s.t.} \quad & z_i \geq \underline{G}_i(y_i - v_{1i}), \ i = 1, \ldots, d \\ & z_i \geq \overline{G}_i(y_i - v_{1i}), \ i = 1, \ldots, d \\ & \sum_{j=1}^{m} \lambda_j = 1 \\ & y = \sum_{j=1}^{m} \lambda_j v_j \\ & \lambda_j \geq \delta, j = 1, \ldots, m, \end{aligned} \tag{7}$$

where $\delta > 0$ is a small accuracy, e.g. $\delta = 0.1^{-6}$. If the result is negative, we have proven we can reject faces that include vertex v_1 from consideration. If such a direction does not exist the solution will be $y = v_1$ and the objective function value is $\sum_{i=1}^{d} z_i = 0$.

Example 5. Using the vertex set $V_2 := \{v_1, v_5, v_6, v_7, v_8\}$ we will illustrate LP (7) taking in the ordered set as first vertex v_1. It feels that the result for w_7 and w_8 is more obvious due to the graphical observation in Fig. 3. Running LP (7) with $\delta = 10^{-6}$ gives an objective function value of $\sum_{i=1}^{d} z_i = -0.058$ and $y = (0.00, 0.33, 0.54, 0.0, 0.69, 0.89)^T$. To be more precise $y_1 = 2.7 * 10^{-6}$, yielding an interior point of S_2. This illustrates that for this example all of subset S_2 can be removed from consideration.

4 Lower Bounds in a Polytopal Subset and the Algorithm

Refining the partition can in general be done in many ways like using bisection or multi-section. Using a radial partition or a hyperplane to split parts. The idea of following a box (rectangular) shape seems attractive from a bounding point of view as distances within the partition set diminish and possibly underestimation of the objective function value is tighter. A generic pseudo-code of a B&B method based on bisection using monotonicity is provided in Algorithm 1. We sketch various ways to generate lower bounds in this section and discuss several options for the refinement in Sect. 5.

Algorithm 1. Polytopal branch and bound($f,\ P,\ \alpha$)

Require:
f: the d dimensional continuously differentiable objective function.
P: feasible set $P = \text{conv}(\{w_1, \ldots, w_q\})$
α: accuracy

Store P in Λ ▷ Set of partition sets
$X = \{w_1, \ldots, w_q\}$ ▷ List of points used as vertices
Evaluate and store $f(x)$ for all $x \in X$
$\overline{f} = \min_{x \in X} f(x)$ ▷ Incumbent value
$\underline{f} = \underline{f}(P)$
while $\overline{f} - \underline{f} > \alpha$ **do**
  Extract S from Λ ▷ Retrieve S from Λ with lowest value for $\underline{f}(S)$
  Evaluate gradient enclosure G of S
  if $0 \in G$ **then** Divide = true ▷ $0 \notin G$ is a necessary not sufficient condition
  else ▷ Trying to exploit monotonicity
    Divide = CheckMonotonicity($f,\ S,\ G, \Lambda$) ▷ If monotone store subsets in Λ
  if Divide **then**
    $\{S_1, S_2, \ldots, S_p\}$ = Refine(S) evaluating points x ▷ Refinement rule
    if $x \notin X$ **then**
      Evaluate and store $f(x)$ and add x to X
      if $f(x) < \overline{f}$ **then**
        $\overline{f} = f(x)$
        Λ = CutOff(Λ) ▷ Remove subsets $S \in \Lambda$ with $\underline{f}(S) > \overline{f}$
    for each new subset S_j **do**
      Evaluate $\underline{f}(S_j)$
      if $\underline{f}(S_j) \leq \overline{f}$ **then** ▷ RangeUp test
        Store S_j in Λ ▷ Store S_j and its bounds in Λ
  $\underline{f} = \min_{S \in \Lambda} \underline{f}(S)$
return $\cup_{S \in \Lambda} S$ and $[\underline{f}, \overline{f}]$

An overview of concepts for lower bounding in B&B is provided in the book [8]. More specifically, we discussed lower bounds on a simplicial feasible set based on bounds on the derivative G in [9]. The basis is provided by the Taylor view provided a (or some) base point $b \in S$

$$f(x) \geq f(b) + \underline{(x-b)^T \nabla f(b)} \qquad x \in S. \tag{8}$$

That study used several small full dimensional instances from [11] and showed how an LP using the function values in the vertices of the enclosing box gave most effective bounds. With the example in mind, this looks very unattractive as soon as the dimension of P is far less than d. Specifically, in the example case, the function value and also the derivatives are far higher in absolute value than that at the vertices. Therefore, we will use a small illustration of a lower bound from [9] based on a center form that uses only the centroid of P as base point, although it is less sophisticated than an LP. Given a gradient range $[\underline{\nabla f(S)}, \overline{\nabla f(S)}]$, the lower bound of the directional derivative in direction $x - c$,

$$\underline{(x-c)^T \nabla f(S)} = \sum_{i=1}^{n} \min\{(x_i - c_i)\underline{\nabla_i f(S)}, (x_i - c_i)\overline{\nabla_i f(S)}\}. \tag{9}$$

As (9) is concave in x, its minimum is taken in one of the vertices. Notice that this requires evaluation of the objective function at the centroid:

$$\varphi_c(S) := f(c) + \min_{v \in V} \underline{(v-c)^T \nabla f(S)}. \tag{10}$$

Example 6. The function value in the centroid of P is $f(c) = 0.245$. Using $[\underline{\nabla f(P)}, \overline{\nabla f(P)}]$, the lower bound yields $\varphi_c(P) = -1.52$. After the partition we have the function value at the centroid of S_1 being $f(c) = 0.155$. Actually, this value improves the incumbent best value $\overline{f} := \min_{w \in W} f(w) = f(w_3) = 0.204$. The gradient bounds $[\underline{\nabla f(S_1)}, \overline{\nabla f(S_1)}]$ tighten and also the maximum distance to the centroid gets smaller yielding a lower bound of $\varphi_c(S_1) = -1.12$. For the partition S_2, we have $f(c) = 0.53$ and using gradient bounds $[\underline{\nabla f(S_2)}, \overline{\nabla f(S_2)}]$ the lower bound yields a value of $\varphi_c(S_2) = -1.05$.

The example illustrates how the gradient bounds tighten and also the lower bound increases when bisection is applied. However, notice that the centroid form (10) does not guarantee that the lower bound increases, as the function values in the centroid do not increase with a refinement.

5 Ideas for Refining Subsets

When lower bounding and monotonicity checks are not sufficient to remove a subset, we have to divide it into two (bisection) or more subsets. There are several possibly conflicting criteria to keep in mind:

1. Preferably a subset should be "round" to keep bounds tight
2. We like polytopal subsets to have as few vertices as possible
3. Division cuts should preferably follow coordinate planes for getting tight interval hull bounds on subsets
4. It should be easy to keep track of the faces of the subset for the dimension reduction in case of monotonicity.

5.1 Radial Refinement

One of the refinements promoted by [10] is that of using a radial refinement along the centroid instead of bisecting the subset. The concept is sketched for the 2D example in Fig. 4. The procedure is to connect the centroid of the subset to all faces. It may be clear, that this way of refinement does not promote "round" subsets as the longest edge is not made shorter. For the example, the number of vertices is drastically reduced and one could proceed with a simplicial B&B based on longest edge bisection (LEB).

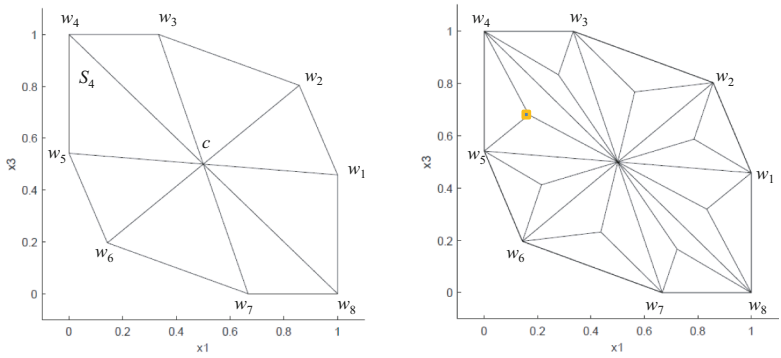

Fig. 4. Radial refinement of the 2D polytope

Example 7. For the used example, we have the radial refinement as sketched in Fig. 4 This refinement fits the lower bounding calculation of Sect. 4. Indeed, one would find a new incumbent, as the centroid of subset conv$\{w_4, w_5, c\}$) has a function value of 0.05. However, all lower bounds do not exceed the value of -0.18, such that no subset can be eliminated due to a cut-off and further refinement is necessary to the right part of the figure which contains 24 subsets.

It is important to recognise, that the convergence towards simplicial subsets is not guaranteed, as one of the facets may contain vertices that do not imply a set of affine independent points. An extreme case is the unit box and its face graph as sketched in Fig. 5.

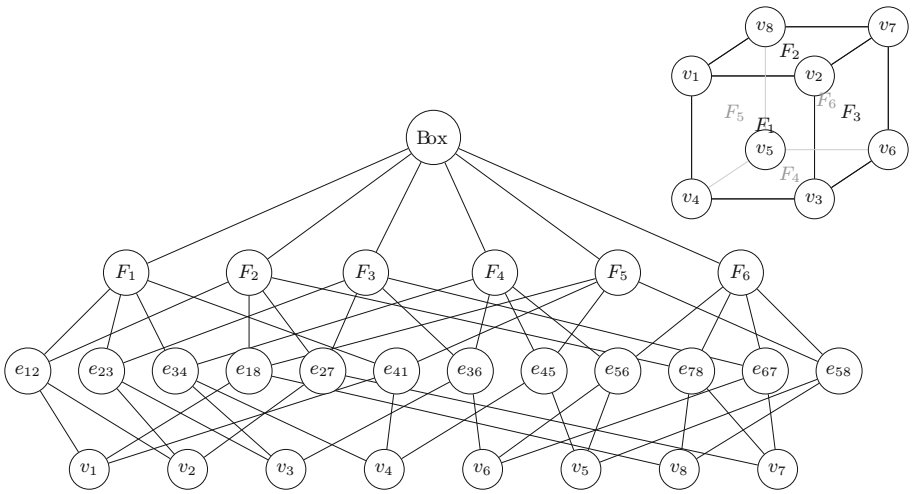

Fig. 5. Face graph of 3D box as polytopal feasible set

5.2 Component Wise Refinement

Interval arithmetic algorithms rely on bisecting (or multi-secting) an enclosing box (interval) along the longest edge. This certainly avoid needle shaped subsets. As sketched in Fig. 6, bisecting along component c_i of the centroid of the enclosing box implies finding the facets of S that include c_i and cutting them along the edges. This generates more vertices. The component wise width is halved after d bisections.

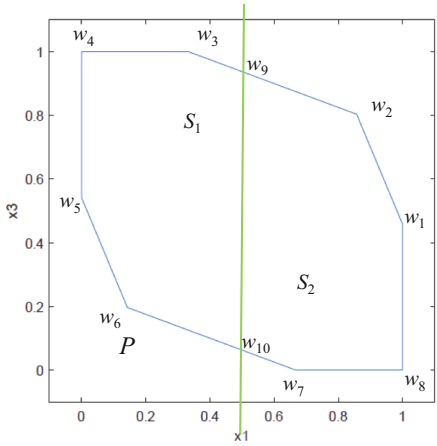

Fig. 6. Component wise bisection along c_1

Example 8. For the used example, facets $\text{conv}(\{w_2, w_3\})$ and $\text{conv}(\{w_6, w_7\})$ include $c_1 = 0.5$ and are split along new vertices $w_9 = (0.5, 1, 0.94, 0, 69, 0, 79, 0.21)^T$ and $w_{10} = (0.5, 0, 0.06, 0.31, 0.21, 0.79)^T$ respectively generating two subsets, $S_1 = \text{conv}(\{w_3, w_4, w_5, w_6, w_9, v_{10}\})$ and $S_2 = \text{conv}(\{w_1, w_2, w_7, w_8, w_9, w_{10}\})$. The evaluated vertices can be renumbered within the subsets of course. Actually for the generic case, it is not known how many new vertices are generated with a box bisection.

5.3 Vertex Wise Bisection Reducing Number of Vertices

An alternative which focuses on vertex reduction is to use n vertices that are not in the same facet and of which one of the components is as close to the centroid as possible to force volume reduction. The idea to select vertices is that in the end, we end up with subsets with $m = n + 1$ vertices and from there can use simplicial bisection of the longest edge. There is still some difficulty with degeneracy though; more than n vertices can lay on the separating hyperplane leading to non-simplicial facets.

Let $U := \{u_1, u_2, \ldots, u_\ell\}$ be groups of n affine independent vertices $u_j \subset V, |u_j| = n$ that are not in a facet of S. The subset S is then split into S_1, S_2

using the normal vector p of u_j (see, [9]) and the hyperplane $x^T p = p^T v_\ell, v_\ell \in u_j$. Consider the simplex conv(u), within subset conv(V), a vertex in the selected subset $v_\ell \subset u$ and a vertex of S outside of u, $v \in V \setminus u$. Construct a set of vectors $\mathcal{Y} := \{y - v_\ell, y \in u \setminus \{v_\ell\}\}$ with corresponding matrix representation Y. The normal vector of conv(u) in the direction of v can be expressed by defining

$$p := \left[I - Y(Y^T Y)^{-1} Y^T\right](v - v_\ell). \tag{11}$$

For finding the best subset u we can take as selection criterion to find vertices relatively close to the centroid with respect to one of the components

$$\min_{u \in U} \min_{i=1,\ldots,d} \max_{v \in u} \frac{|v_i - c_i|}{\overline{x}_i - \underline{x}_i},$$

where $\overline{x}_i - \underline{x}_i$ is the component width of the enclosing box of S.

Example 9. This rule is illustrated in Fig. 7 for subset S_1 assuming that S_2 is rejected due to monotonicity. Initially $u = \{v_1, v_5\}$ had been selected to bisect S into S_1, S_2. For $S_1, U = \{\{v_1, v_3\}, \{v_1, v_4\}, \{v_2, v_4\}, \{v_2, v_5\}, \{v_3, v_5\}\}$. The plane through v_1, v_4 is relatively closest (value 0.157 of the criterion) to c_2 (component 2). Further bisection is done through v_1, v_3 which splits component $i = 6$ best. After these bisections, S_1 has been partitioned into simplices. It is not directly clear from the x_1, x_3 projection that this is the best way to proceed, such that we depict in the figure also the x_2, x_6 projection. From the final partition, a simplicial B&B can be started, where it is easier to keep track of the facets.

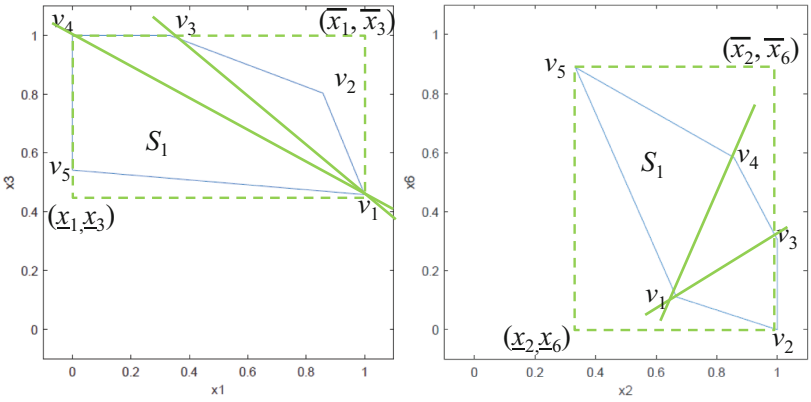

Fig. 7. Bisection along vertex hyperplanes close to c. The same content left and right, other 2D projection.

For the illustration of the calculation of the normal vector which defines the bisection along v_1, v_4, we can use reference vectors $v = v_5$ and $v_\ell = v_1$. This provides us with normal vector $p = (-0.10, -0.51, -0.41, -0.27, -0.24, 0.35)^T$, which is perpendicular to the plane through v_1, v_4.

If degeneracy occurs, more than n vertices are located in the separating hyperplane. This is illustrated in Fig. 8 for splitting the unit box. This means that the best group u is not unique. However, we can still define the corresponding hyperplane and normal vector.

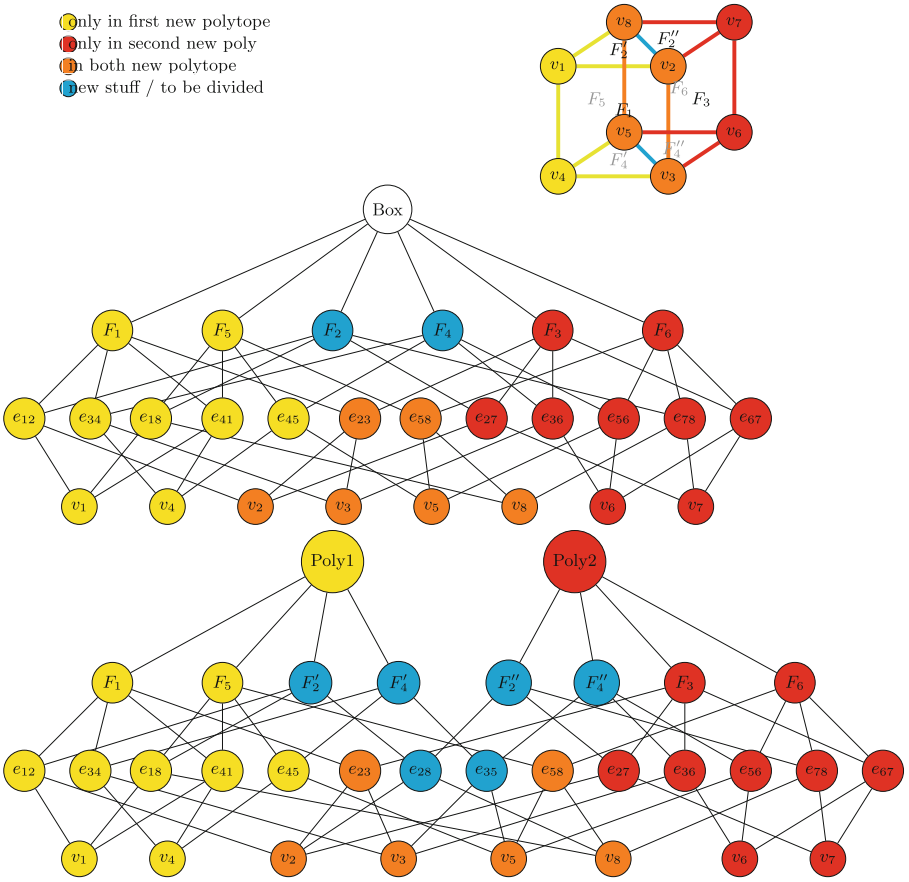

Fig. 8. Face graph of bisected 3D box

5.4 Bisecting Coordinates Along One Vertex

Using only vertices has as characteristic that we do not follow the coordinate wise splitting to promote sharp enclosures. Moreover, focusing on reduction of the width of the enclosing box does not take care of scaling with respect to the gradients. One target is to try to promote monotonicity to have dimension reduction. We can do so by taking one one hand the width of $\overline{G}_i - \underline{G}_i$ into account and on the other hand look for a vector coordinate closest to to the centroid

$$\min_{v \in V} \min_{i=1,\ldots,d} \frac{|v_i - c_i|}{\overline{G}_i - \underline{G}_i}$$

and use $x_i = v_i$ as bisection hyperplane. This does not require using the normal vector expression (11) and generates at most $n-1$ new vertices in each iteration. This procedure is an intermediate between coordinate wise bisection and using vertices. It also converges to a simplicial B&B.

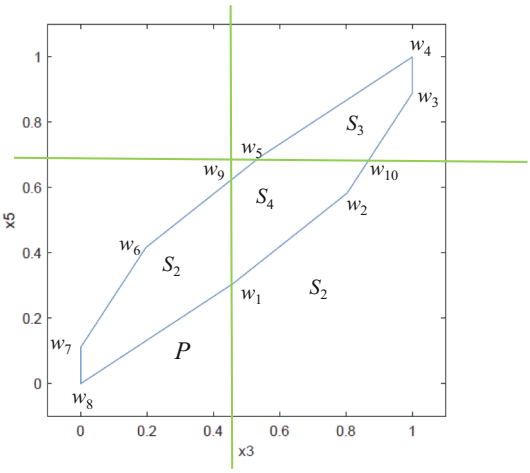

Fig. 9. Bisection along one vertex along a coordinate close to c.

Example 10. This rule is illustrated in Fig. 9. First of all, the criterion gives that we can bisect using the coordinate $i = 3$ of vertex v_1. This is similar as the bisection along vertices into S_1 and S_2, such that S_2 provides a monotonicity and can be removed. The example is very symmetric and there are two other candidates that could have been used with the same criterion value. The difference with a hyperplane supported by vertices is that we now generate a new vertex w_9; in total $n - 1 = 1$ vertices. We now focus on the resulting subset S_1 to be split into S_3 and S_4. There is less symmetry in the gradient bounds and the criterion provides a unique bisection along component $i = 5$ of w_5 generating new vertex w_{10}. To illustrate this, we adapted the projection in the figure. Although not visible, $0 \notin [\underline{\nabla} f(S_4), \overline{\nabla} f(S_4)]$. However, this desired effect is still not sufficient to find a monotonic direction according to (6). It is interesting to see that the number of vertices of the subsets is decreasing when we go deeper into the B&B tree.

6 Conclusions

Our question deals with the use of polytopes as feasible set and partition sets in global optimization branch and bound. The findings of monotonicity of simplicial B&B can be extended, although keeping track of facets to be used as subsets is a bigger challenge. Ideas of lower bounding can be based on vertex evaluations,

but also on vertices of an enclosing box and the centroid. What is the best way to refine the partition sets requires a systematic investigation. One option is to split along vertex hyperplanes reducing the number of vertices and converge to simplicial B&B. Another option is to follow interval bisection rules which may provide tighter bounds, but this results in an increase in the number of vertices for the subsets. Another rule is to combine the two ways of providing a bisection. The idea is to promote convergence to a simplicial B&B for which effective bounding has been defined. These theoretical findings provoke further investigation into the effectiveness of rules in a computational setting.

References

1. Casado, L.G., G.-Tóth, B., Hendrix, E.M.T., Messine, F.: On monotonicity detection in simplicial branch and bound over a simplex. In: Gervasi, O., Murgante, B., Misra, S., Rocha, A.M.A.C., Garau, C. (eds.) ICCSA 2022. LNCS, vol. 13378, pp. 113–126. Springer, Cham (2022). https://doi.org/10.1007/978-3-031-10562-3_9
2. Casado, L.G., G.-Tóth, B., Hendrix, E.M.T., Messine, F.: Local search versus linear programming to detect monotonicity in simplicial branch and bound. J. Glob. Optim. (2023)
3. Casado, L.G., G.-Tóth, B., Messine, F., Hendrix, E.M.T.: Directional derivative bounds and border facets in simplicial B&B monotonicity tests. In: SCAN 2020: The 19th International Symposium on Scientific Computing, Computer Arithmetic and Verified Numerical Computations, pp. 18–19. Szeged (Hungary) (2021)
4. G.-Tóth, B., Casado, L.G., Hendrix, E.M.T., Messine, F.: On new methods to construct lower bounds in simplicial branch and bound based on interval arithmetic. J. Glob. Optim. **80**(4), 779–804 (2021)
5. G.-Tóth, B., Hendrix, E.M.T., Casado, L.G.: On monotonicity and search strategies in face based copositivity detection algorithms. Central Eur. J. Oper. Res. **30**, 1071–1092 (2021)
6. G.-Tóth, B., Hendrix, E.M.T., Messine, F., Casado, L.G.: On dealing with minima at the border of a simplicial feasible area in simplicial branch and bound. J. Optim. Theory Appl. (2024). https://doi.org/10.1007/s10957-024-02480-9
7. Hansen, E., Walster, W.: Global Optimization Using Interval Analysis, 2nd edn. Marcel Dekker Inc., New York (2004)
8. Hendrix, E.M.T., B.-Tóth, G.: Introduction to Nonlinear and Global Optimization. Springer, New York (2010). https://doi.org/10.1007/978-0-387-88670-1
9. Hendrix, E.M.T., G.-Tóth, B., Messine, F., Casado, L.G.: On derivative based bounding for simplicial branch and bound. RAIRO **55**(3), 2023–2034 (2021)
10. Horst, R.: On generalized bisection of n-simplices. Math. Comput. **66**(218), 691–699 (1997)
11. Karhbet, S.D., Kearfott, R.B.: Range bounds of functions over simplices, for branch and bound algorithms. Reliable Comput. **25**, 53–73 (2017). Reliable-Computing-journal
12. Kearfott, R.B.: An interval branch and bound algorithm for bound constrained optimization problems. J. Global Optim. **2**(3), 259–280 (1992)

13. Moore, R.E., Kearfott, R.B., Cloud, M.J.: Introduction to Interval Analysis. Society for Industrial and Applied Mathematics, USA (2009)
14. Rall, L.B.: Examples of software for automatic differentiation and generation of Taylor coefficients. In: Rall, L.B. (ed.) Automatic Differentiation: Techniques and Applications. LNCS, vol. 120, pp. 54–90. Springer, Heidelberg (1981). https://doi.org/10.1007/3-540-10861-0_5

Author Index

A
Aktas, Cevat 23
Alflahi, Adam A. E. 194
Almeida, Nuno 131
Al-Noor, Nadia Hashim 284
Alsammani, Abdallah 194
Alvelos, Filipe 313
Andrade, Marina A. P. 162, 219
Anelli, Angelo 3
Averyanova, Yuliya 206

B
Bezkorovainyi, Yurii 206
Bovdui, Ihor 206

C
Carolino, E. 177
Casado, L. G. 397
Cherednichenko, Kostiantyn 206
Choraś, Michał 100
Ciloglugil, Birol 23
Costa, Lino A. 313
Costa, Lino 370

D
D'Angelo, Gianni 53
D'Antonio, Salvatore 100
de Fátima Pina, Maria 247, 266
Dias, Joana 324
dos Santos, Francisco 370

E
Elobaid, Rafida M. 284

F
Farinha, João 247, 266
Farsimadan, Eslam 83
Ferreira, Brígida 324
Ficco, Massimo 71
Filipe, Vitor 341
Fusco, Pietro 71

G
G.-Tóth, B. 397
Góis, Inês 144
Gomazkova, Yulia 37
Gomes, H. T. 355
Gonçalves, Rui 313
Gumerov, Marat 37

H
Harabaglia, Paolo 3
Hendrix, E. M. T. 397
Holubnychyi, Oleksii 206

I
Ivannikova, Viktoriia 206

K
Kogeda, Okuthe P. 113
Kozik, Rafał 100
Kuznetsov, Borys 206

L
Lima, J. 355
Lucena, Rui 131

M
Manyama, Mashako D. 113
Martinho, Domingos 144
Martins, Rui 247, 266
Matos, Marina A. 313, 383
Messine, F. 397
Mohammed, Mohammed A. Y. 194
Moradi, Leila 83
Moscatelli, Massimiliano 3

© The Editor(s) (if applicable) and The Author(s), under exclusive license to Springer Nature Switzerland AG 2024
O. Gervasi et al. (Eds.): ICCSA 2024 Workshops, LNCS 14816, pp. 415–416, 2024.
https://doi.org/10.1007/978-3-031-65223-3

N
Neves, Joana 324
Nikitina, Tatyana 206

O
Obaiys, Suzan J. 284
Ody, Christopher 177
Oliveira, Teresa A. 219, 235
Ostroumov, Ivan 206

P
Paiva, Emerson J. 383
Palmieri, Francesco 53, 83
Pawlicki, Marek 100
Pereira, A. I. 355
Pimentel, Carina 299
Pinto, Gonçalo 341
Pratas, António 144

R
Ramos, M. Rosário 177
Ribeiro, Ana 299
Rimoli, Gennaro Pio 71
Robustelli, Antonio 53
Rocha, Ana Maria A. C. 313, 383
Rocha, Humberto 324

S
Santos, Francisca 299
Santos, Jaime 247
Silva, A. M. T. 355
Silva, A. S. 355
Simões, Paula 131
Sobreiro, Pedro 144
Sokolova, Olena 206
Solomentsev, Oleksandr 206
Sushchenko, Olha 206
Sychev, Oleg 37

T
Teixeira, Ana 341
Teixeira, Beatriz 341
Teodoro, M. Filomena 162, 219
Teodoro, Maria Filomena 235

U
Uccello, Federica 100

V
Varela, Leonilde 370
Voliansky, Roman 206
Vona, Marco 3

Z
Zaliskyi, Maksym 206